

# **Organocatalytic activation of renewable resources for the synthesis of polyesters and non-isocyanate polyurethanes**

Zur Erlangung des akademischen Grades einer

**DOKTORIN DER NATURWISSENSCHAFTEN**

(Dr. rer. nat.)

von der KIT-Fakultät für Chemie und Biowissenschaften

des Karlsruher Instituts für Technologie (KIT)

genehmigte

**DISSERTATION**

von

**M. Sc. Frieda Clara Marei Scheelje**

aus Kiel

1. Referent: Prof. Dr. Michael A. R. Meier

2. Referent: Prof. Dr. Joachim Podlech

Tag der mündlichen Prüfung: 22.04.2024



Meinen Großeltern

*Annerose und Günther Müffelman,*

die schon lange vor mir Doktor und Chemikerin waren.





*“Love of learning is the most necessary passion... in it lies our happiness. It’s a sure remedy for what ails us, an unending source of pleasure.”*

- *Émilie du Châtelet*



# DECLARATION OF AUTHORSHIP

Die vorliegende Arbeit wurde von November 2020 bis März 2024 unter Anleitung von Prof. Dr. Michael A. R. Meier am Institut für Organische Chemie (IOC) des Karlsruher Instituts für Technologie (KIT) angefertigt.

## Erklärung

Hiermit versichere ich, dass ich die Arbeit selbstständig angefertigt, nur die angegebenen Quellen und Hilfsmittel benutzt und mich keiner unzulässigen Hilfe Dritter bedient habe. Insbesondere habe ich wörtlich oder sinngemäß aus anderen Werken übernommene Inhalte als solche kenntlich gemacht. Die Satzung des Karlsruher Instituts für Technologie (KIT) zur Sicherung wissenschaftlicher Praxis habe ich beachtet. Des Weiteren erkläre ich, dass ich mich derzeit in keinem laufenden Promotionsverfahren befinde, und auch keine vorausgegangenen Promotionsversuche unternommen habe. Die elektronische Version der Arbeit stimmt mit der schriftlichen Version überein und die Primärdaten sind gemäß Abs. A (6) der Regeln zur Sicherung guter wissenschaftlicher Praxis des KIT beim Institut abgegeben und archiviert.

Karlsruhe, den 06.03.2024

---

Clara Scheelje



# ACKNOWLEDGEMENTS

Zuerst möchte ich **Mike** für die Betreuung meiner Doktorarbeit danken. Danke, dass du mir so viele Freiheiten gelassen hast, meine eigenen Ideen umzusetzen, und bei Fragen trotzdem jederzeit konstruktiv zur Verfügung standest. Danke auch dafür, dass du immer sehr verständnisvoll warst, sodass ich meine Grenzen kommunizieren konnte und gleichzeitig immer motiviert war, mein Bestes zu geben, und so wachsen und meine Stärken erproben konnte.

Mein besonderer Dank gilt allen im **Arbeitskreis**, die mich in dieser Zeit begleitet haben. Erstmal natürlich danke an **Bohni**, meinen dreijährigen Labor- und Büro-nachbarn und treuen Mitstreiter der Anti-Karriero-Fraktion, für viel gemeinsames Leiden, aber auch lange Verratsch-Einheiten mit Lieferando-Support, ständige Hilfe bei meinen Fragen und für alles, was wir gemeinsam auf die Beine gestellt haben, wie die Alumni-Konferenz und die Website, und allgemein dafür, dass du mein erster Freund im AK warst und mich aktiv integriert hast. **Anja**, danke für eine von Anfang bis Ende gemeinsam durchgestandene Zeit, deine wertvollen Small-talk-Fähigkeiten in großen Kaffeepausen und viele schöne Abende in Bordeaux, Freiburg und Karlsruhe, die mit dir in der Runde immer direkt witziger waren. Danke **Jonas** für deine stete und kompetente Hilfe, den NMR-Finder, dein angenehmes Gehtempo, für deine ansteckende Freude am Denken und Lernen und dafür, dass du mich bekräftigt hast, ins Ausland zu gehen. **Qianyu**, eine sehr gute Nachfolgerin für den Platz mir gegenüber im Büro, danke für deinen herrlichen Humor und deine absolut nüchterne Kompetenz und Zuverlässigkeit. Das gleiche gilt für **Sandra**, danke für dein großes Engagement in der Gruppe von Anfang an und deine Art, deine Meinung ohne Scheu zu vertreten – schade, dass ihr beide erst so spät dazukamt. Ein großer Dank geht auch an **Roman** für lange Nachrichten mit viel wertvollem Input nach jedem einzelnen Lab Report und sowieso zu jeder Zeit, wenn ich Rat brauchte, deine Selbstverständlichkeit, mit der du alle integrierst und respektierst und deine herrliche Art, andere Leute nachzumachen und damit den ganzen Raum zu unterhalten. **Dani**, auch wenn du leider viel zu schnell weg warst, danke ich dir für deine Geduld während unserer Youtube-Nachhilfe und während des Drehs der Videos für den Girls' Day, als wir zehn Anläufe für eine einzige Aufzugfahrt gebraucht haben, weil ich jedes Mal

lachen musste. Auch großen Dank an **Michi**, mich hat immer fasziniert, wie du in einem Moment gnadenlos Sprüche raushauen kannst und aber immer sofort konstruktiv und lieb bist, sobald man mit dir zusammenarbeitet, danke für deine Ehrlichkeit, für viele lustige Tischtennisrunden und ein paar Runden Rage Cage, in denen du tapfer für mich getrunken hast. Danke **Henni** für gemeinsame Critical-Mass-Besuche und für deine stete Bereitschaft, die Gruppe wie es nur geht zu unterstützen, ich hoffe, du verzeihst uns, dass wir dich ununterbrochen abgelenkt und danach dir die Schuld für die Ablenkung gegeben haben. Thank you **Francesca** for great team work in the review, valuable terpene input and exchange of frustration in all times. Danke **Pete**, dass du mich in meiner Sturheit geduldig vom 1:2:1-Verhältnis überzeugt hast, während du mein Theorem im Tischtennis in zwei Sekunden geblickt hast, danke fürs Brückenschlagen zum IOC und für stets kompetenten Input. Und dir und **Leon** auch einen großen Dank für die Top-Snackversorgung im Tiny Store während meiner Schreibphase. **Timo**, danke für deine wertvolle Polymer-Perspektive auf meine Projekte und für deine stets liebe Art. Thank you **Celeste** for being the best Aperol bartender, for your good taste in music and for teaching me “Fresca, fresca, l’aqua di bide” on one of many fun nights in the AK. Thank you **Caitlyn** for supplying me with enough scrungies for a lifetime, for your “Friday” euphoria and for always taking care that there are enough pictures of the activities. Obrigada **Nichollas** por todas as boas sugestões para meus projetos e minhas apresentações e por tanta paciência com meu português. Thanks to **Federico Ferrari** for a successful Girls’ Day and for always being extremely helpful and polite. Danke **Dennis** für eine schöne Zeit in Bordeaux und danke **Marc**, dass du mich für den AK rekrutiert hast. Danke **Pinar** für deine große Unterstützung mit der Alumni-Konferenz und auch allgemein mit allem Organisatorischen. Darüber hinaus danke ich **Eren, Marie, Anni, Pia, Maxi, Kevin, Jonas Wenzel, Larissa, Julian, Becci, Luca Filippi, Iuliana, Alessandro, Conni, Andreas, Michelle, Luis, Sarah, Benni, Dennis, Silas, Federico Mundo, Florian, Leonie, Svenja, Tina, Luca Narducci, Yannis** und **Shilpa** für die gemeinsame Zeit im AK, für viele lustige Abende, Unternehmungen und Pausen. Further I would like to thank **Haritz Sardon** for giving me the possibility to do a research stay in his group and for always giving valuable input. I would also like to thank **Mercedes Fernandez** for helping me with all the rheology experiments and always patiently explaining everything. A great thanks also to the entire group for

making me feel comfortable and welcome from the first day on, and special thanks to **Marta** for showing me everything and always helping with my project and **Giulia** for a lot of patience with my rheology samples. Danke außerdem an das Karlsruhe House of Young Scientists (**KHYS**) für die finanzielle Förderung meines Auslandsaufenthalts.

Viele der Ergebnisse, die ich erhalten habe, waren insbesondere möglich durch die tatkräftige Unterstützung von Studierenden und Auszubildenden, mit denen ich die Freude hatte zusammenzuarbeiten. Ich danke natürlich vor allem **Michelle** für die lange synthetische Unterstützung, und außerdem **Klaus, Henni** und **Johanna**, die ihr mit euren Projekten wertvolle ergänzende Arbeit geleistet habt und euch wacker mit der Terpen-Chemie herumgeschlagen habt. Des Weiteren danke ich **Elin, Natalia, Elsa** und **Julian** für tatkräftige und sehr eigenständige Zuarbeit.

Ein großer Dank geht außerdem an alle Mitarbeitenden der analytischen Abteilung des IOC: **Pia Lang, Tanja Ohmer, Despina Savvidou** und **Andreas Rapp** für die stets zuverlässige Betreuung des NMRs, **Angelika Möhle** und **Lara Hirsch** für das Messen zahlreicher Massenspektren, **Richard von Budberg** für die Reparatur von Glasgeräten, **Sina Zimmermann** für Hilfe in der Werkstatt und **Christoph Götz** und **Nathalie Schmitt** für stets freundliche Betreuung der Ausgabe.

Ein großes Dankeschön gilt den fleißigen Korrekturlesern **Pete, Jonas, Celeste, Nichollas, Timo, Anja, Francesca, Roman, Andreas, Henni, Sandra, Qianyu** und **Bohni**, dafür, dass ihr euch Zeit für meine zum Teil chaotischen und kurzfristig gesendeten Texte genommen und mir viel hilfreichen Input gegeben habt.

Während der Jahre meiner Promotion war ich sehr dankbar über meine **Freundschaften**, die mich in schwierigen Zeiten unterstützt haben und ein wichtiger Ausgleich zum Laboralltag waren. Insbesondere danke ich der **Flauschigen Lerngruppe** und **Hannah** dafür, dass ich bei euch immer sichere Häfen hatte und immer komplett ich selbst sein konnte, für viele unvergessliche Momente und natürlich auch für die gemeinsam durchgestandene Studienzzeit. Außerdem danke ich natürlich meiner **Familie** für die bedingungslose Unterstützung, euren Glauben an mich und eure Begeisterung für alles, was ich so mache, insbesondere **Freia** und **Luci**, ihr seid meine wichtigsten Anker und einfach ganz wunderbar, ich bin unendlich dankbar, dass ich euch habe. Und natürlich: "Last but not least, I want to thank **me**, for believing in me, for doing all this hard work, for never quitting."





# ABSTRACT

In the face of global challenges, such as climate change and environmental pollution, increasing research effort has been directed towards establishing more sustainable chemical protocols. This also concerns the production of polymeric materials, which are currently mostly petroleum-based and often rely on hazardous synthesis routes. The twelve principles of Green Chemistry offer a framework for more sustainable approaches to chemical synthesis, including e.g. the use of renewable resources, less toxic chemical reagents, and catalysis.

Within this work, the application of thiourea catalysts in the synthesis of renewable polymers was investigated. Several thiourea compounds were synthesized using a multicomponent reaction and tested in different synthesis approaches towards polyesters and *non-isocyanate polyurethanes* (NIPUs).

Establishing a route towards polyesters, different thioureas were used as cocatalysts in combination with organobases for the ring-opening polymerization of  $\epsilon$ -caprolactone, achieving narrow dispersity values ( $\overline{D} \leq 1.07$ ) even after long reaction times of up to 72 h. Thiourea catalysts bearing sulfone or ester moieties showed comparable performance to the classically used  $\text{CF}_3$  motif. Moreover, the synthesis of a renewable bicyclic lactone based on  $\alpha$ -pinene as starting material was achieved.

Secondly, the use of thiourea catalysts for the synthesis of renewable NIPUs was investigated. Test reactions of transurethanization and cyclic carbonate opening approaches showed the latter route to be efficiently catalyzed by addition of thiourea compounds. Based on terpenes as renewable resources, a scope of five-membered cyclic carbonates was synthesized and opened with allylamine or fatty acid-based dec-9-en-1-amine under thiourea catalysis. Expanding this approach, renewable erythritol bis(cyclic carbonate) was introduced as sugar-based feedstock for urethane monomer synthesis. Reaction and work-up conditions of the aminolysis reaction were optimized and compared regarding their sustainability.

In this way, seven urethane monomers containing two terminal double bonds were obtained, thus representing AA monomers. Afterwards, linear non-isocyanate polyurethanes were synthesized via step-growth thiol-ene polyaddition with different

dithiols. Variation of the dithiol and urethane allowed for the synthesis of NIPUs with different properties, with molecular weights of up to  $31 \text{ kg}\cdot\text{mol}^{-1}$  and  $T_g$  values ranging from 1 to  $29 \text{ }^\circ\text{C}$ .

Lastly, the synthesized terpene- and erythritol-based urethane monomers were used to produce NIPU thermosets via thiol-ene cross-linking. The curing conditions were optimized to obtain NIPU foils containing a limonene-based and an erythritol-based urethane monomer in different ratios. For selected materials, the implementation of a Lewis acid catalyst to promote exchange reactions was achieved. The use of a mixture of bifunctional and trifunctional thiols allowed for improved reprocessability of the obtained materials.

# KURZZUSAMMENFASSUNG

Angesichts globaler Herausforderungen wie dem Klimawandel und zunehmender Umweltverschmutzung konzentrieren sich aktuelle Forschungsanstrengungen zunehmend darauf, nachhaltigere chemische Protokolle zu etablieren. Dies betrifft auch die Herstellung polymerer Materialien, die derzeit größtenteils auf Erdöl basieren und oft auf risikobehafteten Synthesewegen beruhen. Die zwölf Prinzipien der Grünen Chemie bieten einen Rahmen für nachhaltigere chemische Syntheseansätze, einschließlich der Verwendung erneuerbarer Ressourcen, weniger giftiger chemischer Reagenzien und der Nutzung von Katalyse.

Im Rahmen dieser Arbeit wurde die Anwendung von Thioharnstoffkatalysatoren für die Synthese erneuerbarer Polymere untersucht. Mehrere Thioharnstoffe wurden mithilfe einer Multikomponentenreaktion hergestellt und in verschiedenen Ansätze zur Herstellung von Polyestern und nicht-isocyanatbasierten Polyurethanen (NIPUs) untersucht.

Bei der Etablierung einer Route zu Polyestern wurden verschiedene Thioharnstoffe als Kokatalysatoren in Kombination mit Organobasen für die Ringöffnungspolymerisation von  $\epsilon$ -Caprolacton verwendet, wobei auch nach langen Reaktionszeiten von bis zu 72 h niedrige Dispersitäten ( $D \leq 1.07$ ) erreicht wurden. Thioharnstoffkatalysatoren mit Sulfon- oder Estergruppen zeigten eine vergleichbare Leistung wie das klassisch verwendete  $CF_3$ -Motiv. Darüber hinaus wurde die Synthese eines erneuerbaren bicyclischen Lactons auf Basis von  $\alpha$ -Pinen als Ausgangsmaterial erreicht.

Zudem wurde die Verwendung von Thioharnstoffkatalysatoren für die Synthese erneuerbarer NIPUs untersucht. Testreaktionen zur Transurethanisierung und zur Ringöffnung von cyclischen Carbonaten zeigten, dass letztere effizient durch Zugabe von Thioharnstoffverbindungen katalysiert wurde. Basierend auf Terpenen als erneuerbare Ressourcen wurden eine Reihe fünfgliedriger cyclischer Carbonate synthetisiert und unter Thioharnstoffkatalyse mit Allylamin oder fettsäurebasiertem Dec-9-en-1-amin geöffnet. Durch die Erweiterung dieses Ansatzes wurde erneuerbares Erythritolbis(cyclocarbonat) als zuckerbasierter Ausgangsstoff für die Synthese von Urethanmonomeren eingeführt. Reaktions- und Aufarbeitungs-

bedingungen der Aminolyse-Reaktion wurden optimiert und hinsichtlich ihrer Nachhaltigkeit verglichen.

Auf diese Weise wurden sieben Urethanmonomere mit je zwei terminalen Doppelbindungen erhalten, die folglich AA-Monomere darstellen. Anschließend wurden lineare nicht-isocyanatbasierte Polyurethane über eine Stufenwachstums-Thiol-En-Polyaddition mit verschiedenen Dithiolen synthetisiert. Die Variation des Dithiols und des Urethanmonomers ermöglichte die Synthese von NIPUs mit unterschiedlichen Eigenschaften, mit Molekulargewichten von bis zu  $31 \text{ kg} \cdot \text{mol}^{-1}$  und  $T_g$ -Werten im Bereich von 1 bis  $29 \text{ }^\circ\text{C}$ .

Abschließend wurden die synthetisierten terpen- und erythritolbasierten Urethanmonomere zur Herstellung von NIPU-Thermosets über eine Vernetzung mittels Thiol-En-Reaktion verwendet. Die Aushärtebedingungen wurden optimiert, um NIPU-Filme ausgehend von einem auf Limonen basierenden und einem auf Erythritol basierenden Urethanmonomer in unterschiedlichen Verhältnissen zu erhalten. Für ausgewählte Materialien wurde die Implementierung eines Lewis-Säure-Katalysators zur Förderung von Austauschreaktionen erreicht. Die Verwendung einer Mischung aus bifunktionalen und trifunktionalen Thiolen ermöglichte eine verbesserte Wiederaufarbeitung der erhaltenen Materialien.

# TABLE OF CONTENTS

<b>Declaration of authorship</b> .....	I
<b>Acknowledgements</b> .....	III
<b>Abstract</b> .....	VII
<b>Kurzzusammenfassung</b> .....	IX
<b>1. Introduction</b> .....	1
<b>2. Theoretical Background</b> .....	3
2.1. Green Chemistry .....	3
2.2. Non-isocyanate polyurethanes .....	8
2.3. Thermoplastic polyesters .....	16
2.4. Covalent adaptable networks .....	21
2.5. Renewable resources for polymer synthesis .....	26
2.5.1. Plant oils .....	26
2.5.2. Carbohydrate-based erythritol bis(cyclic carbonate) .....	30
2.5.3. Cyclic terpenes .....	32
2.6. Organocatalysis in polymer synthesis .....	37
2.6.1. Organic superbases TBD and DBU .....	38
2.6.2. Thiourea organocatalysts .....	41
<b>3. Aim of the Thesis</b> .....	45
<b>4. Results and Discussion</b> .....	47
4.1. Synthesis of a set of thiourea catalysts .....	47
4.2. Thiourea-catalyzed ring-opening polymerization .....	51
4.2.1. Ring-opening polymerization of cyclic carbonates .....	52
4.2.2. Ring-opening polymerization of $\epsilon$ -caprolactone .....	54
4.2.3. Synthesis and ring-opening polymerization of terpene-based lactones .....	59
4.3. Thiourea catalysts in transurethanization reactions .....	70

4.4.	Linear non-isocyanate polyurethanes from terpenes via thiourea organocatalysis and thiol-ene-chemistry.....	74
4.4.1.	Synthesis of terpene-based cyclic carbonates .....	74
4.4.2.	Ring-opening of cyclic carbonates.....	78
4.4.3.	Synthesis of linear NIPUs.....	88
4.5.	Linear non-isocyanate polyurethanes from EBCC.....	94
4.5.1	Monomer synthesis .....	94
4.5.2	Linear NIPU synthesis.....	101
4.6.	Synthesis of PHU networks .....	110
<b>5.</b>	<b>Conclusion.....</b>	<b>123</b>
<b>6.</b>	<b>Experimental Section.....</b>	<b>125</b>
6.1.	Methods.....	125
6.1.1.	Materials.....	125
6.1.2.	General Methods and Instrumentation .....	126
6.2.	Experimental Procedures .....	130
6.2.1.	Synthesis of thiourea catalysts .....	130
6.2.2.	Synthesis and ring-opening polymerization of cyclic carbonate and lactone monomers.....	154
6.2.3.	Synthesis and transurethanization of model urethanes.....	167
6.2.4.	Non-isocyanate polyurethanes from terpenes .....	172
6.2.5.	Synthesis of erythritol-based linear PHUs and PHU networks ....	230
<b>7.</b>	<b>Appendix.....</b>	<b>242</b>
7.1.	List of abbreviations.....	242
7.2.	List of publications .....	244
7.3.	List of conference contributions .....	244
<b>8.</b>	<b>References.....</b>	<b>245</b>

# 1. INTRODUCTION

While the importance of the chemical industry for ubiquitous products of daily life is unquestionable, it is also associated with the highly polluting and energy-consuming production of potentially hazardous materials. Indeed, the chemical industry significantly contributes to climate change,<sup>1</sup> biodiversity loss<sup>2,3</sup> and out-of-equilibrium phosphorus<sup>4</sup> and nitrogen cycles.<sup>5</sup> At the same time, the chemical industry is necessary to produce materials that enable innovations for a more sustainable economy.<sup>6</sup> If societies aim to make an impactful effort to stop the stressing of these planetary boundaries, a fundamental change of the chemical industry is crucial.<sup>7</sup>

Facing this challenge, guidelines promoting a greener and more sustainable chemistry were introduced within the last decades.<sup>8–10</sup> These directives encouraged various research areas to develop strategies that surpass the limitations of previous approaches with regard to sustainability,<sup>11</sup> which is an ongoing task that requires broad and cooperative research efforts.<sup>12,13</sup>

To answer the question how future materials should look like, Zimmermann et al. summarized the principle aims of sustainable chemistry such that chemicals and chemical processes should be non-depleting, non-toxic and non-persistent in the environment.<sup>14</sup> These three concepts serve as framework for research projects targeting applications within a future industry and also offer a guidance for the research presented in this work.

When looking at polymers, it can be stated that these three terms – non-depleting, non-toxic and non-persistent – do not apply for the majority of polymeric products used to this day.<sup>15</sup> Not only does the production of polymers largely depend on fossil resources such as crude oil and gas,<sup>16</sup> their synthesis routes also often require the use of hazardous chemicals, such as isocyanates in the case of polyurethanes.<sup>17,18</sup> Further, apart from critical amounts of plastic waste,<sup>19</sup> even polymers that are collected back for repeated use cannot always be efficiently recycled.<sup>20</sup> This is especially the case for thermoset materials, whose mechanical properties are highly desirable for certain applications, but which are not reproces-

sable and thus not straightforward to implement in Circular Economy approaches.<sup>21</sup>

This work aims to develop strategies for polymer synthesis that take the aforementioned concepts for more sustainable materials as a guideline. Renewable feedstock is used to develop less depleting materials, organocatalytic approaches and the choice of less harmful reagents aim for less toxic synthesis pathways, and finally efforts to enhance the reprocessability of the obtained materials work towards enabling closed-loop recycling.



## 2. THEORETICAL BACKGROUND

### 2.1. Green Chemistry

After the challenges of societies depending on an ever-expanding industry had been pointed out by the Club of Rome in 1972 in the release of their report on the “Limits to Growth”,<sup>22</sup> and after the threads of climate change had been distinguished,<sup>23</sup> international committees such as the *Advisory Group on Greenhouse Gases*<sup>24</sup> and its successor, the *Intergovernmental Panel on Climate Change*,<sup>25</sup> have been founded and since then emphasized the risks of planetary boundaries. In this context, the concept of *Green Chemistry* was introduced in the 1990s,<sup>8</sup> with twelve main principles giving guidance on how to design processes and chemical products more sustainably (**Figure 1**).<sup>9</sup>

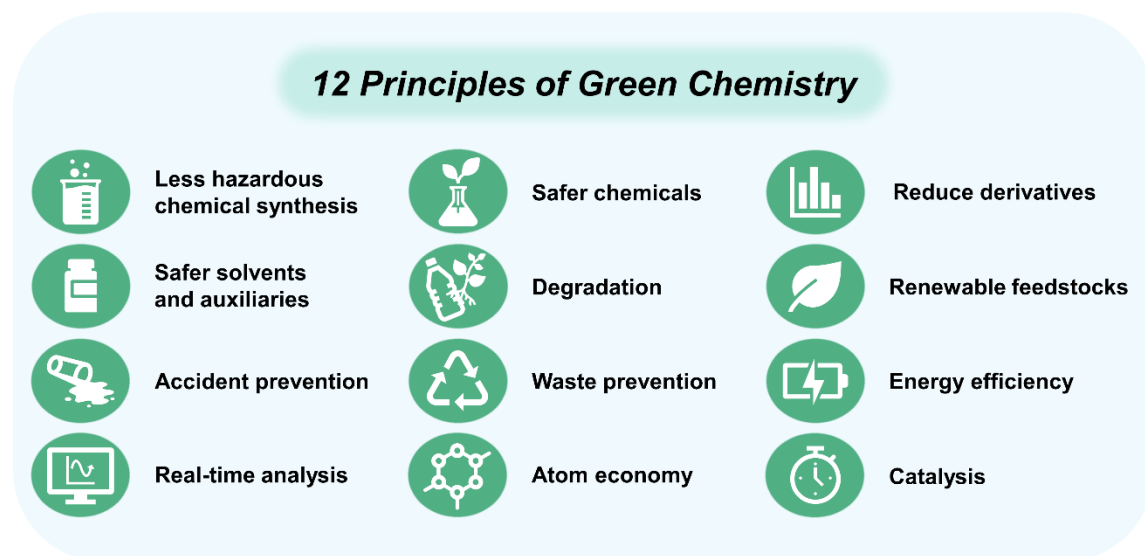


**Figure 1.** The twelve principles of Green Chemistry.<sup>9</sup>

Since then, the principles of Green Chemistry have influenced chemical research in various areas. Further, international treaties, such as the *Kyoto Protocol*<sup>26</sup> and the *Paris Agreement*,<sup>27</sup> have been brought forward to express political motivation for a transition towards a more sustainable industry.<sup>28</sup> In this chapter, the twelve principles of Green Chemistry will be introduced briefly based on examples from current research efforts.

Having established that the production of many chemicals poses a health hazard to humans and the environment,<sup>3</sup> a main focus of Green Chemistry is set on reducing the hazard of chemical processes and materials. As such, the principle of *less hazardous chemical synthesis* aims to develop more efficient and cleaner protocols, including all chemical substances that are used during the synthesis, as well as their precursors. For instance, avoiding the use of toxic phosgene<sup>29</sup> in the production of polyurethane monomers is a broad field of current research<sup>30–34</sup> and will be discussed in more detail in section 2.2.

Reducing the hazard of chemical syntheses is further connected to the use of *safer solvents and auxiliaries*. Extensive research describes the development of more sustainable solvent systems as they often contribute significantly not only to the overall waste<sup>35</sup> and pollution of processes, but also to hazardousness due to the toxicity, flammability or corrosiveness of the majority of solvents.<sup>36</sup> Thus, it is desirable to develop chemical syntheses that do not require any solvent.<sup>37,38</sup> For cases in which solvents cannot be avoided, however, solvent selection guides were published, in which a range of different solvents is ranked based on factors such as safety, health and effect on the environment.<sup>36,39</sup>

In cases where the use of hazardous chemicals is still necessary, it is crucial to ensure that measurements for *accident prevention* are taken to protect the workers and the environment. Important tools for this are safety trainings of workers,<sup>40</sup> and further the ability of *real-time analysis*, which can further prevent the release of toxic chemicals into the environment.

In the same way that chemicals used within a process should pose minimal hazard to the environment, the end products should not be harmful during the consumer phase and afterwards. Therefore, the design of inherently *safer chemicals* must include profound knowledge about the toxicology of the products. At the same time, consumer products should show *biodegradability* into benign substances whenever possible, as collection for recycling cannot always be guaranteed. This concept is of great importance in the development of polymers, as the immense amount of plastic waste poses environmental problems.<sup>19</sup> Especially in the field of polyesters, considerable progress has already been achieved with respect to biodegradability.<sup>41,42</sup> This group of polymers will be further discussed in section 2.3.

The degradability of materials is directly linked to another aspect that is connected to several principles of Green Chemistry, which is the *prevention of waste*. It

includes avoiding the formation of by- and side products, but also considers the use of solvents and reactants, as depicted above. An indication for the amount of waste inherently produced during a reaction is the *atom economy* (AE),<sup>43</sup> defined in Equation (1).

$$AE = \frac{M_{\text{product}}}{M_{\text{reactants}}} \quad (1)$$

The atom economy thus describes the weight percentage of atoms that end up in the final product. It gives an preliminary estimate of the waste that might be produced by a reaction per se, with no possibility to decrease it via process optimization. However, a considerable amount of waste produced in chemical syntheses derives from factors that cannot be directly distinguished from the chemical equation, such as conversion, solvent waste, by- and side products, and reactants used for the work-up. Thus, more extensive metrics were introduced,<sup>44</sup> one commonly used metric being the *environmental factor* (E-Factor) that was proposed by Sheldon.<sup>45</sup> It describes the mass of produced waste divided by the mass of desired products, as described in Equation (2).

$$\text{Environmental Factor} = \frac{m_{\text{waste}}}{m_{\text{product}}} \quad (2)$$

The calculation of the E-Factor depends on the definition of waste, making it difficult to compare published E-Factors directly. For more clarity, a more recent common differentiation is made between the *simple E-Factor* (sEF), considering only the waste due to yield losses and reagents, and the *complete E-Factor* (cEF), including solvent and water waste.<sup>46</sup>

Industrial E-Factors, considering multiple reaction steps, are in the range of <1 to 5 for bulk chemicals, 5 to >50 for fine chemicals and 25 to >100 for pharmaceuticals.<sup>10</sup> Notably, lower E-Factors are required in cases where high amounts are produced to decrease the absolute amount of waste.

To reduce the E-Factor of a reaction, its components have to be considered precisely. Next to new concepts for solvent use, as mentioned above, it is crucial

to *reduce derivatives*, which includes classical chemical tools such as over-stoichiometric reagents or protecting groups.

In general, high yields and conversions are crucial to achieve a low E-Factor not only by a lower contribution of side products, but also by less required work-up. Thus, examples for reactions that fulfill several requirements of Green Chemistry are multicomponent reactions and tandem reactions, which do not only often show high atom economy, but also avoid work-up steps.<sup>47</sup> As such, multicomponent reactions have also been shown to be highly useful in polymer synthesis.<sup>48</sup>

Preventing waste is a possibility to expose less chemicals to the environment, but it also contributes to less material being needed in general, since less material input is necessary for the same amount of product, and further recycled materials can be used instead of raw materials. In this context, the ideal concept of a Circular Economy (Figure 2)<sup>49</sup> was developed within the last decades.<sup>50</sup> It aims to keep materials in the supply chains as long as possible.<sup>51–53</sup>

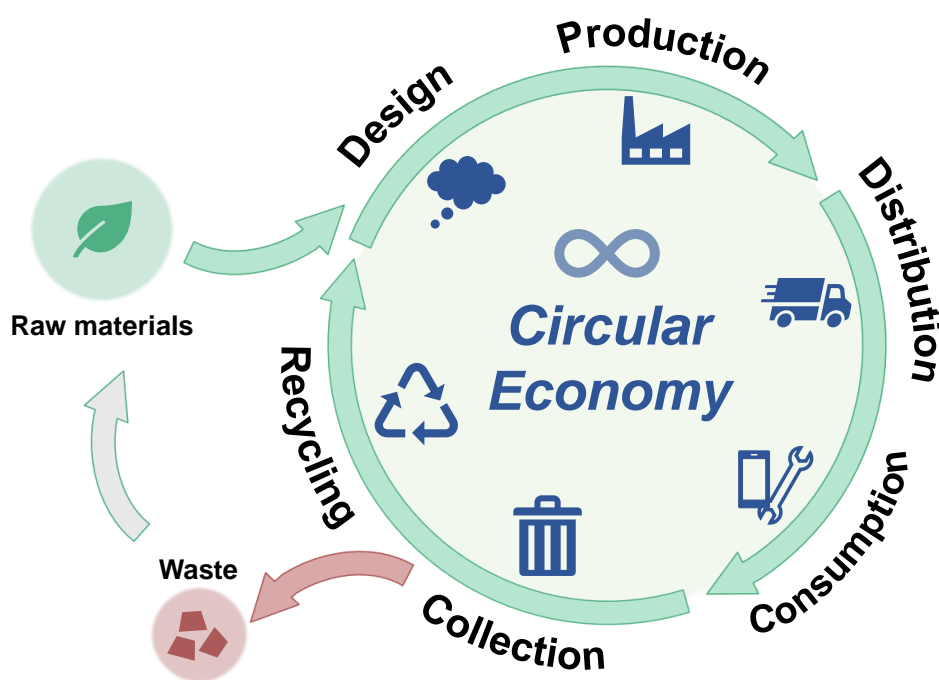


**Figure 2.** Scheme of the Circular Economy concept.<sup>49</sup>

The design and production should thus mainly be sourced from reusing and recycling of used goods and partly from *renewable feedstock* if necessary. This opens possibilities to produce without the need for crude oil and gas.<sup>54</sup> Less

depletion and consumption of non-renewable resources is an essential aspect of sustainable approaches.

This requires all aspects of economy to be thought in a holistic concept, starting from designing more sustainable products and adjusting production processes, and further including the collection and recycling of the consumed products, which relates to the concept of waste prevention described above. The idea is that materials should be developed in a way that their value can be taken advantage of still after their consumption. In that way, the use of raw materials as well as the release of products into the environment are to be minimized.

Next to the raw materials that are consumed primarily in the synthesis of chemical products, depletion of resources is further linked to the high energy consumption of chemical processes. Therefore, design for *energy efficiency* is key to achieving greener synthesis conditions. To avoid harsh reaction conditions, *catalysis* can further be an effective tool, as catalysts lower the activation energy required for a process.<sup>55</sup> Furthermore, suitable catalysts often provide highly selective reaction conditions, thus, the formation of side products and therefore of overall waste can be decreased. In this context, the field of organocatalysis will be discussed in more detail in section 2.6.

Since the twelve principles of Green Chemistry are in many cases connected, it is important to take all aspects into account when assessing the overall sustainability of a process.<sup>56</sup> They offer a frame for the design of chemicals and chemical procedures that cause less hazard, depletion, and waste production than state-of-the-art procedures. Within the field of polymer chemistry, they are key to bring forward a fundamental change towards more sustainability.<sup>57</sup>

## 2.2. Non-isocyanate polyurethanes

The production of *polyurethanes* (PUs) reaches back to the 1940s, and has since then increased and diversified immensely to result in a widely used class of polymers with various applications.<sup>18,58</sup> Chemically, PUs are characterized by the presence of urethane linkages in the polymeric backbone, which can give rise to desirable properties, e.g. due to hydrogen bonding.<sup>59</sup> Industrially, polyurethane formulations find applications for instance in coatings, adhesives, or sealants.<sup>60</sup> Industrially, PUs are obtained via polyaddition of diisocyanates and polyols. A schematic illustration of PU synthesis is depicted in **Figure 3**.<sup>61</sup> As a high variety of polyols and additives is industrially accessible, the respective PUs cover a wide range of properties.<sup>62</sup>

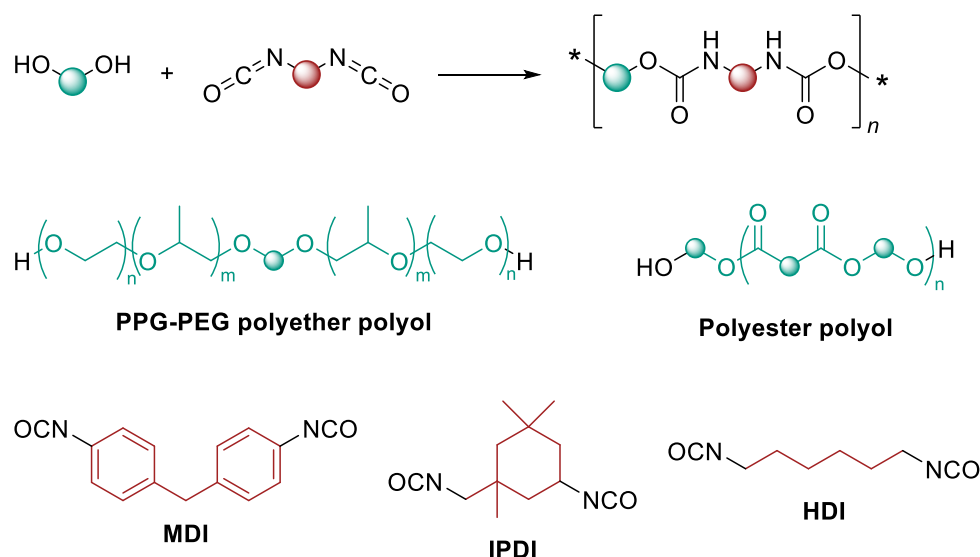


**Figure 3.** Polyurethane synthesis *via* polyaddition of polyol and diisocyanate, as well as examples for commercially used diols and diisocyanates. PPG = polypropylene glycol; PEG = polyethylene glycol; MDI = methylene diphenyl diisocyanate; IPDI = isophorone diisocyanate; HDI = hexamethylene diisocyanate.

The use of difunctional monomers can yield thermoplastic PUs.<sup>63</sup> They usually consist of a soft segment, allowing e.g. for elongation and elasticity,<sup>64</sup> which depends mostly on the polyol structure, as well as a hard segment containing the diisocyanate block, which can act as physical cross-link through intramolecular interactions and thus contributes to the stiffness, tensile strength, and the impact resistance of the material.<sup>65</sup> Multifunctional monomers, on the other hand, allow for

chemically cross-linked PUs towards thermoset materials.<sup>66</sup> Further, secondary reactions of the isocyanates by dimerization or trimerization<sup>67,68</sup> or by the reaction with other present functional groups, such as urethane or urea moieties,<sup>69</sup> can yield cross-linked structures.

An important secondary reaction is the hydrolysis of isocyanate groups, releasing CO<sub>2</sub> and forming an amine end group that then can react with another isocyanate to yield a urea linkage. This mechanism for CO<sub>2</sub> release is taken advantage of in the production of PU foams.<sup>70</sup> While flexible PU foams with open cells find application for example as cushion and sponge materials,<sup>71</sup> closed foam cells result in a rigid structure in which the gases formed during the foaming are enclosed, thus showing good insulation properties.<sup>72,73</sup> If foam formation is avoided, elastomeric PUs can be obtained,<sup>74</sup> which find application as cellular elastomers, synthetic leather, and elastomeric fibers, among others.

With regard to sustainability, the presented synthesis route contains clear drawbacks. The majority of the building blocks for PU synthesis is obtained from fossil-based resources, which is addressed by increased implementation of biobased monomers, especially biobased polyols,<sup>75–77</sup> but the use of diisocyanates in general is questionable due to their origin from toxic phosgene<sup>78</sup> and their inherent health hazard.<sup>79,80</sup> In fact, the use of diisocyanates has already been restricted within the European Union since 2023.<sup>81</sup>

With this in mind, several approaches have been developed to access alternative *non-isocyanate polyurethanes* (NIPUs).<sup>82–84</sup> Notably, some presented procedures do enable an isocyanate-free synthesis, but they still often rely on the use of phosgene-based reagents for the introduction of the urethane functional groups. This is for instance the case for the majority of approaches of NIPU synthesis by ring-opening polymerization of cyclic urethanes.<sup>85,86</sup> The main phosgene-free strategies to access polyurethane structures are summarized in **Figure 4**.

One possibility to obtain NIPUs is the *ring-opening copolymerization* of aziridines with CO<sub>2</sub>. In this process, the homopolymerization of aziridines is a competing side reaction and may decrease the urethane content, which was addressed by using supercritical CO<sub>2</sub>.<sup>87,88</sup> However, aziridines are hazardous compounds<sup>89,90</sup> and therefore still represent a health risk, even if avoiding isocyanates. An alternative ring-opening approach is the synthesis and polymerization of cyclic urethanes from

the depolymerization of oligourethane precursors instead of their often applied synthesis from phosgene derivatives.<sup>91</sup>

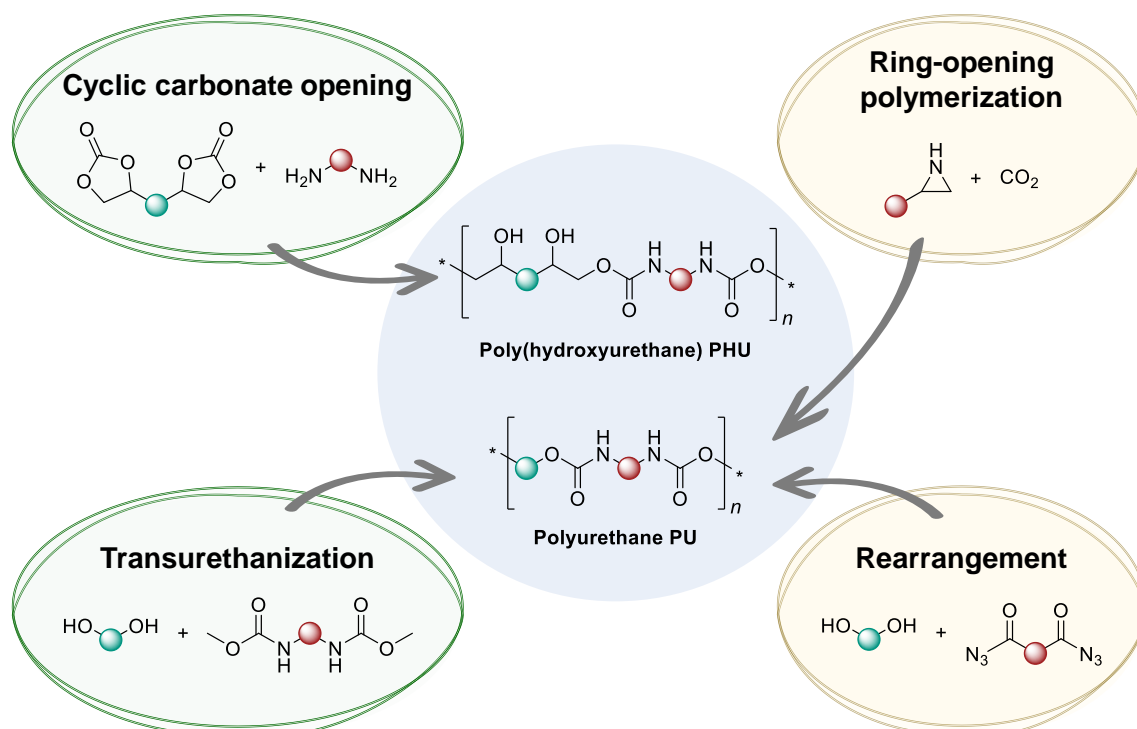


**Figure 4.** Phosgene-free routes to poly(hydroxyurethanes) and polyurethanes.<sup>82–84</sup>

A second synthesis route towards NIPUs is by *rearrangement* and subsequent polyaddition with diols. The isocyanate group is formed in situ and phosgene-free during the reaction, making the handling safer. Since no isolation of hazardous isocyanate compounds is necessary, the resulting polymers are referred to as NIPUs within this context. Several rearrangement reactions are suitable to yield isocyanate groups in situ,<sup>92</sup> with the Curtius rearrangement shown in **Figure 4**.<sup>93,94</sup> This approach can also be applied to the synthesis of AB-type monomers containing both functional groups.<sup>95</sup> Still, the starting materials of the reaction, in this case acyl azides, continue to be harmful and are therefore not as desirable to replace isocyanates.<sup>96</sup>

If urethane moieties are already present in linear monomers, NIPUs can be obtained by *transurethanization* with diols (see **Figure 5**). This is a step-growth polymerization mechanism based on an equilibrium condensation reaction in which an alcohol equivalent is released in each step. Several routes have been described to yield urethane monomers without the need for isocyanate groups,<sup>97–100</sup> for



instance the methoxycarbonylation of amines<sup>101,102</sup> or the aminolysis of ethylene carbonate.<sup>91</sup> One common strategy to achieve efficient polymer synthesis is to use *dimethyl carbonate* (DMC) and a diamine to generate diurethane precursors, which upon polycondensation with a diol release methanol as a volatile compound (see **Figure 5**).<sup>103,104</sup> DMC is attractive as a benign reagent<sup>105</sup> for which synthesis methods with improved sustainability have been developed,<sup>106,107</sup> for example based on CO<sub>2</sub> and methanol.<sup>108,109</sup> Applying high temperatures and high vacuum conditions to remove the formed methanol is necessary to shift the reaction towards high conversions and therefore high molecular weights.

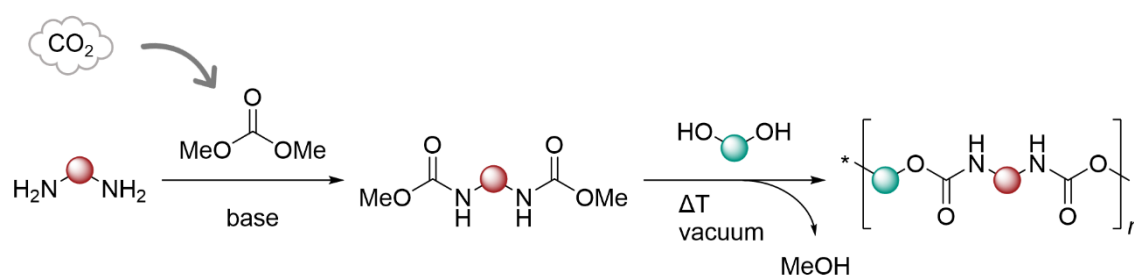


**Figure 5.** Synthesis of urethane monomers from diamines and CO<sub>2</sub> and subsequent polyaddition with a diol to yield NIPUs.

The required monomers for this approach can be obtained from the same polyamines that yield the industrially used isocyanates. Therefore, it is possible to mimic the structure of classical PUs. For instance, a study by Zheng and Li compared the structures and properties of NIPUs obtained via transurethanization with their isocyanate-based counterparts.<sup>110</sup> In the NIPU structures, an increased urea content was observed, resulting in inferior thermal and mechanical properties. The formation of urea bonds was attributed to urethane metathesis and further to a possible side reaction between alcohol and urethane groups, releasing carbonate and amine groups, the latter of which could then react with urethane groups to form urea moieties. Although urea bonds also occur in PUs obtained from diisocyanates, these side reactions have to be taken into account to develop more selective procedures. Still, transurethanization represents one of the most promising approaches for thermoplastic NIPU synthesis.

Similarly, linear dicarbonate monomers can be reacted with diamines in a polycondensation method.<sup>111</sup> However, in that case, selective reaction to the urethane with

little urea formation is a challenge. As an alternative, the *opening of cyclic carbonates* with amines has found increased use in the synthesis of NIPUs.<sup>112</sup> The ring-opening of a cyclic carbonate with an amine upon nucleophilic substitution yields a hydroxyurethane moiety in two different regioisomers (see **Figure 6**).<sup>113,114</sup> Therefore, if polyfunctional cyclic carbonates and amines are used, it leads to the formation of *poly(hydroxyurethanes)* (PHUs). The regioselectivity of the ring-opening varies depending on the substitution pattern of the cyclic carbonates, and the final polymer may contain both isomeric groups.

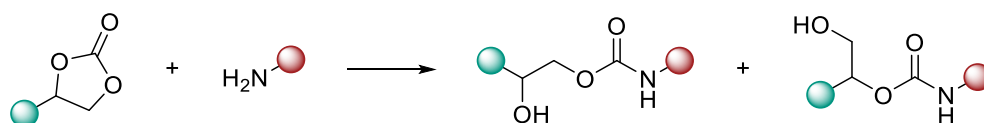


**Figure 6.** Ring-opening of cyclic carbonate with amine yielding two different regioisomers of hydroxyurethanes.

By the introduction of an additional hydroxy group per urethane unit, the obtained structures inherently vary from classically used PU materials and are not a straightforward replacement. Further, during the opening of cyclic carbonates by amines, several side reactions can occur, such as urea formation or dehydration, thus limiting the molecular weight of the obtained PHUs.<sup>115,116</sup> However, in optimized approaches, the additional functionalities may be beneficial for certain applications, e.g. achieving improved adhesion properties due to the additional hydroxy groups<sup>117</sup> or taking advantage of the reactive groups for the synthesis of *graft-copolymers*.<sup>118</sup>

Sustainable routes towards polyfunctional cyclic carbonates and amines as suitable precursors for NIPUs have been investigated extensively.<sup>119,120</sup> Polyamines are already industrially available and used in PU synthesis. They can be obtained via common approaches such as reductive amination, Gabriel synthesis, or by reduction of nitro compounds, amide derivatives, or nitriles.<sup>121</sup> For a transformation towards a greener chemical industry, the synthesis of polyamines from renewable feedstock without the need for harsh reaction conditions is a considerable challenge<sup>122,123</sup> that will not be addressed in this work.

Five-membered cyclic carbonates are accessible from abundant chemical groups such as epoxides, double bonds, and 1,2-diols. **Figure 7** depicts a selection of

routes towards five-membered cyclic carbonates, focusing on routes in which more benign substrates and reagents can be used instead of e.g. halohydrins or halogenated carbonates.

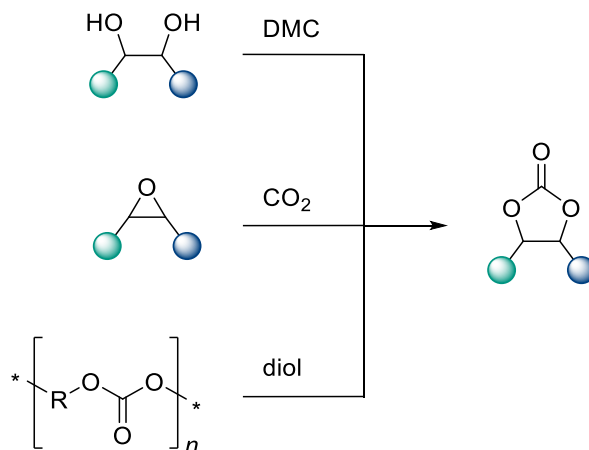


**Figure 7.** Selection of halogen-free routes to five-membered cyclic carbonates.

1,2-Diols are abundant in naturally occurring compounds, for example in carbohydrates and their fermentation products, which will be discussed in more detail in section 2.5.2. The reaction of 1,2-diols with carbonyl compounds was shown to yield cyclic carbonates effectively. Several carbonyl derivatives, such as alkyl carbonates,<sup>124–126</sup> urea,<sup>127</sup> or CO<sub>2</sub>,<sup>128,129</sup> can be reacted with 1,2-diols, upon which DMC represents an attractive reactant, being more benign and accessible from renewable feedstock.<sup>130</sup>

The insertion of CO<sub>2</sub> into an epoxide group is another common strategy to obtain five-membered cyclic carbonates.<sup>131–133</sup> The reaction can be catalyzed, e.g., by adding tetrabutylammonium salts of halogenides (see **Figure 8**). In this case, the halogenide attacks the epoxide as a nucleophile, generating an alkoxide ion that can react with CO<sub>2</sub>, with the resulting carbonate ion being able to substitute the halogenide catalyst under ring formation.<sup>134–136</sup> The addition of metal complexes can activate the epoxide group further and therefore improve the performance.<sup>137,138</sup> Other catalyst systems that have been investigated include the use of metal-organic frameworks,<sup>139</sup> porphyrins,<sup>140</sup> alkali metal salts,<sup>141,142</sup> or imidazolium salts.<sup>143,144</sup>

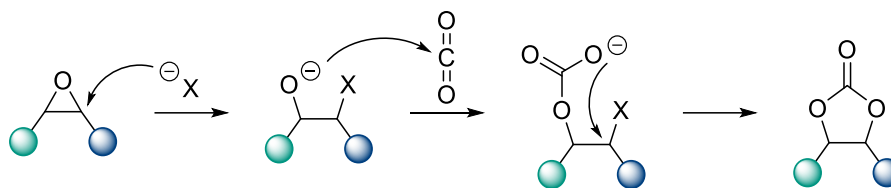


**Figure 8.** Mechanism of cyclic carbonate synthesis from epoxide and CO<sub>2</sub> using a halogenide ion based catalyst. X = Cl, Br, I.

A possible reagent to introduce reactive epoxy groups into monomers is epichlorohydrin,<sup>145–147</sup> however, the use of this chlorinated reagent limits the sustainability of such approaches, and especially epichlorohydrin is highly toxic. Alternatively, epoxides are accessible from the oxidation of double bonds, and since double bonds occur in a variety of substrate classes, this approach has widely been used for the synthesis of a broad range of cyclic carbonates as precursors for NIPUs.<sup>134</sup> For certain substrates, reacting double bonds directly with CO<sub>2</sub> and O<sub>2</sub> under addition of transition metal complexes or metal oxides is an attractive possibility,<sup>148,149</sup> which is being investigated as alternative route.

The third approach to synthesize five-membered cyclic carbonates without the need for halogenated reagents that is shown in **Figure 7** is by depolymerization of polycarbonates with a short diol. This has already been shown in early investigations by Carothers.<sup>150</sup> However, the scope of cyclic carbonate structures obtainable by this method is limited and moreover, only monofunctional cyclic carbonates are accessible. Although also monofunctional cyclic carbonates have been successfully used in the synthesis of NIPUs,<sup>151</sup> at least two functionalities within the molecule are favorable for the synthesis of polymeric structures. The aforementioned strategies based on 1,2-diols or epoxides enable the formation of polyfunctional cyclic carbonates as monomers for NIPU synthesis.

Their straightforward synthesis has led to a wide use of five-membered cyclic carbonates for the synthesis of NIPUs, but their reactivity is limited due to a low ring strain. The reactivity can be increased either by additional electron-withdrawing groups or by introducing an endocyclic or exocyclic double bond<sup>152</sup> that contributes to a higher ring strain and further traps the leaving alcohol group as ketone moiety. Such vinylene or exovinylene carbonates can be used for efficient NIPU synthesis,<sup>153</sup> however, their synthesis usually relies on the metal-catalyzed

conversion of propargylic alcohols<sup>154,155</sup> and the implementation of more benign reaction conditions remains a challenge.

As further alternative, six-membered cyclic carbonates possess a higher ring strain than their five-membered counterparts.<sup>156</sup> Analogous to the routes towards five-membered cyclic carbonates depicted in **Figure 7**, six-membered cyclic carbonates can be obtained via the reaction of 1,3-diols with alkyl carbonates<sup>157,158</sup> or CO<sub>2</sub>,<sup>159</sup> or by insertion of CO<sub>2</sub> into oxetanes.<sup>160</sup> Both 1,3-diols and oxetanes are less straightforward to synthesize from abundant resources than 1,2-diols and epoxides. Further, their increased reactivity also complicates the isolation of six-membered cyclic carbonates, which contributes to the higher focus on five-membered cyclic carbonates with regard to NIPU synthesis.

Overall, the aminolysis of cyclic carbonates is a promising approach for more sustainable PU applications, nevertheless further research is necessary for a successful implementation.<sup>161</sup> For instance, as was discussed in the beginning of this section, one of the main applications of PUs is the production of PU foams, which results from a side reaction between the isocyanate groups and water. With the absence of isocyanate groups in NIPU syntheses, this poses a challenge for the design of materials that are suited for industrial use. Increased research within the last years has led to several approaches for the synthesis of NIPU foams.<sup>32</sup>

The overall sustainability of PUs can be improved by the use of less harmful monomers, but also by aiming towards biobased starting materials.<sup>162–165</sup> The use of renewable feedstock for the synthesis of polyurethane precursors will be discussed in section 2.5. Further, the use of catalysts can be beneficial<sup>166</sup> and will be treated in section 2.6.

The biodegradation of polyurethane materials is limited and depends highly on the used monomers.<sup>167</sup> It can be increased in the presence of labile moieties such as ester bonds.<sup>168,169</sup> As high material stability can also be desirable, a main focus upon including polyurethanes in circular approaches is laid on methods for their reprocessing<sup>170</sup> and recycling.<sup>171</sup> Next to thermo-chemical processing to obtain low molecular weight feedstock and physical recycling to generate fillers for composite materials, chemical recycling includes hydrolysis, glycolysis, and alcoholysis to generate polyol compounds that might be reused.<sup>172</sup>

## 2.3. Thermoplastic polyesters

Polyester materials are defined by the presence of ester linkages in their polymeric backbone. They are among the most abundant polymeric materials, mostly used in form of fibers,<sup>173</sup> leading to an annual production volume of 63.3 million tons polyester fibers in 2022.<sup>174</sup> Besides the use in the synthetic fiber industry, polyesters find application in packaging, bottles, and photographic films, among others.<sup>175</sup> The majority of produced polyesters are linear polymers with thermoplastic behavior,<sup>176</sup> but also hyperbranched and dendritic structures have been developed.<sup>177,178</sup>

One classic route towards polyesters is via polycondensation, in which a carboxylic acid or derivative reacts with an alcohol group under release of a low molecular weight molecule, which is in most cases either water, methanol, or HCl.<sup>150,179</sup> The use of diacid derivatives as monomers opens a toolbox for various polymer structures.<sup>180</sup> As already described in section 2.2, polycondensation reactions usually require harsh reaction conditions to obtain high conversions and thus high molecular weight polymers because they follow a step-growth mechanism. Low molecular weight molecules need to be removed from the reaction mixture to shift the equilibrium towards high conversion, requiring the use of vacuum (<1 mbar) and high reaction temperatures (>120 °C).

Two common products synthesized industrially via polycondensation are *polyethylene terephthalate* (PET) and *polybutylene terephthalate* (PBT),<sup>176</sup> two high-performance thermoplastic polyesters that find wide application in packaging and textile fibers.<sup>181</sup> The synthesis route to PET and PBT is based on *terephthalic acid* (TPA) and ethylene glycol or 1,4-butanediol, respectively, as shown in **Figure 9**.

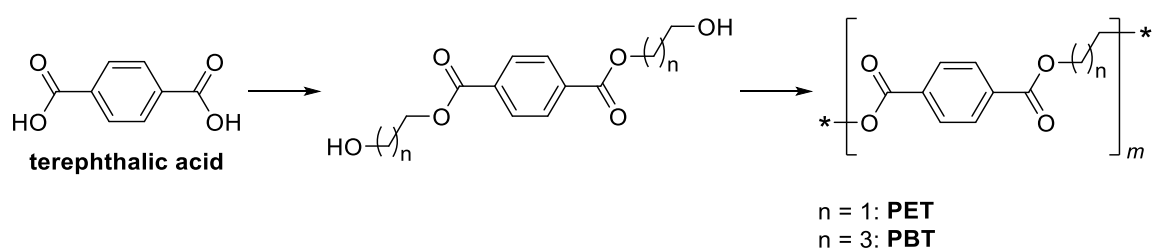


**Figure 9.** Schematic representation of the industrial two-step synthesis route towards PET and PBT starting from terephthalic acid.

In the industrial synthesis of PET and PBT, a diester of TPA and the respective diol is formed either by transesterification or direct esterification.<sup>182</sup> Afterwards, the dimer is converted to the polymer in a polycondensation process. Both processes are usually catalyzed by the addition of metal salts.<sup>183</sup>

The production of PET has been established industrially since the 1950s, using TPA and ethylene glycol produced from fossil feedstock.<sup>184</sup> Nowadays, EG is also accessible from renewable resources such as starch or xylitol.<sup>185–187</sup> TPA has also been investigated to be produced from renewable resources,<sup>188</sup> yet additional focus has been set on replacing TPA for instance by furandicarboxylic acid that can be obtained from fermentation or catalytic transformation of sugar feedstock.<sup>189,190</sup> Alternatively, the aromatic unit can also be replaced by aliphatic blocks, as is the case for *poly(butylene succinate)* (PBS)<sup>191,192</sup> or *poly(butylene succinate adipate)* (PBSA).<sup>193,194</sup> However, this leads to significantly different properties and application possibilities.

Besides polycondensation, the *ring-opening polymerization* (ROP) of lactones represents another widely used route towards polyesters.<sup>195</sup> Lactones of a ring size of below or above five possess a ring strain. In addition to entropic gain, this favors ring-opening after the attack of a nucleophilic initiator, releasing a new nucleophilic group to contribute to a growing polymer chain.

This polymerization method proceeds under mild reaction conditions and follows a chain-growth or living/ controlled mechanism.<sup>196</sup> Thus, in contrast to polycondensation, high molecular weights are achievable without the necessity for very high conversions<sup>197</sup> and further, the obtained dispersities are often narrower.<sup>198</sup> These features allow for targeted synthesis of specific polymeric architectures.<sup>199</sup> Two prominent examples of polyesters that can be accessed by ROP are *poly(lactic acid)* (PLA) and *poly( $\epsilon$ -caprolactone)* (PCL), as depicted in **Figure 10**.

The repeating unit of PLA, lactic acid, reacts with itself to form its cyclic dimer lactide,<sup>200</sup> which then can undergo ROP. In the lactide monomer (**Figure 10a**), the ring strain is enhanced due to the presence of two opposite carbonyl groups.<sup>201</sup> As lactide can be produced in a large scale from renewable resources,<sup>202,203</sup> PLA found applications in the medical field due to its biocompatibility,<sup>204</sup> in fiber production,<sup>205</sup> and in packaging as biobased alternative to other commodity polymers.<sup>206</sup>

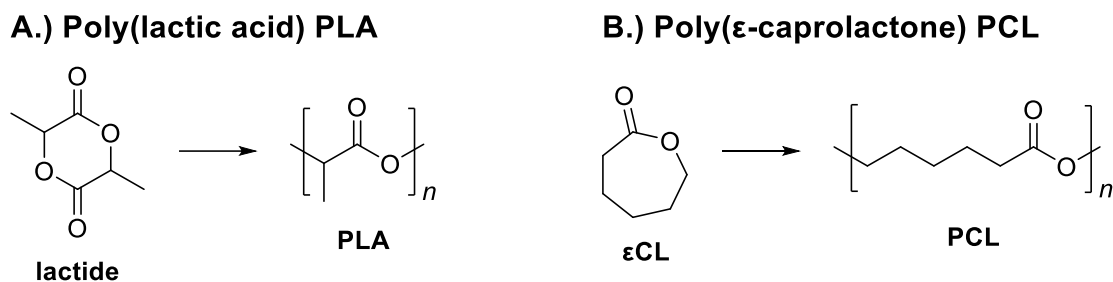


**Figure 10.** Schematic representation of the synthesis of PLA and PCL based on the ring-opening of lactone monomers.

The ring-opening of lactide can be initialized by a variety of compounds such as alcohols,<sup>207</sup> and catalyzed for example by the use of metal catalysts.<sup>208,209</sup> Lactic acid can display two different enantiomers, with L-lactic acid occurring predominantly in nature. Depending on the monomer mixture, PLA can be synthesized with different contents of D-lactic acid, which influences the tacticity and therefore the mechanical properties of the polymer.<sup>210</sup>

The synthesis of PCL is another widely used ROP route (see **Figure 10b**), typically starting from  $\epsilon$ -caprolactone ( $\epsilon$ CL). PCL has found use e.g. in medical applications,<sup>211</sup> with its biocompatibility and the miscibility with other polymeric compounds offering important advantages. In the following discussion, mechanistic steps will be depicted based on  $\epsilon$ CL polymerization, but the activation modi are similar for PLA and PCL.

Various approaches for ROP towards polyesters and suitable catalyst systems have been presented, including metal-based catalysts, organocatalysts, and enzymes. Depending on the choice of reaction conditions and the used catalyst, ROP can proceed via different reaction mechanisms, such as anionic, cationic, radical, or coordination insertion.<sup>212</sup> For example, Brønsted acids, methylating agents, or acylating agents can promote cationic ROP via introduction of a delocalized positive charge into the carbonyl moiety.<sup>213</sup>

A commonly used catalyst system for the ROP of lactones is tin (II) 2-ethylhexanoate in combination with an alcohol initiator.<sup>214,215</sup> The mechanism described in the literature proceeds via coordination insertion<sup>216,217</sup> and is shown for PCL in **Figure 11**. To achieve efficient polymerization, elevated temperatures are often necessary,<sup>208</sup> which favor possible transesterification side reactions and therefore result in broader dispersities than in other described living polymerizations. One



possibility to address this challenge was presented by Okada et al., introducing triflate instead of alkoxide ligands, thus increasing the acidity of the metal center and allowing for a polymerization at lower temperatures.<sup>218,219</sup> Another strategy was published in which metal catalysts such as aluminum oxides are used since these show less reactivity towards aliphatic polyester chains.<sup>220</sup> Next to metal catalysts, ROP of lactones can also be promoted by enzymes<sup>221</sup> or organo-catalysts,<sup>222–224</sup> the latter of which will be discussed in more detail in section 2.6.

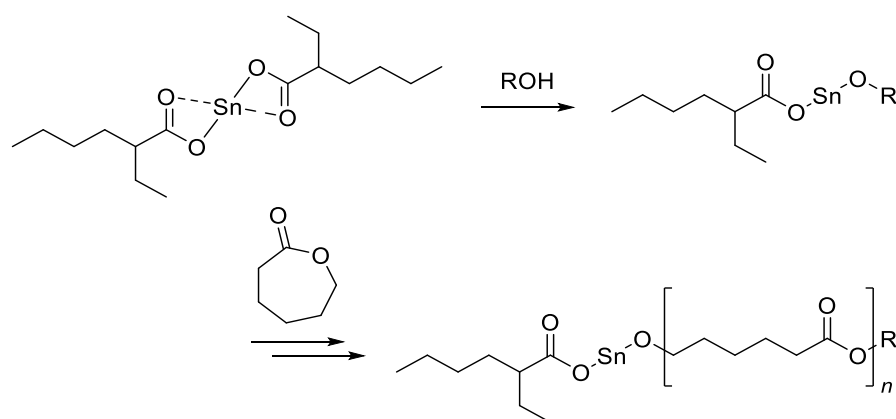


**Figure 11.** ROP of  $\epsilon$ CL, catalyzed by tin (II) octanoate.<sup>216,217</sup>

A third approach to polyester materials that has recently gained increased attention is the *ring-opening copolymerization* (ROCOP) of epoxides and cyclic anhydrides.<sup>225</sup> In this strategy, the alkoxide species that is released by the initial opening of the epoxide monomer attacks the cyclic anhydride, and the released carboxylate species opens another epoxide group during chain propagation.<sup>226</sup> This process is commonly metal-catalyzed and results in the formation of alternating copolymers.<sup>227</sup> The use of two different monomers enables facilitated fine-tuning of the desired properties, such as elasticity or tensile strength. Further, this route opens the possibility to produce controllable semi-aromatic polyesters.<sup>228</sup>

Because of their cleavable ester linkages, polyesters have been investigated as potentially degradable alternatives to polyolefins, as the mechanical and thermal properties are comparable in many cases.<sup>229</sup> PLA has been implemented as degradable alternative in packaging, with increased attention being directed on controlling its crystallinity to ensure sufficient thermal resistance.<sup>230</sup>

During degradation, the ester bond in polyester structures can be hydrolyzed by naturally occurring enzymes and microorganisms.<sup>231,232</sup> This is especially the case

for aliphatic polyesters.<sup>233</sup> PBS and PBSA, for instance, show efficient degradation when exposed to water and elevated temperatures or composting conditions, the efficiency of the degradation depending on the crystallinity of the polymer and on the particle size.<sup>192</sup> Naturally occurring polyhydroxyalkanoates are another example of degradable polyester compounds<sup>234</sup> and have found increased industrial use.<sup>235</sup> Aromatic polyesters such as PET, on the other side, are less prone to degrade under biological conditions.

Additional to biodegradation, research effort has been put into the efficient recycling of polyester materials, which has been implemented especially in the case of PET.<sup>236</sup> Due to the cleavable ester moieties, chemical recycling by depolymerization can be performed.<sup>237</sup> It was also shown that introducing ester bonds into long aliphatic chains via polycondensation of fatty acid methyl esters enabled to mimic the properties of polyolefins, ensuring high stability while also introducing breaking point for polymer deconstruction.<sup>238,239</sup> Which strategy is suited in order to make use of the value of the respective polyester waste depends on the specific application.

Combining these aspects, polyesters represent a promising class of polymers for the development of more sustainable materials. Regarding renewable starting materials, a variety of approaches has been presented to obtain biobased polyesters.<sup>240-242</sup> Different groups of renewable feedstock will be discussed in more detail in section 2.5.

## 2.4. Covalent adaptable networks

Thermosetting polymers consist of a covalently cross-linked network and usually do not change shape upon heating.<sup>243</sup> Thus, thermosets often show enhanced mechanical properties, such as high toughness, form stability, and durability.<sup>244</sup> However, they often represent end-of-life products, therefore posing a challenge for Circular Economy goals.<sup>21</sup> Up to the present day, approaches exist to recycle thermoset materials thermally, mechanically, and chemically.<sup>245</sup> The latter concept involves the introduction of cleavable bonds for polymer deconstruction by implementation of possibly cleavable functional groups, such as esters (see section 2.3), acetals, or imines.<sup>246</sup>

In spite of such aims towards recyclability, thermoset materials suffer from limited processability if compared to thermoplastics since thermosets usually do not flow when applying heat, and physical damage in the network is often not healable. To address this, the concept of cleavable bonds can be expanded to covalent dynamic bonds, therefore introducing the possibility to break and reform bonds reversibly upon a trigger to reshape the network structure.<sup>247</sup> Such materials are referred to as *covalent adaptable networks* (CANs), containing covalent dynamic bonds that can be reconfigured without loss of the 3D network (see **Figure 12**).<sup>248</sup> The trigger can be of different nature, such as by thermal or UV light activation or by change of pH.

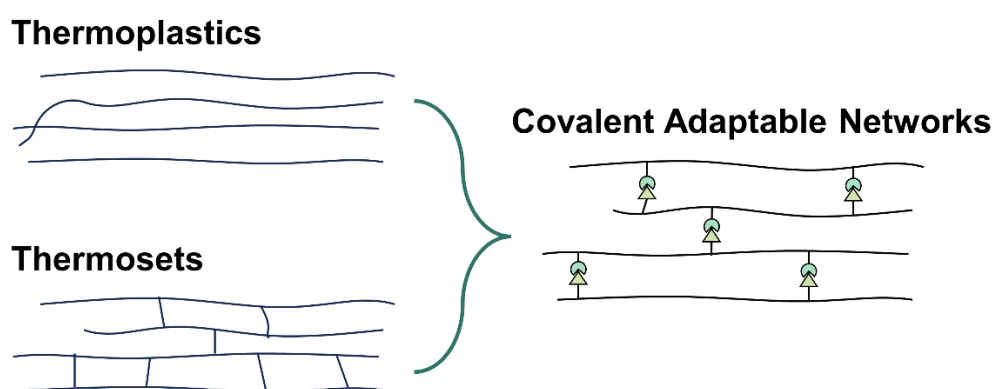


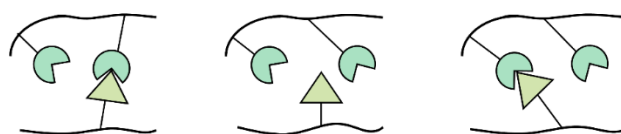
**Figure 12.** Covalent adaptable networks combining desirable properties of thermoplastics and thermosets.

CANs combine the superior robustness and solvent resistance of thermoset materials with the adaptability of thermoplastics.<sup>249</sup> The introduction of dynamic bonds into a 3D polymer network can thus lead to desirable properties,<sup>250</sup> such as reprocessability,<sup>251</sup> self-healing,<sup>252</sup> responsiveness,<sup>253</sup> or shape-memory behavior.<sup>254</sup>

The potential dynamic behavior of polymeric networks is usually investigated via stress relaxation experiments.<sup>255</sup> Commonly, thermoplastics are able to change their shape upon external strain, and thus reduce the induced stress with time, i.e. leading to stress relaxation. The polymeric chains within thermoset materials barely possess the ability to rearrange, resulting in thermoset materials not showing any relevant stress relaxation. In CANs, the triggering of reversible covalent chemistry can enable the reduction of stress with time.

In general, dynamic chemistry within a polymer network can follow different mechanisms, with a common distinction being made between a dissociative mechanism and an associative mechanism (see **Figure 13**). In the dissociative pathway, bonds can be cleaved upon a trigger and subsequently be reformed with another accessible functional group to restore the network linkages (see **Figure 13a**). Alternatively, following an associative route, an additional functional group can associate to an existing bond, forming a new linkage upon releasing the other functional group (see **Figure 13b**).

#### A.) Dissociative mechanism



#### B.) Associative mechanism

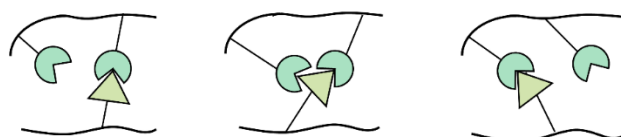


**Figure 13.** Dissociative and associative mechanisms as two types of dynamic chemistry.

The main difference between the two mechanisms in **Figure 13** is that the cross-linking density varies over time in the dissociative pathway, while it stays constant

in the associative one. This has an influence on the viscoelastic properties of the respective networks. CANs that rely on the associative pathway for topology reconfiguration are commonly referred to as vitrimers due to their glass-like fluidity.<sup>256,257</sup> Because of the cross-linking density remaining approximately constant, the change of viscosity with temperature is more gradual than in dissociative networks,<sup>258</sup> enabling better control of mechanical properties while also possibly resulting in less easy reprocessing e.g. via extrusion.<sup>259</sup> At the same time, several CANs have been described in the literature that exhibit both associative and dissociative bonds. A selection of functional groups that can show dynamicity is depicted in **Figure 14**. Generally, according to the different mechanisms of dynamic behavior, the depicted groups can be rearranged in different ways, such as by metathesis reactions between two linkages, by reaction with an additional dangling functional group, or by dissociation and subsequent reformation.

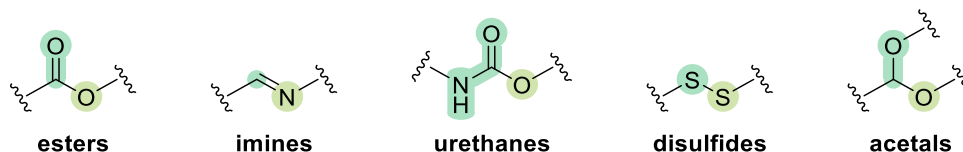


**Figure 14.** Examples for moieties that can show dynamic behavior.

*Ester* linkages are among the longest known dynamic bonds, with transesterification reactions having been used in polymer chemistry from early on. If hydroxy groups are present in networks containing ester linkages, dynamic behavior can be observed at elevated temperatures following an associative mechanism.<sup>260</sup> The group of Leibler introduced this concept with the synthesis of epoxy acid networks, observing glass-like malleability at 240–260 °C while maintaining desirable mechanical properties.<sup>261</sup> Their investigations inspired the development of various vitrimers containing dynamic ester bonds.<sup>262,263</sup> The possible implementation of this concept into the synthesis of well-established epoxy resins allow for a wide application of vitrimers containing ester bonds, such as in 3D printing<sup>264</sup> or photo-welding.<sup>265</sup> However, high temperatures as well as the addition of catalysts remain necessary to achieve good performances.

*Imines* are a second example of dynamic covalent bonds, either by reversible hydrolysis in the presence of water, by associative transamination in presence of

other amine groups, or by imine metathesis.<sup>266</sup> Thus, the mechanism can be associative or dissociative, and the resulting polymers are often water-sensitive. The use of dynamic imine linkages has found wide application in polymer design,<sup>267</sup> e.g. for the synthesis of malleable resins.<sup>268,269</sup>

In *urethane* networks, transurethanization exchange reactions can occur and result in dynamic behavior.<sup>270</sup> This especially concerns PHU materials, which inherently contain hydroxy groups that can act as nucleophiles. As one of the first examples, Cramer, Hillmyer, Dichtel et al. introduced the formation of PHU networks by ring-opening of six-membered cyclic carbonates with amines allowing for reprocessing at 160 °C.<sup>271</sup> Mechanistical investigations showed that transurethanization reactions leading to dynamic behavior proceeded mainly via an associative mechanism. In 2019, the group of Torkelson presented the synthesis of biobased PHU networks obtained from the opening of five-membered cyclic carbonates with amines. The obtained materials displayed the potential for multiple dynamic exchange reactions, which were observed to be a combination of transurethanization, reversible cyclic carbonate aminolysis, and transesterification.<sup>272</sup> In general, since such transurethanization rearrangements often require elevated temperatures of above 160 °C to reach relaxation times within 10<sup>3</sup> s necessary for efficient reprocessing,<sup>271</sup> urethane linkages can be combined with other covalent dynamic bonds.<sup>273–277</sup>

The exchange reaction of *disulfide* bonds can occur via anionic, radical, or metathesis pathways.<sup>278,279</sup> Since the dynamic behavior can be triggered under comparably mild conditions of below 120 °C,<sup>280</sup> disulfide linkages have found application especially in self-healing polymers.<sup>281,282</sup>

Dynamic *acetal* groups can be introduced into polymer networks by a click-reaction between vinyl ethers and hydroxy groups.<sup>283</sup> Subsequently, the acetal linkages can undergo exchange reactions via transacetalization or acetal metathesis. The cleavable acetal moieties can further lead to degradability of the respective CANs.<sup>284</sup>

Dynamic reactions can be promoted by the presence of catalysts. For instance, transesterification reactions can be catalyzed by various compounds, such as tertiary amines,<sup>285,286</sup> Brønsted acids,<sup>287</sup> or Lewis acids.<sup>288,289</sup> For PHUs, on the other hand, Lewis-acidic catalysts were shown to be significantly more active in the promotion of dynamic transurethanization reactions than the tested organocata-

lysts.<sup>290</sup> As an alternative to the external addition of catalysts to the network, internal catalysis can promote reactions in the vicinity selectively and reduce catalyst leaching.<sup>291,292</sup>

Besides the examples shown in **Figure 14**, a variety of other motifs have been shown to introduce dynamic behavior, such as Diels-Alder adducts,<sup>293,294</sup> thioesters,<sup>295</sup> vinylogous urethanes<sup>296,297</sup> and ureas,<sup>298</sup> boronic esters,<sup>299,300</sup> alkylated thioethers,<sup>301</sup> triazolinediones,<sup>302</sup> and others. The implementation of dynamic linkages into high-performance materials to address the drawbacks of cross-linked materials is a field of ongoing exploration.<sup>303</sup>

To further improve the sustainability of materials, it has also been investigated to synthesize CANs based on renewable resources.<sup>304</sup> In principle, all dynamic chemistries presented in **Figure 14** are applicable to renewable feedstock, thus opening a wide range of possibility for further sustainable material development. The use of renewable feedstock for the synthesis of polymers, especially in NIPUs, polyesters, and CANs, will be discussed in more detail in the following section.

## 2.5. Renewable resources for polymer synthesis

To work towards a Circular Economy or bioeconomy, increased research effort has been directed towards the use of renewable feedstock in the chemical industry.<sup>305</sup> This includes the development of biobased polymers,<sup>306–309</sup> for instance polyesters,<sup>240–242</sup> polyurethanes,<sup>164,165,172</sup> or covalent adaptable networks,<sup>304,310</sup> which were discussed in sections 2.2–2.4 and on which this work is focused.

Biobased polymers can either rely on naturally occurring polymeric structures, which can be found e.g. in cellulose, hemicellulose, starch, or lignin, or on the polymerization of renewable monomers.<sup>311</sup> While also CO<sub>2</sub> can be used directly in carbon capture and utilization approaches,<sup>312</sup> the main focus for polymer synthesis from biobased monomers focuses on the use of small organic molecules.<sup>308</sup> In the following sections, three classes of renewable molecules will be discussed, namely plant oils, carbohydrates, and terpenes. Special focus will be laid upon the use of these compounds for the synthesis of polyesters and polyurethanes.

### 2.5.1. Plant oils

Plant oils occur naturally in a variety of renewable feedstock such as seeds and nuts.<sup>313</sup> Within the last decades, their potential for a future chemical industry has been emphasized.<sup>314,315</sup> Next to established applications of plant oil feedstock in the chemical industry, which include surfactants,<sup>316</sup> cosmetics,<sup>317</sup> coatings,<sup>318</sup> and lubricants,<sup>319</sup> its use in the synthesis of polymers has gained increased attention.<sup>320</sup> Prominent examples of more abundant plant oils are sunflower oil, palm oil, rapeseed oil, soybean oil, or castor oil. They consist of mixtures of triglycerides, which are esters of glycerol and varying *fatty acid* (FA) chains. Next to the free FAs, *fatty acid methyl esters* (FAMES) are often used as starting point for further functionalization.<sup>321</sup>

The composition of FAs within the triglyceride mixture depends on the respective plant oil source and influences the properties of the oil. While the saturated palmitic acid and stearic acid are among the most abundant fatty acids, the presence of double bonds within unsaturated fatty acids open the possibility for additional chemical functionalization.<sup>322</sup> Some unsaturated fatty acids that available in larger quantities for the chemical industry are shown in **Figure 15**.



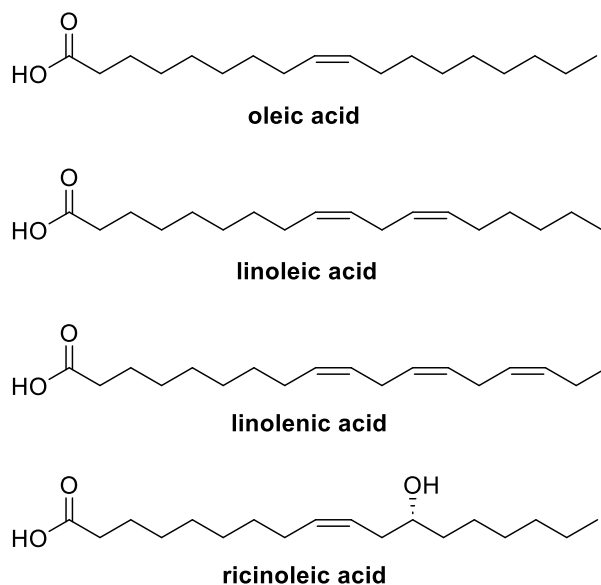


**Figure 15. Selection of abundant unsaturated fatty acids.**

Thus, the two main functionalities found in plant oil feedstock are on the one hand the double bonds that are found in unsaturated FAs and on the other hand the ester or acid moieties. Although historically the carbonyl function has been preferentially used for chemical applications,<sup>323</sup> manifold investigations have been directed to the valorization of the double bonds.<sup>314</sup>

Besides the double bond moiety, ricinoleic acid, (see **Figure 15**), which especially occurs in castor oil, further contains a hydroxy group that can contribute additional reactivity.<sup>324</sup> Industrial pyrolysis of methyl ricinoleate yields heptanal and methyl 10-undecenoate selectively via retro-Alder-ene reaction as valuable platform chemicals, as shown in Figure 16.<sup>325</sup>

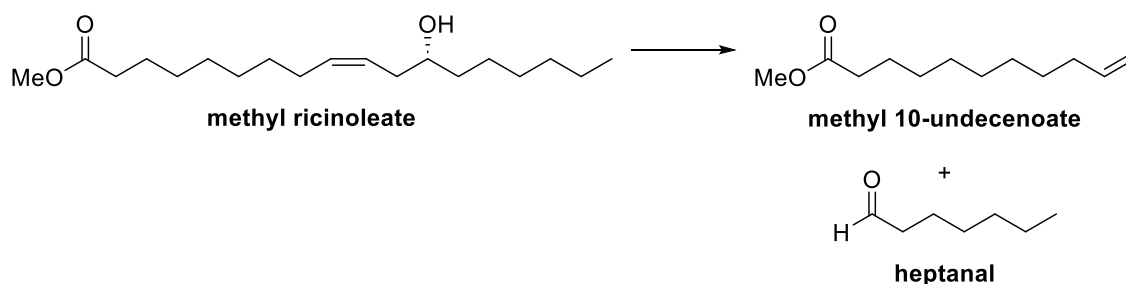


**Figure 16. Pyrolysis of ricinoleic acid methyl ester to yield methyl 10-undecenoate and heptanal as platform chemicals.**<sup>325</sup>

Methyl 10-undecenoate finds industrial application in the production of the bio-based polyamide Nylon-11.<sup>326</sup> Further, its terminal double bond results in increased reactivity for further functionalization.

The reactivity of the double bonds within the FA chains can be addressed in different ways. Thiol-ene addition, for instance, can enable the introduction of additional functionalities under mild conditions.<sup>327,328</sup> Meanwhile, metathesis reactions can be used to obtain polyfunctional monomers.<sup>329–331</sup> Another possibility to use the double bond functionalities chemically is by oxidation. As such, e.g. Wacker oxidation and photo-peroxidation have been described, including subsequent Baeyer-Villiger oxidation.<sup>332</sup> Further, the epoxidation of the double bonds has been investigated with increased focus for the efficient and mild valorization of double bonds in plant oil-derived feedstock.<sup>333</sup> Some epoxidized forms of plant oil are well established and commercially available.

Epoxidized plant oil derivatives can be used for the synthesis of biobased polyols,<sup>334,335</sup> for polyester synthesis by *ring-opening copolymerization* (ROCOP) with cyclic anhydrides,<sup>336</sup> or as monomers for epoxy resins.<sup>337</sup> Besides, as described in section 2.2, epoxides represent suitable precursors for the synthesis of cyclic carbonates for NIPU synthesis.<sup>131,133</sup>

Different catalytic systems have been described that convert epoxidized FA derivatives into their respective cyclic carbonates.<sup>338,339</sup> For instance, 10-undecenoic acid-based terminal epoxides were synthesized and used for the generation of cyclic carbonates.<sup>340</sup> If triglyceride feedstock is used, efficient epoxidation and subsequent carbonation can lead to suitable monomers for the synthesis of cross-linked materials. For example, carbonated soybean oil, which shows a high density of functional groups, has been used for the synthesis of different NIPU thermosets.<sup>341,342</sup> The introduction of dynamic bonds into such materials enables reprocessability while maintaining high mechanical performance.<sup>343,344</sup>

In addition to the double bond moieties, the reactivity of the ester bonds can also be a starting point for further functionalization or polymerization. By combination of both reactivities, monomers for the synthesis of polyurethanes and polyesters via polycondensation methods can be obtained.<sup>345</sup> Different approaches to obtain long-chain aliphatic polyesters via step-growth approaches from FA feedstock have

been described, enabling the tuning of the mechanical properties to resemble those of classic polyolefins.<sup>239</sup>

The carboxylic acid moiety of fatty acid derivatives can also be taken advantage of for the introduction of urethane groups. A possible route towards urethanes starting from carbonyl compounds proceeds via rearrangement reactions. For instance, a catalytic version of the Lossen rearrangement was shown to transform hydroxamic acids derived from plant oil feedstock into urethanes.<sup>346</sup> In a previous work from our group, this was applied to the synthesis of monomers for NIPUs from methyl oleate and methyl 10-undecenoate, as shown in **Figure 17**.<sup>347</sup>

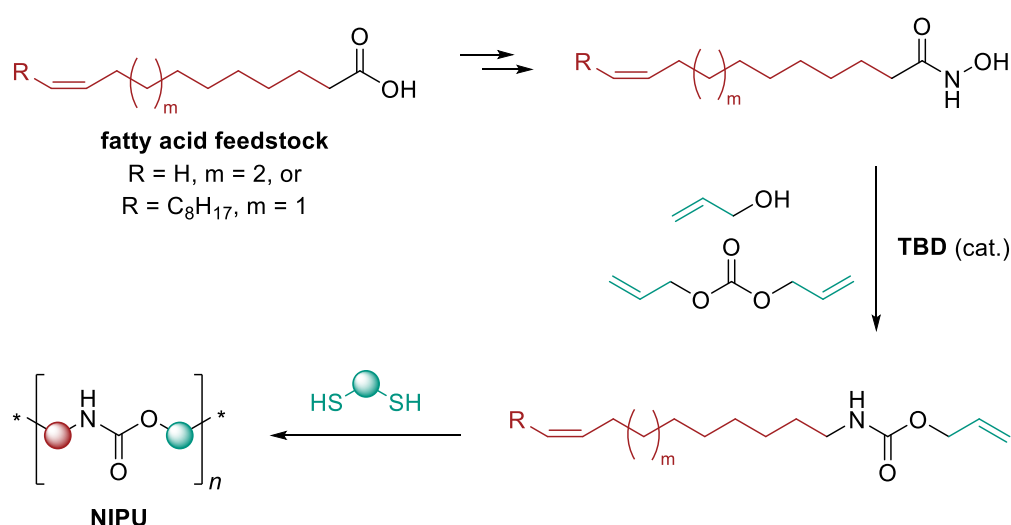


**Figure 17.** Synthesis of urethane moieties and linear NIPUs via catalytic Lossen rearrangement of fatty hydroxamic acids and subsequent thiol-ene polyaddition.<sup>347</sup>

By choosing allyl alcohol and diallyl carbonate as reagents in the catalytic Lossen rearrangement, the resulting urethane compounds contained two double bonds, thus representing AA monomers. Subsequent thiol-ene polyaddition with different biobased dithiols led to the formation of linear NIPUs with molecular weights of up to  $26 \text{ kg}\cdot\text{mol}^{-1}$ . Notably, the resulting polymers thus contain additional thioether linkages within the polymeric backbone.

Lastly, transesterification of triglycerides yields not only FAMES, but also glycerol as valuable platform chemical. Glycerol finds wide application in cosmetics, food industry, and pharmaceuticals.<sup>348</sup> Further, its three hydroxy groups can be exploited chemically for the synthesis of various chemical products.<sup>349</sup> For example, the

1,2-diol moiety can be carbonated by DMC or CO<sub>2</sub> to yield glycerol carbonate,<sup>350</sup> which could serve as building block for NIPU synthesis.<sup>116,351</sup>

### 2.5.2. Carbohydrate-based erythritol bis(cyclic carbonate)

Carbohydrates are the most abundant class of biomolecules in nature and therefore have potential to replace fossil-based hydrocarbons in chemical processes.<sup>352</sup> In nature, they mostly occur in the form of polysaccharides. Thus, for the exploitation of carbohydrate feedstock in polymer synthesis, one possibility is the direct use or chemical modification of polysaccharides to obtain the desired materials.<sup>353</sup> For this, e.g. cellulose represents a promising candidate, not competing for food or feed and occurring abundantly in plant cell walls.<sup>354</sup> Cellulose derivatives such as cellulose nitrates,<sup>355</sup> esters,<sup>356</sup> and ethers<sup>357</sup> have found wide application in coatings, films, and others.

Instead of using polysaccharides in their polymeric form, they can be split into smaller building units using biorefinery concepts,<sup>358</sup> of which a small selection will be presented in this section. Biorefinery of carbohydrate feedstock is considered an essential tool for the supply of platform chemicals such as ethanol, organic acids, or sugar alcohols.<sup>359</sup> For example, reduction of carbohydrate feedstock can be used for the production of biobased polyols,<sup>185–187</sup> which find use in polyurethane and polyester synthesis (see sections 2.2 and 2.3).

Generally, carbohydrate feedstock plays an important role for the development of biobased polyesters. Lactide, the monomer of PLA, can be obtained from corn feedstock,<sup>203</sup> which is widely available. Further, furan dicarboxylic acid, which is a promising substitute for terephthalic acid,<sup>360</sup> can be synthesized from fermentation products of pentoses and hexoses.<sup>189,190</sup>

Meanwhile, carbohydrate-based monomers in their reduced form as sugar alcohols represent natural polyols.<sup>361</sup> Three examples of sugar alcohols are shown in **Figure 18**.

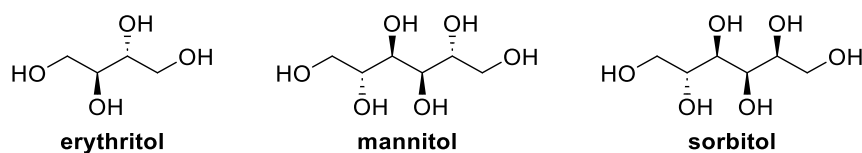


**Figure 18.** Examples of sugar alcohols as natural polyols.

The vicinal hydroxy groups can be used for the introduction of five-membered cyclic carbonate moieties, which are possible starting materials for the synthesis of NIPUs (see section 2.2). As such, NIPU materials were produced successfully from cyclic carbonates of mannitol<sup>362</sup> and sorbitol.<sup>362–364</sup>

In this work, focus was laid on the use of erythritol as renewable feedstock, which therefore will be discussed in this section. The synthesis of *erythritol bis(cyclic carbonate)* (EBCC) has been described e.g. by using diphenyl carbonate as reagent.<sup>365</sup> To avoid the phosgene-based diphenyl carbonate, an organocatalytic synthesis with DMC and *1,5,7-triazabicyclo[4.4.0]dec-5-ene* (TBD) was described previously in our group, as shown in **Figure 19**.<sup>366</sup>

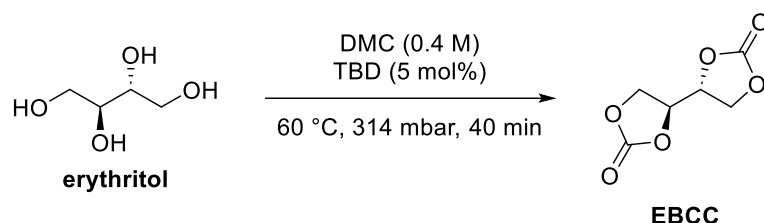


**Figure 19.** Organocatalytic synthesis of EBCC from erythritol and DMC.<sup>366</sup>

Applying reduced pressure and elevated temperature in a rotary evaporator, the product EBCC was yielded after 40 minutes in high purity after simple washing with DMC. Thus, this represents an attractive route regarding sustainability, comprising mild reaction conditions and low production of waste.

Several works have shown the use of EBCC in NIPU synthesis. For instance, in a recent work Gao et al. used the opening of EBCC with diamines to synthesize prepolymers for curing with epoxides to yield epoxyurethane networks.<sup>367</sup>

In a work by Bruchmann and Mülhaupt et al., the melt polycondensation of EBCC with three different diamines was described, yielding thermoplastic copolymers with molecular weights of around 10 kDa, with varying softness due to hard and soft segments attributed to the respective diamines.<sup>365</sup> They observed the formation of two isomeric forms during EBCC ring-opening, with secondary hydroxy groups being formed predominantly.

A study by Grau, Vidil, Cramail et al. thoroughly investigated the opening of the cyclic carbonate groups in EBCC by amines, observing that the opening of the first

carbonate group is significantly faster due to the vicinal cyclic carbonate group increasing the reactivity of EBCC.<sup>368</sup> Further, a regioselectivity for the formation of secondary alcohol groups was confirmed. These findings were used for the synthesis of NIPUs with tunable stereo- and regioselectivity and emphasize the potential of EBCC as a highly reactive monomer for NIPU synthesis.

### 2.5.3. Cyclic terpenes

Terpenes are a class of renewable compounds consisting of isoprene units.<sup>369</sup> They occur in different plants as secondary metabolites and find biological use as toxins, attractants, repellants, or messenger molecules.<sup>370,371</sup> Their biosynthesis involves the implementation of C<sub>5</sub> building blocks and subsequent modification to yield a broad variety of cyclic and acyclic structures.<sup>372</sup> A selection of cyclic terpene structures is shown in **Figure 20**.

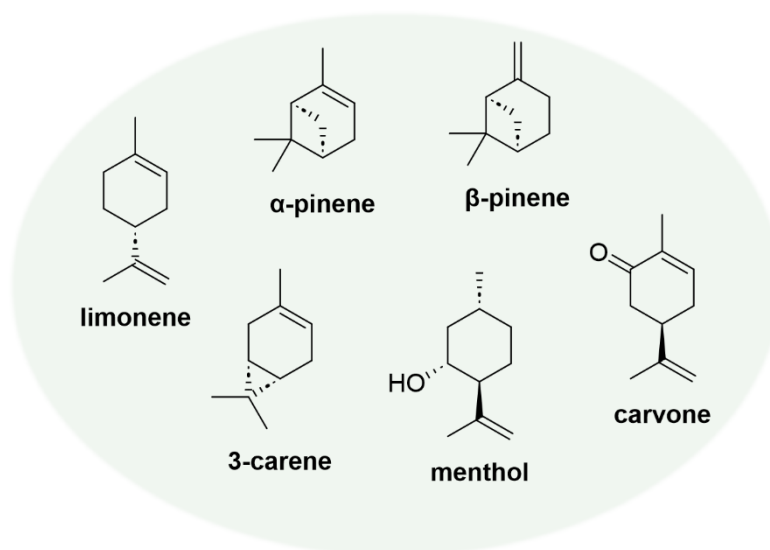


**Figure 20.** Selection of cyclic terpene derivatives.

Cyclic terpene structures are usually chiral, with one enantiomeric form being more abundant in most cases. Therefore, chemical modification of terpenes often results in the formation of several diastereomeric structures. At the same time, the stereocenters can be exploited as attractive features in terpene-derived materials, e.g. as bioactive compounds.<sup>373</sup>

Although terpenes only occur in small amounts within plant feedstock, they can be extracted on an industrial scale and have gained increasing research interest

e.g. for the production of fragrances,<sup>374,375</sup> fine chemicals,<sup>376</sup> pharmaceutical products,<sup>377,378</sup> biofuels,<sup>379</sup> and polymeric materials.<sup>380–383</sup> One major source of terpene feedstock, and especially of pinenes, is turpentine, a byproduct produced in the pulp and paper industry.<sup>384</sup> This accessibility of pinenes from non-edible plant parts has inspired research towards their use in polymer synthesis.<sup>385</sup> Limonene on the other hand occurs as byproduct in the citrus fruit production.<sup>386,387</sup> Industrially, it is mainly applied as flavor and fragrance additive in food and cosmetics.<sup>388</sup> As another example, carvone can be extracted from spearmint or caraway oils and finds application in the fragrance industry and as sprouting inhibitor.<sup>389</sup>

In order to exploit terpene feedstock as organic starting materials, a possible strategy is to address the double bonds. In terpenoid structures containing heteroatoms, such as carvone or menthol (see **Figure 20**), additional functional groups are present. Within this section, strategies for the use of terpene feedstock in the synthesis of polyesters and NIPUs will be presented.

The cyclic structure of terpene compounds makes them attractive precursors for polymer synthesis via *ring-opening polymerization* (ROP) approaches. For this, cyclic ketone structures are accessible by taking advantage of existing functional groups, as in menthol or carvone or by oxidation of double bonds. These cyclic ketones can then be used for the synthesis of seven-membered lactams and lactones, which are monomers for the synthesis of polyamides and polyesters via ROP.<sup>390</sup>

The synthesis and polymerization of terpene-based lactams opens the possibility to synthesize linear polyamide structures from terpenes.<sup>391</sup> The nitrogen can be introduced by Beckmann rearrangement of oximes.<sup>392,393</sup> Upon ring-opening, the stereocenters are retained,<sup>394</sup> often resulting in higher  $T_g$  values than in commercial polyamides. Copolymerization of different monomers opens the possibility to obtain materials with a broad range of properties.<sup>395</sup> These strategies have allowed for the synthesis of various polyamide materials from terpene feedstock.<sup>396–401</sup>

In a similar way, terpene-based lactones are accessible via *Baeyer-Villiger* (BV) oxidation of terpene-based cyclic ketones. For instance, menthone,<sup>402–404</sup> carvone,<sup>405–407</sup> and pinene<sup>408,409</sup> have been used for the synthesis of lactone monomers. As an early example, Tolman and Hillmyer et al. showed the use of oxidized dihydrocarvone as comonomer for the synthesis of linear polyesters.<sup>410</sup> **Figure 21**

shows a work of the same group, i.e. the BV oxidation of carvone-derived carvomenthone to the seven-membered lactone carvomenthide, which was then used as monomer for ROP towards linear polyester structures.<sup>411</sup>

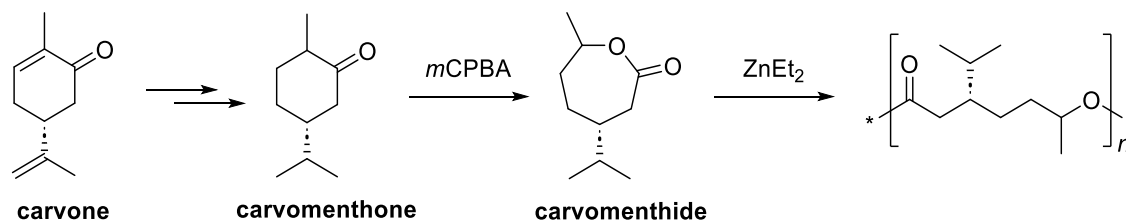


**Figure 21.** ROP of carvone-derived carvomenthide to obtain linear polyesters.<sup>411</sup>

Besides the route shown in **Figure 21**, the exocyclic double bond could also be retained and used for post-polymerization modification. In both cases, good control over the molecular weight and the dispersity was possible, confirming the potential of terpenes as renewable feedstock for ROP monomers. To increase the sustainability of such approaches, BV oxygenases can be used for selective oxidation.<sup>412</sup> Due to their diverse functionalities, terpenes did not only find application in ROP, but also in the synthesis of polymers via step-growth approaches. For this, especially limonene is an attractive feedstock since it is abundant and contains two double bonds for functionalization towards bifunctional monomers.<sup>413</sup> Oxidation of the double bond enabled the synthesis of limonene-based diols and hydroxy acids that could be used for the synthesis of polyester materials via polycondensation.<sup>414</sup> Another approach investigated the synthesis of  $\beta$ -hydroxy amines from limonene for the use in NIPU thermosets.<sup>415</sup>

An efficient tool to address the double bond moieties within terpenes is the thiol-ene click reaction.<sup>416</sup> This enables the introduction of heteroatoms<sup>417</sup> and therefore the synthesis of a broad range of platform chemicals.<sup>418</sup> Taking advantage of the two reactive double bonds within limonene, a previous work from our group described the synthesis of a limonene-based diamine via thiol-ene addition of cysteamine hydrochloride for subsequent synthesis of polyamides and NIPUs.<sup>103</sup> The same amine was used in following approaches for the synthesis of vinylogous urethane vitrimers<sup>419</sup> and epoxy-amine resins.<sup>420–422</sup>

Thiol-ene chemistry can also be used for the addition of thioacetic acid to limonene.<sup>423</sup> Saponification of the resulting thioester moieties yields a limonene-



based dithiol.<sup>424</sup> This can be used e.g. for the synthesis of polymers by thiol-ene polyaddition to comonomers containing multiple double bonds.<sup>347,424,425</sup>

Another widely used method to address the double bond moieties in terpene feedstock is by epoxidation,<sup>426,427</sup> analogous to fatty acid-based feedstock (see section 2.5.1). **Figure 22** exemplarily shows the epoxidation products accessible from limonene.

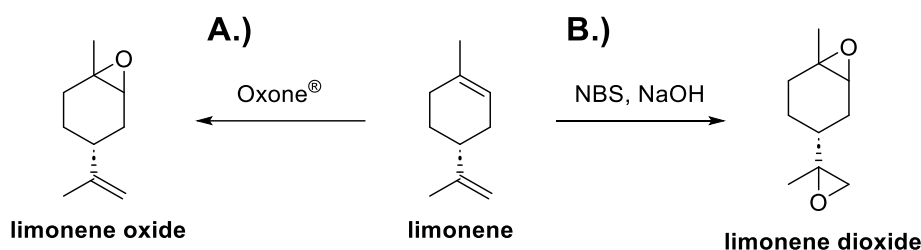


**Figure 22.** Different epoxides accessible from the oxidation of limonene.

As depicted, the endocyclic double bond in limonene can be epoxidized selectively (see **Figure 22a**).<sup>428</sup> As oxidant for this double bond, a system of *N-bromo succinimide* (NBS) and NaOH can be used.<sup>429,430</sup> More sustainable methods involve the use of molecular oxygen as oxidant<sup>431,432</sup> and the implementation of enzyme catalysis.<sup>433,434</sup> The resulting limonene oxide can be used in *ring-opening copolymerization* (ROCOP) approaches with cyclic anhydrides towards polyesters.<sup>435</sup> In a similar way, ROCOP with CO<sub>2</sub> as comonomer can be used to yield polycarbonates.<sup>436,437</sup> Various catalyst systems have been developed for this use of limonene oxide,<sup>438,439</sup> with the remaining double bond allowing for further functionalization.<sup>440–444</sup>

When choosing different oxidation conditions, limonene can be oxidized to a bis-epoxide (see **Figure 22b**). For this, e.g. Oxone<sup>®</sup> can be used as less hazardous oxidant.<sup>445,446</sup> The resulting bifunctional derivative can be applied as monomer in thermosetting polycarbonates<sup>447</sup> or epoxy resins.<sup>448–452</sup> Alternatively, upon carbonation with CO<sub>2</sub>, a bis(cyclic carbonate) LBCC can be obtained. Notably, especially the endocyclic epoxide group shows less reactivity towards carbonation than more accessible epoxides, requiring harsh reaction conditions of temperatures around 120–140 °C and CO<sub>2</sub> pressure of ~30 bar for a successful product formation.<sup>453,454</sup> Alternatively, additional metal catalysts can be used to increase the conversion.<sup>138,455</sup>

As described in section 2.2, bifunctional cyclic carbonate structures represent suitable monomers for the synthesis of NIPUs via ring-opening with polyamines. As such, in works by the group of Mülhaupt, the bis(cyclic carbonate) LBCC derived from limonene was used for the synthesis of NIPU structures, as shown in **Figure 23**.<sup>453,456</sup> Due to limited reactivity of the bis(cyclic carbonate), low molecular weight polymers were obtained, which could be used as prepolymers for the synthesis of thermoplastic NIPUs or cross-linked structures.

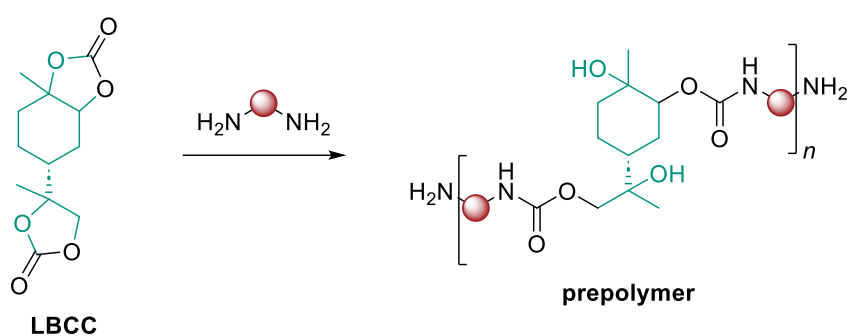


**Figure 23.** Synthesis of hydroxyurethane prepolymers via aminolysis of bis(cyclic carbonate) LBCC.<sup>456</sup>

The strategies described within this section concerning the functionalization of limonene can be also extended to other terpene derivatives. In a similar way to limonene, the terpene feedstock  $\beta$ -elemene was used for epoxidation and ROCOP towards polyesters<sup>457</sup> and for the synthesis of a bis(cyclic carbonate) as precursor for isocyanate-free oligourethane prepolymers.<sup>458</sup> However, limonene presents an attractive feedstock due to its abundance.

Summarized, terpenes are promising naturally occurring precursors for monomers in polymer synthesis such as polyamides, polyesters, and polyurethanes. The structure of cyclic terpenes makes them suitable for an application in ROP approaches and in step-growth polymerization methods. Furthermore, their cyclic structures can result in desirable mechanical and thermal properties of the resulting polymers. At the same time, the limited reactivity of terpene derivatives towards polymerization remains an ongoing challenge.

## 2.6. Organocatalysis in polymer synthesis

The use of catalysis in chemical synthesis is one of the twelve main principles of Green Chemistry (see **Figure 1**) that has been implemented in chemical processes from early on.<sup>459</sup> A catalyst decreases the activation energy of the reaction by offering an alternative reaction pathway and therefore decreases the energy demand.<sup>460</sup> The catalyst is not consumed during the reaction and can thus be used in substoichiometric amounts. Further, the activation by the catalyst is often stronger for one species of product, resulting in increased selectivity where several products or isomers can be formed.<sup>71</sup>

There are several criteria to divide catalysts into different groups, one of the most common distinctions being the one between heterogeneous and homogeneous catalysis.<sup>461</sup> Heterogeneous catalysts can be removed easily from the reaction mixture and are thus generally more straightforward to reuse. Homogeneous catalysts on the other hand offer a broader range of catalyzed reactions and often a higher selectivity. Introduction of a chiral center into the catalyst structure can be used to precisely tune the enantioselectivity of a reaction. However, the separation of a homogeneous catalyst from the reaction mixture can be challenging. With different advantages depending on the field of application, both heterogeneous and homogeneous catalysis are key technologies to develop chemical procedures.

Homogeneous catalysis has found applications throughout very different reaction types.<sup>462</sup> With the first use in established fermentation processes,<sup>463</sup> enzymatic catalysis enables non-hazardous processes with high selectivity for specific applications.<sup>464</sup> Metal-based catalysts on the other hand open the possibility for addressing a large substrate scope, with selective catalyst design due to a broad range of available metals and ligands at hand.<sup>465</sup> For example, metal complexes can serve as Lewis acids,<sup>466</sup> activating electrophilic compounds for nucleophilic attack. At the same time, the use of metals very often poses a potential health hazard and further often relies on limited and expensive resources.<sup>78</sup>

As an addition to enzymes and metal-based catalysts, organocatalysis was investigated, with early examples reaching back to the beginning of last century,<sup>467</sup> but the main breakthrough starting around 2000.<sup>468</sup> A significant focus on organocatalysis was established in works by the groups of List<sup>469,470</sup> and MacMillan,<sup>471,472</sup> resulting in the awarding of the Nobel Prize of Chemistry for

organocatalysis in asymmetric synthesis in 2021.<sup>473</sup> The advantages of organocatalysis are (i) the lower cost of such small molecules without costly metal components, (ii) the typically lower hazard when compared to metal-based counterparts, with most organocatalysts being environmentally benign, and (iii) their typical insensitivity to air and moisture.<sup>472</sup> Whether lower E-Factors are achievable by the use of organocatalysts, depends mainly on their synthesis route.<sup>474</sup> Further, efficient activation often requires higher catalyst loading if compared to metal catalysts, and the activation is often less strong, resulting in possibly lower selectivity. Which catalyst choice is the most promising one to achieve more sustainable chemical processes has to be evaluated for every reaction accordingly.<sup>475</sup>

The activation of reactants by organocatalysts can proceed in various ways, such as by protonation/ deprotonation, nucleophilic attack, and hydrogen bonds. It is also possible for several activation modes to occur at the same time, enhancing the activation by synergistic effects.

Organocatalytic methods have been used in various asymmetric synthesis pathways.<sup>476</sup> In polymer synthesis, organocatalytic methods have found wide application,<sup>477</sup> in step-growth<sup>478</sup> as well as in chain-growth and living polymerization approaches.<sup>479,480</sup> As one of the first examples, 4-dimethylaminopyridine was used as nucleophilic catalyst in the ROP of lactones towards polyesters,<sup>481</sup> which has inspired further extensive research in this field. This chapter will focus on organobases as Lewis-basic catalysts and thioureas as hydrogen-bonding catalysts.

### 2.6.1. Organic superbases TBD and DBU

Two prominent examples of Lewis-basic organocatalysts are *1,5,7-triazabicyclo[4.4.0]dec-5-ene* (TBD) and *1,8-diazabicyclo[5.4.0]undec-7-ene* (DBU),<sup>482</sup> which are shown in **Figure 24**. TBD and DBU are both strong organic bases, with TBD exhibiting a slightly higher basicity.<sup>91–94</sup>

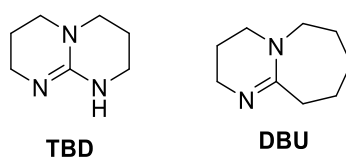


**Figure 24.** TBD and DBU as common organic superbases used in polymer synthesis.

Both bases exhibit Lewis-basic tertiary amine groups, and upon protonation the resulting charge is delocalized between the different nitrogen atoms. The guanidine base TBD further contains an additional NH-moiety which can undergo hydrogen bonding. By reaction with vinyl acetate, the acylation of TBD was observed,<sup>483</sup> as the lack of a back reaction enabled the isolation of acylated TBD. The successful acylation confirms that TBD acts as a nucleophilic catalyst and attacks at carbonyl centers. At the same time, calculations showed that due to steric hindrance, the formed acylated TBD is not planar and therefore more reactive towards subsequent nucleophilic attack if compared to, for example, *1,4,6-triazabicyclo-[3.3.0]oct-4-ene* (TBO).<sup>95</sup>

The combination of high basicity, nucleophilicity, and the activation of the acylated intermediates in reactions with carbonyl centers makes TBD all in all a very versatile and efficient catalyst that can be used in a variety of reactions. Whether the activation of substrates proceeds via nucleophilic attack, proton abstraction, or hydrogen bonding, can vary and has to be analyzed for each case.

The amidine base DBU is less nucleophilic due to a lower electron density and is more expensive than TBD, which can be synthesized from inexpensive chemicals.<sup>484</sup> However, the lower reactivity of DBU and the lack of hydrogen bonding can be beneficial for certain reactions or to achieve higher selectivity and, moreover, its liquid state in contrast to the solid form of TBD makes it easier to handle. In many cases, both bases can be used in an equivalent way.

In the synthesis of NIPUs (see section 2.2) and polyesters (see section 2.3), the shown organobases can be used as catalysts in different ways since, in principle, all of the routes towards NIPUs shown in **Figure 4** involve reactions at a carbonyl center. For example, the formation of urethane moieties via Lossen rearrangement can be catalyzed by tertiary amine bases.<sup>485</sup> Further, in several pathways including polycondensation via transurethanization, TBD was used as catalyst.<sup>103,486–488</sup>

**Figure 25** shows an example of a terpene-based polyurethane obtained from TBD-catalyzed transurethanization.<sup>103</sup> Via thiol-ene reaction, amine groups were introduced into limonene as renewable starting material, and the reaction of the resulting diamine with DMC yielded an AA monomer for NIPU synthesis with different diols. Both the methoxycarbonylation of the diamine and the polyaddition

to the NIPU could be catalyzed by addition of TBD, underlining the versatility of this type of catalyst.

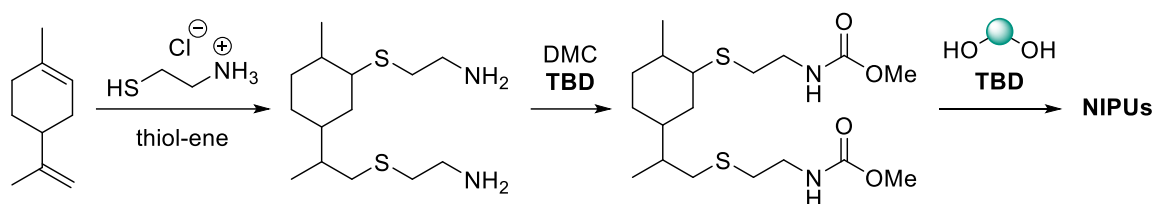


**Figure 25.** Synthesis of linear NIPUs from limonene via TBD-catalyzed transurethanization.<sup>98</sup>

The opening of cyclic carbonates as the most investigated route towards NIPUs (see **Figure 4**) can also be catalyzed by addition of TBD or DBU.<sup>489</sup> TBD was shown to promote the reaction by a nucleophilic opening of the cyclic carbonate,<sup>490</sup> and further by activating the nucleophile and stabilizing the intermediates by the proton-donating NH-group.<sup>491</sup> This was used for the synthesis of NIPUs in presence of TBD.<sup>490,492–495</sup> The reactivity of TBD towards the resulting urethane moieties was shown to favor the formation of urea linkages, which could be taken advantage of to achieve improved properties.<sup>496</sup>

The activation of carbonyl centers by TBD and DBU can also be used in a similar way for the substitution of carbonates and esters.<sup>497–499</sup> In various previous works from our group, this was applied for the synthesis of polyamides,<sup>103,328,500–506</sup> polycarbonates,<sup>130</sup> and polyesters<sup>327,505,507</sup> from renewable resources via step-growth polycondensation.

Apart from polycondensation, the main route towards polyesters involves a ROP of lactones (see section 2.3), which can also be catalyzed by guanidine and amidine bases.<sup>508,509</sup> Calculations showed that TBD acts as bifunctional catalyst, activating both the carbonyl group by nucleophilic attack and the initiator alcohol group by Lewis base catalysis,<sup>483,508</sup> forming an intermediate as shown in **Figure 26** for the ROP of  $\epsilon$ -caprolactone.<sup>508</sup> The high activity of TBD, however, is also the cause of transesterification side reactions, resulting in broadened molecular weight distributions.

Instead of TBD, DBU can be used in ROP for example of L-lactide,<sup>510,511</sup> but no bifunctional catalysis is possible due to a lack of the additional NH-group. Therefore, for other lactones than lactide, DBU is often combined with hydrogen bonding catalysts such as thioureas during ROP reactions.<sup>508</sup> The formation of

polymers using such a catalyst system was shown to be considerably slower compared to TBD, however at the same time the lower reactivity results in less background transesterification and can possibly yield less disperse polymeric products.<sup>126</sup>

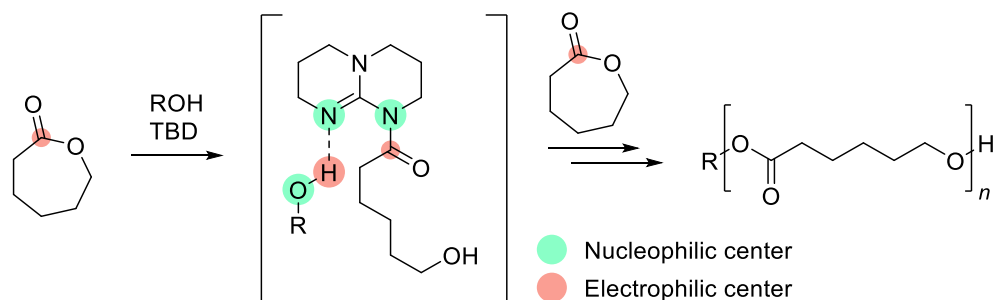


**Figure 26.** TBD as bifunctional catalyst in the ROP of  $\epsilon$ -caprolactone.<sup>122</sup>

### 2.6.2. Thiourea organocatalysts

Another compound group that has often been used in the synthesis of NIPUs and polyesters are thioureas, which coordinate to carbonyl groups<sup>512</sup> via bidentate hydrogen bonding and therefore can activate them for nucleophilic attack (see **Figure 27**).<sup>513,514</sup> Thioureas possess lower  $pK_A$  values than their urea counterparts, resulting in better hydrogen bond donor properties.<sup>130</sup>

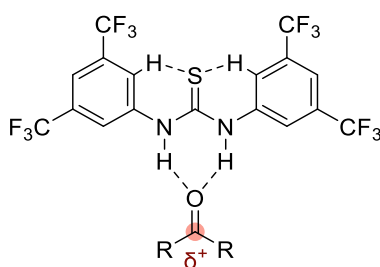


**Figure 27.** Carbonyl activation by thiourea, increasing the electrophilicity of the carbonyl center.

For efficient hydrogen bonding, electron-withdrawing substituents are beneficial, as a lower electron density increases the acidity. Further, aromatic residues can increase the activation by preorganization due to interactions between the *ortho*-protons and the thiocarbonyl group,<sup>515,516</sup> as shown in **Figure 27** for the well-established Schreiner catalyst. This preorganization favors the formation of hydro-

gen bridges between thioureas and hydrogen bonding acceptors by lessening the entropic sacrifice upon association. As such, the 3,5-bis(trifluoromethyl) phenyl group is often used in thiourea catalysts,<sup>516</sup> but can also be substituted by other electron-withdrawing groups.<sup>517–521</sup>

Generally activating carbonyl groups, thiourea compounds can be used for the aminolysis of cyclic carbonates.<sup>489,490,492,522</sup> As an example, the group of Caillol used a thiourea catalyst for the synthesis of NIPU foams from trimethylolpropane tris-carbonate, polypropylene oxide bis-carbonate, and a commercial diamine, with a poly(methylhydrogenosiloxane) as blowing agent, as shown in **Figure 28**.<sup>139</sup>

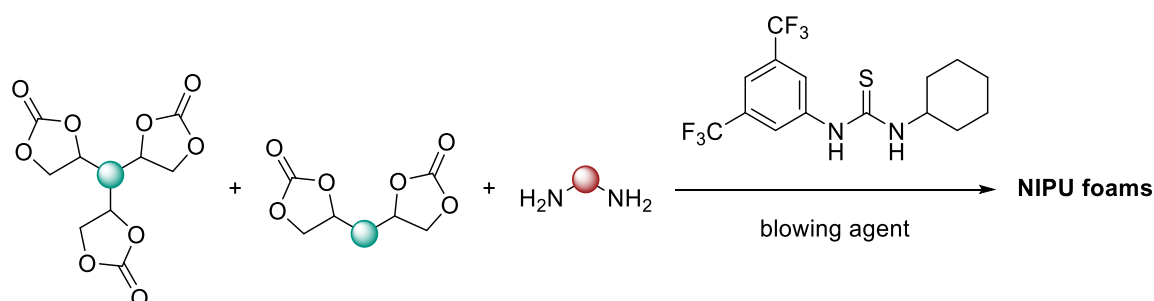


**Figure 28.** Thiourea-catalyzed synthesis of NIPU foams.<sup>139</sup>

This enabled the synthesis of foams at room temperature with a low catalyst loading of 1 mol%. The specific catalyst structure was chosen as it had previously been shown to be active in the opening of cyclic carbonates and due to its solubility in the formulation.<sup>522</sup> The obtained results suggest the potential of more research on this sort of organocatalyst in NIPU synthesis.

Besides, the activation of carbonyls by thioureas can also be taken advantage of in the synthesis of further carbonyl-based polymers. In ROP towards polyesters and polycarbonates, thioureas showed catalytic activity, however, for efficient polymerization, a Lewis base is often added to activate the nucleophilic moiety.<sup>508,523</sup> This Lewis-basic group can be part of the thiourea catalyst,<sup>524</sup> as for instance in the bifunctional catalyst developed in the group of Takemoto (see **Figure 29a**).<sup>525,526</sup> Such bifunctional catalysts were shown to promote the ROP of lactones effectively and selectively,<sup>524,527</sup> as the opening of the ester is preferred over transesterification of ester groups within the growing polymer chain. Further,



when introducing the nucleophilic group within a chiral backbone, this approach can enable stereoselective synthesis.<sup>514</sup>

By deprotonation of the thiourea moiety, a bifunctional catalyst system can be generated (see **Figure 29b**), which is able to activate both the nucleophile and the electrophile. The group of Waymouth developed a catalytic system consisting of thioureas and metal alkoxides, resulting in thiourea anions (thioimidates).<sup>528</sup> Like this, they were able to polymerize L-lactide by synergistic activation of the carbonyl group of the lactone and the alcohol group of the initiator, as confirmed by computational studies. Depending on the choice of thiourea and base, the transition between the initiator being activated by a thiourea anion or by the base as co-catalysis is fluid and can be tuned to achieve maximum activity.<sup>529</sup> The same concept can be found in the cooperative catalysis of analogous urea compounds and organic superbases, yielding a bifunctional imidate catalyst system that showed high activity in the ROP of lactones.<sup>530–533</sup>

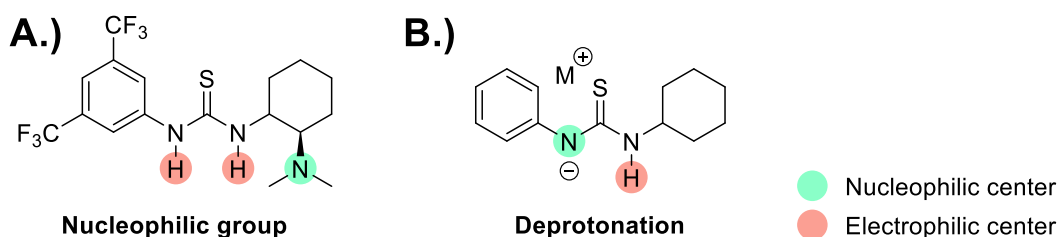


**Figure 29.** Possibilities to introduce bifunctionality into thiourea catalysts. A.) Introduction of a nucleophilic group into the thiourea substituents; B.) deprotonation of thiourea group.

The versatility in the mild activation of carbonyl groups by thioureas renders them potentially attractive catalysts in more sustainable chemical processes. Yet, to establish their use in procedures that aim for improved sustainability, the synthesis of thiourea compounds has to be taken into account.

Thioureas can be prepared by addition of amines to isothiocyanates.<sup>534</sup> Classically, isothiocyanate compounds are synthesized from amines and thiophosgene<sup>535</sup> or CS<sub>2</sub>,<sup>536,537</sup> which presents a drawback with regard to sustainability because of the high intrinsic toxicity of isothiocyanates and thiophosgene or CS<sub>2</sub>. A less hazardous method involves the addition of elemental sulfur to often non-toxic isocyanides.<sup>538</sup> This was implemented in a three-component reaction approach for the synthesis of thioureas, where an amine that is present in the reaction mixture can add to the

isothiocyanate formed in situ from the isocyanide and elemental sulfur.<sup>539</sup> In previous work from our group, this was applied for the synthesis of a scope of thiourea catalysts with alternative electron-withdrawing groups to the 3,5-bis(trifluoromethyl) phenyl group,<sup>521</sup> as fluorinated groups limit the sustainability of the catalyst synthesis. High yields and simple purification further contribute to a greener process. A selection of the thiourea structures that were synthesized in one to five steps is shown in **Figure 30**.

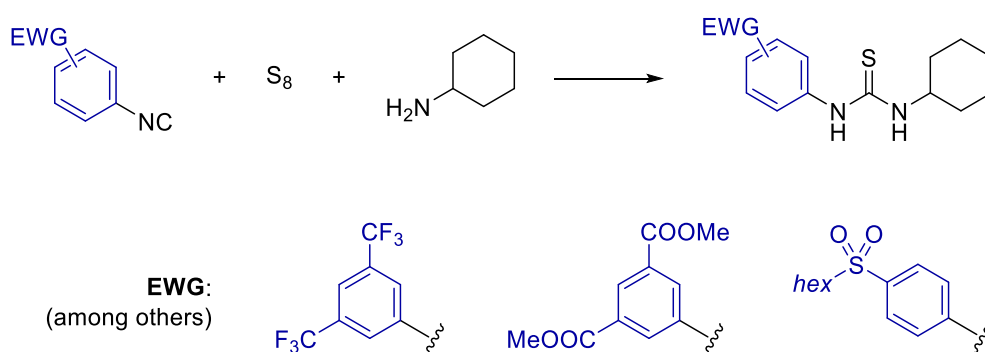


**Figure 30.** Selection of a scope of thioureas by a multi-component reaction of an aryl isocyanide with elemental sulfur and cyclohexyl amine.<sup>521</sup>

With this greener synthesis method at hand, thiourea compounds represent an attractive catalyst class for the sustainable synthesis of polymers, in which various applications remain to be explored.

### 3. AIM OF THE THESIS

The aim of this work was to develop organocatalytic strategies for the functionalization of renewable feedstock towards potential monomers for polyester and NIPU synthesis. Special focus was put on the use of thiourea organocatalysts, conveniently and more sustainably accessible via a multicomponent approach, as well as on utilizing terpenes and erythritol as renewable resources. **Figure 31** summarizes these objectives.

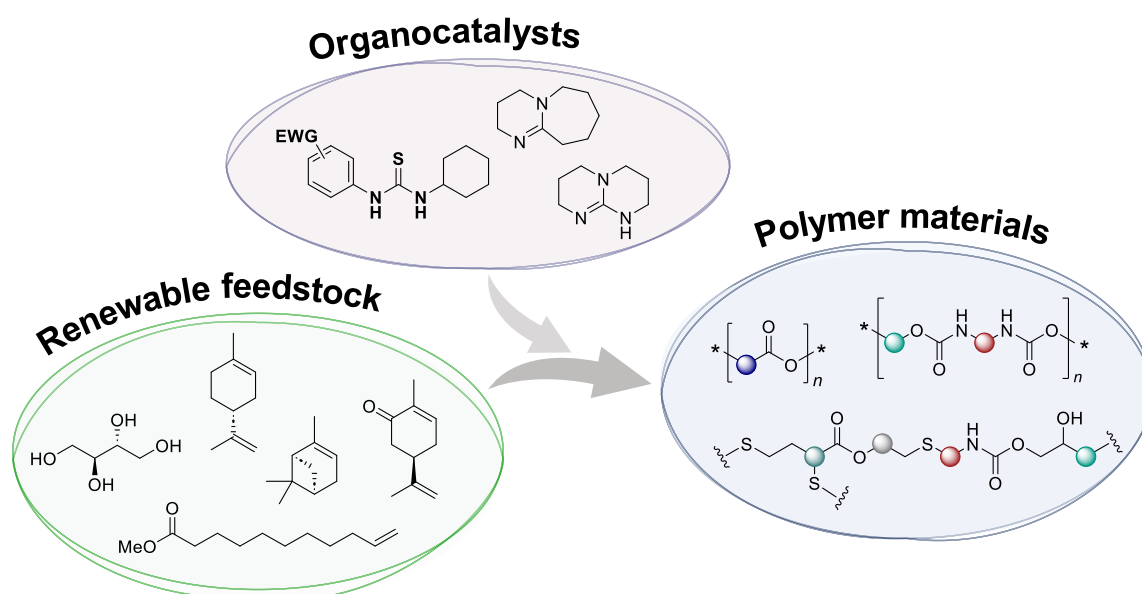


**Figure 31.** Summarized aim of this work, including the organocatalytic transformation of renewable feedstock towards polyester and NIPU materials.

Based on previously established protocols,<sup>521,539</sup> a set of thiourea catalysts was to be synthesized and tested for the activation of different renewable monomers, at the same time comparing their performance with other organocatalysts such as organobases.

In a first project, the terpenes carvone and  $\alpha$ -pinene were chosen to elaborate potentially organocatalyzed ROP routes towards linear polyesters. For this purpose, synthesis routes to obtain terpene-based lactones as ROP monomers were to be addressed. Different catalytic systems should be compared based on model substrates to develop a suitable approach.

Secondly, the use of thiourea catalysts for the synthesis of NIPUs was to be investigated. The performance of selected thioureas was to be tested for transurethanization and cyclic carbonate opening approaches, both being promising routes to obtain NIPUs. Especially the aminolysis of cyclic carbonates should be addressed due to the possibility to use terpene- and erythritol-based cyclic carbonates as renewable substrates for the synthesis of linear NIPUs.

Further, the implementation of terpene and erythritol derivatives into thermoset materials was aimed at. The goal was to establish curing protocols to obtain NIPU networks that potentially display dynamic properties.

Throughout all projects addressed within this work, the twelve principles of Green Chemistry were used as guidelines to establish potentially more sustainable procedures. Different approaches developed in this thesis should be evaluated and compared regarding aspects of sustainability such as renewability, energy consumption, waste production, safety hazard, and the use of catalysts. In this way, the aim was to contribute to the ongoing research towards the development of more sustainable polymeric materials.

## 4. RESULTS AND DISCUSSION

### 4.1. Synthesis of a set of thiourea catalysts

As illustrated in the previous section, one of the aims of this work is to investigate the use of thiourea organocatalysts in polymer synthesis. To achieve this, at first a set of thiourea catalysts, with varying substituents that influence the hydrogen-bonding and thus catalytic activity, was synthesized (see **Figure 32**).<sup>521</sup>

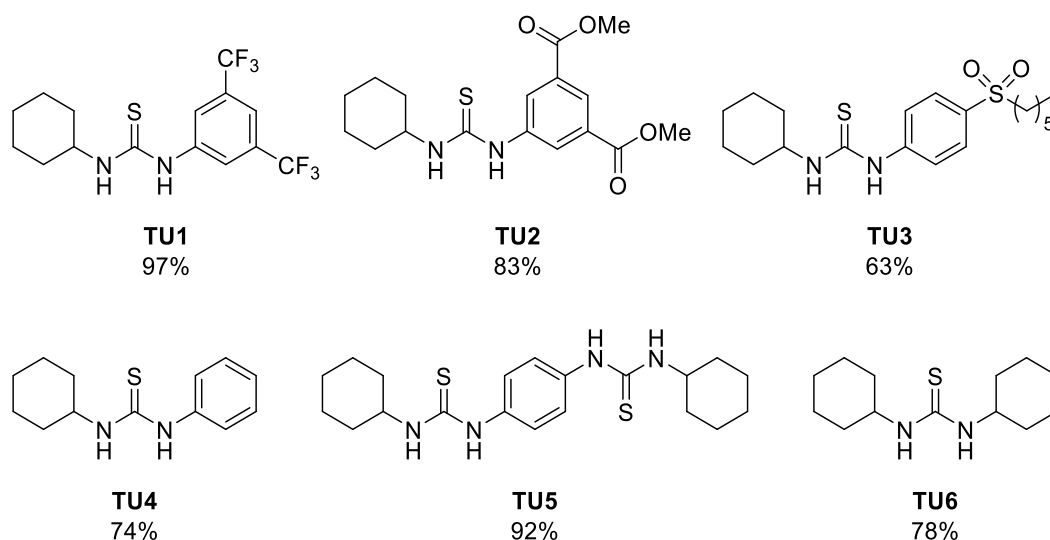


**Figure 32.** Thiourea catalysts synthesized within this work. The reaction conditions were chosen based on a previously described approach (see **Figure 30**).<sup>521</sup>

All catalysts **TU1**–**TU6** contain one cyclohexyl residue and a second residue that varies in its electron-withdrawing ability, which represents a combination used before to combine good solubility and hydrogen bond donor ability.<sup>539</sup> **TU1** contains the often used 3,5-bis(trifluoromethyl)phenyl group that is also present in the so-called Schreiner catalyst.<sup>513,515</sup> This moiety leads to efficient hydrogen bond activation<sup>516</sup> and therefore, **TU1** as easily accessible thiourea was used within this work as reference and to observe if reactions could be facilitated by thiourea catalysis. At the same time, the trifluoromethyl groups limit a potentially sustainable synthesis of this catalyst.<sup>540</sup> One of the aims of this work (see section 3) was to develop more sustainable approaches for polymer synthesis, for which also the synthesis route of the catalysts has to be considered. Thus, based on previous work on a more sustainable synthesis of thiourea catalysts,<sup>521</sup> alternative electron-

withdrawing groups were introduced in **TU2** and **TU3**. Further, thiourea compounds with less electron-withdrawing groups **TU4–TU6** were synthesized within this set. For the formation of these more sustainable thiourea compounds **TU2–TU6**, a multicomponent reaction involving elemental sulfur, cyclohexyl amine, and the respective isocyanide was used, as illustrated in section 2.6.2.<sup>521,539</sup> The yields of the obtained thioureas are given in **Figure 32**.

One possibility to substitute the trifluoromethyl groups is by introducing electron-withdrawing ester groups in *meta*-position, as shown in **TU2**. This catalyst was successfully synthesized from the aryl isocyanide, however, its use is limited to reaction conditions in which no transesterification of the ester groups can occur. Another more benign electron-withdrawing group is represented by the sulfone moiety as in **TU3**. Previously, a route towards **TU3** by oxidation of an aromatic thioether was developed (see **Figure 33**).<sup>521</sup> In this, the thioether moiety of the precursor **1** is oxidized by hydrogen peroxide, yielding the sulfone **2**, which is then converted into the formamide **4** by reacting the amine group with formic acid. Alternatively, the amine group of **1** can be converted into a formamide **3** by reacting with formic acid, and then **3** can be oxidized to **4** by hydrogen peroxide.

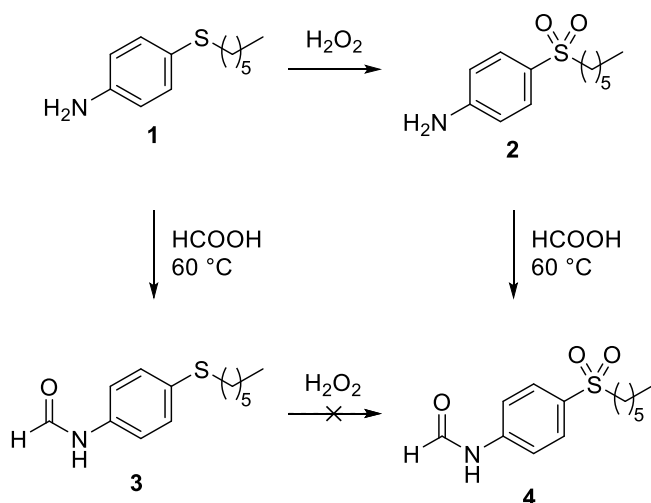


**Figure 33.** Formation of sulfone **2** and formamide **4** from thioether **1**, as well as possible alternative route via formamide **3**.

During the oxidation of **1**, however, the formation of an aromatic side product was observed via <sup>1</sup>H NMR spectroscopy (see **Figure 34**). The amount of side product formed during the reaction varied in different batches. To achieve higher sustainability within the synthesis route, purification via column chromatography should be avoided. Thus, to minimize the formation of the side product, test reactions were

performed at lower temperatures. Yet, also at 30 °C and 40 °C, the side product was observed via *thin layer chromatography* (TLC) and  $^1\text{H}$  NMR spectroscopy (see **Figure 34**). Further,  $\text{MnSO}_4$  and Oxone<sup>®</sup> were tested as alternative oxidants, but in both cases, the formation of higher amounts of side products was observed if compared to using hydrogen peroxide.

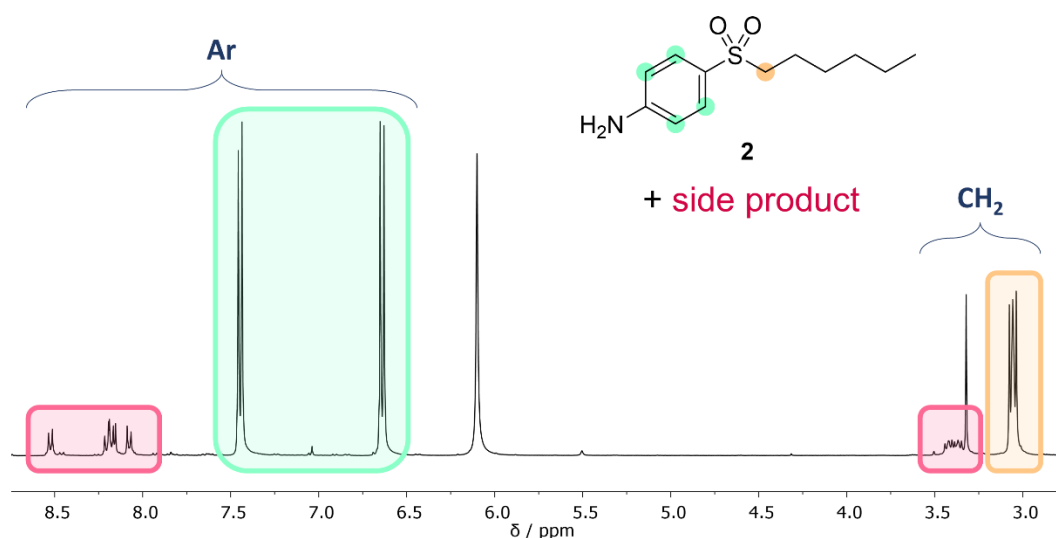


**Figure 34.** Observation of side product in the NMR spectrum of isolated sulfone **2**.

To overcome this challenge, a varied synthesis route for the formamide **4** was tested (see **Figure 33**), in which the thioether **1** containing an amine group was first converted into the formamide **3**, which was subsequently reacted with hydrogen peroxide with the aim to obtain compound **4**. However, while the formamide **3** was obtained successfully, its oxidation did not lead to successful formation of the product **4**. Therefore, this route was not investigated further. Instead, the sulfone intermediate **2** was used for the next synthesis steps without further purification. While in the isolated **4**, the impurity was still detectable (see **Supplementary Figure 10**), the subsequent conversion to the isocyanide prior to the thiourea synthesis required purification via column chromatography, which ultimately resulted in separation of the impurity from the desired compound (see **Supplementary Figure 12**).

Besides the discussed thiourea compounds **TU1–TU3** containing electron-withdrawing moieties, the less electron-poor **TU4–TU6** were synthesized via the same multicomponent approach as **TU2** and **TU3**. This created a set of thiourea catalysts with different hydrogen bonding abilities, which could be compared regarding their

activities in the investigated reactions. The use of the bifunctional thiourea **TU5** was included to investigate a possible increase of activation by a higher number of functional groups. Further, for approaches involving catalysis via thiourea anions, a higher electron density within the thiourea moiety as in **TU4–TU6** might even be beneficial.<sup>530</sup>

The set of thiourea organocatalysts **TU1–TU6** was used throughout this work to test reactions for activation via thioureas. As such, reactions involving a nucleophilic attack at carbonyl centers were investigated, since thiourea compounds were shown to interact with carbonyl moieties via hydrogen bonding.<sup>512,513</sup> With novel synthetic routes to more sustainable polymers being the central aim of this work, the investigations thus mainly focused on the synthesis of polyesters and non-isocyanate polyurethanes.



## 4.2. Thiourea-catalyzed ring-opening polymerization

Part of the experiments of this chapter were performed by Hendrik Kirchhoff and Johanna Rietschel during a practical course (Vertiefungspraktikum) and Bachelor thesis under the co-supervision of the author. The respective experiments are highlighted with footnotes. The interpretation and discussion of the results were written by the author.

The *ring-opening polymerization* (ROP) of lactones is one of the main strategies to yield polyesters,<sup>195</sup> as already discussed in section 2.3. Besides, the ROP of cyclic carbonates with a ring size above five represents a common route towards polycarbonates.<sup>541</sup> These two polymerization methods show similar mechanisms and modes of activation and thus will be treated jointly in this section.

Next to the use of metal catalysts for ROP,<sup>208</sup> organocatalytic approaches have gained increased attention due to the possibility to use cheap and benign catalysts.<sup>222,224</sup> Organocatalysts that can promote ROP of lactones include for example *N*-heterocyclic carbenes.<sup>542,543</sup> However, their high sensitivity to air and moisture makes their handling challenging. As alternatives, guanidine bases or amidine bases in combination with thiourea compounds were investigated, as well as catalyst systems from thioureas and bases, as discussed in section 2.6.<sup>508</sup> The synthesis of the thiourea derivatives **TU1–TU6**, as described in section 4.1,<sup>521</sup> opens the potential to improve the sustainability of organocatalytic ROP of lactones and cyclic carbonates.

Within this work, it was aimed to develop thiourea-catalyzed ROP procedures of terpene derivatives. Terpenes were chosen as renewable starting materials since they were already shown to be suitable precursors for ROP approaches<sup>380</sup> and their use is attractive due to their occurrence as waste materials (see section 2.5.3).

To investigate a possible catalytic effect of the synthesized thioureas **TU1–TU6** on the ROP of terpene-based cyclic carbonates and lactones, model substrates were used at first to develop a suitable procedure that could subsequently be applied to terpene derivatives. Further, the synthesis of ROP monomers from terpene feed-stock was investigated.

### 4.2.1. Ring-opening polymerization of cyclic carbonates

The ROP of cyclic carbonate compounds enables the synthesis of polycarbonate materials. A wide range of terpene-based five-membered cyclic carbonates has been established,<sup>138</sup> but due to low ring strain, five-membered cyclic carbonates showed no reactivity in ROP towards polycarbonates.<sup>544</sup> In contrast, six-membered cyclic carbonates can act as monomers for polycarbonate synthesis via ROP, but they are less straightforward to synthesize.<sup>545,546</sup> A possible access is the reaction of DMC with 1,3-diols, which in turn can be obtained via classic organic reactions, such as Michael addition or aldol addition and subsequent reduction. For the present work, a model six-membered cyclic carbonate was synthesized to analyze whether such substrates are suited for polymerization using thiourea catalysis. In **Figure 35**, the synthesis of the model cyclic carbonate **6** starting from the commercially available 1,3-diol **5** is shown.

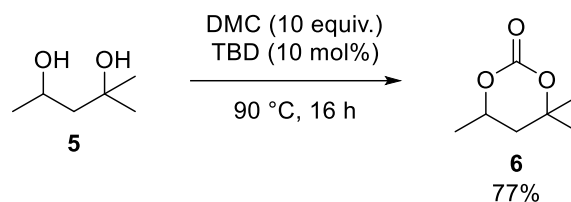


**Figure 35.** Synthesis of model six-membered cyclic carbonate **6**.

The choice of **6** as a model substrate was made based on the availability of the corresponding diol **5** and the simple synthesis that was previously reported.<sup>545</sup> While six-membered cyclic carbonates are not as easily obtained as their five-membered counterparts (see section 2.2), the synthesis of **6** is facilitated by the Thorpe-Ingold effect due to the geminal substituents. At the same time, the hence decreased reactivity of **6** towards ROP due to several substituents resembles potential monomers that could be accessible from terpenes. The product was obtained in a yield of 77% after recrystallization.

For the potential ROP of **6**, three different organocatalytic systems were investigated. The results are summarized in **Table 1**. The first investigated system was TBD (**Table 1**, entry 1), secondly DBU in presence of **TU1** was tested (**Table 1**, entries 2 and 4), and thirdly a cooperative system of **TU1** and potassium methoxide (**Table 1**, entries 3 and 5). In the approaches using TBD or DBU, benzyl alcohol

was used as nucleophilic initiator. No benzyl alcohol was required as initiator when **TU1** was combined with an alcoholate base, as the alcoholate can initiate the reaction itself. All experiments were conducted under air and water exclusion.

**Table 1.** Test reactions of polycarbonate synthesis from **6** using different catalyst systems. Samples were taken after 1 d and analyzed via SEC.

entry	BnOH	base	TU1	T / °C	M <sub>n</sub> / kDa
1	BnOH	TBD	-	r.t.	n. d.
2	BnOH	DBU	5 mol%	r.t.	n. d.
3	-	KOMe	5 mol%	r.t.	n. d.
4	BnOH	DBU	5 mol%	70	n. d.
5	-	KOMe	5 mol%	70	n. d.
6	-	BF <sub>3</sub> OEt	5 mol%	70	n. d.

As shown in **Table 1**, all of the selected reaction conditions did not enable the successful synthesis of polycarbonates. In all cases, solely the monomer was detected via SEC after one day of stirring at room temperature (**Table 1**, entries 1-3). Performing the reaction at higher temperatures (**Table 1**, entries 4 and 5) or the use of an alternative alkoxide base (**Table 1**, entry 6) also did not lead to the formation of polymeric species.

Since no polymerization of the test substrate **6** was observed under the chosen reaction conditions, no further investigations on the ROP of cyclic carbonates using thiourea catalyst systems were performed. Notably, the number of performed experiments is not sufficient to exclude the possibility that there might be reaction conditions that can transform **6** to a polycarbonate via thiourea organocatalysis. The concentrations and equivalents of the used substrates and reagents were not varied within the scope of this work. Also, the chosen model substrate **6** might not be reactive enough to see satisfying results. Correlated to the stability of the monomer **6**, the entropic and enthalpic gain upon ring-opening is expected to be

comparably low. The use of sterically less demanding cyclic carbonates for facilitated nucleophilic attack and higher entropy gain or of vicinal functional groups instead to increase the angular and conformational ring strain might be possible strategies for future experiments.

At the same time, one of the aims of this work was to use terpene-based substrates, and the synthesis of cyclic carbonate monomers from terpenes, which should further possess little steric demand, has not been described. The use of terpenes for polycarbonate synthesis has been established in the ring-opening copolymerization of terpene oxides with CO<sub>2</sub>.<sup>437,447</sup> Since no efficient activation was observed within the first test reactions, the indication that a more sustainable polycarbonate synthesis might be possible were not sufficient to continue with these investigations.

To sum up, no promising results were obtained for the ROP of cyclic carbonates using the reaction conditions tested in **Table 1**, therefore for further experiments a higher focus was set on the organocatalyzed synthesis of polyesters from seven-membered lactones that will be described in the following two chapters.

#### 4.2.2. Ring-opening polymerization of $\epsilon$ -caprolactone

Next to polycarbonates, ROP strategies can be used for the controlled synthesis of polyesters. In this context, terpene derivatives have already been used as starting materials.<sup>409</sup> Terpenoid structures that consist of six-membered cyclic ketones can be transformed into seven-membered lactones by *Baeyer-Villiger* (BV) oxidation, which were shown to be precursors for ROP towards polyesters (see section 2.5.3).<sup>409</sup>

To test the performance of the synthesized thiourea catalysts (see section 4.1) in the ROP of seven-membered lactones,  $\epsilon$ CL was used as model compound, since it is commercially available, and its polymerization has been widely studied before.<sup>212</sup> The catalyst system of **TU1** and DBU has been investigated for this reaction previously.<sup>508</sup> Therefore, the aim was to analyze the effect of alternative electron-withdrawing groups present in **TU2** and **TU3**, which can be introduced in a more sustainable fashion. Additionally, the thiosemicarbazone **TSC** was tested as potential cocatalyst, which can be obtained from the condensation of a

thiosemicarbazide and the corresponding aldehyde and was synthesized previously in our group.<sup>521</sup>

**Table 2** summarizes the results of the test polymerizations of  $\epsilon$ CL using DBU and **TU1–TU3** or **TSC**.<sup>†</sup> As nucleophilic initiator, pyrene butanol was used, which has been used in previous studies in favor of end group detection, thus enabling a comparison of the results with literature examples.<sup>508</sup> All experiments were carried out in toluene as solvent and under air and water exclusion.

**Table 2.** Test reactions of the ROP of  $\epsilon$ CL with a catalyst system of DBU and **TU1–TU3** or **TSC** as cocatalysts. The molecular weight  $M_n$  and the dispersity  $\mathcal{D}$  were determined via oligo-SEC taking aliquots after the respective reaction time and quenching with benzoic acid.

entry	cocatalyst	time / h	$M_n / \text{kg}\cdot\text{mol}^{-1}$	$\mathcal{D}$
<b>1</b>	<b>TU1</b>	2	0.4	n. d.
<b>2</b>	<b>TU1</b>	72	14.1	1.07
<b>3</b>	<b>TU2</b>	48	7.3	1.05
<b>4</b>	<b>TU3</b>	48	12.9	1.06
<b>5</b>	<b>TSC</b>	48	n. d.	n. d.

After two hours of reaction time using DBU in combination with **TU1** (**Table 2**, entry 1), the formation of oligomeric species was observed. After stirring for three days

<sup>†</sup> The experiment was performed by Hendrik Kirchhoff under co-supervision of the author.

(**Table 2**, entry 2), the molecular weight was determined to be  $14.1 \text{ kg}\cdot\text{mol}^{-1}$  via SEC.

The expected molecular weight depends on the ratio of  $\epsilon\text{CL}$  to pyrene butanol as nucleophilic initiator when supposing a chain-growth mechanism. The calculation of the theoretical molecular weight when using 0.05 equiv. pyrene butanol, corresponding to a monomer to initiator ratio of 20:1, is shown in Equation (3).

$$M_{n,\text{theor}} = \frac{M_{\epsilon\text{CL}}}{\text{equiv}_{\text{In.}}} + M_{\text{In.}} = \frac{114.14 \text{ g}\cdot\text{mol}^{-1}}{0.05} + 274.26 \text{ g}\cdot\text{mol}^{-1} = 2.6 \text{ kg}\cdot\text{mol}^{-1} \quad (3)$$

In. = pyrene butanol.

Notably, the determined molecular weights (**Table 2**, entries 3-5) are significantly higher than the theoretical value from Equation (3). Possible reasons for this difference can be found in the low quantities of pyrene butanol, deviation from ideal chain-growth behavior and especially the lacking acuteness of molecular weight determination via SEC, which is calibrated based on poly(methyl methacrylate) standards. A more accurate determination of the molecular weight might be possible using  $^1\text{H}$  NMR experiments via the signals of the pyrene end group, but was not performed within this work. Nevertheless, the effective polymerization of  $\epsilon\text{CL}$  by DBU and **TU1** can be observed qualitatively.

Entries 4 and 5 of **Table 2** show that **TU2** and **TU3** both promote the ROP of  $\epsilon\text{CL}$  as in the case of **TU1**, with the sulfone-based **TU3** exhibiting very similar results to **TU1** already after 48 h. All three thiourea compounds as cocatalysts yielded polymers with narrow dispersities of 1.06–1.07. These results indicate that the thiourea synthesis route from our group that was discussed in section 4.1 can offer more sustainable cocatalysts for a controlled ROP of lactones. The thiosemicarbazone **TSC**, on the other hand, did not lead to polymerization (**Table 2**, entry 5).

As discussed in section 2.6.1, TBD can be used as alternative to DBU and a thiourea and act as bifunctional catalyst in the ROP of lactones.<sup>508</sup> Thus, to put the above results into context, the catalyst system of TBD and thiourea and DBU was

compared with TBD as catalyst. Samples were taken after different time intervals. The results are summarized in **Table 3**.<sup>†</sup>

**Table 3.** Test reactions of the ROP of  $\epsilon$ CL with TBD as catalyst. The molecular weight  $M_n$  and the dispersity  $\mathcal{D}$  were determined via oligo-SEC taking aliquots after the respective reaction time and quenching with benzoic acid.

entry	time / h	$M_n$ / kg·mol <sup>-1</sup>	$\mathcal{D}$
1	1	4.3	1.09
2	2	6.4	1.09
3	3	8.3	1.08
4	6.5	13.5	1.28
5	24	26.8	1.79
6	72	28.5	2.00

It can be seen that TBD promotes the polymerization of  $\epsilon$ CL successfully and considerably faster than the combination of DBU and thiourea. Already after 6.5 hours, the determined molecular is in a similar range as in the best results from **Table 2**. At the same time, though, the measured dispersity values are significantly higher compared to a combination of DBU and thiourea. The broadening of the molecular weight distribution can also be seen in **Figure 36**, which shows the SEC traces of the reaction. The broadening of the SEC traces with time can be attributed to occurring transesterification reactions within the polymer backbone, as was previously described in the literature.<sup>508</sup>

The comparison to TBD confirms that the catalyst system of DBU with a thiourea shows a very high selectivity of ring-opening above transesterification side reactions and is therefore suited to yield defined polymers with narrow molecular weight distributions. Even after reaction times of two or three days, dispersities below 1.1 were obtained when combining DBU with a thiourea catalyst. The substitution of the commonly used CF<sub>3</sub> groups by more benign residues contributes to an increased sustainability of this catalyst system.

<sup>†</sup> The experiment was performed by Hendrik Kirchhoff under co-supervision of the author.

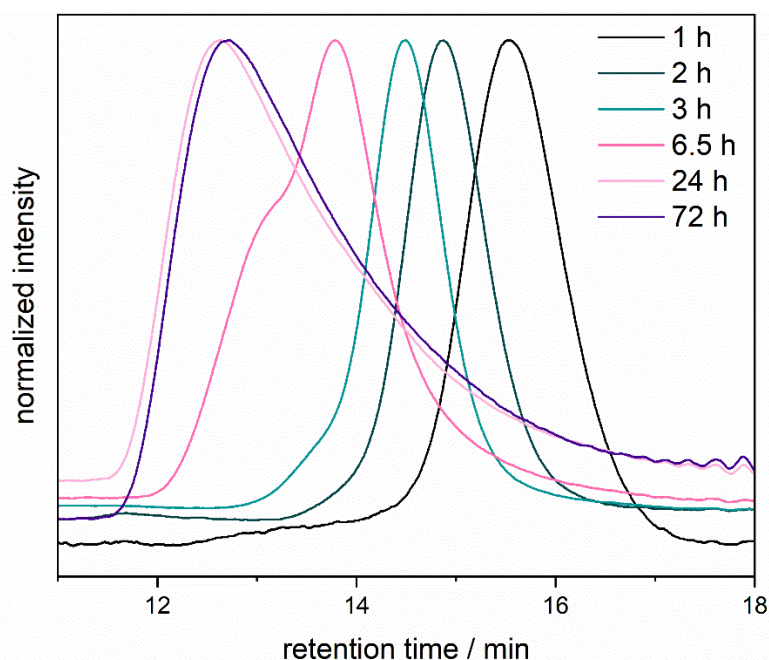


**Figure 36.** SEC traces of the ROP of  $\epsilon$ CL with time, catalyzed by TBD. SEC samples were taken after the respective reaction time and quenched by addition of benzoic acid.

As a third catalyst system, a combination of thiourea and alkoxide was tested, as described in reports by the group of Waymouth.<sup>530</sup> For the described method, the deprotonated thiourea acted as bifunctional catalyst, activating both the nucleophile and the electrophile. Since the thiourea itself is expected to act as nucleophile, it was supposed that electron-withdrawing groups might not be necessary for successful activation, which would enable the use of **TU4–TU6** as cocatalysts. This would provide a benefit concerning sustainability, since their synthesis is more benign or straightforward than that of more electron-poor thioureas. Therefore, the literature-described reaction conditions<sup>530</sup> were applied for the ROP of  $\epsilon$ CL, using potassium methoxide as base and **TU4–TU6** as potential cocatalysts. The results are summarized in **Table 4**.<sup>†</sup>

The chosen reaction conditions did not lead to any successful polymerization of  $\epsilon$ CL. Possible reasons could be a high sensitivity to moisture, although Schlenk techniques were used, or an insufficient activation by the catalytic system.

<sup>†</sup> The experiment was performed by Hendrik Kirchhoff under co-supervision of the author.



**Table 4.** Test reactions of the ROP of  $\epsilon$ CL with a catalyst system of KOMe and **TU4–TU6** as cocatalysts. The samples were analyzed via oligo-SEC taking aliquots after the respective reaction time and quenching with benzoic acid. n. d. = not detected.

entry	cocatalyst	$M_n / \text{kg}\cdot\text{mol}^{-1}$	$\bar{D}$
1	TU4	n. d.	n. d.
2	TU5	n. d.	n. d.
3	TU6	n. d.	n. d.

Therefore, from the investigated approaches, the method using DBU and a thiourea cocatalyst (see **Table 2**) was determined to be the most promising. Within the next section, the transfer of the obtained results from the polymerization of  $\epsilon$ CL as a model compound to the use of terpene substrates is described.

### 4.2.3. Synthesis and ring-opening polymerization of terpene-based lactones

After having established suitable conditions for the organocatalytic ROP of  $\epsilon$ CL as a seven-membered lactone, the aim was to test these reaction conditions for the ROP of renewable substrates. Seven-membered lactones are accessible from terpene feedstock and have been used in several approaches for the synthesis of polyesters.<sup>380,547</sup>

Seven-membered lactones can be obtained via *Baeyer-Villiger* (BV) oxidation of six-membered cyclic ketones. Carvone derivatives are suitable precursors for such ROP monomers. The commercially available 1,2-dihydrocarvone **CK1** can either directly be a substrate for BV oxidation, or it can be reduced to tetrahydrocarvone **CK2** prior to oxidation.

The reduction of 1,2-dihydrocarvone **CK1** to tetrahydrocarvone **CK2** is shown in **Figure 37a**.<sup>†</sup> As reductant, hydrogen was used, with palladium on activated charcoal as heterogeneous catalyst.

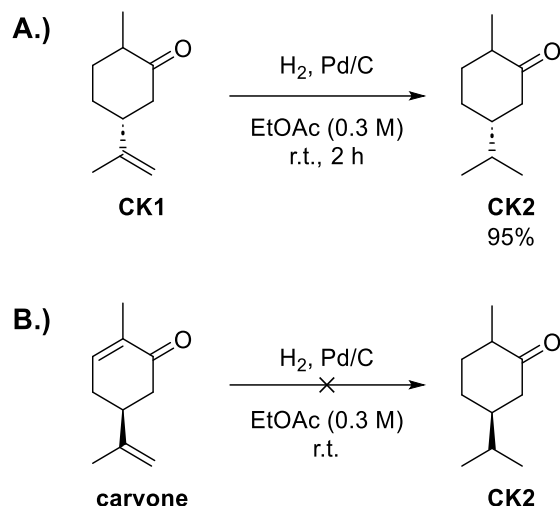


**Figure 37.** A.) Reduction of 1,2-dihydrocarvone **CK1** to tetrahydrocarvone **CK2**; B.) attempted hydrogenation of carvone to tetrahydrocarvone **CK2**.

The chosen reaction conditions yielded the desired tetrahydrocarvone in a high yield and purity. The reaction progress was followed via <sup>1</sup>H NMR spectroscopy, with the decrease of the double bond signals indicating the formation of the product (see **Supplementary Figure 24**).

As 1,2-dihydrocarvone **CK1** is already partially reduced, the same conditions were tested upon carvone as direct substrate. The reaction is shown in **Figure 37b**.<sup>†</sup> No product formation was observed after several hours of stirring. A possible reason for the low reactivity of the double bond towards hydrogenation could be due to a poor accessibility and the lower reactivity of the endocyclic double bond. It might be possible to reduce both double bonds under the same reaction conditions, but as 1,2-dihydrocarvone **CK1** is commercially available, this aim was not further investigated.

Apart from carvone, oxidation products from pinenes can also be potential precursors for terpene-based seven-membered lactones.<sup>409</sup> In a previous Bachelor thesis from our group,<sup>548</sup> the oxidation of  $\alpha$ -pinene via Schenck-Ene addition of oxygen and subsequent work-up with acetic anhydride to yield pinocarvone **CK3**

<sup>†</sup> The synthesis was performed by Johanna Rietschel under co-supervision of the author.

was described. The reaction was reproduced within this project and is shown in **Figure 38**.<sup>I</sup>

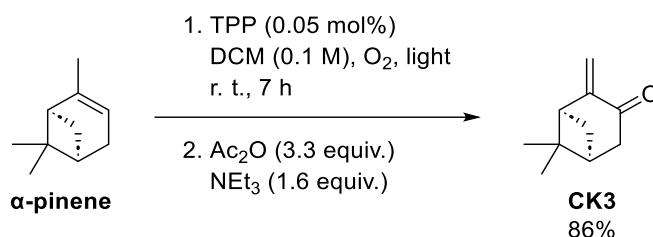


**Figure 38.** Schenck-Ene oxidation of  $\alpha$ -pinene yielding pinocarvone **CK3**.

Within this type of Schenck-Ene reaction, catalytic amounts of the triplet sensitizer *tetraphenyl porphyrine* (TPP) convert <sup>3</sup>O<sub>2</sub> into singlet oxygen <sup>1</sup>O<sub>2</sub>. The latter then undergoes a cycloaddition with the allyl group, which in this case is present in  $\alpha$ -pinene, to form an allyl hydroperoxide. Quenching with acetic anhydride under basic conditions leads to the decomposition of the hydroperoxide to yield an  $\alpha,\beta$ -unsaturated carbonyl moiety.

The product **CK3** was obtained in a yield of 86% after column chromatography. The procedure still contains drawbacks with regard to sustainability, such as the use of DCM as hazardous solvent, overstoichiometric amounts of quenching reagents, and work-up via column chromatography. Nevertheless, compared to other oxidation procedures of pinene towards cyclic ketones, which use several steps,<sup>409</sup> the reaction depicted in **Figure 38** represents an attractive approach due to its good yield, the possibility for a one-pot procedure, and the lacking use of metal catalysts.

To obtain a suitable precursor for lactone synthesis, the reduction of the double bond in **CK3** is necessary, analogously to carvone. The same hydrogenation conditions as shown in **Figure 37a** were applied to obtain the saturated pinene-derived ketone **CK3a** (see **Figure 39**).<sup>II</sup>

The reaction proceeded in a good yield, with the reduction of the double bond being well detectable via <sup>1</sup>H NMR.

<sup>I</sup> The synthesis was performed by Johanna Rietschel under co-supervision of the author.

<sup>II</sup> The synthesis was performed by Hendrik Kirchhoff under co-supervision of the author.

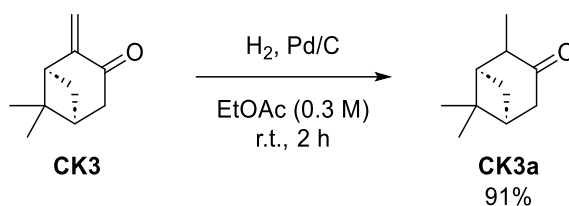


**Figure 39.** Reduction of pinocarvone **CK3** to the saturated cyclic ketone **CK3a**.

With the hydrogenation, a new stereocenter is formed. Since pinocarvone **CK3** is already chiral, the resulting product **CK3a** can consist of two different diastereomeric forms. To determine their ratio, the splitting pattern of the forming CH<sub>3</sub> group in <sup>1</sup>H NMR spectroscopy was analyzed. **Figure 40** shows a zoom of the <sup>1</sup>H NMR spectrum in the region of the CH<sub>3</sub> groups.

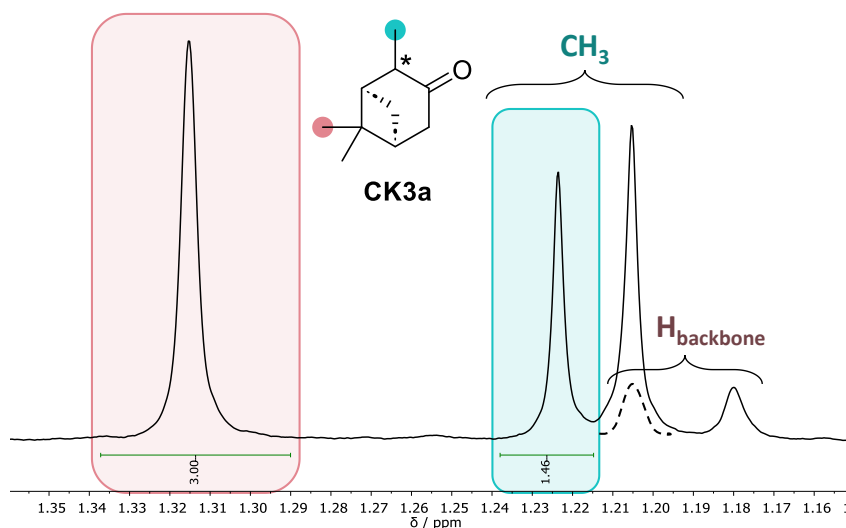


**Figure 40.** Comparison of integral values for CH<sub>3</sub> groups of **CK3a** via <sup>1</sup>H NMR. Since the doublet of the new CH<sub>3</sub> signal overlaps with a signal from the backbone protons, only one of the doublet signals was integrated. The integral value was compared to that of another CH<sub>3</sub> group in the molecule.

The signal that was assigned to the new CH<sub>3</sub> group (**Figure 40**, right) is split, but this was attributed to a *J* coupling with the vicinal CH moiety. The signal intensity of the doublet could not be determined precisely due to overlapping with backbone signals, which could be identified by comparison with the starting material **CK3** and by 2D NMR spectroscopy. Therefore, the left half of the signal from 1.24 to 1.21 ppm without overlap (see **Figure 40**, right box) was compared to the signal of

the second CH<sub>3</sub> group from 1.34 to 1.29 ppm (see **Figure 40**, left box). The integral value of half the signal is around 1.5, indicating that the two CH<sub>3</sub> signals in **Figure 40** approximately occur in a 1:1 ratio. Furthermore, no second new CH<sub>3</sub> signal was observed. These findings lead to the assumption that mainly one diastereomer is formed during the reduction due to steric hindrance. Within the analysis performed in this work, no presumption regarding the nature of the preferred diastereomer can be made, hence compound **CK3a** is depicted without information about the newly formed stereocenter.

**Figure 41** shows an overview of the terpene-based cyclic ketones used in this work that were available for further functionalization.

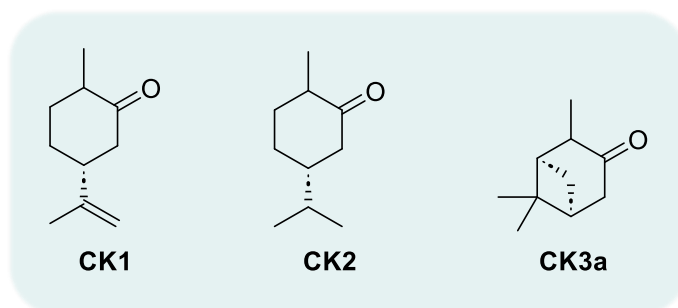


**Figure 41.** Terpene-derived cyclic ketones synthesized within this work.

Subsequently, the BV oxidation of the ketones **CK1–CK3a** towards seven-membered lactones was investigated. For this, different oxidizing agents have been introduced, with two predominantly used examples being *meta*-chloroperoxybenzoic acid (*m*CPBA)<sup>549</sup> and Oxone<sup>®</sup>,<sup>550</sup> the latter of which contains potassium peroxymonosulfate as reactive component. Of these two, Oxone<sup>®</sup> is less hazardous and therefore favorable concerning sustainability.<sup>551</sup> Thus, attempts within this section to obtain the desired seven-membered lactones were performed using Oxone<sup>®</sup> as oxidant.

Notably, when **CK1** was used as substrate, BV oxidation was described to oxidize the double bond towards the epoxide,<sup>410</sup> especially in combination with acetone as solvent.<sup>552</sup> The additional epoxide group can be beneficial for further functionalization. Thus, acetone was chosen as solvent due to its miscibility with water and its ability to promote the epoxidation of the exocyclic double bond in **CK1**. **Figure**

**42** shows the synthesis routes of the conversion of the cyclic ketones **CK1** and **CK2** to their respective BV oxidation products **Lac1** and **Lac2**.<sup>†</sup>

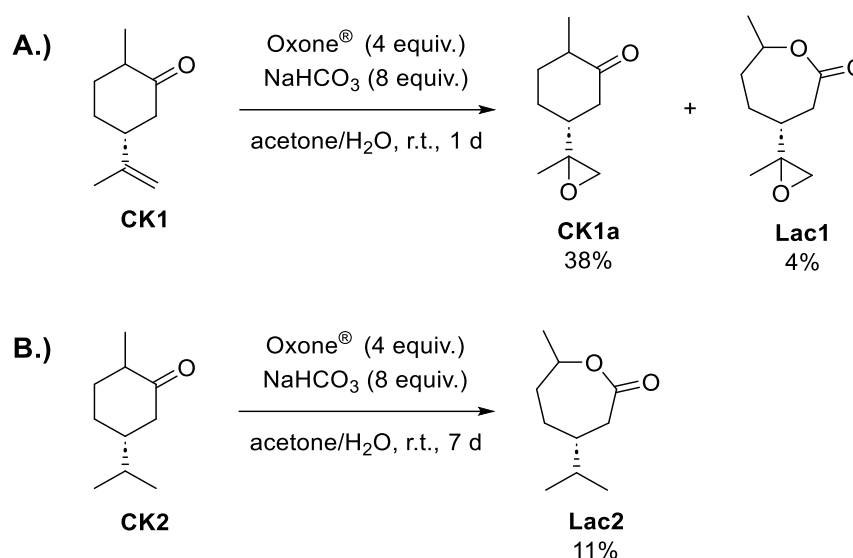


**Figure 42.** BV oxidation of the cyclic ketones **CK1** and **CK2** to obtain the lactones **Lac1** and **Lac2** and the isolated intermediate **CK1a**.

The BV oxidation of **CK1** and **CK2** was described in the literature,<sup>407,410,411</sup> so the reaction could be followed by NMR spectroscopy upon comparing with literature-described spectra. Although the formation of **Lac1** and **Lac2** was observed, low isolated yields were obtained, with 4% and 11% after purification via column chromatography, respectively.

In the case of **CK1**, the intermediate **CK1a**, in which only the double bond was oxidized, was isolated in 38% (see **Figure 42a**). This indicates that the oxidation of the double bond is significantly faster than the BV oxidation of the cyclic ketone. At the same time, other reports described the synthesis of the epoxide **CK1a** from **CK1** using very similar reaction conditions and without observing **Lac1** as side product in a high yield.<sup>552</sup> However, also in the case of **Lac2**, which does not contain a double bond, several days of stirring did not yield the product in a high yield (see **Figure 42b**). Thus, further attempts were directed towards achieving higher yields of the lactones.

Alongside acetone, ethanol and methanol were tested as alternative solvents, which have also been described in the literature for BV oxidation of terpene

<sup>†</sup> The synthesis was performed by Johanna Rietschel under co-supervision of the author.

substrates.<sup>407,411</sup> Regarding sustainability, all three solvents are recommended according to solvent selection guides, with ethanol being the most benign.<sup>39</sup> For this comparison, **Lac2** was chosen since in substrate **Lac1**, a parallel epoxidation complicates the analysis. GC-FID analysis led to partial decomposition of the lactone **Lac2**, therefore <sup>1</sup>H NMR spectroscopy was used for reaction control. Via <sup>1</sup>H NMR, the formation of a lactone moiety could be observed mainly by the appearance of signals assigned to the protons next to the new ester bond. **Figure 43** shows the reaction conditions of the reaction performed in ethanol as well as the <sup>1</sup>H NMR spectrum after stirring for 48 h.

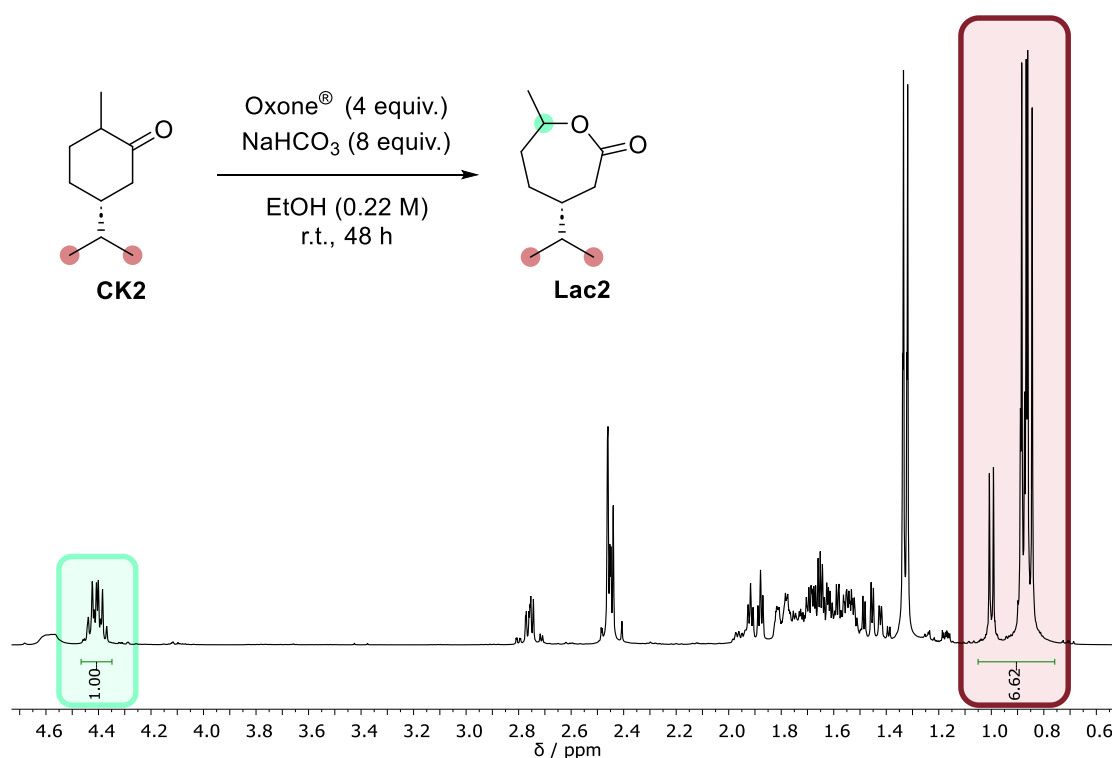


**Figure 43.** <sup>1</sup>H NMR reaction control in the BV oxidation of the cyclic ketone **CK2** to obtain the lactone **Lac2** in ethanol as solvent.

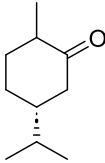
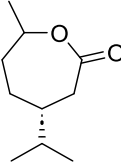
The signal position of the CH<sub>3</sub> protons from the isopropyl group do not differ significantly in the spectra of **CK2** and **Lac2**, therefore the ratio of these six protons and the CH proton next to the ester group could be used to quantify the formation of the lactone.

The oxygen insertion during the BV reaction can occur, in principal, on both sides of the carbonyl group, leading to possible regioisomeric products. However, in all cases, only the new signals corresponding to **Lac2** were observed. This could be

confirmed by 2D NMR spectroscopy. These findings correspond to the literature-described preferential oxygen insertion on the side of the higher substituted residue due to a higher migration velocity.<sup>553</sup>

For the reaction in ethanol after 48 h of stirring, the ratio of the two signals shown in **Figure 43** is only slightly lower than the theoretical one of 1:6, indicating an efficient lactone formation. The ratio of the two signals highlighted in **Figure 43** were calculated for all three tested solvents after a reaction time of 48 h. From the deviation to the theoretical value of 1:6, the conversion of **CK2** to **Lac2** was calculated. The results are summarized in **Table 5**.

**Table 5.** Variation of reaction conditions for the BV oxidation of **CK1**. The conversion was calculated via <sup>1</sup>H NMR spectroscopy comparing the ratio of signal from 4.46–4.35 ppm and the signal from 1.05–0.76 ppm with their theoretical ratio of 1:6 in **Lac2**.

 <b>CK2</b>	Oxone® (4 equiv.) NaHCO <sub>3</sub> (8 equiv.) solvent (0.22 M) r.t., 48 h	 <b>Lac2</b>
entry	solvent	conversion
1	acetone	48%
2	methanol	96%
3	ethanol	91%

The results from **Table 5** show that methanol and ethanol as solvents promote the formation of **Lac2** more efficiently than acetone. However, also in the case of acetone as solvent, significantly higher conversion was observed via NMR spectroscopy than the isolated yield (see **Figure 42b**).

A reason for the low obtained yields could potentially be found in the purification method and an instability of the products towards purification via column chromatography. In literature, multiple vacuum distillations were described as alternative.<sup>407</sup> However, for this method high energy consumption is required, and larger batch sizes are beneficial to obtain satisfying yields, making it not as attractive for the small-scale approaches within this work. Therefore, since the main focus of this work was the use of these literature-known lactones as monomers in ROP towards



polyesters, the product amounts obtained according to **Figure 42**, although low in yield, were taken as they were for further approaches.

Next to the substrates **CK1** and **CK2**, the cyclic ketone **CK3a** was tested for a potential BV oxidation towards the lactone **Lac3** (see **Figure 44**).<sup>1</sup> Since this reaction was not previously described in literature, *m*CPBA was used as oxidant as it showed good performance in the BV oxidation of terpene substrates.<sup>402,404,409</sup>

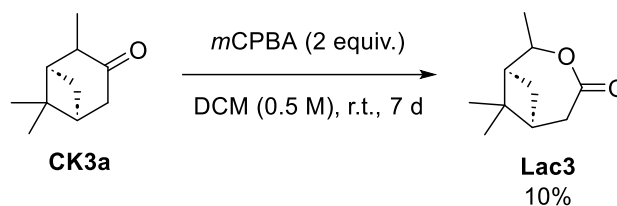


**Figure 44.** BV oxidation of the cyclic ketone **CK3a** to obtain the lactone **Lac3**.

The formation of a lactone moiety could be detected via <sup>1</sup>H NMR spectroscopy. After no further reaction progress was observed, the product **Lac3** was isolated by extraction and subsequent column chromatography in a yield of 10%. A possible explanation for the low obtained yield could be a decreased stability due to the additional four-membered ring, therefore complicating the work-up. Optimization of the reaction conditions and work-up procedure could possibly lead to higher yields of **Lac3**. Further adjustment with regard to sustainability could open a pathway for a new route towards polyester structures from  $\alpha$ -pinene as addition to previously described pinene-based lactones.<sup>554,555</sup>

Despite the low obtained yields, within this section, it was possible to synthesize model lactone compounds from terpene feedstock. The isolated amounts of **Lac1** and **Lac2** were sufficient to be used to test a possible ROP towards polyesters. The reaction conditions were chosen according to **Table 2** using DBU in combination with **TU1** or **TU3** as catalyst system and pyrene butanol as initiator. The results of the test reactions are shown in **Table 6**.<sup>11</sup>

Variation of the reaction conditions within the scope of **Table 6** did not lead to a successful formation of polymers. As solvents, THF and toluene were tested (**Table 6**, entries 1 and 2), but in both cases, no polymeric species were observed via SEC

<sup>1</sup> The synthesis was performed by Hendrik Kirchhoff under co-supervision of the author.

<sup>11</sup> The experiments were performed by Johanna Rietschel under co-supervision of the author.

measurements. Neither **Lac1** nor **Lac2** as monomers and neither **TU1** nor **TU3** (**Table 6**, entries 2-5) could promote the reaction under the chosen conditions, in contrast to the above discussed results for  $\epsilon$ CL. Further, changing the temperature to 50 °C (**Table 6**, entry 6) did also not enable polymerization.

**Table 6.** Test reactions of the ROP of **Lac1** and **Lac2** with a catalyst system of DBU and **TU1** or **TU3** as cocatalysts. For investigation of a potential polymer formation, SEC measurements were performed. r. t. = room temperature; n. d. = not detected.

**TU1**

**TU3**

Entry	substrate	solvent	thiourea	T	polymer formation
1	<b>Lac1</b>	THF	<b>TU1</b>	r. t.	n. d.
2	<b>Lac1</b>	toluene	<b>TU1</b>	r. t.	n. d.
3	<b>Lac1</b>	toluene	<b>TU3</b>	r. t.	n. d.
4	<b>Lac2</b>	toluene	<b>TU1</b>	r. t.	n. d.
5	<b>Lac2</b>	toluene	<b>TU3</b>	r. t.	n. d.
6	<b>Lac2</b>	toluene	<b>TU1</b>	50 °C	n. d.

To conclude, within the scope of this work, no reaction conditions could be found that led to a successful polymerization of **Lac1** or **Lac2** using a catalyst system of DBU and thiourea. Notably, the limited conditions tested within **Table 6** cannot rule out that a polymerization of terpene-based lactones using this catalyst system could be performed. However, the activation might not be strong enough to enable polymerization, since lactones **Lac1** and **Lac2** are deactivated in comparison to

$\epsilon$ CL due to additional substituents, thus potentially making the use of more active metal catalysts necessary.<sup>407,411</sup>

Summing up, the results obtained in this work confirm the promising use of thioureas for the more controlled ROP of substrates such as  $\epsilon$ CL, but no successful activation of terpene-based lactones was observed. The following sections therefore focus on the use of thiourea catalysts for the synthesis of NIPUs as another class of promising polymers.

### 4.3. Thiourea catalysts in transurethanization reactions

Transurethanization is one of the main strategies to access NIPUs (see **Figure 4**)<sup>82–84</sup> and can be catalyzed by the addition of Lewis acids.<sup>556</sup> Since thioureas were shown to activate carbonyl centers in a similar way as Lewis acids (see **Figure 27**), the potential use of thiourea compounds as catalyst for transurethanization approaches was investigated.

In order to activate the carbonyl center efficiently for nucleophilic attack, electron-withdrawing groups are beneficial.<sup>557</sup> Therefore, in this chapter, **TU1–TU3** were tested for a possible activating effect, as well as the commercially available Schreiner's catalyst **TU7** (**Figure UR1**).

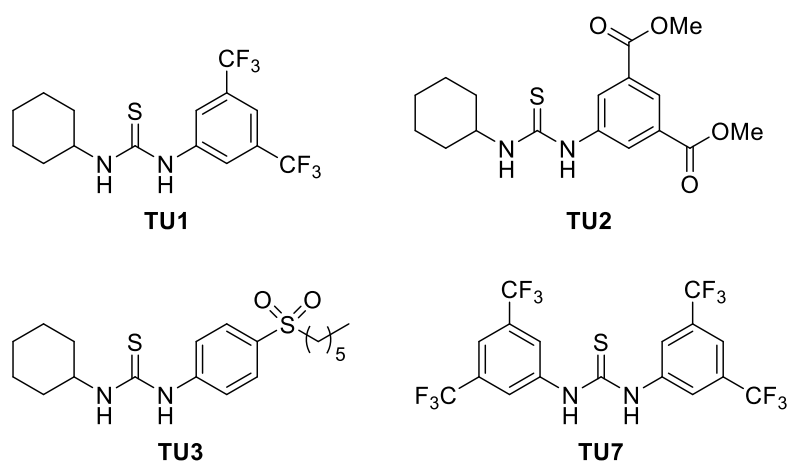


**Figure 45.** Thiourea catalysts with electron-withdrawing substituents tested for the use in transurethanization reactions.

Before testing the catalysts for polymerization of monomers, a model system was developed to investigate if any catalytic effect could be observed. For this, the model substrate **UR1** was synthesized, with methanol as a leaving group, for the reaction with *n*-butanol to yield the model product **UR2** (see **Table 7**). The presence of the two model compounds could be easily followed using GC-FID.

At first, a test reaction was carried out using TBD as organocatalyst, which was used in transurethanization reactions previously. The use of TBD for the formation of **UR2** from **UR1** with *n*-butanol at a temperature of 90 °C led to the formation of 6% product **UR2** compared to **UR1**, determined via GC-FID. Although the conversion was poor, these conditions were used as a starting point to see whether thiourea catalysts showed similar performance to the established catalyst TBD.<sup>103,486</sup>

Thus, the formation of **UR2** from **UR1** with *n*-butanol in the presence of thiourea catalysts was tested in bulk and using different solvents (**Table 7**). The choice of solvents was made based on available green solvent selection guides,<sup>36,39</sup> excluding alcohols and esters that could react with the substrates. Thiourea **TU2** was used for the first test as it showed good solubility in various solvents. In all cases, the mixture was heated to a temperature close to the boiling point of the solvent. In cases where no solvent or high-boiling solvents were used, 90 °C were chosen because the thiourea compounds can decompose above this temperature.<sup>558</sup>

**Table 7.** Test reactions of transurethanization using different solvents. Samples were taken after 3-4 h and analyzed via TLC and GC-FID. The % product were estimated by dividing GC-FID integral of **UR2** by the sum of the integrals of **UR1** and **UR2**. \*TBD was used instead of **TU2**.

CCCCCNC(=O)C  $\xrightarrow[\text{solvent, 3-4 h}]{\text{n-BuOH (1 equiv.)  
TU2 (5 mol%)}}$  CCCCCNC(=O)OCCCC

**UR1**  **UR2**

entry	solvent	molarity	T / °C	% product
<b>1</b>	bulk*	-	90	6
<b>2</b>	bulk	-	90	n. d.
<b>3</b>	cyclohexanone	0.5	90	n. d.
<b>4</b>	butanone	0.5	70	n. d.
<b>5</b>	anisole	0.5	90	n. d.
<b>6</b>	cyclohexane	1.0	80	traces
<b>7</b>	chloroform	1.0	60	traces

The results of **Table 7** show that no efficient product formation was observed under the chosen conditions. Only when using cyclohexane and chloroform, traces of the product were observed. Both solvents are not recommended with regards to sustainability,<sup>39</sup> however, they were chosen for further experiments. **Table 8** shows a selection of varied reaction conditions in chloroform, using higher equivalents of *n*-butanol, alternative thiourea catalysts **TU1**, **TU3** and **TU7** (entries 1–4, **Table 8**), higher catalyst loading of thiourea (entry 5, **Table 8**), and alternative nucleophiles containing amine or thiol groups (entries 6–7, **Table 8**). In none of the cases, the formation of **UR2** or another respective product compound could be observed. For

all batches, further samples were taken after longer reaction times, also showing no product.

**Table 8.** Test reactions of transurethanization using different thiourea catalysts and different nucleophiles.

UR1  $\xrightarrow[\text{CHCl}_3 (1.0 \text{ M}), 60 \text{ }^\circ\text{C}, 3-4 \text{ h}]{n\text{-BuXH (3 equiv.) TU2}}$  UR2

entry	thiourea	mol%	XH	% product
1	TU1	5	OH	n. d.
2	TU2	5	OH	n. d.
3	TU3	5	OH	n. d.
4	TU7	5	OH	n. d.
5	TU2	10	OH	n. d.
6	TU2	10	NH <sub>2</sub>	n. d.
7	TU2	10	SH	n. d.

The unsuccessful activation can be explained by the low reactivity of the urethane moiety. Usually, transurethanization approaches use very high temperatures to enable product formation.<sup>103,486,487</sup> At the same time, at high temperatures the hydrogen bonds between the thiourea and the carbonyl group are less effectively formed because of a higher entropic contribution, and moreover, the thiourea can decompose. Therefore, no higher temperatures were tested.

Further, high vacuum is usually applied during transurethanization to evaporate the small compounds formed during the condensation. Like this, the equilibrium can be shifted towards the product. This strategy could possibly enable a higher conversion also in the investigated conditions, however, as no product formation was observed at all, it can be supposed that the substrates are not activated sufficiently for any reaction to take place. Overall, the results suggest that the use of TBD as organocatalyst in transurethanization approaches is more promising.

To sum up, within the performed experiments, no activation of urethane groups by thiourea compounds for a transurethanization could be observed at 90 °C or below. Additionally, a study published in the meantime by Bakkali-Hassani, Caillol et al. confirmed the herein observed lack of thiourea activation in transurethanization

reactions, stating that activation by Lewis-acidic compounds was significantly stronger.<sup>290</sup> Therefore, further investigation for the use of thiourea compounds in NIPU synthesis focused on the ring-opening of cyclic carbonates with amines, which will be treated in the coming sections.

## 4.4. Linear non-isocyanate polyurethanes from terpenes via thiourea organocatalysis and thiol-ene-chemistry

Parts of this chapter and the associated experimental section are based on previously published results by the author of this thesis:

F. C. M. Scheelje and M. A. R. Meier, Non-isocyanate polyurethanes synthesized from terpenes using thiourea organocatalysis and thiol-ene-chemistry, *Commun. Chem.*, 2023, **6**, 239.<sup>559</sup>

Text, figures, and data are reproduced from this article and were partially edited and extended.

### **Abstract**

The depletion of fossil resources as well as environmental concerns contribute to an increasing focus on finding more sustainable approaches for the synthesis of polymeric materials. In this work, a synthesis route towards non-isocyanate polyurethanes (NIPUs) using renewable starting materials is presented. Based on terpenes as renewable resources, five-membered cyclic carbonates are synthesized and ring-opened with allylamine, using thiourea compounds as benign and efficient organocatalysts. Thus, five renewable AA monomers are obtained, bearing one or two urethane units. Taking advantage of the terminal double bonds of these AA monomers, step-growth thiol-ene polymerization is performed using different dithiols, to yield NIPUs with molecular weights of above 10 kDa under mild conditions. Variation of the dithiol and amine leads to polymers with different properties, exhibiting  $M_n$  of up to 31 kg·mol<sup>-1</sup> and  $T_g$ 's ranging from 1 to 29 °C.

### **Results**

#### **4.4.1. Synthesis of terpene-based cyclic carbonates**

For the synthesis of hydroxyurethane monomers from terpenes, cyclic carbonates of different terpene derivatives were synthesized. As referred to in section 2.5.3, the double bond moieties within terpene feedstock can be modified by epoxidation, generating precursors for cyclic carbonate synthesis. Thus, this chapter describes



the synthesis of cyclic carbonates from the terpene compounds limonene, carvone, and  $\gamma$ -terpinene.

The epoxides **E1** and **E2** (see **Figure 46**) derived from limonene were synthesized on the basis of previous studies.<sup>429,552</sup> With limonene containing two double bonds, it is possible to oxidize either both double bonds using common epoxidizing agents<sup>552</sup> or to oxidize the higher substituted double bond selectively by reaction with *N*-bromo succinimide (NBS) and sodium hydroxide.<sup>429</sup>

Based on this, the cyclic carbonates **CC1** and **CC2** were synthesized from the respective epoxides **E1** and **E2** by insertion of CO<sub>2</sub> using *tetrabutylammonium chloride* (TBACl) as catalyst (see **Figure 46**).<sup>138</sup> Despite recent findings showing high yields for the formation of cyclic carbonates when using aluminum catalysts,<sup>138</sup> the use of catalytic substances was constrained to the halogenide to maintain a simpler approach. Indeed, no additional catalyst was necessary for a sufficient conversion of the epoxides.

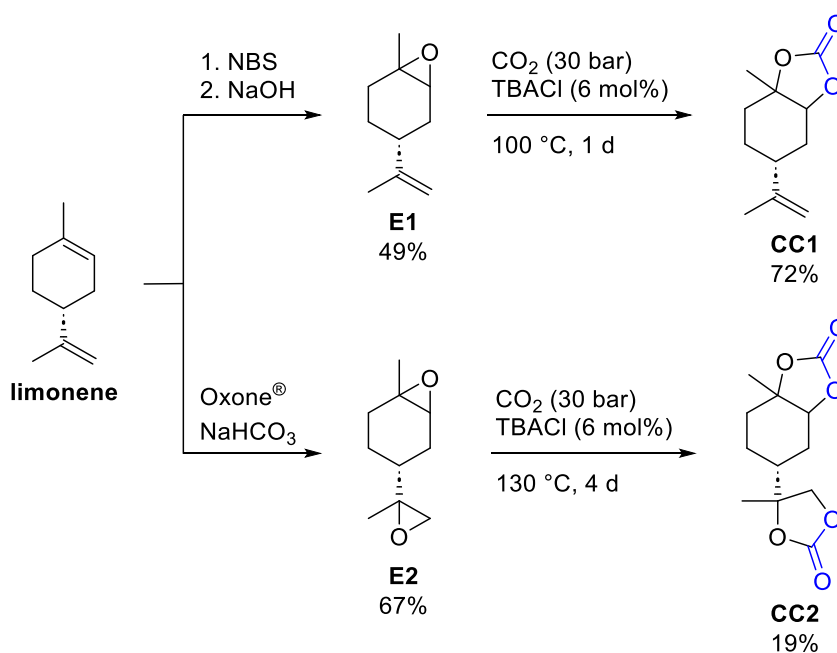


**Figure 46.** Synthesis of cyclic carbonates from limonene.

It must be noted that the reactivity of the endocyclic and exocyclic terpene epoxides varies depending on the substitution pattern. In limonene dioxide **E2**, this could be observed in the formation of a monocarbonate intermediate **CC2a**, in which the epoxide attached to the ring was not yet converted into the carbonate (see **Table 9**). By isolating the intermediate **CC2a**, the ratio of **CC2** to **CC2a** could be

determined and compared with respect to different reaction conditions. As catalysts for the carbonate formation, tetrabutylammonium chloride (**Table 9**, entries 1 and 4), bromide (entry 2) and iodide (entry 3) were used and the ratio of **CC2** to the starting material **E2** and the intermediate product **CC2a** was compared using GC-FID measurements.

**Table 9.** Variation of catalyst, reaction temperature and reaction time in the formation of carbonate **CC2**. GC-FID fractions of **E2**, **CC2a**, and **CC2** are obtained by dividing the GC integral of the respective signal by the sum of the integrals of **E2**, **CC2a**, and **CC2**.

The reaction scheme shows the conversion of **E2** (limonene dioxide) to **CC2** and **CC2a** (carbonate products) using  $\text{CO}_2$  (30 bar) and TBAX (6 mol%) as a catalyst at 100-130 °C. The structures of **E2**, **CC2**, and **CC2a** are shown with their respective stereochemistry.

entry	catalyst	T / °C	t	E2:CC2a:CC2
1	TBACl	100 °C	20 h	1:50:49
2	TBAB	100 °C	20 h	12:57:31
3	TBAI	100 °C	20 h	10:78:12
4	TBACl	130 °C	4 d	0:3:97

It was shown that, in order to obtain full conversion of the limonene dioxide **E2**, stirring at 130 °C for four days with TBACl as catalyst was necessary (**Table 9**, entry 4). This low reactivity of the internal epoxide was not observed in the case of **E1**, for which a conversion of 82% to the carbonate **CC1** was already observed after one day via GC-FID. This difference could be explained by a lower reactivity of **E2** as well as by an increase in viscosity after the carbonation of one epoxide group in **CC2a**, thus making longer stirring and higher temperature necessary for further carbonation towards the final product **CC2**.

When using NBS and sodium hydroxide for the oxidation of only the endocyclic double bond in limonene (see **Figure 46**), one diastereomer of **E1** was formed selectively, fitting to previous findings that the *trans* isomer was mainly observed.<sup>429</sup> The diastereomeric ratio was determined to be 93:7 by GC-FID and <sup>1</sup>H NMR

spectroscopy (see **Supplementary Figure 38** and **Supplementary Figure 39**). During the carbonate formation, the stereocenter was retained, thus also in compound **CC1** one main diastereomer was observed (see **Supplementary Figure 49** and **Supplementary Figure 50**). For the formation of **CC2**, a commercially available diastereomeric mixture of limonene dioxide **E2** was used, and in compound **CC2**, two isomers were observed by  $^1\text{H}$  NMR spectroscopy in a ratio of 51:49 (see **Supplementary Figure 54**). This can further explain the lower isolated yield of **CC2** in comparison to the conversion of the starting material, since the product had to be recrystallized in order to achieve high purity.

Also from carvone, two different epoxides can be synthesized based on previously described procedures.<sup>552</sup> The two double bonds show different reactivity, and it is possible to address them selectively by using either Oxone<sup>®</sup> or hydrogen peroxide as oxidants to obtain the epoxides **E3** or **E4**, respectively. Thus, both epoxide derivatives **E3** and **E4** (see **Figure 47**) were synthesized to enable a comparison.

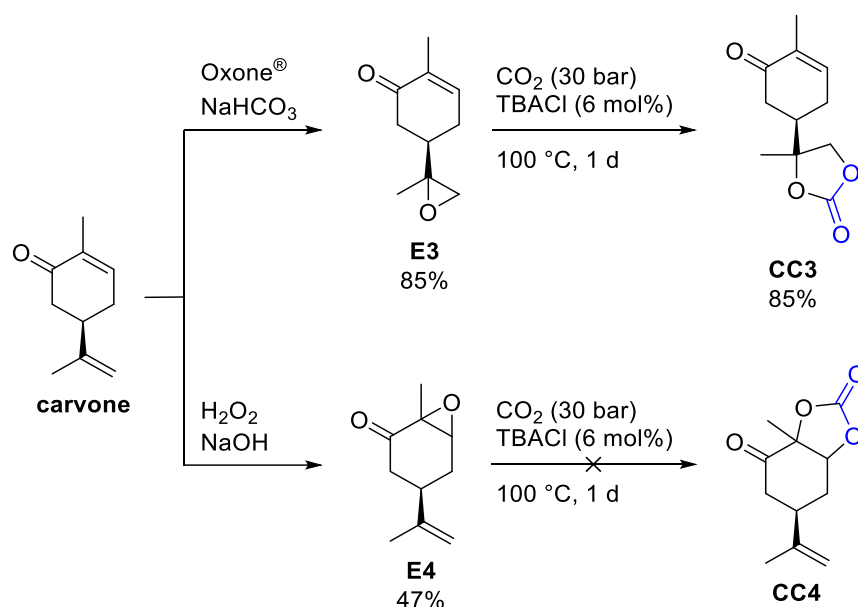


**Figure 47.** Synthesis of cyclic carbonates from carvone.

The oxidation of carvone with Oxone<sup>®</sup> led to the formation of the epoxide **E3**. Two diastereomers were formed in nearly equimolar ratio (see **Supplementary Figure 42** and **Supplementary Figure 43**), which was also preserved in the carbonate formation (see **Supplementary Figure 57** and **Supplementary Figure 58**).

Both the exocyclic epoxide **E3** and the resulting cyclic carbonate **CC3** were synthesized successfully. While also **E4** was successfully synthesized from carvone, the cyclic carbonate **CC4** could not be isolated. Indeed, also previous studies reported a decomposition of the endocyclic carbonate **CC4** upon work-up.<sup>138</sup>

Besides limonene and carvone, also  $\gamma$ -terpinene, which contains two endocyclic double bonds, was tested as substrate for the synthesis of a cyclic carbonate (see **Figure 48**). The synthesis of  $\gamma$ -terpinene-derived epoxide **E5** was described before.<sup>552</sup> To synthesize a cyclic carbonate **CC5** from **E5**, the optimum reaction conditions from **Table 9** were applied for **E5** as substrate.

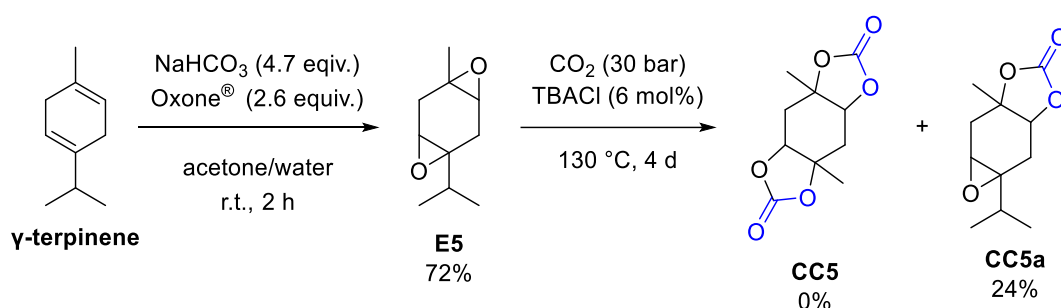


**Figure 48.** Synthesis of cyclic carbonate from  $\gamma$ -terpinene.

Purification of the reaction mixture yielded only monocarbonate **CC5a** as product. The reason for an unsuccessful carbonation of the second epoxide group could be a higher steric hindrance and therefore lower reactivity. Since bifunctional monomers are needed for the synthesis of monomers for NIPUs, this route was not investigated further. Instead, the cyclic carbonates **CC1-CC3** were investigated in ring-opening reactions with allylamine.

#### 4.4.2. Ring-opening of cyclic carbonates

For the application of the cyclic carbonates **CC1-CC3** in the synthesis of NIPUs, they were ring-opened with amines containing double bonds. Like this, AA monomers containing urethane groups and terminal double bonds were generated. For this ring-opening reaction, thioureas were tested as potential organocatalysts. The ring-opening reactions of the endocyclic and exocyclic carbonates were investigated separately to get insight into potential catalysis.

To test if thiourea catalysts can effectively promote the ring-opening of cyclic carbonates **CC1–CC3** with an amine, four different thiourea catalysts **TU1–TU4** were compared with respect to their capability to activate the cyclic carbonate (see **Figure 49**). All of these catalysts are accessible via a multicomponent approach from the respective aromatic isocyanide, elemental sulfur, and cyclohexyl amine (see section 4.1). This is significantly more sustainable than classic synthesis approaches. Depending on the substituents on the aromatic ring, the thiourea derivatives vary in their hydrogen bonding ability, with catalysts **TU1** and **TU3** showing the strongest affinity towards carbonyl groups due to the presence of strong electron-withdrawing groups.<sup>521</sup>

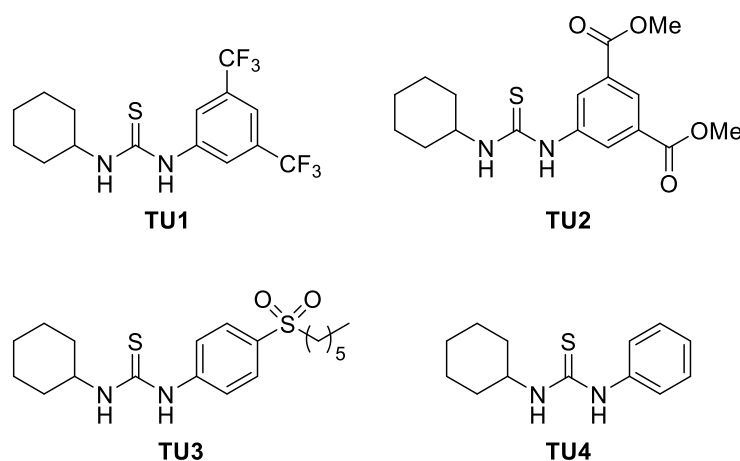


**Figure 49.** Thiourea catalysts tested for the ring-opening of terpene-based cyclic carbonate **CC1**.

The urethane moieties and double bonds that result from ring opening the cyclic carbonates with allylamine make the obtained products suitable building blocks for potential NIPU synthesis.

### Opening of endocyclic carbonate group

For the investigation of a possible catalytic effect upon opening the synthesized carbonates with amines, limonene monocarbonate **CC1** was chosen as model compound to analyze the opening of the endocyclic carbonate attached to the terpene ring structure separately. As nucleophile, allylamine was used. Investigation started using thiourea **TU1**, as it is easily accessible from the commercially available isothiocyanate and was shown to be a promising compound for the activation of carbonyl compounds.<sup>516</sup>

Since in the synthesis of the carbonate **CC1** a high conversion was achieved, the crude reaction mixture could directly be used for the urethane synthesis after washing with brine, without the need for a purification via column chromatography. Further, no solvent was necessary for both the carbonate and the urethane formation, thus contributing to the overall sustainability of the synthesis. The ratio of the urethane monomer **UR3** to the carbonate **CC1** was determined via GC-FID over time, as no other signals were observed, and is shown in **Figure 50** (for exact values, see **Supplementary Table 1**).

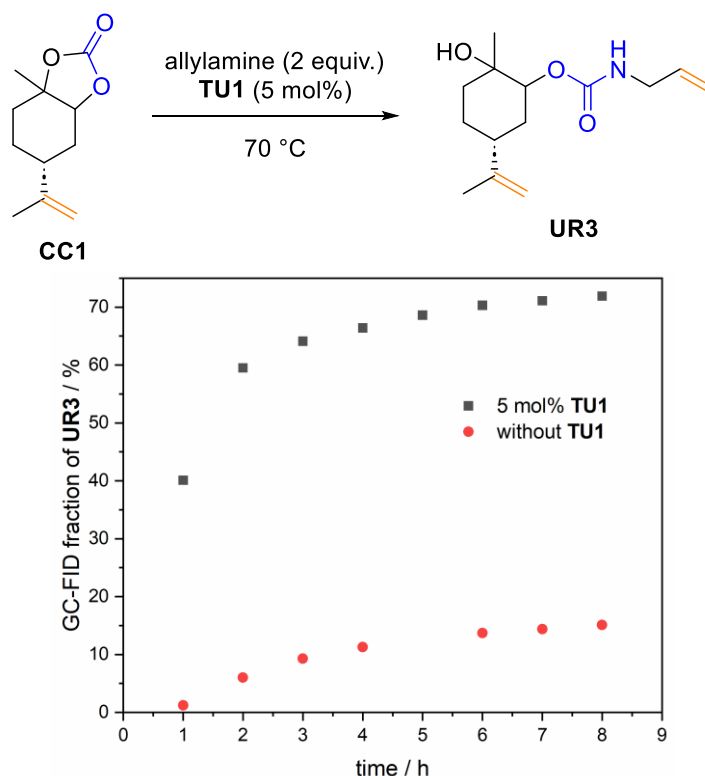


**Figure 50.** Conversion of limonene-derived carbonate **CC1** to urethane monomer **UR3**. The GC-FID fraction of **UR3** is obtained by dividing the GC integral of the signal associated with **UR3** by the sum of the integrals of the signals assigned to **CC1** and **UR3**. Only one of two formed regioisomers of **UR3** is shown for clarity, with the ratio of **UR3:CC1** including both regioisomers.

It can be stated that the reaction is significantly more effective in the presence of thiourea **TU1**, indicating a catalytic effect of the thiourea that positively influences the reaction efficiency. During purification of the urethane monomer **UR3**, the thiourea **TU1** could be recovered, corresponding to 100% of the starting amount, thus further contributing to the sustainability of the presented approach. The

presence of a high percentage of intact thiourea in the final reaction mixture indicates that the thiourea compound is indeed acting as a catalyst.

Since the ring-opening of the endocyclic carbonate **CC1** proceeded successfully, this approach was tested for the synthesis of a urethane monomer from the endocyclic epoxide **E4**. Given that the cyclic carbonate **CC4** could not be isolated, the direct use of the reaction mixture from the carbonation of **E4** for aminolysis to obtain the urethane monomer **UR4** was investigated (see **Figure 51**).

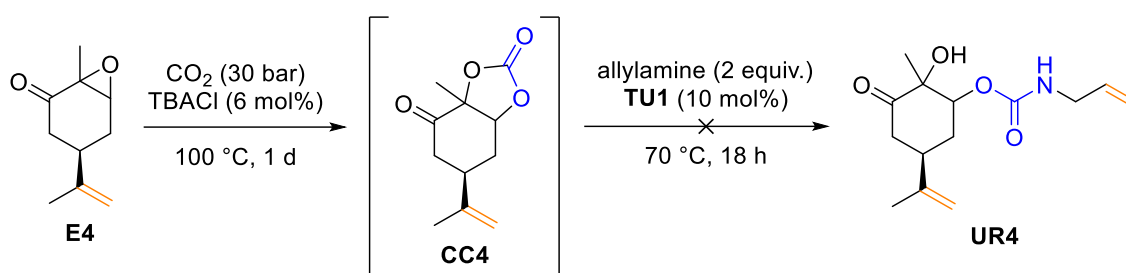


**Figure 51.** Direct use of reaction mixture from the carbonation of **E4** for ring-opening with allylamine for potential isolation of **UR4**.

This way, no exposure of **CC4** to column material is necessary, with urethane **UR4** possibly ensuring higher stability. However, isolation of **UR4** from the reaction mixture was not possible. Therefore, no further investigations on **E4** as starting material were performed. On the other hand, the synthesis of urethane monomer **UR3** derived from **CC1** represents a promising approach towards NIPUs. Therefore, the reaction conditions for the aminolysis of **CC1** were optimized before applying them to the opening of the cyclic carbonates **CC2** and **CC3**.

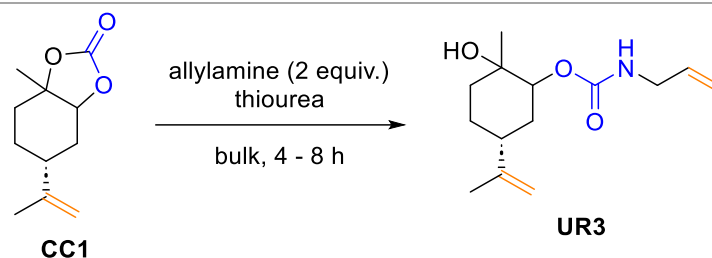
### Optimization of reaction conditions

To optimize the reaction conditions, equivalents and temperature were varied (see **Table 10**, entries 1–5). Further, alternative thiourea compounds **TU2–TU4** were tested next to compound **TU1**, displaying a range of stronger and weaker electron-withdrawing groups (entries 6–8, **Table 10**).

As can be seen from entry 2 in **Table 10**, it is possible to reduce the amount of catalyst used, but higher yields were obtained for 5 mol%. Thus, further experiments were carried out using this catalyst loading. Reduction to only one equivalent of allylamine led to a lower conversion (entry 3, **Table 10**), probably due to the volatility of the amine. Further, the initial choice of  $70\text{ }^\circ\text{C}$  (entry 1, **Table 10**) proved

to be the most suited for the investigated reaction if compared to temperatures of 60 and 80 °C (see entries 4 and 5, **Table 10**).

**Table 10.** Variation of thiourea concentration, reaction temperature and choice of thiourea catalysts in the carbonate ring-opening of **CC1**. The GC-FID fraction of **UR3** is obtained by dividing the GC integral of the signal associated with **UR3** by the sum of the integrals of the signals assigned to **CC1** and **UR3**. Only one of two formed regioisomers of **UR3** is shown for clarity, with the ratio of **UR3:CC1** including both regioisomers.



entry	thiourea	mol%	equiv.	T / °C	UR3:CC1	UR3:CC1
		thiourea	amine		(4 h)	(8 h)
1	TU1	5.0	2.0	70	61:39	76:24
2	TU1	2.5	2.0	70	45:55	57:43
3	TU1	5.0	1.0	70	27:73	37:63
4	TU1	5.0	2.0	60	55:45	68:32
5	TU1	5.0	2.0	80	58:42	66:34
6	TU2	5.0	2.0	70	49:51	64:36
7	TU3	5.0	2.0	70	40:60	55:45
8	TU4	5.0	2.0	70	28:72	42:58

The use of alternative catalysts **TU2–TU4** also led to the formation of product, with electron withdrawing ester (entry 6, **Table 10**) and sulfone groups (entry 7, **Table 10**) resulting in higher conversions than in the case of a simple phenyl substituent (entry 8, **Table 10**). However, catalyst **TU1** bearing two CF<sub>3</sub> groups still showed the highest activity. This confirmed the choice of catalyst **TU1** for further experiments, yet catalysts **TU2** and **TU3** remain valid options that can be obtained more sustainably.

The investigations proved the initial reaction conditions from entry 1 (**Table 10**) to be the most suited for the opening of the endocyclic carbonate group. As this functionality is assumed to be the less reactive one, the same conditions were



chosen for a closer look into the opening of the exocyclic carbonate groups in the terpene derivatives **CC2** and **CC3**.

### Opening of exocyclic carbonate groups

To analyze the influence of the thiourea catalyst on the conversion of the exocyclic carbonate group found in compounds **CC2** and **CC3**, the carbonate **CC3** based on carvone was chosen as model substrate as it does not contain an additional endocyclic carbonate group.

For the opening of the carbonate, the optimized conditions of the opening of **CC1** (see **Table 10**, entry 1) were used. The conversion was detected via GC-FID as in the case before and the comparison of the reactions with and without the presence of thiourea **TU1** is shown in **Table 11**.

**Table 11.** Carbonate ring-opening of **CC3** with and without thiourea catalyst. The GC-FID fraction of **UR5** is obtained by dividing the GC integral of the signal associated with **UR5** by the sum of the integrals of the signals assigned to **CC3** and **UR5**. Only one of two formed regioisomers of **UR5** is shown for clarity, with the ratio of **UR5:CC3** including both regioisomers

Reaction scheme: **CC3** + allylamine (2 equiv.) + thiourea → **UR5** (bulk, 4 - 8 h)

entry	mol% TU1	UR5:CC3 (4 h)	UR5:CC3 (8 h)
1	5.0	83:17	90:10
2	0	78:22	96:4

In general, a higher conversion to the respective urethane **UR5** is observed, as expected, than in the case of the endocyclic carbonate (see **Table 10**), which can be attributed to a lower steric hindrance. Already without the addition of thiourea, high conversions are obtained (entry 2, **Table 11**). Addition of thiourea does not significantly influence the conversion (see entry 1, **Table 11**), thus no activation is necessary to obtain the urethane monomer **UR5** from carbonate **CC3**.

Compound **CC2** bears two carbonate groups, which show different reactivities as demonstrated before. Therefore, thiourea catalyst **TU1** was used for the activation of especially the endocyclic carbonate. The general reaction conditions for the opening of **CC2** towards diurethane **UR6** were chosen as in **Table 10** (entry 1), using double the amount of allylamine and thiourea **TU1** (see **Figure 52**).

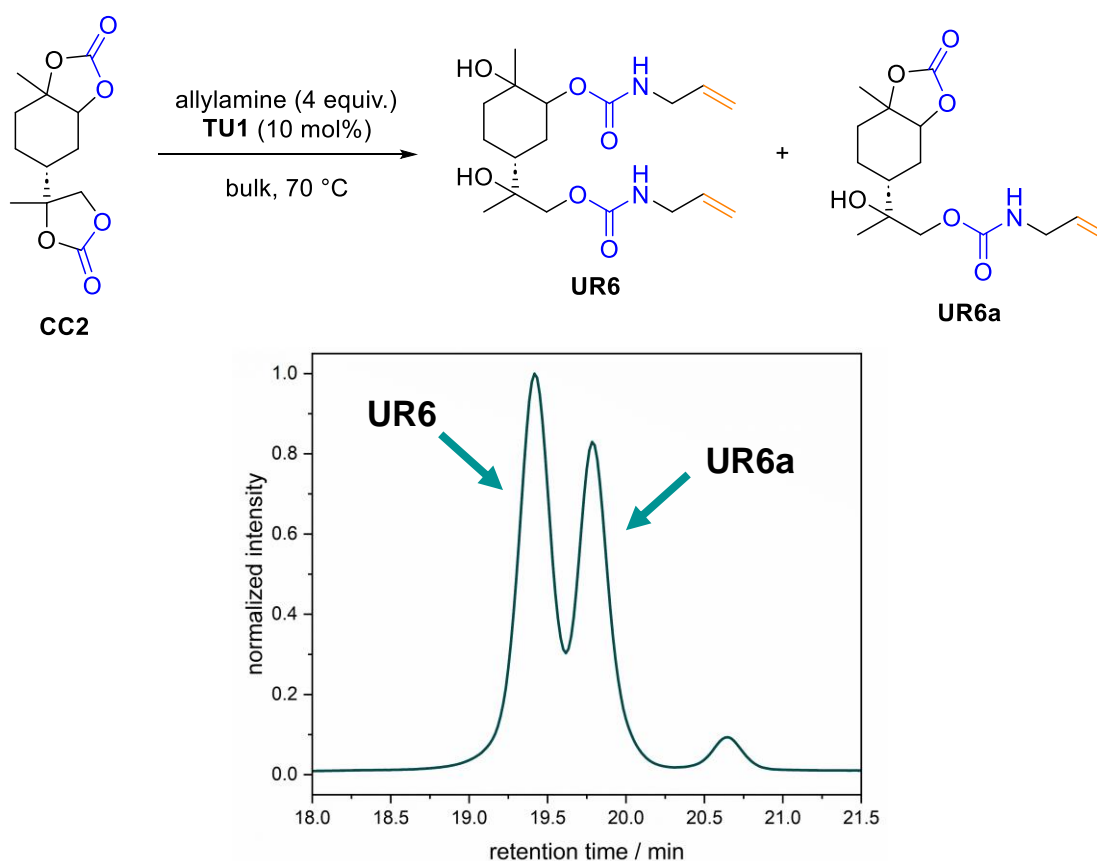


**Figure 52.** Ring-opening of limonene carbonate **CC2** to bifunctional urethane **UR6** and monofunctional urethane **UR6a**, analyzed via SEC. The SEC chromatogram was measured after 2 h reaction time, still showing presence of the intermediate **UR6a**. The signal at 20.7 min is a system peak and does not correspond to any compound found in the mixture. In the chemical equation, only one regioisomer of each **UR6** and **UR6a** is shown for clarity.

As intermediate, the monourethane **UR6a** could be observed via SEC measurements (see **Figure 52**) and isolated, confirming the observation that the endocyclic carbonate group is less reactive. The chemical similarity between the monourethane **UR6a** and the diurethane **UR6** results in a difficult separation via column chromatography, requiring a gradient column that hampers the recyclability of the solvent mixture. In order to facilitate the work-up, the reaction progress was

monitored over time (see **Supplementary Table 2**), also investigating whether it is possible to push the reaction to a quantitative conversion of **CC2** and **UR6a** by adding further allylamine after a certain amount of time. The low volatility of **UR6** required the use of SEC instead of GC-FID for monitoring, nevertheless enabling a qualitative observation of the presence of unreacted **UR6a** within the mixture. In entries 1b-7b (**Supplementary Table 2**), an additional equivalent of allylamine was added after 6 h. However, no difference in yield was observed compared to the batch where no allylamine was added at a later stage (see entries 1a-7a, **Supplementary Table 2**), and in both cases, full conversion of **UR6a** was not observed. The occurring of this structurally similar intermediate, which is not straightforward to isolate from the product, represents a drawback of the bifunctional monomer **UR6** when compared to monomer **UR3**. When stopping the reaction after one day, most of the intermediate was converted, and after purification via column chromatography the product was isolated in 85% yield.

### Regioselectivity of the carbonate ring-opening

As discussed in section 2.2 (see **Figure 6**), the opening of unsymmetric cyclic carbonates can generate two different regioisomers. To analyze this for the compounds **UR3**, **UR5** and **UR6**, GC-FID and 2D NMR experiments (COSY, HDSC, and HMBC) were performed. **Figure 53** shows the detection of the different regioisomers of the urethane monomers **UR3**, **UR5**, and **UR6** via  $^1\text{H}$  NMR spectroscopy.

For the limonene-derived monourethane **UR3**, two different regioisomers were assigned in the corresponding  $^1\text{H}$  NMR spectra. From GC-FID measurements (see **Supplementary Figure 71**), their ratio was determined to be 53:47, indicating low regioselectivity. For an analysis via NMR spectroscopy, the signals  $\text{CH}_3$  groups within **UR3** were compared. Due to overlapping signals in these NMR spectra, no exact integral values could be obtained (see **Figure 53a**), but a ratio of  $\sim 1:1$  of the two regioisomers can be deduced from comparable signal intensities.

Similar to compound **UR3**, the exocyclic cyclic carbonate in carvone-derived **UR5** can in principle be opened on two different sides, leading to two possible regioisomers. Via GC-FID and NMR measurements, two different diastereomers are distinguishable, related to the low diastereoselectivity of the epoxide formation, but only one regioisomer was observed. Based on  $^1\text{H}$  NMR data (see **Figure 53b**), a

CH<sub>2</sub> group adjacent to the urethane group could be assigned, corresponding to the regioisomeric product shown in **Figure 53b**. This can be related to the two sides of the carbonate group in **CC3** differing stronger in steric demand than in the case of **CC1**.

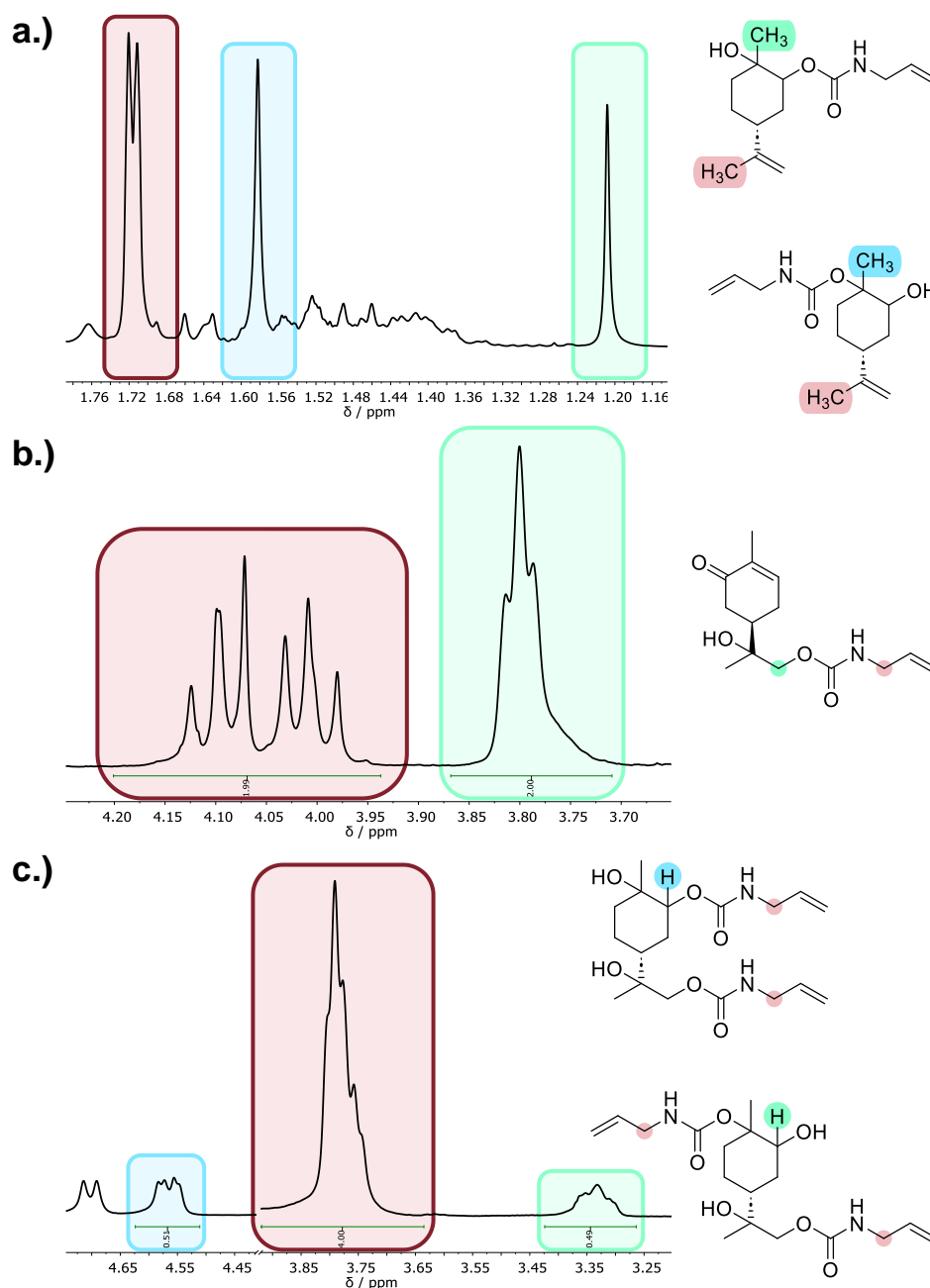


**Figure 53.** Determination of different regioisomers formed upon ring-opening of the cyclic carbonates **CC1–CC3** via NMR spectroscopy. a.) The ratio between the CH<sub>3</sub> groups in **UR3** indicates low regioselectivity for the endocyclic carbonate. b.) The ratio between the signals of the CH<sub>2</sub> groups indicates the formation of mainly one regioisomer for compound **UR5**. c.) According to the previously observed regioselectivities, two regioisomers are observed in the synthesis of **UR6**.

Regarding the regioselectivity of the aminolysis of limonene-derived bis(cyclic carbonate) **CC2** towards diurethane **UR6**, an analogous trend to compounds **UR3** and **UR5** was observed in the endocyclic and exocyclic carbonate groups. The exocyclic carbonate was opened selectively on the sterically less demanding side, whereas in the case of the endocyclic carbonate, both regioisomers were formed in a ratio of 49:51 as determined by  $^1\text{H}$  NMR measurements (see **Figure 53c**), comparing the CH signals adjacent to the tertiary hydroxy or ester group. Since compound **UR6** was not volatile enough for analysis via GC-FID, the ratio can be determined less accurately due to overlapping signals in the  $^1\text{H}$  NMR spectrum. Nevertheless, the observations match the previous findings for **UR3** and **UR5**.

### Introduction of a fatty acid-based amine

Considering the toxicity of allylamine as well as solubility issues in the case of the substrate **UR6**, it is desirable to look for alternative amines containing a terminal double bond. As such, fatty acid-based derivatives are desirable, being still simple in their structure. In a previous work from our group, it was shown that fatty acid-derived undecenoic acid can be used as starting material for the synthesis of decenyl amine **7** (see **Figure 54**) via esterification, substitution with hydroxyl amine, Lossen rearrangement, and subsequent saponification.<sup>485</sup> The amine **7** was thus synthesized according to the procedure described in that work. The introduction of this building block into the urethane monomers was first investigated using limonene monocarbonate **CC1** (see **Figure 54**).

Analogous reaction conditions as in the case of allylamine were chosen (see **Table 10**, entry 1). Also in this case, two equivalents of the amine were used to enable higher conversion, and thiourea **TU1** was added to activate the endocyclic carbonate. The monomer **UR7** was obtained in a yield of 55%, the carbonate opening was thus less effective in comparison to the reaction with allylamine, which can be attributed to the lower reactivity of the amine due to its higher molecular weight.<sup>114</sup> Further, limonene dicarbonate **CC2** was opened with **7** using analogous reaction conditions, yielding the diurethane monomer **UR8** in a yield of 15%. The low yield can be attributed to both the carbonate and the amine being less reactive than their respective counterparts, as discussed above.

Concerning the regioselectivity of the aminolysis with **7**, the formation of two different regioisomers was observed for both **UR7** and **UR8** via  $^1\text{H}$  NMR spec-

troscopy (see **Supplementary Figure 79** and **Supplementary Figure 82**), analogous to the urethane monomers **UR3** and **UR6** from allylamine. Due to overlapping signals, no definite value for the regioisomeric ratio could be determined, but the signal intensities indicate high regioselectivity for the exocyclic carbonate and low regioselectivity in the case of the endocyclic carbonate group.

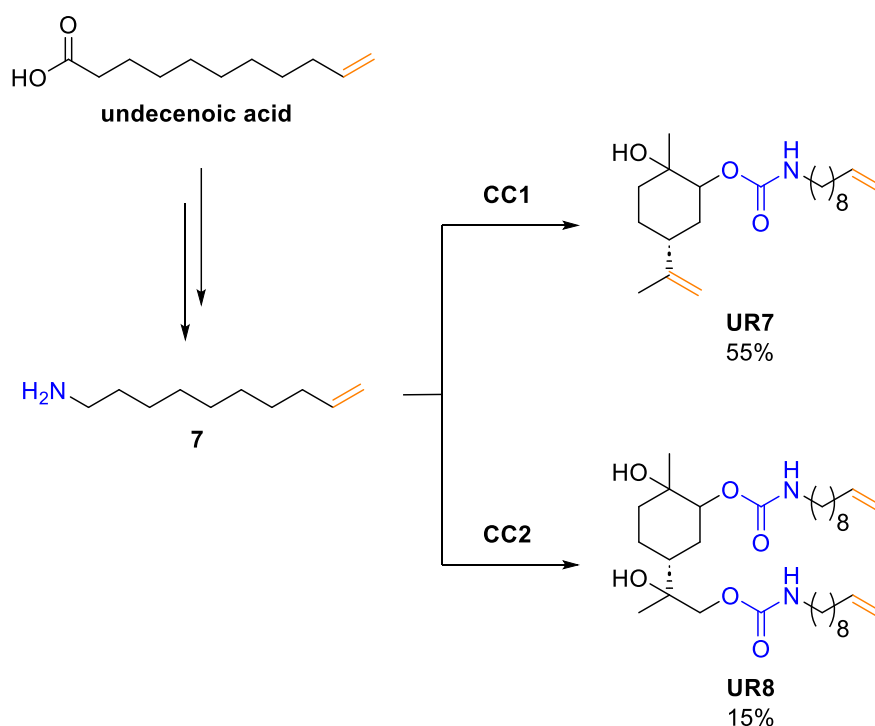


**Figure 54.** Synthesis of fatty acid-based amine **7** and subsequent carbonate opening of **CC1** and **CC2** to urethane monomers **UR7** and **UR8**. Only one regioisomer of each **UR7** and **UR9** is shown for clarity.

#### 4.4.3. Synthesis of linear NIPUs

To demonstrate a possible application of the synthesized urethane monomers for polymer synthesis, the substrates **UR3**, **UR4**, and **UR5–UR8** were reacted with dithiols in a step-growth thiol-ene polymerization to obtain linear NIPUs. To promote a radical formation, *2,2-dimethoxy-2-phenylacetophenone* (DMPA) was added as initiator and the reaction mixture was irradiated with UV light of 365 nm. As promising substrate, limonene monourethane **UR3** was chosen as it showed good solubility in various solvents. Among commercially available dithiols, 1,10-decanedithiol **T1** was chosen for first test reactions. It contains a linear spacer that is expected to keep the polar urethane moieties at a sufficient distance to

enable a certain degree of solubility. Test reactions were performed in chloroform, a solvent shown suitable in previous studies,<sup>347</sup> and 2-methyl tetrahydrofuran (2-Me-THF), which represents a less hazardous and furthermore renewable solvent. A concentration of 0.5 M was found to be a good compromise between not using too much solvent and yet dissolving the monomers well enough to enable efficient stirring. The results of the polymerization reactions are shown in **Table 12** and **Supplementary Figure 86**, revealing that efficient formation of polymers with molecular weights  $>10 \text{ kg}\cdot\text{mol}^{-1}$  takes place at the chosen conditions. Both solvents led to the formation of polymers (see **Table 12**, entries 1 and 2), with higher molecular weights being achieved in the case of the more sustainable 2-Me-THF.

**Table 12.** Thiol-ene polymerization of limonene-based urethane monomer **UR3** and 1,10-decanedithiol **T1**. The average molecular weight  $M_n$  and the dispersity  $\mathcal{D}$  were obtained from SEC from the crude reaction mixture using THF as solvent. Only one of two regioisomers of **UR3** is shown for clarity. In. = 2,2'-dimethoxy-2-phenylacetophenone.

entry	solvent	[In.] / mol%	$M_n$ / $\text{kg}\cdot\text{mol}^{-1}$	$\mathcal{D}$
1	$\text{CHCl}_3$	5.0	12.5	2.0
2	2-Me-THF	5.0	21.7	1.8
3	2-Me-THF	2.5	14.8	1.6
4	2-Me-THF	0	5.4	1.7

To gain insight into the reaction taking place, control reactions were carried out in absence of either the diene monomer **UR3**, the dithiol **T1**, UV irradiation, or initiator. The results show that both monomers as well as irradiation with UV light are necessary for the formation of polymers. In absence of DMPA, oligomeric species with a molecular weight of  $M_n = 5.4 \text{ kg}\cdot\text{mol}^{-1}$  were observed after two days of irradiation (see **Table 12**, entry 4), confirming that radical addition can also take

place without an initiator. However, significantly higher molecular weights were achieved when adding DMPA to the reaction mixture. A reduction of the initiator concentration to 2.5 mol% also led to the formation of polymers with  $M_n > 10 \text{ kg}\cdot\text{mol}^{-1}$  (see **Table 12**, entry 3). Yet, the molecular weight is lower than when using 5 mol% initiator.

The polymer could be precipitated from the crude mixture by dropping the solution into cold methanol. The  $^1\text{H}$  NMR spectrum of the precipitated polymer (see **Supplementary Figure 90**) confirmed the presence of both the terpene moiety and the aliphatic chain of the dithiol within the material. Further, the IR spectrum of the precipitated polymer (see **Supplementary Figure 95**) shows the presence of characteristic signals corresponding to the present urethane and thioether moieties. Together with the performed control reactions, this undermines the assumption of NIPU formation via thiol-ene polyaddition.

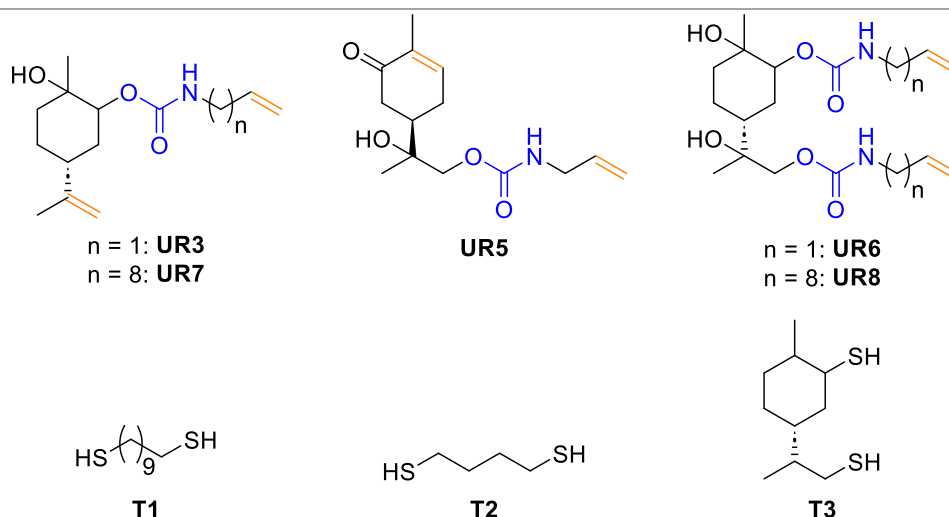
The formation of NIPUs from monomer **UR3** was monitored over time (see **Supplementary Table 4** and **Supplementary Figure 85**), showing that already after 1 h, a molecular weight of  $11.8 \text{ kg}\cdot\text{mol}^{-1}$  was achieved. After 5 h,  $14.1 \text{ kg}\cdot\text{mol}^{-1}$  were observed, indicating that the polymerization can possibly be stopped earlier. Nevertheless, for a comparison between the different monomers, 24 h were kept as fixed reaction time to allow for slower reactions to still be observed.

After the first promising results, the determined reaction conditions were applied for the synthesis of linear NIPUs from all urethane monomers synthesized in this section. Besides the variation of the urethane monomer, a variation of the dithiol can be a possibility to achieve different properties. As renewable alternative to **T1**, dithiol **T3** was synthesized from limonene. A summary of the used dithiols and of the results from the polymerization reactions is shown in **Table 13** and **Supplementary Table 3**. SEC measurements of the obtained polymeric materials were performed (chromatograms are shown in **Supplementary Figure 87–Supplementary Figure 89**) to determine  $M_n$  and  $\mathcal{D}$  (see **Table 13**), revealing mostly high molecular weights and dispersities close to 2, as expected for a step-growth polymerization. In contrast to the results achieved with monomer **UR3**, the use of monomer **UR5** (entry 4, **Table 13**) only led to the formation of oligomeric species, which can be attributed to the reduced reactivity of the double bond in  $\alpha,\beta$ -position to the carbonyl group with respect to radical thiol-ene additions. The urethane monomers **UR3**, **UR6**, and **UR7** could successfully be used for the synthesis of



NIPUs with  $M_n > 10 \text{ kg}\cdot\text{mol}^{-1}$ . When compared to monomer **UR3**, the polymer **PHU6** derived from monomer **UR7** shows slightly higher molecular weight (entry 6, **Table 13**). The observed  $T_g$  of  $1 \text{ }^\circ\text{C}$  is significantly lower than that of polymer **PHU1**, which can be attributed to the longer alkyl chains and thus lower relative amount of urethane moieties. In the case of monomer **UR6**, the molecular weight is limited (entry 5, **Table 13**), which could be related to an increased stiffness. The molecular weight was not sufficiently high for a successful precipitation; thus, the polymer could not be characterized via thermal analysis.

**Table 13.** Variation of dithiol within the synthesis of NIPUs. All reactions were carried out in a 2 mL glass vial in front of a UV-lamp of 365 nm absorption maximum, with reaction conditions according to **Table 12**, entry 2. The average molecular weight  $M_n$  and the dispersity  $\mathcal{D}$  were obtained from SEC measurements of the precipitated polymers using THF as solvent. \* obtained from SEC of the crude reaction mixture, as precipitation of the polymer was not possible.



entry	name	diene	dithiol	$M_n / \text{kg}\cdot\text{mol}^{-1}$	$\mathcal{D}$	$T_g / \text{ }^\circ\text{C}$
1	PHU1	UR3	T1	17.9	2.2	18
2	PHU2	UR3	T2	15.1	1.9	16
3	PHU3	UR3	T3	3.4*	1.5*	-
4	PHU4	UR5	T1	1.3*	2.0*	-
5	PHU5	UR6	T1	10.5*	1.4*	-
6	PHU6	UR7	T1	21.6	1.7	1
7	PHU7	UR7	T3	6.1*	1.5*	-
8	PHU8	UR8	T1	31.2	1.8	23
9	PHU9	UR8	T3	12.8	1.7	29

Monomer **UR8** could also be successfully used for the synthesis of NIPUs. When using dithiol **T1** (entry 8, **Table 13**), the polymer **PHU8** with the highest molecular weight within this work of  $31.2 \text{ kg}\cdot\text{mol}^{-1}$  was obtained after precipitation. Its  $T_g$  of  $23 \text{ }^\circ\text{C}$  is higher than that of **PHU6**, where the same amine was used for the carbonate opening. The higher  $T_g$  can be attributed to increased hydrogen bonding due to the presence of two urethane moieties per repeating unit.

For a variation of the dithiol, the urethane monomer **UR3** was chosen as starting point. The use of dithiol **T2** with a shorter chain length led to a polymer with lower molecular weight (entry 2, **Table 13**), which might be attributed to a less favorable structure in which the terpene units are relatively close. The resulting polymer **PHU2** showed a  $T_g$  of  $16 \text{ }^\circ\text{C}$  that is similar to that of **PHU1**. The renewable dithiol **T3** in combination with monomer **UR3** did not yield a polymer with high molecular weight (entry 3, **Table 13**), supporting the previous assumption of close terpene moieties hampering the formation of longer polymer chains. For this reason, dithiol **T3** was tested for a polymerization with monomers **UR7** and **UR8**, which contain one and two additional decenyl spacers, respectively. Indeed, already the use of monomer **UR7** (entry 7, **Table 13**) with an elongated chain length compared to monomer **UR3** (entry 3, **Table 13**) led to higher molecular weight, yet not high enough for a precipitation of the polymer **PHU7**. Extending this to monomer **UR8** with an additional  $\text{C}_{10}$  chain led to the formation of NIPU **PHU9** with a molecular weight of  $12.8 \text{ kg}\cdot\text{mol}^{-1}$  that could be precipitated (see **Table 13**, entry 9). The observed  $T_g$  of  $29 \text{ }^\circ\text{C}$  is higher than that of **PHU8** with a linear dithiol, corresponding to a higher stiffness of the terpene unit.

## ***Discussion***

This section showed the application of thiourea catalysis for the functionalization of terpene-based carbonates towards urethane building blocks. The presence of a thiourea catalyst significantly improved the opening of the endocyclic carbonate groups by allylamine, whereas no activation was necessary in the case of the exocyclic carbonate structures. This enabled the access to AA monomers for the synthesis of linear NIPUs as potential application in polymer synthesis. By thiol-ene polyaddition with dithiols, NIPUs with molecular weights of up to  $31 \text{ kg}\cdot\text{mol}^{-1}$  were obtained, strongly depending on the structure of the respective monomers.

By elongating the carbon chains within the urethane monomers, it was possible to achieve higher molecular weights and further implement a renewable dithiol from limonene. The  $T_g$  values, ranging from 1 to 29 °C, are slightly higher than those of literature-described terpene-containing NIPUs of similar molecular weight,<sup>103,347,456</sup> which can be attributed to additional OH groups<sup>103,347</sup> or higher terpene content, respectively.<sup>456</sup>

This approach complements previous strategies of introducing urethane moieties into polymers via thiol-ene reaction.<sup>347,560</sup> It should be noted that the obtained materials contain additional thioether linkages as well as hydroxy groups in contrast to industrially used PUs. However, other works also include thioether linkages, e.g. for self-blowing NIPU foams,<sup>561,562</sup> showing the potential of such new structures. Further, this work brings forward the use of thiourea catalysis for NIPU production,<sup>563</sup> as potential strategy to activate more hindered cyclic carbonates. Although several examples have shown the potential of implementing terpene structures into polyurethanes,<sup>103,344,415,453,456,458,564</sup> their number remains limited.

## 4.5. Linear non-isocyanate polyurethanes from erythritol bis(cyclic carbonate)

The results obtained from section 4.4 represent a promising approach for the synthesis of hydroxyurethane building blocks for thiol-ene polyadditions towards PHUs. The concept of first ring-opening cyclic carbonates with functionalized amines and subsequent thiol-ene reaction worked efficiently under mild conditions and was therefore expected to be applicable to other systems besides the terpene-based monomers **UR3–UR8**. An interesting candidate is *erythritol bis(cyclic carbonate)* (EBCC),<sup>365</sup> which can be obtained from the reaction of erythritol and DMC (see **Figure 19**).<sup>366</sup> Within this section, the opening of EBCC with allylamine and the fatty acid-based amine **7** was investigated to obtain di(hydroxyurethane) monomers with terminal double bonds. Afterwards, the synthesis of linear PHUs from these AA monomers was investigated.

### 4.5.1 Monomer synthesis

For the use of EBCC in linear PHUs, the synthesis of the hydroxyurethane monomers needed to be investigated first.

EBCC was synthesized according to a previously established protocol, reacting erythritol with DMC and using TBD as organocatalyst (see **Figure 55**).<sup>366</sup> By leaving the reaction mixture for 40 minutes on the rotary evaporator (60 °C, 300 mbar) and subsequent washing with cold DMC, the product was obtained in a yield of 47%.

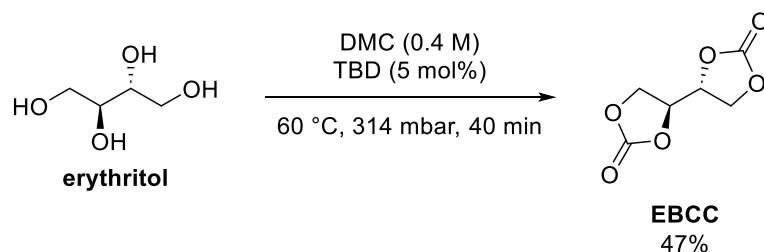


**Figure 55.** Organocatalytic synthesis of EBCC from erythritol and DMC.

The obtained yield is considerably lower than described previously, and the product NMR of the obtained EBCC showed the presence of small impurities. To avoid

tedious work-up, the product was however directly used in the ring-opening reaction.

For the optimization of the aminolysis of EBCC, allylamine, a commercially available compound, was used as nucleophile. The reaction conditions of the ring-opening were chosen to obtain the di(hydroxyurethane) **UR9** (**Figure 56**) in the maximum yield, while aiming to design the synthesis as sustainable as possible. For clarity, only one regioisomeric form of **UR9** is depicted in **Figure 56**.

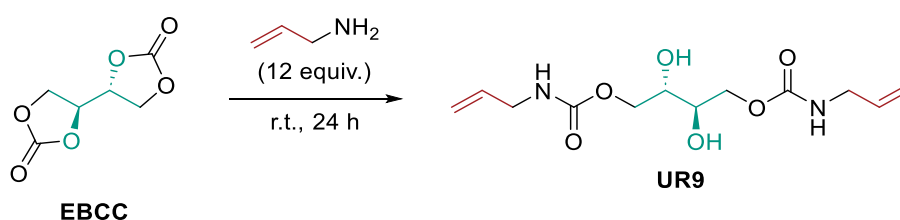


**Figure 56.** Aminolysis of EBCC with allylamine at room temperature. For clarity, only one possible regioisomer of **UR9** is shown.

To avoid the use of solvent during this step, the solubility of EBCC in allylamine was investigated. Indeed, the solid dicarbonate was soluble in  $\geq 12$  equivalents of allylamine, so this was taken as a starting point for the optimization. The reaction was thus stirred at room temperature and thereafter analyzed.

TLC and GC-FID measurements showed full conversion of the cyclic carbonate.<sup>1</sup> Further, in the  $^1\text{H}$  NMR spectrum of the reaction mixture (**Supplementary Figure 105**), the signal of the  $\text{CH}_2$  groups in the cyclic carbonate was not detected, suggesting that the starting material was successfully converted. New signals could be assigned to the desired product.

In a recent work by Grau, Vidil, Cramail et al., the stereochemistry of the ring-opening of EBCC with amines was thoroughly investigated.<sup>368</sup> They observed a high selectivity towards the formation of the product containing secondary hydroxy groups, which was attributed to an activation of the monomer by the neighboring carbonate group. In the ring-opening of the first cyclic carbonate, a regioselectivity of 100% was determined, whereas in the second ring-opening, a selectivity towards the formation of secondary hydroxy groups of 68% was observed. This

<sup>1</sup> GC-FID screenings were performed previous to this work by Dr. Katharina Wetzel.

change was attributed to the decreased activating effect after ring-opening of one carbonate group.

In the approach within this work, a similar trend was expected. To analyze this,  $^1\text{H}$  NMR spectroscopy was used. Within the product mixture, it was possible to compare the signal of the NH groups of the urethane moiety from 7.35–6.82 ppm with one of the signals assigned to the CH<sub>2</sub> groups within the erythritol core from 4.20–4.09 ppm, since there was no signal overlap within these regions (see **Figure 57**). The latter signal was attributed to the isomer **UR9a** bearing secondary hydroxy groups by 2D NMR spectroscopy of the isolated isomer. By calculating the ratio between these two signals, the ratio between the two regioisomeric forms **UR9a** and **UR9b** was estimated.

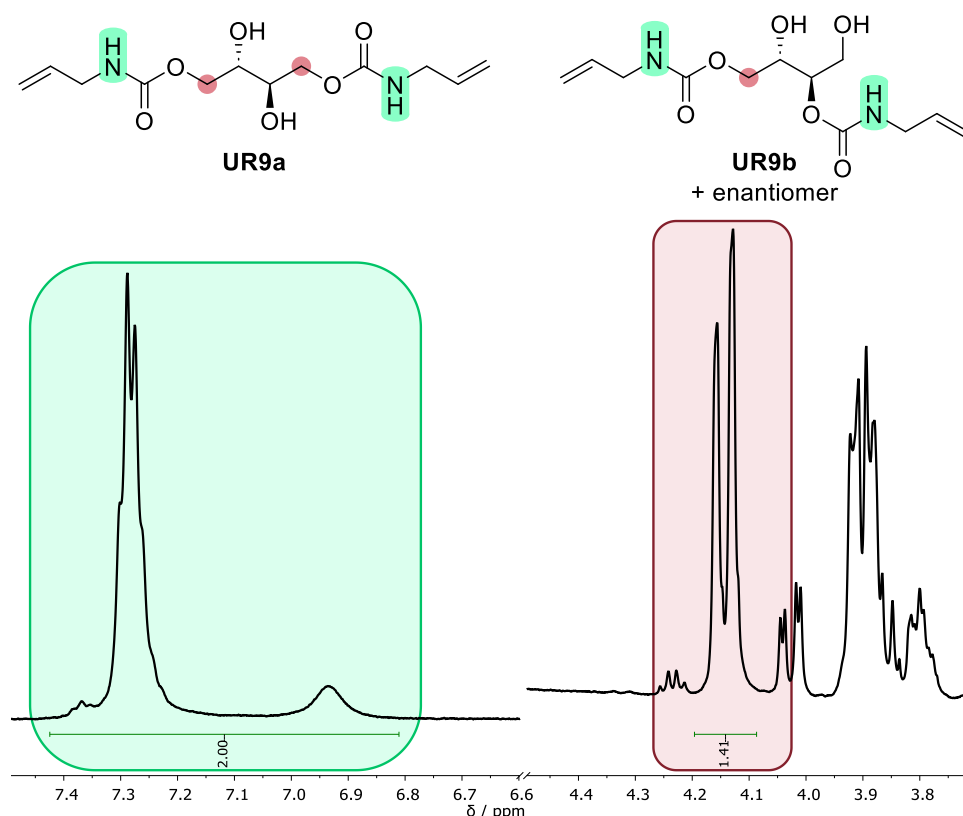


**Figure 57.**  $^1\text{H}$  NMR reaction control of the synthesis of **UR9** by comparing the signal of the NH group at 7.35–6.82 ppm with one signal of the CH<sub>2</sub> protons at 4.20–4.09 ppm. The signal of the NH group splits up due to the presence of rotamers. The theoretical ratio of the signals in 100% **UR9a** is 1:1.

The two compared signals would occur in a 1:1 ratio within the pure isomer **UR9a**, but only a ratio of 2.0:1.4 was observed. Thus, a selectivity towards the isomeric

form showing secondary hydroxy groups of 70% can be estimated. This is in good accordance with the previously reported 68%.<sup>368</sup>

The reaction was performed successfully in 12 equivalents of allylamine. With ongoing reaction progress, partial precipitation of the product was observed as it was less soluble in allylamine. Further, the high excess of allylamine is not desirable with respect to sustainability. Therefore, for comparison, the solubilization of the product and starting material in allylamine at 70 °C, slightly below its boiling point, was analyzed. Six equivalents were sufficient to dissolve both the starting material as well as the amount of product corresponding to 100% yield. Thus, EBCC was stirred in 6 equivalents of allylamine at 70 °C overnight to compare the results. The NMR spectrum of the product mixture showed the signals of the desired product and full conversion of the cyclic carbonate. Additionally, the ratio of regioisomeric forms of the hydroxyurethane units in the reaction mixture stirred at 70 °C was calculated according to **Figure 57**, yielding a ratio of secondary to primary alcohol groups of 60%, corresponding to a less pronounced regioselectivity than when performing the reaction at room temperature (see **Supplementary Figure 106**). However, a higher number of additional signals was observed that could not be assigned (see **Supplementary Figure 106**). Therefore, performing the reaction at room temperature was chosen as synthesis route towards monomer **UR9**.

When purifying the product **UR9** via column chromatography or via extraction and recrystallization, the desired product was obtained in yields of 56% and 47%, respectively. The product signals in the <sup>1</sup>H NMR spectrum corresponded to a high purity of the regioisomer **UR9a** bearing two secondary hydroxy groups. This can explain yield losses during the purification. In any case, the isolated isomeric form in high purity was used for further experiments.

To optimize the reaction with regard to sustainability, the amount of waste produced by the reaction has to be taken into account. A large part of the waste production within chemical syntheses derives from the purification of the products.<sup>9</sup> Since column chromatography makes use of a high amount of solvent and stationary phase, purification methods such as washing and extraction or recrystallization are expected to produce less waste.

In the synthesis of **UR9**, possible impurities after reaction completion were excess allylamine, the starting material EBCC and potential side products or intermediates.

Allylamine is water-soluble and can thus be washed out with water or brine. A possibility to purify the product from the remaining impurities was by recrystallization, since the product was found to be crystalline. For this, it was important that the ratio between product and impurities was high enough to ensure successful separation via recrystallization. At the same time, subsequent washing, extraction, and recrystallization still required a considerable amount of solvent. Further, higher losses in yield were to be expected than when using column chromatography, especially since the product was observed to be partly water-soluble. For this reason, one batch of **UR9** was synthesized and split into two equal parts afterwards, of which one was purified using washing/ extraction and recrystallization and the other one using automatic flash column chromatography. For both cases, the respective amount of solvent use was measured (see **Table 14**). Further, for column chromatography, the used amount of silica gel was determined, and for washing, the amounts of brine and Na<sub>2</sub>SO<sub>4</sub> were counted as waste.

**Table 14.** Contributions of reagents, solvents, and purifying agents to the waste produced through work-up via automatic flash column chromatography or extraction and subsequent recrystallization of **UR9**. The reaction conditions were chosen according to **Figure 56**. Solvent amounts needed to transfer product between flasks were not considered. \* Two contributions from extraction and recrystallization.

entry	contribution	column chromatography	extraction + recrystallization
1	EBCC	2 g	2 g
2	allylamine	8 g	8 g
3	ethyl acetate	600 g	270 g + 90 g*
4	silica	100 g	-
5	brine	-	220 g
6	Na <sub>2</sub> SO <sub>4</sub>	-	20 g
7	cyclohexane	-	62 g
8	$\Sigma m_{\text{waste}}$	710 g	672 g
10	$m_{\text{product}}$	1.86 g	1.57 g



The yield of **UR9** from purification via column chromatography was slightly higher. Yield losses in both cases could be attributed to the poor solubility of the product in ethyl acetate or to the occurring of side products.

For automatic flash column chromatography, significantly more ethyl acetate was necessary, this being the highest contribution to the mass of waste (**Table 14**, entry 3). On the other hand, in the washing step, a considerable amount of brine was necessary to remove the water-soluble impurities efficiently (**Table 14**, entry 5). Additionally, the amount of ethyl acetate needed for initial dissolution of the product and later for extraction of the product from the organic phase contributed significantly to the overall waste (**Table 14**, entry 3). Washing and extraction did not yield the product in a satisfying purity, therefore recrystallization in cyclohexane/ ethyl acetate (1:1.25) was performed subsequently (**Table 14**, entries 3 and 7).

The documented amounts of produced waste could be used to calculate E-factors for both work-up processes. Equation (4) shows the calculation of the E-factor including all produced waste *cEF*.<sup>46</sup>

$$cEF = \frac{\sum m_{\text{waste}} - m_{\text{product}}}{m_{\text{product}}} \quad (4)$$

To further compare both purification methods, the contribution of solvents to the produced sum of waste was calculated as shown in Equation (5).

$$\text{solvent contribution} = \frac{\sum m_{\text{solvents}}}{\sum m_{\text{waste}}} \quad (5)$$

In **Table 15**, the calculated metrics, i.e. yield, *cEF*, and solvent contribution, are summarized for both purification methods.

The results show that the complete E-factor is lower for the purification via column chromatography compared to the procedure using washing, extraction, and recrystallization (**Table 15**, entry 2). This can mainly be attributed to a higher yield (**Table 15**, entry 1) and to a high use of ethyl acetate and brine during washing and extraction (**Table 15**, entries 3 and 5).

**Table 15.** Reaction metrics calculated for the two purification methods compared within this work. The reaction conditions were chosen according to **Figure 56**.

entry	metric	column chromatography	extraction + recrystallization
1	yield	56%	47%
2	<i>cEF</i>	380	430
3	solvent contribution	85%	63%

Moreover, the solvent contribution is higher in the purification via column chromatography (**Table 15**, entry 3). As no solvent mixture was used for the separation, the solvent can possibly be gained from the purified fractions and be reused. In the purification by extraction and recrystallization, the used solvents can also possibly be recovered by evaporation, but the contribution of brine, which is not straightforward to recover due to the presence of organic compounds, resulted in a high amount of overall waste. Excess allylamine could not be easily recovered in either case, since it was dissolved in the aqueous phase during the washing step or retained by the stationary phase during column chromatography. On a larger scale, a partial recovery of allylamine could possibly be achieved by distillation prior to further work-up.

The comparison reveals that both purification methods resulted in relatively high E-factors on a laboratory scale. Purification via extraction and recrystallization did not lead to an improvement in the E-factor compared to column chromatography in the case of monomer **UR9**, which is mainly caused by poor solubility of **UR9** in ethyl acetate as well as by the impurities in water. Therefore, in this case, purification via column chromatography led to less production of waste, especially when recovery of the solvents is taken into account. However, the production of waste is not the only metric to assess the sustainability of a process, as discussed in section 2.1. The safety hazard of reagents also needs to be considered, for instance in the use of silica gel for column chromatography. Thus, overall, both purification methods remained valid options for the presented synthesis route.

The aminolysis of EBCC, as shown in **Figure 56**, can also be extended for the synthesis of further monomers. Analogous to the terpene-based monomers in section 4.4, the introduction of the fatty acid-based amine **7** as substitute for

allylamine was investigated. **Figure 58** shows the synthesis route towards the resulting monomer **UR10**.

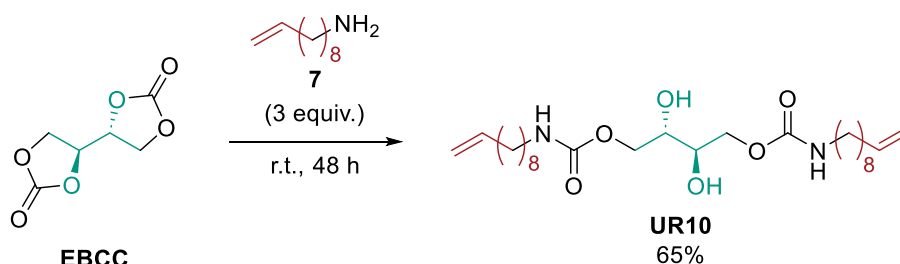


**Figure 58.** Aminolysis of EBCC with fatty acid-based amine **7**.

Only 3 equivalents of amine **7** were used since it was more extensive to synthesize than allylamine.<sup>485</sup> After full conversion of the product was determined via TLC, the reaction mixture was purified via washing and extraction to yield 65% of the product **UR10**. Although less equivalents of the amine were used, the isolated yield was higher than for monomer **UR9**, which can be attributed to less work-up steps and lower solubility in water.

With the two di(hydroxyurethanes) **UR9** and **UR10** at hand, both monomers could subsequently be tested for the use in PHU synthesis by thiol-ene polyaddition. By comparing both monomers, the influence of the chain length for applications in polymer synthesis can possibly be investigated.

#### 4.5.2 Linear NIPU synthesis

Similar to the terpene-based urethane monomers **UR3–UR8** from section 4.4, the synthesis of linear NIPUs from **UR9** and **UR10** was investigated, using the more easily accessible **UR9** for test reactions. As the crystalline monomers were barely soluble in the solvents that were used in section 4.4, i.e. chloroform and 2-methyl tetrahydrofuran, the solubility of **UR9** in more polar solvents was investigated. The respective dilution necessary to dissolve the monomer fully is shown in **Table 16**. While acetone and ethyl acetate only dissolved the monomer poorly, the polar protic solvents methanol and ethanol as well as the polar aprotic solvents DMF and DMSO were more suitable choices.

With respect to the principles of Green Chemistry, methanol and ethanol are preferable as they were recommended by Prat et al. in the CHEM21 solvent

selection guide, whereas DMSO was ranked as problematic and DMF as hazardous.<sup>39</sup>

**Table 16.** Maximum concentration possible to dissolve monomer **UR9** in different polar solvents.

entry	solvent	concentration / mol·L <sup>-1</sup>
1	acetone	0.033
2	EtOAc	0.027
3	MeOH	0.33
4	EtOH	0.50
5	DMSO	0.70
6	DMF	0.70

However, all four solvents from entries 3–6 (**Table 16**) were tested for a possible NIPU synthesis via thiol-ene polyaddition by reacting monomer **UR9** with 1,10-decanethiol (**Figure 59**).

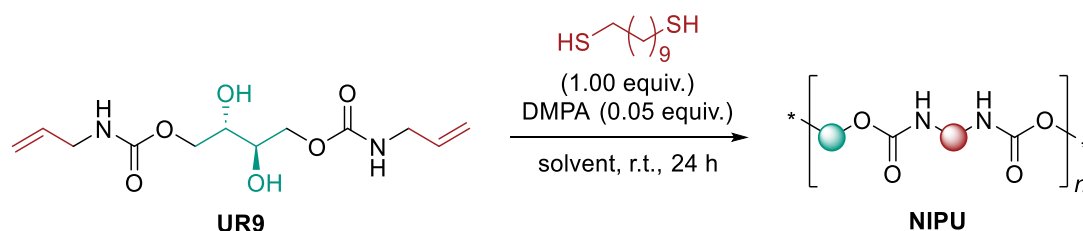


**Figure 59.** Synthesis of linear NIPUs from monomer **UR9**.

Using methanol or ethanol as solvents, colorless precipitates formed during the reaction. This led to the assumption that while the two solvents can dissolve the monomers efficiently, oligomers and polymers were not anymore soluble. The white precipitate was isolated by evaporation of the solvent, but the resulting colorless powders were not soluble in THF, hexafluoroisopropanol, or dimethyl acetamide, which were available solvents for SEC analysis. Since they showed solubility in DMSO, NMR spectroscopy was performed to determine the reaction progress.

**Figure 60** shows an exemplary <sup>1</sup>H NMR spectrum of the polyaddition product obtained from the polymerization in methanol. The signals in the <sup>1</sup>H NMR spectra

could be assigned to the supposed structure of a linear chain as shown in **Figure 60**, but the two signals corresponding to the terminal bonds as found in the urethane monomer **UR9** are still visible.

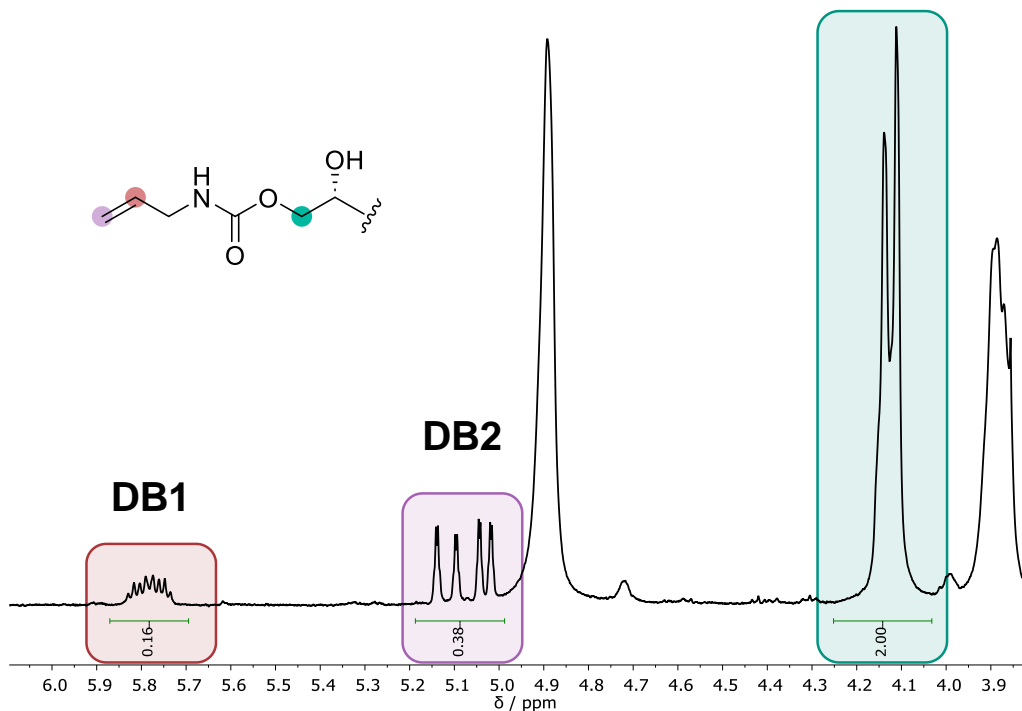


**Figure 60.**  $^1\text{H}$  NMR signals of terminal double bonds compared to  $\text{CH}_2$  signal in the growing polymer chain for the determination of the molecular weight.

Notably, the signal of DB2 consists of two split signals due to different vicinal coupling with of the two terminal olefinic protons. Nevertheless, they were treated as one signal group within this context. Integration of the signals of DB1 and DB2 in comparison to a normalized signal that can be assigned to the backbone enables the calculation of the molecular weight via  $^1\text{H}$  NMR according to Equations (6) and (7).

### Signal DB1

$$M_n(\text{DB1}) = n \cdot M_{\text{repeating unit}} = \frac{1}{I_{\text{DB1}}} \cdot M_{\text{repeating unit}} \quad (6)$$

$n$  = number of repeating units

$I_{\text{DB1}}$  = integral value of signal from 5.87 to 5.69 ppm.

**Signal group DB2**

$$M_n(\text{DB2}) = n \cdot M_{\text{repeating unit}} = \frac{1}{I_{\text{DB2}}} \cdot 2 \cdot M_{\text{repeating unit}} \quad (7)$$

$n$  = number of repeating units

$I_{\text{DB2}}$  = integral value of signal group from 5.19 to 4.99 ppm.

With these equations, the molecular weight values according to both double bond signals were calculated, as shown in **Table 17**.

**Table 17.** Synthesis of linear NIPUs **PHU10** from monomer **UR9** in different solvents and concentrations. The values for  $M_n$  were determined via  $^1\text{H}$  NMR spectroscopy by comparison of the signals of DB1 and DB2 (see **Figure 60**) with the signal from 4.25–4.03 ppm. \* not detected due to no precipitation of the polymer. \*\* not detected due to the absence of end group signals in the  $^1\text{H}$  NMR spectrum.

entry	solvent	concentration / mol·L <sup>-1</sup>	$M_n(\text{DB1})$ / kg·mol <sup>-1</sup>	$M_n(\text{DB2})$ / kg·mol <sup>-1</sup>	$T_g$ / °C
1	MeOH	0.1	3.2	2.6	11
2	EtOH	0.1	3.8	3.5	11
3	DMSO	0.1	3.3	2.1	n. d.*
4	DMSO	0.5	n. d.**	n. d.**	8

The results from entries 1 and 2 (**Table 17**) show that only low molecular weights are achieved when using methanol or ethanol as solvents, with the reaction in ethanol yielding slightly higher molecular weights. Further, precipitation of the obtained oligomeric species was observed. After evaporation of the solvent, the materials were analyzed via DSC to determine their glass transitions. Both precipitates displayed  $T_g$  values below room temperature.

Since the obtained materials were still soluble in DMSO, it was investigated to perform the polyaddition reaction in DMSO as solvent. When using DMSO in the starting concentration of 0.1 mol·L<sup>-1</sup> (**Table 17**, entry 3), no high molecular weight

was obtained. Further, a significant deviation between the two  $M_n$  values for DB1 and DB2 was observed, which can be attributed to overlapping signals in this region. This is especially the case for the signal DB2 (see **Figure 60**), therefore it is supposed that more reliable results are obtained from analyzing the signal DB1. In order to increase the molecular weight of the polymers, the concentration was varied to see a possible influence on the reaction progress. A concentration of  $0.5 \text{ mol}\cdot\text{L}^{-1}$  was chosen which showed efficient polymerization in section 4.4 (see **Table 12**). After stirring for 24 hours, no double bond signals were detectable in the  $^1\text{H}$  NMR spectrum, indicating the formation of higher molecular weight species (**Table 17**, entry 4). For further insights, the reaction progress was followed over time with NMR spectroscopy. The use of deuterated DMSO enabled the observation of the reaction with time. The molecular weight was determined from both the signal of DB1 and the one of DB2. As already after one hour no remaining double bond signals were detected, samples were taken every 5 min. **Table 18** shows the determined values of the molecular weight within the first 20 min and after 40 min.

**Table 18.** Screening of linear NIPU synthesis from monomer **UR9** with time. The values for  $M_n$  were determined via  $^1\text{H}$  NMR spectroscopy by comparison of the signals of DB1 and DB2 (see **Figure 60**) with the signal from 4.25–4.03 ppm. \* not applicable due to negative integral value; \*\* not applicable due to signal overlap.

entry	time / min	$M_n(\text{DB1})$ / $\text{kg}\cdot\text{mol}^{-1}$	$M_n(\text{DB2})$ / $\text{kg}\cdot\text{mol}^{-1}$
1	5	1.3	1.2
2	10	4.5	4.0
3	15	31	16
4	20	n. a.*	47
5	40	200	n. a.**

The stacked NMR signals of DB1 and DB2 within 20 min reaction time are depicted in **Figure 61**. Notably, as higher molecular weights are reached, the error of the signal intensity increases due to a lower signal to noise ratio. Therefore, the values from **Table 18** cannot serve as definite values of the molecular weight, but they can give an impression of the molecular weight range of the obtained polymers.

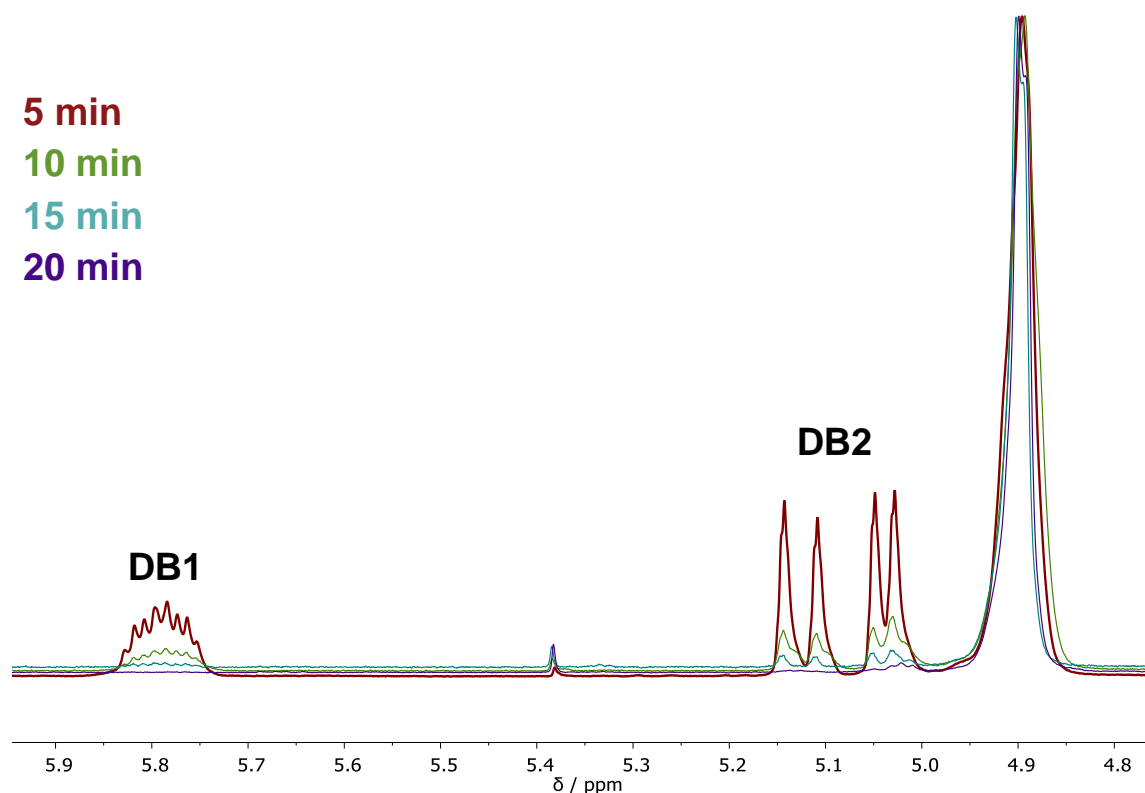


**Figure 61.** Stacked <sup>1</sup>H NMR spectra of NIPU synthesis from **UR9** in DMSO (see **Table 18**) within the first 20 min.

From the NMR characterization, it can be stated that polymer chains of considerable molecular weights were formed already after short reaction times of 20–40 min. The values after 40 min (**Table 18**, entry 5) are likely to contain a high error, but the results after 15 and 20 min (**Table 18**, entries 3 and 4) hint at a possible range. The values from **Table 18** allow for the conclusion that linear NIPUs with molecular weights of  $>30 \text{ kg}\cdot\text{mol}^{-1}$  can be obtained via the reaction conditions in **Table 17**, entry 4, and **Table 18**. This confirms an efficient thiol-ene polyaddition towards the NIPU material **PHU10**.

Further characterization of the polymeric materials was performed using IR spectroscopy and DSC analysis. For this, the polymer had to be isolated from the



reaction mixture. DMSO as solvent could not be removed by evaporation, thus, to isolate the NIPU materials, precipitation in an anti-solvent was investigated. As antisolvents, cyclohexane, 2-methyl THF, methanol, and water were tested.

Cyclohexane represents a less hazardous alternative to other alkanes, such as pentane or *n*-hexane,<sup>39</sup> and it did not dissolve the oligomeric species synthesized in methanol and ethanol as solvents (entries 1 and 2, **Table 17**). However, no precipitation was possible due to phase separation of DMSO and cyclohexane.

2-Methyl THF as antisolvent led to the formation of a colorless precipitate. Yet, on the attempt of isolating the precipitate via phase separation, a solvent residue remained that dissolved the polymer again. A possible explanation could be a poor miscibility of DMSO and 2-methyl THF.

As more polar antisolvents, methanol and water were investigated, which are both miscible with DMSO. By pouring the polymer solution into cold methanol or water, colorless precipitates formed and could be isolated via filtration and drying. For characterization, the material precipitated in methanol was chosen, since methanol is more straightforward to remove from the polymeric material.

In the case of the polymers that could be isolated, DSC measurements were performed to analyze their thermal transitions. It can be noted that the materials exhibited similar glass transitions around 10 °C (**Table 17**, entries 1, 2, and 4). Besides, IR spectroscopy of the precipitated **PHU10** under the reaction conditions of **Table 17**, entry 4 was measured, with the IR spectrum exhibiting characteristic signals of urethane, hydroxy, and thioether moieties as expected (see **Supplementary Figure 108**).

Although the low solubility of the monomer **UR9** limited the possibility to analyze the obtained NIPUs thoroughly, the synthesis of NIPUs with molecular weights of  $>30 \text{ kg}\cdot\text{mol}^{-1}$  was possible under mild reaction conditions in short reaction times. Thus, the approach from **Table 17** was applied for the second erythritol-based diurethane **UR10** containing longer aliphatic chains. The synthesis of the material **PHU11** is shown in **Figure 62**.

During the reaction, the formation of a colorless precipitate was observed. Pouring of the reaction mixture into cold methanol led to the formation of a colorless precipitate that would correspond to 60% yield and which was not soluble in DMSO in order to perform NMR analysis.

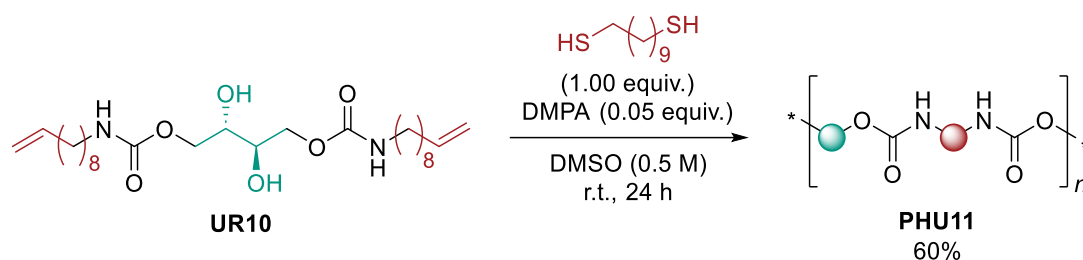


**Figure 62.** Synthesis of linear NIPU **PHU11** from monomer **UR10**.

The IR spectrum of the material **PHU11** confirms the presence of urethane, hydroxy, and thioether moieties (see **Figure 63**). These observations lead to the conclusion that the polymerization of **UR9** towards linear NIPUs was most likely successful, however, the limited data represent a drawback of this material. The use of alternative dithiols, e.g. containing ether bonds, might lead to better solubilization and will be object of further research on this topic.

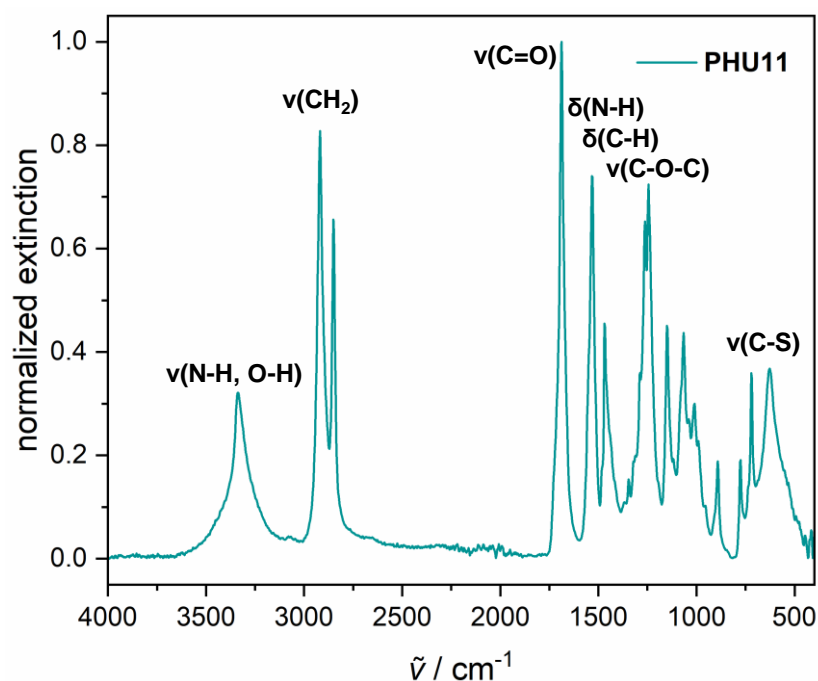


**Figure 63.** IR spectrum of the NIPU material **PHU11** synthesized according to **Figure 62**.

To sum up, the substrate EBCC based on renewable erythritol represents a potent monomer for the synthesis of linear NIPUs via cyclic carbonate opening and subsequent thiol-ene polyaddition. The optimization of yields within the monomer synthesis as well as a larger scope of dithiols may be a focus of further investigations, establishing the use of EBCC in such approaches.

Further, the efficiency of the polyaddition reaction via thiol-ene chemistry makes the monomers **UR9** and **UR10** attractive building blocks for different sorts of NIPU materials, also possibly including cross-linked materials. Therefore, the synthesis of NIPU thermosets based on the urethane monomers from sections 4.4 and 4.5 was investigated within the following section.

## 4.6. Synthesis of PHU networks

Besides linear NIPUs, as presented in the previous sections, the urethane monomers **UR3** and **UR5–UR10** represent potential building blocks for a synthesis of thermosets by polyaddition with polythiols. Such PHU networks could possibly show dynamic behavior by transurethanization reactions, as reported in the literature previously (see section 2.4).<sup>271,272</sup>

Within this section, the focus was laid mainly on the limonene-based mono-urethane **UR3** and the sugar-based diurethane **UR9** as monomers for PHU network synthesis, since they were readily synthesized without tedious work-up steps (see sections 4.4 and 4.5), thus also representing more sustainable monomers at this point of research. As polythiols, the compounds **T4** and **T5** (**Figure 64**) are commercially available and have already been applied for thermoset synthesis via thiol-ene cross-linking.<sup>565–568</sup>

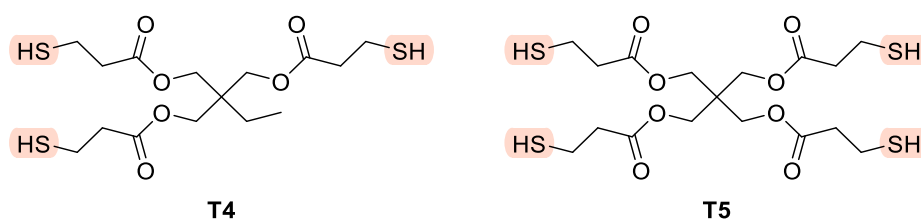


**Figure 64.** Commercially available polythiols **T4** and **T5** containing ester linkages.

Notably, the thiols **T4** and **T5** contain several ester groups. Thus, materials that are obtained upon cross-linking of monomer urethanes **UR3** and **UR9** with **T4** and **T5** will contain ester linkages besides urethane moieties and hydroxy groups. Potential dynamic behavior could therefore not only arise from transurethanization, but also from transesterification reactions.<sup>260</sup> This does not represent a drawback with respect to the material synthesis, but potential dynamicity would have to be investigated concerning its mechanism.

First attempts to obtain cross-linked materials were performed using the terpene-based monomer **UR3** (see **Figure 65**). It was determined to be miscible with the thiols **T4** and **T5** and further, the mixture was able to dissolve DMPA as photo-initiator. Thus, both polythiols were tested for possible cross-linking with **UR3** in the presence of 5 mol% DMPA.

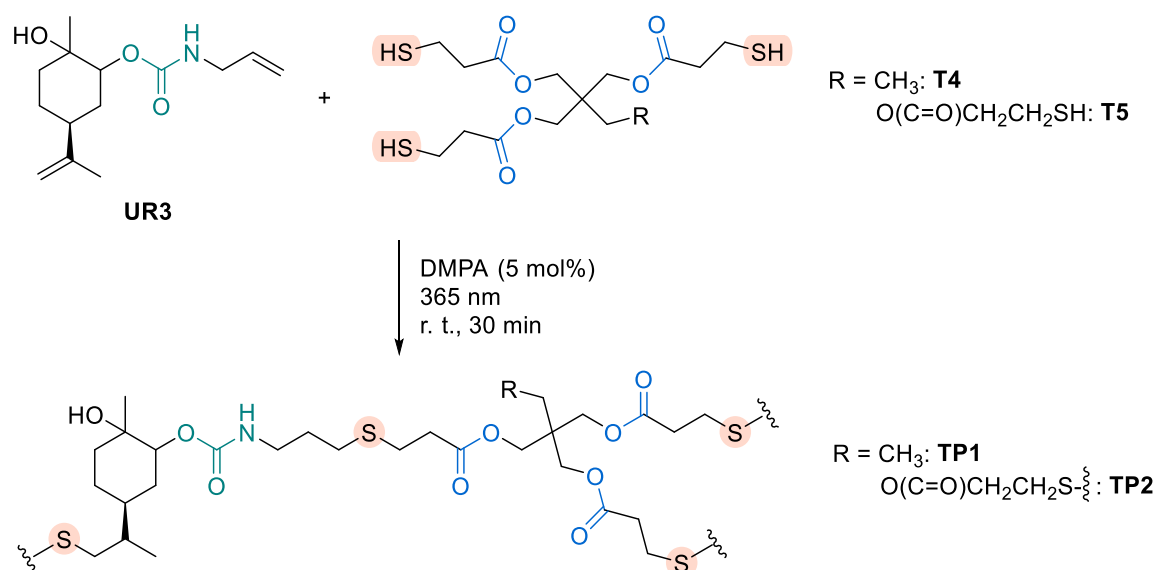


**Figure 65.** PHU networks **TP1** and **TP2** obtained from terpene-based monomer **UR3** and polythiols **T4** or **T5** via UV curing.

In the first attempt, irradiation with 365 nm UV light for 2 h at room temperature yielded transparent insoluble materials in both cases. With time, no further curing could be observed via IR spectroscopy. After 24 h, DSC measurements of both materials were performed. The results showed a  $T_g$  of the material **TP1** of 20 °C, thus slightly below room temperature, whereas the  $T_g$  of the material **TP2** was measured to be 28 °C. A curing above the  $T_g$  is favorable to achieve a higher conversion, therefore thiol **T4** was chosen for further experiments as they were performed at room temperature.

For further experiments, silicon molds were used to produce foils directly by irradiation. Moreover, the amount of photoinitiator was decreased to 1 wt.% since it remained in the cured material, and instead of DMPA, Irgacure<sup>®</sup> 819 was used as UV photoinitiator for further test reactions as it was well soluble in all formulations. **Figure 66** shows a picture of a transparent foil obtained from the curing of monomer **UR3** with trithiol **T4** for 30 minutes at room temperature.

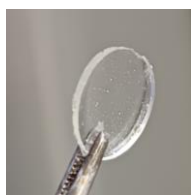


**Figure 66.** Picture of PHU network **TP1** after irradiation with 365 nm UV light for 30 min.

The fast and efficient curing to yield a transparent cross-linked material confirms monomer **UR3** as a promising building block for thermoset synthesis. Applications of the use of monomer **UR3** e.g. in 3D printing would be interesting for further investigations. For the synthesis of dynamic PHU networks, however, the use of sugar-based monomer **UR9** is more attractive due to a higher density of urethane and hydroxy groups and further a possibly higher accessibility of the secondary hydroxy groups. **Figure 67** shows the synthesis of a potential network from **UR9** and **T4**.

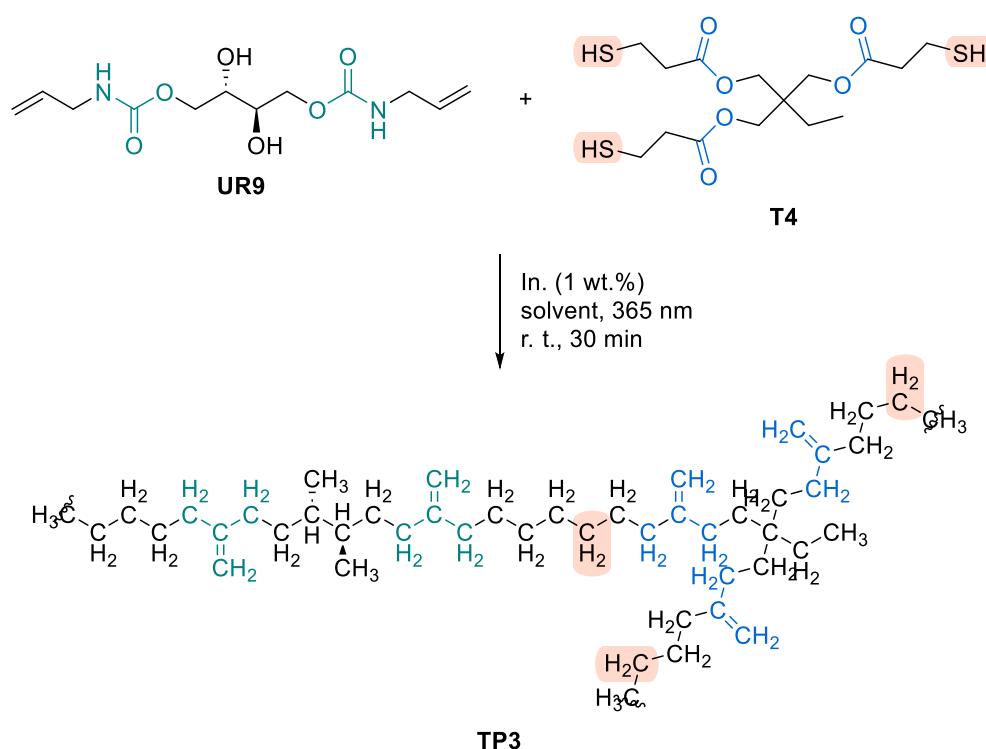


**Figure 67.** PHU network **TP3** obtained from sugar-based monomer **UR9** and polythiol **T4** via UV curing. In. = Irgacure® 819.

The sugar-based monomer **UR9** was not as straightforward to implement into cross-linked materials as the monomer **UR3** since its poor solubility and high melting point did not allow for a polymerization in bulk. Therefore, different solvents were tested for the polymerization. For this, similar solvents that could dissolve the monomers and the initiator were used. Similar to the synthesis of linear PHUs in **Table 17**, the polar protic solvents methanol and ethanol were tested next to the polar aprotic solvents DMSO and DMF, the latter of which were able to dissolve monomer **UR9** in a higher concentration, but are less straightforward to be

removed from the resulting network. Further, acetone was tested as potential solvent. The results of the curing test reactions with monomer **UR9** are shown in **Table 19**.

**Table 19.** Synthesis of PHU networks from monomers **UR9** and **T4** in different solvents. The values of the concentrations correspond to the maximum concentration that **UR9** was soluble in, respectively. In. = Irgacure® 819.

entry	solvent	concentration / mol·L <sup>-1</sup>	observation	opacity	name
1	acetone	0.033	precipitation	n. d.	
2	MeOH	0.5	foil formation	opaque	<b>TP3a</b>
3	EtOH	0.33	precipitation	n. d.	
4	DMSO	0.7	foil formation	transparent	<b>TP3b</b>
5	DMF	0.7	foil formation	transparent	<b>TP3c</b>

If methanol was used as solvent, the formation of an opaque foil was observed that was thereafter insoluble, indicating successful cross-linking, but at the same time resulting in precipitation of parts of the polymer (**Table 19**, entry 2).

In DMSO and DMF as solvents, the formation of transparent foils was observed after curing with UV light (**Table 19**, entries 4 and 5). This was taken as a starting point for further investigation. In order to make use of the cross-linked materials, the removal of the used solvent is necessary. For DMF, this was possible via evaporation at elevated temperature under reduced pressure. For the removal of DMSO, on the other hand, another strategy had to be applied. The DMSO within the network was removed by solvent exchange with methanol. For this, the material was left to swell in an excess of methanol for 15 minutes. Subsequently, the swelling solution was replaced with pure methanol and the same procedure was repeated five times. Afterwards, the remaining methanol was removed in a vacuum oven over night. Subsequent IR spectra and TGA analysis did not show any remaining solvent (see **Figure 68** and **Supplementary Figure 109**).

**Figure 68** shows the IR spectrum of the PHU network **TP3b** synthesized in DMSO as solvent according to **Table 19**, entry 4. In the IR spectrum, relevant signals from the PHU network structure could be assigned, such as the stretching vibrations  $\nu(\text{C}=\text{O})$  and  $\nu(\text{C}-\text{O}-\text{C})$  and the deformation vibration  $\delta(\text{N}-\text{H})$  belonging to the ester and urethane groups, as well as the stretching vibration of the thioether linkages,  $\nu(\text{C}-\text{S})$ .

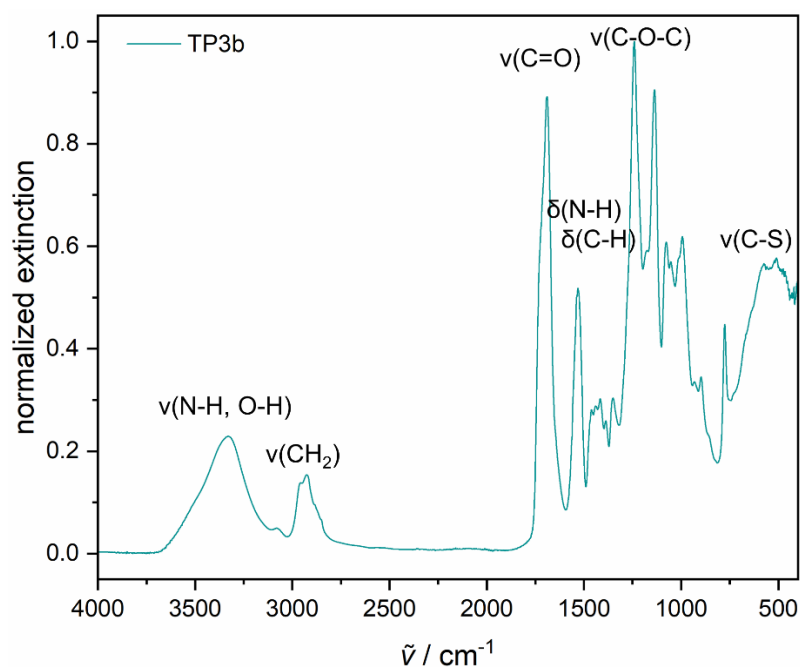


**Figure 68.** IR spectrum of **TP3b** synthesized in DMSO as solvent according to **Table 19**, entry 4, and subsequent solvent exchange with methanol.

With this procedure at hand, it was possible to synthesize cross-linked polymers in DMSO as solvent, which is preferable to DMF concerning health hazards. At the same time, attempts were directed towards strategies to avoid even the use of DMSO, since the methanol necessary for solvent exchange creates extra waste, and further the solvent exchange is also expected to remove the gel content of the material. One possible strategy for a material synthesis without DMSO as solvent was to use mixtures of the monomers **UR3** and **UR9**, thus decreasing the concentration of the poorly soluble monomer **UR9**. As such, different mixtures of **UR3** and **UR9** were cured in a 0.5 M methanol solution in the presence of 1 wt% Irgacure<sup>®</sup> 819. The resulting polymeric foils are shown in **Figure 69**.



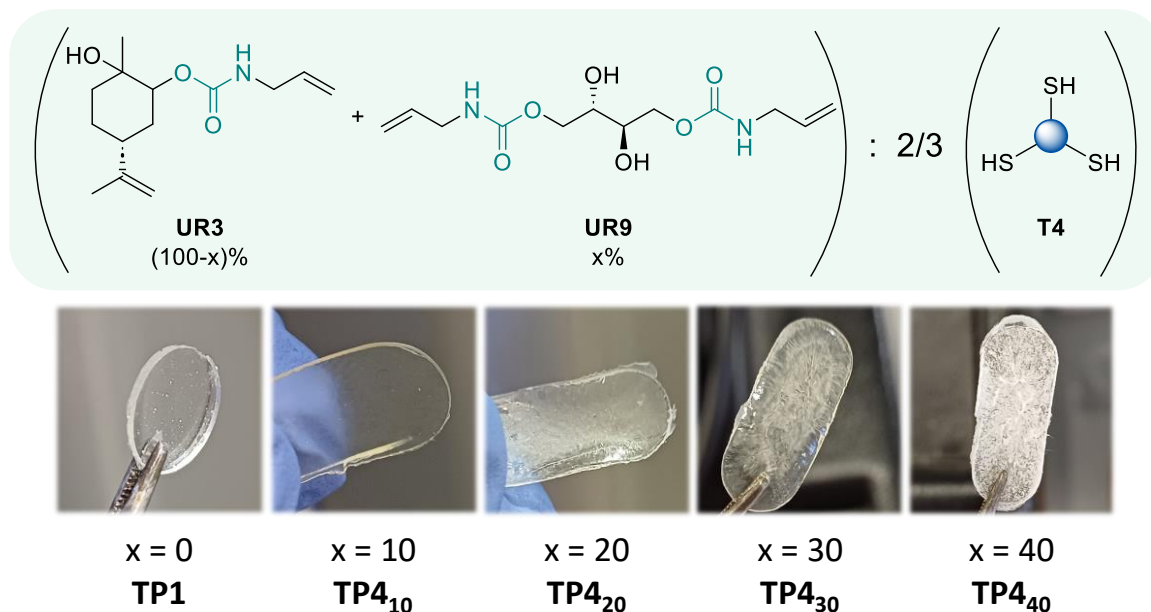


**Figure 69.** Cross-linked materials obtained from monomer mixtures of **UR3** and **UR9** with polythiol **T4** in different ratios. The monomers and 1 wt% Irgacure® 819 were dissolved in methanol (0.5 M with respect to **UR9**) and irradiated with UV light (365 nm) for 30 minutes.

While 10% of monomer **UR9** led to the formation of homogeneous foil **TP4<sub>10</sub>**, some inhomogeneities are visible in the case of 20% **UR9** in **TP4<sub>20</sub>** and especially in **TP4<sub>30</sub>** with 30% monomer **UR9**. Starting from a ratio of 40:60, precipitation of the material was visible, and no homogeneous thermoset could be obtained.

The incorporation of the monomers **UR3** and **UR9** into PHU networks **TP1** and **TP4** was followed via IR spectroscopy. **Figure 70** shows the decrease of the double bond related signals of the C-H and C-H stretching vibrations.

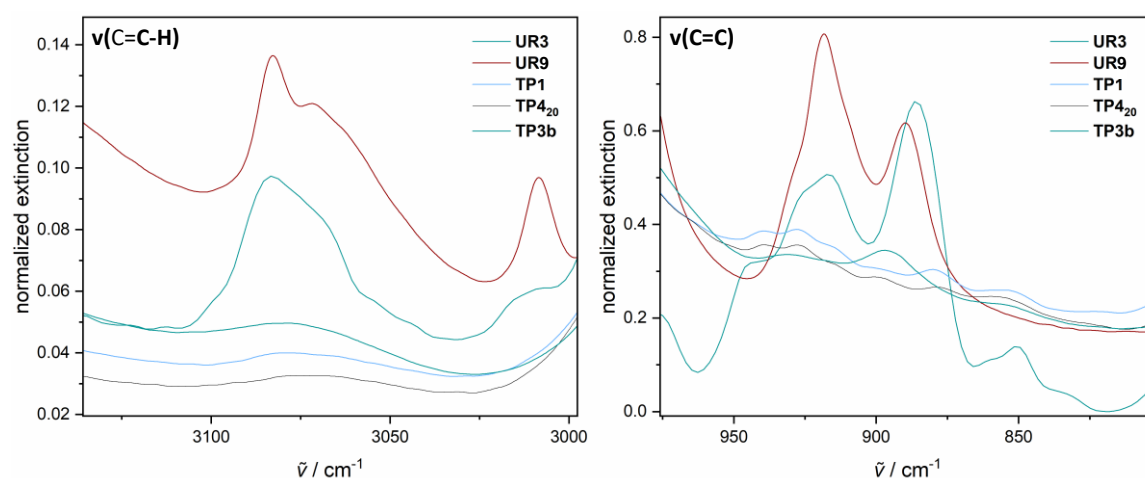


**Figure 70.** IR spectra of double bond signals in monomers **UR3** and **UR9** as well as in the cross-linked materials using ratios **UR9:UR3** of 0:100 (**TP1**), 20:80 (**TP4<sub>20</sub>**), and 100:0 (**TP3b**).

The double bond signals are clearly visible in both monomers but decrease upon cross-linking. This confirms a successful thiol-ene reaction.

The different contents of monomer **UR9** in the polymers **TP4<sub>10</sub>-TP4<sub>30</sub>** influence the signal intensities due to different composition. As such, the relative urethane content in monomer **UR9** is higher than in monomer **UR3**, so the corresponding signals of the urethane groups increase in intensity with higher **UR9** content. This can be seen e.g. in the N-H deformation vibration,  $\delta(\text{N-H})$ , as shown in **Figure 71**, compared for the sugar-based monomer **UR9** and the cross-linked materials **TP4<sub>10</sub>-TP4<sub>30</sub>**. For comparison, the IR spectrum of the trithiol monomer **T4** within the same area is shown. In **T4**, which does not contain urethane linkages, the  $\delta(\text{N-H})$  signal is absent.

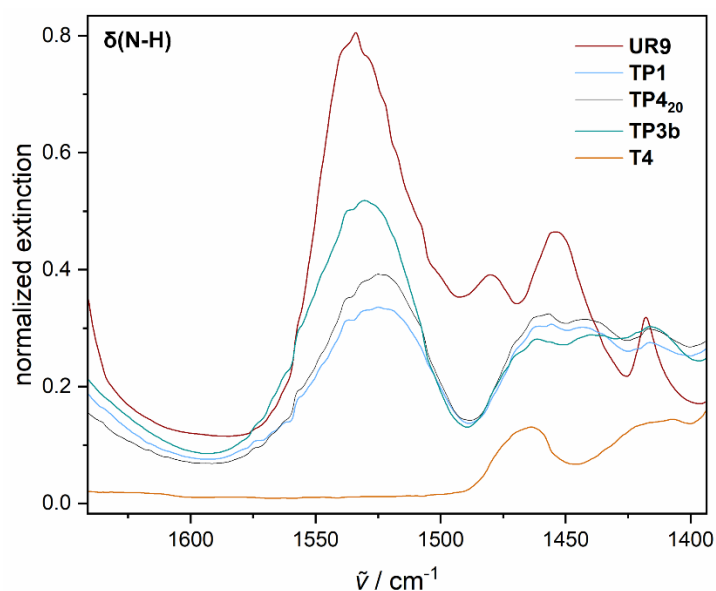


**Figure 71.** IR band of N-H deformation vibration in monomers **UR9** and **T4** as well as in the cross-linked materials using ratios **UR9:UR3** of 0:100 (**TP1**), 20:80 (**TP4<sub>20</sub>**), and 100:0 (**TP3b**).

Besides IR spectroscopy for the analysis of the synthesized PHU networks, DSC analysis was used to determine thermal transitions. **Figure 72** shows the DSC traces of cross-linked materials **TP3a** and **TP3b** using methanol or DMSO as solvent, **TP4<sub>10</sub>-TP4<sub>30</sub>** with different contents of monomer **UR9**, and of **TP1** derived from the terpene-based monomer **UR3**.

From the DSC curves, no clear trend of  $T_g$  values depending on the percentage of monomer **UR9** could be observed, but all materials showed  $T_g$  values slightly above room temperature. In the material **TP3a** cured in methanol as well as in

**TP4<sub>30</sub>** containing 30% of monomer **UR9** as urethane monomer, lower values of  $T_g$  were observed, which can possibly be attributed to lower cross-linking due to precipitation during the UV curing. The  $T_g$  value of **TP1** containing only the terpene monomer is slightly higher than in the first test experiments, which could be due to more efficient cross-linking in the foil.

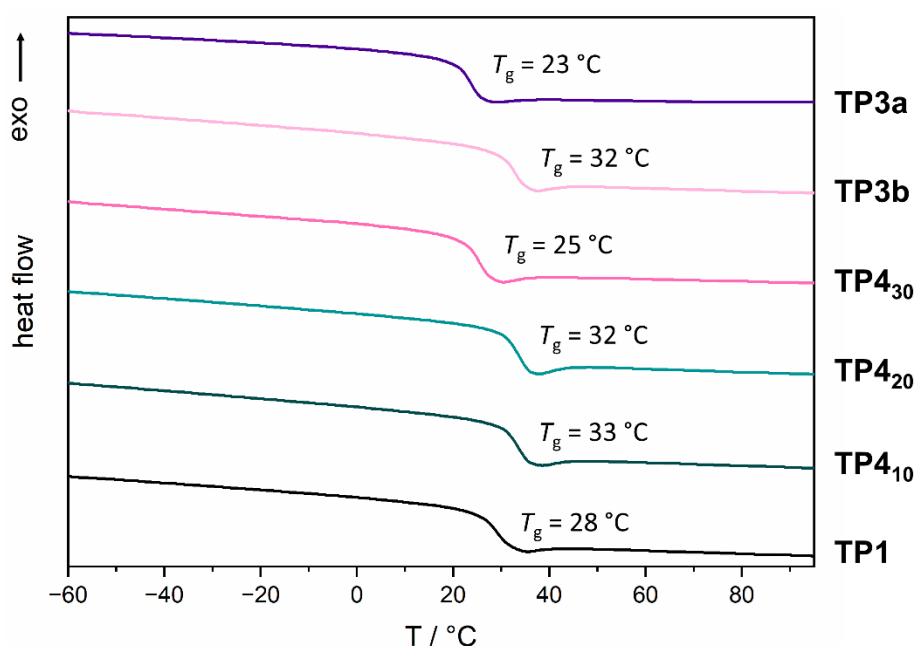


**Figure 72.** DSC traces of PHU network **TP3** cured in methanol (**TP3a**) or DMSO (**TP3b**) as solvents as well as materials **TP4<sub>10</sub>**-**TP4<sub>30</sub>** with different contents of monomer **UR9**, and material **TP1** from the terpene-based monomer **UR3**.

The results show that by adding a second monomer, the diurethane **UR9** can be incorporated into PHU networks without the use of high-boiling solvents like DMSO or DMF.

Besides the dilution of the monomer **UR9** to achieve increased solubility, a second strategy that was explored within this work was a possible protection of the hydroxy groups. This way, the hydroxy groups would not be available for hydrogen bond interactions, thus contributing to a better solubility of the monomer **UR9**. A protection of **UR9** as cyclic ketal with acetone as abundant and benign reagent was attempted to obtain the protected monomer **UR9a** (see **Figure 73**). Stirring at reflux using molecular sieves yielded a product mixture of **UR9** and **UR9a**, as shown in the  $^1\text{H}$  NMR spectrum in **Figure 73**. The content of **UR9a** was determined to be 83–87% based on the signal ratio in the NMR spectrum.

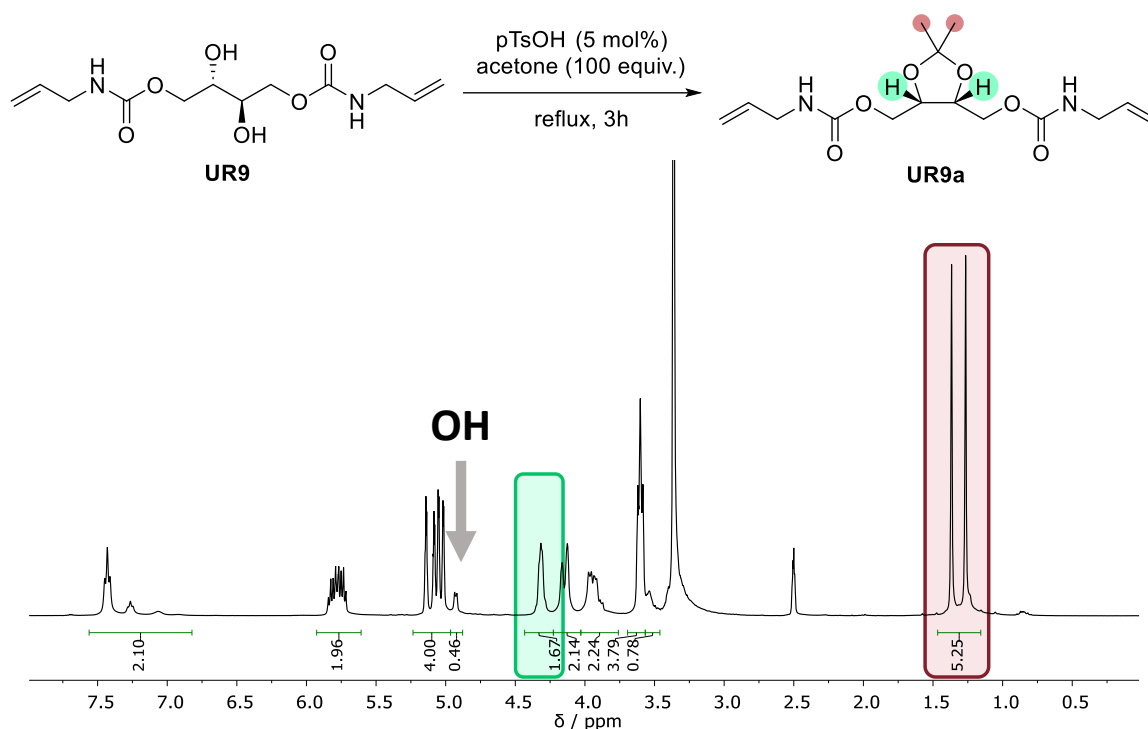


**Figure 73.** Conversion of monomer **UR9** to the protected **UR9a** and the  $^1\text{H}$  NMR spectrum of the resulting product mixture, exhibiting characteristic signals of **UR9a**.

The decreased content of hydroxy groups can possibly improve the solubility of **UR9a**, however, the obtained mixture was still crystalline. This results in a necessity of solvent for a possible network formation. Together with the more complicated procedure of introducing a protecting group and having to remove it after the network formation, this approach did not represent a more sustainable alternative to the use of DMSO as solvent and was therefore no longer pursued. Nevertheless, the possibility of protecting the hydroxy groups within **UR9** was shown and might be extended to the synthesis of acetals with possibly longer alkyl chains to improve solubility.

In a next step, a potential dynamic behavior of these materials in the sense of CANs (see section 2.4) was investigated. For this, stress relaxation experiments were performed, which are a common method to determine dynamicity within thermoset materials. The reconfiguration of dynamic bonds within CANs can lead to a relaxation of stress upon applied strain.

The materials **TP1** and **TP4** were synthesized as foils, therefore they could in principal directly be used for stress relaxation measurements in a rheometer with

a parallel plate geometry. First test experiments of the materials at elevated temperatures showed that the starting value of the relaxation modulus  $G(t)$  increased significantly throughout experiments with increasing temperature, which indicates that the material still reacted. After leaving the materials at 110 °C overnight, a stable value for the modulus was determined. However, this pretreatment caused a coloring of the material, as shown in **Figure 74**.

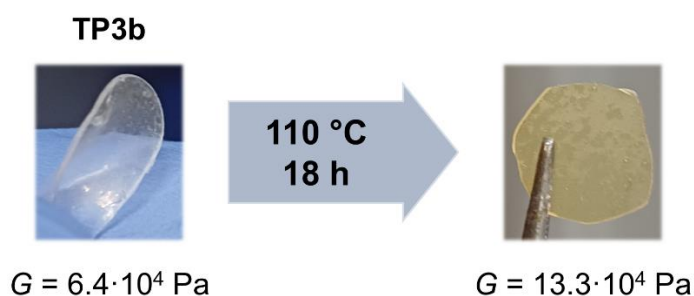


**Figure 74.** Change in color and shear modulus of material **TP3b** after heating to 110 °C overnight.

The preheated samples were used for stress relaxation experiments at 110–120 °C, a temperature range chosen to avoid degradation of the urethane groups. However, no stress relaxation fast enough to be within the range of material reprocessability could be observed. Further, cutting of the material **TP3b** and hot-pressing at 150 °C and 5 MPa did not lead to any reprocessing.

The lack of dynamicity can possibly be attributed to a rigid network of the PHU networks in which the reactive functional groups were not mobile enough to undergo transurethanization or transesterification reactions. Thus, the use of a dithiol as comonomer to lower the cross-linking density was investigated, as shown in **Figure 75**. As linear dithiols, commercially available 1,10-decanedithiol **T1** and 3,6-dioxa-1,8-octanedithiol **T6** were tested.

When using **T1** as comonomer in a ratio of 1:1 to **T4** concerning the double bond equivalents in DMSO as solvent, a transparent foil of **TP5** was obtained that became opaque upon solvent removal. This could possibly be attributed to phase separation due to the different polarity of the monomers. Therefore, **T6** was tested as alternative comonomer for the material **TP6**, leading to the formation of a homogeneous foil even after solvent exchange and drying in vacuum oven.

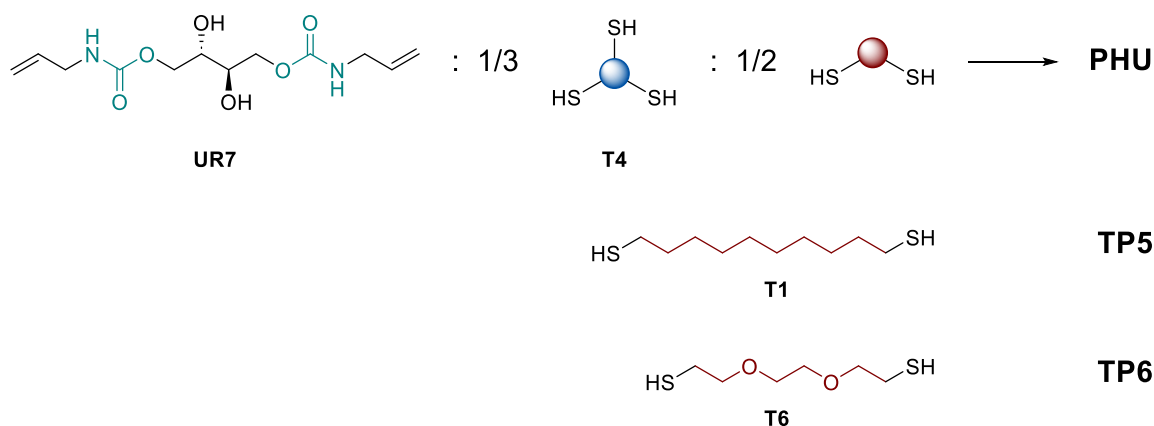


**Figure 75.** PHU network formation using a mixture of trithiol and dithiols **T1** or **T6**, yielding the polymeric materials **TP5** and **TP6**, respectively.

In a parallel approach, the addition of a catalyst to the reaction mixture was investigated. Since the materials from the sugar-based monomer **UR9** required solvent exchange after curing, this strategy was tested for the material **TP1** from the monomer **UR3** without the use of solvent. As catalyst,  $\text{Ti}(\text{OBu})_4$  was tested. 2 wt.% of  $\text{Ti}(\text{OBu})_4$  could successfully be implemented into the material by adding it to the reaction mixture before curing, yielding the material **TP7**.

Hot-pressing of **TP6** and **TP7** at 130 °C and 3 MPa showed a partial reprocessability, as shown in **Figure 76**.

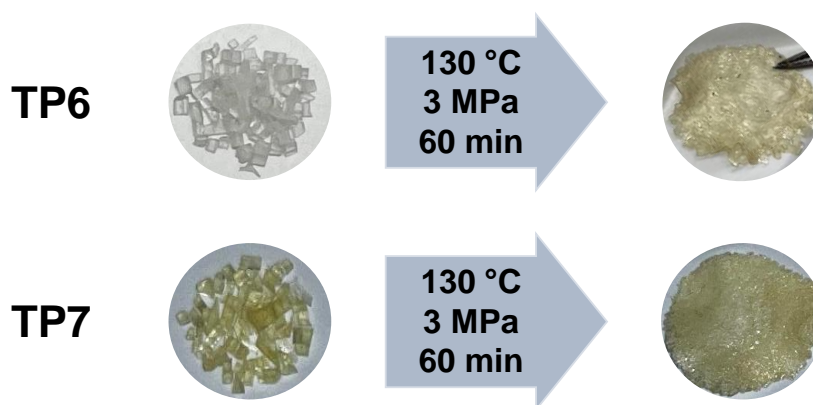


**Figure 76.** Reprocessing of the materials **TP6** and **TP7** under elevated temperature and pressure.

This can be seen as a starting point to obtain CANs from monomers **UR3** and **UR9**, but further optimization of the synthesis procedures and thorough characterizations are necessary to underline these findings. Possibly, a combination of several approaches investigated within this section could lead to suitable materials for

applications involving reprocessability. The use of monomer mixtures of **UR3** and **UR9**, as shown in **Figure 69**, results in a higher density of possibly dynamic hydroxyurethane groups compared to using only **UR3** as monomer (see **Figure 71**) and further enables the use of methanol as solvent, which can be removed by evaporation. Implementation of catalysts into these materials might lead to a higher dynamicity. Next to  $\text{Ti}(\text{OBu})_4$ , other Lewis acids or organic Brønsted acids can be tested as catalysts to catalyze potential transesterification reactions. Moreover, creating a more mobile network by adding dithiol comonomers can be tested for different dithiol to trithiol ratios to optimize the reprocessability of the materials. These challenges remain to be addressed in future work, for which the investigations within this section lay the groundwork.





## 5. CONCLUSION

In this work, different strategies for more sustainable approaches towards polyester and NIPU materials were investigated. For this, benign functionalization of renewable feedstock was addressed, especially focusing on the use of organocatalysis to activate carbonyl compounds.

For the synthesis of polyesters,  $\epsilon$ CL was polymerized efficiently, either using TBD as organocatalyst or a catalyst system of DBU and electron-poor thioureas, the latter of which were synthesized via an established, more sustainable multi-component reaction approach. It was shown that thioureas carrying sulfone or ester moieties, both more benign functional groups compared to typically applied  $\text{CF}_3$  groups, could substitute the commonly used  $\text{CF}_3$  motif as cocatalysts to achieve polyesters with narrow dispersity values ( $D \leq 1.07$ ). This represents an improvement with regard to sustainability as a possibility to avoid fluorinated reagents. Future work on this subject could include the use of more sustainable guanidine or amidine bases to substitute TBD and DBU. Furthermore, additional research may open the possibility to extend the developed approach to the use of renewable terpene-derived substrates as ROP monomers, for which different attempts were already addressed within this work.

The use of thiourea organocatalysts was further investigated for different strategies towards NIPU materials. Thus, thiourea catalysts enabled the activation of terpene-based cyclic carbonates to obtain hydroxyurethane monomers with two terminal double bonds. The catalytic effect of the thiourea catalysts was especially observed for limonene-derived endocyclic carbonate groups. For the exocyclic carbonate groups as well as for the synthesis of an erythritol-based di(hydroxyurethane) monomer, no activation by thioureas was necessary. The regioselectivity of the carbonate opening was studied thoroughly for all substrates.

The obtained hydroxyurethane monomers derived from limonene and erythritol were used successfully for the synthesis of linear NIPUs with molecular weights between 6 and 31  $\text{kg}\cdot\text{mol}^{-1}$ . Thiol-ene polyaddition with different dithiols proved to be a suitable tool to obtain NIPUs efficiently at room temperature. The obtained results thus bring forward the implementation of terpene and erythritol derivatives into polyurethane structures without the need for isocyanates. For this purpose, the

showcased approaches using a combination of thiourea catalysis and thiol-ene reaction enable the use of less activated cyclic carbonates. Moreover, no use of polyamines is needed, whose sustainable synthesis from renewable feedstock remains a challenge.

In general, the synthesized renewable hydroxyurethane monomers represent promising building blocks for the synthesis of PHU materials. As such, investigations towards the synthesis of PHU networks by thiol-ene curing with polythiols were performed within this work, establishing suitable reaction conditions for successful cross-linking at room temperature. Considering future work, the exploitation of the hydroxyurethane and ester groups within these networks to achieve possible dynamic behavior remains to be investigated. The implementation of a Lewis acid as well as the use of monomer mixtures of dithiols and trithiols were shown to increase the reprocessability of the PHU networks and are therefore starting points for further optimization.

Overall, the approaches investigated within this work represent fundamental research on more sustainable polymer synthesis. The twelve principles of Green Chemistry were used as a guiding philosophy in all developed strategies, with special focus on the use of organocatalysis, renewable feedstock, and non-toxic reagents, with the aim to contribute to a possible transition towards a greener economy.

## 6. EXPERIMENTAL SECTION

### 6.1. Methods

#### 6.1.1. Materials

(*R*)-(+)-limonene (Sigma Aldrich, 97%), (*R*)-(+)-dihydrocarvone (Acros Organics, 98%) (*S*)-(+)-carvone (Sigma Aldrich, 98%), 1,10-decanedithiol (TCI, >98%), 1-isothiocyanato-3,5-bis(trifluoromethyl)benzene (fluorochem), 1,4-butanedithiol (Sigma Aldrich, >97%), 1,5,7-triazabicyclo[4.4.0]dec-5-ene (TCI, >98%), 1,8-diazobicyclo[5.4.0]-7-undecene (TCI, >98.0%), 1-bromohexane (fluorochem), 1-butanol (Sigma Aldrich, ≥99%), 2,2'-dimethoxy-2-phenylacetophenone (Sigma Aldrich, 99%), 2-butanone (Sigma Aldrich, ≥99%), 2-methyl tetrahydrofuran (Acros Organics, anhydrous, stabilized), 2-methylpentane-2,4-diol (Fluka, >99%), 3,6-dioxo-1,8-octanethiol (Sigma Aldrich, 95%), 4-aminothiophenol (fluorochem), 10-undecenoic acid (Sigma Aldrich, 98%), α-(+)-pinene (Sigma Aldrich, 98%), γ-terpinene (Sigma Aldrich, >97%) acetic acid (Fluka, >99.8%), acetone (Honeywell, ≥99.8%), acetonitrile (Fisher Scientific, HPLC gradient grade), allylamine (abcr, 98%), allyl isocyanate (Fisher Scientific, 98%), ammonium chloride (technical grade, BASF), anisole (Sigma Aldrich, 99%), aniline (Acros Organics, 98%), bis-(bis-3,5-(trifluoromethyl)phenyl) thiourea (>98%, TCI), butane-1,4-diol (Acros Organics, 99+%), chloroform (Fisher Scientific, >99.8%), chloroform-*d* (Eurisotop, 99.8% D), cyclohexane (VWR, HPLC grade), cyclohexylamine (Sigma Aldrich, ≥99.9%), cyclohexyl isocyanide (Sigma Aldrich, 98%), dichloromethane (Fisher Scientific, HPLC grade, ≥99.8%), diethyl ether (technical grade, VWR), diisopropylamine (Sigma Aldrich, >99.5%), dimethyl carbonate (Sigma Aldrich, 99%), dimethyl formamide (Fisher Scientific, ≥99%) dimethyl sulfoxide (Fisher Scientific, ≥99.9%), dimethyl sulfoxide-*d*<sub>6</sub> (Eurisotop, 99.80% D), erythritol (Alfa Aesar, 99%), ethanol (Fisher Scientific, ≥99.8%), ethyl acetate (VWR, HPLC grade), formic acid (Carl Roth, ≥98%), hexan-1-amine (Sigma Aldrich, 99%), hydrochloric acid (37 % solution in water, Acros Organics), hydrogen peroxide solution (30%), hydrogen (Air Liquide, 99.999%), hydroxylamine hydrochloride (Acros Organics, >99%), *meta*-chloroperoxybenzoic

acid (Sigma Aldrich,  $\geq 77\%$ ), methanol (VWR, HPLC grade), *N*-bromo succinimide (abcr, 99%), *n*-hexane (technical grade), Oxone<sup>®</sup> (Sigma Aldrich), oxygen (Air Liquide, 99.5%), palladium on activated charcoal (Sigma Aldrich, 10% Pd basis), Pentaerythritol-tetrakis(3-mercaptopropionate) (Sigma Aldrich, 97%), phosphorus oxychloride (Acros Organics, 99%), potassium hydroxide (Bernd Kraft, for analysis), sodium bicarbonate (Sigma Aldrich,  $>95\%$ ), sodium chloride (Fisher Scientific, 99.5%), sodium hydroxide (Carl Roth,  $\geq 99\%$ ), sodium sulfate anhydrous (Acros Organics, 99%), sodium sulfite (anhydrous), sodium thiosulfate (technical grade), sulfur (elemental, technical grade), tetrabutylammonium bromide (Acros Organics, 98%), tetrabutylammonium chloride (Sigma Aldrich,  $\geq 97.0\%$ ), tetrabutylammonium iodide (Sigma Aldrich,  $\geq 99.0\%$ ), tetrahydrofuran (Sigma Aldrich,  $\geq 99.9\%$ ), tetraphenyl porphyrine (TCI), thioacetic acid (Alfa Aesar, 97%), toluene (Acros Organics, 99.85%), triethylamine (Sigma Aldrich,  $\geq 99.5\%$ ), trimethylolpropane tris(3-mercaptopropionate) (Sigma Aldrich,  $\geq 95\%$ ).

### 6.1.2. General Methods and Instrumentation

#### Thin Layer Chromatography (TLC)

TLC was performed on aluminium plates coated with silica gel of the type 60 F<sub>254</sub> from Sigma Aldrich. The compounds on the plates were visualised via fluorescence quenching with 254 nm UV light or by staining with Seebach solution (2 g cerium(IV) sulfate, 5 g phosphomolybdic acid hydrate, 16 mL concentrated sulfuric acid, 200 mL water), vanillin solution (15 g vanillin, 2.5 mL concentrated sulfuric acid, 250 mL ethanol), or KMnO<sub>4</sub> staining solution (1.5 g KMnO<sub>4</sub>, 10 g K<sub>2</sub>CO<sub>3</sub>, 1.25 mL 10% NaOH and 200 mL water).

#### Flash Column Chromatography

Flash Column Chromatography was performed with silica gel 60 purchased from Sigma Aldrich. For automatic flash column chromatography, a Biotage<sup>®</sup> Isolera<sup>™</sup> One Flash Column equipped with a UV-Vis detector (200 × 800 nm) with Biotage<sup>®</sup> Sfär Silica HC Duo Columns was used. All solvents were used in HPLC grade.

## Nuclear Magnetic Resonance (NMR) Spectroscopy

$^1\text{H}$  and  $^{13}\text{C}$  NMR spectra were recorded at ambient temperature with a Bruker AVANCE DPX 400 spectrometer at 400 MHz for  $^1\text{H}$  NMR and 101 MHz for  $^{13}\text{C}$  NMR or with a Bruker AVANCE DPX 500 spectrometer at 500 MHz for  $^1\text{H}$  NMR and 126 MHz for  $^{13}\text{C}$  NMR. Chemical shifts  $\delta$  are reported in ppm relative to the solvent signal of  $\text{CDCl}_3$  (7.26 ppm for  $^1\text{H}$  and 77.16 ppm for  $^{13}\text{C}$  spectra) or  $\text{DMSO-}d_6$  (2.50 ppm for  $^1\text{H}$  and 39.52 ppm for  $^{13}\text{C}$  spectra). Spin multiplicity and corresponding signal patterns were reported as follows: s = singlet, d = doublet, t = triplet, q = quartet, m = multiplet and br = broadened. Coupling constants ( $J$ ) are reported in Hertz (Hz). For full assignment of the signals to the measured structure,  $^1\text{H}$ - $^1\text{H}$  Correlated Spectroscopy ( $^1\text{H}$ - $^1\text{H}$ -COSY),  $^1\text{H}$ - $^{13}\text{C}$  Heteronuclear Single Quantum Coherence ( $^1\text{H}$ - $^{13}\text{C}$ -HSQC), and  $^1\text{H}$ - $^{13}\text{C}$  Heteronuclear Multiple Bond Correlation ( $^1\text{H}$ - $^{13}\text{C}$ -HMBC) were used.

## Fourier-Transformation Infrared (FT-IR) Spectroscopy

FT-IR spectra were recorded using a Bruker Alpha-P instrument applying ATR technology in a range of  $\tilde{\nu} = 400\text{--}4000\text{ cm}^{-1}$  with 24 scans per measurement.

## High-Resolution Mass Spectrometry (HRMS)

Mass spectra were recorded on a Q Exactive (Orbitrap) mass spectrometer (Thermo Fisher Scientific, San Jose, CA, USA) equipped with an atmospheric pressure ionization source operating in the nebulizer assisted electrospray mode. Calibration of the instrument was done in the  $m/z$ -range 150–2000 using a standard containing caffeine, Met-Arg-Phe-Ala acetate and a mixture of fluorinated phosphazenes (Ultramark 1621) (all from Sigma-Aldrich). A constant spray voltage of 3.5 kV, a dimensionless sheath gas of 6 and a sweep gas flow rate of 2 were applied. The capillary voltage and the S-lens RF level were set to 68.0 V and 320 °C, respectively.

## Gas Chromatography – Flame Ionization Detector (GC-FID)

GC-FID screenings were conducted using a Bruker 430 GC instrument with a capillary column FactorFour™ VF-5ms (30 m × 0.25 mm × 0.25 mm) and a flame ionization detector (FID). The measurements proceeded via standard measurement method: initial temperature 95 °C, heat to 200 °C with 15 °C·min<sup>-1</sup>, hold 200 °C for 4 min, heat to 300 °C with 15 °C·min<sup>-1</sup> and then hold 300 °C for 2

min. The sample preparation consisted of dissolving 1.5–3.0 mg of the compound in 1.5 mL of ethyl acetate. The mixture was filtered by syringe filter prior to use to avoid plugging of the injection setup or the column.

For the determination of isomeric ratios, GC-FID measurements were performed using an Agilent 8860 gas chromatograph with a HP-5 column (30 m × 0.32 mm × 0.25 μm) and a flame ionization detector (FID). The measurements were carried out using the following heating program of the oven: initial temperature 95 °C, hold for 1 min, ramp up to 200 °C with a rate of 15 °C·min<sup>-1</sup>, hold 200 °C for 4 min, ramp up to 300 °C with a rate of 15 °C·min<sup>-1</sup>, and then hold at 300 °C for 2 min. Measurements were performed in split-split mode using nitrogen as the carrier gas (flow rate 30 mL·min<sup>-1</sup>) and were recorded for 20 min in total. For sample preparation, 1.5 mg of the substances were dissolved in 1.5 mL ethyl acetate and filtrated by syringe filter to avoid plugging of the injection setup or the column. The injection volume was set to 1 μL and the injection temperature to 220 °C.

### **Size Exclusion Chromatography (SEC)**

For reaction monitoring of monomer synthesis, SEC measurements were performed in THF on a PSS SECcurity<sup>2</sup> GPC system based on Agilent infinity 1260 II hardware. The system was equipped with an autosampler SECcurity<sup>2</sup>, a SECcurity<sup>2</sup> isocratic pump, a column oven (Bio)SECcurity<sup>2</sup> column compartment TCC6500, and a refractive index detector SECcurity<sup>2</sup> RI. Analysis was performed using two PSS SDV analytical columns (3 μm, 300 × 8.0 mm<sup>2</sup>, 1000 Å) with a PSS SDV analytical precolumn (3 μm, 50 × 8.0 mm<sup>2</sup>). The flow rate for measurements was set to 1 mL·min<sup>-1</sup>. The system was calibrated with narrow linear poly(methyl methacrylate) standards (Polymer Standards Service, PSS, Germany) ranging from 102 to 62200 Da.

Polymer samples were characterized on a Shimadzu SEC system equipped with a Shimadzu isocratic pump model LC-20AD, a Shimadzu refractive index detector (24 °C) model RID-20A, a Shimadzu autosampler model SIL-20A, and a Varian column oven model 510 (50 °C). For separation, a three-column setup was used with one SDV 3 μm, 8 × 50 mm precolumn and two SDV 3 μm, 1000 Å, 3 × 300 mm columns supplied by PSS, Germany. THF stabilized with 250 ppm butylated hydroxytoluene (BHT, ≥99.9%) supplied by Sigma-Aldrich was used at a

flow rate of  $1.0 \text{ mL}\cdot\text{min}^{-1}$ . For sample preparation, the amount of sample corresponding to 1.5 mg of expected polymer was dissolved in 1.5 mL of the mobile phase and filtrated by syringe filter to avoid plugging of the injection setup or the column. For calibration, six poly(methyl methacrylate) standards (Agilent) ranging from 1102 Da to 62200 Da were used. The peak around 20.15 min is a system peak and does not belong to any impurities. The values of  $M_n$ ,  $M_w$  and  $\bar{D}$  were determined by integration of the peaks in LabSolution software based on the performed calibration.

SEC measurements of higher molecular weight polymers were performed on a Shimadzu SEC system equipped with a Shimadzu isocratic pump (LC-20AD), a Shimadzu refractive index detector (30 °C) (RID-20A), a Shimadzu autosampler (SIL-20A) and a Shimadzu column oven (30 °C). The column system comprised a SDV 5  $\mu\text{m}$ , 8  $\times$  50 mm precolumn, a SDV 5  $\mu\text{m}$ , 1,000 Å, 8  $\times$  300 mm column and a SDV 5  $\mu\text{m}$ , 100000 Å, 8  $\times$  300 mm column supplied by PSS, Germany. A mixture of THF stabilized with 250 ppm butylated hydroxytoluene (BHT,  $\geq 99.9\%$ ) and 2 vol.% triethylamine ( $\geq 99.5\%$ ) supplied by Sigma Aldrich was used at a flow rate of  $1.00 \text{ mL}\cdot\text{min}^{-1}$ . For sample preparation, the amount of sample corresponding to 1.5 mg of expected polymer was dissolved in 1.5 mL of the mobile phase and filtrated by syringe filter to avoid plugging of the injection setup or the column. Calibration was carried out by injection of ten poly(methyl methacrylate) standards ranging from 1102 Da to 981000 Da. The values of  $M_n$ ,  $M_w$  and  $\bar{D}$  were determined by integration of the peaks in LabSolution software based on the performed calibration.

### Differential Scanning Calorimetry (DSC)

DSC measurements were performed on a Mettler Toledo DSC1 instrument equipped with a sample robot. Samples of 5–10 mg were loaded in a 100  $\mu\text{L}$  aluminum crucible with pierced lid, and the measurements were performed under nitrogen atmosphere with a flow rate of  $50 \text{ mL}\cdot\text{min}^{-1}$ . The DSC thermograms were recorded at a heating/cooling rate of  $10 \text{ K}\cdot\text{min}^{-1}$  using the following heating/cooling program: first heating from 20 to 110 °C, then cooling from 110 to  $-70$  °C, and a final heating step from  $-70$  to 110 °C. The data from the last heating step are shown in the DSC curves.

## 6.2. Experimental Procedures

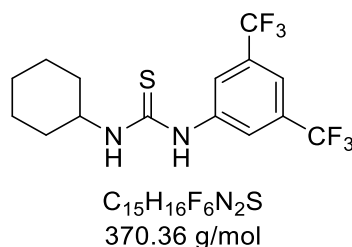
### 6.2.1. Synthesis of thiourea catalysts

Compounds **TU2**, **1**, **2**, **3**, **4**, **8**, **11**, **TU5**, and **TU6** were synthesized by the author of this thesis.

Compounds **TU1** and **TU3** were synthesized by Michelle Karsten under co-supervision of the author of this thesis.

Compounds **9**, **10**, and **TU4** were synthesized by Hendrik Kirchhoff under co-supervision of the author of this thesis.

#### ***N*-(3,5-Bis(trifluoromethyl)phenyl)-*N'*-cyclohexyl thiourea **TU1****



2.00 g (7.38 mmol, 1.00 equiv.) 1-Isothiocyanato-3,5-bis(trifluoromethyl)benzene were dissolved in 7.5 mL ethyl acetate. 0.94 mL (810 mg, 8.1 mmol, 1.1 equiv.) cyclohexylamine were added and the mixture was stirred at room temperature until TLC (cyclohexane/ ethyl acetate 2:1) detected full conversion. Afterwards, 10 mL water and 10 mL ethyl acetate were added, and the phases were separated. The aqueous phase was extracted with ethyl acetate (2 × 25 mL) and washed with water (2 × 25 mL). After drying over  $Na_2SO_4$ , the solvent was removed under reduced pressure and 2.65 g (7.16 mmol, 97%) of the product were obtained as colorless solid.

$R_f$  (cyclohexane/ethyl acetate 2:1) = 0.72, visualized by staining with  $KMnO_4$  solution.

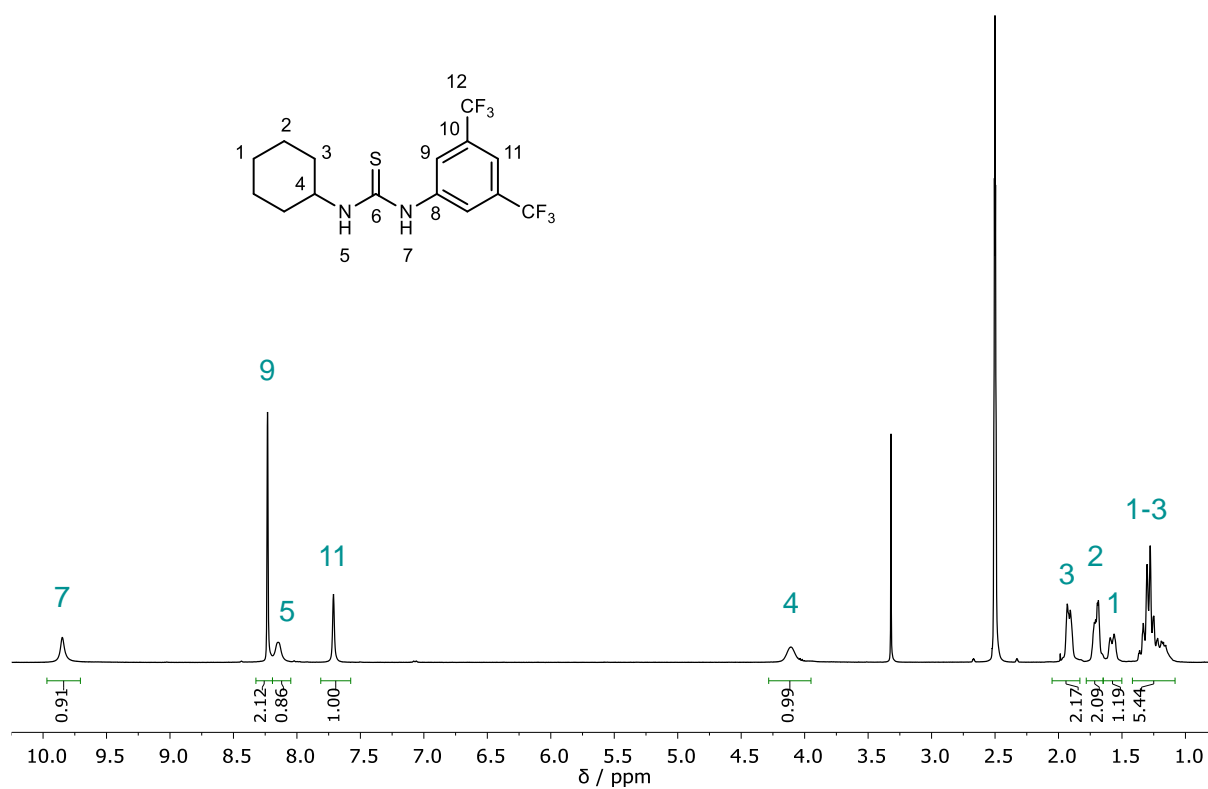
$^1H$  NMR (400 MHz,  $DMSO-d_6$ )  $\delta$  / ppm = 9.85 (br s, 1H, **H7**), 8.23 (s, 2H, **H9**), 8.14 (br s, 1H, **H5**), 7.71 (s, 1H, **H11**), 4.10 (m, 1H, **H4**), 2.05–1.83 (m, 2H, **H3**), 1.78–1.65 (m, 2H, **H2**), 1.66–1.50 (m, 1H, **H1**), 1.42–1.09 (m, 5H, **H1–3**).

$^{13}C$  NMR (101 MHz,  $DMSO-d_6$ )  $\delta$  / ppm = 179.2 (**C6**), 142.0 (**C8**), 130.1 (q,  $^2J = 32.2$  Hz, **C10**), 123.2 (q,  $^1J = 273.6$  Hz, **C12**), 121.7 (**C9**), 115.8 (**C11**), 52.3 (**C4**), 31.6 (**C3**), 25.1 (**C1**), 24.4 (**C2**).

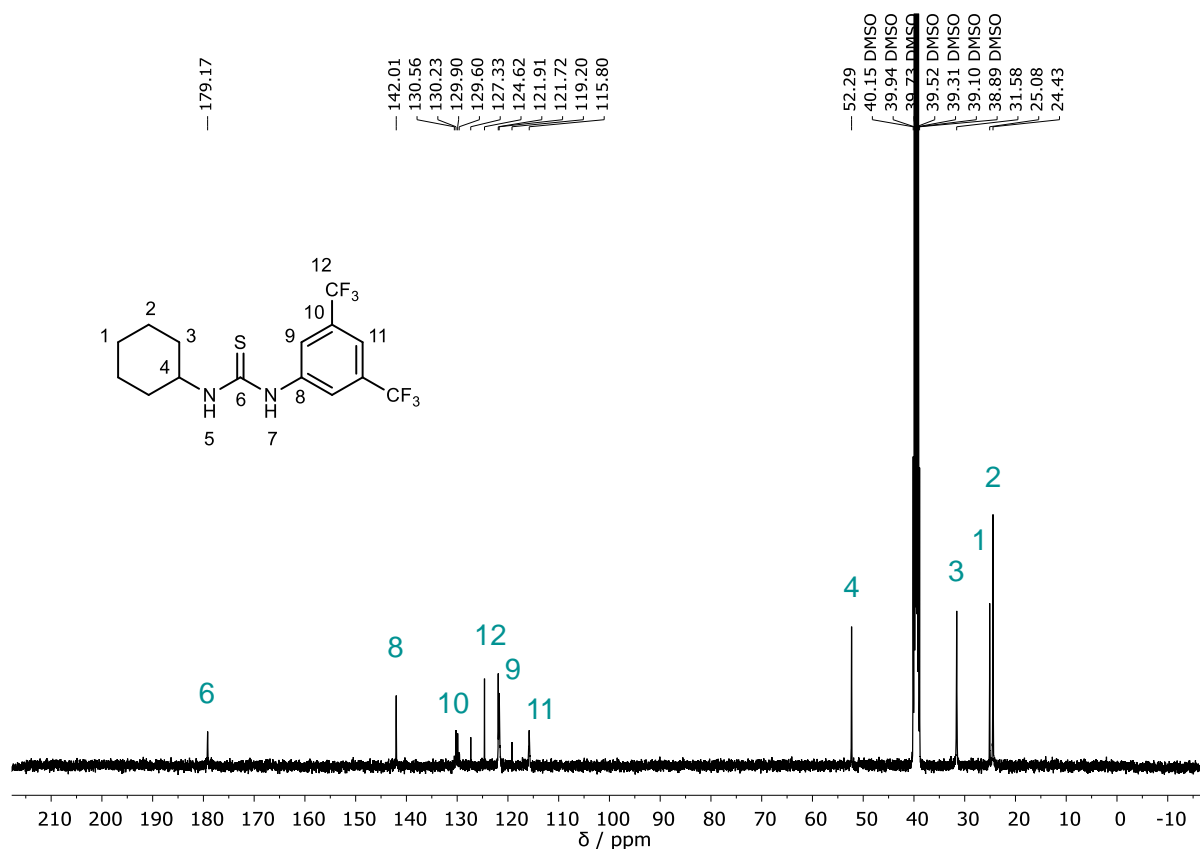


**IR (ATR platinum diamond):**  $\tilde{\nu}$  /  $\text{cm}^{-1}$  = 3281, 3189, 3163, 3040, 3001, 2933, 2860, 1791, 1622, 1553, 1526, 1467, 1437, 1382, 1364, 1336, 1269, 1176, 1127, 1105, 1039, 1024, 941, 904, 888, 862, 847, 810, 754, 706, 679, 618, 587, 516, 468, 454, 420.

**ESI-MS:**  $[\text{M}+\text{H}]^+$  calc. 371.1011, detected 371.1003.

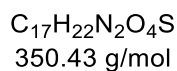
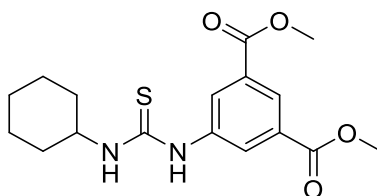


**Supplementary Figure 1.**  $^1\text{H}$  NMR spectrum of TU1, measured in  $\text{DMSO}-d_6$  at 400 MHz.



**Supplementary Figure 2.**  $^{13}\text{C}$  NMR spectrum of TU1, measured in  $\text{DMSO}-d_6$  at 101 MHz.

### *N*-(5-(Dimethylisophthalate))-*N'*-cyclohexyl thiourea TU2



5-Isocyano dimethylisophthalate was synthesized previously by Roman Nickisch. The product was prepared according to a literature-known procedure.<sup>521</sup>

To a dispersion of 164 mg (0.639 mmol, 0.140 equiv.) elemental sulfur in 5.06 mL methanol (0.90 M corresponding to isocyanide), 575  $\mu\text{L}$  (498 mg, 5.02 mmol, 1.10 equiv.) cyclohexylamine were added. 1.00 g (4.56 mmol, 1.00 equiv.) 5-isocyano dimethylisophthalate were added and the reaction mixture was stirred at room temperature for 4 days. Afterwards, 13 mL methanol were added and the mixture was left to crystallize for 3 days at room temperature. Filtration of the

product, washing with a minimal amount of methanol, and removal of the solvent yielded 1.33 g (3.80 mmol, 83%) of the product as a slightly yellow powder.

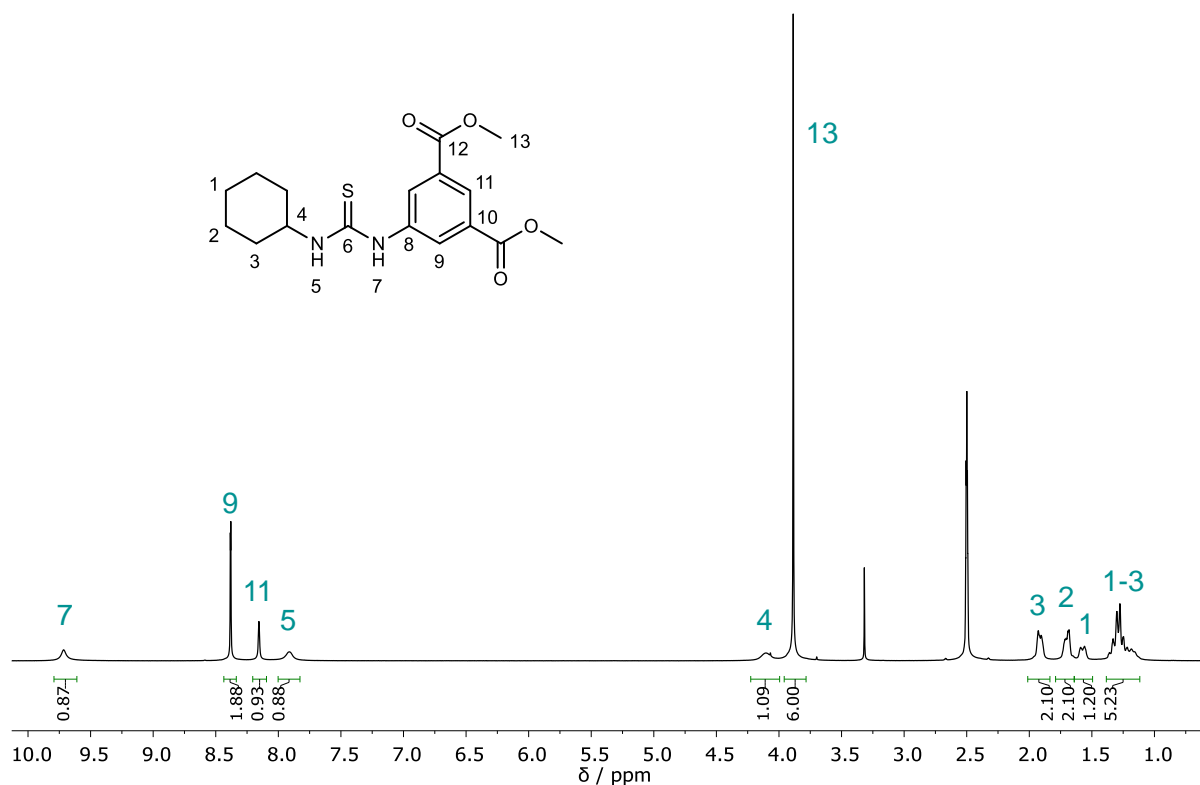
$R_f$  (cyclohexane/ethyl acetate 3:1) = 0.17, visualized by staining with vanillin solution.

$^1\text{H NMR}$  (400 MHz,  $\text{DMSO-}d_6$ )  $\delta$  / ppm = 9.72 (bs, 1H, **H7**), 8.43–8.34 (m, 2H, **H9**), 8.16 (s, 1H, **H11**), 7.92 (bs, 1H, **H5**), 4.14–4.04 (m, 1H, **H4**), 3.89 (s, 6H, **H13**), 1.96–1.87 (m, 2H, **H3**), 1.74–1.66 (m, 2H, **H2**), 1.60–1.54 (m, 1H, **H1**), 1.36–1.13 (m, 5H, **H1–3**).

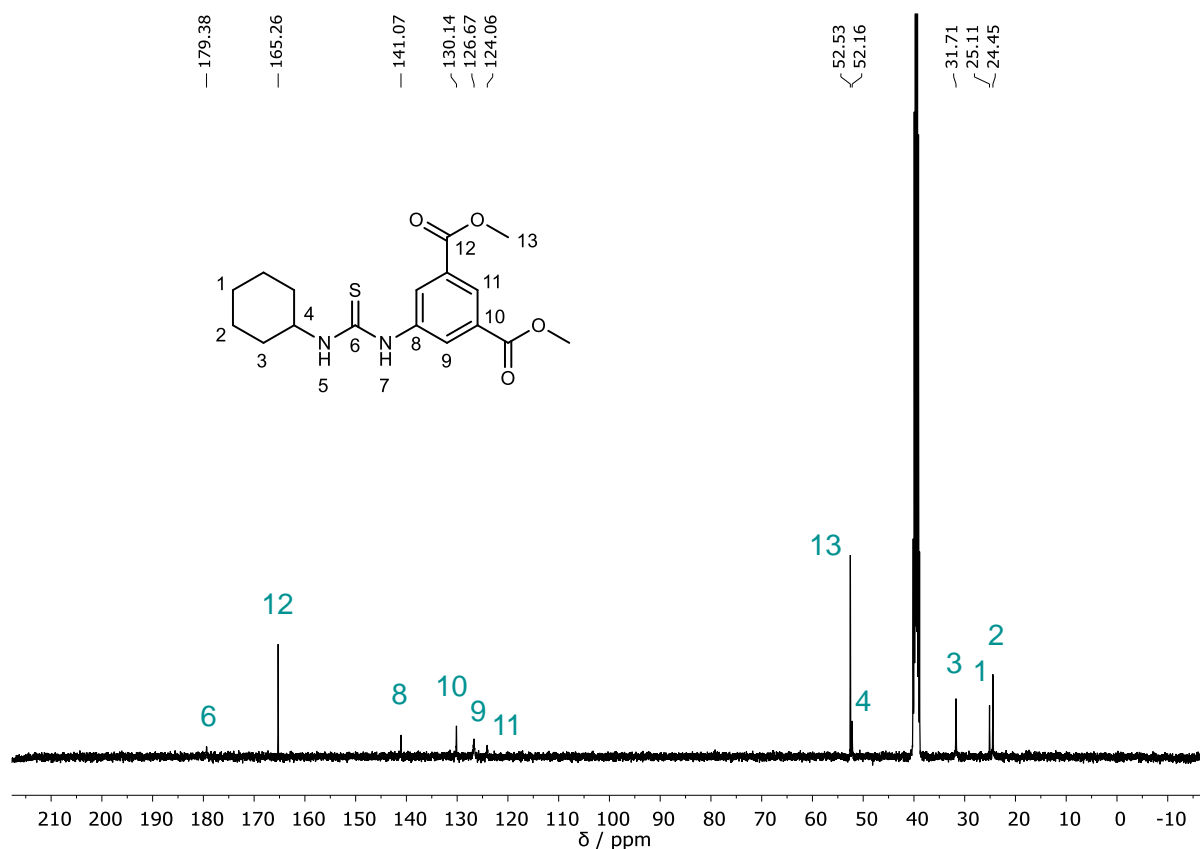
$^{13}\text{C NMR}$  (101 MHz,  $\text{DMSO-}d_6$ )  $\delta$  / ppm = 179.4 (**C6**), 165.3 (**C12**), 141.1 (**C8**), 130.1 (**C10**), 126.7 (**C9**), 124.1 (**C11**), 52.5 (**C13**), 52.2 (**C4**), 31.7 (**C3**), 25.1 (**C1**), 24.4 (**C2**).

**IR (ATR platinum diamond):**  $\tilde{\nu}$  /  $\text{cm}^{-1}$  = 3329, 3162, 3020, 2927, 2857, 2847, 1727, 1711, 1598, 1530, 1435, 1383, 1344, 1312, 1250, 1197, 1184, 1144, 1110, 997, 981, 908, 892, 852, 821, 793, 756, 723, 690, 666, 633, 606, 548, 510, 485, 454, 433.

**ESI-MS:**  $[\text{M}+\text{H}]^+$  calc. 351.1373, detected 351.1368.



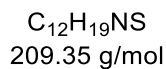
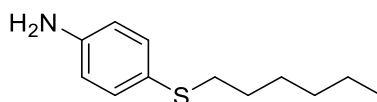
**Supplementary Figure 3.**  $^1\text{H NMR}$  spectrum of TU2, measured in  $\text{DMSO-}d_6$  at 400 MHz.



**Supplementary Figure 4.**  $^{13}\text{C}$  NMR spectrum of **TU2**, measured in  $\text{DMSO-}d_6$  at 101 MHz.

## Synthesis of thiourea **TU3**

### 4-(*n*-Hexylthio) aniline **1**



The product was prepared according to a literature-known procedure.<sup>521</sup>

6.02 g (48.1 mmol, 1.00 equiv.) 4-amino thiophenol were dissolved in 150 mL ethanol (0.33 M). To this solution, 1.90 g (47.5 mmol, 0.988 equiv.) NaOH were added. Afterwards, 6.70 mL (7.91 g, 47.9 mmol, 1.00 equiv.) 1-bromohexane were added within the course of 1 h. The mixture was stirred at room temperature overnight and afterwards poured into 360 mL ice-cold water. The product was extracted with diethyl ether. The organic phase was washed with saturated  $\text{Na}_2\text{CO}_3$  solution (3  $\times$  160 mL) and with aqueous  $\text{NH}_4\text{Cl}$  (3  $\times$  160 mL) solution and dried over  $\text{Na}_2\text{SO}_4$ . After removal of the solvent under reduced pressure, the brown oil

was purified via column chromatography (cyclohexane/ethyl acetate 95:5  $\rightarrow$  7:3). The product was yielded as brownish oil in a yield of 7.20 g (34.4 mmol, 71%).

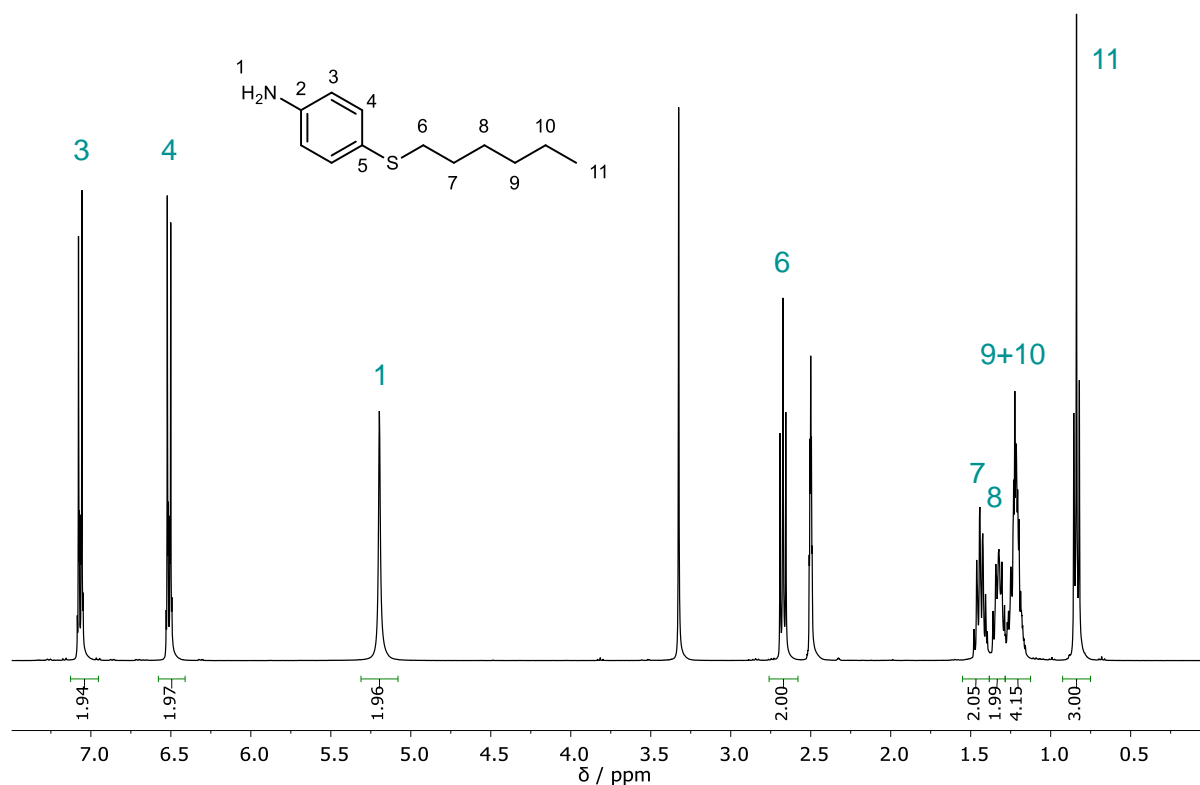
$R_f$  (cyclohexane/ethyl acetate 7:3) = 0.71, visualized by staining with vanillin solution.

$^1\text{H NMR}$  (400 MHz,  $\text{DMSO-}d_6$ )  $\delta$  / ppm = 7.13–7.03 (m, 2H, **H3**), 6.58–6.41 (m, 2H, **H4**), 5.20 (s, 2H, **H1**), 2.67 (t,  $J = 7.2$  Hz, 2H, **H6**), 1.55–1.38 (m, 2H, **H7**), 1.33 (ddt,  $J = 13.9, 9.3, 6.3$  Hz, 2H, **H8**), 1.28–1.13 (m, 4H, **H9**, **H10**), 0.93–0.75 (m, 3H, **H11**).

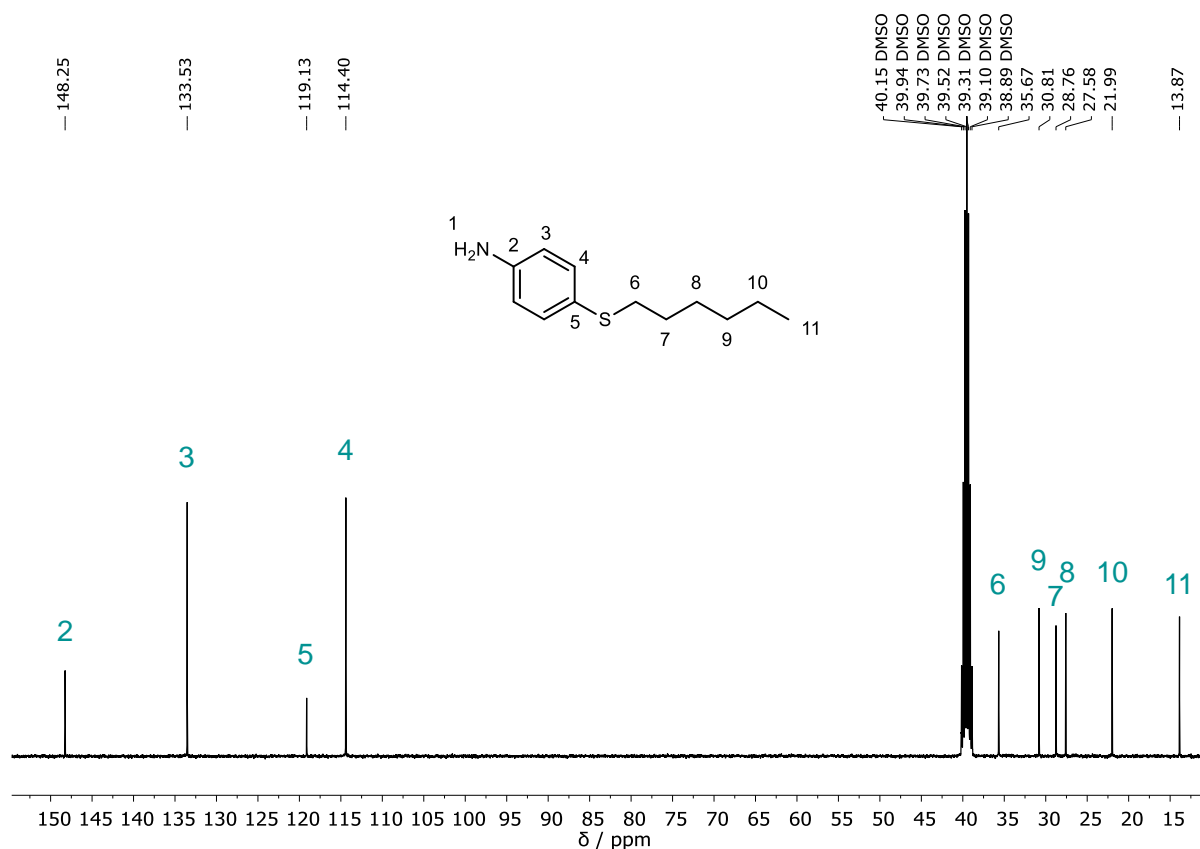
$^{13}\text{C NMR}$  (101 MHz,  $\text{DMSO-}d_6$ )  $\delta$  / ppm = 148.2 (**C2**), 133.5 (**C3**), 119.1 (**C5**), 114.4 (**C4**), 35.7 (**C6**), 30.8 (**C9**), 28.8 (**C7**), 27.6 (**C8**), 22.0 (**C10**), 13.9 (**C11**).

**IR (ATR platinum diamond):**  $\tilde{\nu}$  /  $\text{cm}^{-1}$  = 3452, 3360, 3211, 3025, 2953, 2924, 2854, 1730, 1619, 1597, 1494, 1464, 1422, 1376, 1277, 1176, 1124, 1096, 1010, 820, 725, 681, 623, 514.

**ESI-MS:**  $[\text{M}+\text{H}]^+$  calc. 210.1311, detected 210.1306.

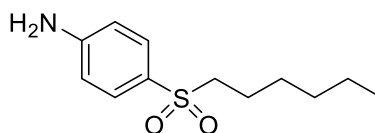


**Supplementary Figure 5.**  $^1\text{H NMR}$  spectrum of **1**, measured in  $\text{DMSO-}d_6$  at 400 MHz.



**Supplementary Figure 6.**  $^{13}\text{C}$  NMR spectrum of 1, measured in  $\text{DMSO-}d_6$  at 101 MHz.

#### 4-(*n*-Hexylsulfonyl) aniline 2



$\text{C}_{12}\text{H}_{19}\text{NO}_2\text{S}$   
241.35 g/mol

The product was prepared according to a literature-known procedure.<sup>521</sup>

4.00 g 4-(*n*-hexylthio) aniline 1 (19.1 mmol, 1.00 equiv.) were dissolved in 38 mL acetonitrile (0.5 M) and 19.5 mL of aqueous hydrogen peroxide solution (30 wt% in water, 22 g, 191 mmol, 10.0 equiv.) were added. The reaction mixture was stirred at 40 °C for 23 hours. Then, the reaction mixture was cooled to room temperature, the same amount of hydrogen peroxide was added, and the mixture was stirred further at 40 °C for 17 hours. Afterwards, 38 mL of saturated  $\text{Na}_2\text{SO}_3$  solution were added slowly, while cooling the mixture with a water bath. The organic phase was separated, and the aqueous phase was extracted with ethyl acetate (2 × 40 mL). The combined organic phases were dried over  $\text{Na}_2\text{SO}_4$ , and the solvent was removed under reduced pressure. Because of the formation of two

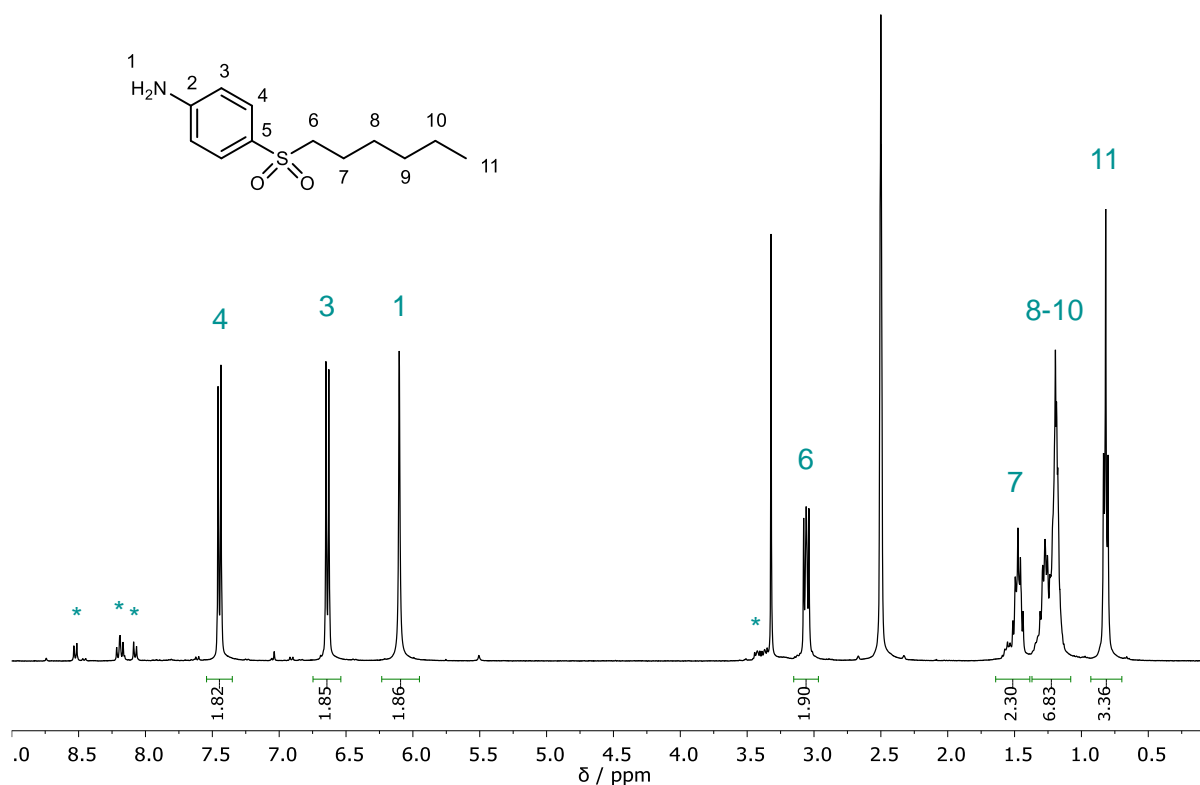
phases during evaporation, the mixture was diluted with dichloromethane, washed with water, and the aqueous phase was extracted with dichloromethane (2 × 30 mL). The combined organic phases were dried over Na<sub>2</sub>SO<sub>4</sub>, and the solvent was again removed under reduced pressure. 4.61 g (19.1 mmol, quant.) of the product were obtained as a brown solid.

*R<sub>f</sub>* (cyclohexane/ethyl acetate 2:1) = 0.25, visualized by staining with vanillin solution.

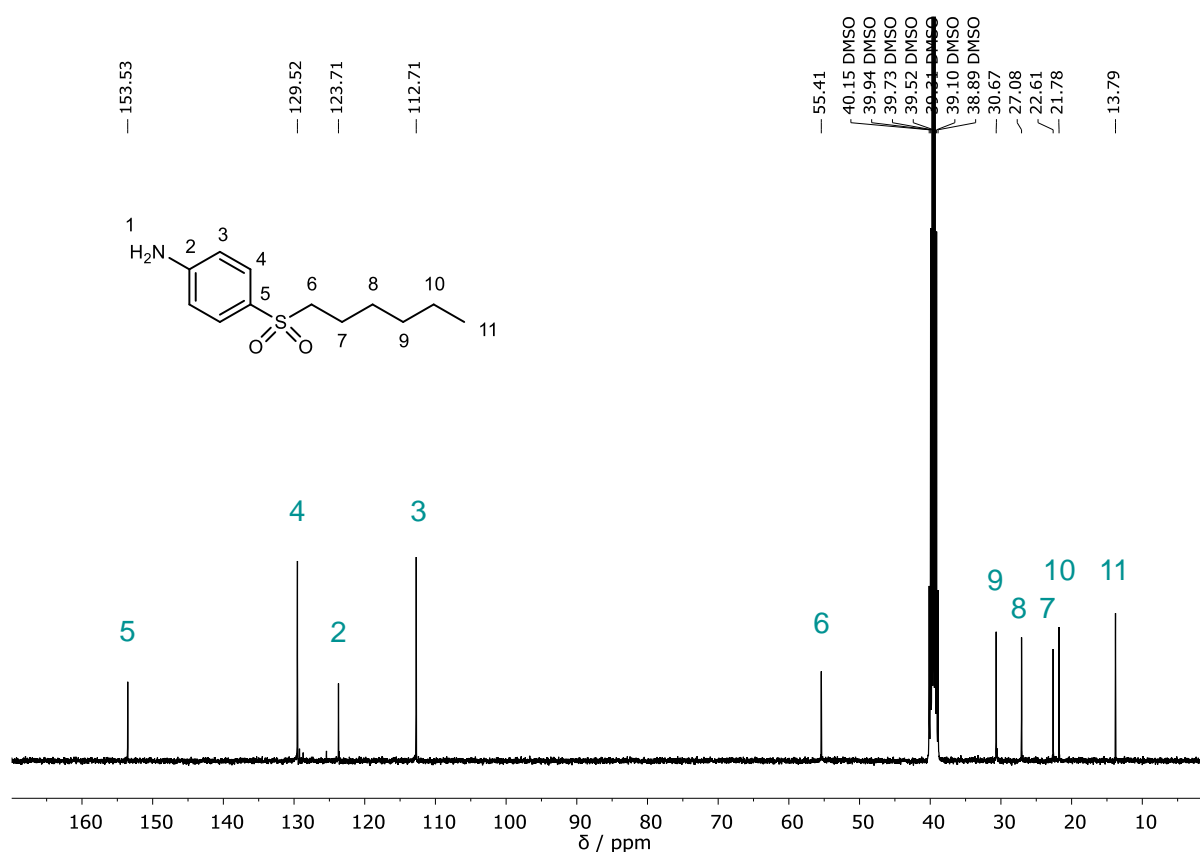
<sup>1</sup>H NMR (400 MHz, DMSO-*d*<sub>6</sub>) δ / ppm = 7.54–7.35 (m, 2H, **H4**), 6.75–6.54 (m, 2H, **H3**), 6.10 (s, 2H, **H1**), 3.15–2.97 (m, 2H, **H6**), 1.64–1.39 (m, 2H, **H7**), 1.37–1.08 (m, 6H, **H8-10**), 0.82 (t, *J* = 6.7 Hz, 3H, **H11**).

<sup>13</sup>C NMR (100 MHz, DMSO-*d*<sub>6</sub>) δ / ppm = 153.5 (**C5**), 129.5 (**C4**), 123.7 (**C2**), 112.7 (**C3**), 55.4 (**C6**), 30.7 (**C9**), 27.1 (**C8**), 22.6 (**C7**), 21.8 (**C10**), 13.8 (**C11**).

IR (ATR platinum diamond):  $\tilde{\nu}$  / cm<sup>-1</sup> = 3468, 3372, 3247, 3223, 2954, 2923, 2871, 2857, 1906, 1630, 1594, 1503, 1459, 1438, 1410, 1378, 1322, 1301, 1271, 1241, 1217, 1184, 1127, 1084, 1013, 964, 945, 828, 767, 726, 701, 681, 633, 593, 563, 526, 489, 441, 421.

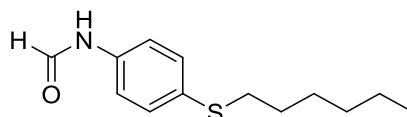


Supplementary Figure 7. <sup>1</sup>H NMR spectrum of **2**, measured in DMSO-*d*<sub>6</sub> at 400 MHz.



Supplementary Figure 8.  $^{13}\text{C}$  NMR spectrum of **2**, measured in  $\text{DMSO-}d_6$  at 101 MHz.

### *N*-(4-(hexylthio)phenyl)formamide **3**



$\text{C}_{13}\text{H}_{19}\text{NOS}$   
237.36 g/mol

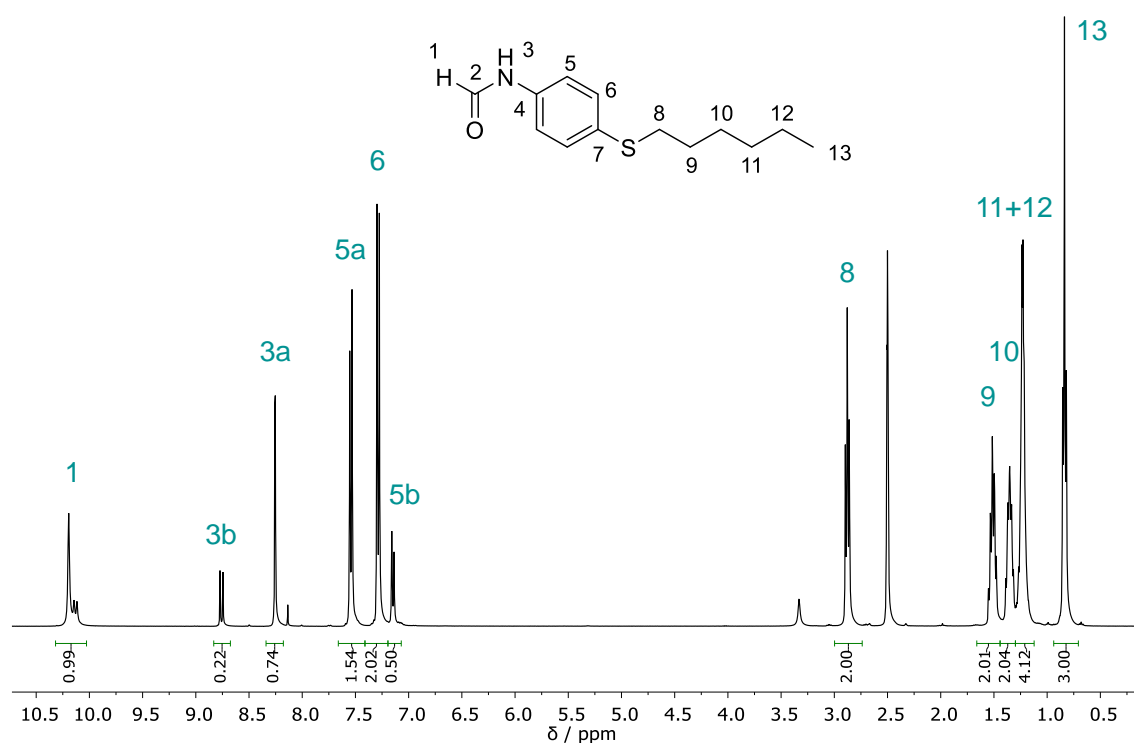
To 4.48 g (21.4 mmol, 1.00 equiv.) of 4-(*n*-hexylthio) aniline **1**, 8.07 mL (9.84 g, 214 mmol, 10.0 equiv.) formic acid were added. The mixture was stirred at 60 °C for 27 h. Subsequently, the remaining formic acid and water were removed under reduced pressure. Afterwards, 5.05 g (21.3 mmol, 99%) of the product were obtained as a colorless solid.

$^1\text{H}$  NMR (400 MHz,  $\text{DMSO-}d_6$ )  $\delta$  / ppm = 10.31–10.03 (m, 1H, **H1**), 8.76 (d,  $J$  = 5.5 Hz, **H3b**), 8.26 (d,  $J$  = 1.9 Hz, **H3a**), 7.66–7.41 (m, **H5a**), 7.41–7.19 (m, 2H, **H6**), 7.19–7.07 (m, **H5b**), 2.99–2.74 (m, 2H, **H8**), 1.66–1.44 (m, 2H, **H9**), 1.35 (p,  $J$  = 7.0 Hz, 2H, **H10**), 1.30–1.12 (m, 4H, **H11**, **H12**), 0.94–0.71 (m, 3H).



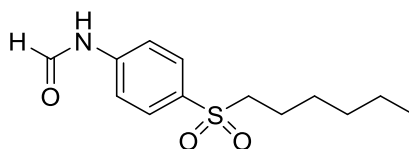
Due to the occurrence of rotamers, no integral values are given for the aromatic  $^1\text{H}$  NMR signals. The sum of integrals matches the expected number of protons. The signals of the rotamers are labelled with a and b for the major and minor rotamer, respectively.

**ESI-MS:**  $[\text{M}+\text{H}]^+$  calc. 238.1260, detected 238.1257.



**Supplementary Figure 9.**  $^1\text{H}$  NMR spectrum of **3**, measured in  $\text{DMSO}-d_6$  at 400 MHz.

#### 4-(*n*-Hexylsulfonyl) formamidobenzene **4**



$\text{C}_{13}\text{H}_{19}\text{NO}_3\text{S}$   
269.36 g/mol

To 4.61 g (19.1 mmol, 1.00 equiv.) of 4-(*n*-hexylsulfonyl) aniline **2**, 7.21 mL (8.80 g, 191 mmol, 10.0 equiv.) formic acid were added. The mixture was stirred at 60 °C for 24 h. Subsequently, the remaining formic acid and water were removed under reduced pressure. Afterwards, 5.11 g (19.0 mmol, 99%) of the product were obtained as a brown solid. The product was used directly for the synthesis of **8** without further purification.

$R_f$  (cyclohexane/ethyl acetate 2:1) = 0.10, visualized by staining with vanillin solution.

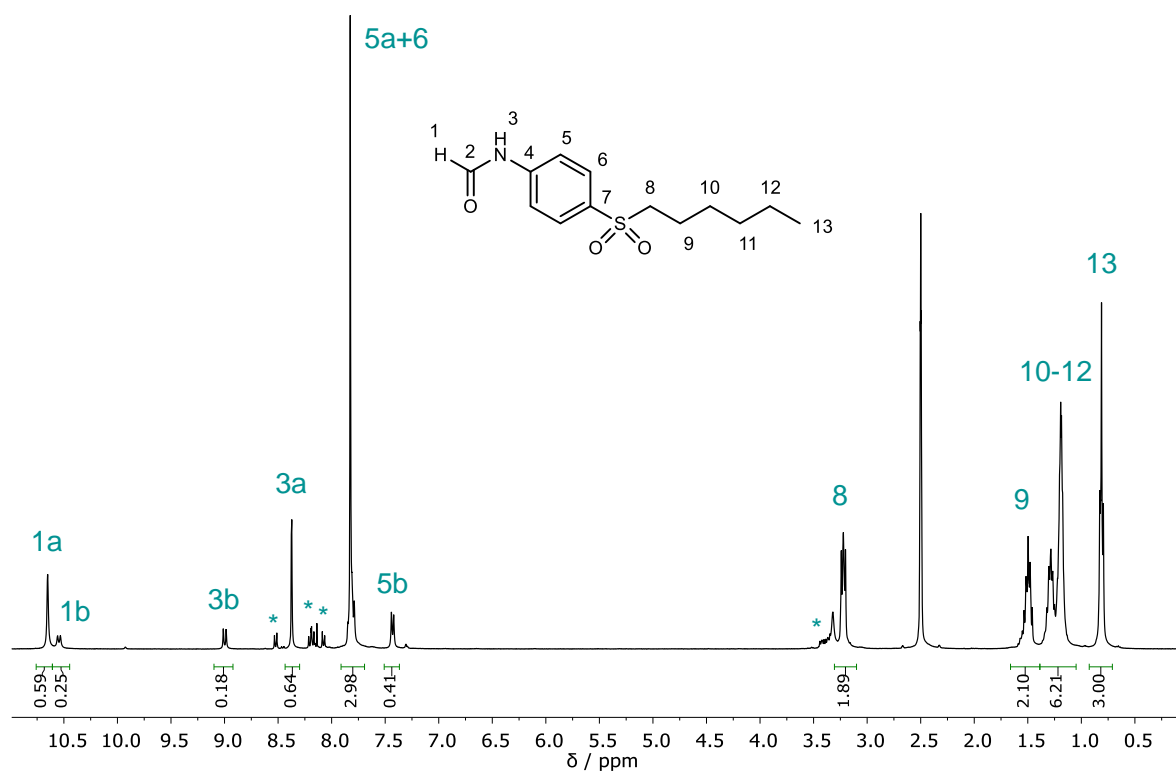
**$^1\text{H}$  NMR (400 MHz, DMSO- $d_6$ )**  $\delta$  / ppm = 10.65 (s, **H1a**), 10.54 (d,  $J$  = 10.6 Hz, **H1b**), 9.00 (d,  $J$  = 10.6 Hz, **H3b**), 8.37 (d,  $J$  = 1.7 Hz, **H3a**), 7.91–7.70 (m, **H5a**, **H6**), 7.51–7.37 (m, **H5b**), 3.31–3.10 (m, 2H, **H8**), 1.66–1.39 (m, 2H, **H9**), 1.39–1.05 (m, 6H, **H10–12**), 0.93–0.71 (m, 3H, **H13**).

Due to the occurrence of rotamers, no integral values are given for the aromatic and carbonyl  $^1\text{H}$  NMR signals. The sum of integrals matches the expected number of protons. The signals of the rotamers are labelled with a and b for the major and minor rotamer, respectively.

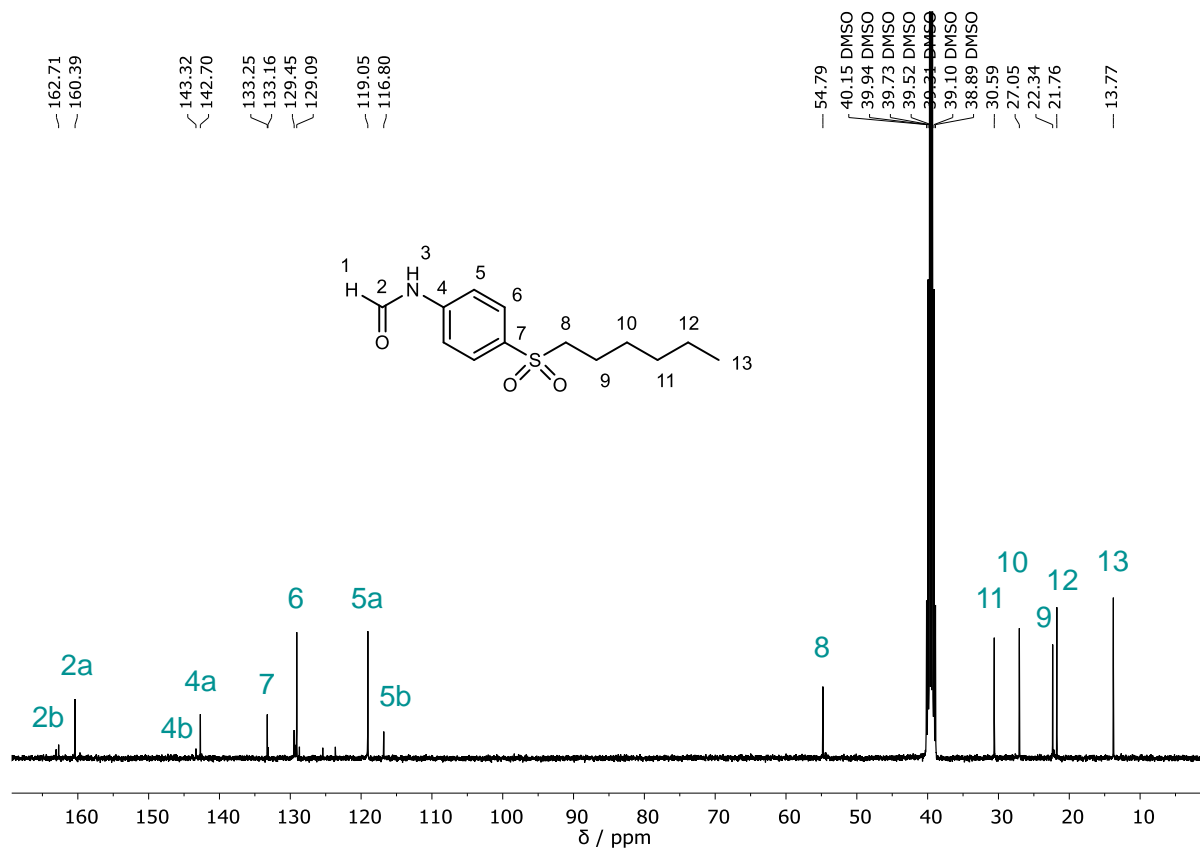
**$^{13}\text{C}$  NMR (101 MHz, DMSO- $d_6$ )**  $\delta$  / ppm = 162.7 (**C2b**), 160.4 (**C2a**), 143.3 (**C4b**), 142.7 (**C4a**), 133.3 (**C7a**), 133.2 (**C7b**), 129.4 (**C6b**), 129.1 (**C6a**), 119.1 (**C5a**), 116.8 (**C5b**), 54.8 (**C8**), 30.6 (**C11**), 27.1 (**C10**), 22.3 (**C9**), 21.8 (**C12**), 13.8 (**C13**).

**IR (ATR platinum diamond):**  $\tilde{\nu}$  /  $\text{cm}^{-1}$  = 3360, 3263, 3202, 3070, 3030, 2993, 2953, 2934, 2921, 2871, 2858, 1750, 1682, 1590, 1519, 1490, 1468, 1456, 1416, 1380, 1273, 1236, 1217, 1193, 1135, 1084, 1033, 1012, 966, 948, 915, 889, 833, 813, 767, 744, 724, 707, 688, 618, 592, 565, 536, 496, 462, 441, 423.

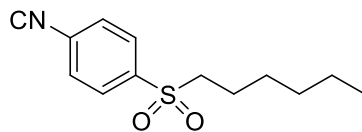
**ESI-MS:**  $[\text{M}+\text{H}]^+$  calc. 270.1158, detected 270.1155.



**Supplementary Figure 10.**  $^1\text{H}$  NMR spectrum of **4**, measured in  $\text{DMSO-}d_6$  at 400 MHz.



**Supplementary Figure 11.**  $^{13}\text{C}$  NMR spectrum of **4**, measured in  $\text{DMSO-}d_6$  at 101 MHz.

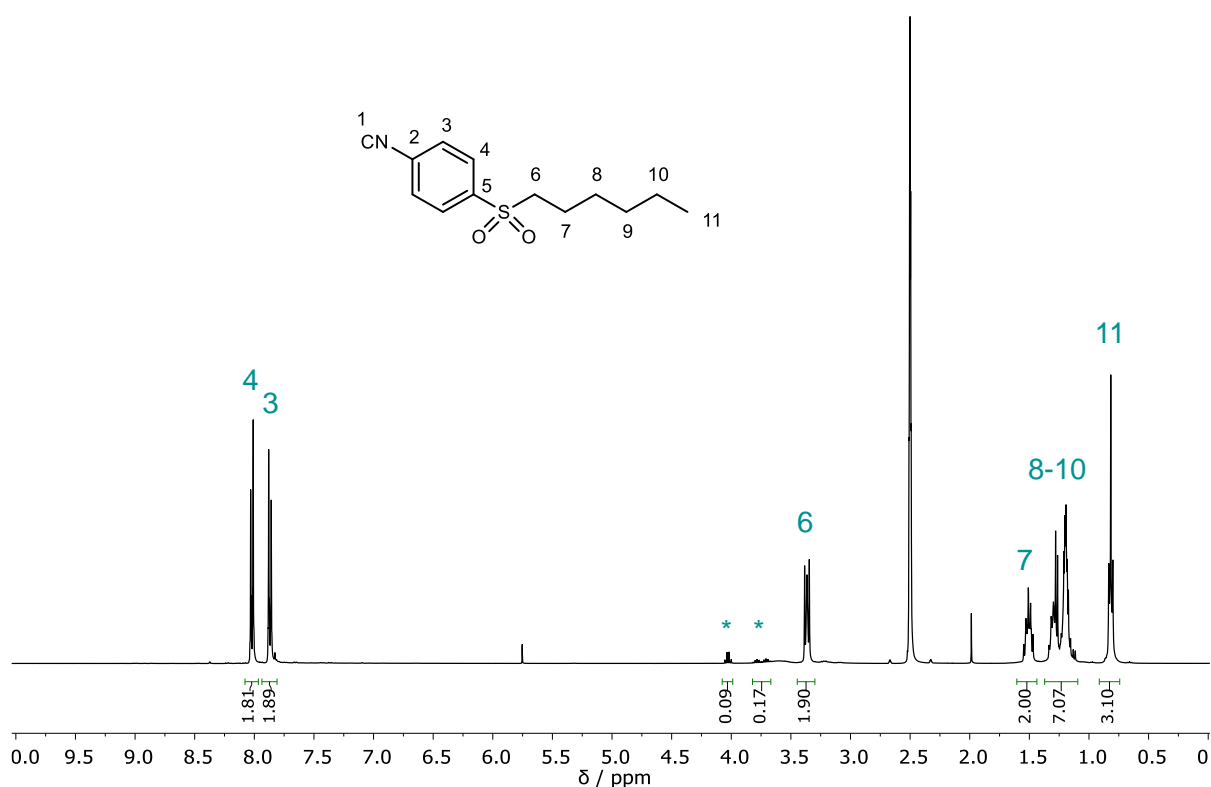
**4-(*n*-Hexylsulfonyl) isocyanobenzene 8**

C<sub>13</sub>H<sub>17</sub>NO<sub>2</sub>S  
251.34 g/mol

1.76 g (6.55 mmol, 1.00 equiv.) 4-(*n*-hexylsulfonyl) formamidobenzene **4** were dissolved in 20 mL dichloromethane (0.33 M) and 2.85 mL (2.05 g, 20.3 mmol, 3.10 equiv.) diisopropylamine (DIPA) were added. The reaction mixture was cooled to 0 °C and 777 μL (1.31 g, 8.51 mmol, 1.30 equiv.) phosphorus oxychloride were added dropwise while keeping the temperature at 0 °C. Afterwards, the reaction was stirred at room temperature for 2 hours. Purification was performed via flash column chromatography, in which the reaction mixture was added dropwise directly onto the dry silica loaded column (height ca. 10 cm, ø ca. 5 cm) to quench the remaining phosphorus oxychloride. Then, the product was purified by eluting with dichloromethane with 3 vol.% triethylamine. 1.20 g (9% impurity of DIPA, corresponds to 4.60 mmol, product, 70%) of the product were obtained as dark red solid.

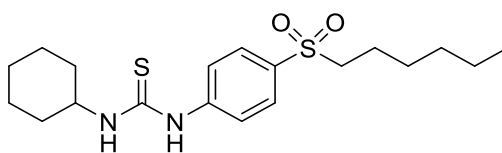
**<sup>1</sup>H NMR (400 MHz, DMSO-*d*<sub>6</sub>)** δ / ppm = 8.08–7.97 (m, 2H, **H4**), 7.94–7.81 (m, 2H, **H3**), 3.45–3.30 (m, 2H, **H6**), 1.61–1.44 (m, 2H, **H7**), 1.37–1.09 (m, 6H, **H8-10**), 0.91–0.74 (m, 3H, **H11**).

Further analysis was not performed due to the sensitivity of the product.



**Supplementary Figure 12.**  $^1\text{H}$  NMR spectrum of **8**, measured in  $\text{DMSO-}d_6$  at 400 MHz.

### ***N*-(4-(*n*-Hexylsulfonyl)phenyl)-*N'*-cyclohexyl thiourea TU3**



$\text{C}_{19}\text{H}_{30}\text{N}_2\text{O}_2\text{S}_2$   
382.58 g/mol

197 mg (771  $\mu\text{mol}$ , 0.125 equiv.) elemental sulfur were suspended in 6.9 mL methanol (0.90 M corresponding to isocyanide) and 711  $\mu\text{L}$  (612 mg, 6.17 mmol, 1.00 equiv.) cyclohexylamine were added. 1.55 g (6.17 mmol, 1.00 equiv.) 4-(*n*-hexylsulfonyl) isocyanobenzene **8** were added and the reaction mixture was stirred at room temperature for 17 hours. Afterwards, the solvent was removed under reduced pressure and the product was purified via column chromatography (cyclohexane/ethyl acetate 6:4  $\rightarrow$  3:1). 1.49 g (3.89 mmol, 63%) of the product were obtained as slightly red solid.

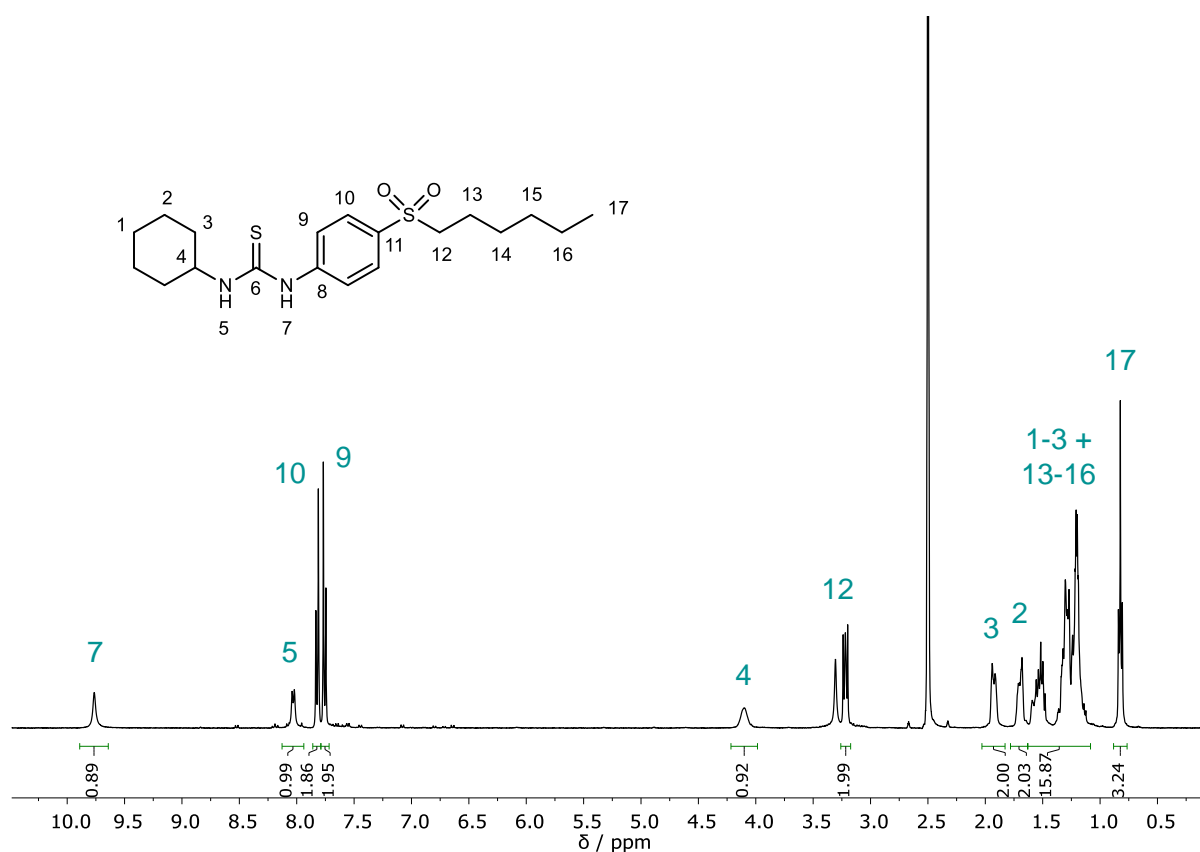
$R_f$  (cyclohexane/ethyl acetate 2:1) = 0.32, visualized by staining with vanillin solution.

**$^1\text{H}$  NMR (400 MHz, DMSO- $d_6$ )**  $\delta$  / ppm = 9.77 (bs, 1H, **H7**), 8.12–7.97 (m, 1H, **H5**), 7.85–7.79 (m, 2H, **H10**), 7.78–7.73 (m, 2H, **H9**), 4.18–4.04 (m, 1H, **H4**), 3.26–3.17 (m, 2H, **H12**), 1.99–1.84 (m, 2H, **H3**), 1.76–1.65 (m, 2H, **H2**), 1.64–1.09 (m, 18H, **H1-3**, **H13-16**), 0.88–0.77 (m, 3H, **H17**).

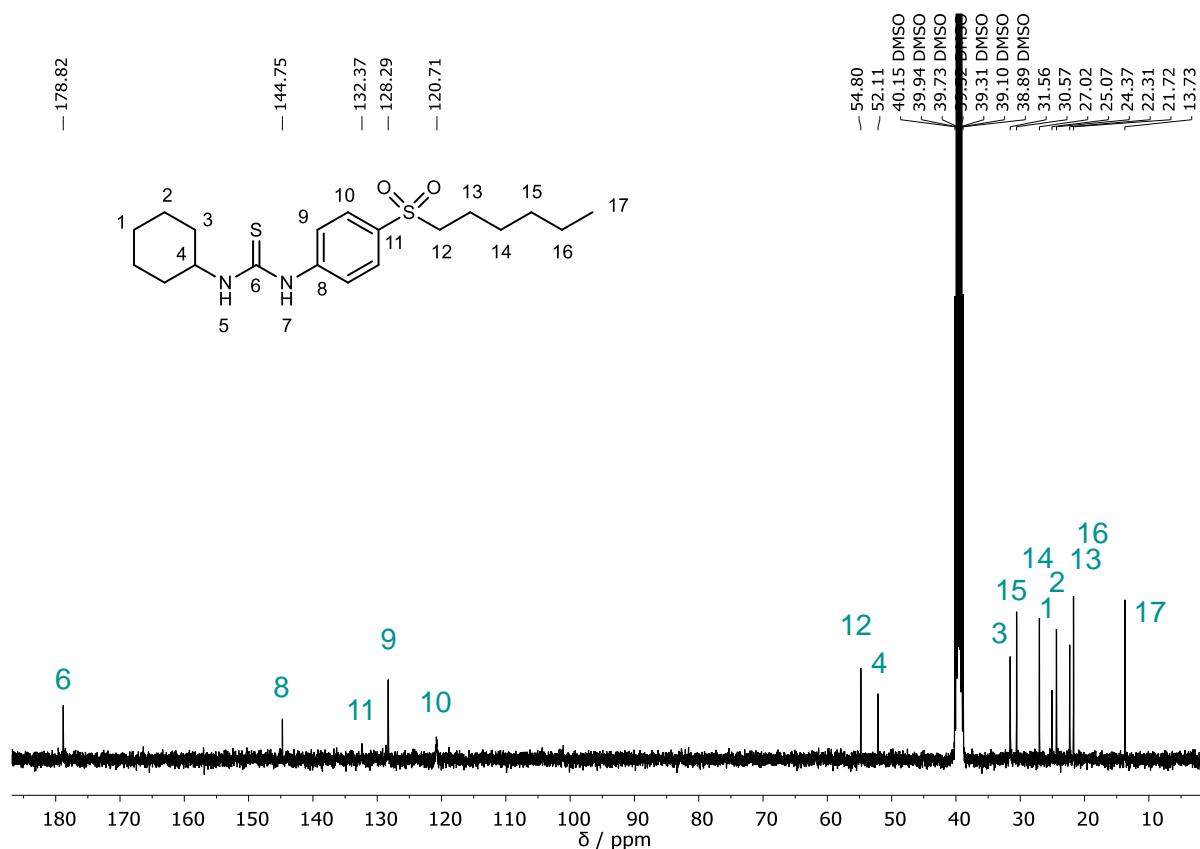
**$^{13}\text{C}$  NMR (101 MHz, DMSO- $d_6$ )**  $\delta$  / ppm = 178.8 (**C6**), 144.7 (**C8**), 132.4 (**C11**), 128.3 (**C9**), 120.7 (**C10**), 54.8 (**C12**), 52.1 (**C4**), 31.6 (**C3**), 30.6 (**C15**), 27.0 (**C14**), 25.1 (**C1**), 24.4 (**C2**), 22.3 (**C13**), 21.7 (**C16**), 13.7 (**C17**).

**IR (ATR platinum diamond):**  $\tilde{\nu}$  /  $\text{cm}^{-1}$  = 3340, 3224, 3181, 3087, 3063, 2929, 2852, 1911, 1623, 1596, 1532, 1497, 1449, 1419, 1333, 1299, 1273, 1251, 1212, 1181, 1135, 1111, 1086, 1011, 981, 889, 876, 832, 772, 740, 722, 688, 666, 649, 621, 596, 573, 550, 530, 490, 443.

**ESI-MS:**  $[\text{M}+\text{H}]^+$  calc. 383.1821, detected 383.1818.



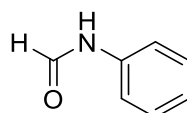
**Supplementary Figure 13.**  $^1\text{H}$  NMR spectrum of **TU3**, measured in DMSO- $d_6$  at 400 MHz.



Supplementary Figure 14.  $^{13}\text{C}$  NMR spectrum of TU3, measured in  $\text{DMSO-}d_6$  at 400 MHz.

## Synthesis of thiourea TU4

### *N*-phenylformamide 9



$\text{C}_7\text{H}_7\text{NO}$   
121.14 g/mol

1.96 mL (21.5 mmol, 1.00 equiv., 2.00 g) of aniline were added to 8.1 mL (220 mmol, 10 equiv., 9.9 g) formic acid. The reaction mixture was stirred for 24 h at 60 °C. After cooling down, the solution was diluted in ethyl acetate and washed with brine. The organic layer was dried over  $\text{MgSO}_4$ . The solvent was removed under reduced pressure. The product was obtained as a brown solid with a yield of 2.25 g (18.6 mmol, 87%).

$R_f$  (cyclohexane/ethyl acetate 4:1) = 0.14, visualized by UV light quenching.

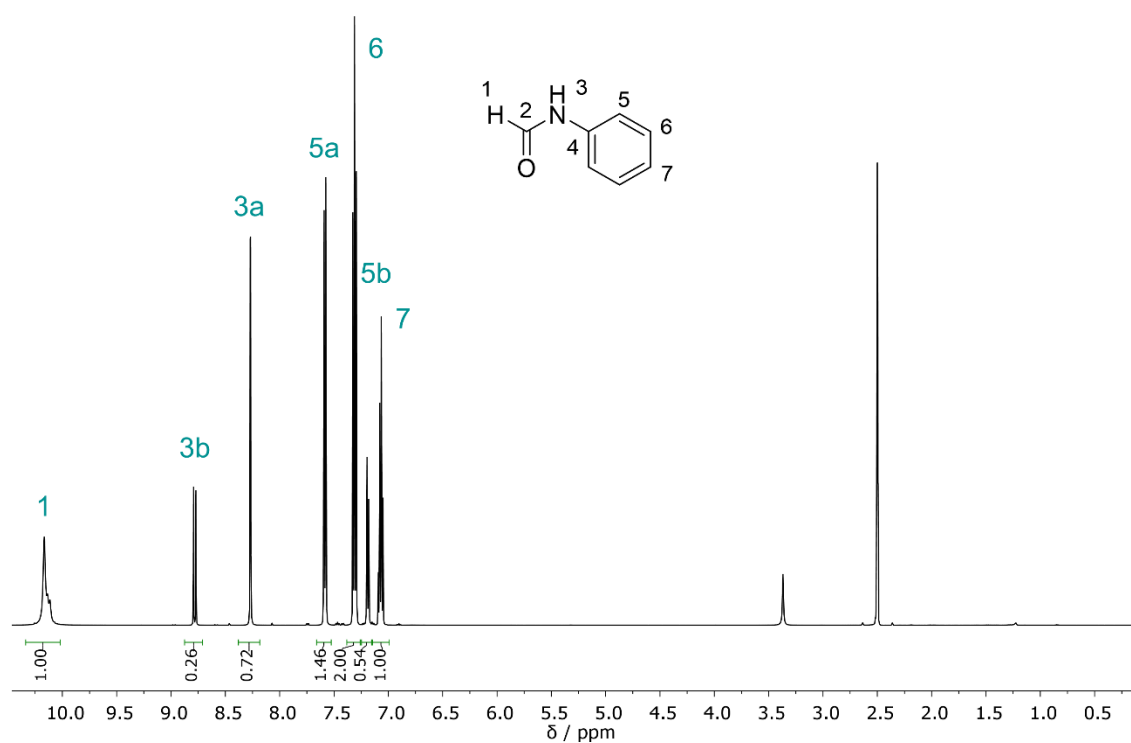
$^1\text{H}$  NMR (500 MHz,  $\text{DMSO-}d_6$ )  $\delta$  / ppm = 10.35–9.96 (m, 1H, H1), 8.78 (d,  $J$  = 11.0 Hz, H3b), 8.27 (d,  $J$  = 2.0 Hz, H3a), 7.66–7.53 (m, H5a), 7.38–7.26 (m, 2H, H6), 7.25–7.16 (m, H5b), 7.15–6.99 (m, 1H, H7).

Due to the occurrence of rotamers, no integral values are given for the split  $^1\text{H}$  NMR signals. The sum of integrals matches the expected number of protons. The signals of the rotamers are labelled with a and b for the major and minor rotamer, respectively.

$^{13}\text{C}$  NMR (126 MHz,  $\text{DMSO-}d_6$ )  $\delta$  / ppm = 162.5 (**C2b**), 159.6 (**C2a**), 138.4 (**C4b**), 138.2 (**C4a**), 129.4 (**C6b**), 128.9 (**C6a**), 123.6 (**C7**), 119.1 (**C5a**), 117.5 (**C5b**).

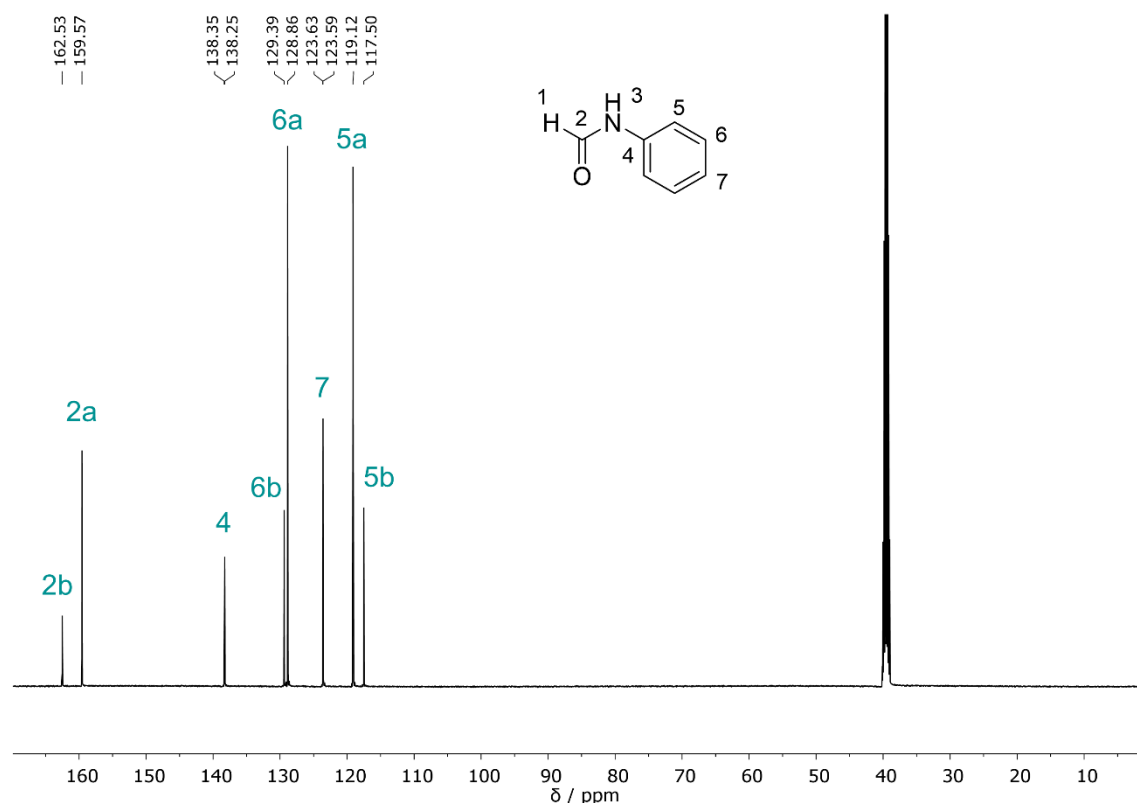
IR (ATR platinum diamond):  $\tilde{\nu}$  /  $\text{cm}^{-1}$  = 3259, 3194, 3134, 3076, 3055, 3021, 2945, 2911, 2881, 1664, 1651, 1594, 1550, 1492, 1443, 1397, 1312, 1256, 1184, 1155, 1077, 1023, 997, 907, 896, 882, 834, 821, 745, 690, 656, 617, 522, 500, 462, 408.

ESI-MS:  $[\text{M}+\text{H}]^+$  calc. 122.0600, detected 122.0600.



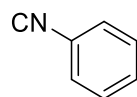
Supplementary Figure 15.  $^1\text{H}$  NMR spectrum of **9**, measured in  $\text{DMSO-}d_6$  at 500 MHz.





**Supplementary Figure 16.**  $^{13}\text{C}$  NMR spectrum of **9**, measured in  $\text{DMSO-}d_6$  at 126 MHz.

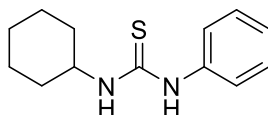
### Phenyl isocyanide **10**



$\text{C}_7\text{H}_5\text{N}$   
103.12 g/mol

1.00 g (8.25 mmol, 1.00 equiv.) *N*-phenylformamide **9** were dissolved in 5 mL dichloromethane. 3.60 mL (2.59 g, 25.6 mmol, 3.10 equiv.) diisopropylamine were added and the solution was cooled down to 0 °C with an ice bath. 979  $\mu\text{L}$  (1.65 g, 10.7 mmol, 1.30 equiv.) phosphoryl chloride were added dropwise and the reaction mixture was stirred at room temperature for 2 h. Afterwards, the reaction was quenched by pouring the mixture directly on a silica-packed column ( $h = 5$  cm) and flushing with dichloromethane. The product was obtained as a yellow liquid in a yield of 728 mg (7.06 mmol, 86%) and directly used for the synthesis of the thiourea **TU4**.

$R_f$  (DCM) = 0.75, visualized by staining with vanillin solution.

***N*-phenyl-*N'*-cyclohexyl thiourea TU4**

C<sub>13</sub>H<sub>18</sub>N<sub>2</sub>S  
234.36 g/mol

728 mg (7.06 mmol, 1.00 equiv.) phenyl isocyanide **10** were dissolved in 7 mL methanol (1.0 M corresponding to isocyanide). 896  $\mu$ L (770 mg, 7.77 mmol, 1.10 equiv.) cyclohexylamine and 250 mg (990  $\mu$ mol, 0.14 equiv.) elemental sulfur were added. The reaction mixture was stirred at 60 °C for 18 h. After cooling down, the suspension was filtrated and washed carefully with methanol. The solvent of the filtrate was removed under reduced pressure. The obtained solid was washed one more time with methanol. The product was obtained as a yellow solid in a yield of 1.23 g (5.25 mmol, 74%).

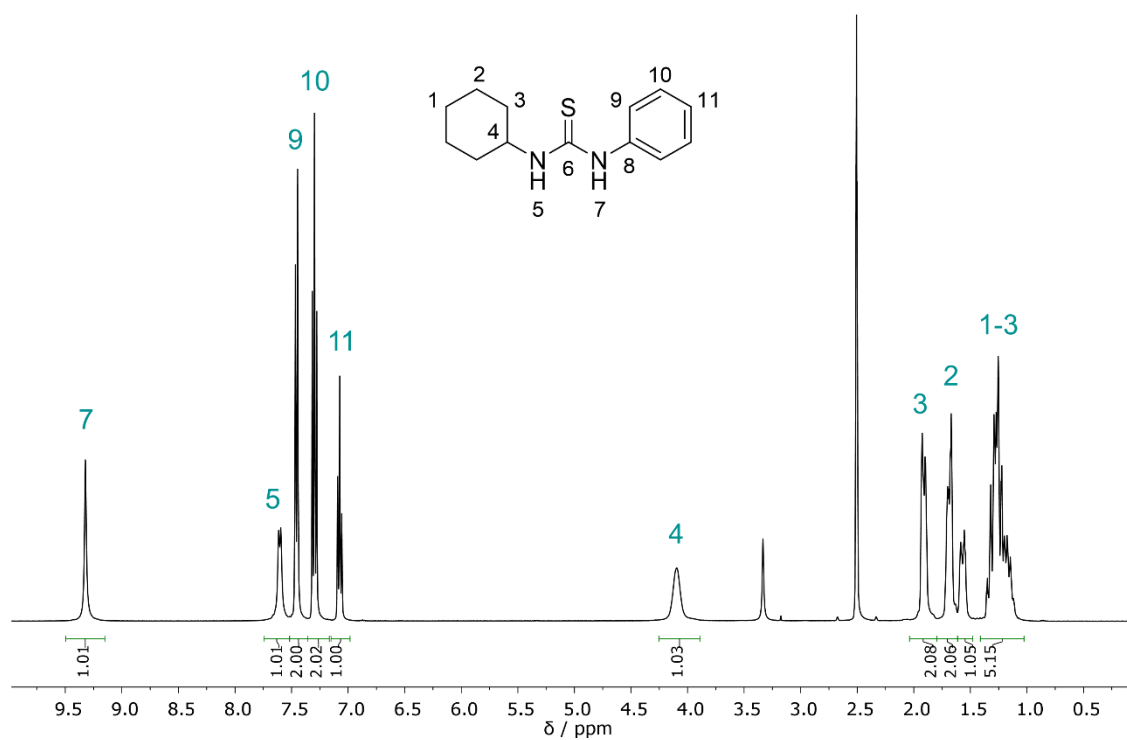
**R<sub>f</sub>** (cyclohexane/ethyl acetate 1:1) = 0.80, visualized by staining with Seebach solution.

**<sup>1</sup>H NMR (400 MHz, DMSO-*d*<sub>6</sub>)**  $\delta$  / ppm = 9.32 (s, 1H, **H7**), 7.60 (d, *J* = 8.0 Hz, 1H, **H5**), 7.52–7.53 (m, 2H, **H9**), 7.36–7.17 (m, 2H, **H10**), 7.07 (t, *J* = 7.3 Hz, 1H, **H11**), 4.25–3.89 (m, 1H, **H4**), 2.04–1.79 (m, 2H, **H3**), 1.79–1.61 (m, 1H, **H2**), 1.61–1.48 (m, 1H, **H1**), 1.41–1.03 (m, 5H, **H1–3**).

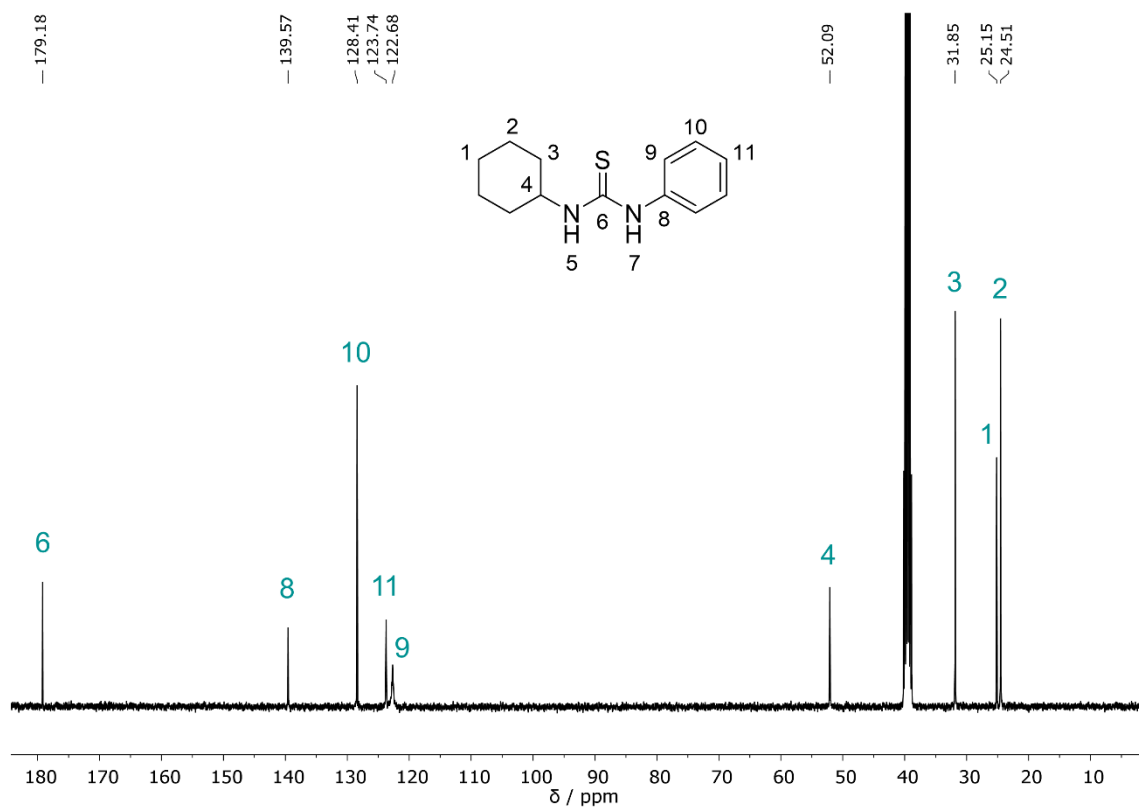
**<sup>13</sup>C NMR (101 MHz, DMSO-*d*<sub>6</sub>)**  $\delta$  / ppm = 179.2 (**C6**), 139.6 (**C8**), 128.4 (**C10**), 123.7 (**C11**), 122.7 (**C9**) 52.1 (**C4**), 31.8 (**C3**), 25.2 (**C1**), 24.5 (**C2**).

**IR (ATR platinum diamond):**  $\tilde{\nu}$  / cm<sup>-1</sup> = 3237, 3027, 3011, 2938, 2852, 1590, 1539, 1505, 1491, 1449, 1395, 1356, 1311, 1290, 1236, 1199, 1182, 1146, 1110, 1073, 1049, 1024, 920, 984, 892, 854, 840, 823, 789, 739, 691, 653, 621, 599, 574, 535, 487, 420.

**ESI-MS:** [M+H]<sup>+</sup> calc. 235.1263, detected 235.1260.



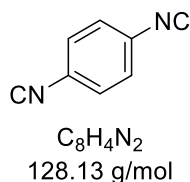
**Supplementary Figure 17.**  $^1\text{H}$  NMR spectrum of **TU4**, measured in  $\text{DMSO-}d_6$  at 400 MHz.



**Supplementary Figure 18.**  $^{13}\text{C}$  NMR spectrum of **TU4**, measured in  $\text{DMSO-}d_6$  at 101 MHz.

## Synthesis of thiourea TU5

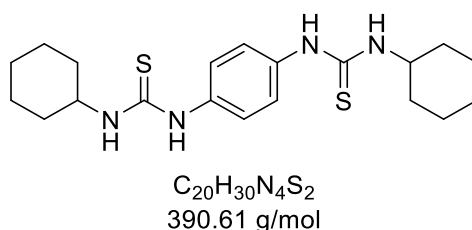
### 1,4-Diisocyanobenzene **11**



1,4-Diformamidobenzene was synthesized previously by Roman Nickisch. 3.00 g (18.3 mmol, 1.00 equiv.) 1,4-diformamidobenzene were dissolved in 55 mL dichloromethane (0.33 M) and 15.8 mL (11.5 g, 113 mmol, 6.20 equiv.) diisopropylamine were added. The reaction mixture was cooled to 0 °C and 4.44 mL (7.28 g, 47.5 mmol, 2.60 equiv.) phosphorus oxychloride were added dropwise while keeping the temperature at 0 °C. Afterwards, the reaction was stirred at room temperature for 2 h. Purification was performed via flash column chromatography, in which the reaction mixture was added dropwise directly onto the dry silica loaded column (height 10 cm, ø 5 cm) to quench the remaining phosphorus oxychloride. Then, the product was purified by eluting with dichloromethane. 2.61 g (quant.) of impure product were obtained and used directly for the synthesis of **TU5** due to the sensitivity of the product.

$R_f$  (cyclohexane/ethyl acetate 3:2) = 0.73, visualized by staining with vanillin solution.

### 1,1'-(1,4-Phenylene)bis(3-cyclohexylthiourea) **TU5**



352 mg (1.37 mmol, 0.280 equiv.) elemental sulfur were suspended in 4.9 mL methanol (1.0 M corresponding to isocyanide), and 1.24 mL (1.07 g, 10.8 mmol, 2.20 equiv.) cyclohexylamine were added. Afterwards, 627 mg (4.90 mmol, 1.00 equiv.) 1,4-diisocyanobenzene **11** were added, and the reaction mixture was stirred at 80 °C for 15 min. The solvent was removed under reduced pressure. The crude product was washed with 5 mL methanol at 60 °C for several minutes and then left to cool down to room temperature. After filtration and washing with minimal

amount of methanol, the solvent was evaporated to obtain 1.77 g (4.53 mmol, 92%) of the product as slightly yellow solid.

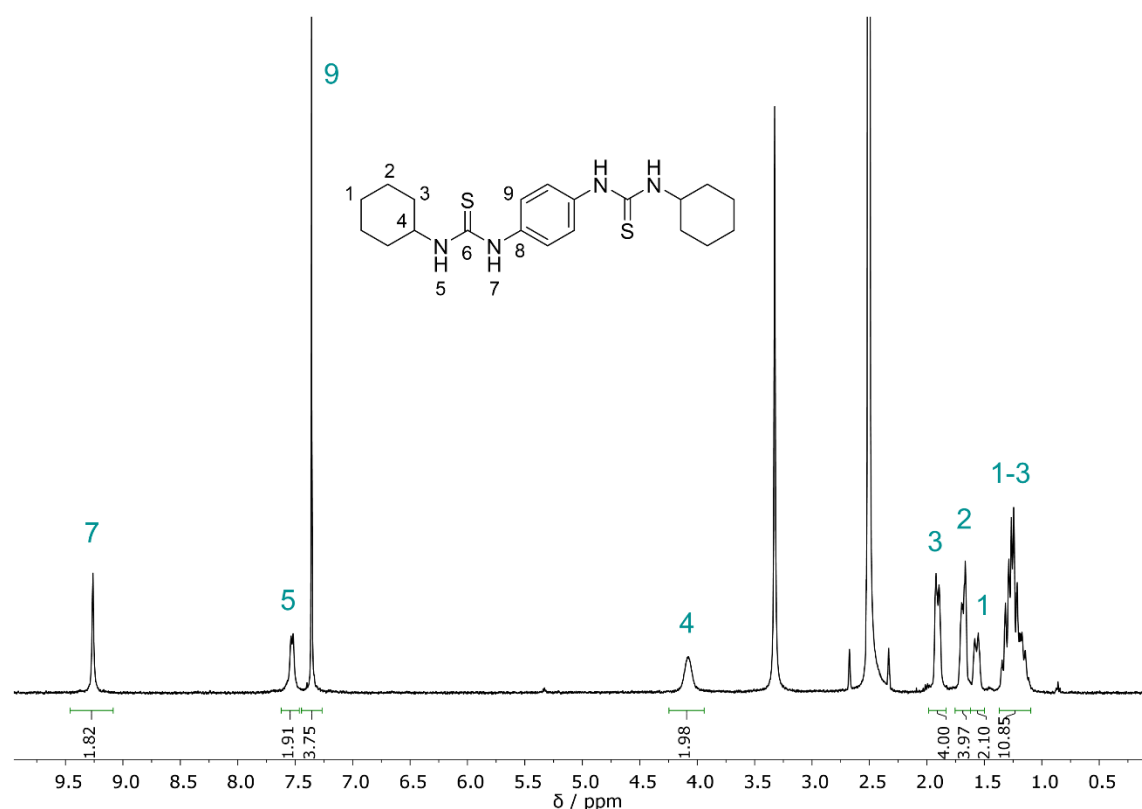
$R_f$  (cyclohexane/ethyl acetate 1:1) = 0.49, visualized by UV light quenching.

$^1\text{H NMR}$  (400 MHz,  $\text{DMSO-}d_6$ )  $\delta$  / ppm = 9.26 (s, 2H, **H7**), 7.53 (d,  $J = 7.9$  Hz, 2H, **H5**), 7.36 (s, 4H, **H9**), 4.24–3.94 (s, 2H, **H4**), 1.98–1.83 (m, 4H, **H3**), 1.75–1.62 (m, 4H, **H2**), 1.62–1.50 (m, 2H, **H1**), 1.37–1.09 (m, 10H, **H1–3**).

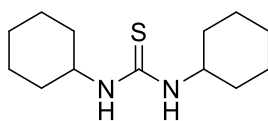
$^{13}\text{C NMR}$  analysis was not performed due to poor solubility of the product.

**IR (ATR platinum diamond):**  $\tilde{\nu}$  /  $\text{cm}^{-1}$  = 3378, 3287, 3223, 2926, 2850, 1543, 1516, 1505, 1447, 1429, 1383, 1355, 1303, 1251, 1226, 1200, 1151, 1106, 1013, 982, 891, 864, 842, 813, 797, 780, 649, 541, 502, 416.

**ESI-MS:**  $[\text{M}+\text{H}]^+$  calc. 391.1985, detected 391.1977.



**Supplementary Figure 19.**  $^1\text{H NMR}$  spectrum of **TU5**, measured in  $\text{DMSO-}d_6$  at 400 MHz.

**1,3-Dicyclohexylthiourea TU6**

$C_{13}H_{24}N_2S$   
240.41 g/mol

59 mg (230  $\mu$ mol, 0.13 equiv.) elemental sulfur, 232  $\mu$ L (200 mg, 2.02 mmol, 1.10 equiv.) cyclohexylamine and 200 mg (1.83 mmol, 1.00 equiv.) cyclohexyl isocyanide were stirred at room temperature for 5 min. Then, 1.5 mL ethanol were added, and the mixture was stirred overnight. The crude product was filtered off and washed with ethanol (1 mL). After removal of the remaining solvent, the product was obtained as a colorless solid in a yield of 344 mg (1.43 mmol, 78%).

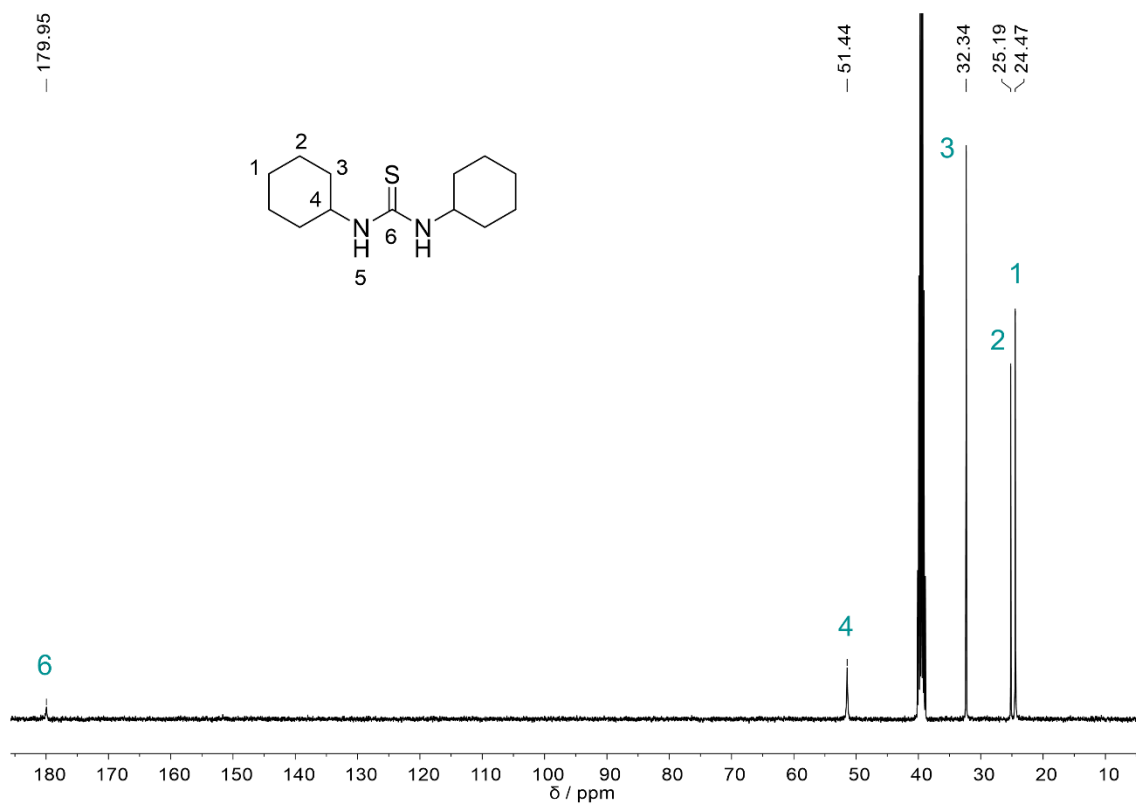
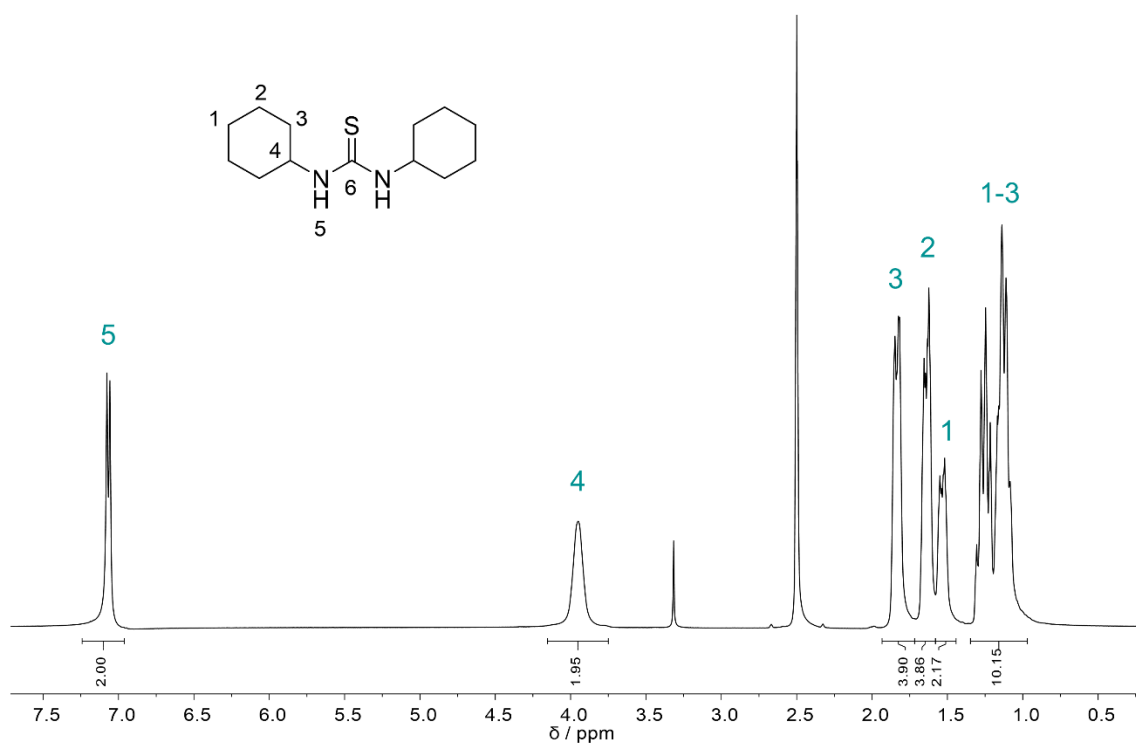
$R_f$  (cyclohexane/ethyl acetate 3:1) = 0.39, visualized by staining with vanillin solution.

$^1H$  NMR (400 MHz, DMSO- $d_6$ )  $\delta$  / ppm = 7.07 (d,  $J$  = 8.0 Hz, 2H, **H5**), 4.15–3.75 (m, 2H, **H4**), 1.93–1.72 (m, 4H, **H3**), 1.72–1.58 (m, 4H, **H2**), 1.58–1.44 (m, 2H, **H1**), 1.35–0.97 (m, 10H, **H1–3**).

$^{13}C$  NMR (101 MHz, DMSO- $d_6$ )  $\delta$  / ppm = 180.0 (**C6**), 51.4 (**C4**), 32.3 (**C3**), 25.2 (**C1**), 24.5 (**C2**).

IR (ATR platinum diamond):  $\tilde{\nu}$  /  $cm^{-1}$  = 3289, 2926, 2852, 1551, 1503, 1450, 1410, 1379, 1360, 1342, 1296, 1275, 1255, 1227, 1186, 1154, 1111, 1076, 1029, 983, 886, 848, 815, 772, 588, 551.

ESI-MS:  $[M+H]^+$  calc. 241.1733, detected 241.1730.



## 6.2.2. Synthesis and ring-opening polymerization of cyclic carbonate and lactone monomers

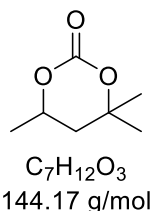
### Synthesis of monomers

Compound **6** was synthesized by the author of this thesis.

Compounds **CK2**, **Lac2**, and **CK3** were synthesized by Johanna Rietschel under co-supervision of the author of this thesis.

Compounds **CK3a** and **Lac3** were synthesized by Hendrik Kirchhoff under co-supervision of the author of this thesis.

### 4,4,6-trimethyl-1,3-dioxan-2-one **6**



In a 25 mL round bottom flask, 1.00 g (8.46 mmol, 1.00 equiv.) 2-methylpentane-2,4-diol, 7.12 mL (7.62 g, 84.6 mmol, 10.0 equiv.) DMC and 120 mg (0.85 mmol, 0.10 equiv.) TBD were stirred at 90 °C. After 16 h of stirring, excess methanol and DMC were removed under reduced pressure. The crude product mixture was dissolved in ethyl acetate (80 mL), washed with brine (3 × 30 mL), and the combined organic phases were dried over Na<sub>2</sub>SO<sub>4</sub>. After removal of the solvent under reduced pressure, the white solid was recrystallized in cyclohexane yielding 942 mg (6.53 mmol, 77%) of the product as white crystals.

*R<sub>f</sub>* (cyclohexane/ethyl acetate 1:1) = 0.26, visualized via staining with Seebach solution.

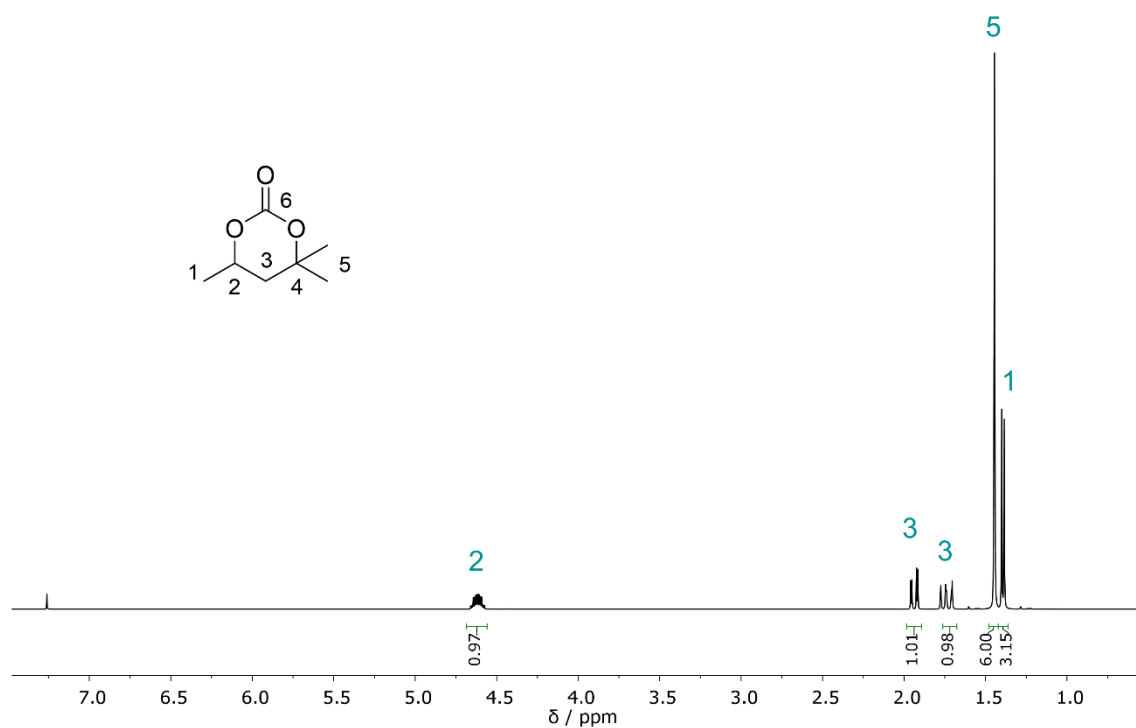
<sup>1</sup>H NMR (400 MHz, CDCl<sub>3</sub>) δ / ppm = 4.68–4.56 (m, 1H, **H2**), 1.99–1.89 (m, 1H, **H3**), 1.77–1.68 (m, 1H, **H3**), 1.47 (s, 6H, **H5**), 1.42–1.36 (d, *J* = 6.2 Hz, 3H, **H1**).

<sup>13</sup>C NMR (101 MHz, CDCl<sub>3</sub>) δ / ppm = 149.6 (**C6**), 80.9 (**C4**), 72.4 (**C2**), 40.7 (**C3**), 30.0 (**C5**), 26.7 (**C5**), 21.3 (**C1**).

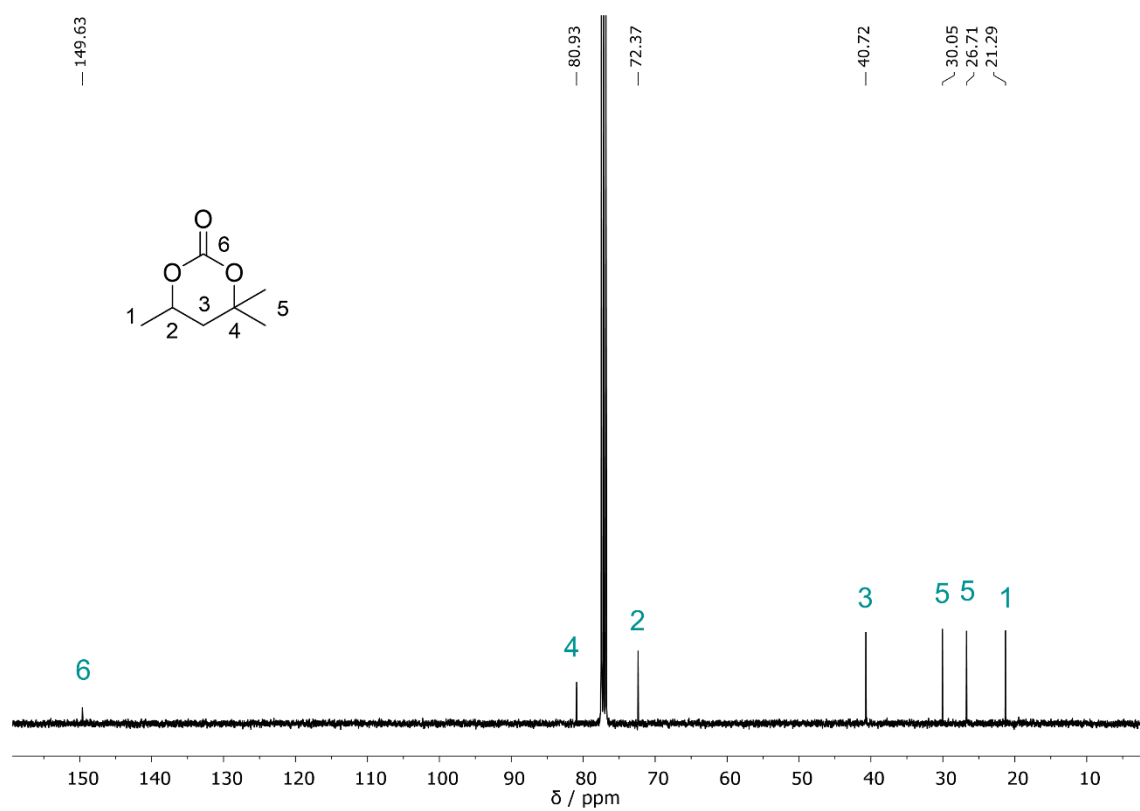
IR (ATR platinum diamond):  $\tilde{\nu}$  / cm<sup>-1</sup> = 2979, 2937, 2882, 1712, 1545, 1453, 1390, 1364, 1293, 1274, 1223, 1139, 1096, 1073, 1027, 1011, 977, 944, 916, 889, 830, 772, 631, 551, 484, 447.

ESI-MS: [M+H]<sup>+</sup> calc. 145.0859, detected 145.0856.

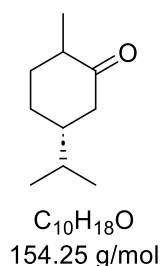




**Supplementary Figure 22.** <sup>1</sup>H NMR spectrum of **6**, measured in CDCl<sub>3</sub> at 400 MHz.



**Supplementary Figure 23.** <sup>13</sup>C NMR spectrum of **6**, measured in CDCl<sub>3</sub> at 101 MHz.

**Carvomenthone CK2**

5.00 g (32.8 mmol, 1.00 equiv.) (+)-dihydrocarvone were dissolved in 130 mL ethyl acetate (0.3 M) and 490 mg (4.6 mmol, 0.14 eq.) palladium on carbon (10 wt.%) were added. Hydrogen was bubbled through the reaction mixture at atmospheric pressure for 1 min. The suspension was stirred for 2 h under hydrogen atmosphere. Afterwards, the reaction mixture was filtered through a short column of silica gel (5 cm of silica gel) and flushed with ethyl acetate. The product was obtained as a colorless liquid in a yield of 4.83 g (31.3 mmol, 95%).

*R<sub>f</sub>* (cyclohexane/ethyl acetate 3:1) = 0.70, visualized by staining with KMnO<sub>4</sub> solution.

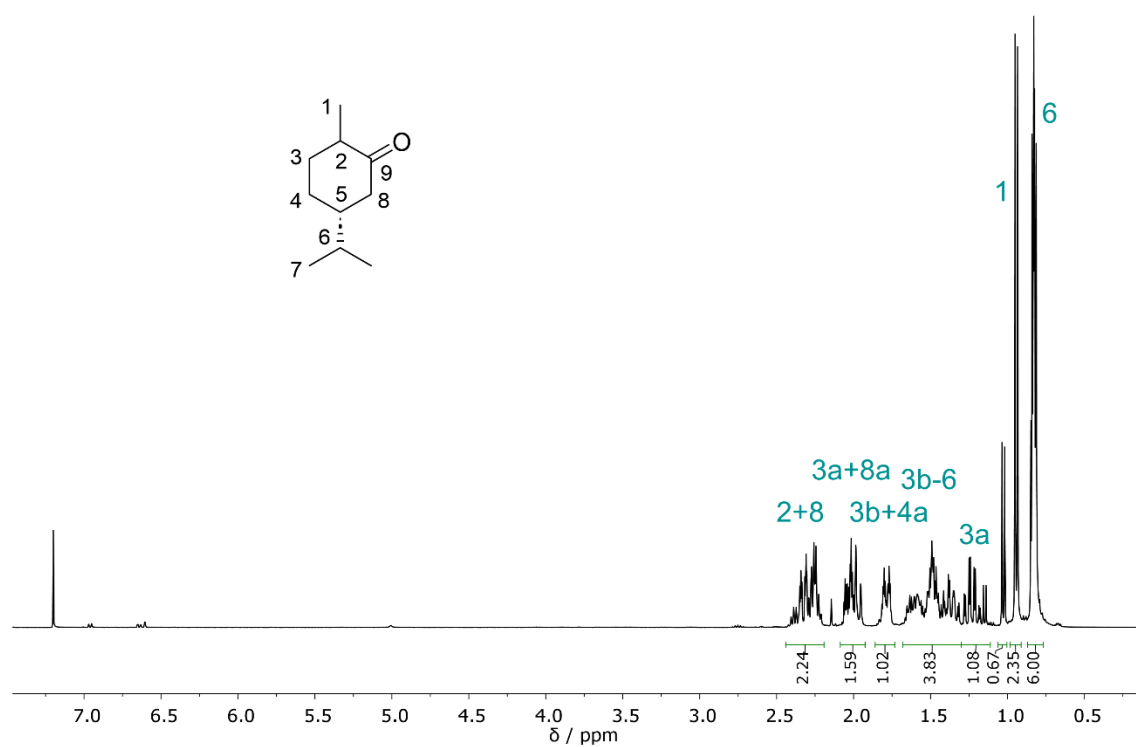
**<sup>1</sup>H NMR (400 MHz, CDCl<sub>3</sub>)** δ / ppm = 2.44–2.19 (m, **H2**, **H8**), 2.09–1.93 (m, **H3a**, **H8a**), 1.86–1.73 (m, **H3b**, **H4a**), 1.69–1.54 (m, **H3b**, **H4b**, **H5b**), 1.54–1.30 (m, **H4a**, **H5a**, **H6**), 1.30–1.11 (m, **H3a**), 1.03 (d, *J* = 7.0 Hz, **H1b**), 0.94 (d, *J* = 6.5 Hz, **H1a**) 0.87–0.77 (m, 6H, **H7**).

Due the occurrence of diastereomers, no integral values are given for the respective NMR signals. The sum of integrals matches the expected number of protons. The signals of the isomeric forms are referred to as a (major isomer) and b (minor isomer).

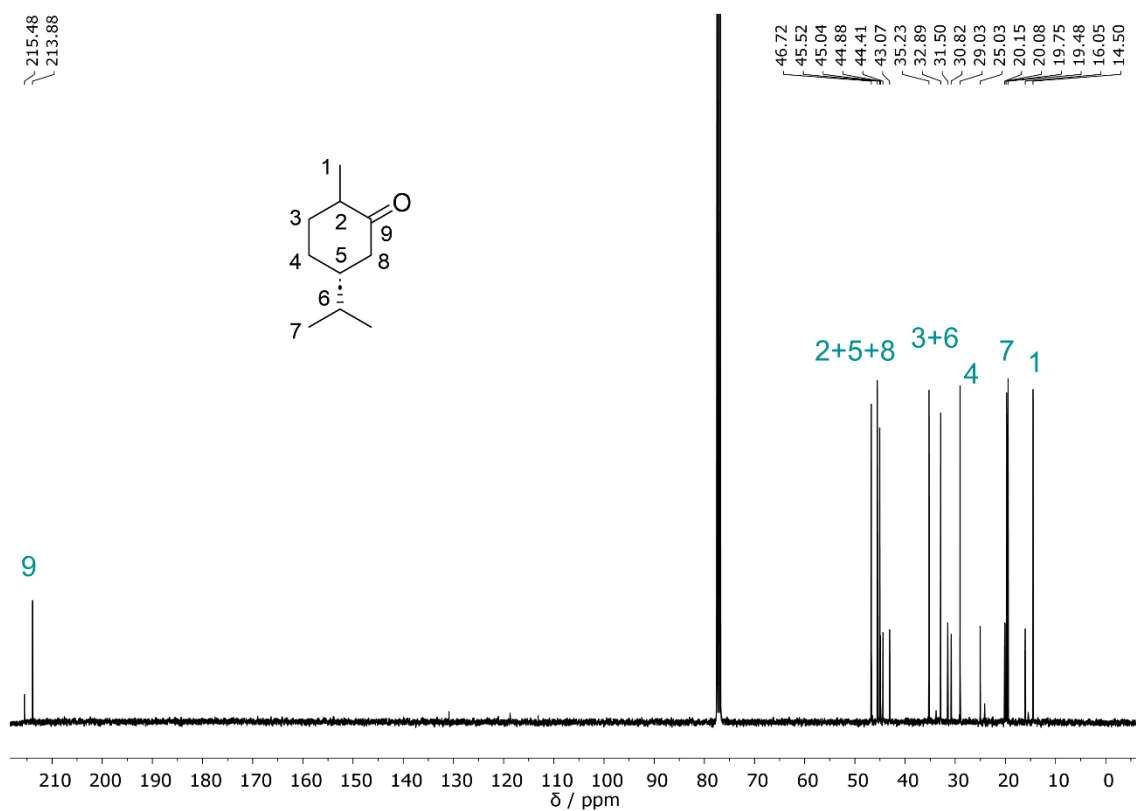
**<sup>13</sup>C NMR (101 MHz, CDCl<sub>3</sub>)** δ / ppm = 215.5 (**C9b**), 213.9 (**C9a**), 46.7 (**C5a**), 45.5 (**C8a**), 45.0 (**C2a**), 44.9 (**C5b**), 44.4 (**C2b**), 43.1 (**C8b**), 35.2 (**C3a**), 32.9 (**C6a**), 31.5 (**C3b**), 30.8 (**C6b**), 29.0 (**C4a**), 25.0 (**C4b**), 20.2 (**C7b**), 20.1 (**C7b**), 19.8 (**C7a**), 19.5 (**C7a**), 16.1 (**C1b**), 14.5 (**C1a**).

**IR (ATR platinum diamond):**  $\tilde{\nu}$  / cm<sup>-1</sup> = 2960, 2930, 2871, 1709, 1454, 1428, 1387, 1368, 1315, 1259, 1241, 1220, 1198, 1149, 1126, 1093, 1061, 1035, 1015, 999, 962, 950, 886, 865, 731, 631, 617, 523, 423.

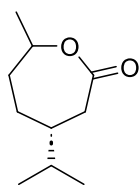
**ESI-MS:** [M+H]<sup>+</sup> calc. 155.1430, detected 155.1427.



Supplementary Figure 24.  $^1\text{H}$  NMR spectrum of CK2, measured in  $\text{CDCl}_3$  at 400 MHz.



Supplementary Figure 25.  $^{13}\text{C}$  NMR spectrum of CK2, measured in  $\text{CDCl}_3$  at 101 MHz.

**(4*R*)-4-Isopropyl-7-methyloxepan-2-one Lac2**

C<sub>10</sub>H<sub>18</sub>O<sub>2</sub>  
170.25 g/mol

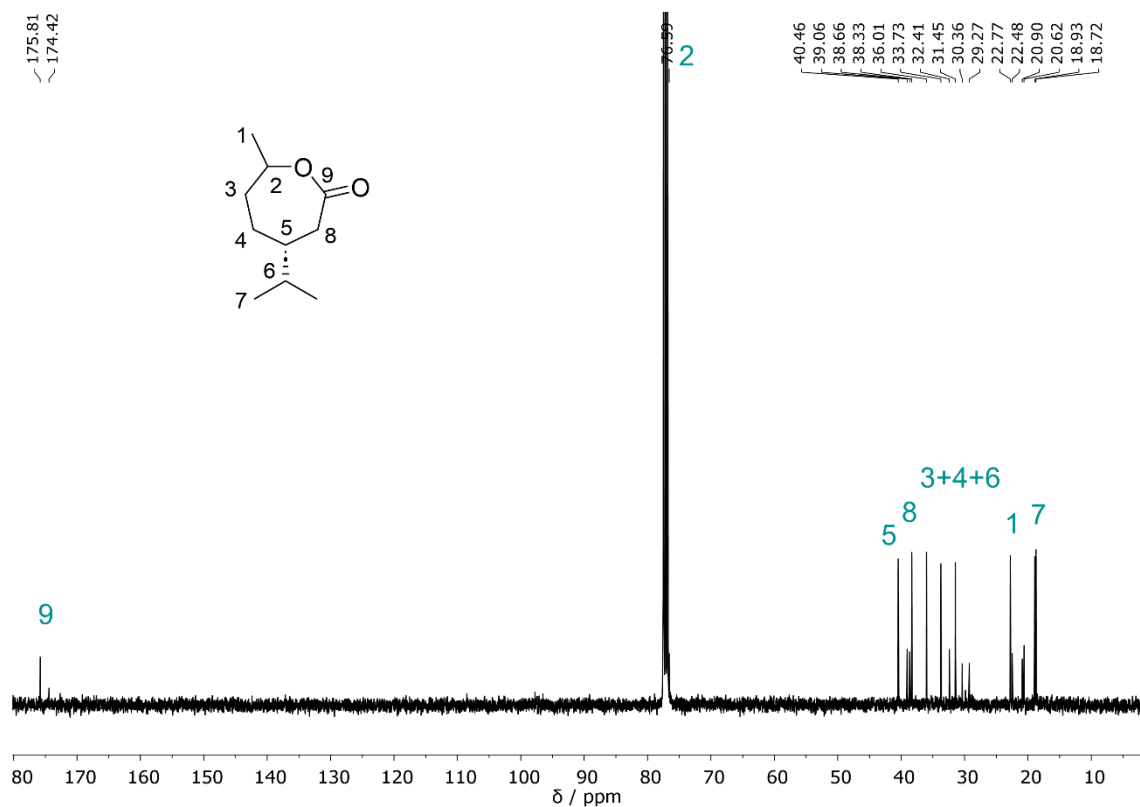
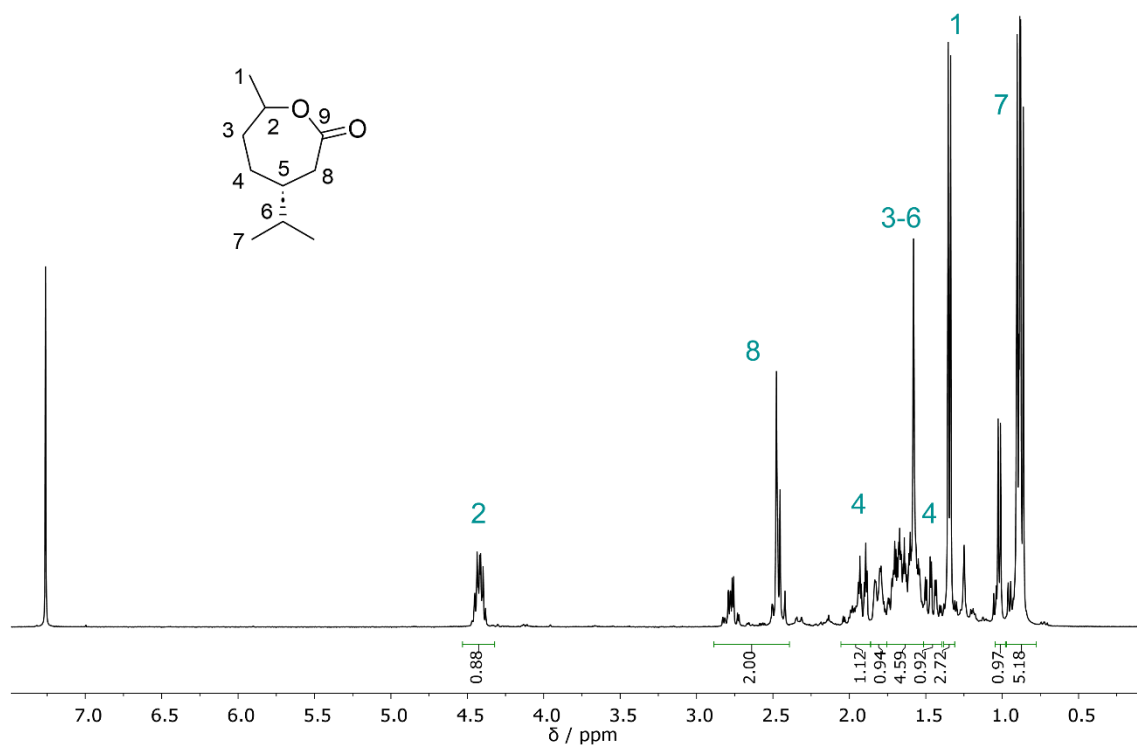
A three-necked flask was charged with 2.00 g (13.0 mmol, 1.00 equiv.) carvomenthone **CK2**, 8.71 g (104 mmol, 8.00 equiv.) NaHCO<sub>3</sub> and 75 mL acetone (0.2 M). 15.9 g (51.9 mmol, 4.00 equiv.) Oxone<sup>®</sup> dissolved in 60 mL water (0.9 M) were added dropwise to the solution. The reaction was stirred at room temperature for 7 d. Afterwards, the reaction mixture was filtered through Celite 545 to remove the solid parts and the filtrate was concentrated under reduced pressure. The mixture was extracted with ethyl acetate and the solvent was removed under reduced pressure. The product was purified by automatic flash column chromatography (cyclohexane/ethyl acetate 9:1 → 0:1), yielding 240 mg (1.41 mmol, 11%) as a colorless liquid.

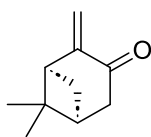
*R<sub>f</sub>* (cyclohexane/ethyl acetate 1:1) = 0.74, visualized by staining with KMnO<sub>4</sub> solution.

<sup>1</sup>H NMR (400 MHz, CDCl<sub>3</sub>) δ / ppm = 4.53–4.32 (m, **H2**), 2.89–2.39 (m, **H8**), 2.06–1.86 (m, **H3**), 1.86–1.75 (m, **H4**), 1.75–1.51 (m, **H3-6**), 1.51–1.40 (m, **H4**), 1.38–1.31 (m, **H1**), 1.05–0.98 (m, **H7b**), 0.97–0.78 (m, **H7a**).

Due the occurrence of diastereomers, no integral values are given for the respective NMR signals. The sum of integrals matches the expected number of protons. The signals of the isomeric forms are referred to as a (major isomer) and b (minor isomer).

<sup>13</sup>C NMR (100 MHz, CDCl<sub>3</sub>) δ / ppm = 175.8 (**C9a**), 174.4 (**C9b**), 76.6 (**C2**), 40.5 (**C5a**), 39.1 (**C5b**), 38.7 (**C8b**), 38.3 (**C8a**), 36.0 (**C3a**), 33.7 (**C6a**), 32.4 (**C4b**), 31.4 (**C4a**), 30.4 (**C3b**), 29.3 (**C6b**), 22.8 (**C1a**), 22.5 (**C1b**), 20.9 (**C7b**), 20.6 (**C7b**), 18.9 (**C7a**), 18.7 (**C7a**).



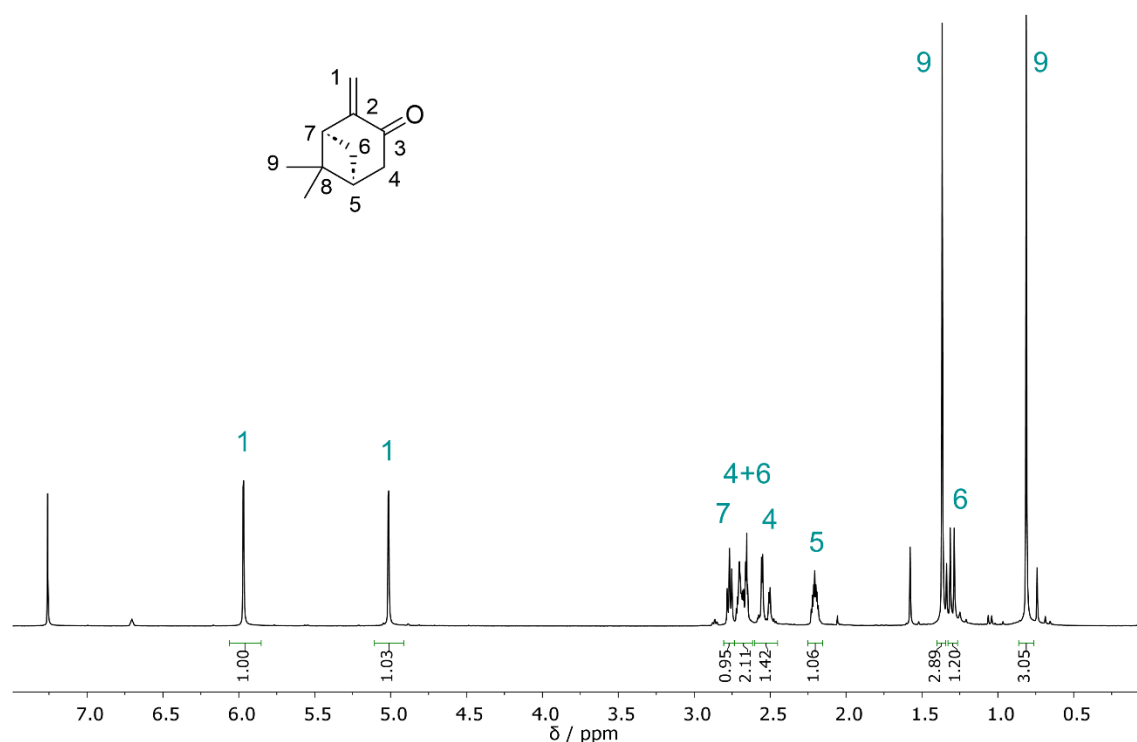
**Pinocarvone CK3**

C<sub>10</sub>H<sub>14</sub>O  
150.22 g/mol

5.00 g (36.7 mmol, 1.00 equiv.)  $\alpha$ -(+)-pinene and 11.3 mg (18.4  $\mu$ mol, 0.05 mol%) tetraphenyl porphyrin were dissolved in 300 mL dichloromethane in a 450 mL standard photochemical reactor. The reaction mixture was stirred for 8 h under irradiation with a 400 W high-pressure sodium vapor lamp. During the reaction, a gentle stream of oxygen bubbled through the stirring mixture. After 7 h, the reaction was quenched by the addition of 11 mL (12 g, 120 mmol, 3.3 equiv.) acetic anhydride and 8.1 mL (5.9 g, 59 mmol, 1.6 equiv.) triethylamine. This mixture was stirred overnight at room temperature. Afterwards, the crude mixture was diluted with ethyl acetate (600 mL) and washed with water (3  $\times$  100 mL), saturated NaHCO<sub>3</sub> solution (3  $\times$  100 mL), 1 M aqueous HCl (3  $\times$  100 mL), and brine (3  $\times$  100 mL). Afterwards, the organic phase was dried over Na<sub>2</sub>SO<sub>4</sub>, and the solvent was removed under reduced pressure. The crude mixture was purified by column chromatography (cyclohexene/ethyl acetate 15:1) to yield 4.75 g (31.6 mmol, 86%) of the product as a red liquid.

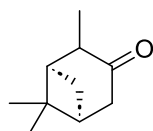
*R<sub>f</sub>* (cyclohexane/ethyl acetate 15:1) = 0.40, visualized by staining with KMnO<sub>4</sub> solution.

<sup>1</sup>H NMR (400 MHz, CDCl<sub>3</sub>)  $\delta$  / ppm = 5.97 (d, *J* = 1.7 Hz, 1H, **H1**), 5.01 (d, *J* = 1.7 Hz, 1H, **H1**), 2.77 (t, *J* = 6.0 Hz, 1H, **H7**), 2.74–2.62 (m, 2H, **H4**, **H6**), 2.60–2.45 (m, 1H, **H4**), 2.26–2.15 (m, 1H, **H5**), 1.37 (s, 3H, **H9**), 1.33–1.26 (m, 1H, **H6**), 0.81 (s, 3H, **H9**).



**Supplementary Figure 28.**  $^1\text{H}$  NMR spectrum of **CK3**, measured in  $\text{CDCl}_3$  at 400 MHz.

**(1*R*,5*S*)-2,6,6-trimethylbicyclo[3.1.1]heptan-3-one CK3a**



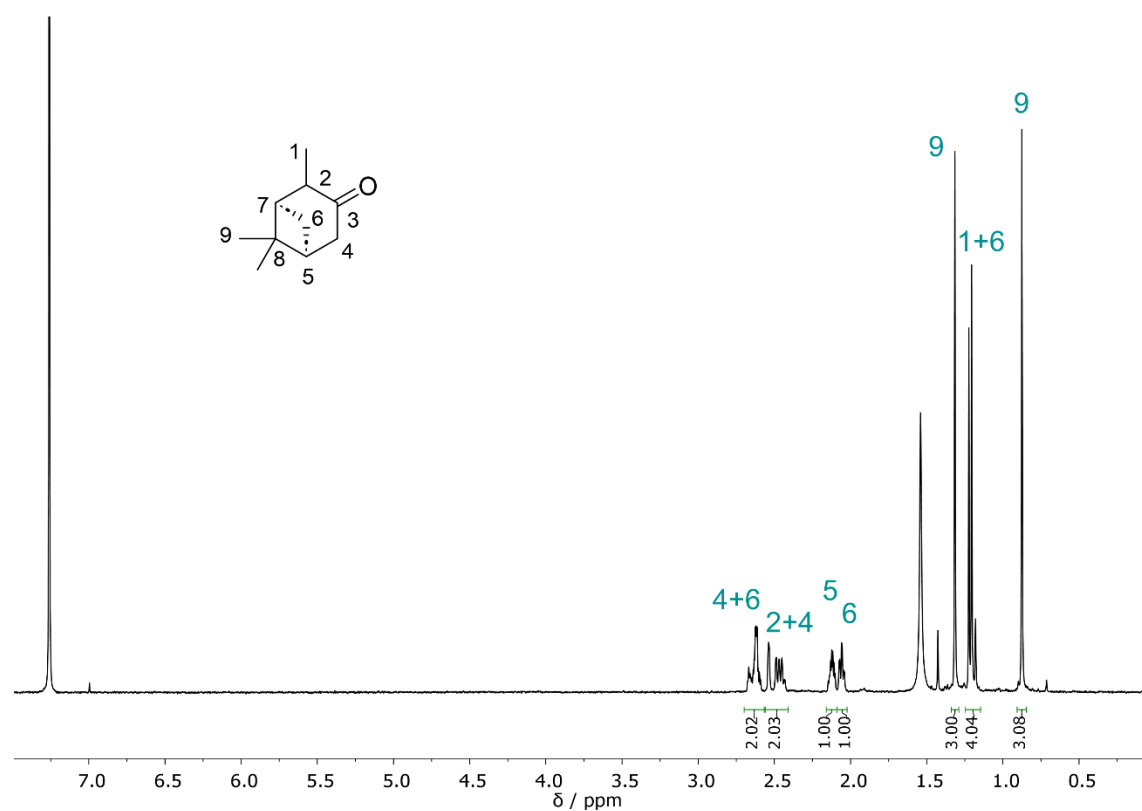
$\text{C}_{10}\text{H}_{16}\text{O}$   
152.24 g/mol

1.00 g (6.66 mmol, 1.00 equiv.) pinocarvone **CK3** was dissolved in 25 mL ethyl acetate (0.3 M). 100 mg (0.94 mmol, 0.14 equiv.) of palladium on carbon (10 wt.%) were added and hydrogen was bubbled through the reaction mixture for 1 min at atmospheric pressure. The suspension was stirred for 2 h under hydrogen atmosphere. Afterwards, the reaction mixture was filtered through a short column (5 cm of silica gel) and flushed with ethyl acetate. The product was obtained as a yellow liquid in a yield of 921 mg (6.05 mmol, 91%).

$R_f$  (cyclohexane/ethyl acetate 15:1) = 0.75, visualized by staining with Seebach solution.

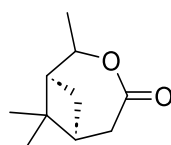
$^1\text{H}$  NMR (400 MHz,  $\text{CDCl}_3$ )  $\delta$  / ppm = 2.70–2.56 (m, 2H, **H4**, **H6**), 2.56–2.41 (m, 2H, **H2**, **H4**), 2.16–2.09 (m, 1H, **H5**), 2.09–2.02 (m, 1H, **H7**), 1.31 (s, 3H, **H9**), 1.25–1.15 (m, 4H, **H1**, **H6**), 0.88 (s, 3H, **H9**).

$^{13}\text{C}$  NMR (100 MHz,  $\text{CDCl}_3$ )  $\delta$  / ppm = 215.4 (**C3**), 51.4 (**C2**), 45.1 (**C7**), 44.9 (**C4**), 39.1 (**H5**), 34.5 (**C6**), 27.2 (**C9**), 22.1 (**C9**), 17.0 (**C1**).



**Supplementary Figure 29.**  $^1\text{H}$  NMR spectrum of **CK3a**, measured in  $\text{CDCl}_3$  at 400 MHz.

### (1*S*,6*S*)-2,7,7-Trimethyl-3-oxabicyclo[4.1.1]octan-4-one Lac3



$\text{C}_{10}\text{H}_{16}\text{O}_2$   
168.24 g/mol

200 mg (1.31 mmol, 1.00 equiv.) (1*R*,5*S*)-2,6,6-trimethylbicyclo[3.1.1]heptan-3-one **CK3a** were dissolved in 2.6 mL of DCM (0.5 M). 453 mg (3.42 mmol, 2.00 equiv.) *m*CPBA were added to the solution. The reaction mixture was stirred at room temperature for 7 d. The reaction was quenched by the addition of 20% aqueous  $\text{Na}_2\text{S}_2\text{O}_3$  solution. Afterwards, the emulsion was diluted with diethyl ether and washed subsequently with sat.  $\text{NaHCO}_3$  solution and water. The organic layer



was dried over Na<sub>2</sub>SO<sub>4</sub> and purified by column chromatography (cyclohexane/ethyl acetate 5:1), yielding 22.8 mg (136 μmol, 10%) of the product as a yellow liquid.

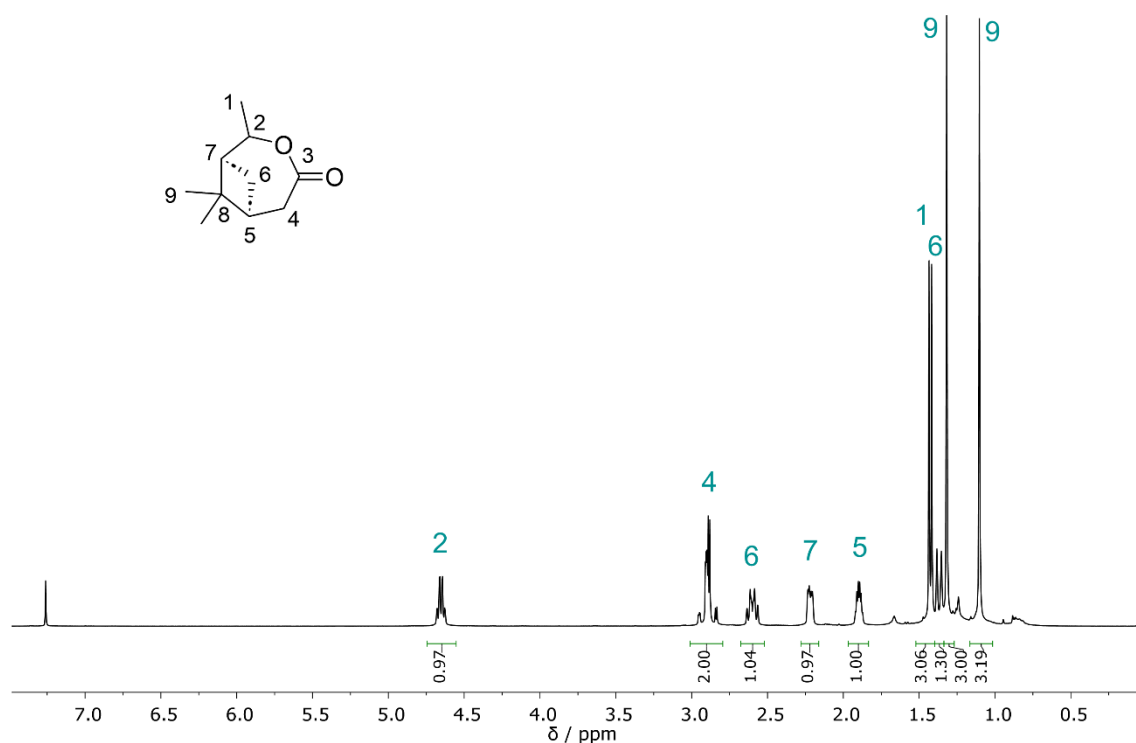
*R<sub>f</sub>* (cyclohexane/ethyl acetate 5:1) = 0.40, visualized by staining with Seebach solution.

**<sup>1</sup>H NMR (400 MHz, CDCl<sub>3</sub>)** δ / ppm = 4.65 (qd, *J* = 6.9, 1.7 Hz, 1H, **H2**), 3.01–2.79 (m, 2H, **H4**), 2.67–2.52 (m, 1H, **H6**), 2.28–2.15 (m, 1H, **H7**), 1.96–1.83 (m, 1H, **H5**), 1.42 (d, *J* = 6.9 Hz, 3H, **H1**), 1.39–1.34 (m, 1H, **H6**), 1.32 (s, 3H, **H9**), 1.10 (s, 3H, **H9**).

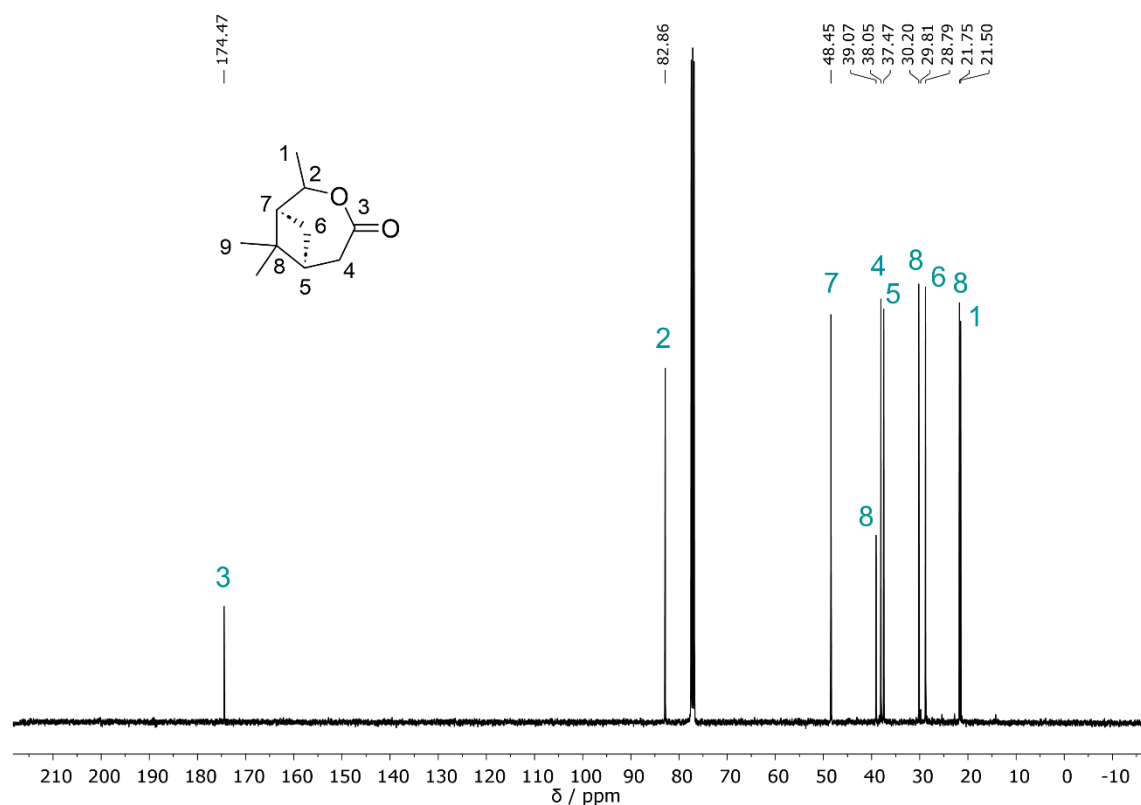
**<sup>13</sup>C NMR (101 MHz, CDCl<sub>3</sub>)** δ / ppm = 174.5 (**C3**), 82.9 (**C2**), 48.4 (**C7**), 39.1 (**C8**), 38.0 (**C4**), 37.5 (**C5**), 30.2 (**C8**), 28.8 (**C6**), 21.8 (**C9**), 21.5 (**C1**).

**IR (ATR platinum diamond):**  $\tilde{\nu}$  / cm<sup>-1</sup> = 2979, 2911, 2873, 1703, 1469, 1412, 1369, 1356, 1319, 1282, 1247, 1209, 1188, 1166, 1130, 1089, 1070, 1007, 945, 922, 877, 859, 834, 797, 728, 666, 634, 609, 554, 520, 475, 421.

**ESI-MS:** [M+H]<sup>+</sup> calc. 169.1223, detected 169.1223.



**Supplementary Figure 30.** <sup>1</sup>H NMR spectrum of Lac3, measured in CDCl<sub>3</sub> at 400 MHz.



**Supplementary Figure 31.**  $^{13}\text{C}$  NMR spectrum of **Lac3**, measured in  $\text{CDCl}_3$  at 101 MHz.

### General procedures for ring-opening polymerizations

All test reaction for ring-opening polymerizations were carried out under air and water exclusion. As preparation, all glassware was heated up under high vacuum before usage and stored under Argon.

Solvents and DBU were previously distilled and kept over activated molecular sieves and Argon atmosphere.

TBD was dried under high vacuum for 1 d and stored under Argon atmosphere for further use.

The lactones **Lac1** and **Lac2** were dissolved in THF,  $\text{CaH}_2$  was added, and the respective mixture was stirred overnight. After filtration and removal of the solvent, the lactones were stored under argon atmosphere.

All remaining reactants were dried by addition and evaporation of toluene for  $\geq 5$  times. Remaining solvent was removed under high vacuum.

Reaction mixtures were degassed three times using the *freeze-pump-thaw* method before starting the reactions.

### Polymerization test reactions of cyclic carbonate **6**

1.2 mL dry dichloromethane was added to a vial charged with the respective base (see **Table 1**; 28  $\mu\text{mol}$ , 6.0 mol%) and 52.4 mg (14  $\mu\text{mol}$ , 30 mol%) thiourea **TU1**. The mixture was stirred until fully dissolved. 0.21 mL of this solution were added to a vial containing 100 mg (694  $\mu\text{mol}$ , 1.00 equiv.) of cyclic carbonate **6** in 0.2 mL dichloromethane to initiate the polymerization. The reaction was stirred at ambient temperature for 18 h.

### Polymerization of $\epsilon$ -caprolactone using a DBU/ thiourea catalyst system

439  $\mu\text{L}$  (452 mg, 3.96 mmol, 1.00 equiv.) of  $\epsilon$ -caprolactone were added to a solution of 30  $\mu\text{L}$  (30 mg, 200  $\mu\text{mol}$ , 5.0 mol%) DBU, 200  $\mu\text{mol}$  (5.0 mol%) of the corresponding thiourea (see **Table 2**) and 73.3 mg (198  $\mu\text{mol}$ , 5.00 mol%) pyrene butanol in 2 mL dry toluene (2 M). The reaction mixture was placed on a pulsating panel. After distinguished time intervals, aliquots of 7  $\mu\text{L}$  (corresponding to 1.5 mg  $\epsilon$ -caprolactone) were taken and quenched with benzoic acid. The sample was dried on air and the remaining residue was dissolved in 1.5 mL of THF for SEC measurements.

### TBD-catalyzed polymerization of $\epsilon$ -caprolactone

439  $\mu\text{L}$  (452 mg, 3.96 mmol, 1.00 equiv.) of  $\epsilon$ -caprolactone were added to a solution of 2.8 mg (20  $\mu\text{mol}$ , 5.0 mol%) TBD, 200  $\mu\text{mol}$  (5.0 mol%) of the corresponding thiourea (see **Table 3**) and 73.3 mg (198  $\mu\text{mol}$ , 5.00 mol%) pyrene butanol in 2 mL dry toluene (2 M). The reaction mixture was placed on a pulsating panel. After distinguished time intervals, aliquots of 7  $\mu\text{L}$  (corresponding to 1.5 mg  $\epsilon$ -caprolactone) were taken and quenched with benzoic acid. The sample was dried on air and the remaining residue was dissolved in 1.5 mL of THF for SEC measurements.

### Polymerization tests of $\epsilon$ -caprolactone using a KOMe/ thiourea catalyst system

A solution of 1.8 mg (26  $\mu\text{mol}$ , 5.0 mol%) potassium methoxide and 74.9  $\mu\text{mol}$  (15 mol%) of the corresponding thiourea (see **Table 4**) in 1 mL dry THF was prepared. 0.2 mL of this solution were added to a solution of 55  $\mu\text{L}$  (57 mg, 500  $\mu\text{mol}$ , 1.00 equiv.)  $\epsilon$ -caprolactone in 0.25 mL of THF. The reaction mixtures were placed on a pulsating panel. After distinguished time intervals, aliquots of 7  $\mu\text{L}$  (correspon-

ding to 1 mg  $\epsilon$ -caprolactone) were taken and quenched with benzoic acid. The sample was dried on air and the remaining residue was dissolved in 1.5 mL of THF for SEC measurements.

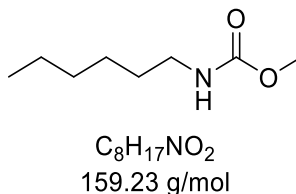
**Polymerization tests of terpene-based lactones Lac1 and Lac2 using a DBU/thiourea catalyst system**

A mixture of 100 mg (1.00 equiv.) lactone, thiourea (5.0 mol%) and pyrene butanol (5.00 mol%) was degassed in a sealed vial. Subsequently, toluene (2 M) and DBU (5.0 mol%) were added. The reaction mixture was stirred at the respective temperature (see **Table 6**). After distinguished time intervals, aliquots of 9  $\mu$ L (corresponding to 1.5 mg  $\epsilon$ -caprolactone) were taken and quenched with benzoic acid. The sample was dried on air and the remaining residue was dissolved in 1.5 mL of THF for SEC measurements.

### 6.2.3. Synthesis and transurethanization of model urethanes

#### Synthesis of model urethanes

##### Methyl hexylcarbamate UR1



In a 50 mL round bottom flask, 1.97 mL (1.52 g, 15.0 mmol, 1.00 equiv.) hexan-1-amine, 12.6 mL (13.5 g, 150 mmol, 10.0 equiv.) DMC, and 160 mg (1.1 mmol, 0.075 equiv.) TBD were stirred at 80 °C. After 5 h of stirring, another 104 mg (0.75 mmol, 0.050 equiv.) TBD were added, and the mixture was stirred overnight. Afterwards, the residue was diluted with ethyl acetate (100 mL) and washed subsequently with saturated  $NH_4Cl$  solution (2 × 60 mL) and brine (60 mL). After drying over  $Na_2SO_4$ , the crude mixture was concentrated and purified via column chromatography (cyclohexane/ethyl acetate 9:1 → 4:1), yielding 2.36 g (14.8 mmol, 99%) of the product as colorless oil.

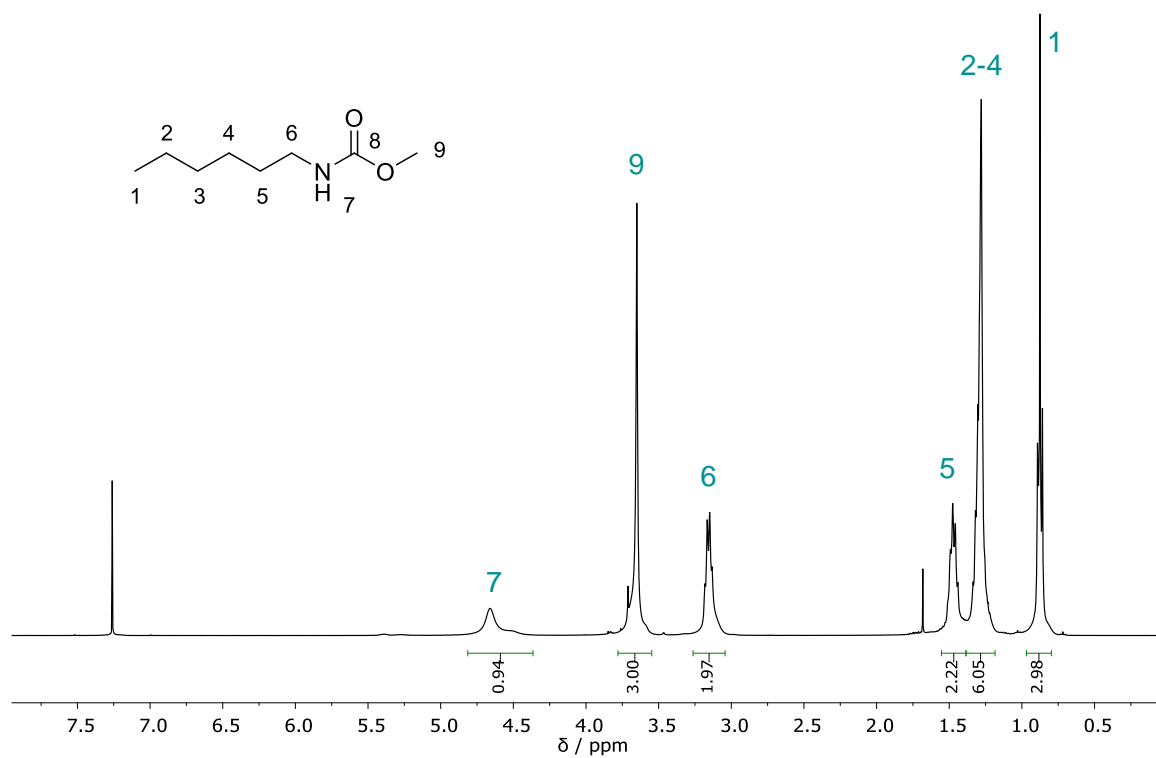
$R_f$  (cyclohexane/ethyl acetate 3:2) = 0.46, visualized by staining with  $KMnO_4$  solution.

$^1H$  NMR (400 MHz,  $CDCl_3$ )  $\delta$  / ppm = 4.81–4.36 (m, 1H, **H7**), 3.65 (s, 3H, **H9**), 3.26–3.04 (m, 2H, **H6**), 1.56–1.38 (m, 2H, **H5**), 1.38–1.17 (m, 6H, **H2-4**), 0.97–0.79 (m, 3H, **H1**).

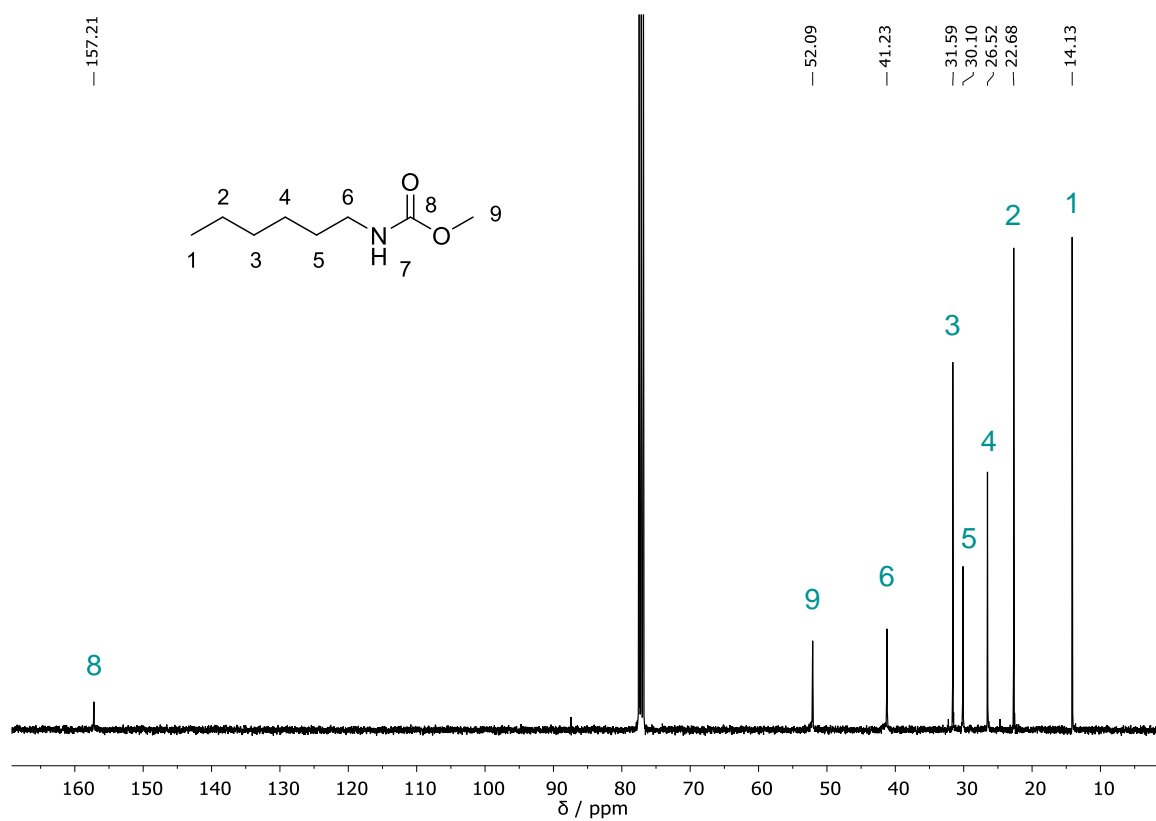
$^{13}C$  NMR (101 MHz,  $CDCl_3$ )  $\delta$  / ppm = 157.2 (**C8**), 52.1 (**C9**), 41.2 (**C6**), 31.6 (**C3**), 30.1 (**C5**), 26.5 (**C4**), 22.7 (**C2**), 14.1 (**C1**).

IR (ATR platinum diamond):  $\tilde{\nu}$  /  $cm^{-1}$  = 3331, 2955, 2928, 2858, 1697, 1531, 1461, 1378, 1342, 1249, 1145, 1042, 936, 876, 779, 725, 633.

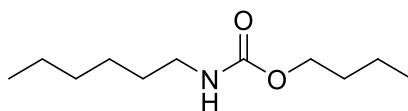
ESI-MS:  $[M+H]^+$  calc. 160.1332, found 160.1330.



Supplementary Figure 32. <sup>1</sup>H NMR spectrum of UR1, measured in CDCl<sub>3</sub> at 400 MHz.



Supplementary Figure 33. <sup>13</sup>C NMR spectrum of UR1, measured in CDCl<sub>3</sub> at 101 MHz.

**Butyl hexylcarbamate UR2**

$C_{11}H_{23}NO_2$   
201.31 g/mol

In a 5 mL pressure vial, 200 mg (1.26 mmol, 1.00 equiv.) methyl hexylcarbamate **UR1**, 1.2 mL (930 mg, 13 mmol, 10 equiv.) *n*-butanol, and 18 mg (0.13 mmol, 0.10 equiv.) TBD were stirred at 90 °C. After 9 h of stirring, the residue was diluted with ethyl acetate (75 mL) and washed subsequently with saturated  $NH_4Cl$  solution (2 × 25 mL) and brine (25 mL). After drying over  $Na_2SO_4$ , the crude mixture was concentrated and purified via column chromatography (cyclohexane/ethyl acetate 1:0 → 7:3), yielding 46 mg (0.23 mmol, 18%) of the product as colorless oil.

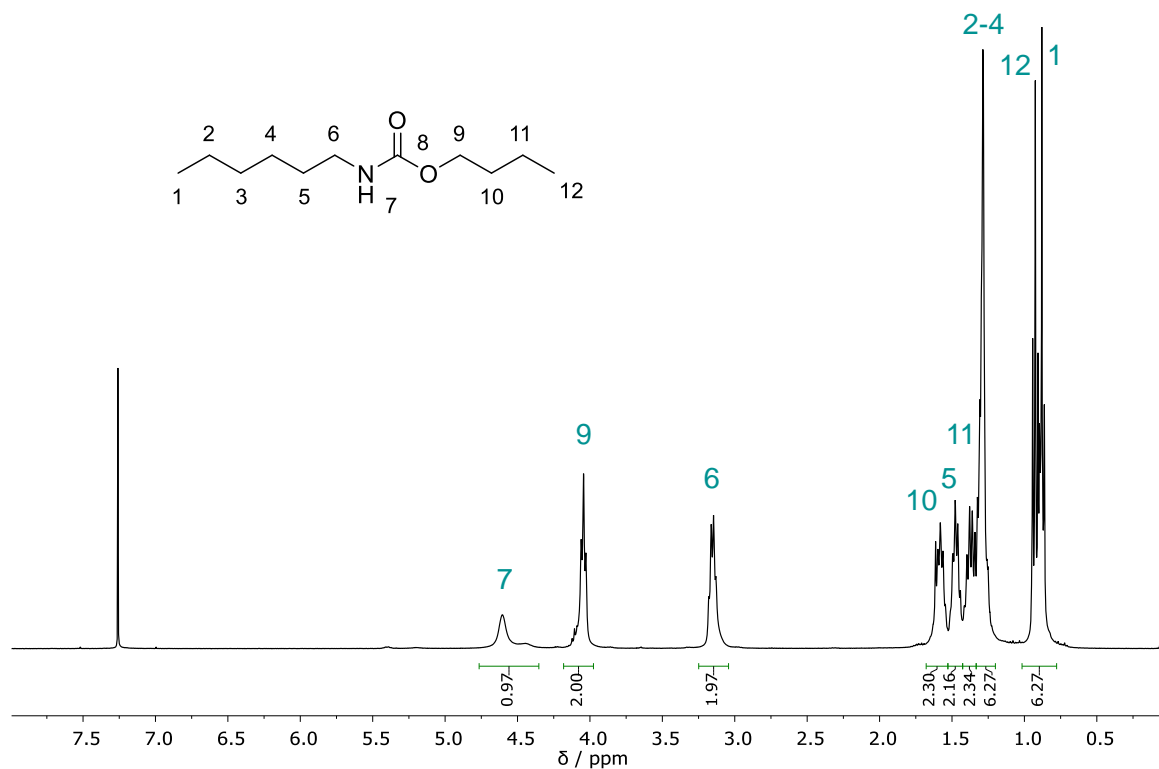
$R_f$  (cyclohexane/ethyl acetate 7:3) = 0.58, visualized by staining with  $KMnO_4$  solution.

$^1H$  NMR (400 MHz,  $CDCl_3$ )  $\delta$  / ppm = 4.76–4.35 (m, 1H, **H7**), 4.17–3.97 (m, 2H, **H9**), 3.25–3.04 (m, 2H, **H6**), 1.68–1.53 (m, 2H, **H10**), 1.53–1.43 (m, 2H, **H5**), 1.43–1.33 (m, 2H, **H11**), 1.33–1.20 (m, 6H, **H2-4**), 1.00–0.80 (m, 6H, **H1**, **H12**).

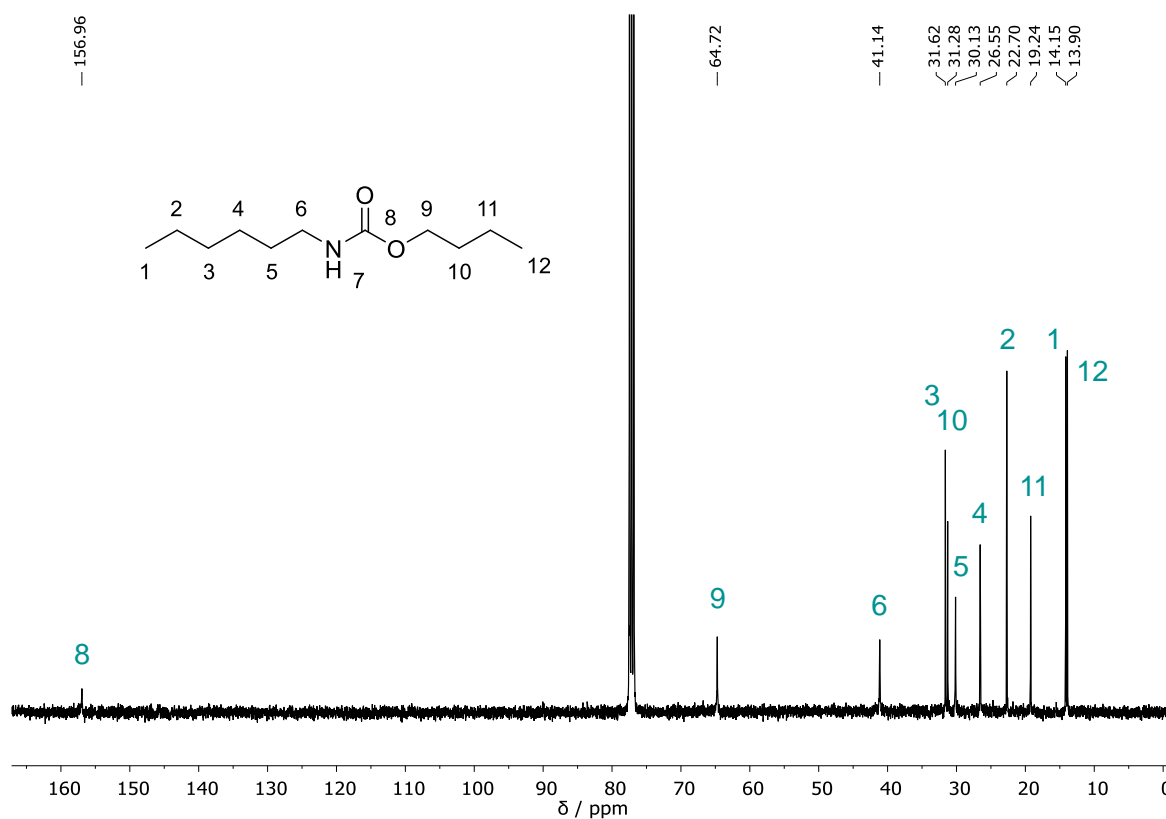
$^{13}C$  NMR (101 MHz,  $CDCl_3$ )  $\delta$  / ppm = 157.0 (**C8**), 64.7 (**C9**), 41.1 (**C6**), 31.6 (**C3**), 31.3 (**C10**), 30.1 (**C5**), 26.6 (**C4**), 22.7 (**C2**), 19.2 (**C11**), 14.2 (**C1**), 13.9 (**C12**).

IR (ATR platinum diamond):  $\tilde{\nu}$  /  $cm^{-1}$  = 3330, 2957, 2929, 2860, 1693, 1532, 1465, 1378, 1247, 1143, 1065, 1037, 779, 726, 632, 505.

ESI-MS:  $[M+H]^+$  calc. 202.1802, found 202.1798.



Supplementary Figure 34. <sup>1</sup>H NMR spectrum of UR2, measured in CDCl<sub>3</sub> at 400 MHz.



Supplementary Figure 35. <sup>13</sup>C NMR spectrum of UR2, measured in CDCl<sub>3</sub> at 101 MHz.



### Transurethanization test reactions

All test reactions were carried out in sealed glass vials. 100 mg (628  $\mu\text{mol}$ , 1.00 equiv.) **UR1**, 57.5  $\mu\text{L}$  (46.6 mg, 628  $\mu\text{mol}$ , 1.00 equiv.) *n*-butanol, and thiourea (5–10 mol%) were dissolved in solvent (0.5–1.0 M) and heated to reflux or up to 90 °C (see **Table 7** and **Table 8**). After distinguished time intervals, aliquots corresponding to 1.5 mg **UR1** were taken for GC-FID measurements.

## 6.2.4. Non-isocyanate polyurethanes from terpenes

### Synthesis of monomers

Compounds **E3**, **CC1**, **CC2**, **CC3**, **CC5**, **UR3**, **UR5**, **UR6**, **UR7**, and **8** were synthesized by the author of this thesis.

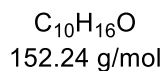
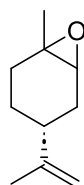
Compounds **E1**, **E4**, and **E5** were synthesized by Michelle Karsten under co-supervision of the author of this thesis.

Compounds **UR8**, **13**, **14**, and **T3** were synthesized by Elsa Brudy under co-supervision of the author of this thesis.

Compound **12** was synthesized by Laura Seidling under co-supervision of the author of this thesis.

### Synthesis of terpene-based epoxides

#### Limonene oxide **E1**



The product was synthesized according to a literature-known procedure.<sup>429</sup>

In a three-necked round-bottom flask, 20.0 g (146 mmol, 1.00 equiv.) (*R*)-limonene were added to a solution of 20 mL water and 90 mL acetone and cooled to 0 °C. Then, 27.4 g (153 mmol, 1.05 equiv.) NBS were slowly added over a period of 30 min. After full conversion was detected via TLC, acetone was removed under reduced pressure. The mixture was diluted with 60 mL diethyl ether and the phases were separated. The organic phase was washed with 100 mL water and dried over  $Na_2SO_4$ . After removing the solvent, 40 mL aqueous sodium hydroxide (6 M) solution were added, and the mixture was stirred at 60 °C for 90 min. After diluting with 60 mL diethyl ether, the phases were separated, and the organic layer was washed with 30 mL saturated sodium bicarbonate solution and 30 mL water. The solvent was removed, and the product was purified by column chromatography (cyclohexane/ethyl acetate 20:1). The product was obtained as a colorless liquid in a yield of 9.71 g (63.8 mmol, 49%).

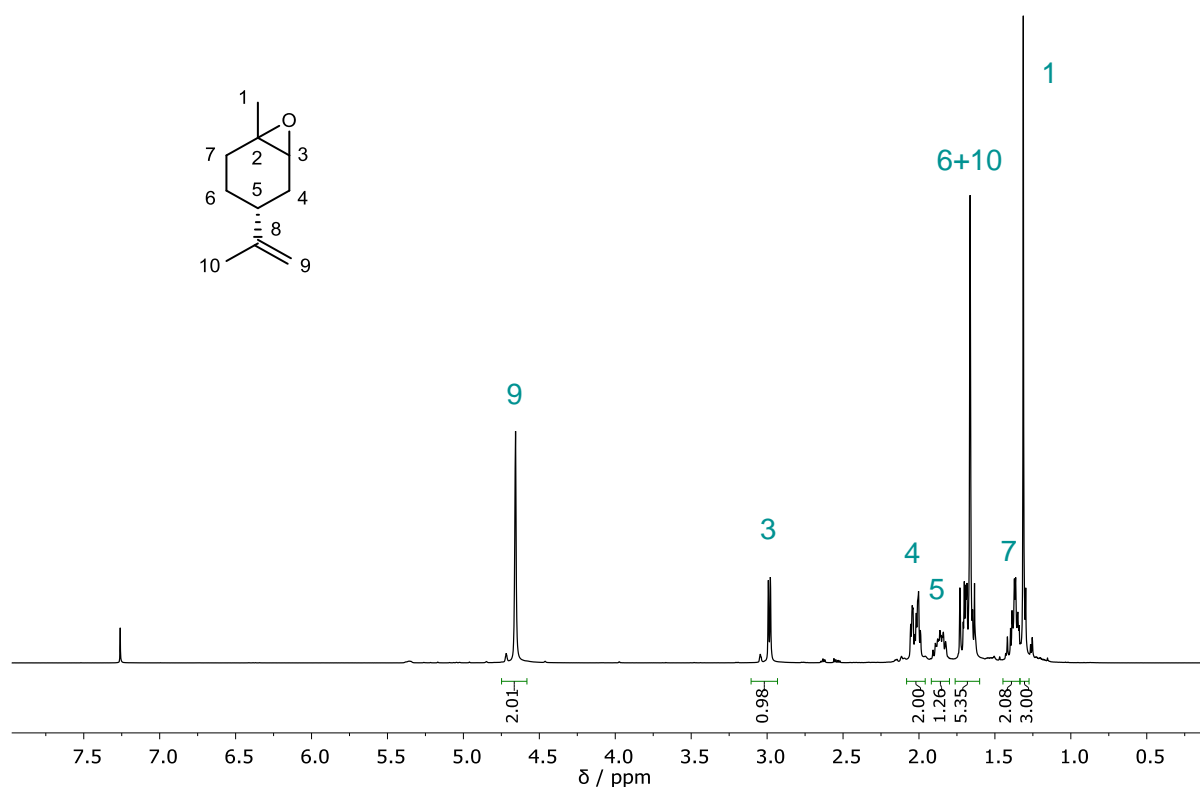
$R_f$  (cyclohexane/ethyl acetate 20:1) = 0.30, visualized by staining with Seebach solution.

$^1\text{H NMR}$  (400 MHz,  $\text{CDCl}_3$ )  $\delta$  / ppm = 4.67–4.58 (m, 2H, **H9**), 3.09–2.92 (m, 1H, **H3**), 2.09–1.95 (m, 2H, **H4**), 1.95–1.79 (m, 1H, **H5**), 1.78–1.58 (m, 5H, **H6**, **H10**), 1.40–1.34 (m, 2H, **H7**), 1.33–1.27 (s, 3H, **H1**).

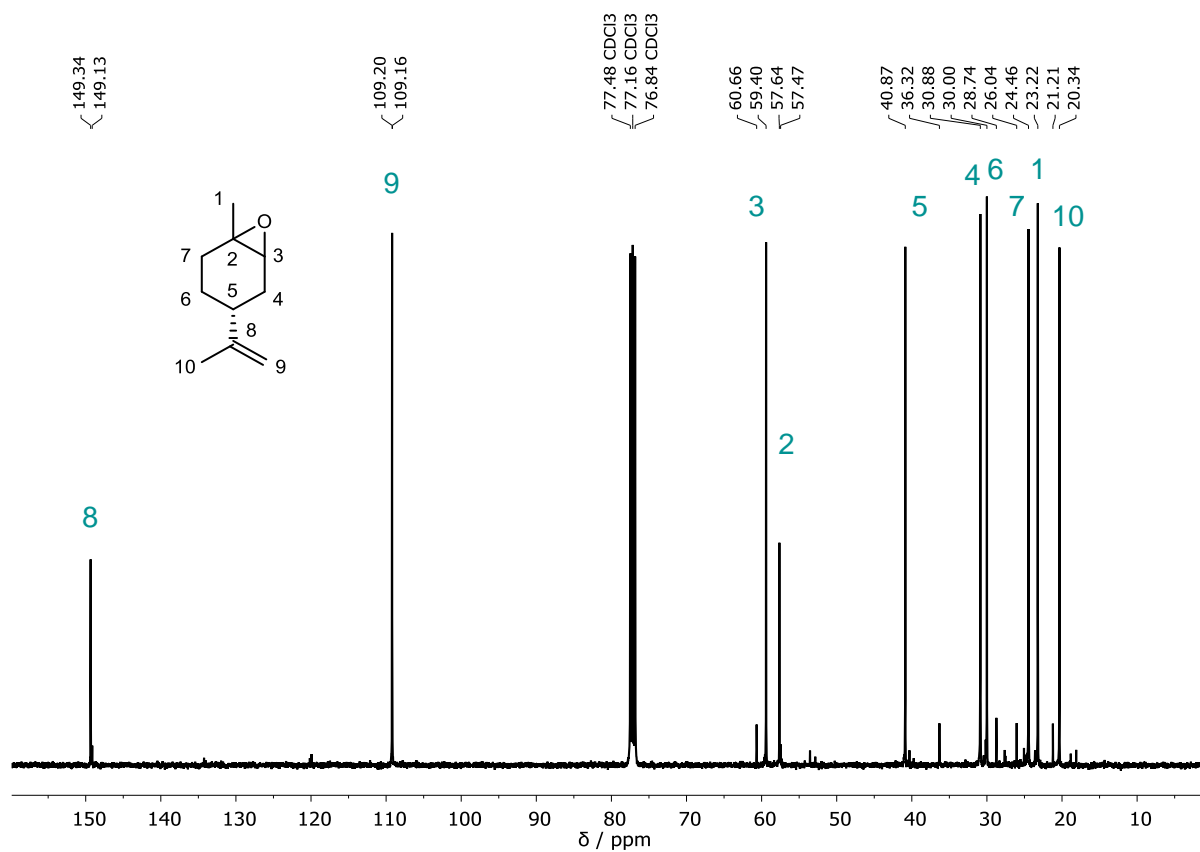
$^{13}\text{C NMR}$  (101 MHz,  $\text{CDCl}_3$ )  $\delta$  / ppm = 149.3 (**C8**) 149.1 (**C8**), 109.2 (**C9**), 60.7 (**C3**) 59.4 (**C3**), 57.6 (**C2**), 57.5 (**C2**), 40.9 (**C5**), 36.3 (**C5**), 30.9 (**C4**), 30.0 (**C6**), 28.7 (**C6**), 26.0 (**C7**), 24.5 (**C7**), 23.2 (**C1**), 21.2 (**C10**), 20.3 (**C10**).

**IR (ATR platinum diamond):**  $\tilde{\nu}$  /  $\text{cm}^{-1}$  = 3073, 2969, 2931, 2861, 1741, 1645, 1449, 1433, 1378, 1360, 1312, 1252, 1209, 1182, 1119, 1097, 1038, 1024, 1013, 970, 885, 841, 806, 758, 671, 611, 556, 525, 507, 460, 444.

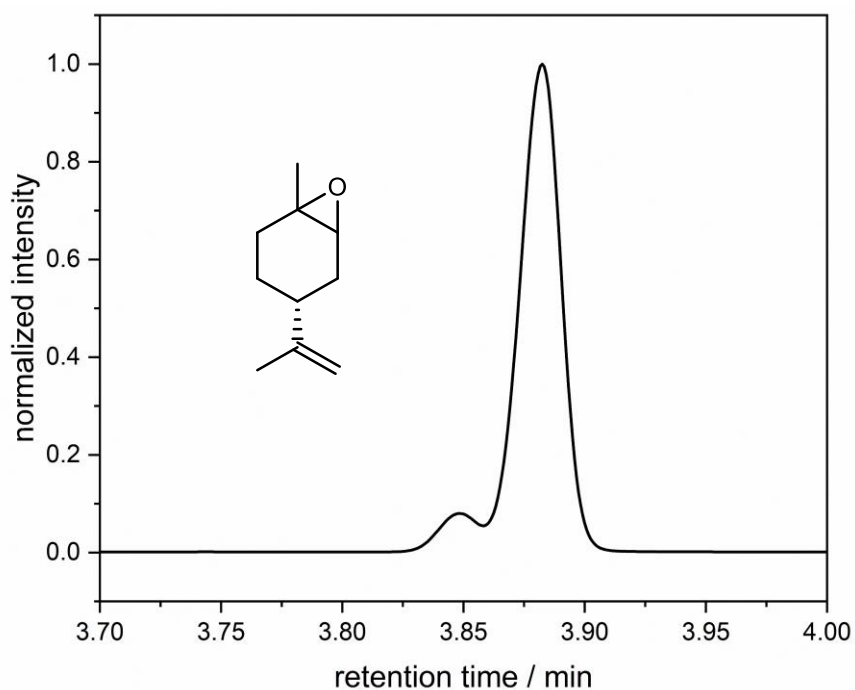
**ESI-MS:**  $[\text{M}+\text{H}]^+$  calc. 153.1274, detected 153.1273.



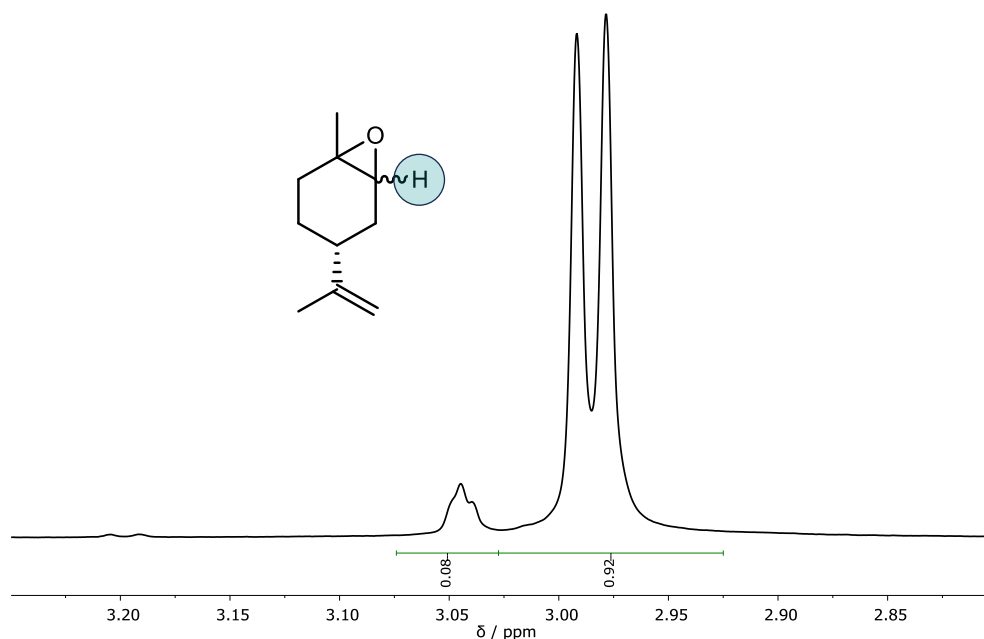
**Supplementary Figure 36.**  $^1\text{H NMR}$  spectrum of **E1**, measured in  $\text{CDCl}_3$  at 400 MHz.



**Supplementary Figure 37.** <sup>13</sup>C NMR spectrum of **E1**, measured in CDCl<sub>3</sub> at 101 MHz.

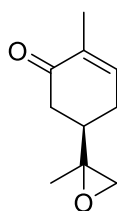


**Supplementary Figure 38.** Determination of diastereomeric ratio of compound **E1** via GC-FID. The calculated diastereomeric ratio is 93:7.



**Supplementary Figure 39.** Determination of diastereomeric ratio of compound **E1** via <sup>1</sup>H NMR spectroscopy. The calculated diastereomeric ratio is 92:8.

### Carvone oxide **E3**



$C_{10}H_{14}O_2$   
166.22 g/mol

The product was synthesized according to a literature-known procedure.<sup>552</sup> 5.00 g (33.3 mmol, 1.00 equiv.) (*S*)-carvone and 13.4 g (160 mmol, 4.80 equiv.) sodium bicarbonate were suspended in 100 mL acetone (0.33 M). 15.3 g (49.9 mmol, 1.50 equiv.) Oxone<sup>®</sup>, dissolved in 100 mL water (0.5 M), were added slowly while stirring. The reaction mixture was stirred at room temperature for 45 min. Afterwards, the mixture was extracted with ethyl acetate (3 × 150 mL). The combined organic phases were washed with water (2 × 100 mL) and dried over Na<sub>2</sub>SO<sub>4</sub>. After removal of the solvent under reduced pressure, the mixture was purified via column chromatography (cyclohexane/ethyl acetate 4:1 → 3:1), yielding 4.69 g (28.2 mmol, 85%) of the product as slightly yellow oil.

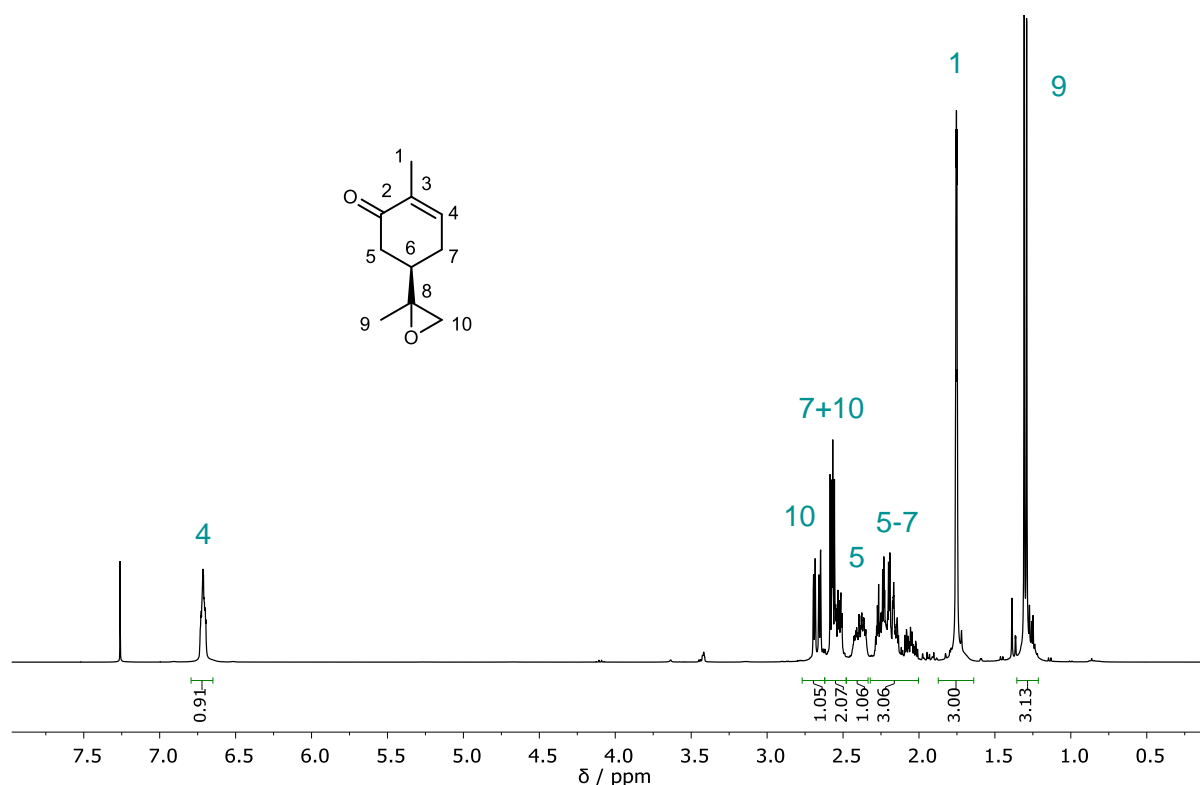
$R_f$  (cyclohexane/ethyl acetate 7:3) = 0.30, visualized by staining with Seebach solution.

$^1\text{H NMR}$  (400 MHz,  $\text{CDCl}_3$ )  $\delta$  / ppm = 6.79–6.65 (m, 1H, **H4**), 2.77–2.62 (m, 1H, **H10**), 2.62–2.48 (m, 2H, **H7**, **H10**), 2.48–2.34 (m, 1H, **H5**), 2.32–2.00 (m, 3H, **H5**, **H6**, **H7**), 1.87–1.70 (m, 3H, **H1**), 1.36–1.21 (m, 3H, **H9**).

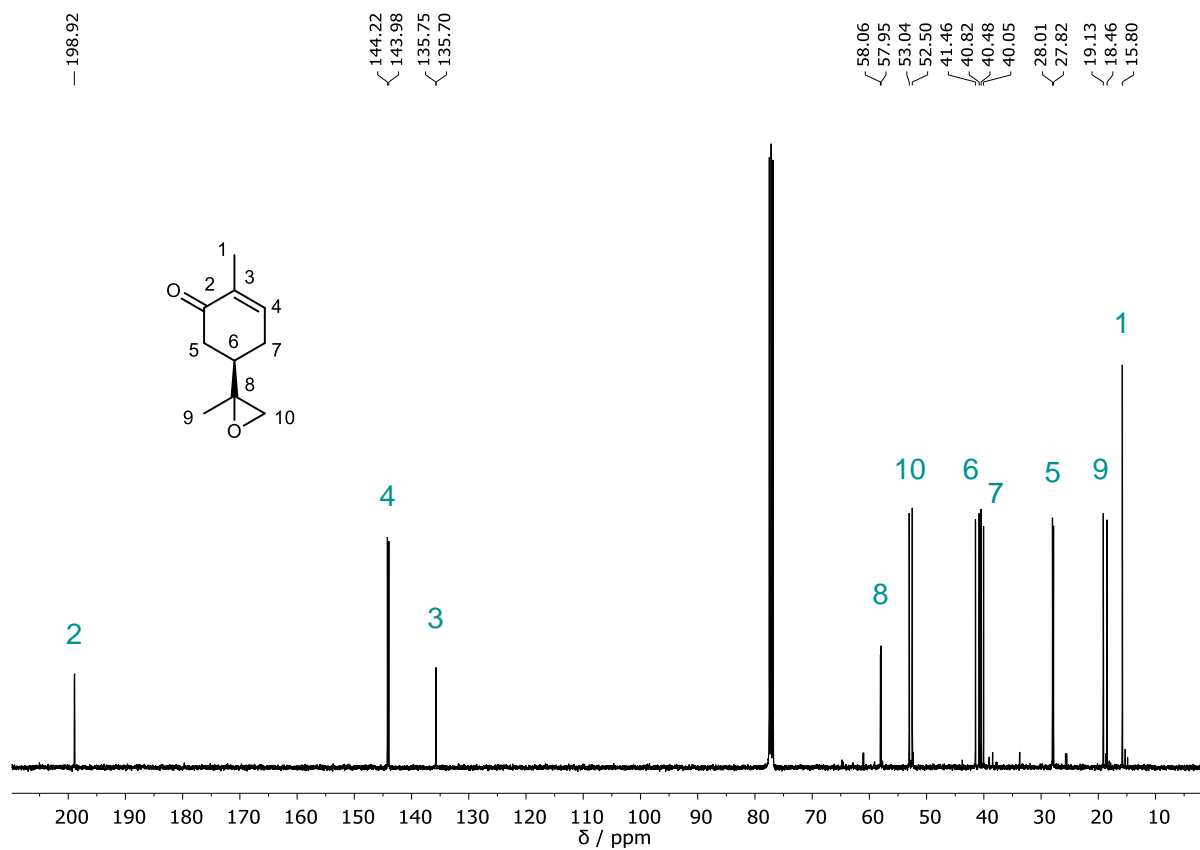
$^{13}\text{C NMR}$  (101 MHz,  $\text{CDCl}_3$ )  $\delta$  / ppm = 198.9 (**C2**), 144.2 (**C4**), 144.0 (**C4**), 135.8 (**C3**), 135.7 (**C3**), 58.1 (**C8**), 58.0 (**C8**), 53.0 (**C10**), 52.5 (**C10**), 41.5 (**C6**), 40.8 (**C6**), 40.5 (**C7**), 40.1 (**C7**), 28.0 (**C5**), 27.8 (**C5**), 19.1 (**C9**), 18.5 (**C9**), 15.8 (**C1**).

**IR (ATR platinum diamond):**  $\tilde{\nu}$  /  $\text{cm}^{-1}$  = 3038, 2975, 2924, 2891, 1710, 1667, 1486, 1450, 1435, 1365, 1249, 1205, 1144, 1106, 1051, 992, 957, 938, 903, 878, 830, 803, 763, 748, 704, 669, 625, 563, 524, 488, 426.

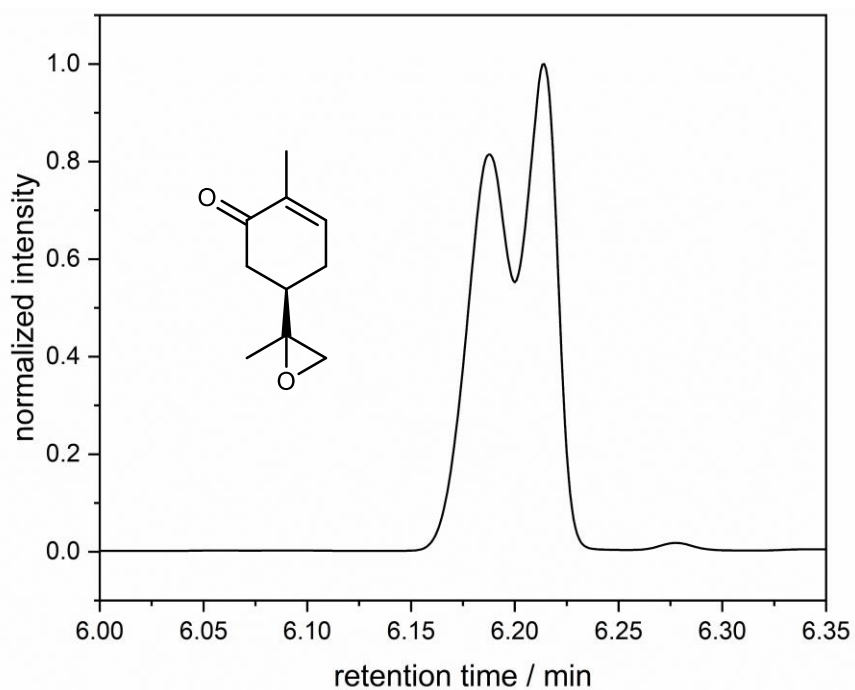
**ESI-MS:**  $[\text{M}+\text{H}]^+$  calc. 167.1067, detected 167.1063.



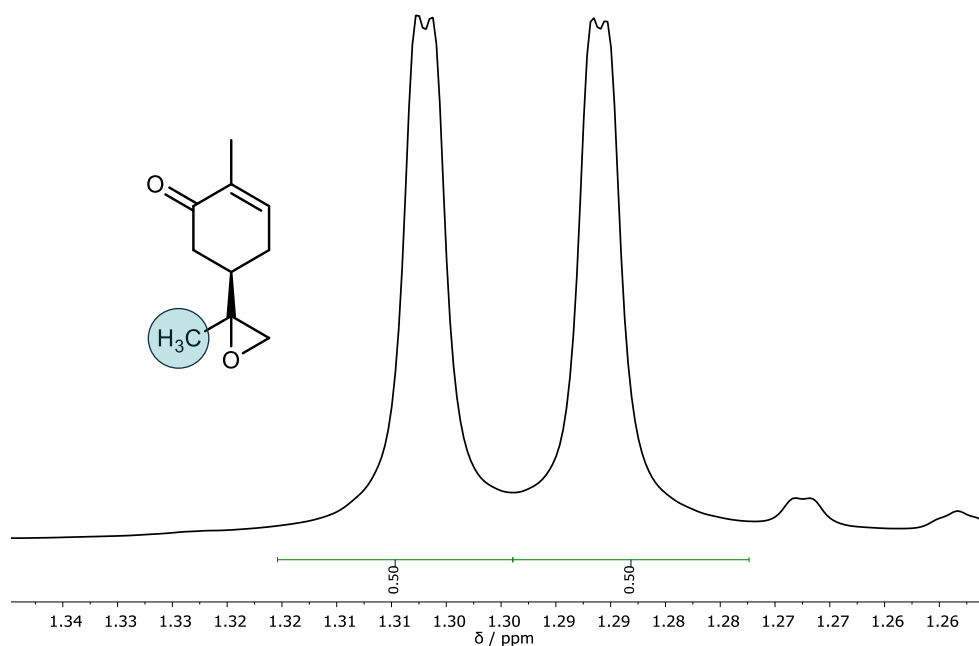
**Supplementary Figure 40.**  $^1\text{H NMR}$  spectrum of **E3**, measured in  $\text{CDCl}_3$  at 400 MHz.



**Supplementary Figure 41.**  $^{13}\text{C}$  NMR spectrum of **E3**, measured in  $\text{CDCl}_3$  at 101 MHz.

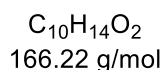
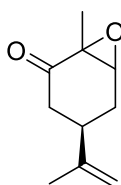


**Supplementary Figure 42.** Determination of diastereomeric ratio of compound **E3** via GC-FID. The calculated diastereomeric ratio is 50:50.



**Supplementary Figure 43.** Determination of diastereomeric ratio of compound **E3** via  $^1\text{H}$  NMR spectroscopy. The calculated diastereomeric ratio is 50:50.

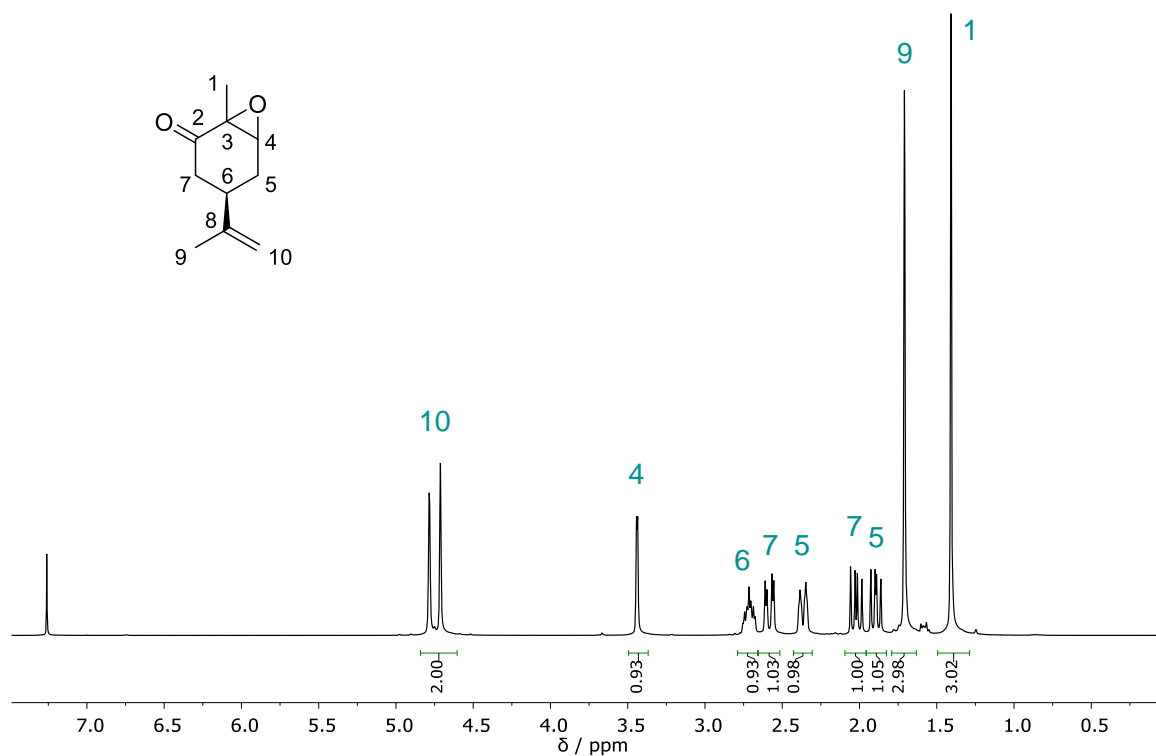
### Carvone oxide **E4**



The product was synthesized according to a literature-known procedure.<sup>552</sup> In a round bottom flask, 3.00 g (20.0 mmol, 1.00 equiv.) (*R*)-(-)-carvone were dissolved in 33 mL methanol. The solution was cooled to 0 °C and 20 mL (10.0 equiv., 20.0 mmol) 30% hydrogen peroxide solution were added to the mixture while stirring. A solution of 1.00 g (1.25 equiv., 25.0 mmol) NaOH in 167 mL water (6 M) was added slowly and the reaction was stirred at 0 °C for 20 min and additional 2.5 h at 40 °C. Afterwards, the reaction mixture was diluted with dichloromethane and washed with water. The organic phase was dried over  $\text{Na}_2\text{SO}_4$  and the solvent was removed under reduced pressure. The crude mixture was purified by column chromatography (cyclohexane/ethyl acetate 9:1) to yield 1.56 g (9.39 mmol, 47%) of the product as a colorless liquid.

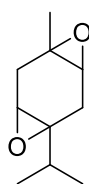


$^1\text{H NMR}$  (400 MHz,  $\text{CDCl}_3$ )  $\delta$  / ppm = 4.84–4.60 (m, 2H, **H10**), 3.49–3.37 (m, 1H, **H4**), 2.78–2.66 (m, 1H, **H6**), 2.66–2.51 (m, 1H, **H7**), 2.43–2.31 (m, 1H, **H5**), 2.09–1.96 (m, 1H, **H7**), 1.96–1.82 (m, 1H, **H5**), 1.79–1.63 (m, 3H, **H9**), 1.50–1.29 (m, 3H, **H1**).



**Supplementary Figure 44.**  $^1\text{H NMR}$  spectrum of **E4**, measured in  $\text{CDCl}_3$  at 400 MHz.

### $\gamma$ -Terpinene epoxide **E5**



$\text{C}_{10}\text{H}_{16}\text{O}_2$   
168.24 g/mol

The product was synthesized according to a literature-known procedure.<sup>552</sup>

5.00 g (36.7 mmol, 1.00 equiv.)  $\gamma$ -terpinene and 14.5 g (173 mmol, 4.70 equiv.)  $\text{NaHCO}_3$  were suspended in 110 mL acetone (0.33 M). 29.3 g (95.4 mmol, 2.60 equiv.) Oxone<sup>®</sup>, dissolved in 184 mL water, were slowly added at 0 °C. The reaction was stirred at room temperature for 2 h. The mixture was diluted with ethyl acetate and the phases were separated. The aqueous phase was extracted with

ethyl acetate and the combined organic phases were washed with water, dried over sodium sulfate, and the solvent was removed under reduced pressure. The crude mixture was purified via column chromatography (cyclohexane/ethyl acetate 95:5  $\rightarrow$  3:1) to yield 4.45 g (26.4 mmol, 72%) of the product as yellow oil.

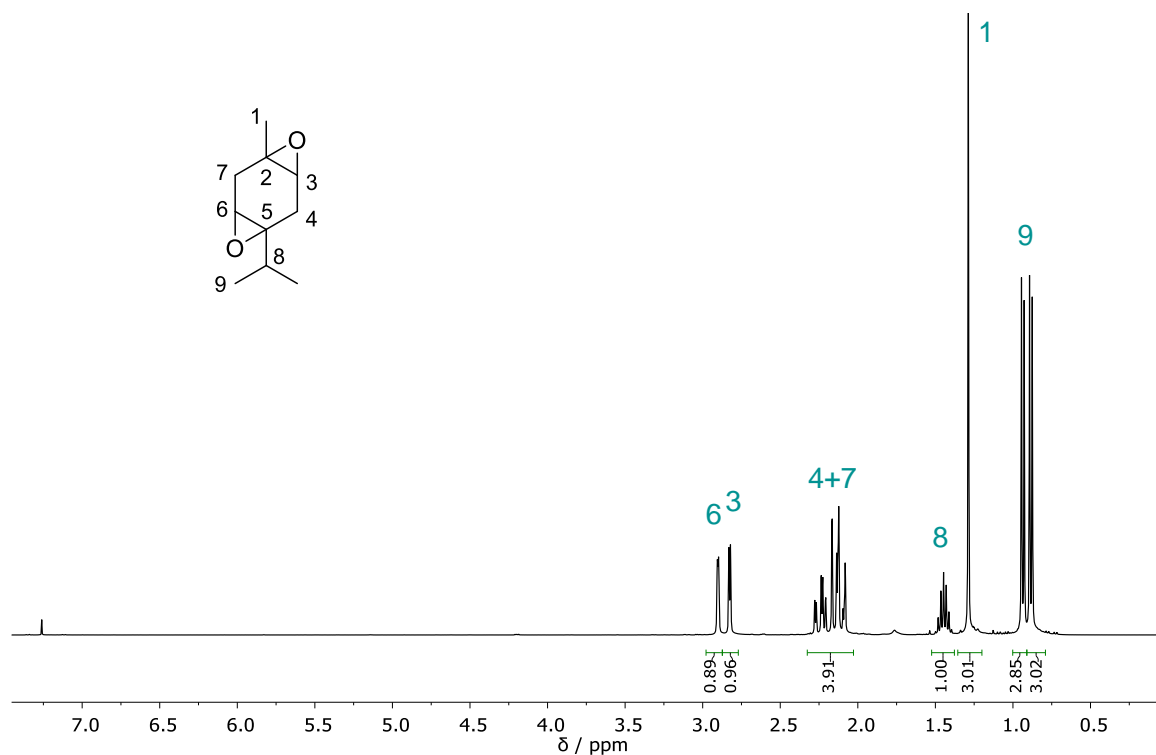
$R_f$  (cyclohexane/ethyl acetate 4:1) = 0.50, visualized by staining with Seebach solution.

$^1\text{H NMR}$  (400 MHz,  $\text{CDCl}_3$ )  $\delta$  / ppm = 2.90 (d,  $J$  = 3.0 Hz, 1H, **H6**), 2.83 (d,  $J$  = 4.0 Hz, 1H, **H3**), 2.33–2.03 (m, 4H, **H4**, **H7**), 1.45 (hept,  $J$  = 6.9 Hz, 1H, **H8**), 1.29 (s, 3H, **H1**), 0.94 (d,  $J$  = 6.8 Hz, 3H, **H9**), 0.88 (d,  $J$  = 7.0 Hz, 3H, **H9**).

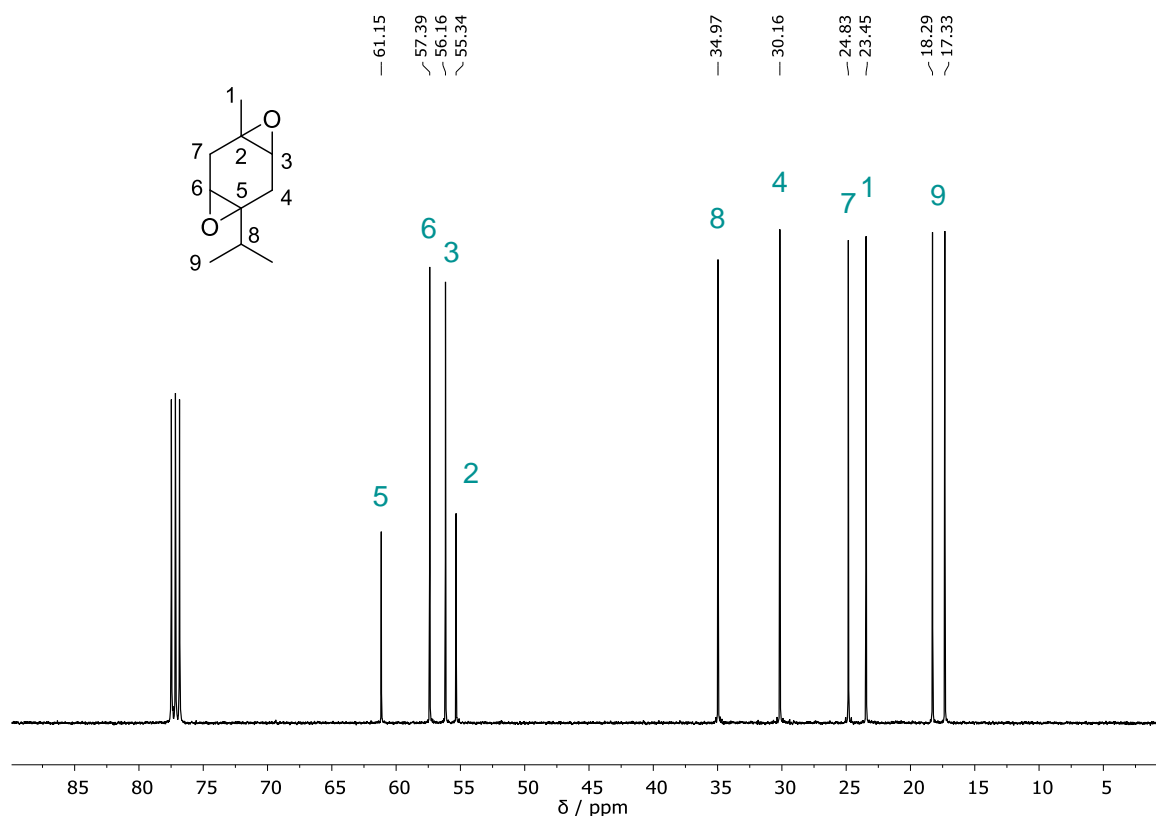
$^{13}\text{C NMR}$  (101 MHz,  $\text{CDCl}_3$ )  $\delta$  / ppm = 61.2 (**C5**), 57.4 (**C6**), 56.2 (**C3**), 55.3 (**C2**), 35.0 (**C8**), 30.2 (**C4**), 24.8 (**H7**), 23.4 (**C1**), 18.3 (**C9**), 17.3 (**C9**).

**IR (ATR platinum diamond):**  $\tilde{\nu}$  /  $\text{cm}^{-1}$  = 2962, 2916, 2876, 1467, 1448, 1419, 1385, 1368, 1334, 1312, 1283, 1243, 1206, 1167, 1154, 1118, 1068, 1029, 1006, 936, 896, 875, 826, 734, 671, 642, 605, 557, 526, 491, 468, 430, 413.

**ESI-MS:**  $[\text{M}+\text{H}]^+$  calc. 169.1223, detected 169.1220.



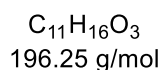
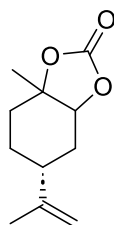
**Supplementary Figure 45.**  $^1\text{H NMR}$  spectrum of **E5**, measured in  $\text{CDCl}_3$  at 400 MHz.



**Supplementary Figure 46.**  $^{13}\text{C}$  NMR spectrum of **E5**, measured in  $\text{CDCl}_3$  at 101 MHz.

## Synthesis of terpene-based cyclic carbonates

### Limonene monocarbonate **CC1**



A stainless-steel reactor with Teflon inset was charged with 8.00 g (52.6 mmol, 1.00 equiv.) limonene oxide **E1**, 876 mg (3.15 mmol, 0.06 equiv.) TBACl and 30 bar  $\text{CO}_2$  pressure. The reaction mixture was stirred and heated to 100 °C for 3 d. After completion of the reaction and cooling to room temperature, the viscous liquid was diluted with ethyl acetate (ca. 200 mL), washed with brine ( $3 \times 100$  mL) and extracted with ethyl acetate (50 mL). The combined organic phases were dried over  $\text{Na}_2\text{SO}_4$ , and the solvent was removed under reduced pressure. 8.23 g of almost pure limonene carbonate **CC1** were obtained, as confirmed by  $^1\text{H}$  NMR and

GC-FID experiments, and was used directly for the synthesis of the urethane monomers **UR3** and **UR7**. For analysis, 1.00 g (12 wt%) of the crude reaction product was purified via column chromatography (cyclohexane/ethyl acetate 94:6  $\rightarrow$  1:1) and 902 mg (4.56 mmol, corresponds to a yield of 72%) of the product were obtained as a colorless liquid.

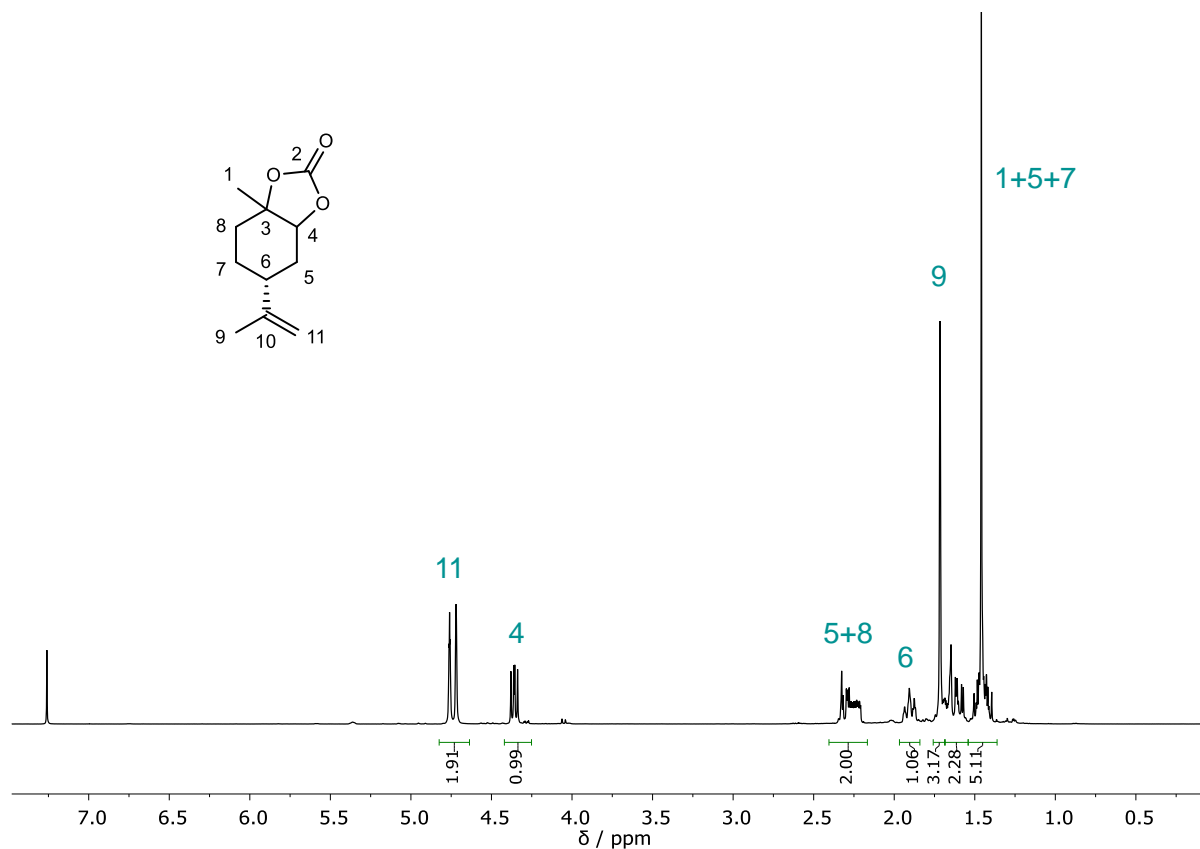
$R_f$  (cyclohexane/ethyl acetate 3:1) = 0.39, visualized by staining with Seebach solution.

$^1\text{H NMR}$  (400 MHz,  $\text{CDCl}_3$ )  $\delta$  / ppm = 4.82–4.68 (m, 2H, **H11**), 4.36 (dd,  $3J = 9.5$ , 7.0 Hz, 1H, **H4**), 2.41–2.17 (m, 2H, **H5**, **H8**), 1.97–1.85 (m, 1H, **H6**), 1.72 (s, 3H, **H9**), 1.69–1.54 (m, 2H, **H7**, **H8**), 1.54–1.37 (m, 5H, **H1**, **H5**, **H7**).

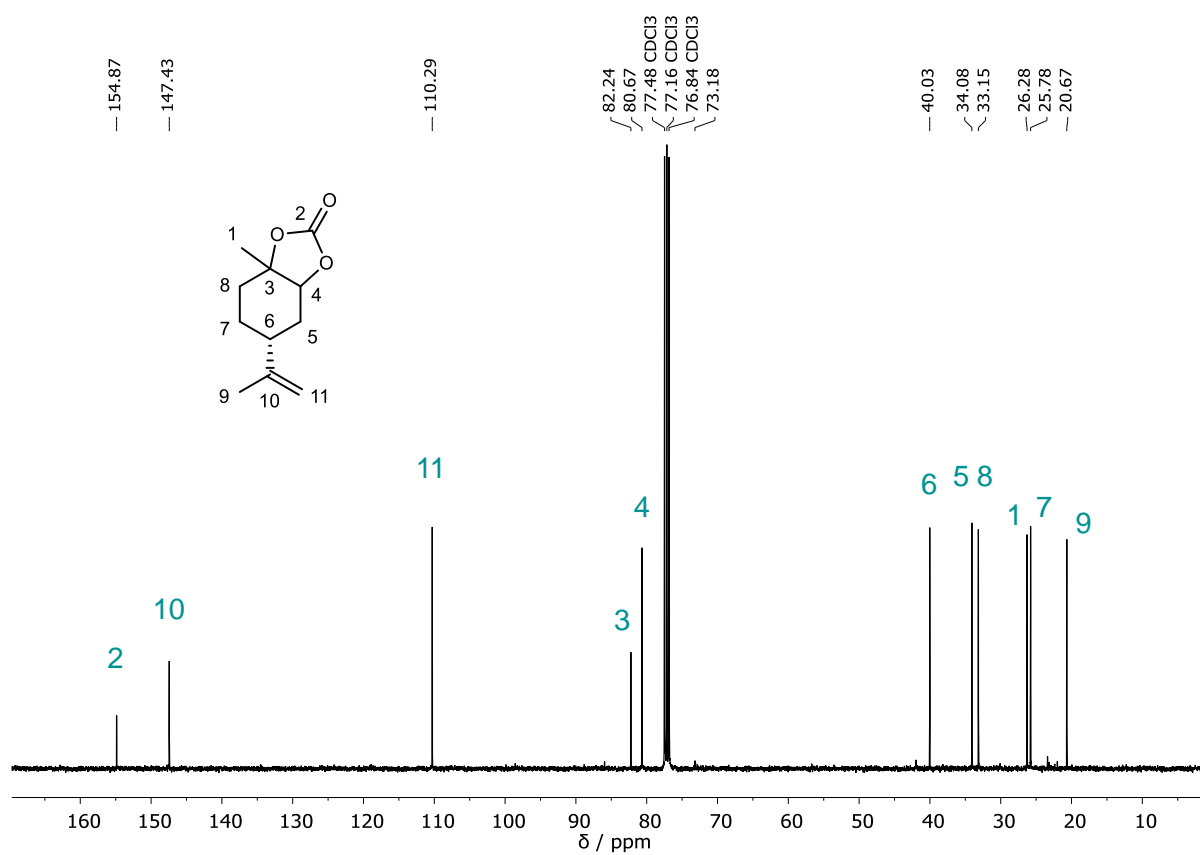
$^{13}\text{C NMR}$  (101 MHz,  $\text{CDCl}_3$ )  $\delta$  / ppm = 154.9 (**C2**), 147.4 (**C10**), 110.3 (**C11**), 82.2 (**C3**), 80.7 (**C4**), 40.0 (**C6**), 34.1 (**C5**), 33.2 (**C8**), 26.3 (**C1**), 25.81 (**C7**), 20.7 (**C9**).

**IR (ATR platinum diamond):**  $\tilde{\nu}$  /  $\text{cm}^{-1}$  = 3082, 2938, 2868, 1789, 1646, 1561, 1455, 1442, 1382, 1348, 1293, 1271, 1247, 1214, 1188, 1150, 1127, 1075, 1024, 1010, 987, 941, 883, 817, 807, 780, 762, 724, 648, 615, 589, 559, 548, 523, 485, 454, 418.

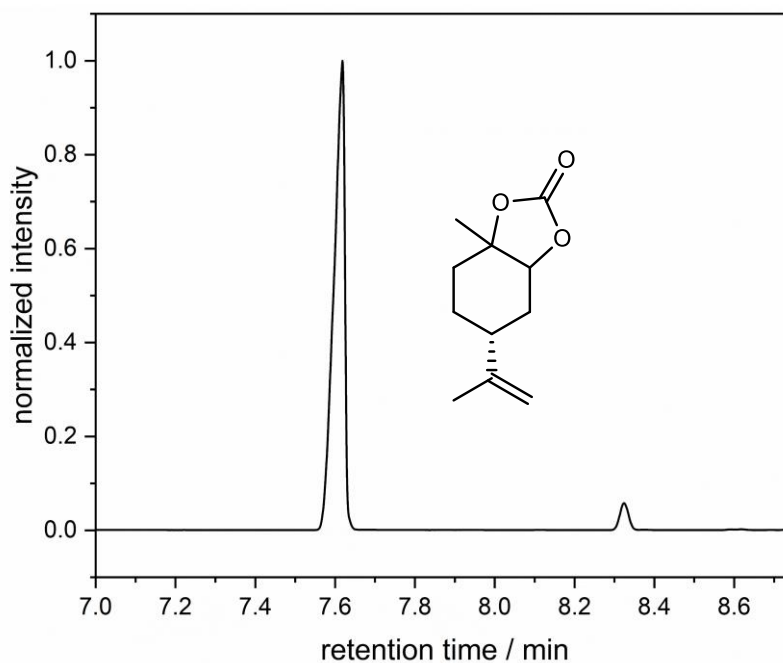
**ESI-MS:**  $[\text{M}+\text{H}]^+$  calc. 197.1172, detected 197.1171.



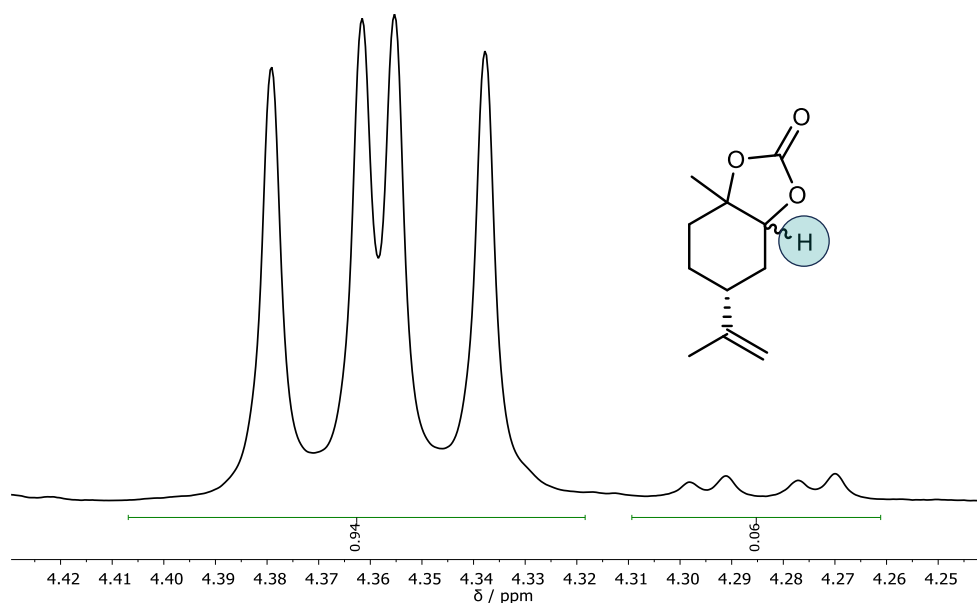
**Supplementary Figure 47.**  $^1\text{H NMR}$  spectrum of **CC1**, measured in  $\text{CDCl}_3$  at 400 MHz.



**Supplementary Figure 48.**  $^{13}\text{C}$  NMR spectrum of **CC1**, measured in  $\text{CDCl}_3$  at 101 MHz.

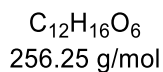
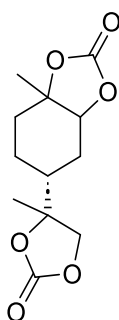


**Supplementary Figure 49.** Determination of diastereomeric ratio of compound **CC1** via GC-FID. The calculated diastereomeric ratio is 95:5.



**Supplementary Figure 50.** Determination of diastereomeric ratio of compound **CC1** via  $^1\text{H}$  NMR spectroscopy. The calculated diastereomeric ratio is 94:6.

### Limonene decarbonate **CC2**



A stainless-steel reactor with Teflon inset was charged with 10.0 g (59.4 mmol, 1.00 equiv.) limonene dioxide **E2**, 991 mg (3.56 mmol, 0.06 equiv.) TBACl and 30 bar  $\text{CO}_2$  pressure. The reaction mixture was stirred and heated to 130 °C for 3 d. After completion of the reaction and cooling to room temperature, the viscous liquid was purified via column chromatography (cyclohexane/ethyl acetate 5:1  $\rightarrow$  1:1) and 13.8 g of a colorless liquid were obtained. The product was further recrystallized in cyclohexane/ethyl acetate to yield 2.95 g (11.5 mmol, 19%) of the product as a colorless solid.

$R_f$  (cyclohexane/ethyl acetate 1:2) = 0.37, visualized by staining with Seebach solution.

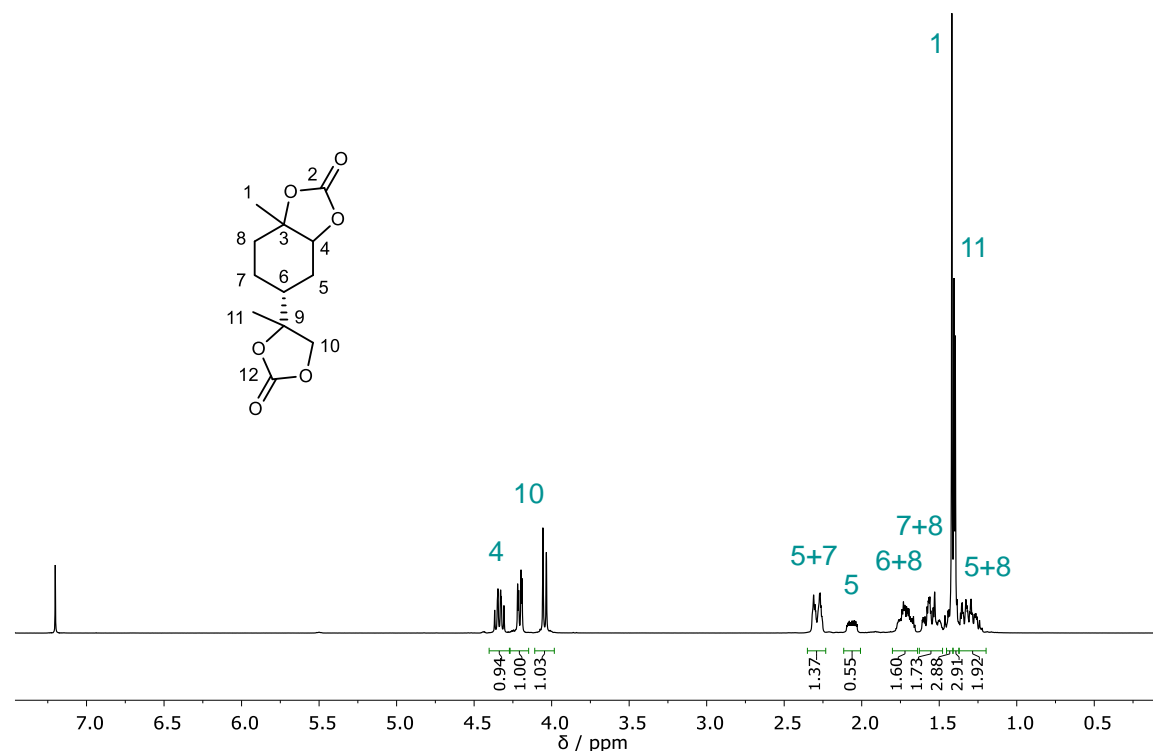
$^1\text{H NMR}$  (400 MHz,  $\text{CDCl}_3$ )  $\delta$  / ppm = 4.40–4.27 (m, **H4**), 4.27–4.15 (m, **H10**), 4.11–3.98 (m, **H10**), 2.35–2.23 (m, **H5**, **H7**), 2.12–2.01 (m, **H5**), 1.80–1.64 (m, **H6**, **H8**), 1.63–1.48 (m, **H7**, **H8**), 1.45–1.41 (m, **H1**), 1.41–1.37 (m, **H11**), 1.37–1.20 (m, **H5**, **H8**).

Due the occurrence of isomers, no integral values are given for the respective NMR signals. The sum of integrals matches the expected number of protons. The purity of the product was confirmed via GC-FID measurements.

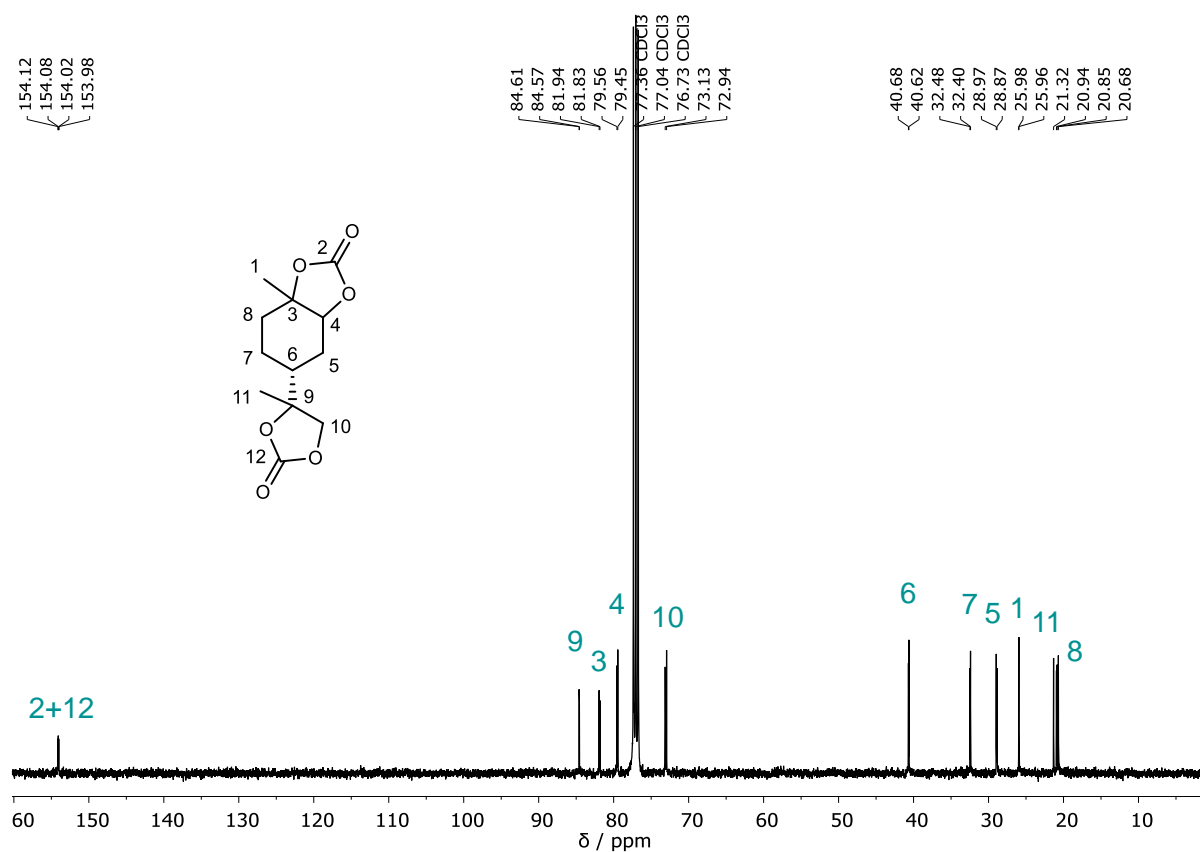
$^{13}\text{C NMR}$  (101 MHz,  $\text{CDCl}_3$ )  $\delta$  / ppm = 154.1 (**C2/C12**), 154.0 (**C2/C12**), 84.6 (**C9**), 81.9 (**C3**), 81.8 (**C3**), 79.6 (**C4**), 79.4 (**C4**), 73.1 (**C10**), 72.9 (**C10**), 40.7 (**C6**), 40.6 (**C6**), 32.5 (**C7**), 32.4 (**C7**), 29.0 (**C5**), 28.9 (**C5**), 26.0 (**C1**), 21.3 (**C11**), 20.9 (**C11**), 20.8 (**C8**), 20.7 (**C8**).

**IR (ATR platinum diamond):**  $\tilde{\nu}$  /  $\text{cm}^{-1}$  = 2983, 2939, 2883, 2871, 1776, 1556, 1481, 1445, 1395, 1359, 1341, 1323, 1301, 1280, 1265, 1247, 1221, 1194, 1171, 1152, 1141, 1105, 1090, 1070, 1054, 1024, 942, 918, 897, 880, 842, 814, 773, 721, 703, 599, 579, 557, 524, 492, 476, 460, 425.

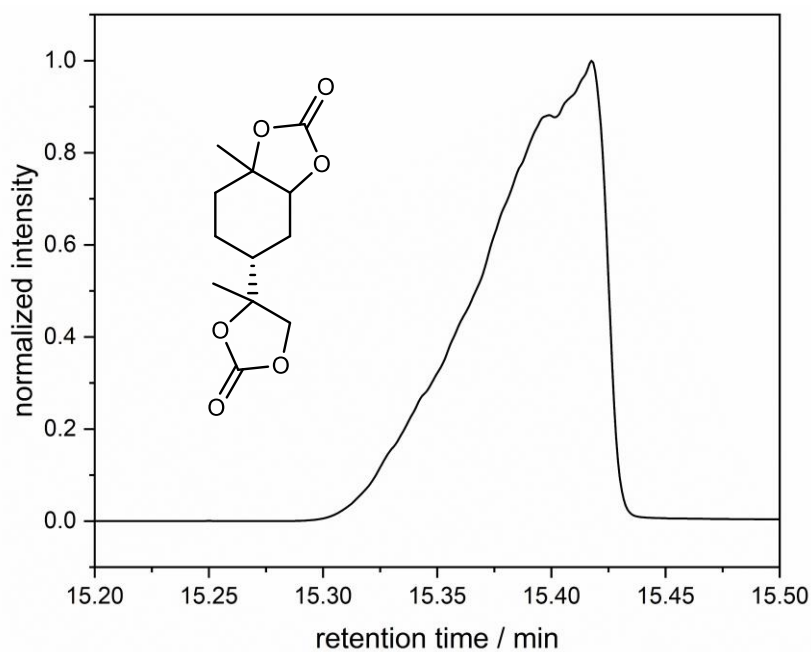
**ESI-MS:**  $[\text{M}+\text{H}]^+$  calc. 257.1020, detected 257.1017.



**Supplementary Figure 51.**  $^1\text{H NMR}$  spectrum of **CC2**, measured in  $\text{CDCl}_3$  at 400 MHz.

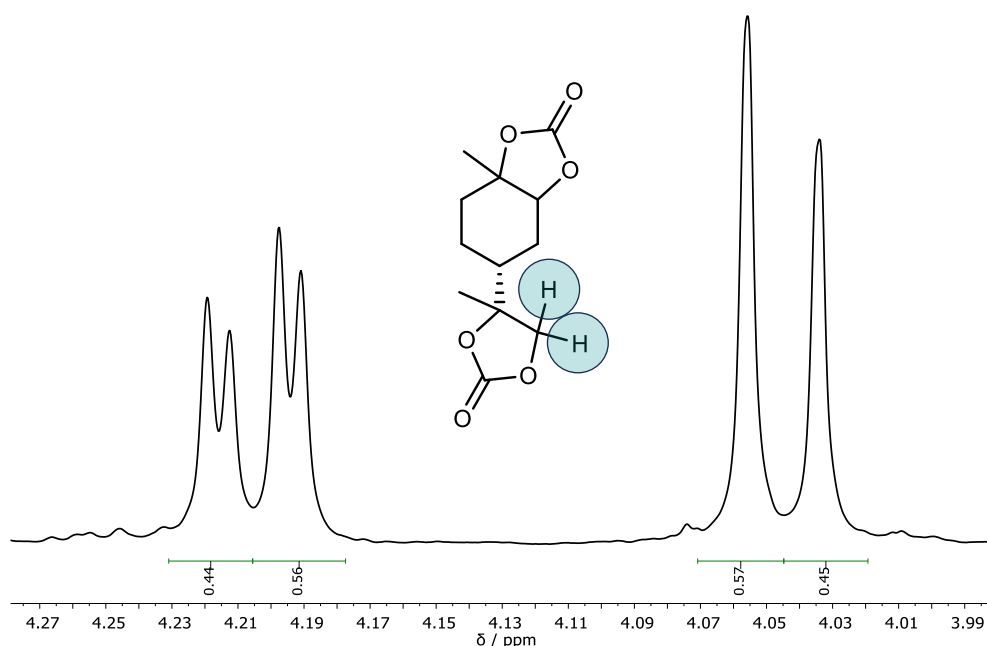


**Supplementary Figure 52.**  $^{13}\text{C}$  NMR spectrum of **CC2**, measured in  $\text{CDCl}_3$  at 101 MHz.



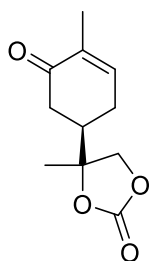
**Supplementary Figure 53.** Determination of diastereomeric ratio of compound **CC2** via GC-FID. The diastereomeric ratio could not be calculated due to insufficient separation of the signals.





**Supplementary Figure 54.** Determination of diastereomeric ratio of compound **CC2** via  $^1\text{H}$  NMR spectroscopy. The calculated diastereomeric ratio is 56:44.

### Carvone carbonate **CC3**



$\text{C}_{11}\text{H}_{14}\text{O}_4$   
210.23 g/mol

A stainless-steel reactor with Teflon inset was charged with 3.00 g (18.0 mmol, 1.00 equiv.) carvone oxide **E3**, 301 mg (1.08 mmol, 0.06 equiv.) TBACl and 30 bar  $\text{CO}_2$  pressure. The reaction mixture was stirred and heated to 100 °C for 40 h. After completion of the reaction and cooling to room temperature, the viscous liquid was diluted with ethyl acetate (ca. 200 mL), washed with brine (3 × 50 mL) and extracted with ethyl acetate (50 mL). The combined organic phases were dried over  $\text{Na}_2\text{SO}_4$ , and the solvent was removed under reduced pressure. The residue was purified via column chromatography (cyclohexane/ethyl acetate 6:1 → 2:1), yielding 3.20 g (15.2 mmol, 85%) of the product as slightly yellow oil.

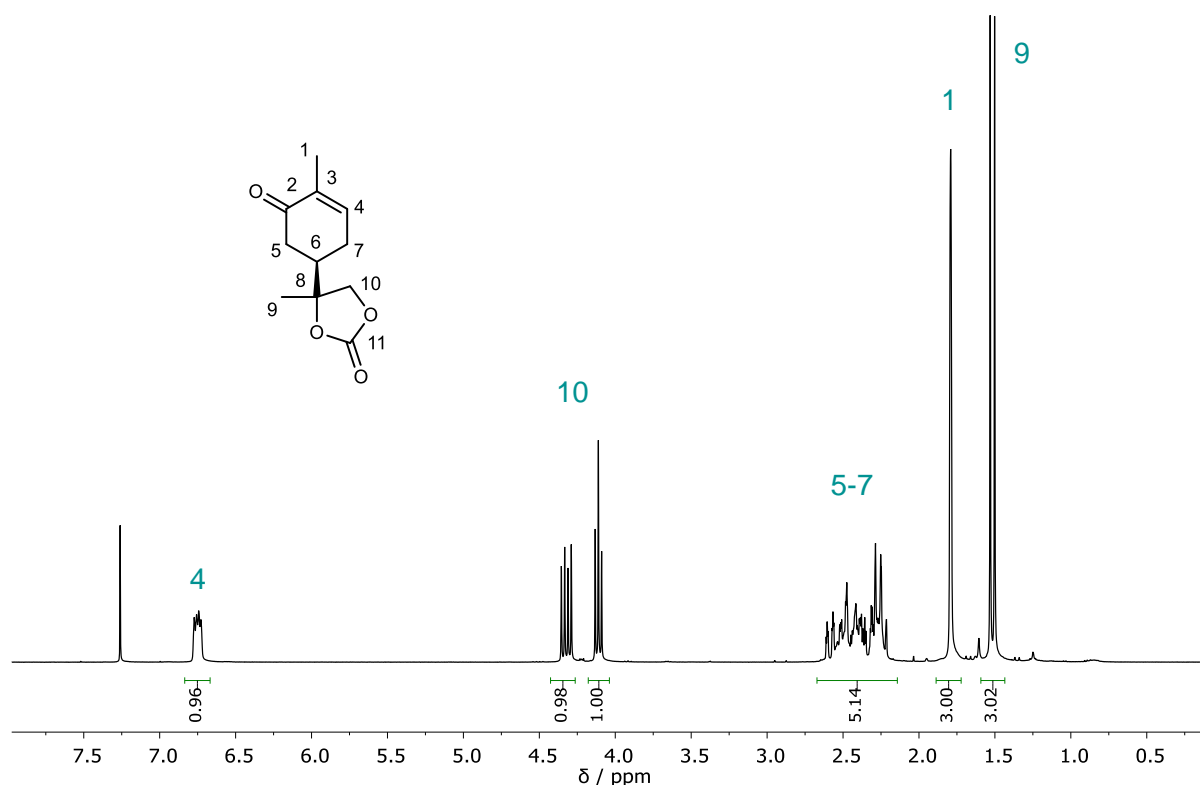
$R_f$  (cyclohexane/ethyl acetate 1:1) = 0.30, visualized by staining with Seebach solution.

$^1\text{H NMR}$  (400 MHz,  $\text{CDCl}_3$ )  $\delta$  / ppm = 6.84–6.67 (m, 1H, **H4**), 4.43–4.26 (m, 1H, **H10**), 4.18–4.04 (m, 1H, **H10**), 2.66–2.18 (m, 5H, **H5-7**), 1.89–1.72 (m, 3H, **H1**), 1.59–1.44 (m, 3H, **H9**).

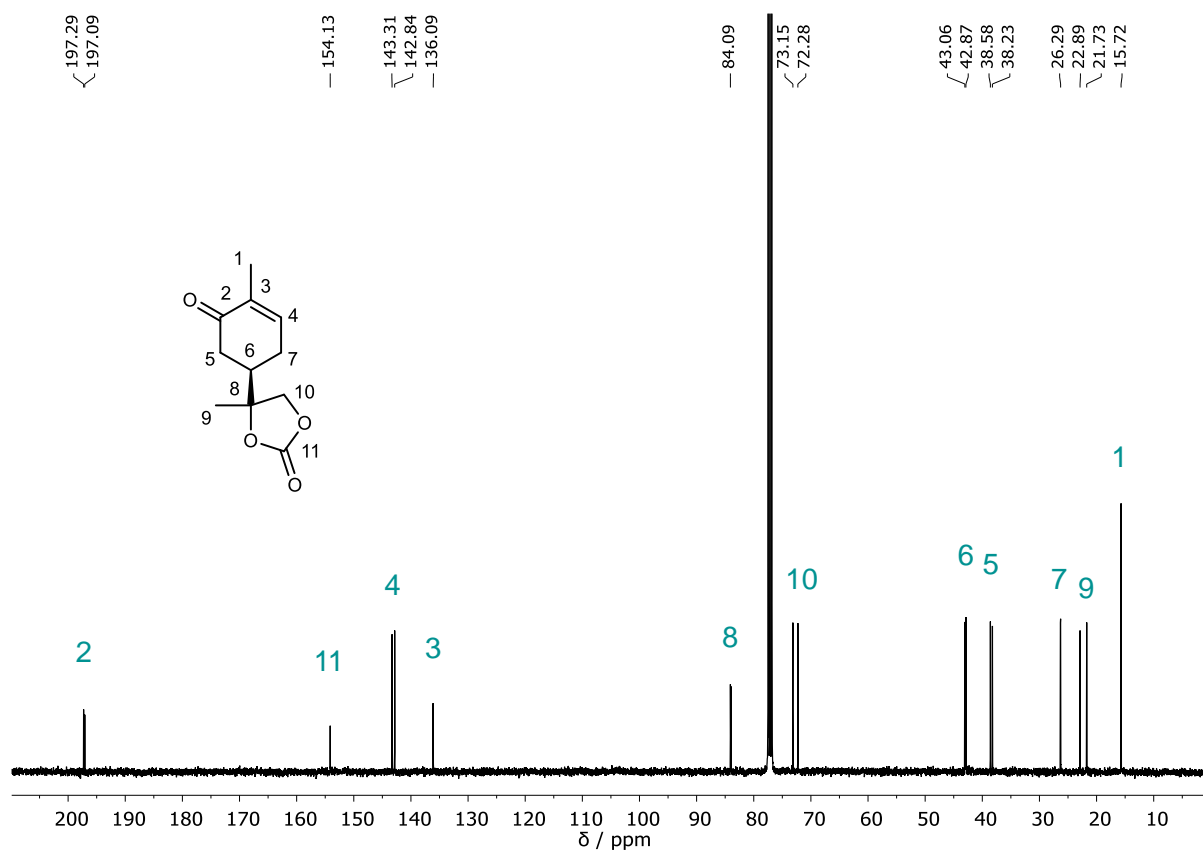
$^{13}\text{C NMR}$  (100 MHz,  $\text{CDCl}_3$ )  $\delta$  / ppm = 197.3 (**C2**), 197.1 (**C2**), 154.1 (**C11**), 143.3 (**C4**), 142.8 (**C4**), 136.1 (**C3**), 84.1 (**C8**), 73.1 (**C10**), 72.3 (**C10**), 43.1 (**C6**), 42.9 (**C6**), 38.6 (**C5**), 38.2 (**C5**), 26.3 (**C7**), 22.9 (**C9**), 21.7 (**C9**), 15.7 (**C1**).

**IR (ATR platinum diamond):**  $\tilde{\nu}$  /  $\text{cm}^{-1}$  = 2981, 2954, 2926, 2902, 2853, 1767, 1670, 1547, 1487, 1452, 1398, 1384, 1363, 1322, 1289, 1260, 1241, 1223, 1186, 1167, 1106, 1057, 1019, 952, 906, 843, 801, 773, 721, 706, 599, 573, 557, 533, 476, 421.

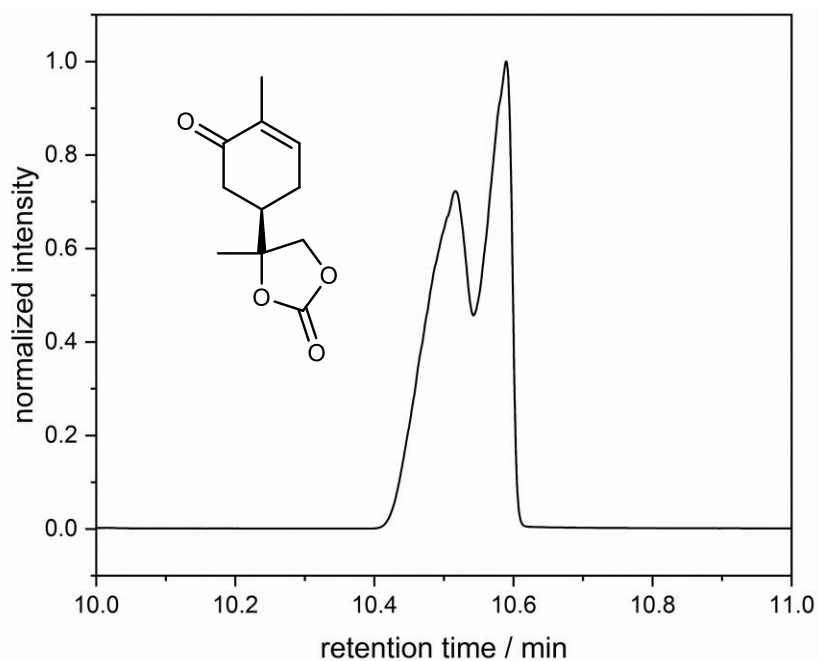
**ESI-MS:**  $[\text{M}+\text{H}]^+$  calc. 211.0965, detected 211.0960.



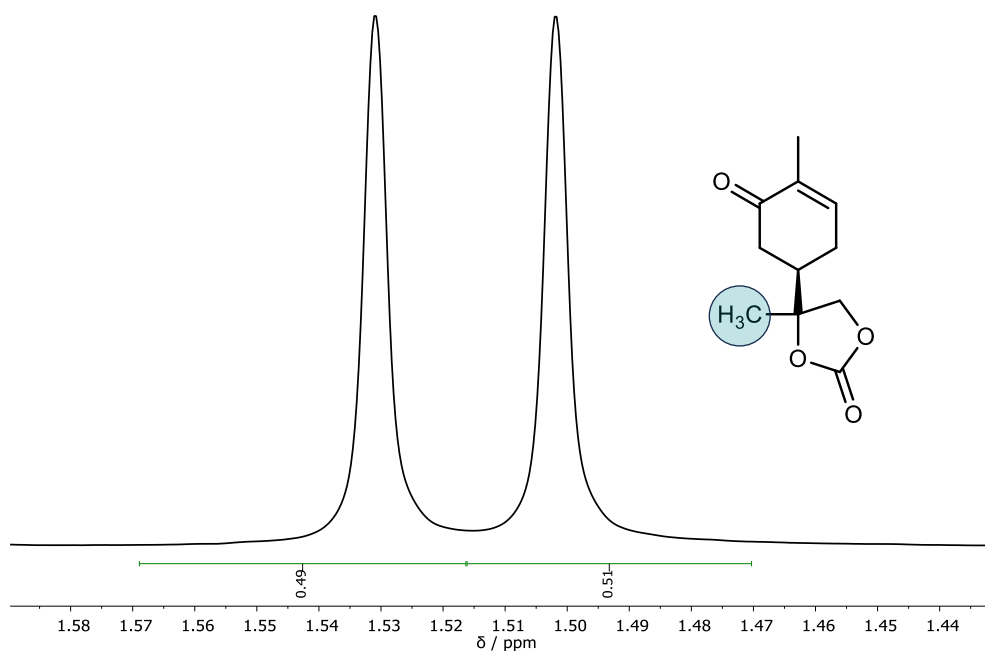
**Supplementary Figure 55.**  $^1\text{H NMR}$  spectrum of **CC3**, measured in  $\text{CDCl}_3$  at 400 MHz.



**Supplementary Figure 56.** <sup>13</sup>C NMR spectrum of **CC3**, measured in CDCl<sub>3</sub> at 101 MHz.

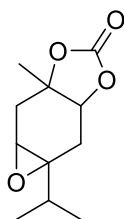


**Supplementary Figure 57.** Determination of diastereomeric ratio of compound **CC3** via GC-FID. The calculated diastereomeric ratio is 53:47.



**Supplementary Figure 58.** Determination of diastereomeric ratio of compound **CC3** via  $^1\text{H}$  NMR spectroscopy. The calculated diastereomeric ratio is 51:49.

### $\gamma$ -Terpinene monocarbonate **CC5a**



$\text{C}_{11}\text{H}_{16}\text{O}_4$   
212.24 g/mol

A stainless-steel reactor with Teflon inset was charged with 1.00 g (5.94 mmol, 1.00 equiv.) carvone oxide **E5**, 60 mg (250  $\mu\text{mol}$ , 0.03 equiv.) TBABr and 30 bar  $\text{CO}_2$  pressure. The reaction mixture was stirred and heated to 130  $^\circ\text{C}$  for 7 d. Afterwards, the mixture was diluted with ethyl acetate (150 mL), washed with brine (2  $\times$  80 mL) dried over  $\text{Na}_2\text{SO}_4$ , and the solvent was removed under reduced pressure. After purification via column chromatography (cyclohexane/ethyl acetate 95:5  $\rightarrow$  1:1), 302 mg (1.42 mmol, 24%) of the product **CC5a** were isolated.

$R_f$  (cyclohexane/ethyl acetate 1:1) = 0.39, visualized by staining with Seebach solution.

$^1\text{H}$  NMR (400 MHz,  $\text{CDCl}_3$ )  $\delta$  / ppm = 4.70–4.30 (m, 1H, **H4**), 3.29–3.02 (m, 1H, **H7**), 2.59 (dd,  $J$  = 16.3, 4.1 Hz, 1H, **H5**), 2.47–2.34 (m, 1H, **H8**), 2.11–1.97 (m, 1H,

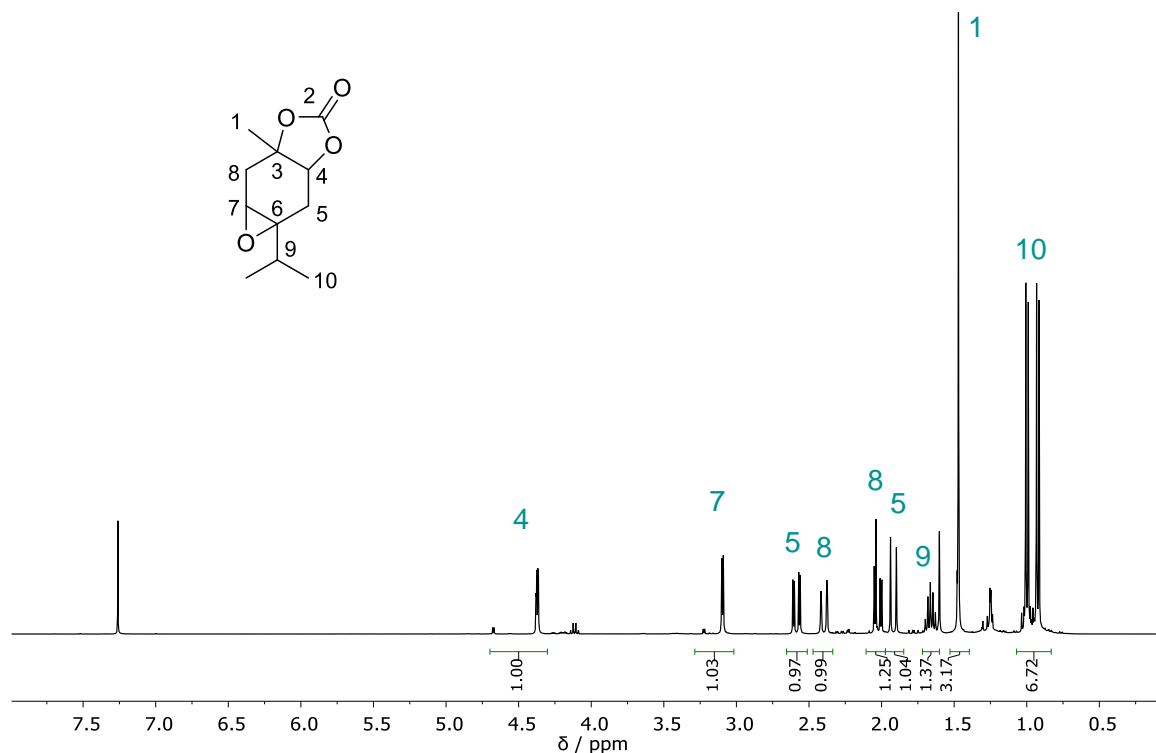
**H8**), 1.92 (d,  $J = 16.3$  Hz, 1H, **H5**), 1.72–1.60 (m, 1H, **H9**), 1.47 (s, 3H, **H1**), 1.00 (d,  $J = 6.8$  Hz, 3H, **H10**), 0.92 (d,  $J = 7.0$  Hz, 6H, **H10**).

Due to the occurrence of isomers, signals of the minor isomer are not entirely assigned. The sum of integrals matches the expected number of protons. The signals of the isomeric forms are referred to as a (major isomer) and b (minor isomer).

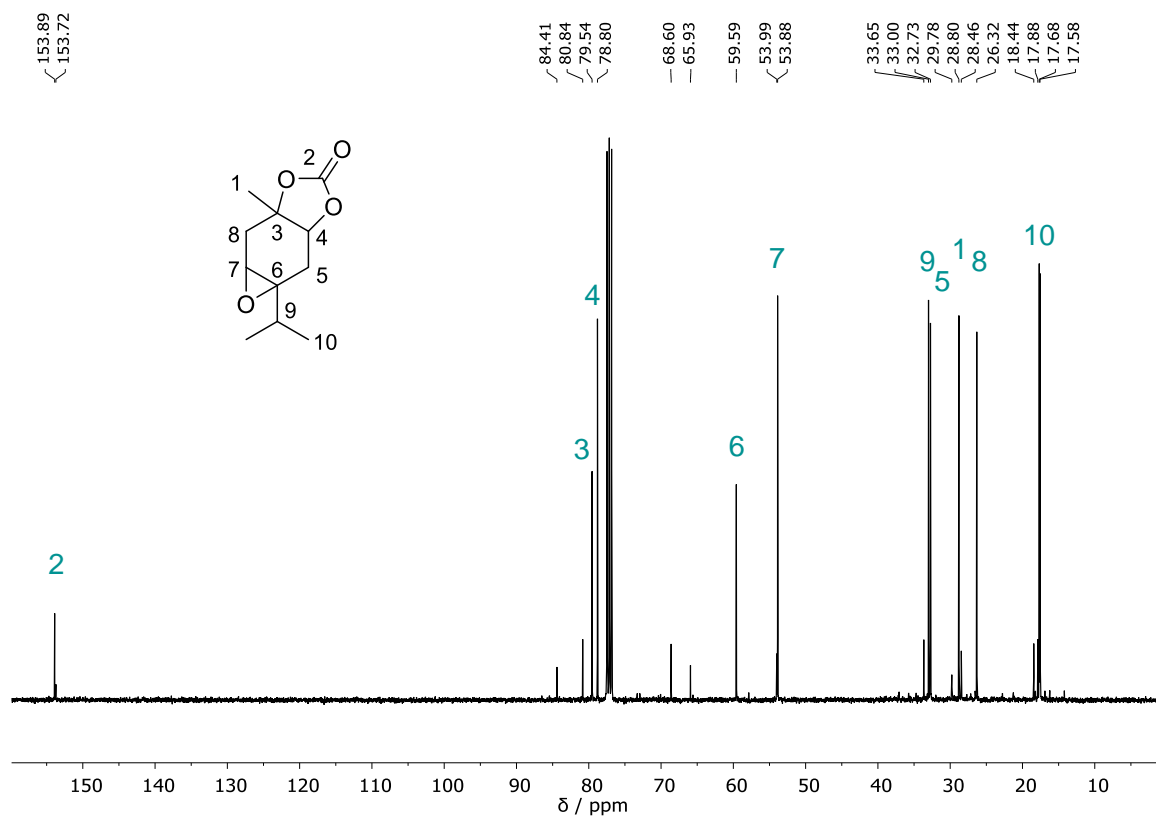
**$^{13}\text{C}$  NMR (101 MHz,  $\text{CDCl}_3$ )  $\delta$  / ppm = 153.9 (**C2a**), 153.7 (**C2b**), 84.4 (**Cb**), 80.8 (**C4b**), 79.5 (**C3**), 78.8 (**C4a**), 68.6 (**Cb**), 65.9 (**Cb**), 59.6 (**C6**), 54.0 (**C7b**), 53.9 (**C7a**), 33.6 (**Cb**), 33.0 (**C9**), 32.7 (**C5**), 29.8 (**Cb**), 28.8 (**C1a**), 28.5 (**Cb**), 26.3 (**C8**), 18.4 (**C1b**), 17.9 (**C10b**), 17.7 (**C10a**), 17.6 (**C10a**).**

**IR (ATR platinum diamond):  $\tilde{\nu}$  /  $\text{cm}^{-1}$  = 2973, 2960, 2931, 2913, 2898, 2877, 2855, 1775, 1535, 1463, 1451, 1426, 1386, 1360, 1342, 1321, 1310, 1263, 1246, 1218, 1165, 1137, 1116, 1076, 1054, 1020, 1010, 946, 933, 905, 871, 832, 767, 715, 678, 666, 631, 585, 570, 522, 481, 460.**

**ESI-MS:**  $[\text{M}+\text{H}]^+$  calc. 213.1121, detected 213.1116.



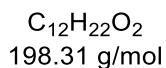
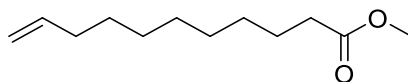
**Supplementary Figure 59.**  $^1\text{H}$  NMR spectrum of **CC5a**, measured in  $\text{CDCl}_3$  at 400 MHz.



**Supplementary Figure 60.**  $^{13}\text{C}$  NMR spectrum of **CC5a**, measured in  $\text{CDCl}_3$  at 101 MHz.

## Synthesis of 10-undecenoic acid-based amine

### Methyl undec-10-enoate **12**



In a round bottom flask, 82.0 g (445 mmol, 1.00 equiv.) undec-10-enoic acid were dissolved in in 200 mL methanol. 5.93 mL (10.9 g, 111 mmol, 0.25 equiv.)  $\text{H}_2\text{SO}_4$  were added, and the reaction mixture was stirred under reflux conditions for 25 h. After cooling to room temperature, the solution was neutralized with sodium bicarbonate (21 g). The solution was filtered, and the solvent was removed under reduced pressure. The residue was diluted in ethyl acetate (200 mL) and washed with saturated  $\text{NaHCO}_3$  solution ( $3 \times 50$  mL), water (50 mL) and brine (50 mL). The organic phase was dried over  $\text{Na}_2\text{SO}_4$ , and the solvent was removed under reduced pressure. The crude mixture was purified via vacuum distillation ( $p = 30$  mbar,  $T = 165$  °C), yielding 71.7 g (362 mmol, 81 %) of the product as a colorless liquid.

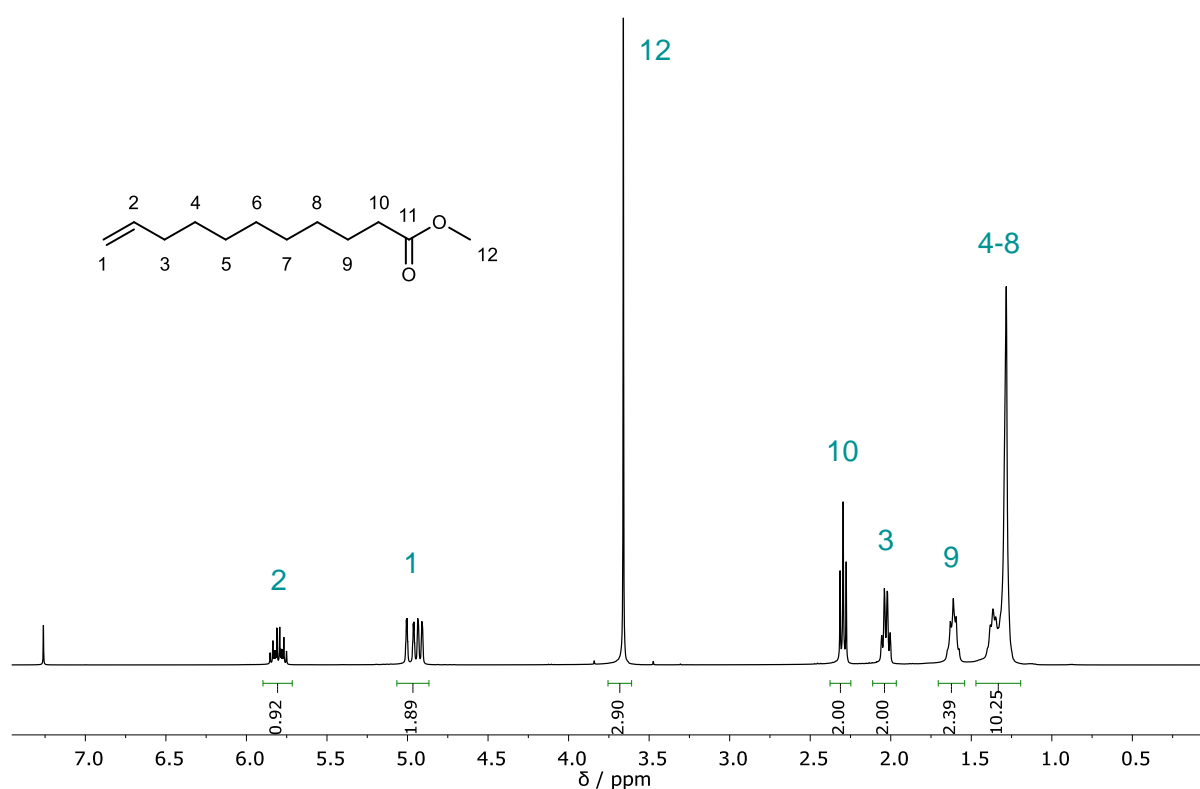
**R<sub>f</sub>** (*n*-hexane/diethyl ether 7:3) = 0.67, visualized by staining with Seebach solution.

**<sup>1</sup>H NMR (400 MHz, CDCl<sub>3</sub>)**  $\delta$  / ppm = 5.80 (ddt,  $J$  = 17.0, 10.2, 6.7 Hz, 1H, **H2**), 5.07–4.87 (m, 2H, **H1**), 3.66 (s, 3H, **H12**), 2.30 (t,  $J$  = 7.6 Hz, 2H, **H10**), 2.03 (tdd,  $J$  = 6.5, 5.3, 1.5 Hz, 2H, **H3**), 1.71–1.54 (m, 2H, **H9**), 1.47–1.19 (m, 10H, **H4–8**).

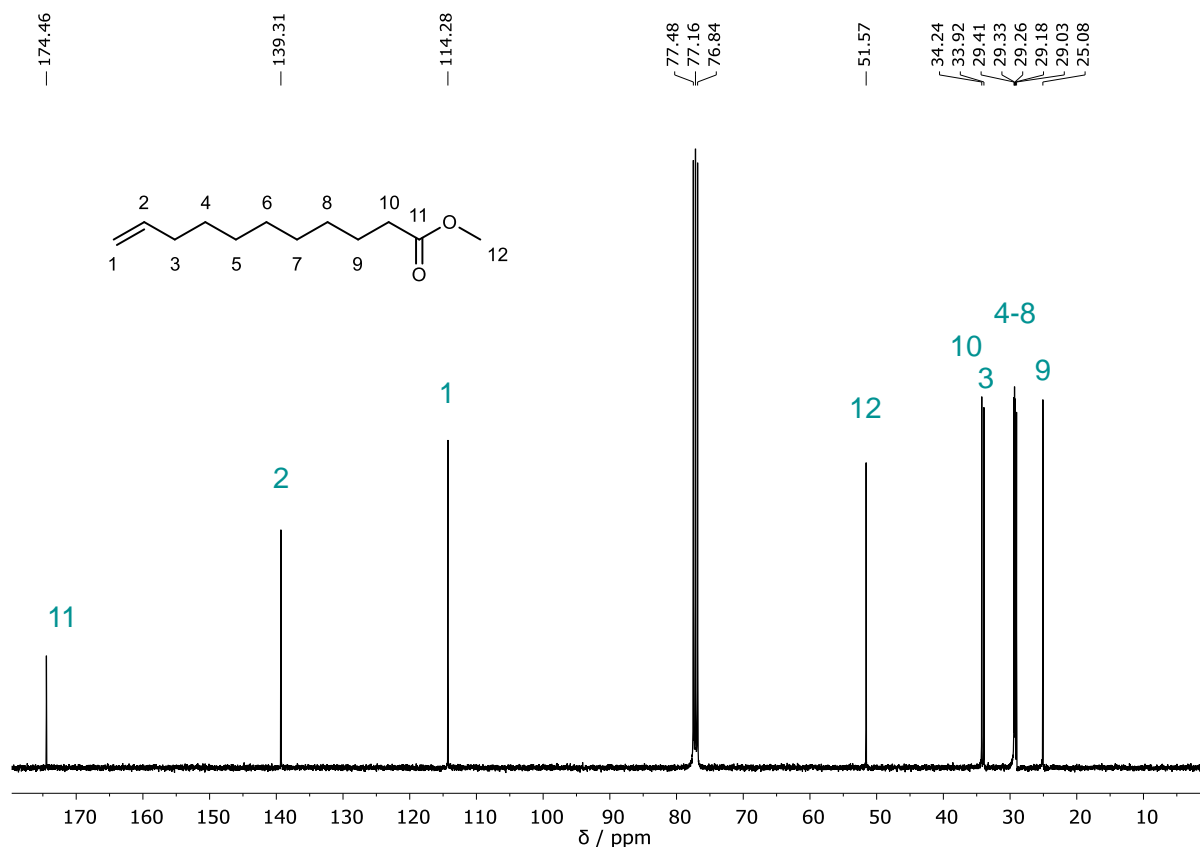
**<sup>13</sup>C NMR (101 MHz, CDCl<sub>3</sub>)**  $\delta$  / ppm = 174.5 (**C11**), 139.3 (**C2**), 114.3 (**C1**), 51.6 (**C12**), 34.2 (**C10**), 33.9 (**C3**), 29.4 (**C4–8**), 29.3 (**C4–8**), 29.2 (**C4–8**), 29.0 (**C4–8**), 25.1 (**C9**).

**IR (ATR platinum diamond):**  $\tilde{\nu}$  / cm<sup>-1</sup> = 3077, 2976, 2926, 2855, 1740, 1641, 1436, 1361, 1318, 1239, 1196, 1169, 1116, 1047, 994, 909, 882, 858, 772, 724, 635, 589, 554, 434.

**ESI-MS:** [M+H]<sup>+</sup> calc. 199.1693, detected 199.1691.

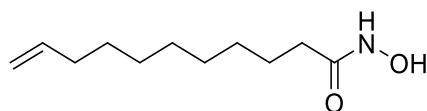


**Supplementary Figure 61.** <sup>1</sup>H NMR spectrum of **12**, measured in CDCl<sub>3</sub> at 400 MHz.



**Supplementary Figure 62.**  $^{13}\text{C}$  NMR spectrum of **12**, measured in  $\text{CDCl}_3$  at 101 MHz.

### ***N*-Hydroxyundec-10-enamide **13****



$\text{C}_{11}\text{H}_{21}\text{NO}_2$   
199.29 g/mol

20.3 g (110 mmol, 1.00 equiv.) methyl 10-undecenoate **12** and 10.7 g (154 mmol, 1.50 equiv.) hydroxylamine hydrochloride were suspended in 460 mL methanol. After adding 17.1 g (305 mmol, 3.00 equiv.) KOH, the mixture was stirred strongly under reflux conditions over night. After completion of the reaction (control via TLC), the mixture was brought to a pH of 5 using 25% acetic acid. Part of the reaction mixture was removed under reduced pressure. The residue was diluted with water (100 mL) and ethyl acetate (300 mL). The organic phase was separated, dried over  $\text{Na}_2\text{SO}_4$  and the solvent was removed under reduced pressure. Recrystallization (*n*-hexane/ethyl acetate 5:1) yielded 7.46 g (39.9 mmol, 36%) of the product as colorless crystals.

$R_f$  (ethyl acetate) = 0.59, visualized by staining with Seebach solution.

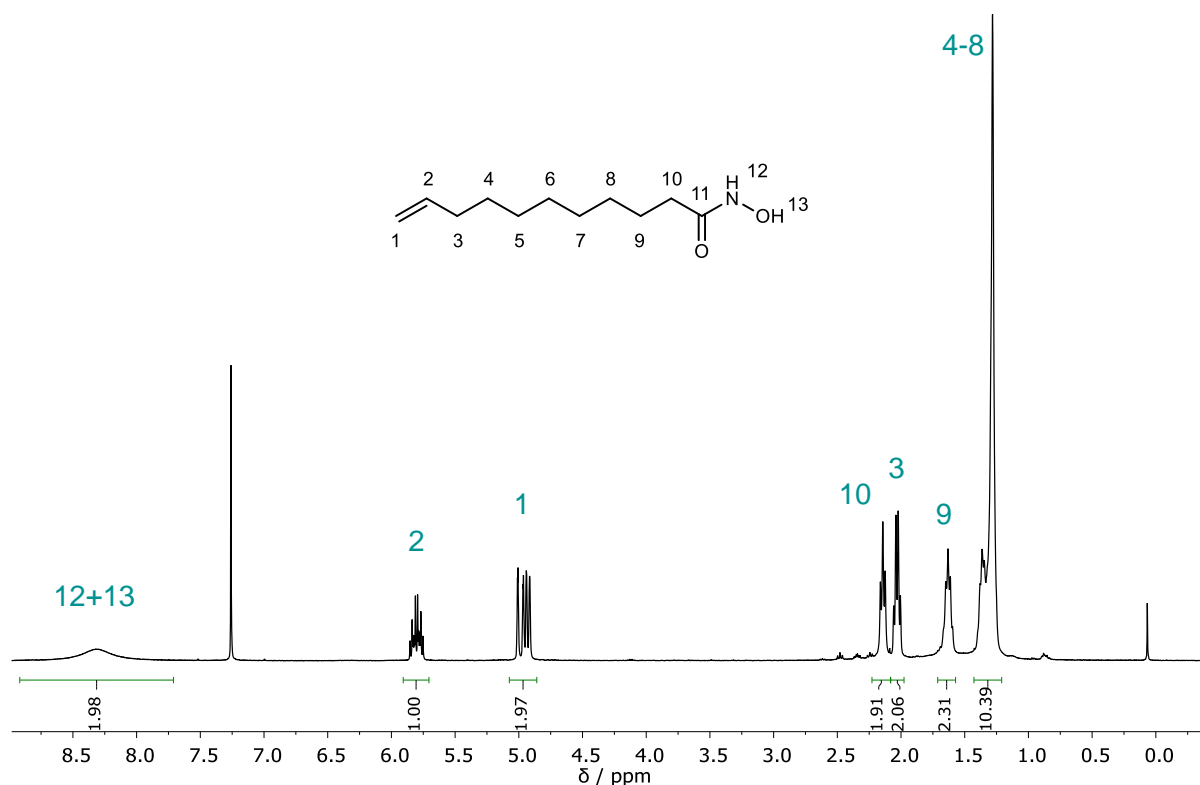


**$^1\text{H}$  NMR (400 MHz,  $\text{CDCl}_3$ )**  $\delta$  / ppm = 8.31 (bs, 2H, **H12**, **H13**), 5.91–5.71 (m, 1H, **H2**), 5.07–4.86 (m, 2H, **H1**), 2.14 (t,  $J = 7.5$  Hz, 2H, **H10**), 2.03 (q,  $J = 6.9$  Hz, 2H, **H3**), 1.72–1.56 (m, 2H, **H9**), 1.42–1.20 (m, 10H, **H4-8**).

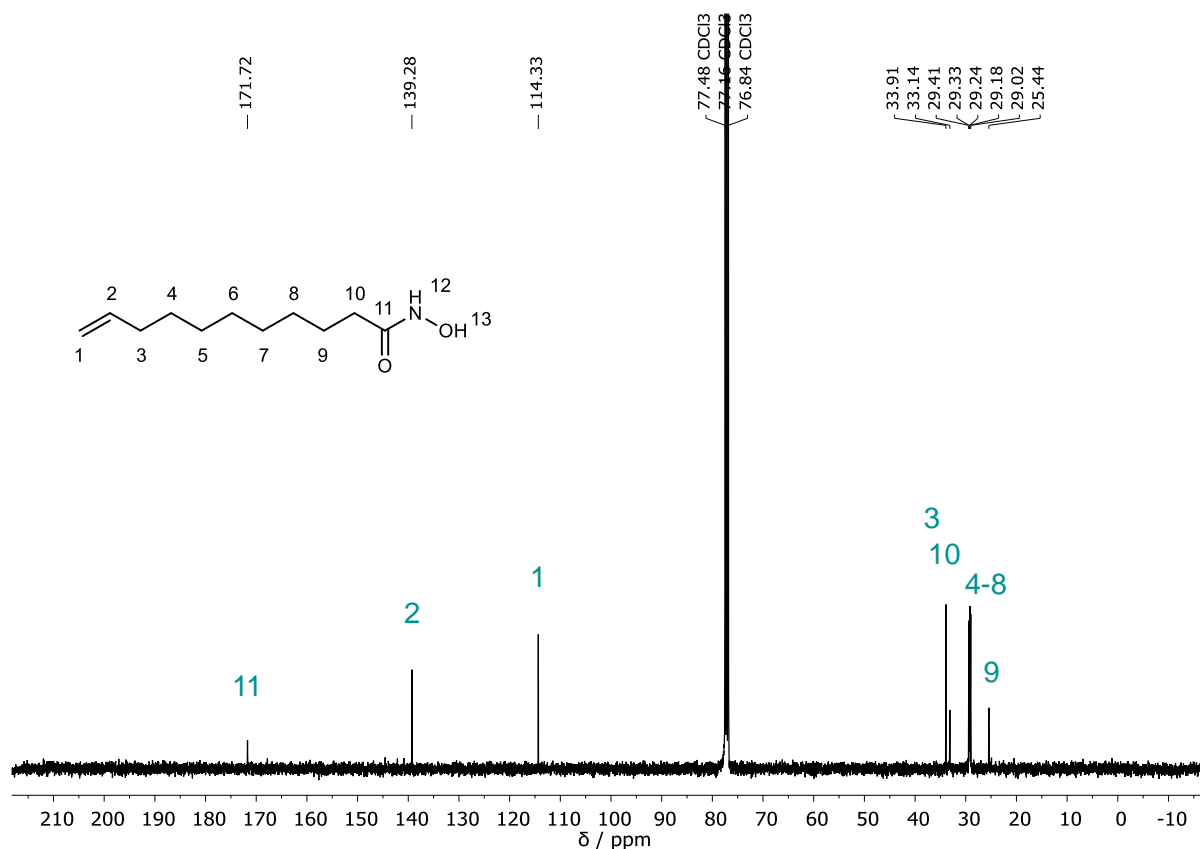
**$^{13}\text{C}$  NMR (101 MHz,  $\text{CDCl}_3$ )**  $\delta$  / ppm = 171.7 (**C11**), 139.3 (**C2**), 114.3 (**C1**), 33.9 (**C3**), 33.1 (**C10**), 29.4 (**C4-8**), 29.3 (**C4-8**), 29.2 (**C4-8**), 29.0 (**C4-8**), 25.4 (**C9**).

**IR (ATR platinum diamond):**  $\tilde{\nu}$  /  $\text{cm}^{-1}$  = 3259, 3081, 3000, 2980, 2945, 2914, 2847, 2701, 1834, 1659, 1642, 1606, 1570, 1468, 1428, 1383, 1327, 1290, 1273, 1234, 1121, 1070, 1043, 1022, 993, 967, 913, 850, 759, 745, 720, 656, 548, 477, 449, 425.

**ESI-MS:**  $[\text{M}+\text{H}]^+$  calc. 200.1645, detected 200.1644.

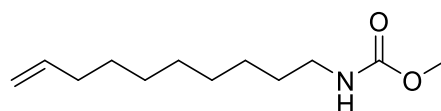


**Supplementary Figure 63.**  $^1\text{H}$  NMR spectrum of **13**, measured in  $\text{CDCl}_3$  at 400 MHz.



**Supplementary Figure 64.**  $^{13}\text{C}$  NMR spectrum of **13**, measured in  $\text{CDCl}_3$  at 101 MHz.

### Methyl dec-9-en-1-ylcarbamate **14**



$\text{C}_{12}\text{H}_{23}\text{NO}_2$   
213.32 g/mol

7.11 g (35.7 mmol, 1.00 equiv.) *N*-hydroxyundec-10-enamide **13** was dissolved in 59 mL (64 g, 700 mmol, 20 equiv.) dimethyl carbonate and 3.0 mL (2.3 g, 70 mmol, 2.0 equiv.) methanol. The mixture was heated under reflux conditions and 980 mg (7.0 mmol, 0.20 equiv.) TBD were added. After completion of the reaction (control via TLC), the mixture was evaporated to dryness. Purification via column chromatography (*n*-hexane/ethyl acetate 9:1  $\rightarrow$  7:3) yielded 4.61 g (21.6 mmol, 61%) of the product as a colorless oil.

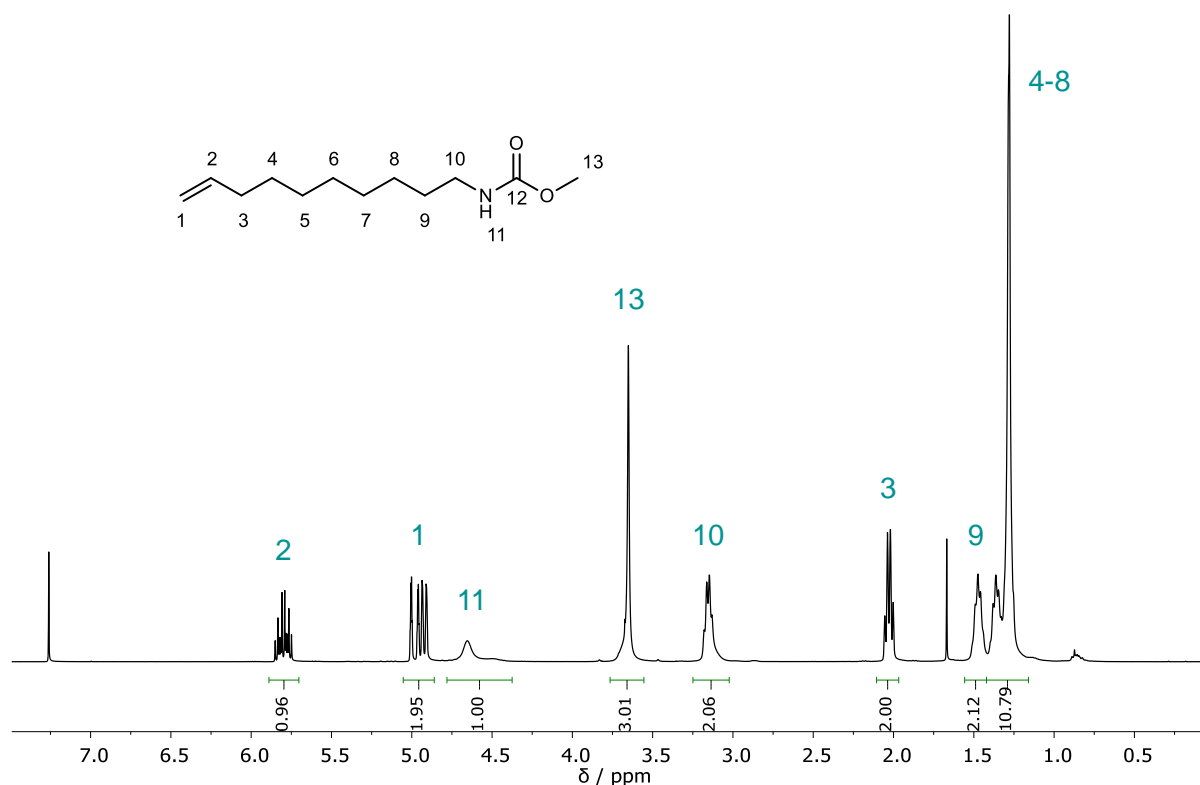
**R<sub>f</sub>** (cyclohexane/ethyl acetate 5:1) = 0.44, visualized by staining with Seebach solution.

**$^1\text{H}$  NMR (400 MHz,  $\text{CDCl}_3$ )**  $\delta$  / ppm = 5.89–5.70 (m, 1H, **H2**), 5.05–4.86 (m, 2H, **H1**), 4.78–4.38 (m, 1H, **H11**), 3.65 (s, 3H, **H13**), 3.25–3.02 (m, 2H, **H10**), 2.11–1.97 (m, 2H, **H3**), 1.56–1.42 (m, 2H, **H9**), 1.42–1.16 (m, 10H, **H4-8**).

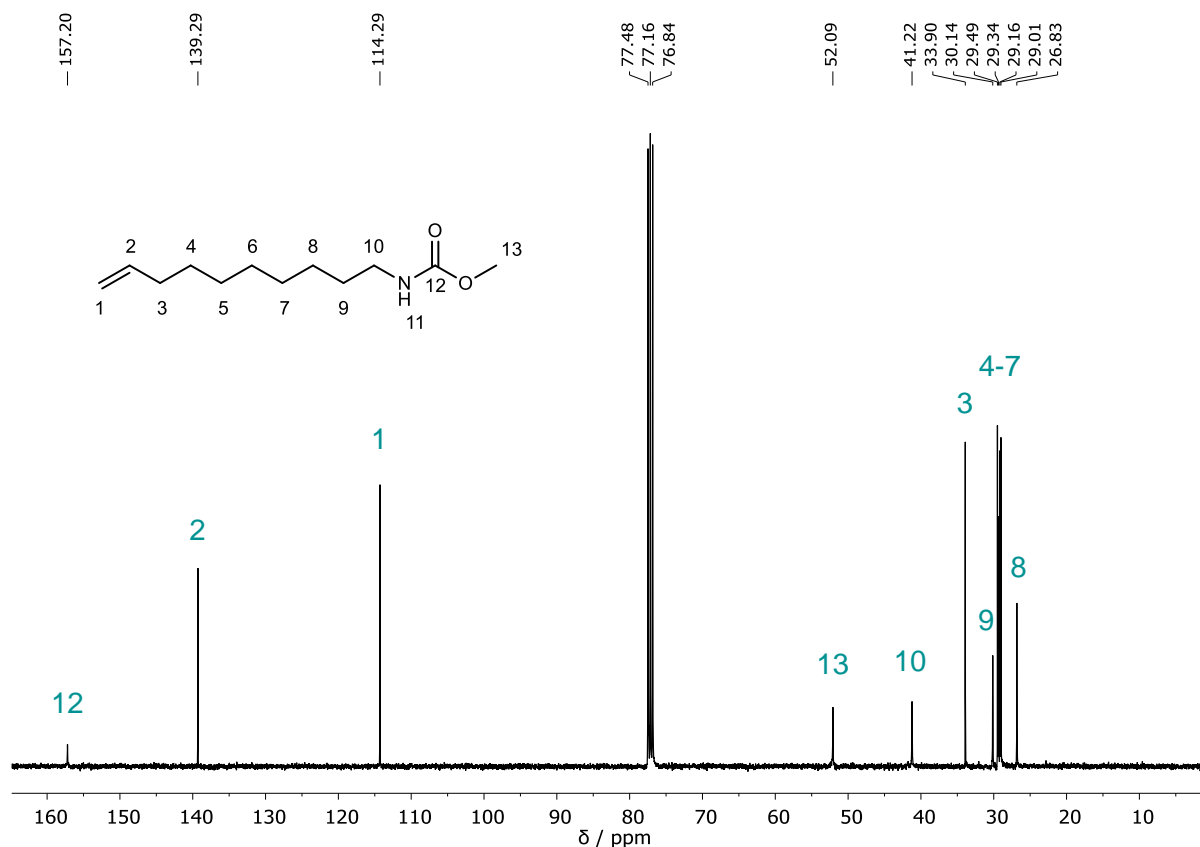
**$^{13}\text{C}$  NMR (101 MHz,  $\text{CDCl}_3$ )**  $\delta$  / ppm = 157.2 (**C12**), 139.3 (**C2**), 114.3 (**C1**), 52.1 (**C13**), 41.2 (**C10**), 33.9 (**C3**), 30.1 (**C9**), 29.5 (**C4-7**), 29.3 (**C4-7**), 29.2 (**C4-7**), 29.0 (**C4-7**), 26.8 (**C8**).

**IR (ATR platinum diamond):**  $\tilde{\nu}$  /  $\text{cm}^{-1}$  = 3334, 3077, 2925, 2854, 1699, 1640, 1532, 1463, 1443, 1367, 1346, 1250, 1193, 1143, 1112, 1037, 994, 908, 851, 779, 723, 687, 634, 555.

**ESI-MS:**  $[\text{M}+\text{H}]^+$  calc. 214.1802, detected 214.1800.

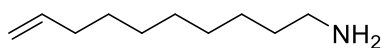


**Supplementary Figure 65.**  $^1\text{H}$  NMR spectrum of **14**, measured in  $\text{CDCl}_3$  at 400 MHz.



**Supplementary Figure 66.**  $^{13}\text{C}$  NMR spectrum of **14**, measured in  $\text{CDCl}_3$  at 101 MHz.

### Dec-9-en-1-amine **7**



$\text{C}_{10}\text{H}_{21}\text{N}$   
155.28 g/mol

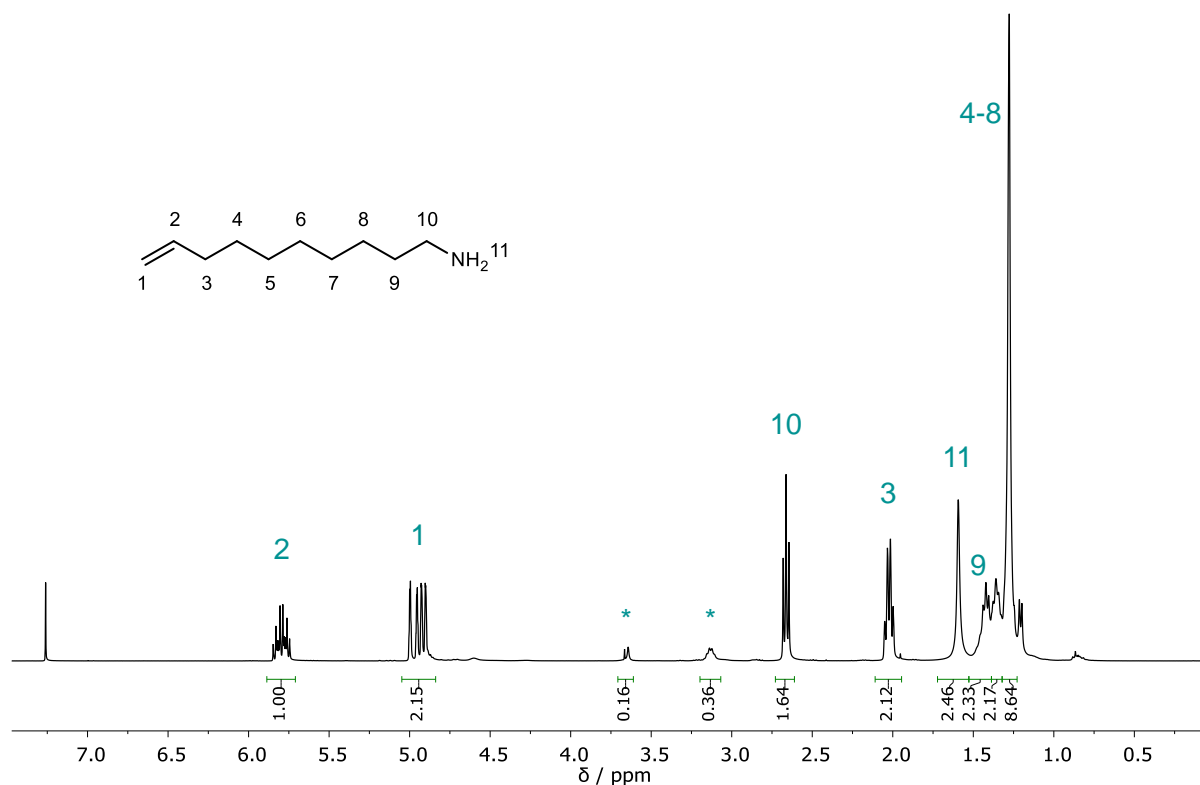
5.00 g (23.4 mmol, 1.00 equiv.) methyl dec-9-enylcarbamate **14** were dissolved in isopropanol (65 mL) and 16 M potassium hydroxide solution (45 mL) was added. With strong stirring, the mixture was heated to reflux for 16 hours until TLC showed full conversion. After cooling to room temperature, diethyl ether (100 mL) and water (50 mL) were added. After separation of the water layer, the organic layer was washed with brine (80 mL). Subsequently, the organic solution was dried over  $\text{Na}_2\text{SO}_4$  and then evaporated to dryness to obtain 3.74 g of dec-9-en-1-amine as colorless oil in a purity of 82% according to measurements with remaining impurity of unreacted **14**, corresponding to a yield of 2.87 g (18.5 mmol, 79%). The mixture was used directly for the synthesis of monomers **UR7**, **UR8**, and **UR10** without further purification.

**$^1\text{H}$  NMR (400 MHz,  $\text{CDCl}_3$ )**  $\delta$  / ppm = 5.80 (ddt,  $J$  = 16.9, 10.2, 6.7 Hz, 1H, **H2**), 5.05–4.84 (m, 2H, **H1**), 2.66 (t,  $J$  = 7.0 Hz, 2H, **H10**), 2.02 (q,  $J$  = 6.9 Hz, 2H, **H3**), 1.70–1.53 (m, 2H, **H11**) 1.52–1.39 (m, 2H, **H9**), 1.39–1.32 (m, 2H, **H4-7**), 1.32–1.23 (m, 8H, **H4-8**).

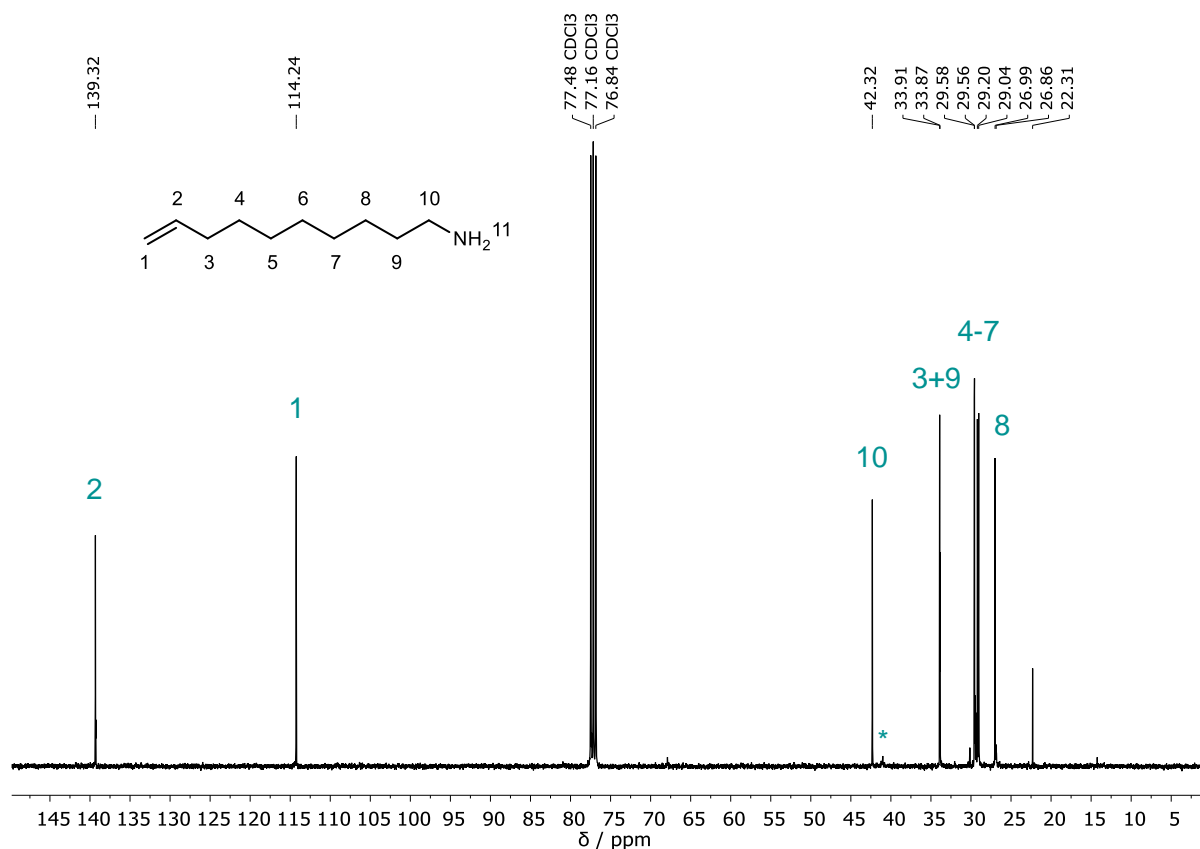
**$^{13}\text{C}$  NMR (101 MHz,  $\text{CDCl}_3$ )**  $\delta$  / ppm = 139.3 (**C2**), 114.2 (**C1**), 42.3 (**C10**), 33.9 (**C3**, **C9**), 29.6 (**C4-7**), 29.2 (**C4-7**), 29.0 (**C4-7**), 27.0 (**C4-7**), 26.9 (**C4-7**), 22.3 (**C8**).

**IR (ATR platinum diamond):**  $\tilde{\nu}$  /  $\text{cm}^{-1}$  = 3374, 3240, 3076, 2976, 2923, 2853, 1822, 1715, 1640, 1557, 1464, 1384, 1371, 1305, 1258, 1178, 1142, 1114, 993, 908, 819, 723, 634, 554, 442, 418.

**ESI-MS:**  $[\text{M}+\text{H}]^+$  calc. 156.1747, detected 156.1746.



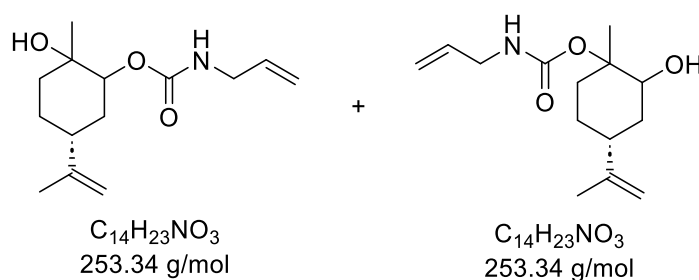
**Supplementary Figure 67.**  $^1\text{H}$  NMR spectrum of **7**, measured in  $\text{CDCl}_3$  at 400 MHz. \* residual **14**.



**Supplementary Figure 68.**  $^{13}\text{C}$  NMR spectrum of **7**, measured in  $\text{CDCl}_3$  at 101 MHz. \* residual **14**.

## Synthesis of terpene-based hydroxyurethane monomers

### Urethane monomer UR3



In a 5 mL pressure vial, 380 mg (1.0 mmol, 5.0 mol%) *N*-(3,5-bis(trifluoromethyl)phenyl)-*N'*-cyclohexyl thiourea **TU1** were added to 4.00 g (20.4 mmol, 1.00 equiv.) limonene carbonate **CC1** and 3.1 mL (2.3 g, 41 mmol, 2.0 equiv.) allylamine. The vial was sealed, and the mixture was stirred at 70 °C overnight. After completion of the reaction (reaction control via TLC), the mixture was diluted with ethyl acetate, washed with brine (3 ×) and extracted with ethyl acetate. The combined organic phases were dried over  $\text{Na}_2\text{SO}_4$ , and the solvent was removed under reduced pressure. The crude product was purified via column chromatography

(cyclohexane/ethyl acetate 3:1) and 4.39 g (17.3 mol, 85%) of the product were obtained as slightly yellow oil.

From GC-FID measurements, two isomers were observed in a ratio of 53:47.

$R_f$  (cyclohexane/ethyl acetate 3:1) = 0.15, visualized by staining with Seebach solution.

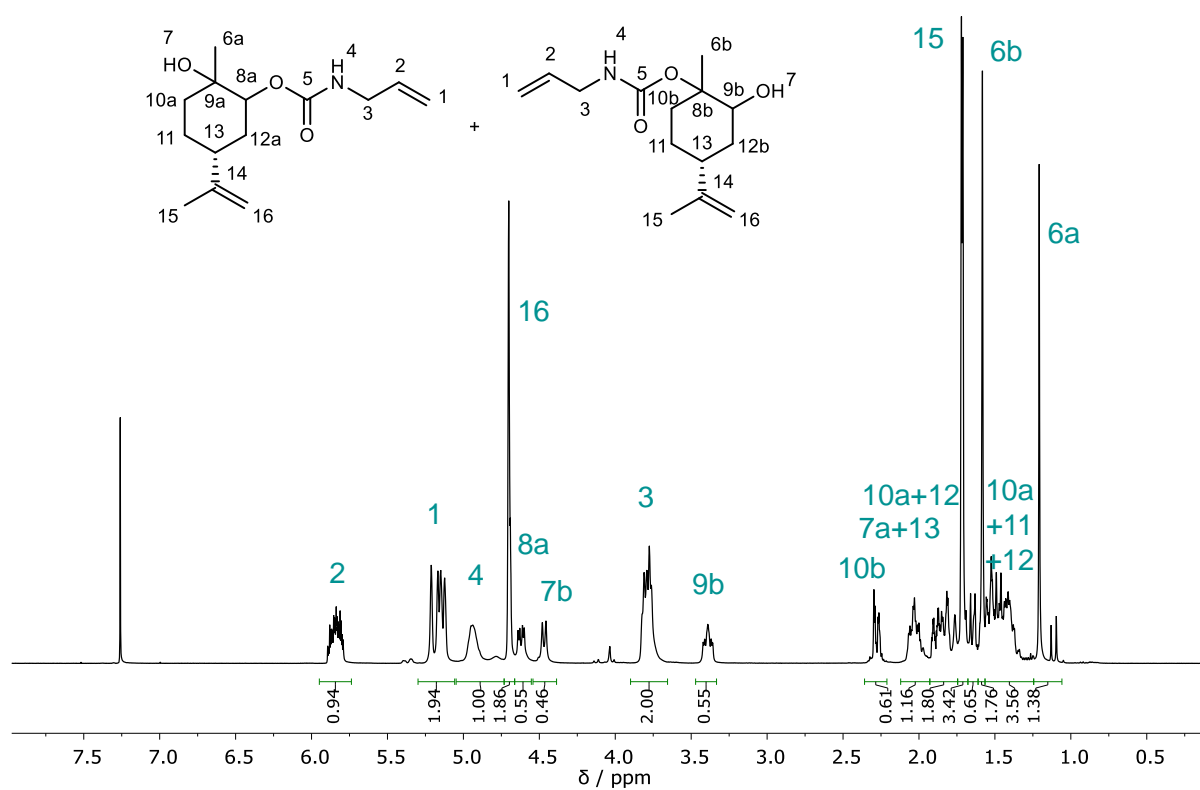
**$^1\text{H NMR}$  (400 MHz,  $\text{CDCl}_3$ )  $\delta$  / ppm =** 5.95–5.74 (m, **H2**), 5.29–5.06 (m, **H1**), 5.04–4.73 (m, **H4**), 4.73–4.66 (m, **H16**), 4.66–4.55 (m, **H8a**), 4.54–4.39 (m, **H7b**), 3.90–3.65 (m, **H3**), 3.47–3.34 (m, **H9b**) 2.36–2.21 (m, **H10b**), 2.12–1.93 (m, **H7a**, **H13**), 1.92–1.74 (m, **H10a**, **H12a**, **H12b**), 1.74–1.68 (m, **H15**), 1.68–1.61 (m, **H12a**), 1.61–1.56 (m, **H6b**), 1.57–1.24 (m, **H10a**, **H11**, **H12b**), 1.24–1.05 (m, **H6a**).

Due to the occurrence of isomers, no integral values are given for the respective NMR signals. The sum of integrals matches the expected number of protons. The purity of the product was confirmed via GC-FID.

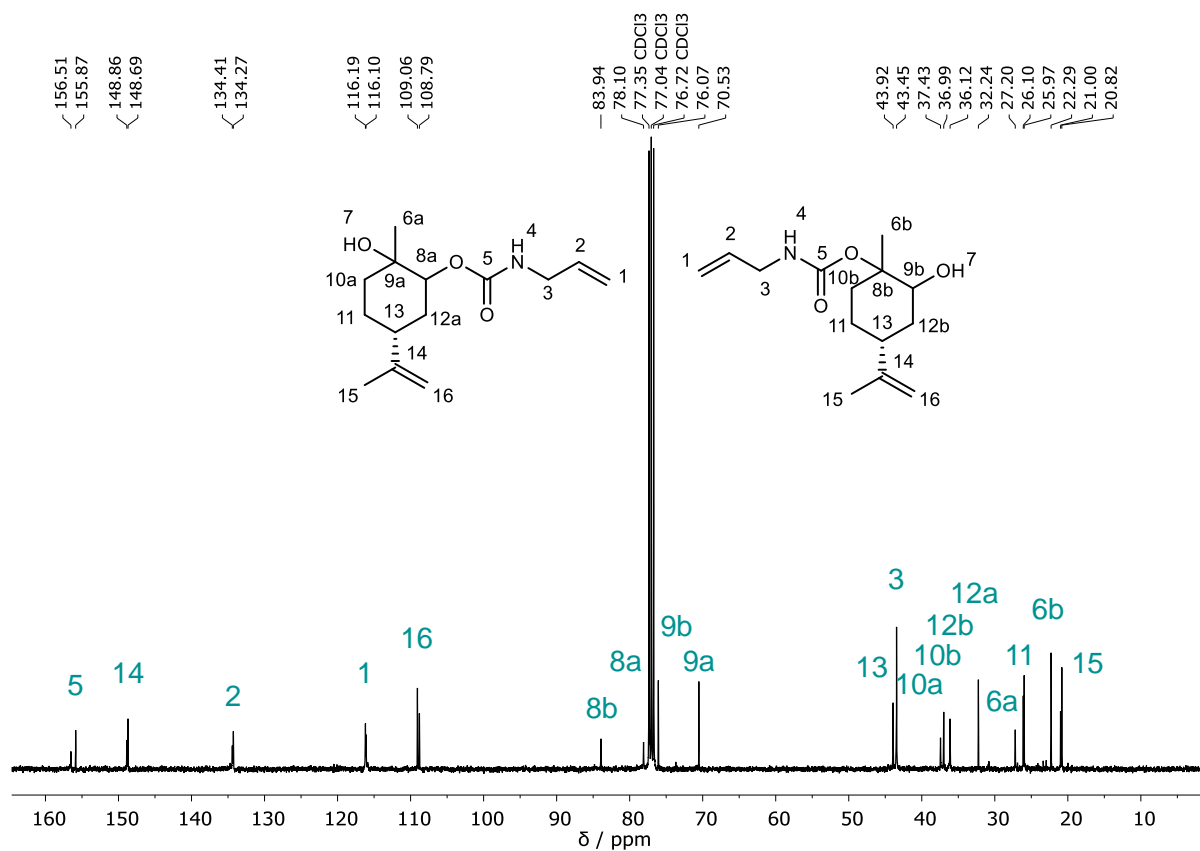
**$^{13}\text{C NMR}$  (101 MHz,  $\text{CDCl}_3$ )  $\delta$  / ppm =** 156.5 (**C5**), 155.9 (**C5**), 148.9 (**C14**), 148.7 (**C14**), 134.4 (**C2**), 134.3 (**C2**), 116.2 (**C1**), 116.1 (**C1**), 109.1 (**C16**), 108.8 (**C16**), 83.9 (**C8b**), 78.1 (**C8a**), 76.1 (**C9b**), 70.5 (**C9a**), 43.9 (**C13**), 43.5 (**C3**), 37.4 (**C10a**), 37.0 (**C10b**), 36.1 (**C12b**), 32.2 (**C12a**), 27.2 (**C6a**), 26.1 (**C11**), 26.0 (**C11**), 22.3 (**C6b**), 21.0 (**C15**), 20.8 (**C15**).

**IR (ATR platinum diamond):**  $\tilde{\nu}$  /  $\text{cm}^{-1}$  = 3330, 3083, 2935, 2863, 1683, 1645, 1525, 1453, 1394, 1375, 1246, 1186, 1141, 1071, 1008, 992, 917, 886, 851, 776, 655, 605, 582, 544, 515, 451.

**ESI-MS:**  $[\text{M}+\text{H}]^+$  calc. 254.1751, detected 254.1747.

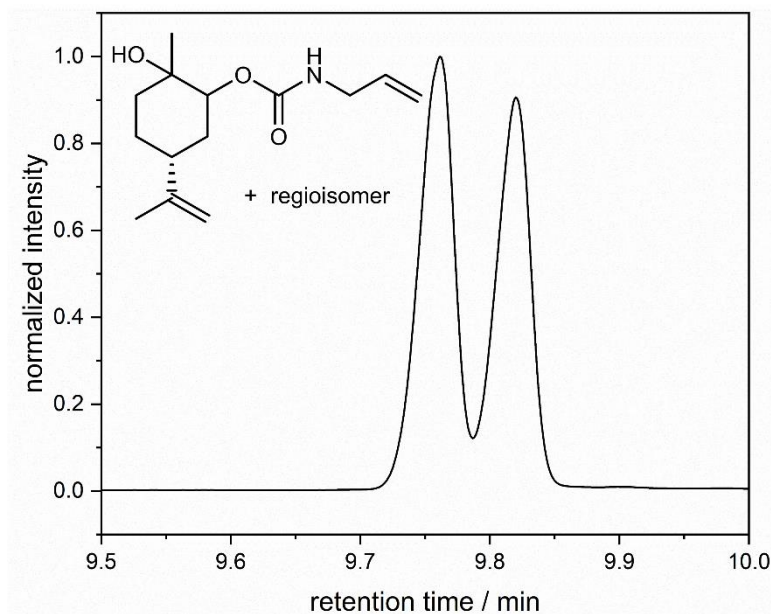


**Supplementary Figure 69.**  $^1\text{H}$  NMR spectrum of UR3, measured in  $\text{CDCl}_3$  at 400 MHz.



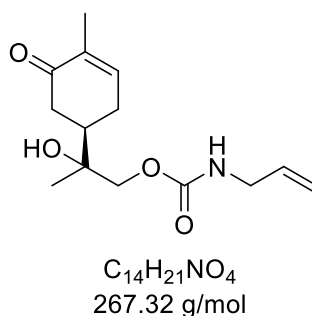
**Supplementary Figure 70.**  $^{13}\text{C}$  NMR spectrum of UR3, measured in  $\text{CDCl}_3$  at 101 MHz.





**Supplementary Figure 71.** Determination of regioisomeric ratio of compound **UR3** via GC-FID. The calculated regioisomeric ratio is 53:47.

### Urethane monomer **UR5**



In a round bottom flask, 300 mg (1.43 mmol, 1.00 equiv.) carvone carbonate **CC3**, 214  $\mu$ L (163 mg, 2.85 mmol, 2.00 equiv.) allylamine, and 110  $\mu$ L (110 mg, 0.71 mmol, 0.50 equiv.) DBU were dissolved in 2.0 mL DMSO (20 equiv.). The mixture was heated to 40 °C and stirred for 6 h. The progress of the reaction was controlled via TLC. The reaction mixture was dissolved in ethyl acetate (~50 mL), washed with brine (3  $\times$ ) and extracted with ethyl acetate. After removal of the solvent, the mixture was purified via column chromatography (cyclohexane/ ethyl acetate 3:1  $\rightarrow$  1:2), yielding 233 mg (0.87 mmol, 61%) of the product as a slightly yellow oil.

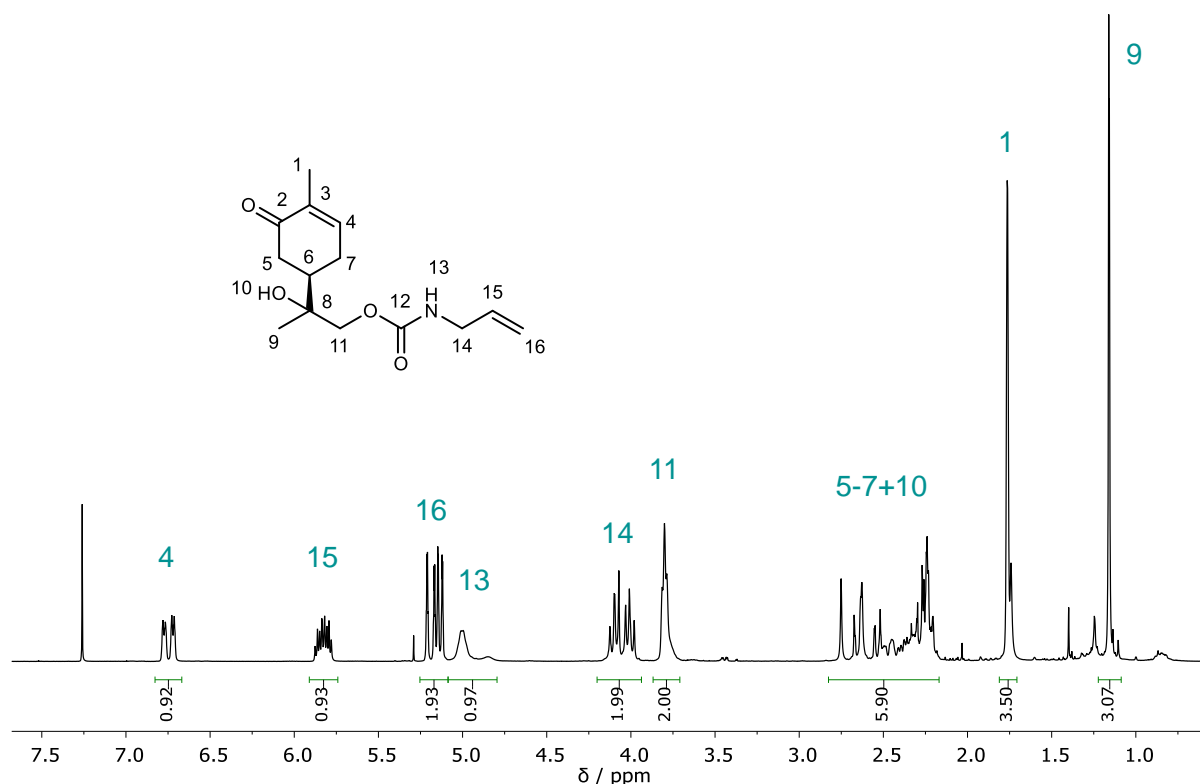
$R_f$  (cyclohexane/ethyl acetate 1:1) = 0.17, visualized by staining with Seebach solution.

**<sup>1</sup>H NMR (400 MHz, CDCl<sub>3</sub>)**  $\delta$  / ppm = 6.83–6.67 (m, 1H, **H4**), 5.91–5.74 (m, 1H, **H15**), 5.25–5.09 (m, 2H, **H16**), 5.09–4.80 (m, 1H, **H13**), 4.21–3.94 (m, 2H, **H11**), 3.86–3.70 (m, 2H, **H14**), 2.83–2.17 (m, 6H, **H5**, **H6**, **H7**, **H10**), 1.82–1.71 (m, 3H, **H1**), 1.21–1.11 (m, 3H, **H9**).

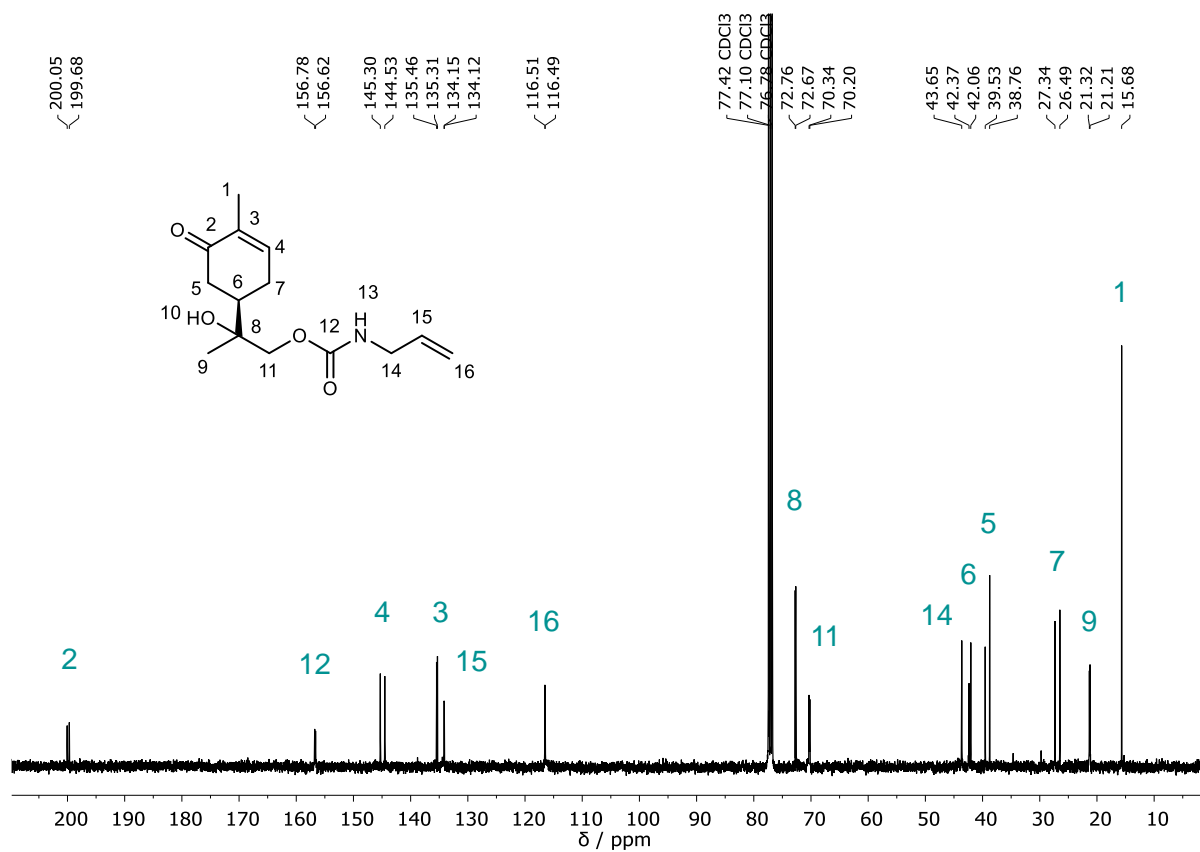
**<sup>13</sup>C NMR (100 MHz, CDCl<sub>3</sub>)**  $\delta$  / ppm = 200.0 (**C2**), 199.7 (**C2**), 156.8 (**C12**), 156.6 (**C12**), 145.3 (**C4**), 144.5 (**C4**), 135.5 (**C3**), 135.3 (**C3**), 134.2 (**C15**), 134.1 (**C15**), 116.5 (**C16**), 72.8 (**C8**), 72.7 (**C8**), 70.3 (**C11**), 70.2 (**C11**), 43.6 (**C14**), 42.4 (**C6**), 42.1 (**C6**), 39.5 (**C5**), 38.8 (**C5**), 27.3 (**C7**), 26.5 (**C7**), 21.3 (**C9**), 21.2 (**C9**), 15.7 (**C1**).

**IR (ATR platinum diamond):**  $\tilde{\nu}$  / cm<sup>-1</sup> = 3342, 3082, 2979, 2952, 2924, 2905, 1699, 1659, 1527, 1452, 1433, 1370, 1242, 1109, 1058, 1017, 994, 922, 832, 801, 776, 711, 634, 556, 468.

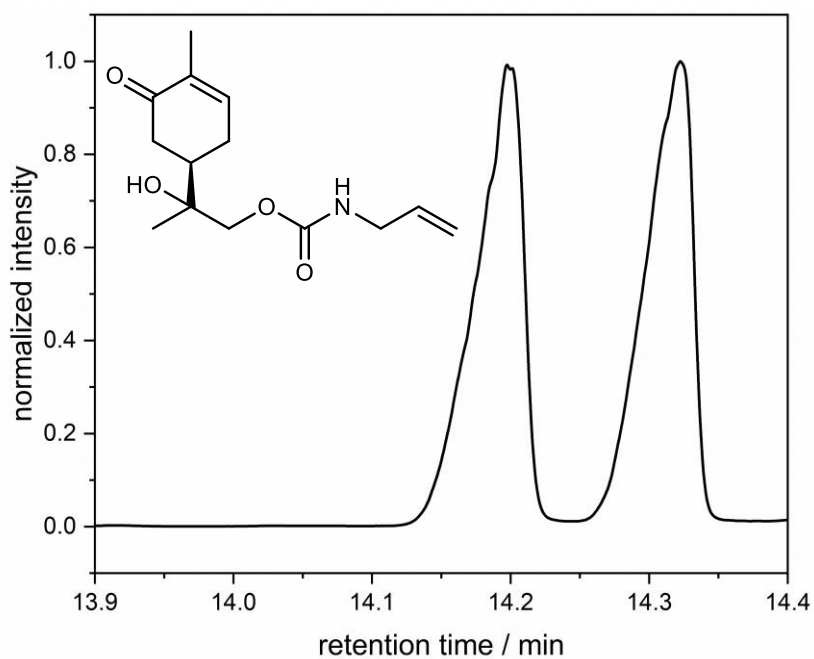
**ESI-MS:** [M+H]<sup>+</sup> calc. 268.1543, detected 268.1541.



**Supplementary Figure 72.** <sup>1</sup>H NMR spectrum of **UR5**, measured in CDCl<sub>3</sub> at 400 MHz.

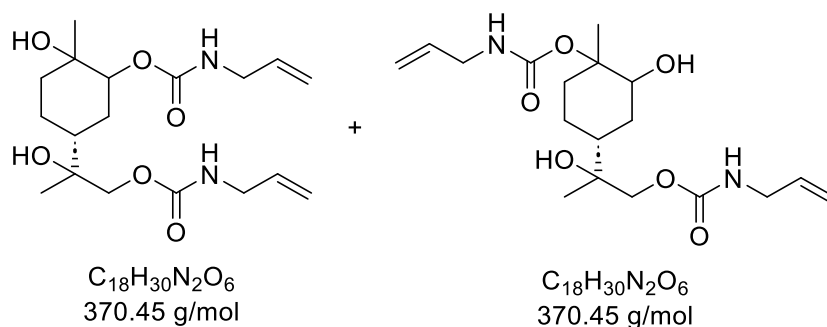


**Supplementary Figure 73.**  $^{13}\text{C}$  NMR spectrum of UR5, measured in  $\text{CDCl}_3$  at 101 MHz.



**Supplementary Figure 74.** Determination of diastereomeric ratio of compound UR5 via GC-FID. The calculated diastereomeric ratio is 50:50.

## Diurethane monomer UR6



In a 5 mL pressure vial, 87 mg (0.23 mmol, 0.10 equiv.) *N*-(3,5-bis(trifluoromethyl)-phenyl)-*N'*-cyclohexyl thiourea **TU1** were added to 600 mg (2.34 mmol, 1.00 equiv.) limonene dicarbonate **CC2** and 1.06 mL (802 mg, 14.1 mmol, 6.00 equiv.) allylamine. The reaction was heated to 70 °C and stirred for 18 h. After complete conversion, the mixture was diluted in 100 mL ethyl acetate and washed with brine (3 ×). The aqueous phase was extracted with ethyl acetate (1 ×) and the combined organic phases were dried over Na<sub>2</sub>SO<sub>4</sub>. The solvent was evaporated and the crude product was purified via column chromatography (cyclohexane/ ethyl acetate 2:1 → 1:4) to yield 735 mg (1.99 mmol, 85%) of the product as slightly yellow, viscous liquid.

*R<sub>f</sub>* (cyclohexane/ethyl acetate 1:1) = 0.15, visualized by staining with Seebach solution.

<sup>1</sup>H NMR (400 MHz, CDCl<sub>3</sub>) δ / ppm = 5.95–5.75 (m, **H2**, **H21**), 5.34–4.82 (m, **H1**, **H4**, **H19**, **H22**), 4.78–4.64 (m, **H7b**), 4.63–4.50 (m, **H9a**), 4.18–3.93 (m, **H17**), 3.91–3.69 (m, **H3**, **H20**), 3.43–3.27 (m, **H9b**), 2.77–2.57 (m, **H14**), 2.34–2.19 (m, **H10–12**), 2.05–1.72 (m, **H10–12**), 1.71–1.22 (m, **H6b**, **H7a**, **H10–13**), 1.18 (s, **H6a**), 1.16–1.06 (m, **H15**).

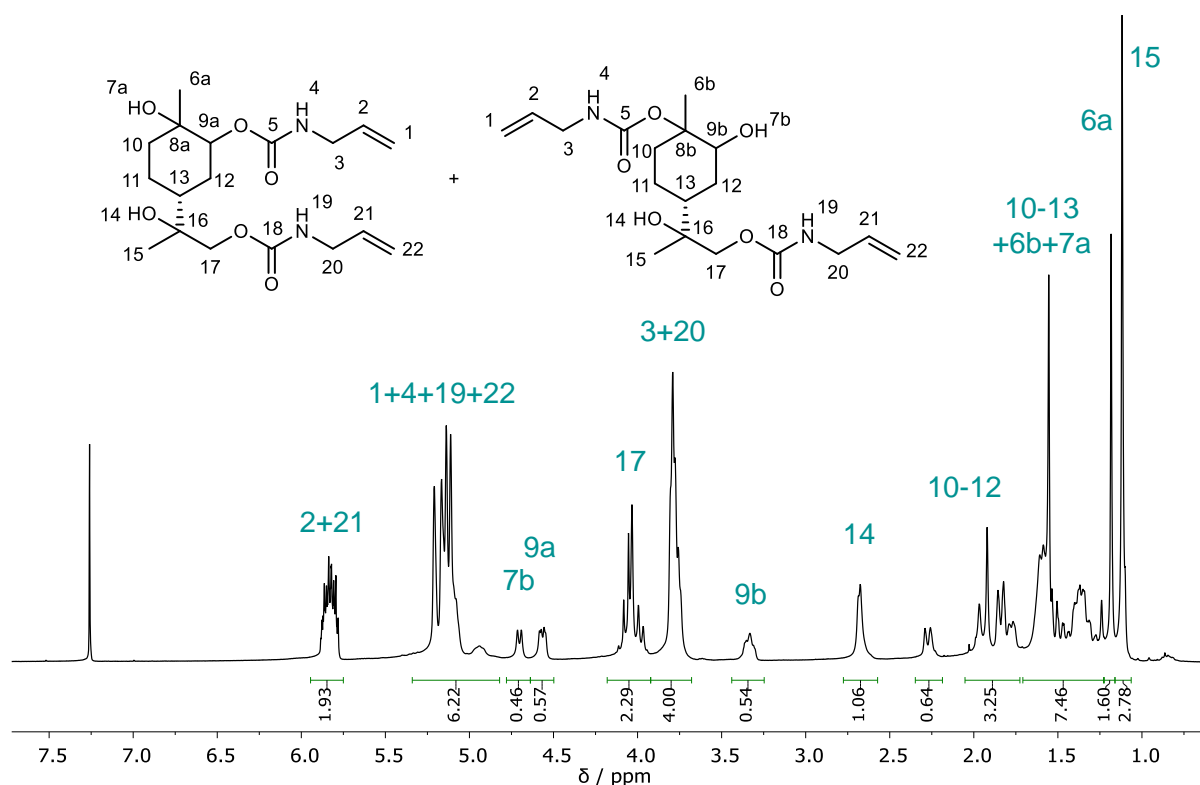
Due to the occurrence of isomers, no integral values are given for the respective signals. The sum of integrals matches the expected number of protons. The purity of the product was confirmed via SEC measurements.

<sup>13</sup>C NMR (101 MHz, CDCl<sub>3</sub>) δ / ppm = 160.0 (**C18**), 156.7 (**C5**), 156.0 (**C5**), 134.5 (**C2/C21**), 134.4 (**C2/C21**), 116.4 (**C1/C22**), 116.2 (**C1/C22**), 83.8 (**C8b**), 78.1 (**C9a**), 77.4 (**C8a**), 76.2 (**C9b**), 73.4 (**C16**), 70.7 (**C17**), 70.6 (**C17**), 43.9 (**C3/C20/C13**), 43.7 (**C3/C20/C13**), 43.6 (**C3/C20/C13**), 43.5 (**C3/C20/C13**), 43.3 (**C3/C20/C13**), 37.3 (**C10-12**), 36.9 (**C10-12**), 32.3 (**C10-12**), 28.5 (**C10-12**), 27.2

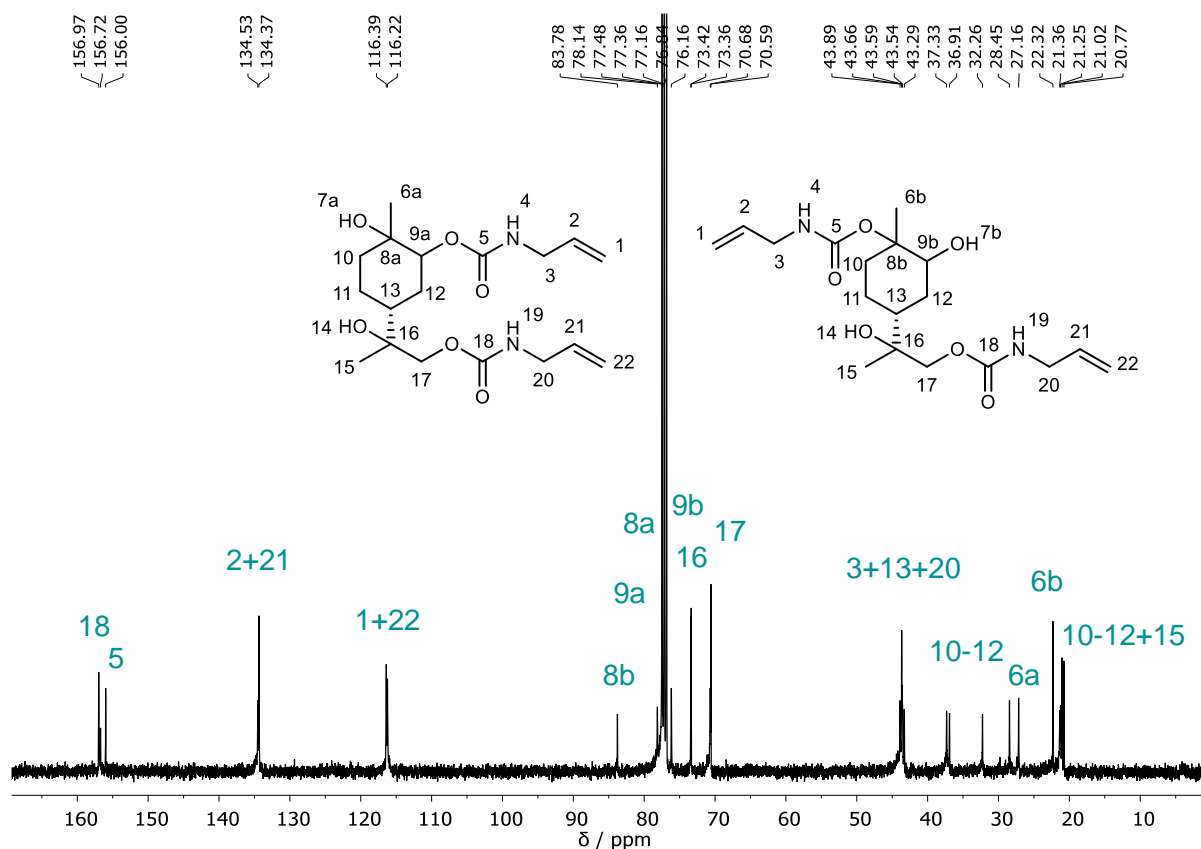
(C6a), 22.3 (C6b), 21.4 (C15/C10-12), 21.2 (C15/C10-12), 21.0 (C15/C10-12), 20.8 (C15/C10-12).

**IR (ATR platinum diamond):**  $\tilde{\nu}$  /  $\text{cm}^{-1}$  = 3326, 3082, 2974, 2937, 2873, 1690, 1645, 1525, 1457, 1421, 1396, 1374, 1240, 1146, 1070, 1044, 1002, 916, 818, 776, 634, 608, 583, 547, 465, 448.

**ESI-MS:**  $[\text{M}+\text{H}]^+$  calc. 371.2177, detected 371.2174.

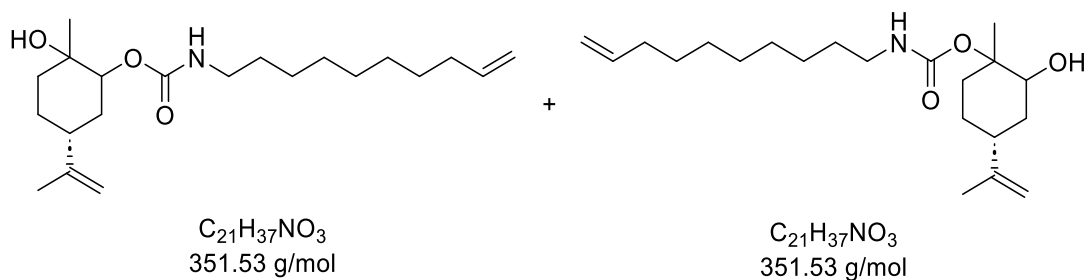


**Supplementary Figure 75.**  $^1\text{H}$  NMR spectrum of UR6, measured in  $\text{CDCl}_3$  at 400 MHz.



Supplementary Figure 76.  $^{13}\text{C}$  NMR spectrum of **UR6**, measured in  $\text{CDCl}_3$  at 101 MHz.

### Urethane monomer **UR7**



In a 5 mL pressure vial, 89 mg (0.241 mmol, 5.0 mol%) *N*-(3,5-bis(trifluoromethyl)-phenyl)-*N'*-cyclohexyl thiourea **TU1** were added to 947 mg (4.83 mmol, 1.00 equiv.) limonene carbonate **CC1**, and 1.50 g (9.66 mmol, 2.00 equiv.) dec-9-en-1-amine **7**. The vial was sealed, and the mixture was stirred at 70 °C. After completion of the reaction (reaction control via TLC), the mixture was purified via column chromatography (cyclohexane/ethyl acetate 20:1  $\rightarrow$  1:1) and 1.17 g (3.34 mol, 69%) of the product were obtained as slightly yellow oil.

**R<sub>f</sub>** (cyclohexane/ethyl acetate 3:1) = 0.25, visualized by staining with Seebach solution.

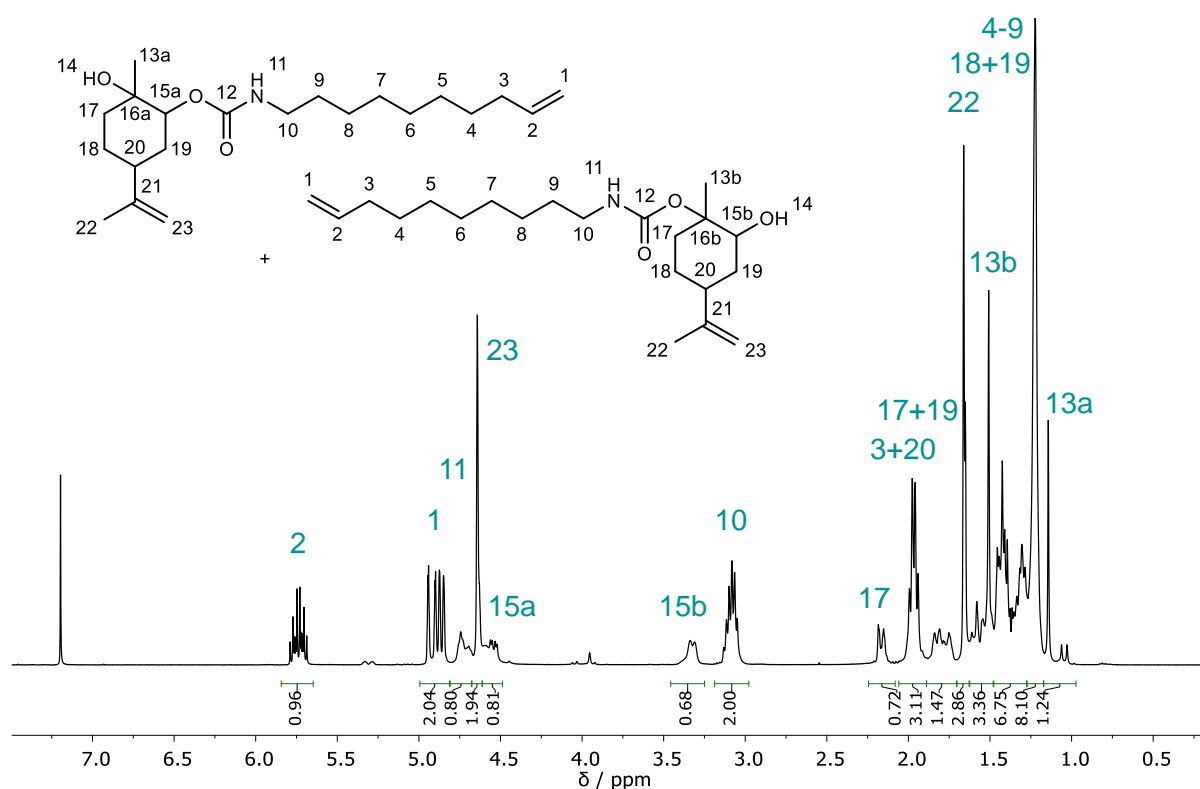
**<sup>1</sup>H NMR (400 MHz, CDCl<sub>3</sub>)**  $\delta$  / ppm = 5.85–5.65 (m, **H2**), 5.01–4.81 (m, **H1**) 4.81–4.68 (m, **H11**), 4.68–4.61 (s, **H23**), 4.61–4.49 (m, **H15a**), 3.46–3.25 (m, **H15b**), 3.18–2.99 (m, **H10**), 2.24–2.08 (m, **H17**), 2.06–1.89 (m, **H3**, **H20**), 1.89–1.70 (m, **H17**, **H19a**, **H19b**), 1.70–1.63 (m, **H22**), 1.62–1.48 (m, **H13b**, **H19a**), 1.48–1.37 (m, **H4–9**, **H18**, **H19b**), 1.37–1.27 (m, **H4–9**, **H17**, **H18**), 1.27–1.17 (m, **H4–9**), 1.17–0.97 (m, **H13a**).

Due to the occurrence of isomers, no integral values are given for the respective NMR signals. The sum of integrals matches the expected number of protons. The purity of the product was confirmed via SEC measurements. The signal corresponding to the OH-proton 14 could not be assigned unambiguously due to overlapping signals.

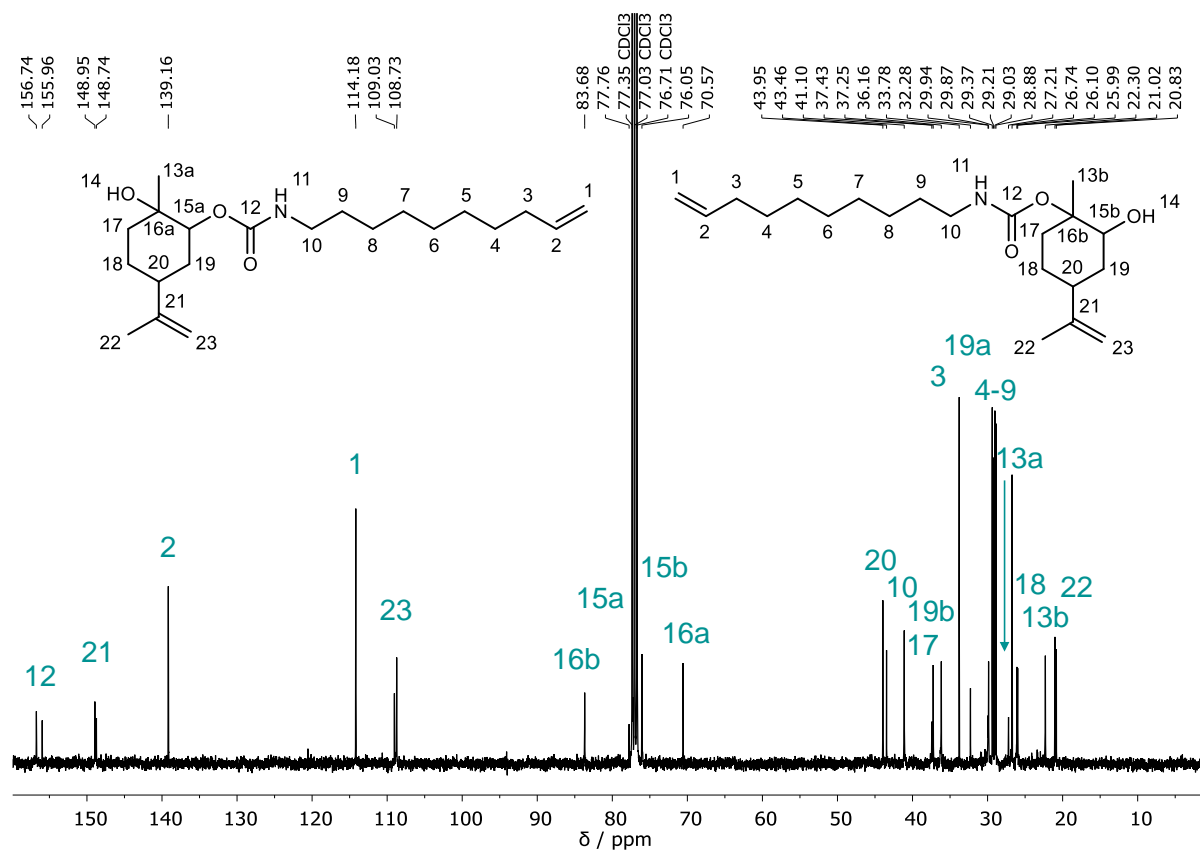
**<sup>13</sup>C NMR (101 MHz, CDCl<sub>3</sub>)**  $\delta$  / ppm = 156.7 (**C12**), 156.0 (**C12**), 149.0 (**C21**), 148.7 (**C21**), 139.2 (**C2**), 114.2 (**C1**), 109.0 (**C23**), 108.7 (**C23**), 83.7 (**C16b**), 77.8 (**C15a**), 76.0 (**C15b**), 70.6 (**C16a**), 44.0 (**C20**), 43.5 (**C20**), 41.1 (**C10**), 37.4 (**C17**), 37.2 (**C17**), 36.2 (**C19b**), 33.8 (**C3**), 32.3 (**C19a**), 29.9 (**C4–9**), 29.4 (**C4–9**), 29.2 (**C4–9**), 29.0 (**C4–9**), 28.9 (**C4–9**), 27.2 (**C13a**), 26.7 (**C4–9**), 26.1 (**C18**), 26.0 (**C18**), 22.3 (**C13b**), 21.0 (**C22**), 20.8 (**C22**).

**IR (ATR platinum diamond):**  $\tilde{\nu}$  / cm<sup>-1</sup> = 3328, 3077, 2926, 2855, 1683, 1643, 1531, 1454, 1440, 1403, 1374, 1248, 1187, 1142, 1076, 1013, 994, 943, 908, 887, 851, 775, 723, 632, 545, 450, 606, 582, 514, 490, 422.

**ESI-MS:** [M+H]<sup>+</sup> calc. 352.2846, detected 352.2842.

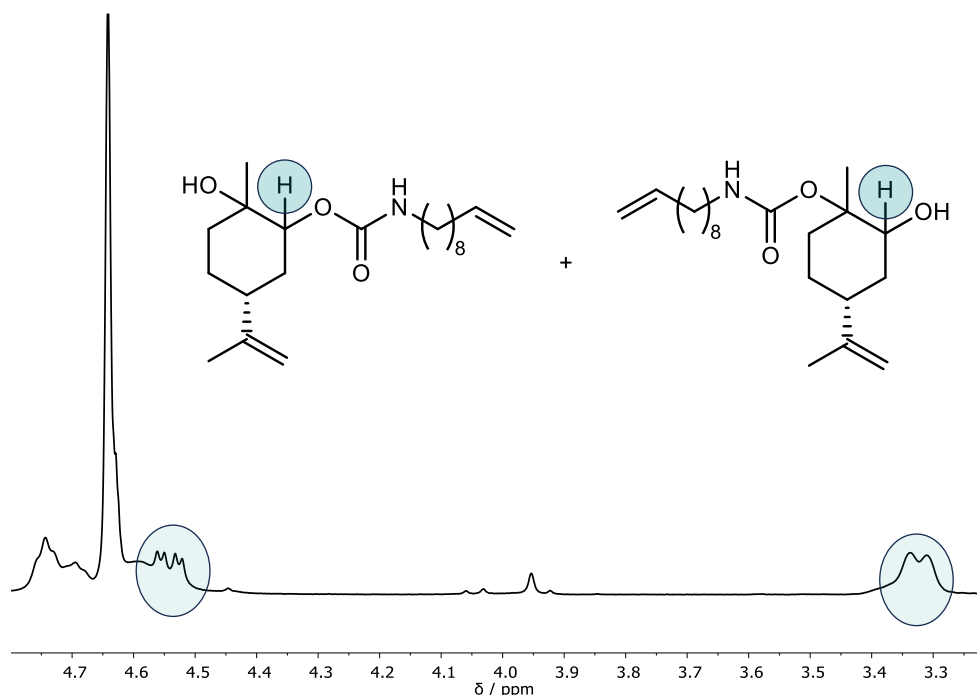


**Supplementary Figure 77.**  $^1\text{H}$  NMR spectrum of UR7, measured in  $\text{CDCl}_3$  at 400 MHz.



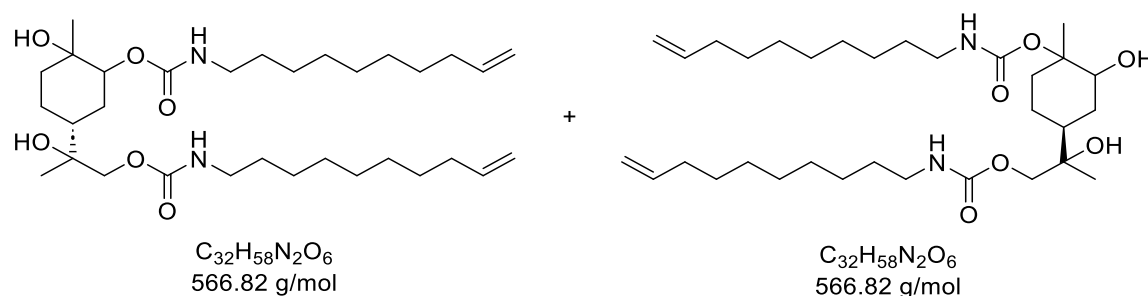
**Supplementary Figure 78.**  $^{13}\text{C}$  NMR spectrum of UR7, measured in  $\text{CDCl}_3$  at 101 MHz.





**Supplementary Figure 79.** Observation of different regioisomers of compound **UR7** via  $^1\text{H}$  NMR spectroscopy.

### Diurethane monomer **UR8**



In a 5 mL pressure vial, 160 mg (0.43 mmol, 10 mol%) *N*-(3,5-bis(trifluoromethyl)-phenyl)-*N'*-cyclohexyl thiourea **TU1** were added to 1.10 g (4.29 mmol, 1.00 equiv.) limonene dicarbonate **CC2** and 2.00 g (12.9 mmol, 3.00 equiv.) dec-9-en-1-amine **7**. The vial was sealed, and the mixture was stirred at 70 °C. After stirring for 6 days and with 334 mg (2.15 mmol, 0.500 equiv.) added after 4 days, the mixture was purified via column chromatography (dichloromethane/acetone 20:1 → 4:1) and 361 mg (0.637 mol, 15%) of the product were obtained as colorless, viscous liquid.  $R_f$  (dichloromethane/acetone 4:1) = 0.38, visualized by staining with vanillin solution.

$^1\text{H}$  NMR (400 MHz,  $\text{CDCl}_3$ )  $\delta$  / ppm = 5.89–5.71 (m, **H2**, **H35**), 5.04–4.89 (m, **H1**, **H36**), 4.89–4.50 (m, **H11**, **H13a**, **H26**), 4.19–3.88 (m, **H24**), 3.43–3.28 (m, **H13b**),

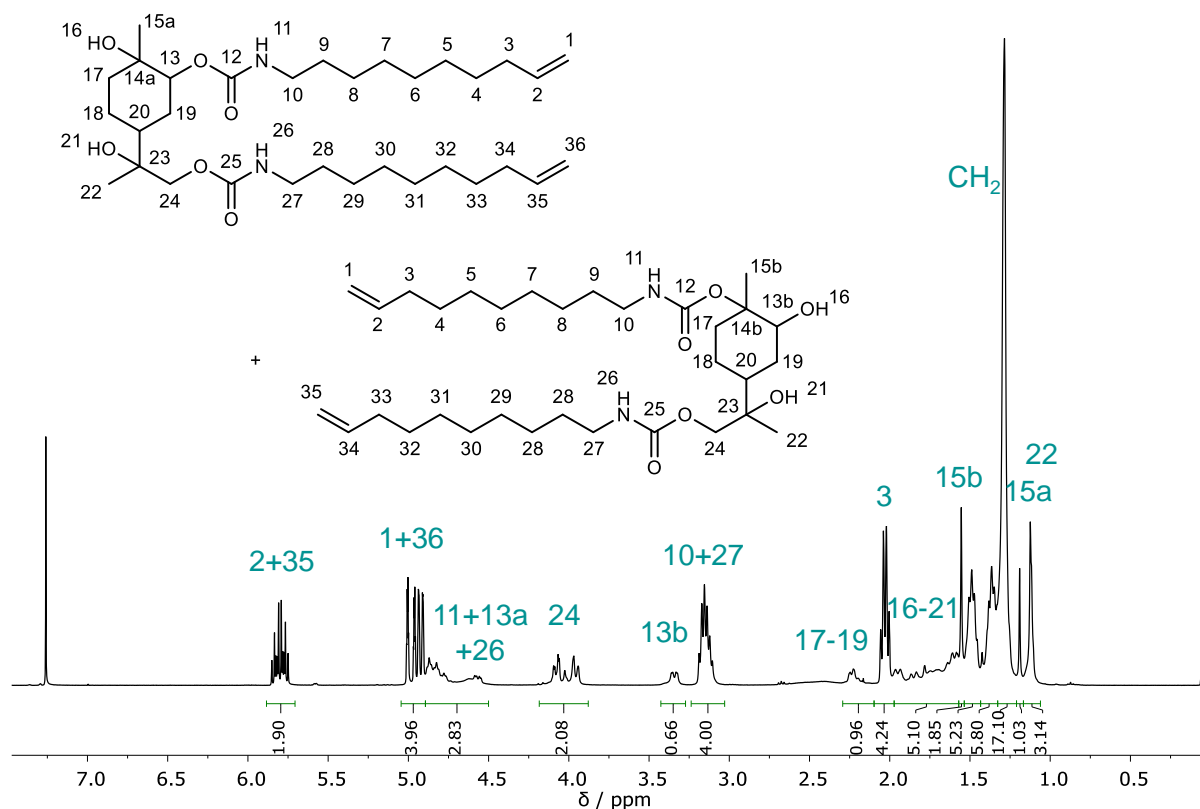
3.24–3.03 (m, **H10**, **H27**), 2.29–2.10 (m, **H17–19**), 2.10–1.97 (m, **H3**), 1.97–1.57 (m, **H16–21**), 1.55 (s, **H15b**), 1.54–1.43 (m, **H17–19**, **H4–9**, **H28–33**), 1.43–1.33 (m, **H17–19**, **H4–9**, **H28–33**), 1.33–1.21 (m, **H17–19**, **H4–9**, **H28–33**), 1.19 (s, **H15a**), 1.17–1.06 (m, **H22**).

Due to the occurrence of isomers, no integral values are given for the respective NMR signals. The sum of integrals matches the expected number of protons. The purity of the product was confirmed via SEC measurements.

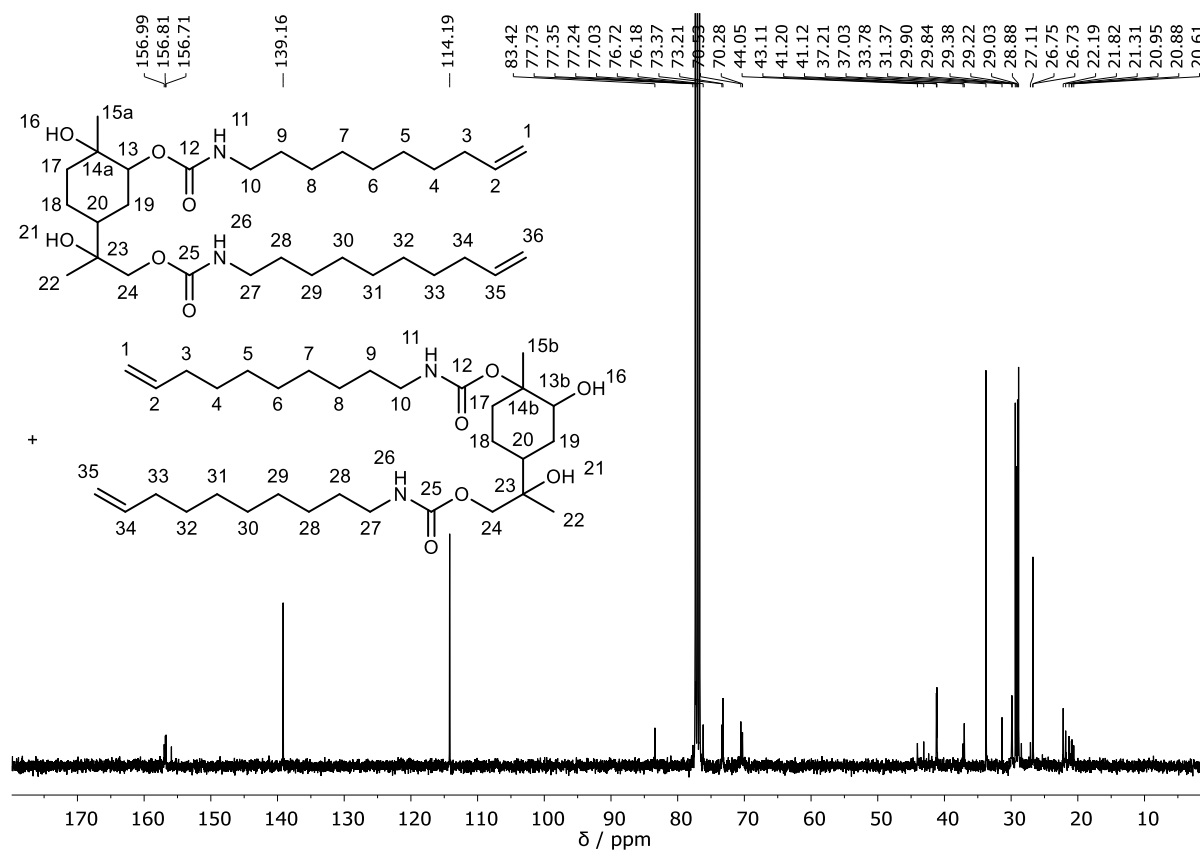
**<sup>13</sup>C NMR (101 MHz, CDCl<sub>3</sub>)**  $\delta$  / ppm = 157.0 (**C12/C25**), 156.8 (**C12/C25**), 156.7 (**C12/C25**), 139.2 (**C2**, **C35**), 114.2 (**C1**, **C36**), 83.4 (**C14b**), 77.7 (**C13a**), 76.2 (**C13b**), 73.4 (**C23**), 73.2 (**C23**), 70.5 (**C14a**), 70.3 (**C24**), 44.0 (**C20**), 43.1 (**C20**), 41.2 (**C10/C27**), 41.1 (**C10/C27**), 37.2 (**C17–19**), 37.0 (**C17/C18**), 33.8 (**C3**), 31.4 (**C19**), 29.9 (**C4–9/C28–33**), 29.8 (**C4–9/C28–33**), 29.4 (**C4–9/C28–33**), 29.2 (**C4–9/C28–33**), 29.0 (**C4–9/C28–33**), 28.9 (**C4–9/C28–33**), 27.1 (**C15a**), 26.8 (**C4–9/C28–33**), 26.7 (**C4–9/C28–33**), 22.2 (**C15b**), 21.8 (**C17–19**), 21.3 (**C22**), 21.0 (**C22**), 20.9 (**C22**), 20.6 (**C17/C18**).

**IR (ATR platinum diamond):**  $\tilde{\nu}$  / cm<sup>-1</sup> = 3331, 3077, 2973, 2925, 2854, 1688, 1641, 1531, 1462, 1444, 1412, 1373, 1248, 1172, 1145, 1072, 1011, 994, 943, 908, 817, 775, 723, 631, 555.

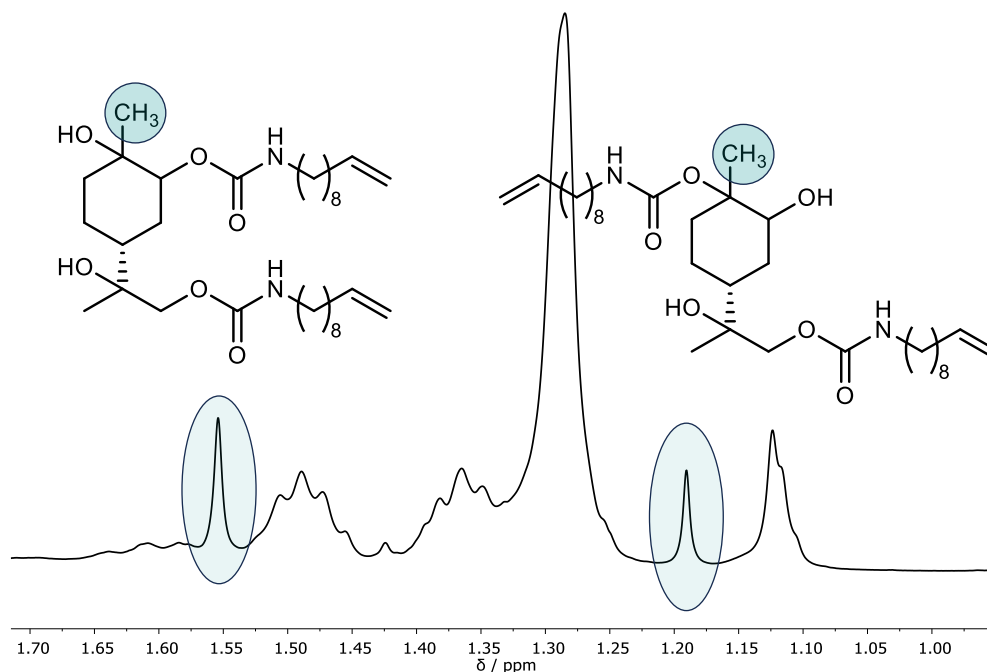
**ESI-MS:** [M+H]<sup>+</sup> calc. 567.4368, detected 567.4362.



**Supplementary Figure 80.**  $^1\text{H}$  NMR spectrum of UR8, measured in  $\text{CDCl}_3$  at 400 MHz.

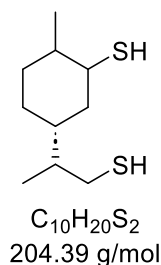


**Supplementary Figure 81.**  $^{13}\text{C}$  NMR spectrum of UR8, measured in  $\text{CDCl}_3$  at 101 MHz.



**Supplementary Figure 82.** Observation of different regioisomers of compound **UR8** via NMR spectroscopy.

### Synthesis of limonene dithiol **T3**



10.0 g (73.4 mmol, 1.00 equiv.) (*R*)-limonene were reacted with 13.1 mL (14.0 g, 184 mmol, 2.50 equiv.) thioacetic acid for 18 h. After complete reaction (control via TLC), the residue was dissolved in ethyl acetate (10 mL) and washed with brine (3 × 20 mL). The aqueous phase was extracted with ethyl acetate (20 mL) and the combined organic phases were dried over  $Na_2SO_4$ . After evaporation of the solvent, the crude dithioacetic ester was transesterified by adding 6.0 mL (1.5 mol, 20 equiv.) methanol and 2.0 g (14.7 mmol, 0.20 equiv.) TBD and stirring under reflux conditions and Argon atmosphere overnight. Excess methanol was removed under reduced pressure. After purification via column chromatography (*n*-hexane/ethyl acetate 30:1), 395 mg (1.93 mmol, 2.6%) of a pure product fraction (99% according to GC-FID) were obtained. A second fraction of 6.08 g containing mainly

the product (90% purity according to GC-FID) was purified by a second column chromatography (*n*-hexane/ethyl acetate 30:1), yielding 378 mg (1.85 mmol, 2.5%) of a pure product fraction (>99% according to GC-FID) were obtained.

From GC-FID measurements, two isomers were observed in a ratio of 89:11.

$R_f$  (dichloromethane) = 0.60, visualized by staining with Seebach solution.

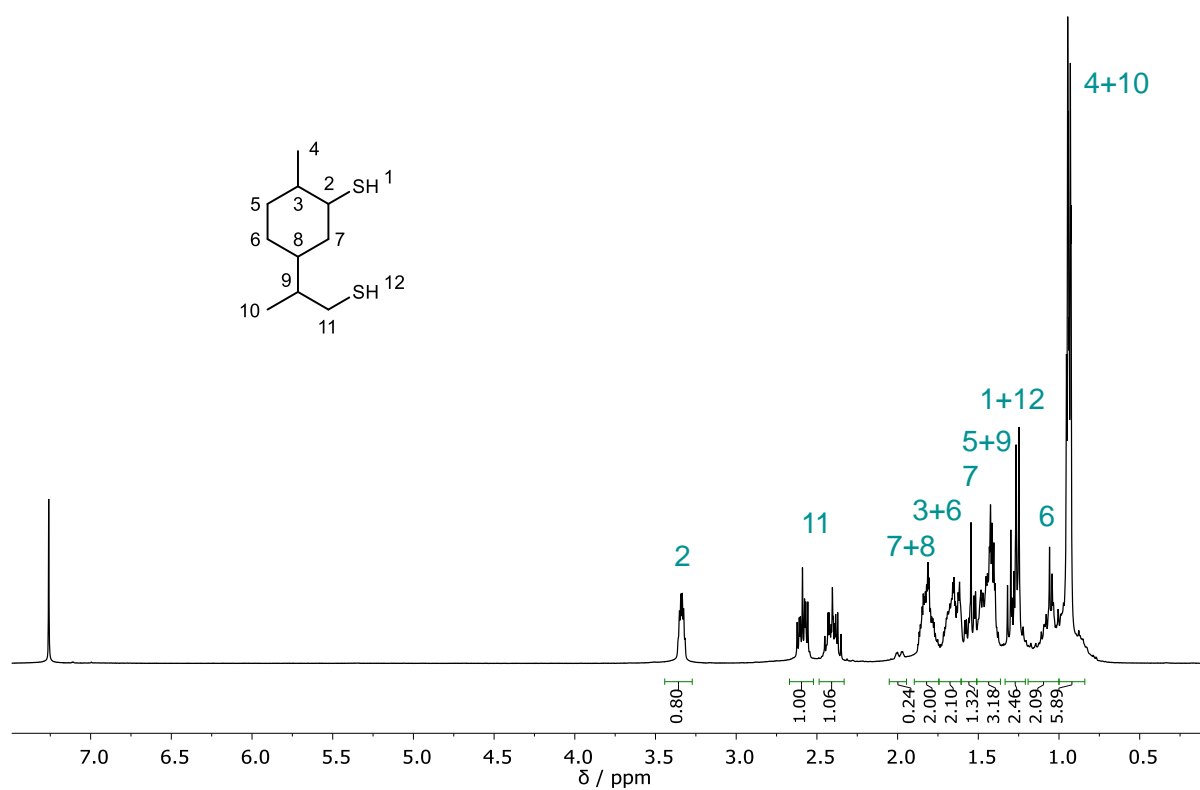
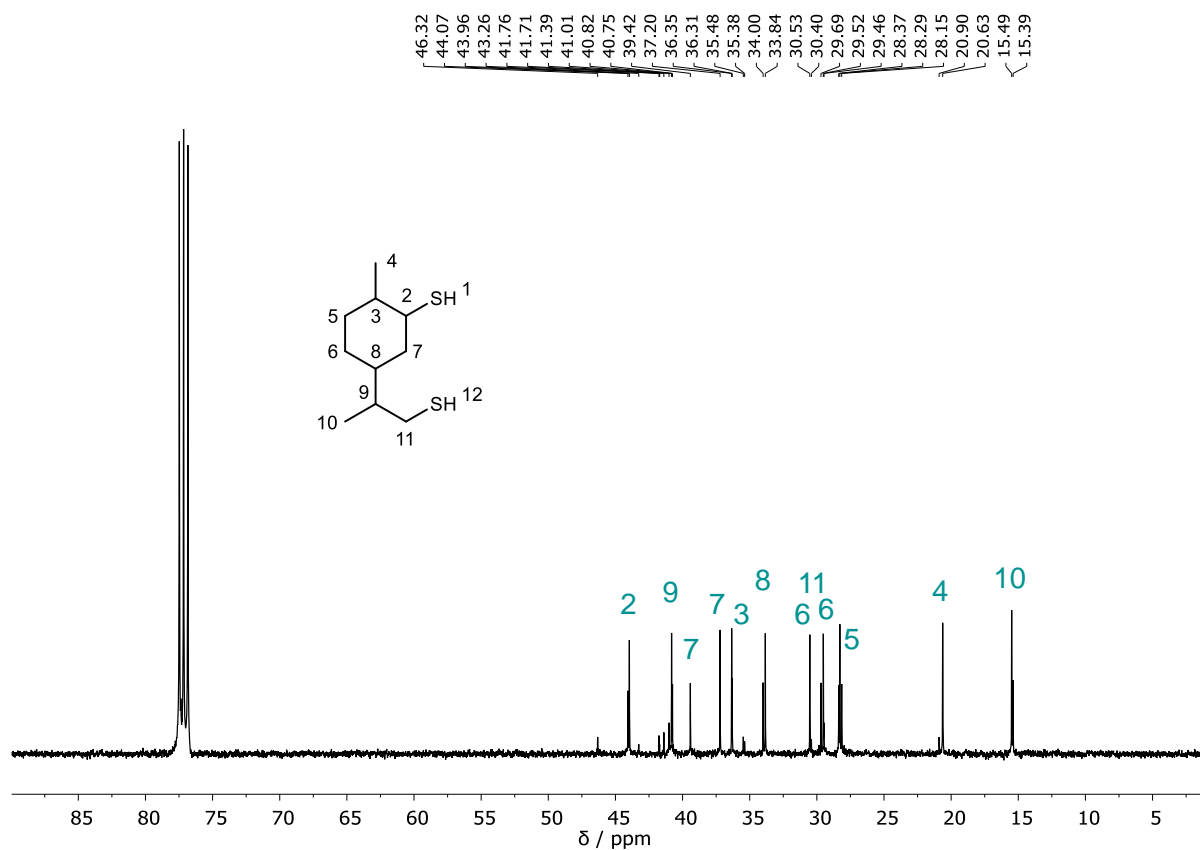
**$^1\text{H}$  NMR (400 MHz,  $\text{CDCl}_3$ )  $\delta$  / ppm = 3.45–3.27 (m, **H2**), 2.67–2.52 (m, **H11**), 2.49–2.33 (m, **H11**), 2.05–1.95 (m, **H<sub>minor</sub>**), 1.90–1.74 (m, **H7**, **H8**), 1.74–1.61 (m, **H3**, **H6**), 1.61–1.51 (m, **H7**), 1.51–1.36 (m, **H5**, **H9**), 1.33–1.21 (m, **H1**, **H12**), 1.19–1.00 (m, **H6**), 1.00–0.84 (m, **H4**, **H10**).**

Due to the occurrence of isomers, no integral values are given for the respective NMR signals and signals of the minor isomer are not assigned. The sum of integrals matches the expected number of protons. The purity of the product was confirmed via GC-FID measurements.

**$^{13}\text{C}$  NMR (101 MHz,  $\text{CDCl}_3$ )  $\delta$  / ppm = 46.3 (**C2**), 44.1 (**C2**), 44.0 (**C2**), 43.3 (**C<sub>minor</sub>**), 41.8 (**C<sub>minor</sub>**), 41.7 (**C<sub>minor</sub>**), 41.4 (**C<sub>minor</sub>**), 41.0 (**C<sub>minor</sub>**), 40.8 (**C9**), 39.4 (**C7**), 37.2 (**C7**), 36.3 (**C3**), 35.5 (**C<sub>minor</sub>**), 35.4 (**C<sub>minor</sub>**), 34.0 (**C8**), 33.8 (**C8**), 30.5 (**C6**), 30.4 (**C<sub>minor</sub>**), 29.7 (**C11**), 29.5 (**C11**), 28.4 (**C6**), 28.3 (**C5**), 28.2 (**C5**), 20.9 (**C<sub>minor</sub>**), 20.6 (**C4**), 15.5 (**C10**), 15.4 (**C10**).**

**IR (ATR platinum diamond):  $\tilde{\nu}$  /  $\text{cm}^{-1}$  = 2955, 2919, 2868, 2852, 2562, 1452, 1375, 1331, 1309, 1292, 1268, 1238, 1170, 1104, 1022, 998, 979, 939, 906, 865, 811, 766, 720, 666, 623, 524, 477, 455, 419.**

**ESI-MS:**  $[\text{M}+\text{H}]^+$  calc. 205.1079, detected 205.1079.

Supplementary Figure 83.  $^1\text{H}$  NMR spectrum of T3, measured in  $\text{CDCl}_3$  at 400 MHz.Supplementary Figure 84.  $^{13}\text{C}$  NMR spectrum of UR8, measured in  $\text{CDCl}_3$  at 101 MHz.

## Small-scale reaction monitoring

### General procedure of carbonate formation screening

To screen the optimum reaction conditions for the formation of limonene dicarbonate **CC2** (see **Table 9**), a stainless-steel reactor with Teflon inset was charged with 1.00 g limonene oxide (5.94 mmol, 1.00 equiv.), 6 mol% tetrabutylammonium halogenide and 30 bar CO<sub>2</sub> pressure. The reactor was heated to 120–180 °C and stirred for 20 h to 3 d. Afterwards, a GC-FID sample was taken to determine the constitution of the mixture.

### General procedure of aminolysis screening

To monitor the reaction progress of carbonate opening over time, reactions were carried out in 1 mL vials. 2.5–5.0 mol% thiourea were added to 100 mg (1.0 equiv.) carbonate and 1.0–4.0 equiv. allylamine. The vial was sealed and the mixture was stirred at 60–80 °C. For reaction control, samples for GC-FID or SEC were taken directly out of the reaction mixture after distinguished time intervals.

**Supplementary Table 1.** Conversion of limonene-derived carbonate **CC1** to urethane monomer **UR3**. The respective GC-FID fractions of **UR3** and **CC1** is obtained by dividing the GC integral of the associated by the sum of the integrals of the signals assigned to **CC1** and **UR3**.

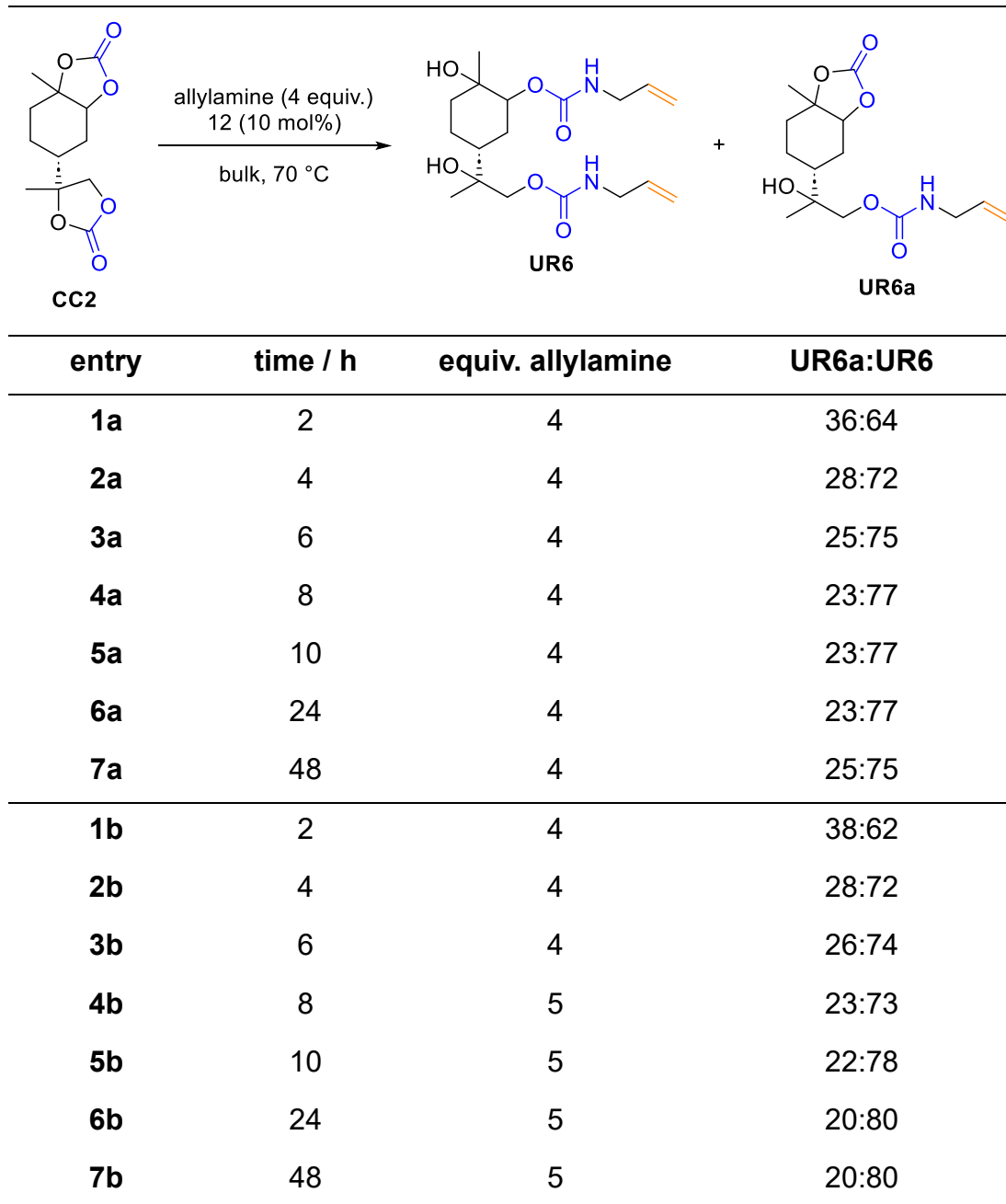
allylamine (2 equiv.)  
TU1 (5 mol%)  
70 °C

**CC1** → **UR3**

entry	time / h	mol% TU1	UR3:CC1
1	1	5	40:60
2	1	0	1:99
3	2	5	60:40
4	2	0	6:94
5	3	5	64:36
6	3	0	9:91
7	4	5	66:34
8	4	0	11:89
9	5	5	69:31
10	6	5	70:30
11	6	0	14:86
12	7	5	71:29
13	7	0	14:86
14	8	5	72:28
15	8	0	15:85



**Supplementary Table 2.** Conversion of limonene-derived carbonate **CC2** to urethane monomer **UR6**. The SEC fractions of **UR6a** and **UR6** are obtained by dividing the SEC integral of the respective signal by the sum of the integrals of the signals assigned to **CC2**, **UR6a**, and **UR6**.



## Synthesis of linear NIPUs

### General procedure of thiol-ene polymerizations

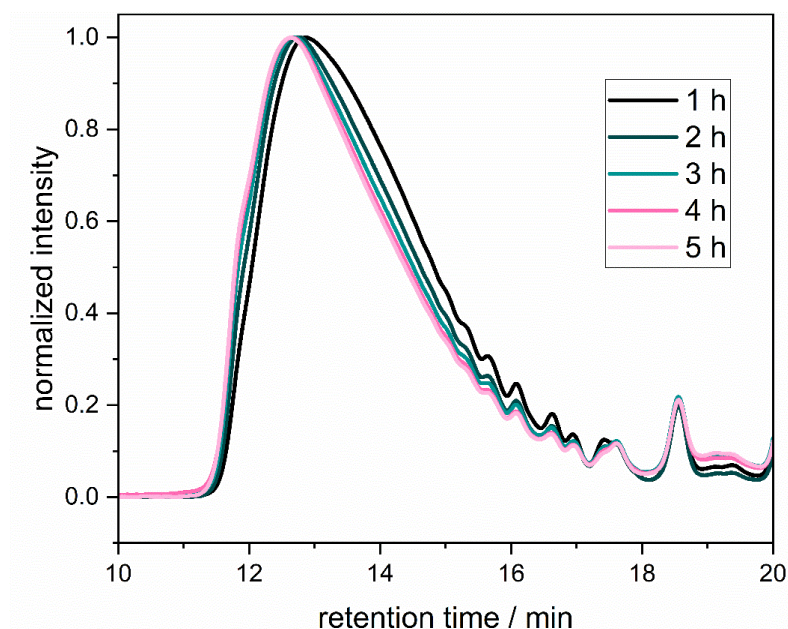
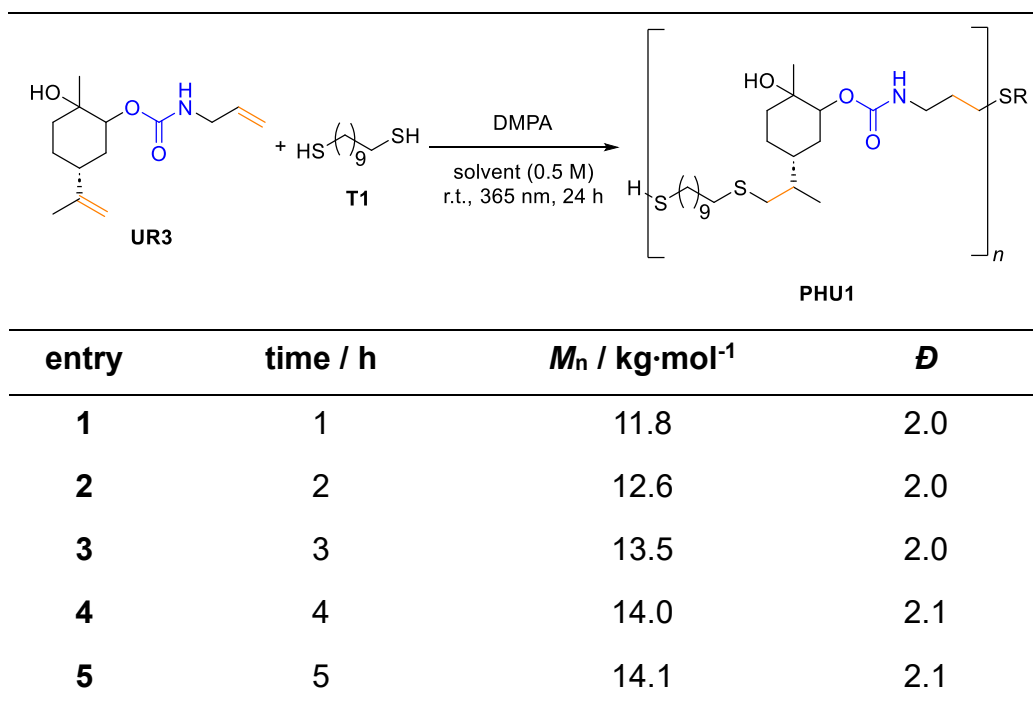
All thiol-ene polyaddition reactions were carried out in 2 mL glass vials. 100 mg of the urethane monomer (1.00 equiv.) and 1.00 equiv. of the dithiol were dissolved in the corresponding solvent (0.5 M) and 2.5–5.0 mol% DMPA were added. If 2-Me-THF was used as solvent, it was filtered over silica through a glass pipette prior to use. The reaction was stirred with a distance of 6 cm in front of a UV-lamp of 365 nm absorption maximum. For reaction control, samples were taken out of the reaction mixture after a previously fixed and documented time. After 24 h, the solvent was evaporated. For precipitation, the polymer was dissolved in THF and poured into ice-cold methanol. After decantation, the precipitated polymer was dried under high vacuum (0.09–0.14 mbar) for 18 h.

**Supplementary Table 3.** Linear NIPUs synthesized within section 4.4. For precipitation, the evaporated crude mixture was dissolved in a minimum amount of THF and poured into 45 mL of anti-solvent, which was previously cooled to -20 °C.

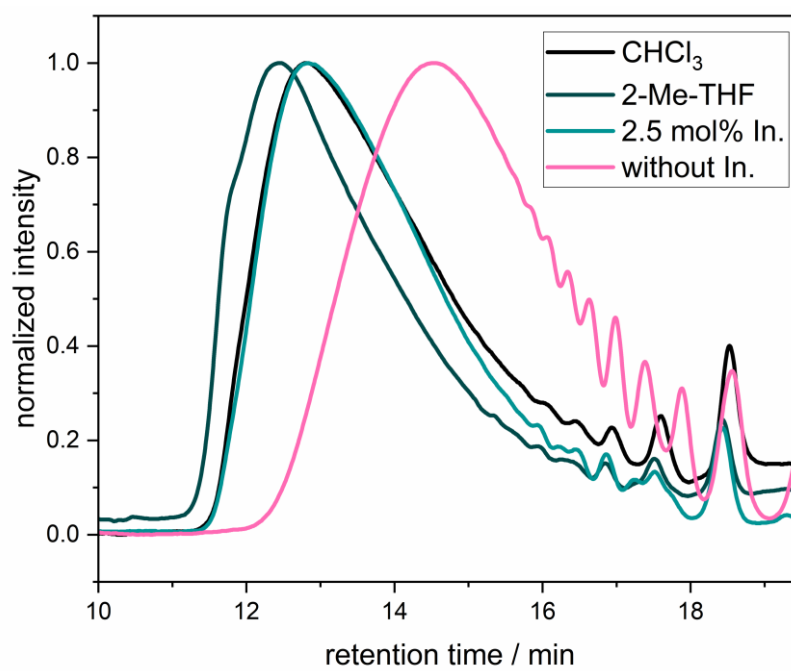
name	diene	dithiol	precipitated in	yield / %
<b>P1</b>	<b>13</b>	<b>20</b>	MeOH	64
<b>P2</b>	<b>13</b>	<b>21</b>	MeOH	26
<b>P3</b>	<b>13</b>	<b>22</b>	-	-
<b>P4</b>	<b>14</b>	<b>20</b>	-	-
<b>P5</b>	<b>15</b>	<b>20</b>	-	-
<b>P6</b>	<b>18</b>	<b>20</b>	MeOH	47
<b>P7</b>	<b>18</b>	<b>22</b>	-	-
<b>P8</b>	<b>19</b>	<b>20</b>	MeOH	40
<b>P9</b>	<b>19</b>	<b>22</b>	MeOH/H <sub>2</sub> O 1:1	39

## Monitoring of reaction progress over time

**Supplementary Table 4.** Thiol-ene polymerization of limonene-based urethane monomer **UR3** and 1,10-decanedithiol **T1** over time. The average molecular weight  $M_n$  and the dispersity  $\mathcal{D}$  were obtained from SEC measurements from the crude reaction mixture. Only one of two regioisomers of **UR3** is shown for clarity.

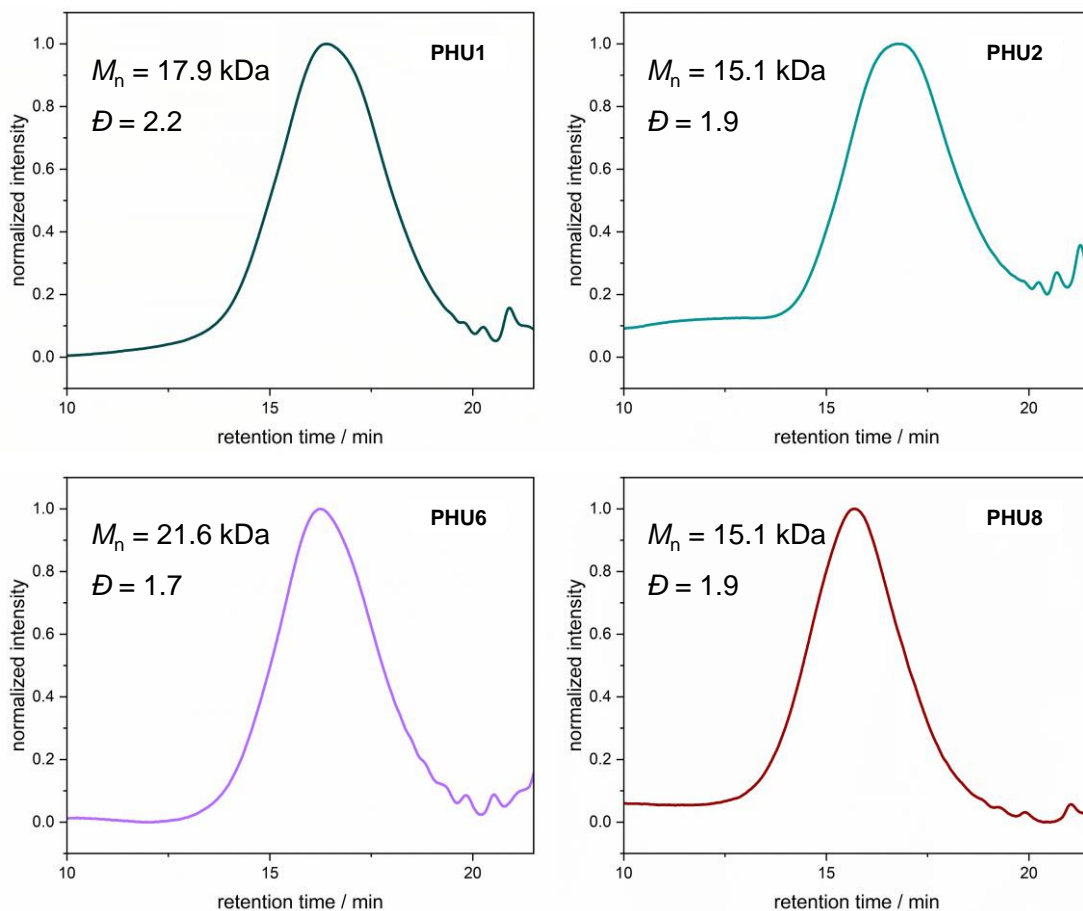
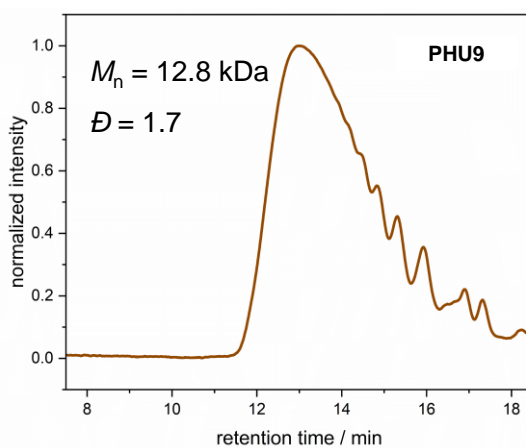


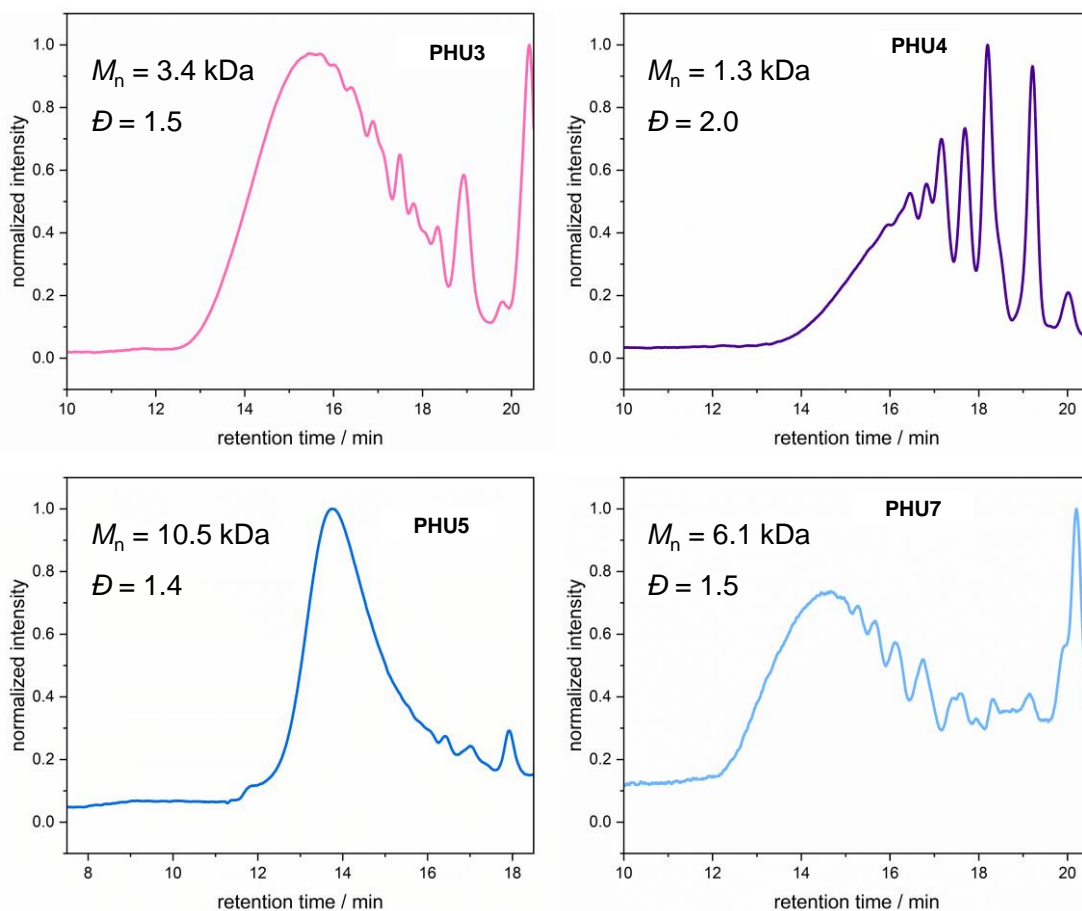
**Supplementary Figure 85.** Oligo-SEC screening over time regarding the polymerization of monomers **UR3** and **T1** (see **Supplementary Table 4**).

**Optimization of reaction conditions**

**Supplementary Figure 86.** Oligo-SEC measurements of crude polymerization tests (see **Table 12**). In. = 2,2'-dimethoxy-2-phenylacetophenone (DMPA).

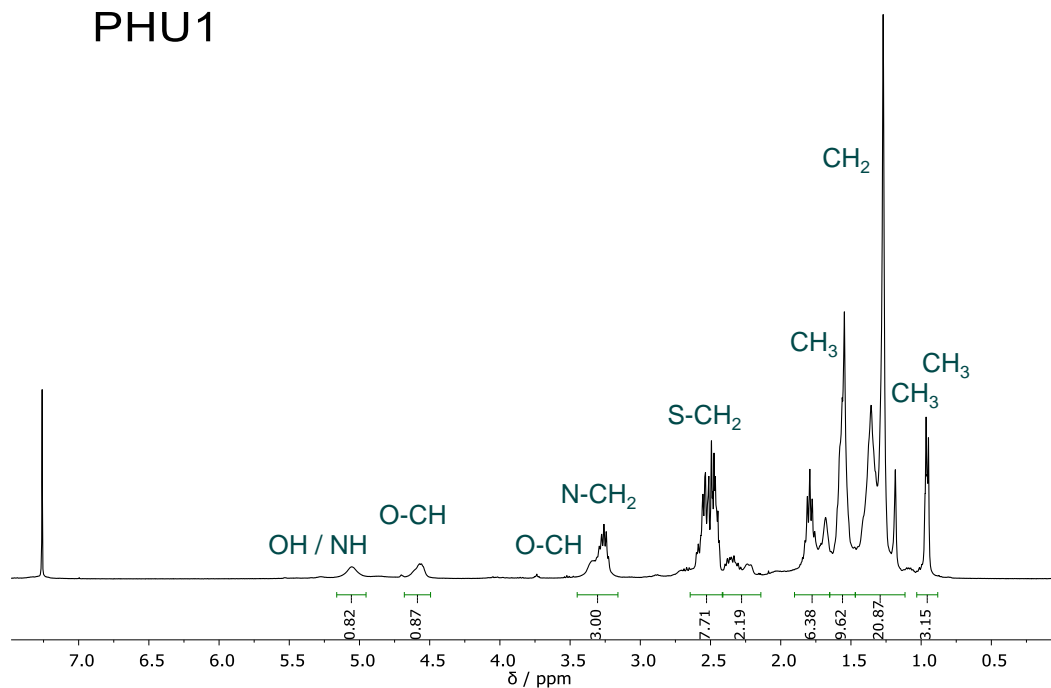
## Characterization of synthesized NIPUs

Supplementary Figure 87. Poly-SEC measurements of polymers **PHU1**, **PHU2**, **PHU6**, and **PHU8**.Supplementary Figure 88. Oligo-SEC measurement of polymer **PHU9**.

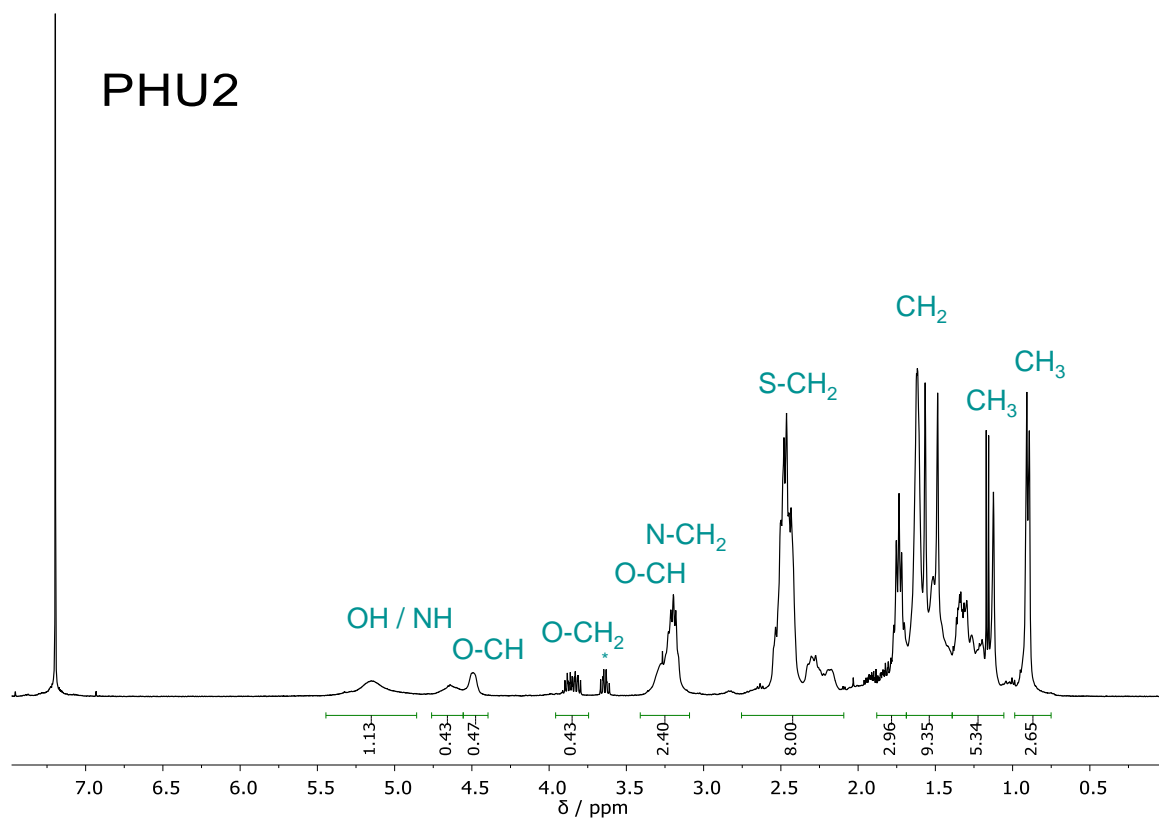


**Supplementary Figure 89.** Crude oligo-SEC measurements of **PHU3**, **PHU4**, **PHU5**, and **PHU7** that could not be precipitated in the anti-solvents tested within this work. The signal at 20.7 min is a system peak and does not correspond to any compound in the mixture.

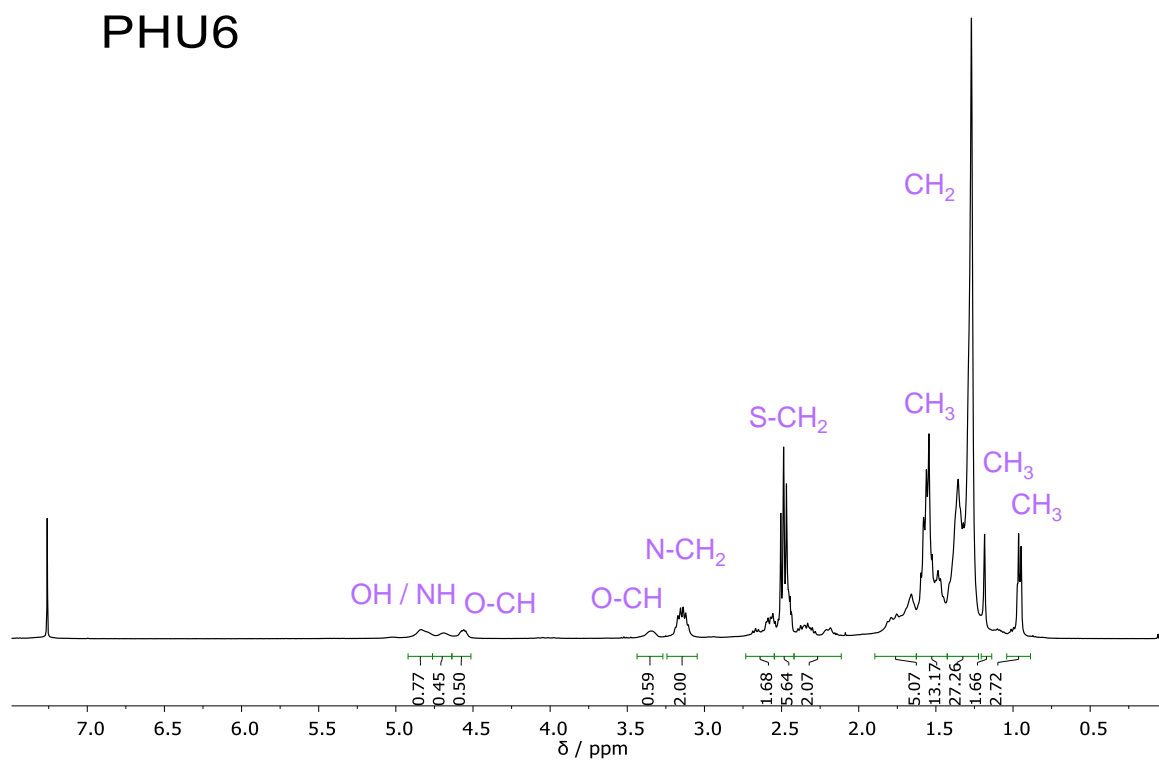
## PHU1



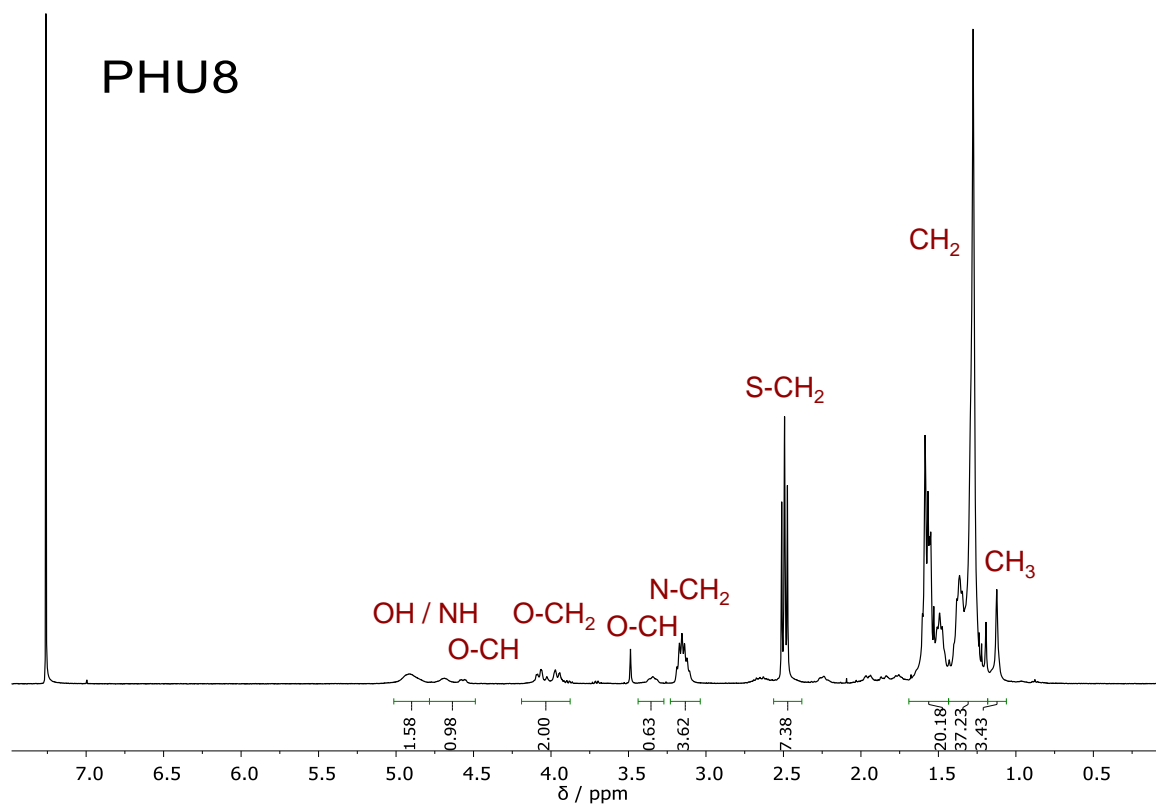
**Supplementary Figure 90.**  $^1\text{H}$  NMR spectrum of **PHU1**, measured in  $\text{CDCl}_3$  at 400 MHz.



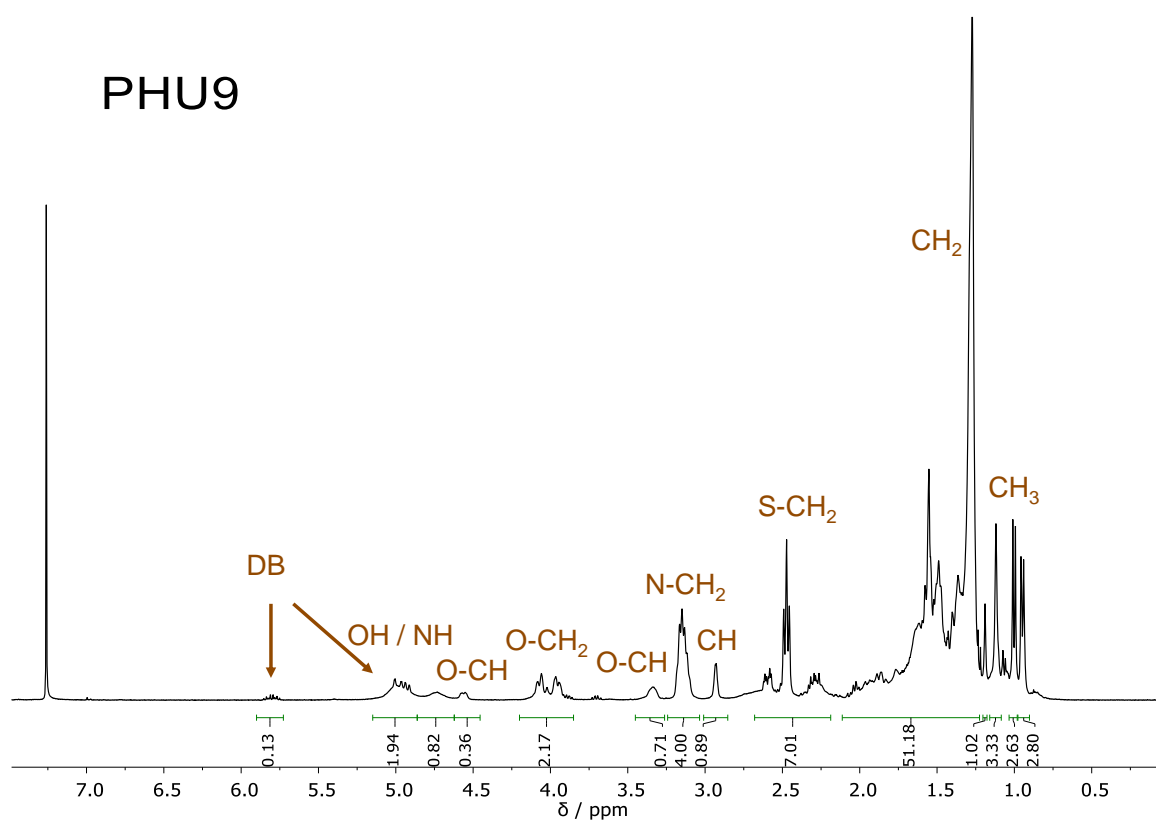
Supplementary Figure 91.  $^1\text{H}$  NMR spectrum of PHU2, measured in  $\text{CDCl}_3$  at 400 MHz.



Supplementary Figure 92.  $^1\text{H}$  NMR spectrum of PHU6, measured in  $\text{CDCl}_3$  at 400 MHz.

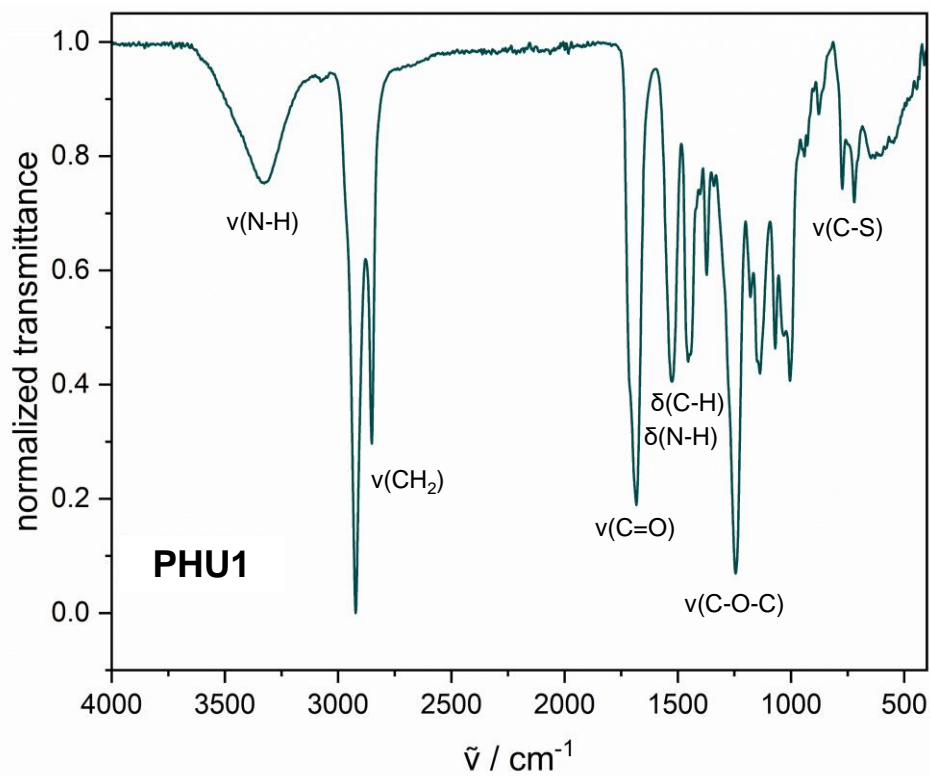


Supplementary Figure 93. <sup>1</sup>H NMR spectrum of PHU8, measured in CDCl<sub>3</sub> at 400 MHz.

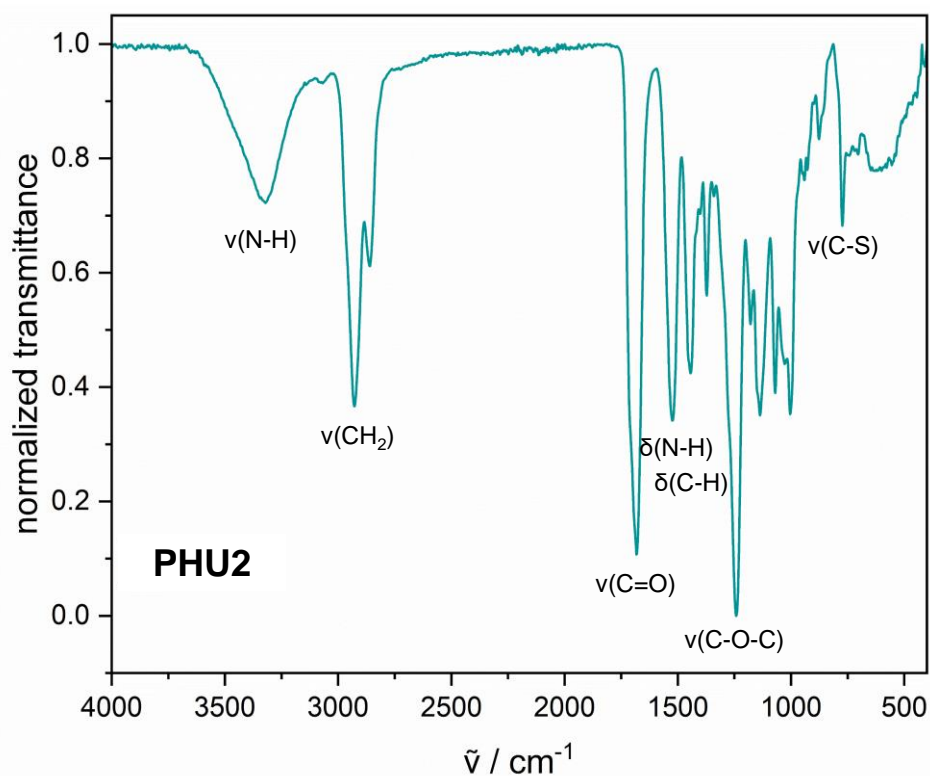


Supplementary Figure 94. <sup>1</sup>H NMR spectrum of PHU9, measured in CDCl<sub>3</sub> at 400 MHz.

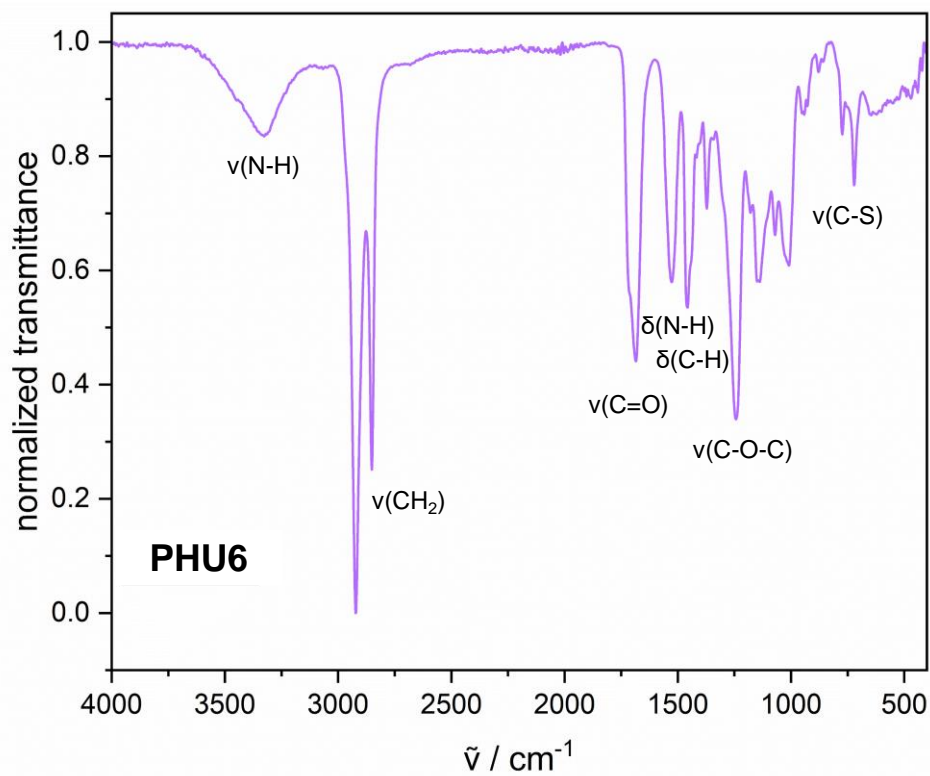




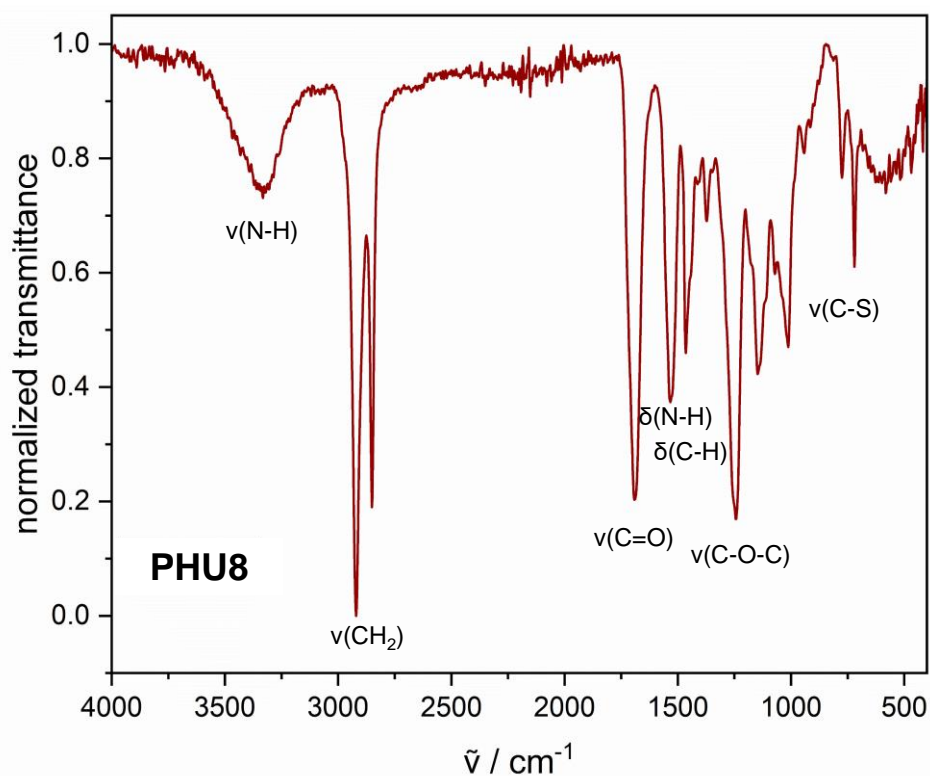
Supplementary Figure 95. IR spectrum of PHU1.



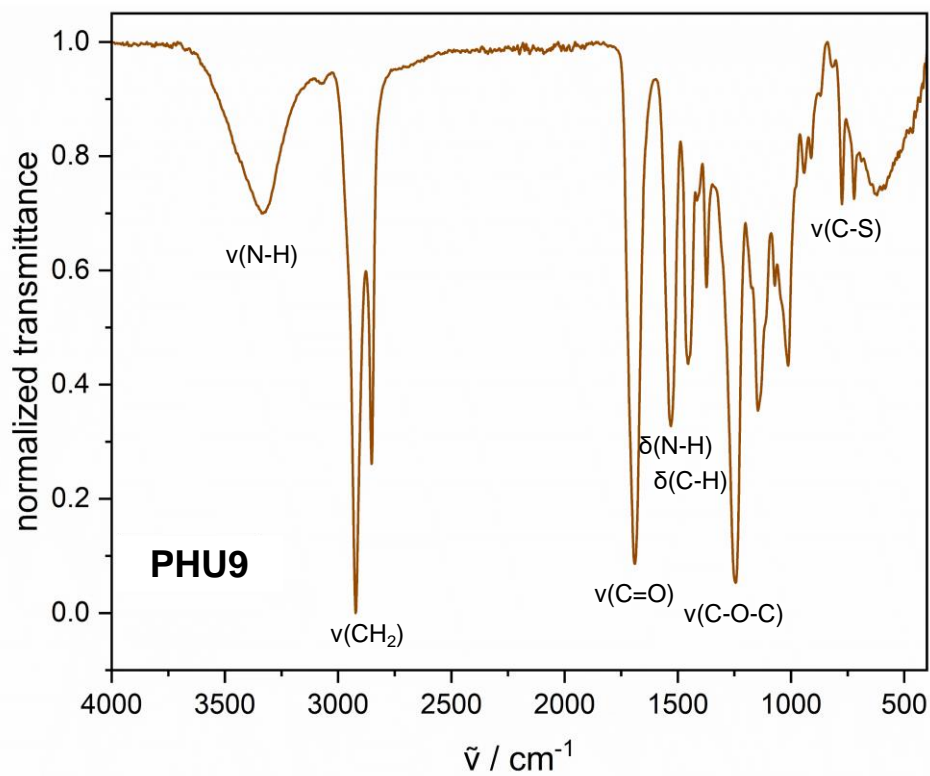
Supplementary Figure 96. IR spectrum of PHU2.



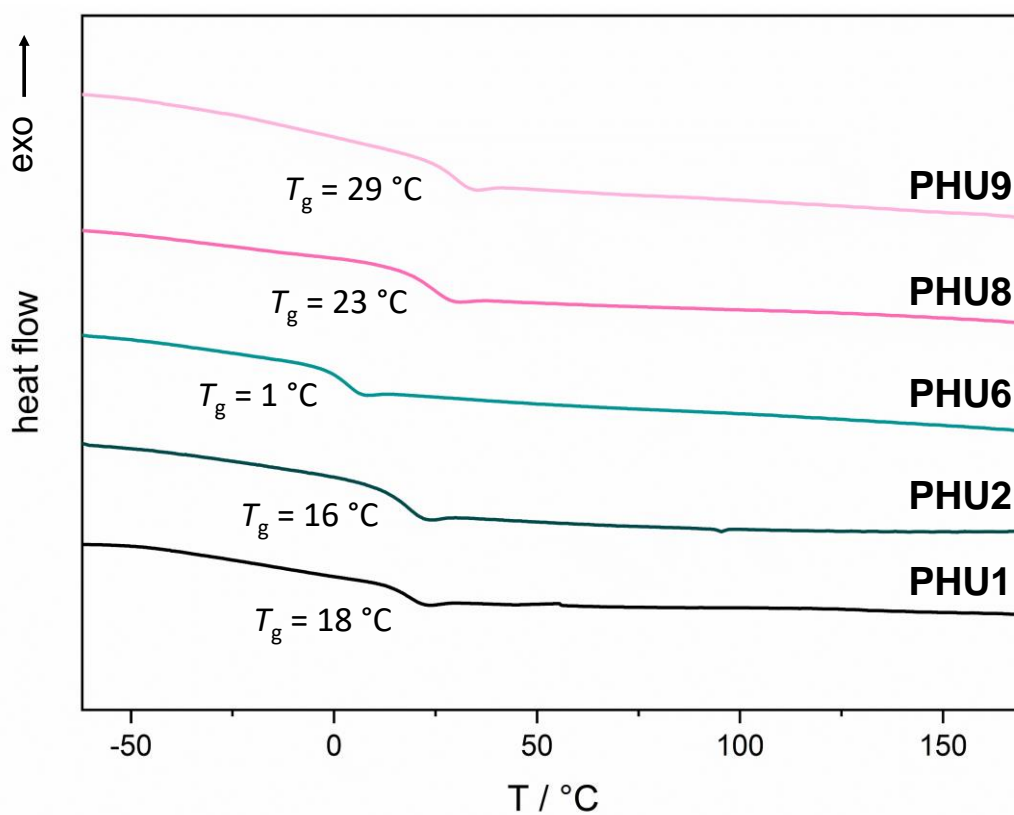
Supplementary Figure 97. IR spectrum of PHU6.



Supplementary Figure 98. IR spectrum of PHU8.



Supplementary Figure 99. IR spectrum of PHU9.

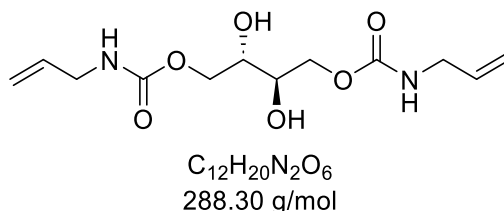


Supplementary Figure 100. DSC curves of precipitated PHU polymers from section 4.4.

## 6.2.5. Synthesis of erythritol-based linear PHUs and PHU networks

### Synthesis of hydroxyurethane monomers

#### Monomer UR9



In a 50 mL glass vial, 2.00 g (11.5 mmol, 1.00 equiv.) of EBCC and 10.4 mL (7.87 g, 138 mmol, 12.0 equiv.) allylamine were stirred at room temperature for 22 h. Afterwards, the crude reaction mixture was purified via column chromatography (ethyl acetate) to yield 1.86 g (6.45 mmol, 56%) of the product as colorless solid.

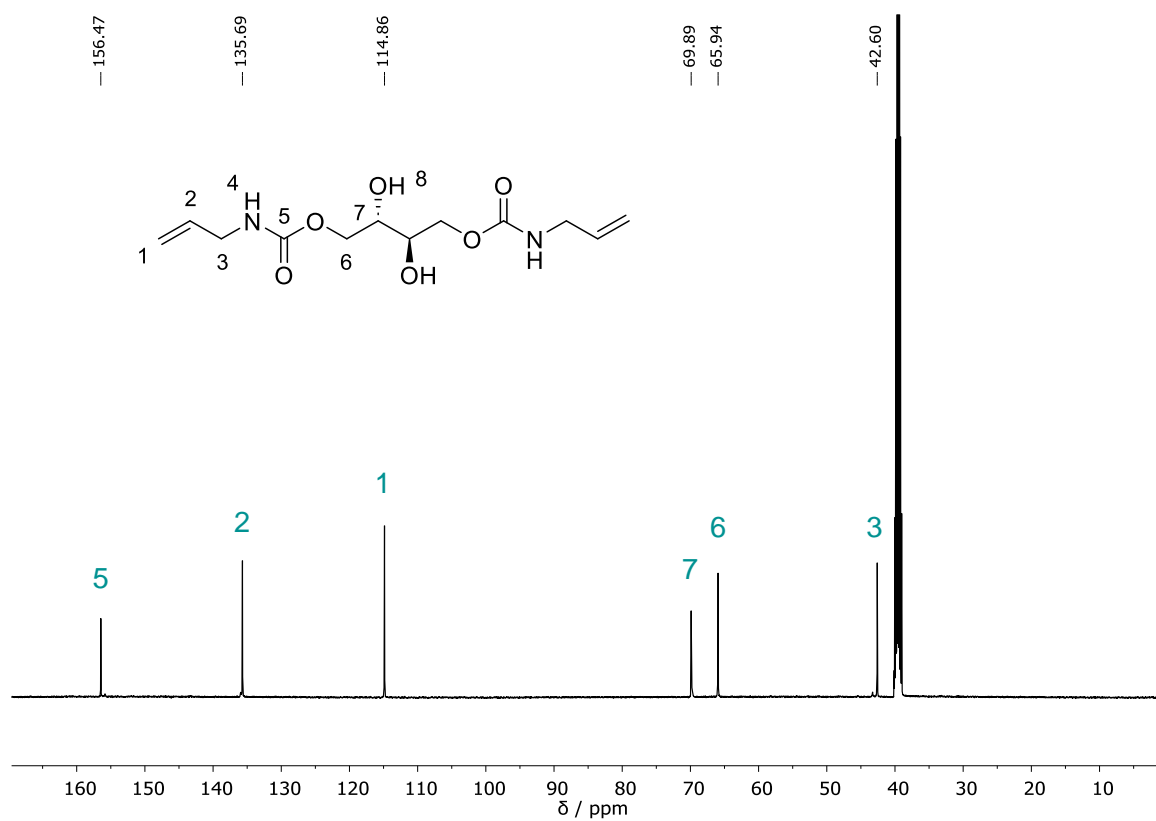
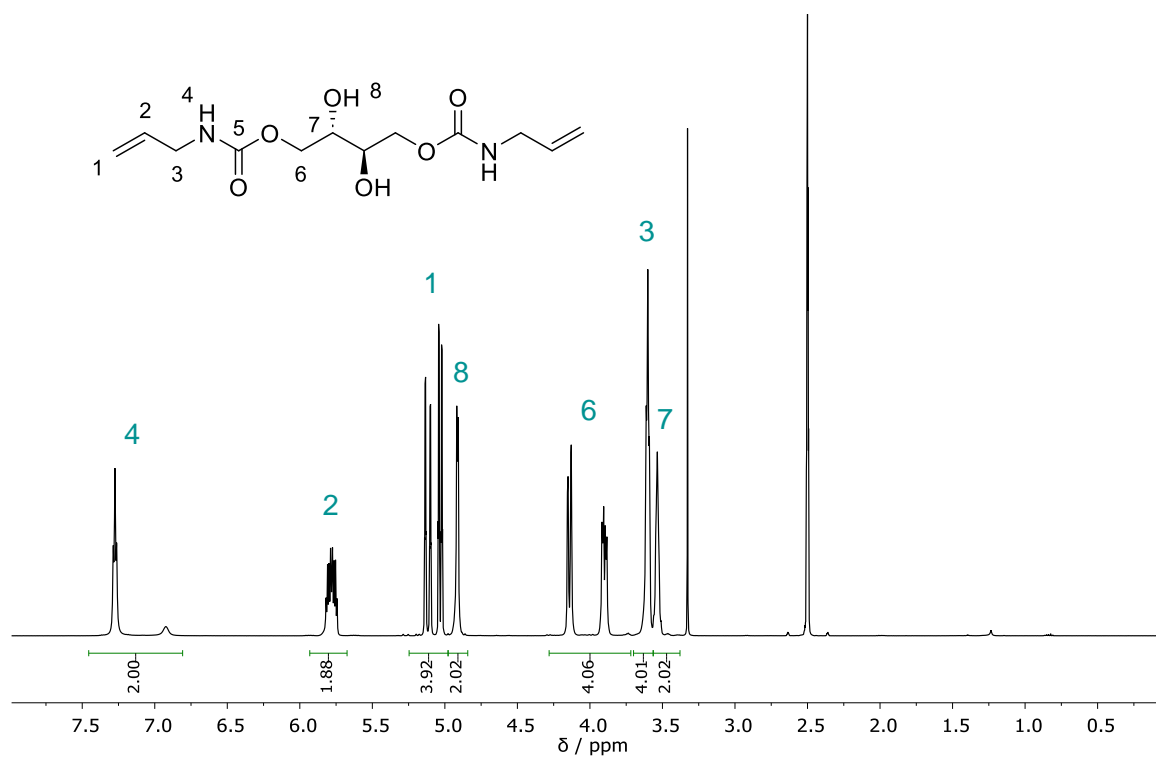
**R<sub>f</sub>** (cyclohexane/ethyl acetate 1:2) = 0.08, visualized by staining with Seebach solution.

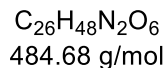
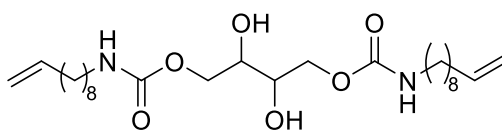
**<sup>1</sup>H NMR (300 MHz, DMSO-*d*<sub>6</sub>)**  $\delta$  / ppm = 7.42–6.78 (m, 2H, **H4**), 5.78 (ddt,  $J$  = 17.2, 10.3, 5.2 Hz, 2H, **H2**), 5.12 (ddq,  $J$  = 17.2, 1.8 Hz, 2H, **H1**), 5.03 (dq,  $J$  = 10.3, 1.7 Hz, 2H, **H1**), 4.98–4.82 (m, 2H, **H8**), 4.22–4.05 (m, 2H, **H6**), 3.99–3.80 (m, 2H, **H6**), 3.71–3.57 (m, 4H, **H3**), 3.57–3.45 (m, 2H, **H7**).

**<sup>13</sup>C NMR (101 MHz, DMSO-*d*<sub>6</sub>)**  $\delta$  / ppm = 156.5 (**C5**), 135.7 (**C2**), 114.9 (**C1**), 69.9 (**C7**), 65.9 (**C6**), 42.6 (**C3**).

**IR (ATR platinum diamond):**  $\tilde{\nu}$  / cm<sup>-1</sup> = 3320, 3083, 3008, 2979, 2957, 2912, 2896, 1685, 1644, 1534, 1480, 1454, 1418, 1387, 1346, 1311, 1250, 1146, 1064, 1027, 982, 918, 890, 775, 647, 593, 509, 458, 446, 432, 415, 406.

**ESI-MS:** [M+H]<sup>+</sup> calc. 289.1394, detected 289.1389.



**Monomer UR10**

In a 50 mL round bottom flask, 1.46 g (8.39 mmol, 1.00 equiv.) of EBCC and 3.91 g (25.2 mmol, 3.00 equiv.) amine **7** were stirred at room temperature for 48 h. Afterwards, the crude reaction mixture was diluted with ethyl acetate (300 mL), washed with brine (3 × 80 mL), and extracted with ethyl acetate (3 × 100 mL). The combined organic phases were dried over Na<sub>2</sub>SO<sub>4</sub>, and the solvent was removed under reduced pressure, yielding 2.63 g (5.43 mmol 65%) of the product as colorless solid.

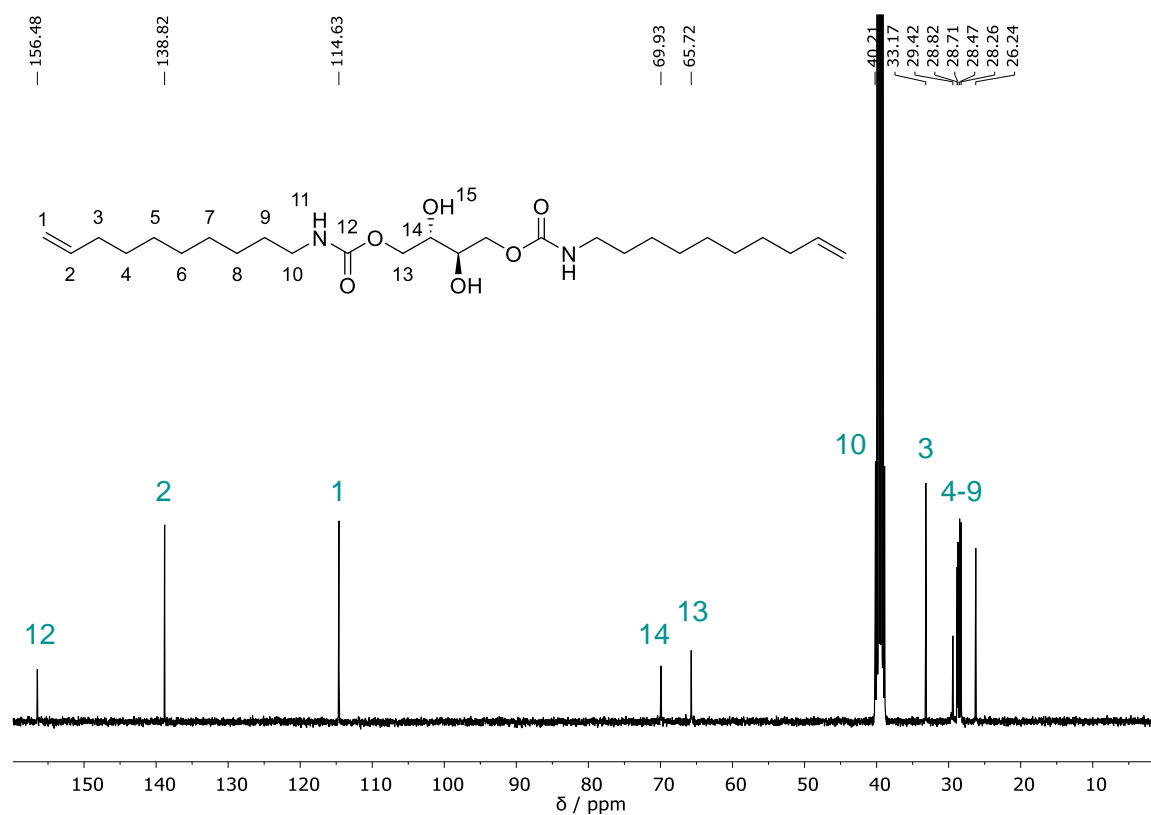
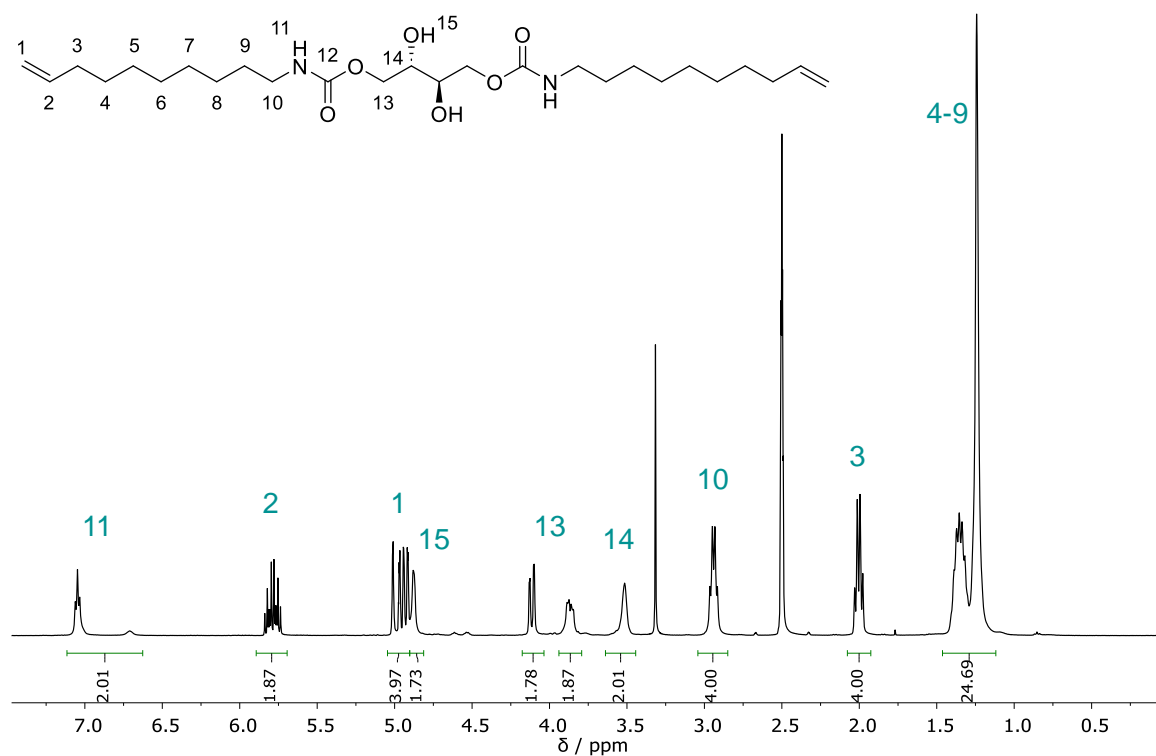
**R<sub>f</sub>** (cyclohexane/ethyl acetate 1:2) = 0.38, visualized by staining with Seebach solution.

**<sup>1</sup>H NMR (400 MHz, DMSO-*d*<sub>6</sub>)** δ / ppm = 7.12–6.63 (m, 2H, **H11**), 5.79 (ddt, *J* = 16.9, 10.2, 6.7 Hz, 2H, **H2**), 4.99 (dq, *J* = 17.2, 1.7 Hz, 2H, **H1**), 4.93 (dq, *J* = 8.9, 2.3, 1.2 Hz, 2H, **H1**), 4.90–4.81 (m, 2H, **H15**), 4.17–4.03 (m, 2H, **H13**), 3.93–3.79 (m, 2H, **H13**), 3.63–3.44 (m, 2H, **H14**), 2.94 (q, *J* = 6.6 Hz, 4H, **H10**), 2.07–1.93 (m, 4H, **H3**), 1.46–1.12 (m, 24H, **H4–9**).

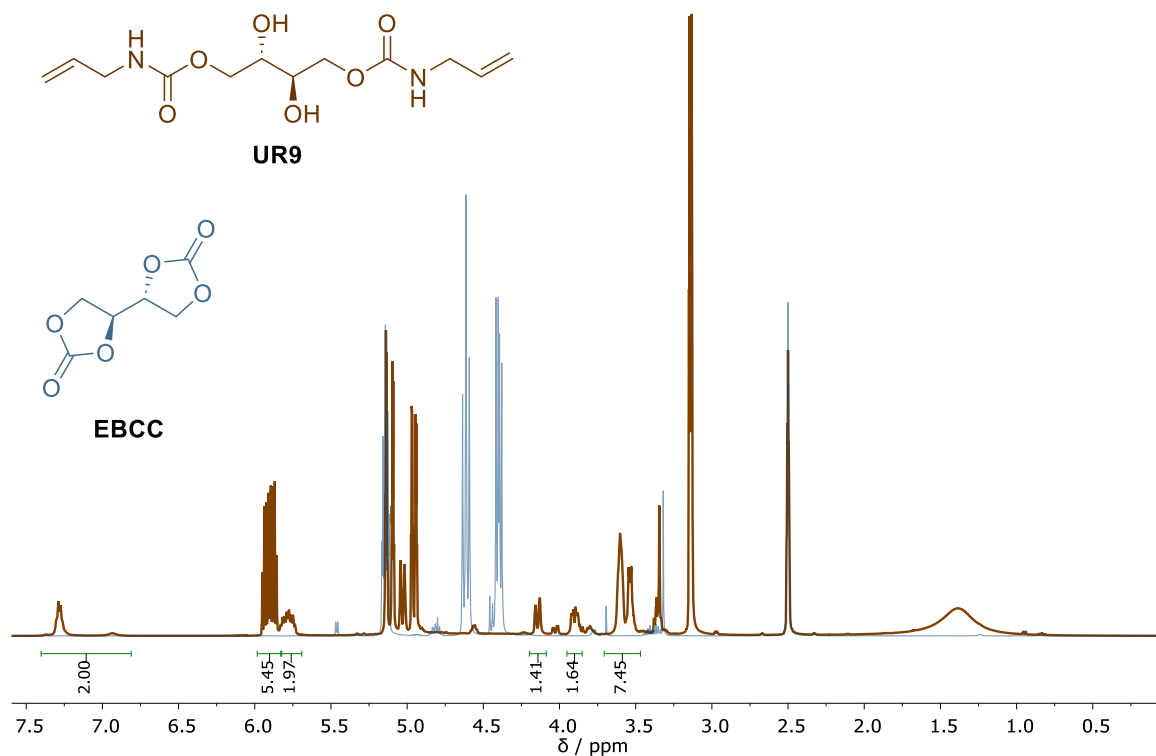
**<sup>13</sup>C NMR (101 MHz, DMSO-*d*<sub>6</sub>)** δ / ppm = 156.5 (**C12**), 138.8 (**C2**), 114.6 (**C1**), 69.9 (**C14**), 65.7 (**C13**), 40.2 (**C10**), 33.2 (**C3**), 29.4 (**C4–9**), 28.8 (**C4–9**), 28.7 (**C4–9**), 28.5 (**C4–9**), 28.3 (**C4–9**), 26.2 (**C4–9**).

**IR (ATR platinum diamond):**  $\tilde{\nu}$  / cm<sup>-1</sup> = 3331, 3079, 2923, 2852, 1687, 1643, 1531, 1481, 1466, 1311, 1284, 1258, 1238, 1147, 1064, 1017, 990, 910, 891, 776, 723, 623, 554, 529, 441, 413.

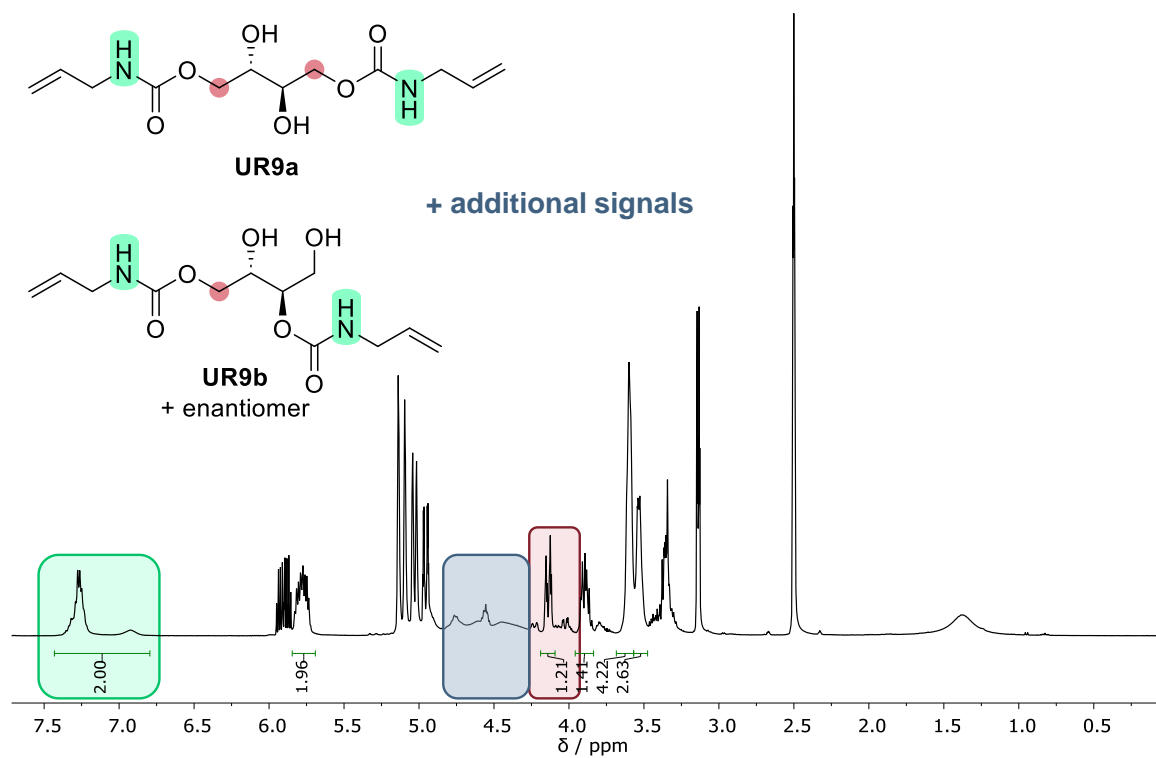
**ESI-MS:** [M+H]<sup>+</sup> calc. 485.3585, 485.3577.



## Reaction control of cyclic carbonate opening



**Supplementary Figure 105.** Reaction control of EBCC aminolysis (Figure 56) after 24 h, showing complete conversion of EBCC.



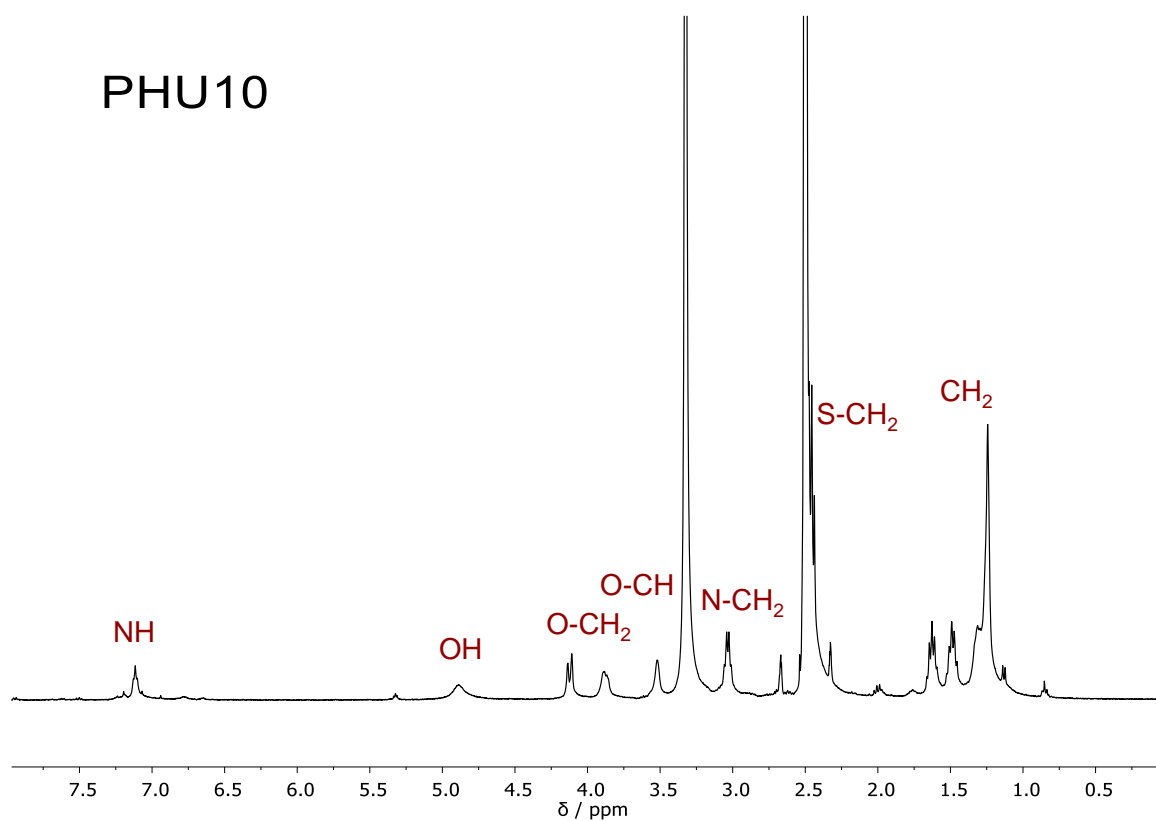
**Supplementary Figure 106.** Reaction control of EBCC aminolysis at 70 °C.



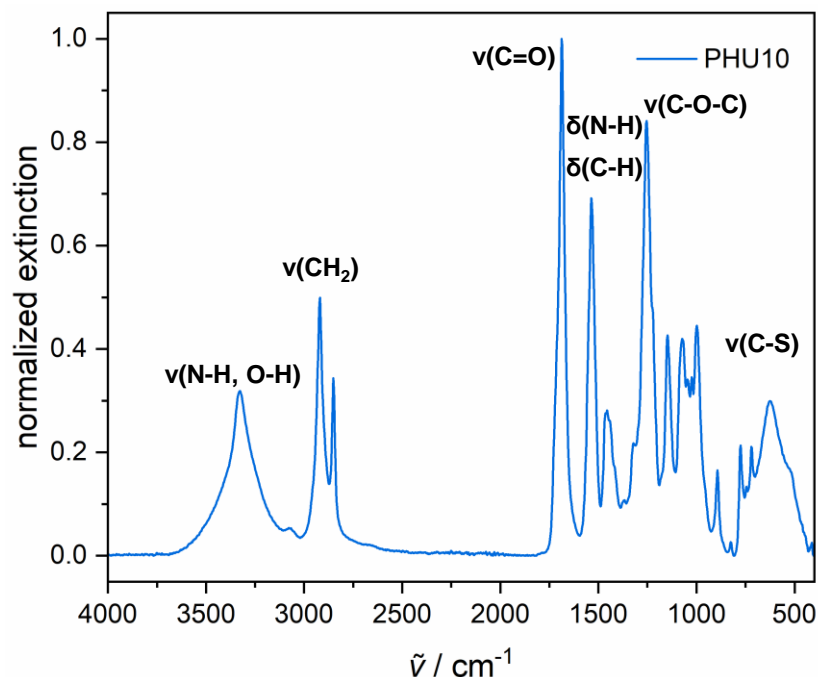
## Synthesis of linear PHUs

Thiol-ene polyaddition reactions towards linear PHUs were carried out in 2 mL or 5 mL glass vials. 100 mg (1.00 equiv.) of the urethane monomer **UR7** or **UR8** and 1.00 equiv. of the dithiol were dissolved in the corresponding solvent (see **Table 17** and **Table 18**) and 5.0 mol% DMPA were added. The reaction was stirred with a distance of 6 cm in front of a UV-lamp of 365 nm absorption maximum. For reaction control, samples were taken out of the reaction mixture after distinguished time intervals. After 24 h, the solvent was evaporated. For precipitation, the polymer was dissolved in DMSO and poured into ice-cold antisolvent. After decantation, the precipitated polymer was dried under vacuum (10 mbar) for 18 h.

## Characterization of PHU10



**Supplementary Figure 107.**  $^1\text{H}$  NMR spectrum of **PHU10**, measured in  $\text{DMSO-}d_6$  at 400 MHz.



**Supplementary Figure 108.** IR spectrum of **PHU10** with characteristic signals assigned.

## Synthesis of terpene-based PHU networks

### TP1

100 mg (395  $\mu\text{mol}$ , 1.00 equiv.) of the urethane monomer **UR3** and 86.7  $\mu\text{L}$  (105 mg, 263  $\mu\text{mol}$ , 0.667 equiv.) of trimethylolpropane tris(3-mercaptopropionate) **T4** were mixed and 1–4 wt.% photoinitiator was added. The reaction mixture was poured into a silica mold and irradiated with a distance of 5 cm in bottom of a UV-lamp of 365 nm absorption maximum.

### TP2

100 mg (395  $\mu\text{mol}$ , 1.00 equiv.) of the urethane monomer **UR3** and 86.7  $\mu\text{L}$  (105 mg, 197  $\mu\text{mol}$ , 0.667 equiv.) of pentaerythritol tetrakis(3-mercaptopropionate) **T5** were mixed and 4 wt.% DMPA was added. The reaction mixture was poured into a silica mold and irradiated with a distance of 5 cm in bottom of a UV-lamp of 365 nm absorption maximum.

### TP7

700 mg (2.67 mmol, 1.00 equiv.) of the urethane monomer **UR3**, 607  $\mu\text{L}$  (734 mg, 1.84 mmol, 0.667 equiv.) of trimethylolpropane tris(3-mercaptopropionate) **T4**, and 29.0  $\mu\text{L}$  (28.7 mg, 2 wt.%)  $\text{Ti}(\text{O}i\text{Bu})_4$  were mixed and 14.3 mg (1 wt.%) Irgacure<sup>®</sup>

819 was added. The reaction mixture was poured into a silica mold and irradiated with a distance of 5 cm in bottom of a UV-lamp of 365 nm absorption maximum.

### Synthesis of PHU networks TP3a–c

20 mg (69.4  $\mu\text{mol}$ , 1.00 equiv.) of the urethane monomer **UR9** and 15.3  $\mu\text{L}$  (18.5 mg, 46.5  $\mu\text{mol}$ , 0.667 equiv.) of trimethylolpropane tris(3-mercaptopropionate) **T4** were dissolved in the corresponding solvent (see **Table 19**). To the solution, 1 wt% photoinitiator was added. The reaction mixture was poured into silica molds and irradiated with a distance of 5 cm in bottom of a UV-lamp of 365 nm absorption maximum. Afterwards, the resulting foil was taken out of the silica mold. In the case of methanol or DMF as solvents, the foils were directly dried overnight (40  $^{\circ}\text{C}$ , 10 mbar). In the case of DMSO as solvent, the foil was left to swell in an excess of methanol for 15 minutes. Subsequently, the swelling solution was replaced with pure methanol and the same procedure was repeated five times. The final material was dried in a vacuum oven (40  $^{\circ}\text{C}$ , 10 mbar) overnight.

### Synthesis of PHU networks TP4<sub>10</sub>–TP4<sub>40</sub>

60–90 mg (0.60–0.90 equiv., see **Figure 69**) of the urethane monomer **UR3** and 0.10–0.40 equiv. of **UR9** were mixed with 86.7  $\mu\text{L}$  (105 mg, 263  $\mu\text{mol}$ , 0.667 equiv. of trimethylolpropane tris(3-mercaptopropionate) and dissolved in methanol (0.5 M with respect to **UR9**). To the solution, 1 wt% photoinitiator was added. The reaction mixture was poured into a silica mold and irradiated with a distance of 5 cm in bottom of a UV-lamp of 365 nm absorption maximum. Afterwards, the resulting foil was taken out of the silica mold and dried in a vacuum oven (40  $^{\circ}\text{C}$ , 10 mbar) overnight.

### Synthesis of PHU networks TP5 and TP6

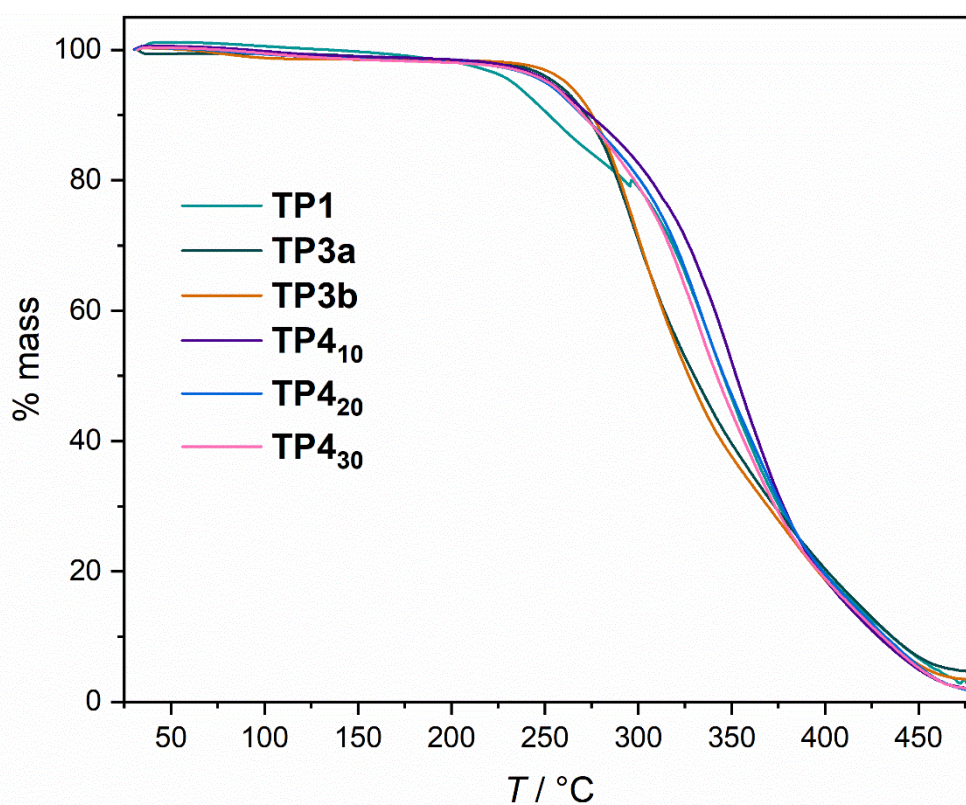
140 mg (486  $\mu\text{mol}$ , 1.00 equiv.) of the urethane monomer **UR9**, 53.3  $\mu\text{L}$  (64.5 mg, 162  $\mu\text{mol}$ , 0.333 equiv.) of trimethylolpropane tris(3-mercaptopropionate) **T4**, and 0.500 equiv. of the dithiol **T1** or **T6** (see **Figure 75**) were dissolved in 0.7 mL DMSO (0.7 M). To the solution, 1 wt% photoinitiator was added. The reaction mixture was poured into a silica mold and irradiated with a distance of 5 cm in bottom of a UV-lamp of 365 nm absorption maximum. The resulting foil was left to swell in an excess of methanol for 15 min. Subsequently, the swelling solution was replaced

with pure methanol and the same procedure was repeated five times. Afterwards, the material was dried in a vacuum oven (40 °C, 10 mbar) overnight.

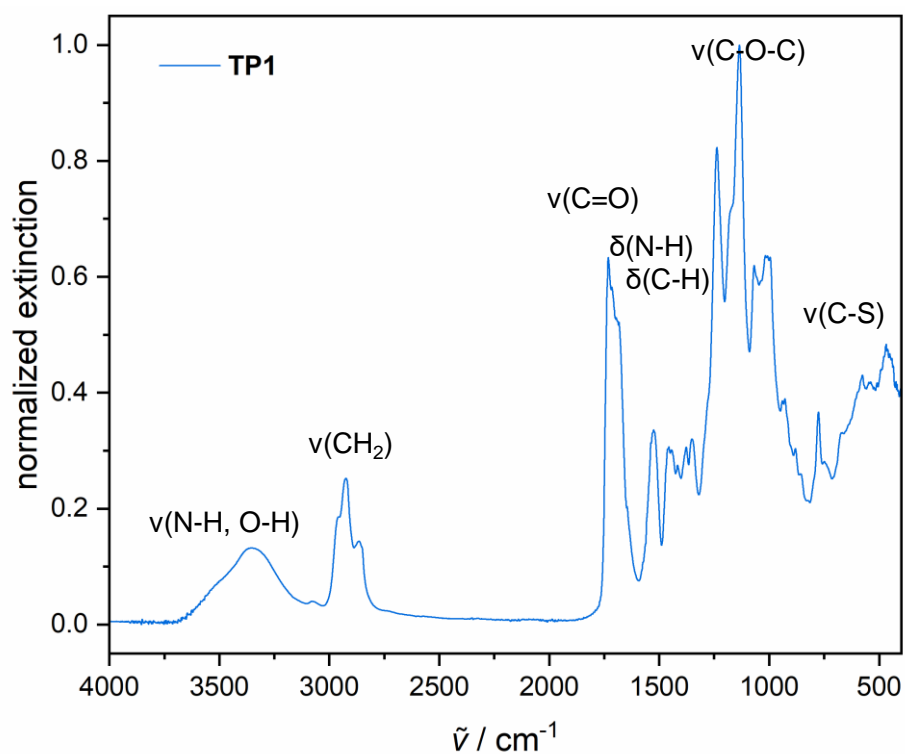
### Protection of hydroxyurethane monomer

In a 25 mL round bottom flask, 500 mg (1.73 mmol, 1.00 equiv.) **UR9** and 13.3  $\mu\text{L}$  (16.5 mg, 86.7  $\mu\text{mol}$ , 5.00 mol%) *p*TsOH were dissolved in 12.8 mL (10.1 g, 173 mmol, 100 equiv.) acetone. After stirring under reflux conditions with molecular sieves implemented into the reflux condenser for 3 h, the product mixture was washed with 1 M NaOH (2  $\times$ ) and extracted with ethyl acetate (2  $\times$ ), and  $^1\text{H}$  NMR of the product mixture was measured (see **Figure 73**).

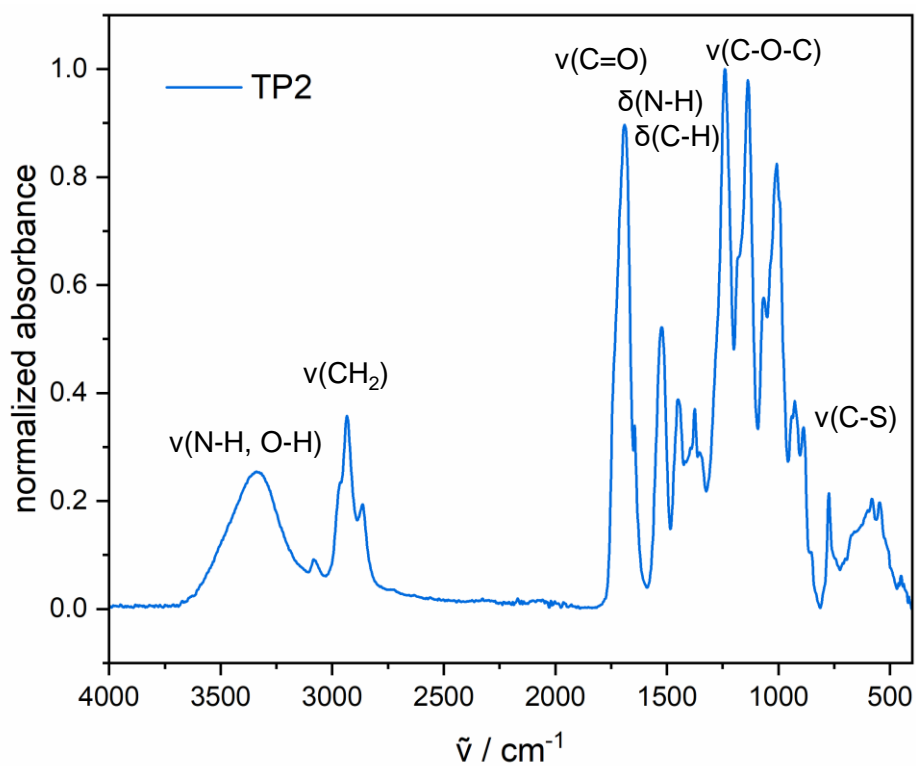
### Characterization of PHU networks



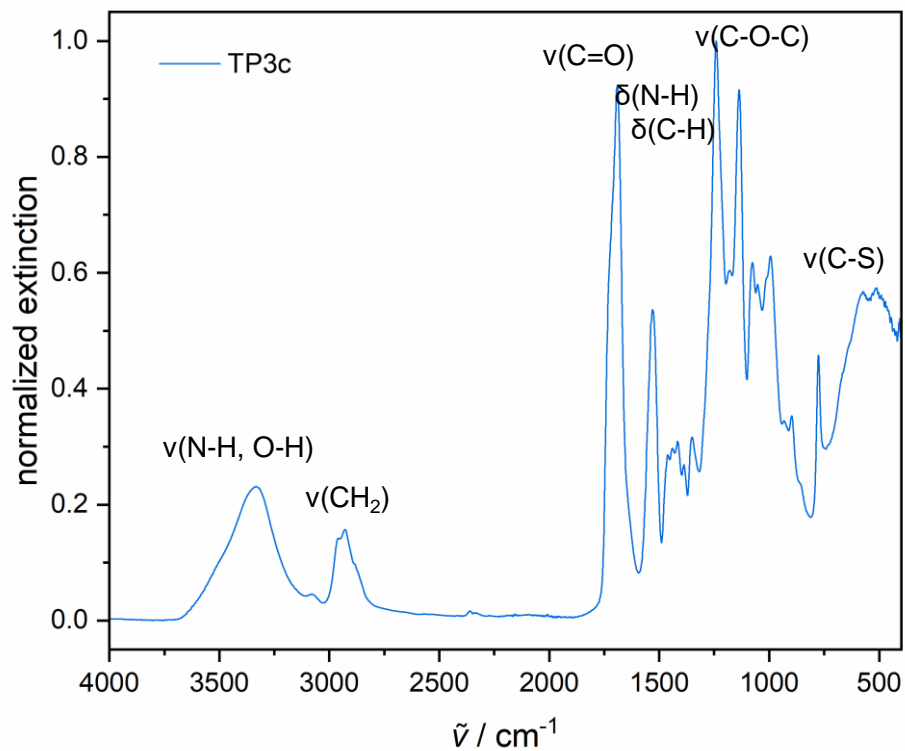
**Supplementary Figure 109.** TGA diagrams of PHU networks. In DMSO and methanol as solvents.



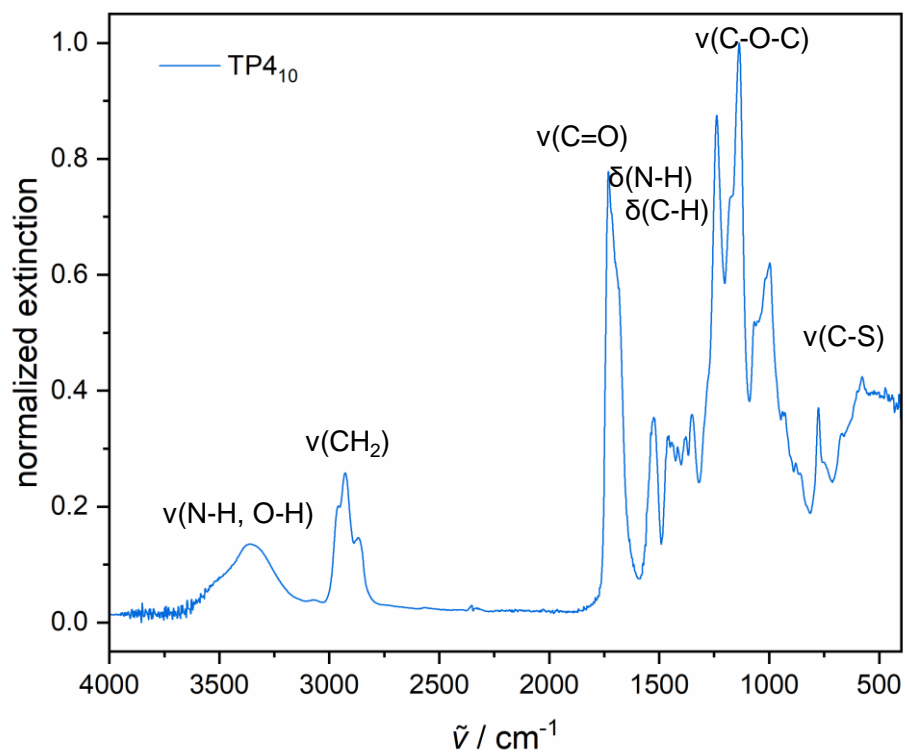
**Supplementary Figure 110.** IR spectrum of TP1 with characteristic signals assigned.



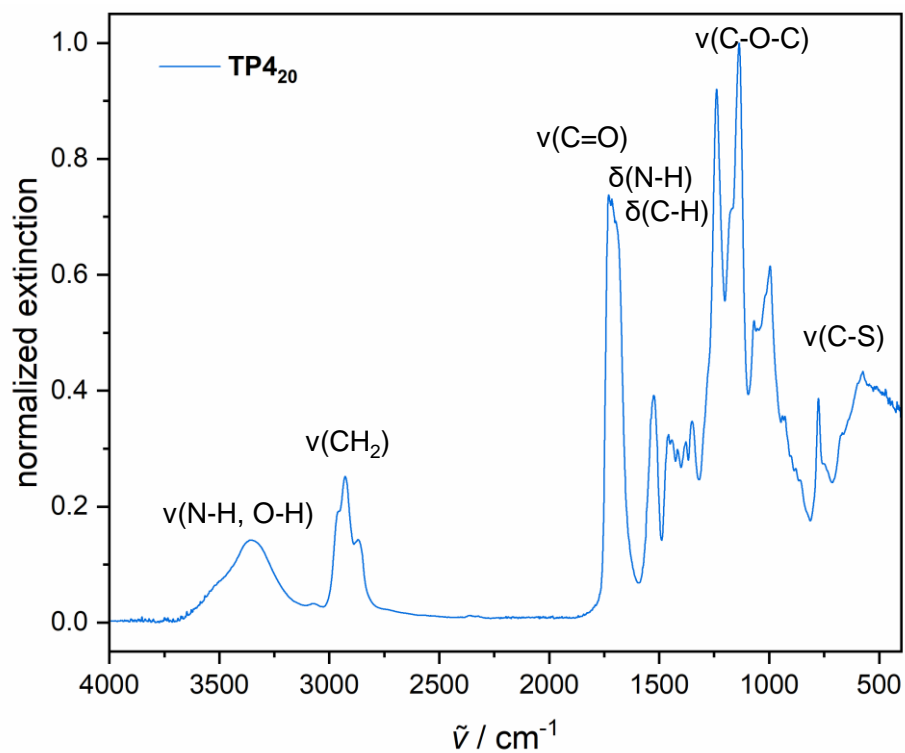
**Supplementary Figure 111.** IR spectrum of TP2 with characteristic signals assigned.



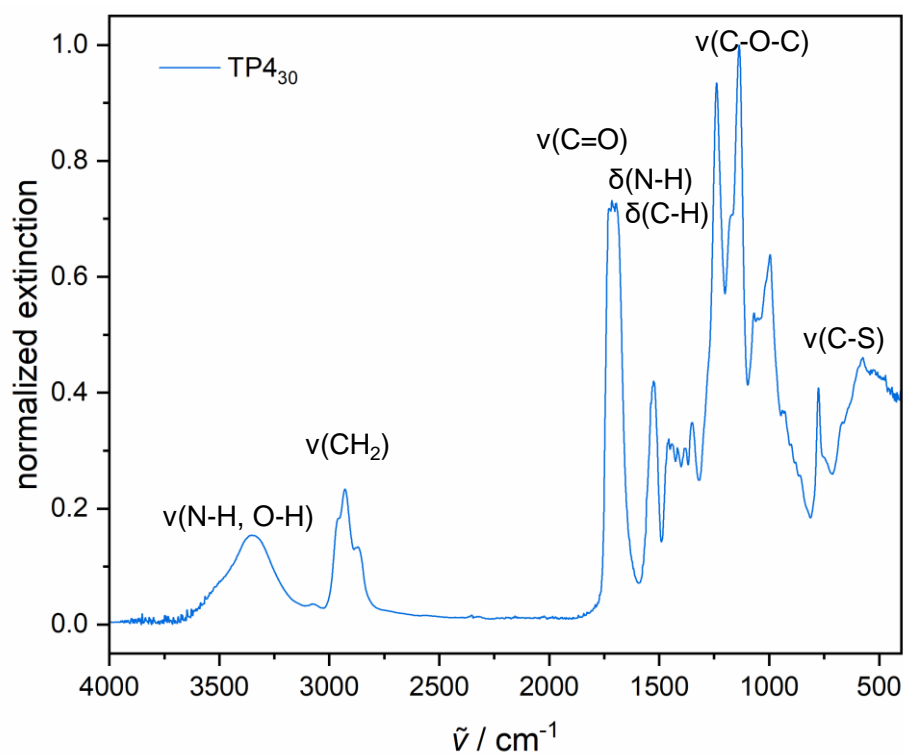
Supplementary Figure 112. IR spectrum of TP3c with characteristic signals assigned.



Supplementary Figure 113. IR spectrum of TP4<sub>10</sub> with characteristic signals assigned.



Supplementary Figure 114. IR spectrum of TP4<sub>20</sub> with characteristic signals assigned.



Supplementary Figure 115. IR spectrum of TP4<sub>30</sub> with characteristic signals assigned.

## 7. APPENDIX

### 7.1. List of abbreviations

AE	<i>Atom economy</i>
ATR	<i>Attenuated total reflection</i>
Bu	<i>Butyl-</i>
BV	<i>Baeyer-Villiger</i>
CAN	<i>Covalent adaptable network</i>
cEF	<i>Complete E-Factor</i>
COSY	<i>Correlated spectroscopy</i>
DBN	<i>1,5-Diazabicyclo[4.3.0]non-5-ene</i>
DBU	<i>1,8-Diazabicyclo[5.4.0]undec-7-ene</i>
DCM	<i>Dichloromethane</i>
DMC	<i>Dimethyl carbonate</i>
DMF	<i>Dimethyl formamide</i>
DMPA	<i>2,2-Dimethoxy-2-phenylacetophenone</i>
DMSO	<i>Dimethyl sulfoxide</i>
DSC	<i>Differential Scanning Calorimetry</i>
EBCC	<i>Erythritol bis(cyclic carbonate)</i>
$\epsilon$ CL	<i><math>\epsilon</math>-Caprolactone</i>
E-Factor	<i>Environmental factor</i>
ESI	<i>Electrospray ionization</i>
Et	<i>Ethyl-</i>
FA	<i>Fatty acid</i>
FAME	<i>Fatty acid methyl ester</i>
FID	<i>Flame ionization detector</i>
FT-IR	<i>Fourier-transformation infrared</i>
GC	<i>Gas chromatography</i>
LBCC	<i>Limonene bis(cyclic carbonate)</i>
HDI	<i>Hexamethylene diisocyanate</i>
HMBC	<i>Heteronuclear multiple bond correlation</i>
HRMS	<i>High resolution mass spectrometry</i>



HSQC	<i>Heteronuclear single quantum coherence</i>
IPDI	<i>Isophorone diisocyanate</i>
mCPBA	<i>meta-chloroperoxybenzoic acid</i>
MDI	<i>Methylene diphenyl diisocyanate</i>
Me	<i>Methyl-</i>
NBS	<i>N-bromo succinimide</i>
NIPU	<i>Non-isocyanate polyurethane</i>
NMR	<i>Nuclear magnetic resonance</i>
PBS	<i>Poly(butylene succinate)</i>
PBSA	<i>Poly(butylene succinate adipate)</i>
PBT	<i>Polybutylene terephthalate</i>
PCL	<i>Poly(<math>\epsilon</math>-caprolactone)</i>
PEG	<i>Polyethylene glycol</i>
PET	<i>Polyethylene terephthalate</i>
PHU	<i>Poly(hydroxyurethane)</i>
PLA	<i>Poly(lactic acid)</i>
PPG	<i>Polypropylene glycol</i>
pTsOH	<i>para-toluenesulfonic acid</i>
PU	<i>Polyurethane</i>
ROCOP	<i>Ring-opening copolymerization</i>
ROP	<i>Ring-opening polymerization</i>
SEC	<i>Size exclusion chromatography</i>
sEF	<i>Simple E-Factor</i>
TBA-	<i>Tetra-n-butylammonium-</i>
TBD	<i>1,5,7-Triazabicyclo[4.4.0]dec-5-ene</i>
TBO	<i>1,4,6-Triazabicyclo[3.3.0]oct-4-ene</i>
TGA	<i>Thermogravimetric analysis</i>
THF	<i>Tetrahydrofuran</i>
TLC	<i>Thin layer chromatography</i>
TMG	<i>1,1,3,3-Tetramethylguanidine</i>
TPA	<i>Terephthalic acid</i>
TPP	<i>Tetraphenyl porphyrine</i>
UV	<i>Ultraviolet</i>

## 7.2. List of publications

1. **F. C. M. Scheelje**, F. C. Destaso, H. Cramail and M. A. R. Meier, Nitrogen-Containing Polymers Derived from Terpenes: Possibilities and Limitations, *Macromol. Chem. Phys.*, 2023, **224**, 2200403.
2. J. Wolfs, **F. C. M. Scheelje**, O. Matveyeva and M. A. R. Meier, Determination of the degree of substitution of cellulose esters via ATR-FTIR spectroscopy, *J. Polym. Sci.*, 2023, **61**, 2697–2707.
3. **F. C. M. Scheelje** and M. A. R. Meier, Non-isocyanate polyurethanes synthesized from terpenes using thiourea organocatalysis and thiol-ene-chemistry, *Commun. Chem.*, 2023, **6**, 239.

## 7.3. List of conference contributions

- Participation at the “Makromolekulares Kolloquium Freiburg 2022”, 23.-25.02.2022, Freiburg, Germany (Online Conference).
- “Renewable Non-Isocyanate Polyurethanes Using Thiourea Catalysis and Thiol-Ene Reaction”: Poster at the Bordeaux Polymer Conference 2022, 13.-16.06.2022, Bordeaux, France.
- “Renewable Non-Isocyanate Polyurethanes Using Thiourea Catalysis and Thiol-Ene Reaction”: Poster at the “GDCh-Fachgruppentagung (Adaptive Polymers and Systems)”, 12.-14.09.2022, Aachen, Germany.
- “Renewable Non-Isocyanate Polyurethanes Using Thiourea Catalysis and Thiol-Ene Reaction”: Poster at the “Makromolekulares Kolloquium Freiburg 2023”, 16.-17.02.2023, Freiburg, Germany.
- “Improving the Sustainability of Polyurethanes”: Oral Contribution at the Conference for the “Center of the Transformation of Chemistry (CTC)” 2023, 04.-08.09.2023, Rottach-Egern, Germany.

## 8. REFERENCES

- 1 H. Ritchie, Sector by sector: where do global greenhouse gas emissions come from?, <https://ourworldindata.org/ghg-emissions-by-sector>, (accessed 16 November 2023).
- 2 K. Groh, C. vom Berg, K. Schirmer and A. Tlili, Anthropogenic Chemicals As Underestimated Drivers of Biodiversity Loss: Scientific and Societal Implications, *Environ. Sci. Technol.*, 2022, **56**, 707–710.
- 3 B. A. Demeneix, How fossil fuel-derived pesticides and plastics harm health, biodiversity, and the climate, *Lancet Diabetes Endocrinol.*, 2020, **8**, 462–464.
- 4 P. J. A. Withers, J. J. Elser, J. Hilton, H. Ohtake, W. J. Schipper and K. C. van Dijk, Greening the global phosphorus cycle: how green chemistry can help achieve planetary P sustainability, *Green Chem.*, 2015, **17**, 2087–2099.
- 5 C. J. Stevens, Nitrogen in the environment, *Science*, 2019, **363**, 578–580.
- 6 R. Schlögl, Chemistry's Role in Regenerative Energy, *Angew. Chem. Int. Ed.*, 2011, **50**, 6424–6426.
- 7 T.-L. Chen, H. Kim, S.-Y. Pan, P.-C. Tseng, Y.-P. Lin and P.-C. Chiang, Implementation of green chemistry principles in circular economy system towards sustainable development goals: Challenges and perspectives, *Sci. Total Environ.*, 2020, **716**, 136998.
- 8 P. T. Anastas and T. C. Williamson, in *Green Chemistry*, ed. P. T. Anastas, American Chemical Society, Washington, DC, 1998, pp. 1–17.
- 9 P. Anastas and N. Eghbali, Green chemistry: principles and practice, *Chem. Soc. Rev.*, 2010, **39**, 301–312.
- 10 R. A. Sheldon, E factors, green chemistry and catalysis: an odyssey, *Chem. Commun.*, 2008, 3352–3365.
- 11 J. Clark, R. Sheldon, C. Raston, M. Poliakoff and W. Leitner, 15 years of Green Chemistry, *Green Chem.*, 2014, **16**, 18–23.
- 12 J. Liu, H. Mooney, V. Hull, S. J. Davis, J. Gaskell, T. Hertel, J. Lubchenco, K. C. Seto, P. Gleick, C. Kremen and S. Li, Systems integration for global sustainability, *Science*, 2015, **347**, 1258832.

- 13 S. A. Matlin, G. Mehta, H. Hopf and A. Krief, One-world chemistry and systems thinking, *Nat. Chem.*, 2016, **8**, 393–398.
- 14 J. B. Zimmerman, P. T. Anastas, H. C. Erythropel and W. Leitner, Designing for a green chemistry future, *Science (New York, N.Y.)*, 2020, **367**, 397–400.
- 15 R. Geyer, J. R. Jambeck and K. L. Law, Production, use, and fate of all plastics ever made, *Sci. Adv.*, 2017, **3**, e1700782.
- 16 F. Ciardelli, M. Bertoldo, S. Bronco and E. Passaglia, *Polymers from Fossil and Renewable Resources*, Springer International Publishing, Cham, 2019.
- 17 O. Bayer, Das Di-Isocyanat-Polyadditionsverfahren (Polyurethane), *Angew. Chem.*, 1947, **59**, 257–288.
- 18 J. O. Akindoyo, M. D. H. Beg, S. Ghazali, M. R. Islam, N. Jeyaratnam and A. R. Yuvaraj, Polyurethane types, synthesis and applications – a review, *RSC Adv.*, 2016, **6**, 114453–114482.
- 19 J. R. Jambeck, R. Geyer, C. Wilcox, T. R. Siegler, M. Perryman, A. Andrady, R. Narayan and K. L. Law, Marine pollution. Plastic waste inputs from land into the ocean, *Science*, 2015, **347**, 768–771.
- 20 H. Jung, G. Shin, H. Kwak, L. T. Hao, J. Jegal, H. J. Kim, H. Jeon, J. Park and D. X. Oh, Review of polymer technologies for improving the recycling and upcycling efficiency of plastic waste, *Chemosphere*, 2023, **320**, 138089.
- 21 W. Post, A. Susa, R. Blaauw, K. Molenveld and R. J. I. Knoop, A Review on the Potential and Limitations of Recyclable Thermosets for Structural Applications, *Polym. Rev.*, 2020, **60**, 359–388.
- 22 D. H. Meadows, D. L. Meadows, J. Randers and W. W. Behrens III, *The Limits to Growth. A report for Club of Rome's project on the predicament of mankind*, Universe Books, New York, 1972.
- 23 E. Robinson and R. C. Robbins, *Sources, abundance, and fate of gaseous atmospheric pollutants. Final report and supplement.*, United States, 1968.
- 24 T. D. Potter, Advisory Group on Greenhouse Gases Established Jointly by WMO, UNEP, and ICSU, *Envir. Conserv.*, 1986, **13**, 365.
- 25 Intergovernmental Panel on Climate Change, About the IPCC, <https://www.ipcc.ch/about/>, (accessed 11 November 2023).
- 26 United Nations Framework Convention on Climate Change, The Kyoto protocol, <https://www.statistiques.developpement->

- durable.gouv.fr/sites/default/files/2018-10/eng5%20reperes%202010%20eng-partie%205.pdf, (accessed 11 November 2023).
- 27 United Nations Framework Convention on Climate Change, Paris Agreement, *Treaty Series*, 2015, **3156**, 79.
- 28 P. Schwager, N. Decker and I. Kaltenecker, Exploring Green Chemistry, Sustainable Chemistry and innovative business models such as Chemical Leasing in the context of international policy discussions, *Curr. Opin. Green Sustain. Chem.*, 2016, **1**, 18–21.
- 29 *Phosgene*, Airgas, Air Liquide, Radnor, PA, 75th edn., 2019, <https://www.airgas.com/msds/001139.pdf>, (accessed 23 December 2023).
- 30 A. Gomez-Lopez, F. Elizalde, I. Calvo and H. Sardon, Trends in non-isocyanate polyurethane (NIPU) development, *Chem. Commun.*, 2021, **57**, 12254–12265.
- 31 A. Cornille, R. Auvergne, O. Figovsky, B. Boutevin and S. Caillol, A perspective approach to sustainable routes for non-isocyanate polyurethanes, *Eur. Polym. J.*, 2017, **87**, 535–552.
- 32 S. El Khezraji, H. Ben Youcef, L. Belachemi, M. A. Lopez Manchado, R. Verdejo and M. Lahcini, Recent Progress of Non-Isocyanate Polyurethane Foam and Their Challenges, *Polymers*, 2023, **15**. DOI: 10.3390/polym15020254.
- 33 H. Khatoon, S. Iqbal, M. Irfan, A. Darda and N. K. Rawat, A review on the production, properties and applications of non-isocyanate polyurethane: A greener perspective, *Prog. Org. Coat.*, 2021, **154**, 106124.
- 34 P. Stachak, I. Łukaszewska, E. Hebda and K. Pielichowski, Recent Advances in Fabrication of Non-Isocyanate Polyurethane-Based Composite Materials, *Materials*, 2021, **14**. DOI: 10.3390/ma14133497.
- 35 A. D. Curzons, D. N. Mortimer, D. J. C. Constable and V. L. Cunningham, So you think your process is green, how do you know? — Using principles of sustainability to determine what is green – a corporate perspective, *Green Chem.*, 2001, **3**, 1–6.
- 36 R. K. Henderson, C. Jiménez-González, D. J. C. Constable, S. R. Alston, G. G. A. Inglis, G. Fisher, J. Sherwood, S. P. Binks and A. D. Curzons, Expanding GSK's solvent selection guide – embedding sustainability into solvent selection starting at medicinal chemistry, *Green Chem.*, 2011, **13**, 854.

- 37 K. Tanaka, *Solvent-free organic synthesis*, Wiley-VCH, Weinheim, 2nd edn., 2009.
- 38 G. W. V. Cave, C. L. Raston and J. L. Scott, Recent advances in solventless organic reactions: towards benign synthesis with remarkable versatility, *Chem. Commun.*, 2001, 2159–2169.
- 39 D. Prat, A. Wells, J. Hayler, H. Sneddon, C. R. McElroy, S. Abou-Shehada and P. J. Dunn, CHEM21 selection guide of classical- and less classical-solvents, *Green Chem.*, 2016, **18**, 288–296.
- 40 F. Ricci, A. Chiesi, C. Bisio, C. Panari and A. Pelosi, Effectiveness of occupational health and safety training, *J. Workplace Learn.*, 2016, **28**, 355–377.
- 41 A. Samir, F. H. Ashour, A. A. A. Hakim and M. Bassyouni, Recent advances in biodegradable polymers for sustainable applications, *npj Mater. Degrad.*, 2022, **6**. DOI: 10.1038/s41529-022-00277-7.
- 42 R. A. Gross and B. Kalra, Biodegradable polymers for the environment, *Science*, 2002, **297**, 803–807.
- 43 B. M. Trost, The Atom Economy - A Search for Synthetic Efficiency, *Science*, 1991, **254**, 1471–1477.
- 44 D. J. C. Constable, A. D. Curzons and V. L. Cunningham, Metrics to 'green' chemistry—which are the best?, *Green Chem.*, 2002, **4**, 521–527.
- 45 R. A. Sheldon, The E Factor: fifteen years on, *Green Chem.*, 2007, **9**, 1273.
- 46 F. Roschangar, R. A. Sheldon and C. H. Senanayake, Overcoming barriers to green chemistry in the pharmaceutical industry – the Green Aspiration Level™ concept, *Green Chem.*, 2015, **17**, 752–768.
- 47 S. E. John, S. Gulati and N. Shankaraiah, Recent advances in multi-component reactions and their mechanistic insights: a triennium review, *Org. Chem. Front.*, 2021, **8**, 4237–4287.
- 48 M. A. R. Meier, R. Hu and B. Z. Tang, Multicomponent Reactions in Polymer Science, *Macromol. Rapid Commun.*, 2021, **42**, e2100104.
- 49 Commonwealth Scientific and Industrial Research Organization (CSIRO), About – Circular Economy, <https://research.csiro.au/circulareconomy/about/>, (accessed 27 November 2023).
- 50 Thibaut Wautelet, *The Concept of Circular Economy: its Origins and its Evolution*, 2018.

- 51 P. Hopkinson, M. Zils, P. Hawkins and S. Roper, Managing a Complex Global Circular Economy Business Model: Opportunities and Challenges, *Calif. Manag. Rev.*, 2018, **60**, 71–94.
- 52 F. Lüdeke-Freund, S. Gold and N. M. P. Bocken, A Review and Typology of Circular Economy Business Model Patterns, *J. Ind. Ecol.*, 2019, **23**, 36–61.
- 53 W. R. Stahel, The circular economy, *Nature*, 2016, **531**, 435–438.
- 54 A. Llevot and M. A. R. Meier, Renewability – a principle of utmost importance!, *Green Chem.*, 2016, **18**, 4800–4803.
- 55 M. North, ed., *Sustainable Catalysis*, Royal Society of Chemistry, Cambridge, 2015.
- 56 A. Llevot, P.-K. Dannecker, M. von Czapiewski, L. C. Over, Z. Söyler and M. A. R. Meier, Renewability is not Enough: Recent Advances in the Sustainable Synthesis of Biomass-Derived Monomers and Polymers, *Chem. Eur. J.*, 2016, **22**, 11510–11521.
- 57 F. M. Haque, J. S. A. Ishibashi, C. A. L. Lidston, H. Shao, F. S. Bates, A. B. Chang, G. W. Coates, C. J. Cramer, P. J. Dauenhauer, W. R. Dichtel, C. J. Ellison, E. A. Gormong, L. S. Hamachi, T. R. Hoye, M. Jin, J. A. Kalow, H. J. Kim, G. Kumar, C. J. LaSalle, S. Liffland, B. M. Lipinski, Y. Pang, R. Parveen, X. Peng, Y. Popowski, E. A. Prebihalo, Y. Reddi, T. M. Reineke, D. T. Sheppard, J. L. Swartz, W. B. Tolman, B. Vlasisavljevich, J. Wissinger, S. Xu and M. A. Hillmyer, Defining the Macromolecules of Tomorrow through Synergistic Sustainable Polymer Research, *Chem. Rev.*, 2022, **122**, 6322–6373.
- 58 A. Das and P. Mahanwar, A brief discussion on advances in polyurethane applications, *Adv. Ind. Eng. Polym. Res.*, 2020, **3**, 93–101.
- 59 E. Delebecq, J.-P. Pascault, B. Boutevin and F. Ganachaud, On the versatility of urethane/urea bonds: reversibility, blocked isocyanate, and non-isocyanate polyurethane, *Chem. Rev.*, 2013, **113**, 80–118.
- 60 F. E. Golling, R. Pires, A. Hecking, J. Weikard, F. Richter, K. Danielmeier and D. Dijkstra, Polyurethanes for coatings and adhesives – chemistry and applications, *Polym. Int.*, 2019, **68**, 848–855.
- 61 *Germany Pat.*, 0193828A1, 1986.

- 62 S. V. Levchik and E. D. Weil, Thermal decomposition, combustion and fire-retardancy of polyurethanes—a review of the recent literature, *Polym. Int.*, 2004, **53**, 1585–1610.
- 63 J. Datta and P. Kasprzyk, Thermoplastic Polyurethanes Derived from Petrochemical or Renewable Resources: A Comprehensive Review, *Polym. Eng. Sci.*, 2018, **58**. DOI: 10.1002/pen.24633.
- 64 U. Šebenik and M. Krajnc, Influence of the soft segment length and content on the synthesis and properties of isocyanate-terminated urethane prepolymers, *Int. J. Adh. Adh.*, 2007, **27**, 527–535.
- 65 K. Kojio, S. Nozaki, A. Takahara and S. Yamasaki, Influence of chemical structure of hard segments on physical properties of polyurethane elastomers: a review, *J. Polym. Res.*, 2020, **27**. DOI: 10.1007/s10965-020-02090-9.
- 66 K.-S. Chen, Y.-S. Chen, T. L. Yu and C.-L. Tsai, Physical Properties of Tri-Isocyanate Crosslinked Polyurethane, *J. Polym. Res.*, 2002, **9**, 119–128.
- 67 P. J. Driest, D. J. Dijkstra, D. Stamatialis and D. W. Grijpma, The Trimerization of Isocyanate-Functionalized Prepolymers: An Effective Method for Synthesizing Well-Defined Polymer Networks, *Macromol. Rapid Commun.*, 2019, **40**, e1800867.
- 68 A. Davis, Dimerisation and Trimerisation of 2,4 Toluene Di-isocyanate, *Makromol. Chem.*, 1963, **66**, 196–204.
- 69 A. Lapprand, F. Boisson, F. Delolme, F. Méchin and J.-P. Pascault, Reactivity of isocyanates with urethanes: Conditions for allophanate formation, *Polym. Degrad. Stab.*, 2005, **90**, 363–373.
- 70 N. V. Gama, A. Ferreira and A. Barros-Timmons, Polyurethane Foams: Past, Present, and Future, *Materials*, 2018, **11**. DOI: 10.3390/ma11101841.
- 71 D. V. Dounis and G. L. Wilkes, Structure-property relationships of flexible polyurethane foams, *Polymer*, 1997, **38**, 2819–2828.
- 72 H.-W. Engels, H.-G. Pirkl, R. Albers, R. W. Albach, J. Krause, A. Hoffmann, H. Casselmann and J. Dormish, Polyurethanes: versatile materials and sustainable problem solvers for today's challenges, *Angew. Chem. Int. Ed.*, 2013, **52**, 9422–9441.
- 73 A. Demharter, Polyurethane rigid foam, a proven thermal insulating material for applications between +130°C and –196°C, *Cryogenics*, 1998, **38**, 113–117.



- 74 Z. S. Petrović and J. Ferguson, Polyurethane elastomers, *Prog. Polym. Sci.*, 1991, **16**, 695–836.
- 75 S. S. Panda, B. P. Panda, S. K. Nayak and S. Mohanty, A Review on Waterborne Thermosetting Polyurethane Coatings Based on Castor Oil: Synthesis, Characterization, and Application, *Polym. Plast. Technol. Eng.*, 2018, **57**, 500–522.
- 76 R. Morales-Cerrada, R. Tavernier and S. Caillol, Fully Bio-Based Thermosetting Polyurethanes from Bio-Based Polyols and Isocyanates, *Polymers*, 2021, **13**. DOI: 10.3390/polym13081255.
- 77 A. S. More, T. Lebarbé, L. Maisonneuve, B. Gadenne, C. Alfos and H. Cramail, Novel fatty acid based di-isocyanates towards the synthesis of thermoplastic polyurethanes, *Eur. Polym. J.*, 2013, **49**, 823–833.
- 78 R. J. Slocombe, E. E. Hardy, J. H. Saunders and R. L. Jenkins, Phosgene Derivatives. The Preparation of Isocyanates, Carbamyl Chlorides and Cyanuric Acid<sup>1</sup>, *J. Am. Chem. Soc.*, 1950, **72**, 1888–1891.
- 79 M. H. Karol and J. A. Kramarik, Phenyl isocyanate is a potent chemical sensitizer, *Toxicol. Lett.*, 1996, **89**, 139–146.
- 80 J. M. Peters and R. L. Murphy, Pulmonary toxicity of isocyanates, *Ann. Intern. Med.*, 1970, **73**, 654–655.
- 81 *Commission Regulation (EU) 2020/1149 of 3 August 2020 amending Annex XVII to Regulation (EC) No 1907/2006 of the European Parliament and of the Council concerning the Registration, Evaluation, Authorisation and Restriction of Chemicals (REACH) as regards diisocyanates. C/2020/5183, 2020.*
- 82 M. Ghasemlou, F. Daver, E. P. Ivanova and B. Adhikari, Bio-based routes to synthesize cyclic carbonates and polyamines precursors of non-isocyanate polyurethanes: A review, *Eur. Polym. J.*, 2019, **118**, 668–684.
- 83 L. Maisonneuve, O. Lamarzelle, E. Rix, E. Grau and H. Cramail, Isocyanate-Free Routes to Polyurethanes and Poly(hydroxy Urethane)s, *Chem. Rev.*, 2015, **115**, 12407–12439.
- 84 G. Rokicki, P. G. Parzuchowski and M. Mazurek, Non-isocyanate polyurethanes: synthesis, properties, and applications, *Polym. Adv. Technol.*, 2015, **26**, 707–761.

- 85 S. Neffgen, H. Keul and H. Höcker, Ring-opening polymerization of cyclic urethanes and ring-closing depolymerization of the respective polyurethanes, *Macromol. Rapid Commun.*, 1996, **17**, 373–382.
- 86 S. Neffgen, H. Keul and H. Höcker, Cationic Ring-Opening Polymerization of Trimethylene Urethane: A Mechanistic Study, *Macromolecules*, 1997, **30**, 1289–1297.
- 87 O. Ihata, Y. Kayaki and T. Ikariya, Synthesis of thermoresponsive polyurethane from 2-methylaziridine and supercritical carbon dioxide, *Angew. Chem. Int. Ed.*, 2004, **43**, 717–719.
- 88 O. Ihata, Y. Kayaki and T. Ikariya, Double stimuli-responsive behavior of aliphatic poly(urethane-amine)s derived from supercritical carbon dioxide, *Chem. Commun.*, 2005, 2268–2270.
- 89 U. Steuerle and R. Feuerhake, in *Ullmann's Encyclopedia of Industrial Chemistry*, Wiley, 2000, p. 2.
- 90 Y. Hata and M. Watanabe, Metabolism of aziridines and the mechanism of their cytotoxicity, *Drug Metab. Rev.*, 1994, **26**, 575–604.
- 91 G. Rokicki and A. Piotrowska, A new route to polyurethanes from ethylene carbonate, diamines and diols, *Polymer*, 2002, **43**, 2927–2935.
- 92 M. Matsugi and T. Shioiri, in *Reference Module in Chemistry, Molecular Sciences and Chemical Engineering*, Elsevier, 2023.
- 93 J. F. Kinstle and L. E. Sepulveda, A novel “apparent sublimation” of a polymer, *J. Polym. Sci. B Polym. Lett. Ed.*, 1977, **15**, 467–469.
- 94 C. N. D. Neumann, W. D. Bulach, M. Rehahn and R. Klein, Water-Free Synthesis of Polyurethane Foams Using Highly Reactive Diisocyanates Derived from 5-Hydroxymethylfurfural, *Macromol. Rapid Commun.*, 2011, **32**, 1373–1378.
- 95 A. S. More, B. Gadenne, C. Alfos and H. Cramail, AB type polyaddition route to thermoplastic polyurethanes from fatty acid derivatives, *Polym. Chem.*, 2012, **3**, 1594.
- 96 A. I. Alfano, S. Pelliccia, G. Rossino, O. Chianese, V. Summa, S. Collina and M. Brindisi, Continuous-Flow Technology for Chemical Rearrangements: A Powerful Tool to Generate Pharmaceutically Relevant Compounds, *ACS Med. Chem. Lett.*, 2023, **14**, 326–337.

- 97 F. Paul, Catalytic synthesis of isocyanates or carbamates from nitroaromatics using Group VIII transition metal catalysts, *Coord. Chem. Rev.*, 2000, **203**, 269–323.
- 98 B. Chen and S. S. C. Chuang, In situ infrared study of oxidative carbonylation of aniline with methanol on Cu-based catalysts, *Green Chem.*, 2003, **5**, 484.
- 99 R. Juárez, A. Corma and H. García, Towards a Phosgene-Free Synthesis of Aryl Isocyanates: Alcoholysis of N-phenylurea to N-phenyl-O-methyl Carbamate Promoted by Basic Metal Oxide Nanoparticles and Organocatalysts, *Top. Catal.*, 2009, **52**, 1688–1695.
- 100 J. Wang, Q. Li, W. Dong, M. Kang, X. Wang and S. Peng, A new non-phosgene route for synthesis of methyl N-phenyl carbamate from phenylurea and methanol, *Appl. Catal. A: Gen.*, 2004, **261**, 191–197.
- 101 N. Lucas, A. P. Amrute, K. Palraj, G. V. Shanbhag, A. Vinu and S. B. Halligudi, Non-phosgene route for the synthesis of methyl phenyl carbamate using ordered AISBA-15 catalyst, *J. Mol. Catal. A. Chem.*, 2008, **295**, 29–33.
- 102 D. Tang, D.-J. Mulder, B. A. J. Noordover and C. E. Koning, Well-defined biobased segmented polyureas synthesis via a TBD-catalyzed isocyanate-free route, *Macromol. Rapid Commun.*, 2011, **32**, 1379–1385.
- 103 M. Firdaus and M. A. R. Meier, Renewable polyamides and polyurethanes derived from limonene, *Green Chem.*, 2013, **15**, 370–380.
- 104 P. Deepa and M. Jayakannan, Solvent-Free and Nonisocyanate Melt Transurethane Reaction for Aliphatic Polyurethanes and Mechanistic Aspects, *J. Polym. Sci. A Polym. Chem.*, 2008, **46**, 2445–2458.
- 105 Y. Ono, Catalysis in the production and reactions of dimethyl carbonate, an environmentally benign building block, *Appl. Catal. A: Gen.*, 1997, **155**, 133–166.
- 106 B. A. V. Santos, V. M. T. M. Silva, J. M. Loureiro and A. E. Rodrigues, Review for the Direct Synthesis of Dimethyl Carbonate, *ChemBioEng Rev.*, 2014, **1**, 214–229.
- 107 H.-Z. Tan, Z.-Q. Wang, Z.-N. Xu, J. Sun, Y.-P. Xu, Q.-S. Chen, Y. Chen and G.-C. Guo, Review on the synthesis of dimethyl carbonate, *Catal. Today*, 2018, **316**, 2–12.

- 108 D. Shi, S. Heyte, M. Capron and S. Paul, Catalytic processes for the direct synthesis of dimethyl carbonate from CO<sub>2</sub> and methanol: a review, *Green Chem.*, 2022, **24**, 1067–1089.
- 109 P. Kongpanna, V. Pavarajarn, R. Gani and S. Assabumrungrat, Techno-economic evaluation of different CO<sub>2</sub>-based processes for dimethyl carbonate production, *Chem. Eng. Res. Des.*, 2015, **93**, 496–510.
- 110 Z. Shen, L. Zheng, C. Li, G. Liu, Y. Xiao, S. Wu, J. Liu and B. Zhang, A comparison of non-isocyanate and HDI-based poly(ether urethane): Structure and properties, *Polymer*, 2019, **175**, 186–194.
- 111 H. Sardon, A. C. Engler, J. M. W. Chan, D. J. Coady, J. M. O'Brien, D. Mecerreyes, Y. Y. Yang and J. L. Hedrick, Homogeneous isocyanate- and catalyst-free synthesis of polyurethanes in aqueous media, *Green Chem.*, 2013, **15**, 1121.
- 112 B. Nohra, L. Candy, J.-F. Blanco, C. Guerin, Y. Raoul and Z. Mouloungui, From Petrochemical Polyurethanes to Biobased Polyhydroxyurethanes, *Macromolecules*, 2013, **46**, 3771–3792.
- 113 J. H. Clements, Reactive Applications of Cyclic Alkylene Carbonates, *Ind. Eng. Chem. Res.*, 2003, **42**, 663–674.
- 114 C. D. Diakoumakos and D. L. Kotzev, Non-Isocyanate-Based Polyurethanes Derived upon the Reaction of Amines with Cyclocarbonate Resins, *Macromol. Symp.*, 2004, **216**, 37–46.
- 115 V. Besse, F. Camara, F. Méchin, E. Fleury, S. Caillol, J.-P. Pascault and B. Boutevin, How to explain low molar masses in PolyHydroxyUrethanes (PHUs), *Eur. Polym. J.*, 2015, **71**, 1–11.
- 116 O. Lamarzelle, P.-L. Durand, A.-L. Wirotius, G. Chollet, E. Grau and H. Cramail, Activated lipidic cyclic carbonates for non-isocyanate polyurethane synthesis, *Polym. Chem.*, 2016, **7**, 1439–1451.
- 117 A. Cornille, G. Michaud, F. Simon, S. Fouquay, R. Auvergne, B. Boutevin and S. Caillol, Promising mechanical and adhesive properties of isocyanate-free poly(hydroxyurethane), *Eur. Polym. J.*, 2016, **84**, 404–420.
- 118 C. Pronoitis, M. Hakkarainen and K. Odellius, Solubility-governed architectural design of polyhydroxyurethane- graft -poly( $\epsilon$ -caprolactone) copolymers, *Polym. Chem.*, 2021, **12**, 196–208.

- 119 O. Kreye, H. Mutlu and M. A. R. Meier, Sustainable routes to polyurethane precursors, *Green Chem.*, 2013, **15**, 1431.
- 120 P. Helbling, F. Hermant, M. Petit, T. Vidil and H. Cramail, Design of Plurifunctional Cyclocarbonates and their Use as Precursors of Poly(hydroxyurethane) Thermosets: A Review, *Macromol. Chem. Phys.*, 2023. DOI: 10.1002/macp.202300300.
- 121 S. A. Lawrence, *Amines. Synthesis, properties and applications*, Cambridge University Press, Cambridge, 2006.
- 122 G. Hibert, O. Lamarzelle, L. Maisonneuve, E. Grau and H. Cramail, Bio-based aliphatic primary amines from alcohols through the 'Nitrile route' towards non-isocyanate polyurethanes, *Eur. Polym. J.*, 2016, **82**, 114–121.
- 123 V. Froidevaux, C. Negrell, S. Caillol, J.-P. Pascault and B. Boutevin, Biobased Amines: From Synthesis to Polymers; Present and Future, *Chem. Rev.*, 2016, **116**, 14181–14224.
- 124 R. I. Khusnutdinov, N. A. Shchadneva and Y. Y. Mayakova, Reactions of diols with dimethyl carbonate in the presence of  $W(CO)_6$  and  $Co_2(CO)_8$ , *Russ. J. Org. Chem.*, 2014, **50**, 948–952.
- 125 Y. N. Lim, C. Lee and H.-Y. Jang, Metal-Free Synthesis of Cyclic and Acyclic Carbonates from  $CO_2$  and Alcohols, *Eur. J. Org. Chem.*, 2014, **2014**, 1823–1826.
- 126 A. Takagaki, K. Iwatani, S. Nishimura and K. Ebitani, Synthesis of glycerol carbonate from glycerol and dialkyl carbonates using hydrotalcite as a reusable heterogeneous base catalyst, *Green Chem.*, 2010, **12**, 578.
- 127 B. M. Bhanage, S. Fujita, Y. Ikushima and M. Arai, Transesterification of urea and ethylene glycol to ethylene carbonate as an important step for urea based dimethyl carbonate synthesis, *Green Chem.*, 2003, **5**, 429.
- 128 F. D. Bobbink, W. Gruszka, M. Hulla, S. Das and P. J. Dyson, Synthesis of cyclic carbonates from diols and  $CO_2$  catalyzed by carbenes, *Chem. Commun.*, 2016, **52**, 10787–10790.
- 129 S. Huang, Liu, Shui, S., J. Li, N. Zhao, W. Wei and Y. Sun, Synthesis of cyclic carbonate from carbon dioxide and diols over metal acetates, *J. Fuel Chem. Technol.*, 2007, **35**, 701–705.

- 130 H. Mutlu, J. Ruiz, S. C. Solleder and M. A. R. Meier, TBD catalysis with dimethyl carbonate: a fruitful and sustainable alliance, *Green Chem.*, 2012, **14**, 1728.
- 131 H. Blattmann, M. Fleischer, M. Bähr and R. Mülhaupt, Isocyanate- and Phosgene-Free Routes to Polyfunctional Cyclic Carbonates and Green Polyurethanes by Fixation of Carbon Dioxide, *Macromol. Rapid Commun.*, 2014, **35**, 1238–1254.
- 132 T. Sakai, N. Kihara and T. Endo, Polymer Reaction of Epoxide and Carbon Dioxide. Incorporation of Carbon Dioxide into Epoxide Polymers, *Macromolecules*, 1995, **28**, 4701–4706.
- 133 M. Schmitt and V. Strehmel, Chemical Reaction of Carbon Dioxide with Bisepoxides for Synthesis of Organic Cyclic Dicarbonates at Ambient Pressure for Polyhydroxy Urethane Synthesis, *Org. Process Res. Dev.*, 2020, **24**, 2521–2528.
- 134 F. D. Bobbink, A. P. van Muyden and P. J. Dyson, En route to CO<sub>2</sub>-containing renewable materials: catalytic synthesis of polycarbonates and non-isocyanate polyhydroxyurethanes derived from cyclic carbonates, *Chem. Commun.*, 2019, **55**, 1360–1373.
- 135 V. Caló, A. Nacci, A. Monopoli and A. Fanizzi, Cyclic Carbonate Formation from Carbon Dioxide and Oxiranes in Tetrabutylammonium Halides as Solvents and Catalysts, *Org. Lett.*, 2002, **4**, 2561–2563.
- 136 F. Chen, T. Dong, T. Xu, X. Li and C. Hu, Direct synthesis of cyclic carbonates from olefins and CO<sub>2</sub> catalyzed by a MoO<sub>2</sub>(acac)<sub>2</sub>-quaternary ammonium salt system, *Green Chem.*, 2011, **13**, 2518.
- 137 C. Miceli, J. Rintjema, E. Martin, E. C. Escudero-Adán, C. Zonta, G. Licini and A. W. Kleij, Vanadium(V) Catalysts with High Activity for the Coupling of Epoxides and CO<sub>2</sub>: Characterization of a Putative Catalytic Intermediate, *ACS Catal.*, 2017, **7**, 2367–2373.
- 138 F. de La Cruz-Martínez, M. Martínez de Sarasa Buchaca, J. Martínez, J. Fernández-Baeza, L. F. Sánchez-Barba, A. Rodríguez-Diéguez, J. A. Castro-Osma and A. Lara-Sánchez, Synthesis of Bio-Derived Cyclic Carbonates from Renewable Resources, *ACS Sustainable Chem. Eng.*, 2019, **7**, 20126–20138.
- 139 M. H. Beyzavi, C. J. Stephenson, Y. Liu, O. Karagiari, J. T. Hupp and O. K. Farha, Metal-organic framework-based catalysts: Chemical fixation of CO<sub>2</sub>

- with epoxides leading to cyclic organic carbonates, *Front. Energy Res.*, 2015, **2**. DOI: 10.3389/fenrg.2014.00063.
- 140 T. Ema, Y. Miyazaki, J. Shimonishi, C. Maeda and J. Hasegawa, Bifunctional porphyrin catalysts for the synthesis of cyclic carbonates from epoxides and CO<sub>2</sub>: structural optimization and mechanistic study, *J. Am. Chem. Soc.*, 2014, **136**, 15270–15279.
- 141 T. Iwasaki, N. Kihara and T. Endo, Reaction of Various Oxiranes and Carbon Dioxide. Synthesis and Aminolysis of Five-Membered Cyclic Carbonates, *Bull. Chem. Soc. Jpn.*, 2000, **73**, 713–719.
- 142 N. Kihara, N. Hara and T. Endo, Catalytic activity of various salts in the reaction of 2,3-epoxypropyl phenyl ether and carbon dioxide under atmospheric pressure, *J. Org. Chem.*, 1993, **58**, 6198–6202.
- 143 F. D. Bobbink, D. Vasilyev, M. Hulla, S. Chamam, F. Menoud, G. Laurenczy, S. Katsyuba and P. J. Dyson, Intricacies of Cation–Anion Combinations in Imidazolium Salt-Catalyzed Cycloaddition of CO<sub>2</sub> Into Epoxides, *ACS Catal.*, 2018, **8**, 2589–2594.
- 144 S. Marmitt and P. F. B. Gonçalves, A DFT Study on the Insertion of CO<sub>2</sub> into Styrene Oxide Catalyzed by 1-Butyl-3-methyl-imidazolium Bromide Ionic Liquid, *J. Comput. Chem.*, 2015, **36**, 1322–1333.
- 145 K. Błażek, H. Beneš, Z. Walterová, S. Abbrent, A. Eceiza, T. Calvo-Correas and J. Datta, Synthesis and structural characterization of bio-based bis(cyclic carbonate)s for the preparation of non-isocyanate polyurethanes, *Polym. Chem.*, 2021, **12**, 1643–1652.
- 146 H.-C. Kang, B. M. Lee, J. Yoon and M. Yoon, Improvement of the phase-transfer catalysis method for synthesis of glycidyl ether, *J. Am. Oil Chem. Soc.*, 2001, **78**, 423–429.
- 147 H. Chen, P. Chauhan and N. Yan, “Barking” up the right tree: biorefinery from waste stream to cyclic carbonate with immobilization of CO<sub>2</sub> for non-isocyanate polyurethanes, *Green Chem.*, 2020, **22**, 6874–6888.
- 148 M. Aresta, A. Dibenedetto and I. Tommasi, Direct synthesis of organic carbonates by oxidative carboxylation of olefins catalyzed by metal oxides: developing green chemistry based on carbon dioxide, *Appl. Organomet. Chem.*, 2000, **14**, 799–802.

- 149 M. Aresta and A. Dibenedetto, Carbon dioxide as building block for the synthesis of organic carbonates, *J. Mol. Catal. A. Chem.*, 2002, **182-183**, 399–409.
- 150 W. H. Carothers, Studies on polymerization and ring formation. I. An introduction to the general theory of condensation polymers, *J. Am. Chem. Soc.*, 1929, **51**, 2283–22591.
- 151 A. Kirchberg, M. Khabazian Esfahani, M.-C. Röpert, M. Wilhelm and M. A. R. Meier, Sustainable Synthesis of Non-Isocyanate Polyurethanes Based on Renewable 2,3-Butanediol, *Macromol. Chem. Phys.*, 2022, **223**, 2200010.
- 152 S. Gennen, B. Grignard, T. Tassaing, C. Jérôme and C. Detrembleur, CO<sub>2</sub>-Sourced  $\alpha$ -Alkylidene Cyclic Carbonates: A Step Forward in the Quest for Functional Regioregular Poly(urethane)s and Poly(carbonate)s, *Angew. Chem. Int. Ed.*, 2017, **56**, 10394–10398.
- 153 S. Dabral, U. Licht, P. Rudolf, G. Bollmann, A. S. K. Hashmi and T. Schaub, Synthesis and polymerisation of  $\alpha$ -alkylidene cyclic carbonates from carbon dioxide, epoxides and the primary propargylic alcohol 1,4-butanediol, *Green Chem.*, 2020, **22**, 1553–1558.
- 154 Y. Sasaki, Reaction of carbon dioxide with propargyl alcohol catalyzed by a combination of Ru<sub>3</sub>(CO)<sub>12</sub> and Et<sub>3</sub>N, *Tetrahedron Lett.*, 1986, **27**, 1573–1574.
- 155 Q.-W. Song, B. Yu, X.-D. Li, R. Ma, Z.-F. Diao, R.-G. Li, W. Li and L.-N. He, Efficient chemical fixation of CO<sub>2</sub> promoted by a bifunctional Ag<sub>2</sub>WO<sub>4</sub>/Ph<sub>3</sub>P system, *Green Chem.*, 2014, **16**, 1633.
- 156 H. Tomita, F. Sanda and T. Endo, Reactivity Comparison of Five- and Six-Membered Cyclic Carbonates with Amines: Basic Evaluation for Synthesis of Poly(hydroxyurethane), *J. Polym. Sci. A Polym. Chem.*, 2001, **39**, 162–168.
- 157 S.-H. Pyo, K. Nuszkiwicz, P. Persson, S. Lundmark and R. Hatti-Kaul, Lipase-mediated synthesis of six-membered cyclic carbonates from trimethylolpropane and dialkyl carbonates: Influence of medium engineering on reaction selectivity, *J. Mol. Catal. B. Enzym.*, 2011, **73**, 67–73.
- 158 S. Sarel and L. A. Pohoryles, The Stereochemistry and Mechanism of Reversible Polymerization of 2,2-Disubstituted 1,3-Propanediol Carbonates, *J. Am. Chem. Soc.*, 1958, **80**, 4596–4599.



- 159 M. Honda, M. Tamura, K. Nakao, K. Suzuki, Y. Nakagawa and K. Tomishige, Direct Cyclic Carbonate Synthesis from CO<sub>2</sub> and Diol over Carboxylation/Hydration Cascade Catalyst of CeO<sub>2</sub> with 2-Cyanopyridine, *ACS Catal.*, 2014, **4**, 1893–1896.
- 160 A. Baba, H. Kashiwagi and H. Matsuda, Cycloaddition of oxetane and carbon dioxide catalyzed by tetraphenylstibonium iodide, *Tetrahedron Lett.*, 1985, **26**, 1323–1324.
- 161 A. Gomez-Lopez, S. Panchireddy, B. Grignard, I. Calvo, C. Jerome, C. Detrembleur and H. Sardon, Poly(hydroxyurethane) Adhesives and Coatings: State-of-the-Art and Future Directions, *ACS Sustainable Chem. Eng.*, 2021, **9**, 9541–9562.
- 162 K. Błażek and J. Datta, Renewable natural resources as green alternative substrates to obtain bio-based non-isocyanate polyurethanes-review, *Crit. Rev. Environ. Sci. Technol.*, 2019, **49**, 173–211.
- 163 M. A. Sawpan, Polyurethanes from vegetable oils and applications: a review, *J. Polym. Res.*, 2018, **25**. DOI: 10.1007/s10965-018-1578-3.
- 164 R. S. Malani, V. C. Malshe and B. N. Thorat, Polyols and polyurethanes from renewable sources: past, present and future—part 1: vegetable oils and lignocellulosic biomass, *J. Coat. Technol. Res.*, 2022, **19**, 201–222.
- 165 R. S. Malani, V. C. Malshe and B. N. Thorat, Polyols and polyurethanes from renewable sources: past, present, and future—part 2: plant-derived materials, *J. Coat. Technol. Res.*, 2022, **19**, 361–375.
- 166 D. K. Chelike and S. A. Gurusamy Thangavelu, Catalyzed and Non-catalyzed Synthetic Approaches to Obtain Isocyanate-free Polyurethanes, *ChemistrySelect*, 2023, **8**. DOI: 10.1002/slct.202300921.
- 167 K. Skleničková, S. Abbrent, M. Halecký, V. Kočí and H. Beneš, Biodegradability and ecotoxicity of polyurethane foams: A review, *Crit. Rev. Environ. Sci. Technol.*, 2022, **52**, 157–202.
- 168 M. Rutkowska, K. Krasowska, A. Heimowska, I. Steinka and H. Janik, Degradation of polyurethanes in sea water, *Polym. Degrad. Stab.*, 2002, **76**, 233–239.
- 169 K. Krasowska, A. Heimowska and M. Rutkowska, in *Thermoplastic Elastomers - Synthesis and Applications*, ed. C. K. Das, InTech, 2015.

- 170 A. Khan, M. Naveed and M. Rabnawaz, Melt-reprocessing of mixed polyurethane thermosets, *Green Chem.*, 2021, **23**, 4771–4779.
- 171 K. M. Zia, H. N. Bhatti and I. Ahmad Bhatti, Methods for polyurethane and polyurethane composites, recycling and recovery: A review, *React. Funct. Polym.*, 2007, **67**, 675–692.
- 172 B. Eling, Ž. Tomović and V. Schädler, Current and Future Trends in Polyurethanes: An Industrial Perspective, *Macromol. Chem. Phys.*, 2020, **221**. DOI: 10.1002/macp.202000114.
- 173 E. M. Aizenshtein, Polyester Fibres: Today and Tomorrow, *Fibre Chem.*, 2017, **49**, 288–293.
- 174 Statista Research Department, Polyester fiber production globally 1975-2022, <https://www.statista.com/statistics/912301/polyester-fiber-production-worldwide/>, (accessed 15 January 2024).
- 175 M. Rabnawaz, I. Wyman, R. Auras and S. Cheng, A roadmap towards green packaging: the current status and future outlook for polyesters in the packaging industry, *Green Chem.*, 2017, **19**, 4737–4753.
- 176 H. C. Lim, in *Brydson's Plastics Materials*, Elsevier, 2017, pp. 527–543.
- 177 H. R. Kricheldorf, Star shaped and hyperbranched aromatic polyesters, *Pure Appl. Chem.*, 1998, **70**, 1235–1238.
- 178 S. Nummelin, M. Skrifvars and K. Rissanen, in *Dendrimers*, ed. A. de Meijere, H. Kessler, S. V. Ley, J. Thiem, F. Vögtle, K. N. Houk, J.-M. Lehn, S. L. Schreiber, B. M. Trost and H. Yamamoto, Springer, Berlin, 2000, pp. 1–67.
- 179 W. H. Carothers and J. A. Arvin, Studies on polymerization and ring formation. II. Poly-esters, *J. Am. Chem. Soc.*, 1929, **51**, 2560–2570.
- 180 U. Edlund and A.-C. Albertsson, Polyesters based on diacid monomers, *Adv. Drug Deliv. Rev.*, 2003, **55**, 585–609.
- 181 M. Jaffe, A. J. Easts and X. Feng, in *Thermal Analysis of Textiles and Fibers*, Elsevier, 2020, pp. 133–149.
- 182 S. K. Gupta and A. Kumar, in *Reaction engineering of step growth polymerization*, ed. S. K. Gupta and A. Kumar, Springer US, Boston, MA, 1987, pp. 241–318.
- 183 K. Ravindranath and R. A. Mashelkar, Polyethylene terephthalate - I. Chemistry, thermodynamics and transport properties, *Chem. Eng. Sci.*, 1986, **41**, 2197–2214.

- 184 O. Olabisi and K. Adewale, *Handbook of Thermoplastics*, CRC Press, Taylor & Francis Group, Boca Raton, 2016.
- 185 W. H. Faveere, S. van Praet, B. Vermeeren, K. N. R. Dumoleijn, K. Moonen, E. Taarning and B. F. Sels, Toward Replacing Ethylene Oxide in a Sustainable World: Glycolaldehyde as a Bio-Based C2 Platform Molecule, *Angew. Chem. Int. Ed.*, 2021, **60**, 12204–12223.
- 186 J. Sun and H. Liu, Selective hydrogenolysis of biomass-derived xylitol to ethylene glycol and propylene glycol on supported Ru catalysts, *Green Chem.*, 2011, **13**, 135–142.
- 187 B. Blanc, A. Bourrel, P. Gallezot, T. Haas and P. Taylor, Starch-derived polyols for polymer technologies: preparation by hydrogenolysis on metal catalysts, *Green Chem.*, 2000, **2**, 89–91.
- 188 M. Volanti, D. Cespi, F. Passarini, E. Neri, F. Cavani, P. Mizsey and D. Fozer, Terephthalic acid from renewable sources: early-stage sustainability analysis of a bio-PET precursor, *Green Chem.*, 2019, **21**, 885–896.
- 189 R.-J. van Putten, J. C. van der Waal, E. de Jong, C. B. Rasrendra, H. J. Heeres and J. G. de Vries, Hydroxymethylfurfural, a versatile platform chemical made from renewable resources, *Chem. Rev.*, 2013, **113**, 1499–1597.
- 190 M. Sajid, X. Zhao and D. Liu, Production of 2,5-furandicarboxylic acid (FDCA) from 5-hydroxymethylfurfural (HMF): recent progress focusing on the chemical-catalytic routes, *Green Chem.*, 2018, **20**, 5427–5453.
- 191 X. Kong, H. Qi and J. M. Curtis, Synthesis and characterization of high-molecular weight aliphatic polyesters from monomers derived from renewable resources, *J. Appl. Polym. Sci.*, 2014, **131**. DOI: 10.1002/app.40579.
- 192 L. Aliotta, M. Seggiani, A. Lazzeri, V. Gigante and P. Cinelli, A Brief Review of Poly (Butylene Succinate) (PBS) and Its Main Copolymers: Synthesis, Blends, Composites, Biodegradability, and Applications, *Polymers*, 2022, **14**. DOI: 10.3390/polym14040844.
- 193 M. S. Nikolic and J. Djonlagic, Synthesis and characterization of biodegradable poly(butylene succinate-co-butylene adipate)s, *Polym. Degrad. Stab.*, 2001, **74**, 263–270.

- 194 X. Dai and Z. Qiu, Synthesis and properties of novel biodegradable poly(butylene succinate-co-decamethylene succinate) copolyesters from renewable resources, *Polym. Degrad. Stab.*, 2016, **134**, 305–310.
- 195 C. Jérôme and P. Lecomte, Recent advances in the synthesis of aliphatic polyesters by ring-opening polymerization, *Adv. Drug Deliv. Rev.*, 2008, **60**, 1056–1076.
- 196 D. Mecerreyes and R. Jérôme, From living to controlled aluminium alkoxide mediated ring-opening polymerization of (di)lactones, a powerful tool for the macromolecular engineering of aliphatic polyesters, *Macromol. Chem. Phys.*, 1999, **200**, 2581–2590.
- 197 A. Löfgren, A.-C. Albertsson, P. Dubois and R. Jérôme, Recent Advances in Ring-Opening Polymerization of Lactones and Related Compounds, *J. Macromol. Sci. C*, 1995, **35**, 379–418.
- 198 G. L. Brode and J. V. Koleske, Lactone Polymerization and Polymer Properties, *J. Macromol. Sci. A*, 1972, **6**, 1109–1144.
- 199 K. M. Stridsberg, M. Ryner and A. C. Albertsson, in *Degradable Aliphatic Polyesters*, ed. A. Abe, Springer Berlin Heidelberg, Berlin, Heidelberg, 2002.
- 200 W. H. Carothers, Polymerization, *Chem. Rev.*, 1931, **8**, 353–426.
- 201 A. Duda and S. Penczek, Thermodynamics of L-Lactide Polymerization. Equilibrium Monomer Concentration, *Macromolecules*, 1990, **23**, 1636–1639.
- 202 J. Lunt, Large-scale production, properties and commercial applications of polylactic acid polymers, *Polym. Degrad. Stab.*, 1998, **59**, 145–152.
- 203 J. Lunt and A. L. Shafer, Polylactic Acid Polymers from Corn. Applications in the Textiles Industry, *J. Ind. Text.*, 2000, **29**, 191–205.
- 204 D. Da Silva, M. Kaduri, M. Poley, O. Adir, N. Krinsky, J. Shainsky-Roitman and A. Schroeder, Biocompatibility, biodegradation and excretion of polylactic acid (PLA) in medical implants and theranostic systems, *Chem. Eng. J.*, 2018, **340**, 9–14.
- 205 B. Gupta, N. Revagade and J. Hilborn, Poly(lactic acid) fiber: An overview, *Prog. Polym. Sci.*, 2007, **32**, 455–482.
- 206 R. G. Sinclair, The Case for Polylactic Acid as a Commodity Packaging Plastic, *J. Macromol. Sci. A: Pure Appl. Chem.*, 1996, **33**, 585–597.

- 207 H. R. Kricheldorf and I. Kreiser-Saunders, Poly lactides - Synthesis, Characterization and Medical Application, *Macromol. Symp.*, 1996, **103**, 85–102.
- 208 H. R. Kricheldorf, M. Ber and N. Scharnagl, Poly(lactones). 9. Polymerization Mechanism of Metal Alkoxide Initiated Polymerizations of Lactide and Various Lactones, *Macromolecules*, 1988, **21**, 281–546.
- 209 H. R. Kricheldorf, S.-R. Lee and S. Bush, Polylactones 36. Macrocyclic Polymerization of Lactides with Cyclic Bu<sub>2</sub>Sn Initiators Derived from 1,2-Ethanediol, 2-Mercaptoethanol, and 1,2-Dimercaptoethane, *Macromolecules*, 1996, **29**, 1375–1856.
- 210 T. Tábi, A. F. Wacha and S. Hajba, Effect of D-lactide content of annealed poly(lactic acid) on its thermal, mechanical, heat deflection temperature, and creep properties, *J. Appl. Polym. Sci.*, 2019, **136**. DOI: 10.1002/app.47103.
- 211 Y. Ikada and H. Tsuji, Biodegradable polyesters for medical and ecological applications, *Macromol. Rapid Commun.*, 2000, **21**, 117–132.
- 212 M. Labet and W. Thielemans, Synthesis of polycaprolactone: a review, *Chem. Soc. Rev.*, 2009, **38**, 3484–3504.
- 213 Y. Shibasaki, H. Sanada, M. Yokoi, F. Sanda and T. Endo, Activated Monomer Cationic Polymerization of Lactones and the Application to Well-Defined Block Copolymer Synthesis with Seven-Membered Cyclic Carbonate, *Macromolecules*, 2000, **33**, 4316–4320.
- 214 P. J. A. In't Veld, E. M. Velner, P. van de Witte, J. Hamhuis, P. J. Dijkstra and J. Feijen, Melt block copolymerization of  $\epsilon$ -caprolactone and L-lactide, *J. Polym. Sci. A Polym. Chem.*, 1997, **35**, 219–226.
- 215 G. Rafler and J. Dahlmann, Biodegradable polymers. 6th comm. Polymerization of  $\epsilon$ -caprolactone, *Acta Polym.*, 1992, **43**, 91–95.
- 216 A. Kowalski, A. Duda and S. Penczek, Mechanism of Cyclic Ester Polymerization Initiated with Tin(II) Octoate. 2. Macromolecules Fitted with Tin(II) Alkoxide Species Observed Directly in MALDI–TOF Spectra, *Macromolecules*, 2000, **33**, 689–695.
- 217 A. Kowalski, A. Duda and S. Penczek, Kinetics and mechanism of cyclic esters polymerization initiated with tin(II) octoate, 1. Polymerization of  $\epsilon$ -caprolactone, *Macromol. Rapid Commun.*, 1998, **19**, 567–572.

- 218 N. Nomura, A. Taira, T. Tomioka and M. Okada, A Catalytic Approach for Cationic Living Polymerization: Sc(OTf)<sub>3</sub>-Catalyzed Ring-Opening Polymerization of Lactones, *Macromolecules*, 2000, **33**, 1497–1499.
- 219 M. Möller, R. Kånge and J. L. Hedrick, Sn(OTf)<sub>2</sub> and Sc(OTf)<sub>3</sub>: Efficient and versatile catalysts for the controlled polymerization of lactones, *J. Polym. Sci. A Polym. Chem.*, 2000, **38**, 2067–2074.
- 220 P. Dubois, N. Ropson, R. Jérôme and P. Teyssié, Macromolecular Engineering of Polylactones and Polylactides. 19. Kinetics of Ring-Opening Polymerization of  $\epsilon$ -Caprolactone Initiated with Functional Aluminum Alkoxides, *Macromolecules*, 1996, **29**, 1965–1975.
- 221 S. Kobayashi, Enzymatic polymerization: A new method of polymer synthesis, *J. Polym. Sci. A Polym. Chem.*, 1999, **37**, 3041–3056.
- 222 N. E. Kamber, W. Jeong, R. M. Waymouth, R. C. Pratt, B. G. G. Lohmeijer and J. L. Hedrick, Organocatalytic Ring-Opening Polymerization, *Chemical reviews*, 2007, **107**, 5813–5840.
- 223 M. K. Kiesewetter, E. J. Shin, J. L. Hedrick and R. M. Waymouth, Organocatalysis: Opportunities and Challenges for Polymer Synthesis, *Macromolecules*, 2010, **43**, 2093–2107.
- 224 C. Thomas and B. Bibal, Hydrogen-bonding organocatalysts for ring-opening polymerization, *Green Chem.*, 2014, **16**, 1687–1699.
- 225 S. Paul, Y. Zhu, C. Romain, R. Brooks, P. K. Saini and C. K. Williams, Ring-opening copolymerization (ROCOP): synthesis and properties of polyesters and polycarbonates, *Chem. Commun.*, 2015, **51**, 6459–6479.
- 226 R. C. Jeske, A. M. DiCiccio and G. W. Coates, Alternating copolymerization of epoxides and cyclic anhydrides: an improved route to aliphatic polyesters, *J. Am. Chem. Soc.*, 2007, **129**, 11330–11331.
- 227 J. M. Longo, M. J. Sanford and G. W. Coates, Ring-Opening Copolymerization of Epoxides and Cyclic Anhydrides with Discrete Metal Complexes: Structure-Property Relationships, *Chem. Rev.*, 2016, **116**, 15167–15197.
- 228 E. Hosseini Nejad, A. Paoniasari, C. E. Koning and R. Duchateau, Semi-aromatic polyesters by alternating ring-opening copolymerisation of styrene oxide and anhydrides, *Polym. Chem.*, 2012, **3**, 1308.

- 229 A. Larrañaga and E. Lizundia, A review on the thermomechanical properties and biodegradation behaviour of polyesters, *Eur. Polym. J.*, 2019, **121**, 109296.
- 230 S. Saeidlou, M. A. Huneault, H. Li and C. B. Park, Poly(lactic acid) crystallization, *Prog. Polym. Sci.*, 2012, **37**, 1657–1677.
- 231 H. Nishida and Y. Tokiwa, Distribution of Poly( $\beta$ -hydroxybutyrate) and Poly( $\epsilon$ -caprolactone) Aerobic Degrading Microorganisms in Different Environments, *J. Environ. Polym. Degrad.*, 1993, **1**, 227–233.
- 232 Y. Tokiwa and T. Suzuki, Hydrolysis of polyesters by lipases, *Nature*, 1977, **270**, 76–78.
- 233 R. Tong, New Chemistry in Functional Aliphatic Polyesters, *Ind. Eng. Chem. Res.*, 2017, **56**, 4207–4219.
- 234 K. Sudesh, H. Abe and Y. Doi, Synthesis, structure and properties of polyhydroxyalkanoates: biological polyesters, *Prog. Polym. Sci.*, 2000, **25**, 1503–1555.
- 235 P. C. Sabapathy, S. Devaraj, K. Meixner, P. Anburajan, P. Kathirvel, Y. Ravikumar, H. M. Zayed and X. Qi, Recent developments in Polyhydroxyalkanoates (PHAs) production - A review, *Bioresour. Technol.*, 2020, **306**, 123132.
- 236 F. Awaja and D. Pavel, Recycling of PET, *Eur. Polym. J.*, 2005, **41**, 1453–1477.
- 237 D. E. Nikles and M. S. Farahat, New Motivation for the Depolymerization Products Derived from Poly(Ethylene Terephthalate) (PET) Waste: a Review, *Macromol. Mater. Eng.*, 2005, **290**, 13–30.
- 238 M. Häußler, M. Eck, D. Rothauer and S. Mecking, Closed-loop recycling of polyethylene-like materials, *Nature*, 2021, **590**, 423–427.
- 239 F. Stempfle, P. Ortmann and S. Mecking, Long-Chain Aliphatic Polymers To Bridge the Gap between Semicrystalline Polyolefins and Traditional Polycondensates, *Chem. Rev.*, 2016, **116**, 4597–4641.
- 240 A. Pellis, E. Herrero Acero, L. Gardossi, V. Ferrario and G. M. Guebitz, Renewable building blocks for sustainable polyesters: new biotechnological routes for greener plastics, *Polym. Int.*, 2016, **65**, 861–871.

- 241 Q. Zhang, M. Song, Y. Xu, W. Wang, Z. Wang and L. Zhang, Bio-based polyesters: Recent progress and future prospects, *Prog. Polym. Sci.*, 2021, **120**, 101430.
- 242 C. Vilela, A. F. Sousa, A. C. Fonseca, A. C. Serra, J. F. J. Coelho, C. S. R. Freire and A. J. D. Silvestre, The quest for sustainable polyesters – insights into the future, *Polym. Chem.*, 2014, **5**, 3119–3141.
- 243 J.-P. Pascault and R. J. J. Williams, in *Handbook of Polymer Synthesis, Characterization, and Processing*, ed. E. Saldívar-Guerra and E. Vivaldo-Lima, Wiley, 2013, pp. 519–533.
- 244 R. L. Quirino, K. Monroe, C. H. Fleischer, E. Biswas and M. R. Kessler, Thermosetting polymers from renewable sources, *Polym. Int.*, 2021, **70**, 167–180.
- 245 E. Morici and N. T. Dintcheva, Recycling of Thermoset Materials and Thermoset-Based Composites: Challenge and Opportunity, *Polymers*, 2022, **14**. DOI: 10.3390/polym14194153.
- 246 K. Saito, T. Türel, F. Eisenreich and Ž. Tomović, Closed-Loop Recyclable Poly(imine-acetal)s with Dual-Cleavable Bonds for Primary Building Block Recovery, *ChemSusChem*, 2023, **16**, e202301017.
- 247 C. J. Kloxin and C. N. Bowman, Covalent adaptable networks: smart, reconfigurable and responsive network systems, *Chem. Soc. Rev.*, 2013, **42**, 7161–7173.
- 248 C. J. Kloxin, T. F. Scott, B. J. Adzima and C. N. Bowman, Covalent Adaptable Networks (CANs): A Unique Paradigm in Crosslinked Polymers, *Macromolecules*, 2010, **43**, 2643–2653.
- 249 W. Alabiso and S. Schlögl, The Impact of Vitrimers on the Industry of the Future: Chemistry, Properties and Sustainable Forward-Looking Applications, *Polymers*, 2020, **12**. DOI: 10.3390/polym12081660.
- 250 P. Chakma and D. Konkolewicz, Dynamic Covalent Bonds in Polymeric Materials, *Angew. Chem. Int. Ed.*, 2019, **58**, 9682–9695.
- 251 K. Yu, P. Taynton, W. Zhang, M. L. Dunn and H. J. Qi, Reprocessing and recycling of thermosetting polymers based on bond exchange reactions, *RSC Adv.*, 2014, **4**, 10108–10117.



- 252 R. H. Aguirresarobe, S. Nevejans, B. Reck, L. Irusta, H. Sardon, J. M. Asua and N. Ballard, Healable and self-healing polyurethanes using dynamic chemistry, *Prog. Polym. Sci.*, 2021, **114**, 101362.
- 253 R. J. Wojtecki, M. A. Meador and S. J. Rowan, Using the dynamic bond to access macroscopically responsive structurally dynamic polymers, *Nat. Mater.*, 2011, **10**, 14–27.
- 254 F. Magliozzi, A. Scali, G. Chollet, D. Montarnal, E. Grau and H. Cramail, Hydrolyzable Biobased Polyhydroxyurethane Networks with Shape Memory Behavior at Body Temperature, *ACS Sustainable Chem. Eng.*, 2020, **8**, 9125–9135.
- 255 M. Guerre, C. Taplan, J. M. Winne and F. E. Du Prez, Vitrimers: directing chemical reactivity to control material properties, *Chem. Sci.*, 2020, **11**, 4855–4870.
- 256 W. Denissen, J. M. Winne and F. E. Du Prez, Vitrimers: permanent organic networks with glass-like fluidity, *Chem. Sci.*, 2016, **7**, 30–38.
- 257 N. J. Van Zee and R. Nicolaÿ, Vitrimers: Permanently crosslinked polymers with dynamic network topology, *Prog. Polym. Sci.*, 2020, **104**, 101233.
- 258 M. Capelot, M. M. Unterlass, F. Tournilhac and L. Leibler, Catalytic Control of the Vitrimer Glass Transition, *ACS Macro Lett.*, 2012, **1**, 789–792.
- 259 C. Bowman, F. Du Prez and J. Kalow, Introduction to chemistry for covalent adaptable networks, *Polym. Chem.*, 2020, **11**, 5295–5296.
- 260 F. I. Altuna, C. E. Hoppe and R. J. J. Williams, Epoxy Vitrimers: The Effect of Transesterification Reactions on the Network Structure, *Polymers*, 2018, **10**. DOI: 10.3390/polym10010043.
- 261 D. Montarnal, M. Capelot, F. Tournilhac and L. Leibler, Silica-Like Malleable Materials from Permanent Organic Networks, *Science*, 2011, **334**, 965–968.
- 262 J. P. Brutman, P. A. Delgado and M. A. Hillmyer, Polylactide Vitrimers, *ACS Macro Lett.*, 2014, **3**, 607–610.
- 263 Y. Yang, S. Zhang, X. Zhang, L. Gao, Y. Wei and Y. Ji, Detecting topology freezing transition temperature of vitrimers by AIE luminogens, *Nat. Commun.*, 2019, **10**, 3165.

- 264 Q. Shi, K. Yu, X. Kuang, X. Mu, C. K. Dunn, M. L. Dunn, T. Wang and H. Jerry Qi, Recyclable 3D printing of vitrimer epoxy, *Mater. Horiz.*, 2017, **4**, 598–607.
- 265 Y. Yang, Z. Pei, X. Zhang, L. Tao, Y. Wei and Y. Ji, Carbon nanotube–vitrimer composite for facile and efficient photo-welding of epoxy, *Chem. Sci.*, 2014, **5**, 3486–3492.
- 266 M. Ciaccia and S. Di Stefano, Mechanisms of imine exchange reactions in organic solvents, *Org. Biomol. Chem.*, 2015, **13**, 646–654.
- 267 M. E. Belowich and J. F. Stoddart, Dynamic imine chemistry, *Chem. Soc. Rev.*, 2012, **41**, 2003–2024.
- 268 A. Chao, I. Negulescu and D. Zhang, Dynamic Covalent Polymer Networks Based on Degenerative Imine Bond Exchange: Tuning the Malleability and Self-Healing Properties by Solvent, *Macromolecules*, 2016, **49**, 6277–6284.
- 269 S. Zhao and M. M. Abu-Omar, Recyclable and Malleable Epoxy Thermoset Bearing Aromatic Imine Bonds, *Macromolecules*, 2018, **51**, 9816–9824.
- 270 C. Bakkali-Hassani, D. Berne, V. Ladmiraal and S. Caillol, Transcarbamoylation in Polyurethanes: Underestimated Exchange Reactions?, *Macromolecules*, 2022, **55**, 7974–7991.
- 271 D. J. Fortman, J. P. Brutman, C. J. Cramer, M. A. Hillmyer and W. R. Dichtel, Mechanically activated, catalyst-free polyhydroxyurethane vitrimers, *J. Am. Chem. Soc.*, 2015, **137**, 14019–14022.
- 272 S. Hu, X. Chen and J. M. Torkelson, Biobased Reprocessable Polyhydroxyurethane Networks: Full Recovery of Crosslink Density with Three Concurrent Dynamic Chemistries, *ACS Sustainable Chem. Eng.*, 2019, **7**, 10025–10034.
- 273 C. Pronoitis, M. Hakkarainen and K. Odelius, Structurally Diverse and Recyclable Isocyanate-Free Polyurethane Networks from CO<sub>2</sub>-Derived Cyclic Carbonates, *ACS Sustainable Chem. Eng.*, 2022, **10**, 2522–2531.
- 274 S. K. Raut, P. K. Behera, T. S. Pal, P. Mondal, K. Naskar and N. K. Singha, Self-healable hydrophobic polymer material having urethane linkages via a non-isocyanate route and dynamic Diels-Alder 'click' reaction, *Chem. Commun.*, 2021, **57**, 1149–1152.

- 275 V. Scholiers, B. Hendriks, S. Maes, T. Debsharma, J. M. Winne and F. E. Du Prez, Trialkylsulfonium-Based Reprocessable Polyurethane Thermosets, *Macromolecules*, 2023. DOI: 10.1021/acs.macromol.3c01270.
- 276 N. van Herck and F. E. Du Prez, Fast Healing of Polyurethane Thermosets Using Reversible Triazolinedione Chemistry and Shape-Memory, *Macromolecules*, 2018, **51**, 3405–3414.
- 277 P. Wu, H. Cheng, X. Wang, R. Shi, C. Zhang, M. Arai and F. Zhao, A self-healing and recyclable polyurethane-urea Diels–Alder adduct synthesized from carbon dioxide and furfuryl amine, *Green Chem.*, 2021, **23**, 552–560.
- 278 H. Otsuka, S. Nagano, Y. Kobashi, T. Maeda and A. Takahara, A dynamic covalent polymer driven by disulfide metathesis under photoirradiation, *Chem. Commun.*, 2010, **46**, 1150–1152.
- 279 S. P. Black, J. K. M. Sanders and A. R. Stefankiewicz, Disulfide exchange: exposing supramolecular reactivity through dynamic covalent chemistry, *Chem. Soc. Rev.*, 2014, **43**, 1861–1872.
- 280 D. J. Fortman, R. L. Snyder, D. T. Sheppard and W. R. Dichtel, Rapidly Reprocessable Cross-Linked Polyhydroxyurethanes Based on Disulfide Exchange, *ACS Macro Lett.*, 2018, **7**, 1226–1231.
- 281 A. Rekondo, R. Martin, A. Ruiz de Luzuriaga, G. Cabañero, H. J. Grande and I. Odriozola, Catalyst-free room-temperature self-healing elastomers based on aromatic disulfide metathesis, *Mater. Horiz.*, 2014, **1**, 237–240.
- 282 J. Canadell, H. Goossens and B. Klumperman, Self-Healing Materials Based on Disulfide Links, *Macromolecules*, 2011, **44**, 2536–2541.
- 283 Q. Li, S. Ma, S. Wang, W. Yuan, X. Xu, B. Wang, K. Huang and J. Zhu, Facile catalyst-free synthesis, exchanging, and hydrolysis of an acetal motif for dynamic covalent networks, *J. Mater. Chem. A*, 2019, **7**, 18039–18049.
- 284 B. Wang, S. Ma, Q. Li, H. Zhang, J. Liu, R. Wang, Z. Chen, X. Xu, S. Wang, N. Lu, Y. Liu, S. Yan and J. Zhu, Facile synthesis of “digestible”, rigid-and-flexible, bio-based building block for high-performance degradable thermosetting plastics, *Green Chem.*, 2020, **22**, 1275–1290.
- 285 Y. Xu, S. Dai, H. Zhang, L. Bi, J. Jiang and Y. Chen, Reprocessable, Self-Adhesive, and Recyclable Carbon Fiber-Reinforced Composites Using a Catalyst-Free Self-Healing Bio-Based Vitrimer Matrix, *ACS Sustainable Chem. Eng.*, 2021, **9**, 16281–16290.

- 286 C. Hao, T. Liu, S. Zhang, W. Liu, Y. Shan and J. Zhang, Triethanolamine-Mediated Covalent Adaptable Epoxy Network: Excellent Mechanical Properties, Fast Repairing, and Easy Recycling, *Macromolecules*, 2020, **53**, 3110–3118.
- 287 J. L. Self, N. D. Dolinski, M. S. Zayas, J. Read de Alaniz and C. M. Bates, Brønsted-Acid-Catalyzed Exchange in Polyester Dynamic Covalent Networks, *ACS Macro Lett.*, 2018, **7**, 817–821.
- 288 G. Rizzo, L. Saitta, S. Dattilo, C. Tosto, E. Pergolizzi, A. Ivankovic and G. Cicala, Thermomechanical Characterization of an Unsaturated Polyester Vitriimer Synthesized Using a Titanium Transesterification Catalyst, *ACS Appl. Polym. Mater.*, 2023, **5**, 8326–8338.
- 289 M. Capelot, D. Montarnal, F. Tournilhac and L. Leibler, Metal-Catalyzed Transesterification for Healing and Assembling of Thermosets, *J. Am. Chem. Soc.*, 2012, **134**, 7664–7667.
- 290 C. Bakkali-Hassani, D. Berne, P. Bron, L. Irusta, H. Sardon, V. Ladmiral and S. Caillol, Polyhydroxyurethane covalent adaptable networks: looking for suitable catalysts, *Polym. Chem.*, 2023, **14**, 3610–3620.
- 291 F. van Lijsebetten, J. O. Holloway, J. M. Winne and F. E. Du Prez, Internal catalysis for dynamic covalent chemistry applications and polymer science, *Chem. Soc. Rev.*, 2020, **49**, 8425–8438.
- 292 L. L. Robinson, E. S. Taddese, J. L. Self, C. M. Bates, J. Read de Alaniz, Z. Geng and C. J. Hawker, Neighboring Group Participation in Ionic Covalent Adaptable Networks, *Macromolecules*, 2022, **55**, 9780–9789.
- 293 X. Chen, M. A. Dam, K. Ono, A. Mal, H. Shen, S. R. Nutt, K. Sheran and F. Wudl, A Thermally Re-mendable Cross-Linked Polymeric Material, *Science*, 2002, **295**, 1698–1702.
- 294 Y.-L. Liu and T.-W. Chuo, Self-healing polymers based on thermally reversible Diels–Alder chemistry, *Polym. Chem.*, 2013, **4**, 2194.
- 295 B. T. Worrell, S. Mavila, C. Wang, T. M. Kontour, C.-H. Lim, M. K. McBride, C. B. Musgrave, R. Shoemaker and C. N. Bowman, A user's guide to the thiol-thioester exchange in organic media: scope, limitations, and applications in material science, *Polym. Chem.*, 2018, **9**, 4523–4534.

- 296 W. Denissen, G. Rivero, R. Nicolaÿ, L. Leibler, J. M. Winne and F. E. Du Prez, Vinylogous Urethane Vitrimers, *Adv. Funct. Mater.*, 2015, **25**, 2451–2457.
- 297 S. Engelen, A. A. Wróblewska, K. de Bruycker, R. Aksakal, V. Ladmiral, S. Caillol and F. E. Du Prez, Sustainable design of vanillin-based vitrimers using vinylogous urethane chemistry, *Polym. Chem.*, 2022, **13**, 2665–2673.
- 298 W. Denissen, I. de Baere, W. van Paepegem, L. Leibler, J. Winne and F. E. Du Prez, Vinylogous Urea Vitrimers and Their Application in Fiber Reinforced Composites, *Macromolecules*, 2018, **51**, 2054–2064.
- 299 O. R. Cromwell, J. Chung and Z. Guan, Malleable and Self-Healing Covalent Polymer Networks through Tunable Dynamic Boronic Ester Bonds, *J. Am. Chem. Soc.*, 2015, **137**, 6492–6495.
- 300 M. Röttger, T. Domenech, R. van der Weegen, A. Breuillac, R. Nicolaÿ and L. Leibler, High-performance vitrimers from commodity thermoplastics through dioxaborolane metathesis, *Science*, 2017, **356**, 62–65.
- 301 B. Hendriks, J. Waelkens, J. M. Winne and F. E. Du Prez, Poly(thioether) Vitrimers via Transalkylation of Trialkylsulfonium Salts, *ACS Macro Lett.*, 2017, **6**, 930–934.
- 302 S. Billiet, K. de Bruycker, F. Driessen, H. Goossens, V. van Speybroeck, J. M. Winne and F. E. Du Prez, Triazolinediones enable ultrafast and reversible click chemistry for the design of dynamic polymer systems, *Nat. Chem.*, 2014, **6**, 815–821.
- 303 F. van Lijsebetten, T. Debsharma, J. M. Winne and F. E. Du Prez, A Highly Dynamic Covalent Polymer Network without Creep: Mission Impossible?, *Angew. Chem. Int. Ed.*, 2022, **61**, e202210405.
- 304 X.-L. Zhao, P.-X. Tian, Y.-D. Li and J.-B. Zeng, Biobased covalent adaptable networks: towards better sustainability of thermosets, *Green Chem.*, 2022, **24**, 4363–4387.
- 305 A. Corma, S. Iborra and A. Velty, Chemical routes for the transformation of biomass into chemicals, *Chem. Rev.*, 2007, **107**, 2411–2502.
- 306 C. Williams and M. Hillmyer, Polymers from Renewable Resources: A Perspective for a Special Issue of Polymer Reviews, *Polym. Rev.*, 2008, **48**, 1–10.

- 307 A. Gandini and T. M. Lacerda, From monomers to polymers from renewable resources: Recent advances, *Prog. Polym. Sci.*, 2015, **48**, 1–39.
- 308 P. F. H. Harmsen, M. M. Hackmann and H. L. Bos, Green building blocks for bio-based plastics, *Biofuel. Bioprod. Bioref.*, 2014, **8**, 306–324.
- 309 Y. Zhu, C. Romain and C. K. Williams, Sustainable polymers from renewable resources, *Nature*, 2016, **540**, 354–362.
- 310 T. Vidil and A. Llevot, Fully Biobased Vitrimers: Future Direction toward Sustainable Cross-Linked Polymers, *Macromol. Chem. Phys.*, 2022, **223**, 2100494.
- 311 R. Mülhaupt, Green Polymer Chemistry and Bio-based Plastics: Dreams and Reality, *Macromol. Chem. Phys.*, 2013, **214**, 159–174.
- 312 P. Gabrielli, M. Gazzani and M. Mazzotti, The Role of Carbon Capture and Utilization, Carbon Capture and Storage, and Biomass to Enable a Net-Zero-CO<sub>2</sub> Emissions Chemical Industry, *Ind. Eng. Chem. Res.*, 2020, **59**, 7033–7045.
- 313 J. M. Dyer, S. Stymne, A. G. Green and A. S. Carlsson, High-value oils from plants, *Plant J.*, 2008, **54**, 640–655.
- 314 U. Biermann, U. T. Bornscheuer, I. Feussner, M. A. R. Meier and J. O. Metzger, Fatty Acids and their Derivatives as Renewable Platform Molecules for the Chemical Industry, *Angew. Chem. Int. Ed.*, 2021, **60**, 20144–20165.
- 315 U. Biermann, W. Friedt, S. Lang, W. Lühs, G. Machmüller, J. O. Metzger, M. Rüscher, H. J. Schäfer and M. P. Schneider, New Syntheses with Oils and Fats as Renewable Raw Materials for the Chemical Industry, *Angew. Chem. Int. Ed.*, 2000, **39**, 2206–2224.
- 316 S. De, S. Malik, A. Ghosh, R. Saha and B. Saha, A review on natural surfactants, *RSC Adv.*, 2015, **5**, 65757–65767.
- 317 N. Poljšak and N. Kočevar Glavač, Vegetable Butters and Oils as Therapeutically and Cosmetically Active Ingredients for Dermal Use: A Review of Clinical Studies, *Front. Pharmacol.*, 2022, **13**, 868461.
- 318 E. Sharmin, F. Zafar, D. Akram, M. Alam and S. Ahmad, Recent advances in vegetable oils based environment friendly coatings: A review, *Ind. Crops. Prod.*, 2015, **76**, 215–229.

- 319 C. Murru, R. Badía-Laíño and M. E. Díaz-García, Oxidative Stability of Vegetable Oil-Based Lubricants, *ACS Sustainable Chem. Eng.*, 2021, **9**, 1459–1476.
- 320 M. A. R. Meier, Plant-Oil-Based Polyamides and Polyurethanes: Toward Sustainable Nitrogen-Containing Thermoplastic Materials, *Macromol. Rapid Commun.*, 2019, **40**, e1800524.
- 321 A. S. Belousov, A. L. Esipovich, E. A. Kanakov and K. V. Otopkova, Recent advances in sustainable production and catalytic transformations of fatty acid methyl esters, *Sustain. Energy Fuels*, 2021, **5**, 4512–4545.
- 322 G. Lewandowski, M. Musik, K. Malarczyk-Matusiak, Ł. Sałaciński and E. Milchert, Epoxidation of Vegetable Oils, Unsaturated Fatty Acids and Fatty Acid Esters: A Review, *Mini Rev. Org. Chem.*, 2020, **17**, 412–422.
- 323 H. Baumann, M. Bühler, H. Fochem, F. Hirsinger, H. Zoebelein and J. Falbe, Natürliche Fette und Öle - nachwachsende Rohstoffe für die chemische Industrie, *Angew. Chem.*, 1988, **100**, 41–62.
- 324 H. Mutlu and M. A. R. Meier, Castor oil as a renewable resource for the chemical industry, *Eur. J. Lipid Sci. Technol.*, 2010, **112**, 10–30.
- 325 F. C. Naughton, Production, chemistry, and commercial applications of various chemicals from castor oil, *J. Am. Oil Chem. Soc.*, 1974, **51**, 65–71.
- 326 M. Genas, Rilsan (Polyamid 11), Synthese und Eigenschaften, *Angew. Chem.*, 1962, **74**, 535–540.
- 327 O. Türünç and M. A. R. Meier, Fatty Acid Derived Monomers and Related Polymers Via Thiol-ene (Click) Additions, *Macromol. Rapid Commun.*, 2010, **31**, 1822–1826.
- 328 O. Türünç, M. Firdaus, G. Klein and M. A. R. Meier, Fatty acid derived renewable polyamides via thiol-ene additions, *Green Chem.*, 2012, **14**, 2577–2583.
- 329 S. Bigot, M. Daghrir, A. Mhanna, G. Boni, S. Pourchet, L. Lecamp and L. Plasseraud, Undecylenic acid: A tunable bio-based synthon for materials applications, *Eur. Polym. J.*, 2016, **74**, 26–37.
- 330 M. Winkler and M. A. R. Meier, Olefin cross-metathesis as a valuable tool for the preparation of renewable polyesters and polyamides from unsaturated fatty acid esters and carbamates, *Green Chem.*, 2014, **16**, 3335–3340.

- 331 U. Biermann, M. A. R. Meier, W. Butte and J. O. Metzger, Cross-metathesis of unsaturated triglycerides with methyl acrylate: Synthesis of a dimeric metathesis product, *Eur. J. Lipid Sci. Technol.*, 2011, **113**, 39–45.
- 332 M. von Czapiewski, M. Rhein and M. A. R. Meier, Fatty Acid Derived Renewable Platform Chemicals via Selective Oxidation Processes, *ACS Sustainable Chem. Eng.*, 2018, **6**, 15170–15179.
- 333 S. M. Danov, O. A. Kazantsev, A. L. Esipovich, A. S. Belousov, A. E. Rogozhin and E. A. Kanakov, Recent advances in the field of selective epoxidation of vegetable oils and their derivatives: a review and perspective, *Catal. Sci. Technol.*, 2017, **7**, 3659–3675.
- 334 A. Cifarelli, L. Boggioni, A. Vignali, I. Tritto, F. Bertini and S. Losio, Flexible Polyurethane Foams from Epoxidized Vegetable Oils and a Bio-Based Diisocyanate, *Polymers*, 2021, **13**. DOI: 10.3390/polym13040612.
- 335 Z. S. Petrović, Polyurethanes from Vegetable Oils, *Polym. Rev.*, 2008, **48**, 109–155.
- 336 A. Brandolese, F. Della Monica, M. À. Pericàs and A. W. Kleij, Catalytic Ring-Opening Copolymerization of Fatty Acid Epoxides: Access to Functional Biopolyesters, *Macromolecules*, 2022, **55**, 2566–2573.
- 337 S. G. Tan and W. S. Chow, Biobased Epoxidized Vegetable Oils and Its Greener Epoxy Blends: A Review, *Polym. Plast. Technol. Eng.*, 2010, **49**, 1581–1590.
- 338 H. Büttner, J. Steinbauer, C. Wulf, M. Dindaroglu, H.-G. Schmalz and T. Werner, Organocatalyzed Synthesis of Oleochemical Carbonates from CO<sub>2</sub> and Renewables, *ChemSusChem*, 2017, **10**, 1076–1079.
- 339 L. Longwitz, J. Steinbauer, A. Spannenberg and T. Werner, Calcium-Based Catalytic System for the Synthesis of Bio-Derived Cyclic Carbonates under Mild Conditions, *ACS Catal.*, 2018, **8**, 665–672.
- 340 J. Martínez, F. de La Cruz-Martínez, M. Martínez de Sarasa Buchaca, J. Fernández-Baeza, L. F. Sánchez-Barba, M. North, J. A. Castro-Osma and A. Lara-Sánchez, Efficient Synthesis of Cyclic Carbonates from Unsaturated Acids and Carbon Dioxide and their Application in the Synthesis of Biobased Polyurethanes, *ChemPlusChem*, 2021, **86**, 460–468.
- 341 P. Helbling, F. Hermant, M. Petit, T. Tassaing, T. Vidil and H. Cramail, Unveiling the reactivity of epoxides in carbonated epoxidized soybean oil and



- application in the stepwise synthesis of hybrid poly(hydroxyurethane) thermosets, *Polym. Chem.*, 2023, **14**, 500–513.
- 342 L. Poussard, J. Mariage, B. Grignard, C. Detrembleur, C. Jérôme, C. Calberg, B. Heinrichs, J. de Winter, P. Gerbaux, J.-M. Raquez, L. Bonnaud and P. Dubois, Non-Isocyanate Polyurethanes from Carbonated Soybean Oil Using Monomeric or Oligomeric Diamines To Achieve Thermosets or Thermoplastics, *Macromolecules*, 2016, **49**, 2162–2171.
- 343 J. Dong, B. Liu, H. Ding, J. Shi, N. Liu, B. Dai and I. Kim, Bio-based healable non-isocyanate polyurethanes driven by the cooperation of disulfide and hydrogen bonds, *Polym. Chem.*, 2020, **11**, 7524–7532.
- 344 X. Liu, X. Yang, S. Wang, S. Wang, Z. Wang, S. Liu, X. Xu, H. Liu and Z. Song, Fully Bio-Based Polyhydroxyurethanes with a Dynamic Network from a Terpene Derivative and Cyclic Carbonate Functional Soybean Oil, *ACS Sustainable Chem. Eng.*, 2021, **9**, 4175–4184.
- 345 A. S. More, L. Maisonneuve, T. Lebarbé, B. Gadenne, C. Alfos and H. Cramail, Vegetable-based building-blocks for the synthesis of thermoplastic renewable polyurethanes and polyesters, *Eur. J. Lipid Sci. Technol.*, 2013, **115**, 61–75.
- 346 O. Kreye, S. Wald and M. A. R. Meier, Introducing Catalytic Lossen Rearrangements: Sustainable Access to Carbamates and Amines, *Adv. Synth. Catal.*, 2013, **355**, 81–86.
- 347 L. Filippi and M. A. R. Meier, Fully Renewable Non-Isocyanate Polyurethanes via the Lossen Rearrangement, *Macromol. Rapid Commun.*, 2021, **42**, 2000440.
- 348 H. W. Tan, A. R. Abdul Aziz and M. K. Aroua, Glycerol production and its applications as a raw material: A review, *Renew. Sust. Energ. Rev.*, 2013, **27**, 118–127.
- 349 M. Pagliaro, R. Ciriminna, H. Kimura, M. Rossi and C. Della Pina, From glycerol to value-added products, *Angew. Chem. Int. Ed.*, 2007, **46**, 4434–4440.
- 350 M. O. Sonnati, S. Amigoni, E. P. Taffin de Givenchy, T. Darmanin, O. Choulet and F. Guittard, Glycerol carbonate as a versatile building block for tomorrow: synthesis, reactivity, properties and applications, *Green Chem.*, 2013, **15**, 283–306.

- 351 C. Duval, N. Kébir, R. Jauseau and F. Burel, Organocatalytic synthesis of novel renewable non-isocyanate polyhydroxyurethanes, *J. Polym. Sci. A Polym. Chem.*, 2016, **54**, 758–764.
- 352 R. A. Sheldon, Chemicals from renewable biomass: A renaissance in carbohydrate chemistry, *Curr. Opin. Green Sustain. Chem.*, 2018, **14**, 89–95.
- 353 A. Gandini, T. M. Lacerda, A. J. F. Carvalho and E. Trovatti, Progress of Polymers from Renewable Resources: Furans, Vegetable Oils, and Polysaccharides, *Chem. Rev.*, 2016, **116**, 1637–1669.
- 354 D. Klemm, B. Heublein, H.-P. Fink and A. Bohn, Cellulose: fascinating biopolymer and sustainable raw material, *Angew. Chem. Int. Ed.*, 2005, **44**, 3358–3393.
- 355 S. C. Rasmussen, From Parkesine to Celluloid: The Birth of Organic Plastics, *Angew. Chem. Int. Ed.*, 2021, **60**, 8012–8016.
- 356 H. Steinmeier, 3. Acetate manufacturing, process and technology 3.1 Chemistry of cellulose acetylation, *Macromol. Symp.*, 2004, **208**, 49–60.
- 357 B. Tosh, Synthesis and Sustainable Applications of Cellulose Esters and Ethers: A Review, *Int. J. Energy Environ. Eng.*, 2014, **1**, 56–78.
- 358 R. A. Sheldon, The Road to Biorenewables: Carbohydrates to Commodity Chemicals, *ACS Sustainable Chem. Eng.*, 2018, **6**, 4464–4480.
- 359 J. J. Bozell and G. R. Petersen, Technology development for the production of biobased products from biorefinery carbohydrates—the US Department of Energy’s “Top 10” revisited, *Green Chem.*, 2010, **12**, 539.
- 360 G. Z. Papageorgiou, V. Tsanaktis and D. N. Bikiaris, Synthesis of poly(ethylene furandicarboxylate) polyester using monomers derived from renewable resources: thermal behavior comparison with PET and PEN, *Phys. Chem. Chem. Phys.*, 2014, **16**, 7946–7958.
- 361 R. L. Bielecki, in *Plant Carbohydrates I*, ed. F. A. Loewus and W. Tanner, Springer Berlin, Berlin, 2013, pp. 158–192.
- 362 M. M. Mazurek-Budzyńska, G. Rokicki, M. Drzewicz, P. A. Guńka and J. Zachara, Bis(cyclic carbonate) based on d-mannitol, d-sorbitol and di(trimethylolpropane) in the synthesis of non-isocyanate poly(carbonate-urethane)s, *Eur. Polym. J.*, 2016, **84**, 799–811.

- 363 P. Furtwengler and L. Avérous, From D-sorbitol to five-membered bis(cyclo-carbonate) as a platform molecule for the synthesis of different original biobased chemicals and polymers, *Sci. Rep.*, 2018, **8**, 9134.
- 364 S. Schmidt, N. E. Göppert, B. Bruchmann and R. Mülhaupt, Liquid sorbitol ether carbonate as intermediate for rigid and segmented non-isocyanate polyhydroxyurethane thermosets, *Eur. Polym. J.*, 2017, **94**, 136–142.
- 365 S. Schmidt, F. J. Gatti, M. Luitz, B. S. Ritter, B. Bruchmann and R. Mülhaupt, Erythritol Dicarboxylate as Intermediate for Solvent- and Isocyanate-Free Tailoring of Bio-Based Polyhydroxyurethane Thermoplastics and Thermoplastic Elastomers, *Macromolecules*, 2017, **50**, 2296–2303.
- 366 P.-K. Dannecker and M. A. R. Meier, Facile and Sustainable Synthesis of Erythritol bis(carbonate), a Valuable Monomer for Non-Isocyanate Polyurethanes (NIPUs), *Sci. Rep.*, 2019, **9**, 9858.
- 367 X. Guo, X. Fang, S. Fan, J. Gao and Q. Gu, Structure–Property Relationships in Epoxyurethane Polymers Based on Erythritol Dicarboxylate, *Macromol. Chem. Phys.*, 2023, **224**. DOI: 10.1002/macp.202200451.
- 368 V. Salvado, M. Dolatkhani, É. Grau, T. Vidil and H. Cramail, Sequence-Controlled Polyhydroxyurethanes with Tunable Regioregularity Obtained from Sugar-Based Vicinal Bis-cyclic Carbonates, *Macromolecules*, 2022, **55**, 7249–7264.
- 369 L. Ruzicka, The Isoprene Rule and the Biogenesis of Terpenic Compounds, *Experientia*, 1953, **9**, 357–396.
- 370 J. Gershenzon and N. Dudareva, The function of terpene natural products in the natural world, *Nat. Chem. Biol.*, 2007, **3**, 408–414.
- 371 V. Ninkuu, L. Zhang, J. Yan, Z. Fu, T. Yang and H. Zeng, Biochemistry of Terpenes and Recent Advances in Plant Protection, *Int. J. Mol. Sci.*, 2021, **22**. DOI: 10.3390/ijms22115710.
- 372 O. Wallach, Zur Kenntniss der Terpene und ätherischen Oele, 1886.
- 373 K. A. Wojtunik-Kulesza, K. Kasprzak, T. Oniszczyk and A. Oniszczyk, Natural Monoterpenes: Much More than Only a Scent, *Chem. Biodiversity*, 2019, **16**, e1900434.
- 374 E. Breitmaier, *Terpenes. Flavors, fragrances, pharmaca, pheromones*, Wiley-VCH, Weinheim, Germany, 2006.

- 375 A. Da Silva-Santos, A. Antunes, L. D'Avila, H. Bizzo and L. Souza-Santos, The Use of Essential Oils and Terpenics/Terpenoids in Cosmetics and Pefumery, *Perfum. flavor.*, 2005, **30**.
- 376 W. Schwab, C. Fuchs and G.-C. Huang, Transformation of terpenes into fine chemicals, *Eur. J. Lipid Sci. Technol.*, 2013, **115**, 3–8.
- 377 M. Zielińska-Błajet, P. Pietrusiak and J. Feder-Kubis, Selected Monocyclic Monoterpenes and Their Derivatives as Effective Anticancer Therapeutic Agents, *Int. J. Mol. Sci.*, 2021, **22**. DOI: 10.3390/ijms22094763.
- 378 S. A. A. Al-Salihi and F. Alberti, Naturally Occurring Terpenes: A Promising Class of Organic Molecules to Address Influenza Pandemics, *Nat. Prod. Bioprospect.*, 2021, **11**, 405–419.
- 379 R. Mewalal, D. K. Rai, D. Kainer, F. Chen, C. Külheim, G. F. Peter and G. A. Tuskan, Plant-Derived Terpenes: A Feedstock for Specialty Biofuels, *Trends Biotechnol.*, 2017, **35**, 227–240.
- 380 F. Della Monica and A. W. Kleij, From terpenes to sustainable and functional polymers, *Polym. Chem.*, 2020, **11**, 5109–5127.
- 381 P. Sahu, A. K. Bhowmick and G. Kali, Terpene Based Elastomers: Synthesis, Properties, and Applications, *Processes*, 2020, **8**, 553.
- 382 M. R. Thomsett, T. E. Storr, O. R. Monaghan, R. A. Stockman and S. M. Howdle, Progress in the synthesis of sustainable polymers from terpenes and terpenoids, *Green Mater.*, 2016, **4**, 115–134.
- 383 M. Winnacker, in *Advances in Polymer Science*, Springer Berlin Heidelberg, Berlin, Heidelberg, 2022.
- 384 L. Canoira, D. Donoso, D. Bolonio, C. Bumharther and M. Lapuerta, Desulfurized and Hydrogenated Crude Sulfate Turpentine (HCST): A Biofuel Derived from a Waste of the Pulp and Paper Industries, *Energy Fuels*, 2023, **37**, 15843–15854.
- 385 M. Winnacker, Pinenes: Abundant and Renewable Building Blocks for a Variety of Sustainable Polymers, *Angew. Chem. Int. Ed.*, 2018, **57**, 14362–14371.
- 386 G. Paggiola, S. van Stempvoort, J. Bustamante, J. M. V. Barbero, A. J. Hunt and J. H. Clark, Can bio-based chemicals meet demand? Global and regional case-study around citrus waste-derived limonene as a solvent for cleaning applications, *Biofuels. Bioprod. Biorefin.*, 2016, **10**, 686–698.

- 387 M. Pourbafrani, G. Forgács, I. S. Horváth, C. Niklasson and M. J. Taherzadeh, Production of biofuels, limonene and pectin from citrus wastes, *Bioresour. Technol.*, 2010, **101**, 4246–4250.
- 388 C. Ravichandran, P. C. Badgujar, P. Gundev and A. Upadhyay, Review of toxicological assessment of d-limonene, a food and cosmetics additive, *Food Chem. Toxicol.*, 2018, **120**, 668–680.
- 389 C. C. C. R. de Carvalho and M. M. R. Da Fonseca, Carvone: Why and how should one bother to produce this terpene, *Food Chem.*, 2006, **95**, 413–422.
- 390 S. Russo and E. Casazza, in *Polymer Science: A Comprehensive Review*, pp. 331–396.
- 391 M. M. Kleybolte, L. Zainer, J. Y. Liu, P. N. Stockmann and M. Winnacker, (+)-Limonene-Lactam: Synthesis of a Sustainable Monomer for Ring-Opening Polymerization to Novel, Biobased Polyamides, *Macromol. Rapid Commun.*, 2022, **43**, e2200185.
- 392 H. Erdtman and S. Thorén, The Beckmann Rearrangement of Some Terpene Ketone Oximes, *Acta Chem. Scand.*, 1970, **24**, 87–92.
- 393 M. Imoto, H. Sakurai and T. Kono, Optically active polymers. I. Polymerization of 4-methyl-7-isopropyl-2-oxohexamethyleneimine, *J. Polym. Sci.*, 1961, **L**, 467–473.
- 394 H. Zhong and J. Deng, Preparation and Chiral Applications of Optically Active Polyamides, *Macromol. Rapid Commun.*, 2021, **42**, e2100341.
- 395 M. Winnacker, D. H. Lamparelli, C. Capacchione, H. H. Güngör, L. Stieglitz, K. S. Rodewald, M. Schmidt and T. F. Gronauer, Sustainable Polyesteramides and Copolyamides: Insights into the Copolymerization Behavior of Terpene-Based Lactams, *Macromol. Chem. Phys.*, 2020, **221**, 2000110.
- 396 P. N. Stockmann, D. L. Pastoetter, M. Woelbing, C. Falcke, M. Winnacker, H. Strittmatter and V. Sieber, New Bio-Polyamides from Terpenes:  $\alpha$ -Pinene and (+)-3-Carene as Valuable Resources for Lactam Production, *Macromol. Rapid Commun.*, 2019, **40**, 1800903.
- 397 M. Winnacker and J. Sag, Sustainable terpene-based polyamides via anionic polymerization of a pinene-derived lactam, *Chem. Commun.*, 2018, **54**, 841–844.

- 398 M. Winnacker, J. Sag, A. Tischner and B. Rieger, Sustainable, Stereoregular, and Optically Active Polyamides via Cationic Polymerization of  $\epsilon$ -Lactams Derived from the Terpene  $\beta$ -Pinene, *Macromol. Rapid Commun.*, 2017, **38**. DOI: 10.1002/marc.201600787.
- 399 P. N. Stockmann, D. van Opdenbosch, A. Poethig, D. L. Pastoetter, M. Hoehenberger, S. Lessig, J. Raab, M. Woelbing, C. Falcke, M. Winnacker, C. Zollfrank, H. Strittmatter and V. Sieber, Biobased chiral semi-crystalline or amorphous high-performance polyamides and their scalable stereoselective synthesis, *Nat. Commun.*, 2020, **11**, 509.
- 400 M. Winnacker, M. Neumeier, X. Zhang, C. M. Papadakis and B. Rieger, Sustainable Chiral Polyamides with High Melting Temperature via Enhanced Anionic Polymerization of a Menthone-Derived Lactam, *Macromol. Rapid Commun.*, 2016, **37**, 851–857.
- 401 M. Winnacker, S. Vagin, V. Auer and B. Rieger, Synthesis of Novel Sustainable Oligoamides Via Ring-Opening Polymerization of Lactams Based on (-)-Menthone, *Macromol. Chem. Phys.*, 2014, **215**, 1654–1660.
- 402 D. Zhang, M. A. Hillmyer and W. B. Tolman, Catalytic Polymerization of a Cyclic Ester Derived from a "Cool" Natural Precursor, *Biomacromolecules*, 2005, **6**, 2091–2095.
- 403 J. Shin, Y. Lee, W. B. Tolman and M. A. Hillmyer, Thermoplastic Elastomers Derived from Menthide and Tulipalin A, *Biomacromolecules*, 2012, **13**, 3833–3840.
- 404 C. L. Wanamaker, L. E. O'Leary, N. A. Lynd, M. A. Hillmyer and W. B. Tolman, Renewable-Resource Thermoplastic Elastomers Based on Polylactide and Polymenthide, *Biomacromolecules*, 2007, **8**, 3634–3640.
- 405 J. Jang, H. Park, H. Jeong, E. Mo, Y. Kim, J. S. Yuk, S. Q. Choi, Y.-W. Kim and J. Shin, Thermoset elastomers covalently crosslinked by hard nanodomains of triblock copolymers derived from carvomenthide and lactide: tunable strength and hydrolytic degradability, *Polym. Chem.*, 2019, **10**, 1245–1257.
- 406 S. C. Knight, C. P. Schaller, W. B. Tolman and M. A. Hillmyer, Renewable carvone-based polyols for use in polyurethane thermosets, *RSC Adv.*, 2013, **3**, 20399.

- 407 J. Yang, S. Lee, W. J. Choi, H. Seo, P. Kim, G.-J. Kim, Y.-W. Kim and J. Shin, Thermoset Elastomers Derived from Carvomenthide, *Biomacromolecules*, 2015, **16**, 246–256.
- 408 M. M. Kleybolte and M. Winnacker,  $\beta$ -Pinene-Derived Polyesteramides and Their Blends: Advances in Their Upscaling, Processing, and Characterization, *Macromol. Rapid Commun.*, 2021, **42**, e2100065.
- 409 H. C. Quilter, M. Hutchby, M. G. Davidson and M. D. Jones, Polymerisation of a terpene-derived lactone: a bio-based alternative to  $\epsilon$ -caprolactone, *Polym. Chem.*, 2017, **8**, 833–837.
- 410 J. R. Lowe, W. B. Tolman and M. A. Hillmyer, Oxidized dihydrocarvone as a renewable multifunctional monomer for the synthesis of shape memory polyesters, *Biomacromolecules*, 2009, **10**, 2003–2008.
- 411 J. R. Lowe, M. T. Martello, W. B. Tolman and M. A. Hillmyer, Functional biorenewable polyesters from carvone-derived lactones, *Polym. Chem.*, 2011, **2**, 702–708.
- 412 M. A. F. Delgove, M. J. L. J. Fürst, M. W. Fraaije, K. V. Bernaerts and S. M. A. de Wildeman, Exploring the Substrate Scope of Baeyer-Villiger Monooxygenases with Branched Lactones as Entry towards Polyesters, *ChemBioChem*, 2018, **19**, 354–360.
- 413 R. Ciriminna, M. Lomeli-Rodriguez, P. Demma Carà, J. A. Lopez-Sanchez and M. Pagliaro, Limonene: a versatile chemical of the bioeconomy, *Chem. Commun.*, 2014, **50**, 15288–15296.
- 414 M. R. Thomsett, J. C. Moore, A. Buchard, R. A. Stockman and S. M. Howdle, New renewably-sourced polyesters from limonene-derived monomers, *Green Chem.*, 2019, **21**, 149–156.
- 415 H. Blattmann and R. Mülhaupt, Multifunctional  $\beta$ -amino alcohols as bio-based amine curing agents for the isocyanate- and phosgene-free synthesis of 100% bio-based polyhydroxyurethane thermosets, *Green Chem.*, 2016, **18**, 2406–2415.
- 416 C. E. Hoyle and C. N. Bowman, Thiol-Ene Click Chemistry, *Angew. Chem. Int. Ed.*, 2010, **49**, 1540–1573.
- 417 C. K. Ranaweera, M. Ionescu, N. Bilic, X. Wan, P. K. Kahol and R. K. Gupta, Biobased Polyols Using Thiol-Ene Chemistry for Rigid Polyurethane

- Foams with Enhanced Flame-Retardant Properties, *J. Renew. Mater.*, 2017, **5**, 1–12.
- 418 M. Firdaus, Thiol-Ene (Click) Reactions as Efficient Tools for Terpene Modification, *Asian J. Org. Chem.*, 2017, **6**, 1702–1714.
- 419 Y. Zhu, F. Gao, J. Zhong, L. Shen and Y. Lin, Renewable castor oil and DL-limonene derived fully bio-based vinylogous urethane vitrimers, *Eur. Polym. J.*, 2020, **135**, 109865.
- 420 N. Mattar, A. R. de Anda, H. Vahabi, E. Renard and V. Langlois, Resorcinol-Based Epoxy Resins Hardened with Limonene and Eugenol Derivatives: From the Synthesis of Renewable Diamines to the Mechanical Properties of Biobased Thermosets, *ACS Sustainable Chem. Eng.*, 2020, **8**, 13064–13075.
- 421 N. Mattar, F. Hübner, M. Demleitner, A. Brückner, V. Langlois, E. Renard, H. Ruckdäschel and A. Rios de Anda, Multiscale Characterization of Creep and Fatigue Crack Propagation Resistance of Fully Bio-Based Epoxy-Amine Resins, *ACS Appl. Polym. Mater.*, 2021, **3**, 5134–5144.
- 422 N. Mattar, V. Langlois, E. Renard, T. Rademacker, F. Hübner, M. Demleitner, V. Altstädt, H. Ruckdäschel and A. Rios de Anda, Fully Bio-Based Epoxy-Amine Thermosets Reinforced with Recycled Carbon Fibers as a Low Carbon-Footprint Composite Alternative, *ACS Appl. Polym. Mater.*, 2021, **3**, 426–435.
- 423 C. S. Marvel and L. E. Olson, Polyalkylene Sulfides. XIII. Polymers from 4-vinyl-1-cyclohexene and d-limonene, *J. Polym. Sci.*, 1957, **26**, 23–28.
- 424 M. Firdaus, M. A. R. Meier, U. Biermann and J. O. Metzger, Renewable copolymers derived from castor oil and limonene, *Eur. J. Lipid Sci. Technol.*, 2014, **116**, 31–36.
- 425 J. Yan, S. Ariyasivam, D. Weerasinghe, J. He, B. Chisholm, Z. Chen and D. Webster, Thiourethane thermoset coatings from bio-based thiols, *Polym. Int.*, 2012, **61**, 602–608.
- 426 E. Louisy, V. Khodyrieva, S. Olivero, V. Michelet and A. Mija, Use of Limonene Epoxides and Derivatives as Promising Monomers for Biobased Polymers, *ChemPlusChem*, 2022, **87**. DOI: 10.1002/cplu.202200190.
- 427 J. D. Tibbetts, W. B. Cunningham, M. Vezzoli, P. Plucinski and S. D. Bull, Sustainable catalytic epoxidation of biorenewable terpene feedstocks using



- H<sub>2</sub>O<sub>2</sub> as an oxidant in flow microreactors, *Green Chem.*, 2021, **23**, 5449–5455.
- 428 Y. Mahamat Ahmat, S. Madadi, L. Charbonneau and S. Kaliaguine, Epoxidation of Terpenes, *Catalysts*, 2021, **11**, 847.
- 429 O. Hauenstein, M. Reiter, S. Agarwal, B. Rieger and A. Greiner, Bio-based polycarbonate from limonene oxide and CO<sub>2</sub> with high molecular weight, excellent thermal resistance, hardness and transparency, *Green Chem.*, 2016, **18**, 760–770.
- 430 A. Rehman, A. M. López Fernández, M. Gunam Resul and A. Harvey, Highly selective, sustainable synthesis of limonene cyclic carbonate from bio-based limonene oxide and CO<sub>2</sub>: A kinetic study, *J. CO<sub>2</sub> Util.*, 2019, **29**, 126–133.
- 431 S. Madadi and S. Kaliaguine, Activated Carbon-Supported Ruthenium as a Catalyst for the Solvent- and Initiator-Free Aerobic Epoxidation of Limonene, *ACS Sustainable Chem. Eng.*, 2021, **9**, 10557–10568.
- 432 S. Madadi, J.-Y. Bergeron and S. Kaliaguine, Kinetic investigation of aerobic epoxidation of limonene over cobalt substituted mesoporous SBA-16, *Catal. Sci. Technol.*, 2021, **11**, 594–611.
- 433 D. M. Biondi, C. Sanfilippo and A. Patti, Stereospecific Epoxidation of Limonene Catalyzed by Peroxygenase from Oat Seeds, *Antioxidants*, 2021, **10**. DOI: 10.3390/antiox10091462.
- 434 M. S. Melchioris, T. Y. Vieira, L. P. S. Pereira, B. A. M. Carciofi, P. H. H. de Araújo, D. de Oliveira and C. Sayer, Epoxidation of (R)-(+)-Limonene to 1,2-Limonene Oxide Mediated by Low-Cost Immobilized *Candida antarctica* Lipase Fraction B, *Ind. Eng. Chem. Res.*, 2019, **58**, 13918–13925.
- 435 E. Hosseini Nejad, A. Paoniasari, C. G. W. van Melis, C. E. Koning and R. Duchateau, Catalytic Ring-Opening Copolymerization of Limonene Oxide and Phthalic Anhydride: Toward Partially Renewable Polyesters, *Macromolecules*, 2013, **46**, 631–637.
- 436 F. Auriemma, C. De Rosa, M. R. Di Caprio, R. Di Girolamo, W. C. Ellis and G. W. Coates, Stereocomplexed Poly(Limonene Carbonate): A Unique Example of the Cocrystallization of Amorphous Enantiomeric Polymers, *Angew. Chem.*, 2015, **127**, 1231–1234.

- 437 C. M. Byrne, S. D. Allen, E. B. Lobkovsky and G. W. Coates, Alternating copolymerization of limonene oxide and carbon dioxide, *J. Am. Chem. Soc.*, 2004, **126**, 11404–11405.
- 438 S. Neumann, L.-C. Leitner, H. Schmalz, S. Agarwal and A. Greiner, Unlocking the Processability and Recyclability of Biobased Poly(limonene carbonate), *ACS Sustainable Chem. Eng.*, 2020, **8**, 6442–6448.
- 439 L. Peña Carrodegua, J. González-Fabra, F. Castro-Gómez, C. Bo and A. W. Kleij, Al(III) -catalysed formation of poly(limonene)carbonate: DFT analysis of the origin of stereoregularity, *Chem. Eur. J.*, 2015, **21**, 6115–6122.
- 440 V. Bonamigo Moreira, J. Rintjema, F. Bravo, A. W. Kleij, L. Franco, J. Puiggali, C. Alemán and E. Armelin, Novel Biobased Epoxy Thermosets and Coatings from Poly(limonene carbonate) Oxide and Synthetic Hardeners, *ACS Sustainable Chem. Eng.*, 2022, **10**, 2708–2719.
- 441 C. Martín and A. W. Kleij, Terpolymers Derived from Limonene Oxide and Carbon Dioxide: Access to Cross-Linked Polycarbonates with Improved Thermal Properties, *Macromolecules*, 2016, **49**, 6285–6295.
- 442 V. B. Moreira, C. Alemán, J. Rintjema, F. Bravo, A. W. Kleij and E. Armelin, A Biosourced Epoxy Resin for Adhesive Thermoset Applications, *ChemSusChem*, 2022, **15**, e202102624.
- 443 O. Hauenstein, S. Agarwal and A. Greiner, Bio-based polycarbonate as synthetic toolbox, *Nat. Commun.*, 2016, **7**, 11862.
- 444 N. Kindermann, À. Cristòfol and A. W. Kleij, Access to Biorenewable Polycarbonates with Unusual Glass-Transition Temperature (T<sub>g</sub>) Modulation, *ACS Catal.*, 2017, **7**, 3860–3863.
- 445 L. Charbonneau, X. Foster and S. Kaliaguine, Ultrasonic and Catalyst-Free Epoxidation of Limonene and Other Terpenes Using Dimethyl Dioxirane in Semibatch Conditions, *ACS Sustainable Chem. Eng.*, 2018, **6**, 12224–12231.
- 446 L. Charbonneau, X. Foster, D. Zhao and S. Kaliaguine, Catalyst-Free Epoxidation of Limonene to Limonene Dioxide, *ACS Sustainable Chem. Eng.*, 2018, **6**, 5115–5121.
- 447 C. Li, R. J. Sablong and C. E. Koning, Chemoselective Alternating Copolymerization of Limonene Dioxide and Carbon Dioxide: A New Highly Functional Aliphatic Epoxy Polycarbonate, *Angew. Chem.*, 2016, **128**, 11744–11748.

- 448 G. Couture, L. Granado, F. Fanget, B. Boutevin and S. Caillol, Limonene-Based Epoxy: Anhydride Thermoset Reaction Study, *Molecules*, 2018, **23**. DOI: 10.3390/molecules23112739.
- 449 F. Kazemi, L. Schutz, J.-Y. Bergeron, E. Gagnon, G. Yap and J. P. Claverie, Lanthanide dodecyl sulfates, a potent family of catalysts for the preparation of biobased epoxy thermosets, *Chem. Commun.*, 2021, **57**, 6784–6787.
- 450 E. Louisy, S. Olivero, V. Michelet and A. Mija, On the Influence of the cis/trans Stereochemistry of Limonene Oxides toward the Synthesis of Biobased Thermosets by Crosslinking with Anhydrides, *ACS Sustainable Chem. Eng.*, 2022, **10**, 7169–7179.
- 451 A. Mija, E. Louisy, S. Lachegur, V. Khodyrieva, P. Martinaux, S. Olivero and V. Michelet, Limonene dioxide as a building block for 100% bio-based thermosets, *Green Chem.*, 2021, **23**, 9855–9859.
- 452 L. Schutz, F. Kazemi, E. Mackenzie, J.-Y. Bergeron, E. Gagnon and J. P. Claverie, Trans -limonene dioxide, a promising bio-based epoxy monomer, *J. Polym. Sci.*, 2021, **59**, 321–328.
- 453 M. Bähr, A. Bitto and R. Mülhaupt, Cyclic limonene dicarbonate as a new monomer for non-isocyanate oligo- and polyurethanes (NIPU) based upon terpenes, *Green Chem.*, 2012, **14**, 1447.
- 454 Y. S. Raupp, Dissertation, Karlsruhe Institute of Technology, 2019.
- 455 G. Fiorani, M. Stuck, C. Martín, M. M. Belmonte, E. Martín, E. C. Escudero-Adán and A. W. Kleij, Catalytic Coupling of Carbon Dioxide with Terpene Scaffolds: Access to Challenging Bio-Based Organic Carbonates, *ChemSusChem*, 2016, **9**, 1304–1311.
- 456 V. Schimpf, B. S. Ritter, P. Weis, K. Parison and R. Mülhaupt, High Purity Limonene Dicarbonate as Versatile Building Block for Sustainable Non-Isocyanate Polyhydroxyurethane Thermosets and Thermoplastics, *Macromolecules*, 2017, **50**, 944–955.
- 457 F. Della Monica and A. W. Kleij, Synthesis and Characterization of Biobased Polyesters with Tunable T<sub>g</sub> by ROCOP of Beta-Elemene Oxides and Phthalic Anhydride, *ACS Sustainable Chem. Eng.*, 2021, **9**, 2619–2625.

- 458 C. Maquilón, A. Brandolese, C. Alter, C. H. Hövelmann, F. Della Monica and A. W. Kleij, Renewable Beta-Element Based Cyclic Carbonates for the Preparation of Oligo(hydroxyurethane)s, *ChemSusChem*, 2022, e202201123.
- 459 J. N. Armor, A history of industrial catalysis, *Catal. Today*, 2011, **163**, 3–9.
- 460 I. Chorkendorff and J. Niemantsverdriet, *Concepts of modern catalysis and kinetics*, Wiley-VCH, Weinheim, 5th edn., 2007.
- 461 E. Farnetti, R. Di Monte and J. Kašpar, *Inorganic and bio-inorganic chemistry*. EOLSS, EOLSS Publ, Oxford, 2009.
- 462 P. W. N. M. van Leeuwen, *Homogeneous Catalysis. Understanding the Art*, Kluwer Acad. Publ, Dordrecht, 2004.
- 463 C. W. Bamforth and D. J. Cook, *Food, Fermentation and Micro-organisms*, John Wiley & Sons, Inc, Hoboken, NJ, 2019.
- 464 E. L. Bell, W. Finnigan, S. P. France, A. P. Green, M. A. Hayes, L. J. Hepworth, S. L. Lovelock, H. Niikura, S. Osuna, E. Romero, K. S. Ryan, N. J. Turner and S. L. Flitsch, Biocatalysis, *Nat. Rev. Methods Primers*, 2021, **1**, 1:46.
- 465 G. P. Chiusoli and P. M. Maitlis, *Metal-catalysis in Industrial Organic Processes*, Royal Society of Chemistry, Cambridge, 2019.
- 466 H. Yamamoto, ed., *Lewis Acids in Organic Synthesis*, Wiley-VCH, Weinheim, New York, 2000.
- 467 P. S. Fiske, Promotionsarbeit, ETH, 1911.
- 468 A. Berkessel and H. Gröger, eds., *Metal-free organic catalysts in asymmetric synthesis*, Wiley-VCH, Weinheim, Cambridge, 2003.
- 469 B. List, Introduction: Organocatalysis, *Chem. Rev.*, 2007, **107**, 5413–5415.
- 470 B. List, R. A. Lerner and C. F. Barbas, Proline-Catalyzed Direct Asymmetric Aldol Reactions, *J. Am. Chem. Soc.*, 2000, **122**, 2395–2396.
- 471 K. A. Ahrendt, C. J. Borths and D. W. C. MacMillan, New Strategies for Organic Catalysis: The First Highly Enantioselective Organocatalytic Diels–Alder Reaction, *J. Am. Chem. Soc.*, 2000, **122**, 4243–4244.
- 472 D. W. C. MacMillan, The advent and development of organocatalysis, *Nature*, 2008, **455**, 304–308.
- 473 B. List and D. W. C. MacMillan, The 2021 Nobel Prize in Chemistry: asymmetric catalysis with small organic molecules, *Curr. Sci.*, 2021, **121**, 1148–1151.

- 474 J. G. Hernández and E. Juaristi, Recent efforts directed to the development of more sustainable asymmetric organocatalysis, *Chem. Commun.*, 2012, **48**, 5396–5409.
- 475 L. C. Branco, A. M. Faisca Phillips, M. M. Marques, S. Gago and P. S. Branco, in *Recent Advances in Organocatalysis*, ed. I. Karame and H. Srour, InTech, 2016.
- 476 O. García Mancheño and M. Waser, Recent Developments and Trends in Asymmetric Organocatalysis, *Eur. J. Org. Chem.*, 2023, **26**, e202200950.
- 477 W. N. Ottou, H. Sardon, D. Mecerreyes, J. Vignolle and D. Taton, Update and challenges in organo-mediated polymerization reactions, *Prog. Polym. Sci.*, 2016, **56**, 64–115.
- 478 A. Bossion, K. V. Heifferon, L. Meabe, N. Zivic, D. Taton, J. L. Hedrick, T. E. Long and H. Sardon, Opportunities for organocatalysis in polymer synthesis via step-growth methods, *Prog. Polym. Sci.*, 2019, **90**, 164–210.
- 479 A. P. Dove, Organic Catalysis for Ring-Opening Polymerization, *ACS Macro Lett.*, 2012, **1**, 1409–1412.
- 480 K. Fukushima and K. Nozaki, Organocatalysis: A Paradigm Shift in the Synthesis of Aliphatic Polyesters and Polycarbonates, *Macromolecules*, 2020, **53**, 5018–5022.
- 481 F. Nederberg, E. F. Connor, M. Möller, T. Glauser and J. L. Hedrick, New Paradigms for Organic Catalysts: The First Organocatalytic Living Polymerization, *Angew. Chem. Int. Ed.*, 2001, **40**, 2712–2715.
- 482 J. E. Taylor, S. D. Bull and J. M. J. Williams, Amidines, isothioureas, and guanidines as nucleophilic catalysts, *Chem. Soc. Rev.*, 2012, **41**, 2109–2121.
- 483 M. K. Kiesewetter, M. D. Scholten, N. Kirn, R. L. Weber, J. L. Hedrick and R. M. Waymouth, Cyclic guanidine organic catalysts: what is magic about triazabicyclodecene?, *J. Org. Chem.*, 2009, **74**, 9490–9496.
- 484 S. Usachev and A. Gridnev, Convenient Preparation of Bicyclic Guanidines, *Synth. Commun.*, 2011, **41**, 3683–3688.
- 485 O. Kreye, D. Kugele, L. Faust and M. A. R. Meier, Divergent Dendrimer Synthesis via the Passerini Three-Component Reaction and Olefin Cross-Metathesis, *Macromol. Rapid Commun.*, 2014, **35**, 317–322.
- 486 M. Unverferth, O. Kreye, A. Prohammer and M. A. R. Meier, Renewable Non-Isocyanate Based Thermoplastic Polyurethanes via Polycondensation of

- Dimethyl Carbamate Monomers with Diols, *Macromol. Rapid Commun.*, 2013, **34**, 1569–1574.
- 487 C. Duval, N. Kébir, A. Charvet, A. Martin and F. Burel, Synthesis and properties of renewable nonisocyanate polyurethanes (NIPUs) from dimethylcarbonate, *J. Polym. Sci. Part A: Polym. Chem.*, 2015, **53**, 1351–1359.
- 488 A. Martin, L. Lecamp, H. Labib, F. Aloui, N. Kébir and F. Burel, Synthesis and properties of allyl terminated renewable non-isocyanate polyurethanes (NIPUs) and polyureas (NIPUreas) and study of their photo-crosslinking, *Eur. Polym. J.*, 2016, **84**, 828–836.
- 489 M. Blain, L. Jean-Gérard, R. Auvergne, D. Benazet, S. Caillol and B. Andrioletti, Rational investigations in the ring opening of cyclic carbonates by amines, *Green Chem.*, 2014, **16**, 4286–4291.
- 490 R. H. Lambeth and T. J. Henderson, Organocatalytic synthesis of (poly)hydroxyurethanes from cyclic carbonates and amines, *Polymer*, 2013, **54**, 5568–5573.
- 491 M. Alves, R. Méreau, B. Grignard, C. Detrembleur, C. Jérôme and T. Tassaing, DFT investigation of the reaction mechanism for the guanidine catalysed ring-opening of cyclic carbonates by aromatic and alkyl-amines, *RSC Adv.*, 2017, **7**, 18993–19001.
- 492 R. H. Lambeth, S. M. Mathew, M. H. Baranoski, K. J. Housman, B. Tran and J. M. Oyler, Nonisocyanate polyurethanes from six-membered cyclic carbonates: Catalysis and side reactions, *J. Appl. Polym. Sci.*, 2017, **134**, 44941.
- 493 A. Z. Yu, R. A. Setien, J. M. Sahouani, J. Docken and D. C. Webster, Catalyzed non-isocyanate polyurethane (NIPU) coatings from bio-based poly(cyclic carbonates), *J. Coat. Technol. Res.*, 2019, **16**, 41–57.
- 494 Q. Chen, K. Gao, C. Peng, H. Xie, Z. K. Zhao and M. Bao, Preparation of lignin/glycerol-based bis(cyclic carbonate) for the synthesis of polyurethanes, *Green Chem.*, 2015, **17**, 4546–4551.
- 495 A. Cornille, S. Dworakowska, D. Bogdal, B. Boutevin and S. Caillol, A new way of creating cellular polyurethane materials: NIPU foams, *Eur. Polym. J.*, 2015, **66**, 129–138.

- 496 A. Bossion, R. H. Aguirresarobe, L. Irusta, D. Taton, H. Cramail, E. Grau, D. Mecerreyes, C. Su, G. Liu, A. J. Müller and H. Sardon, Unexpected Synthesis of Segmented Poly(hydroxyurea–urethane)s from Dicyclic Carbonates and Diamines by Organocatalysis, *Macromolecules*, 2018, **51**, 5556–5566.
- 497 U. Schuchardt, R. Sercheli and R. Matheus Vargas, Transesterification of Vegetable Oils: a Review, *J. Braz. Chem. Soc.*, 1998, **9**, 199–210.
- 498 U. Schuchardt, R. M. Vargas and G. Gelbard, Alkylguanidines as catalysts for the transesterification of rapeseed oil, *J. Mol. Catal. A. Chem.*, 1995, **99**, 65–70.
- 499 J. Sun and D. Kuckling, Synthesis of high-molecular-weight aliphatic polycarbonates by organo-catalysis, *Polym. Chem.*, 2016, **7**, 1642–1649.
- 500 H. Mutlu and M. A. R. Meier, Unsaturated PA X<sub>20</sub> from Renewable Resources via Metathesis and Catalytic Amidation, *Macromol. Chem. Phys.*, 2009, **210**, 1019–1025.
- 501 N. Kolb and M. A. R. Meier, Monomers and their polymers derived from saturated fatty acid methyl esters and dimethyl carbonate, *Green Chem.*, 2012, **14**, 2429–2435.
- 502 M. Winkler and M. A. R. Meier, Highly efficient oxyfunctionalization of unsaturated fatty acid esters: an attractive route for the synthesis of polyamides from renewable resources, *Green Chem.*, 2014, **16**, 1784–1788.
- 503 N. Kolb, M. Winkler, C. Syldatk and M. A. Meier, Long-chain polyesters and polyamides from biochemically derived fatty acids, *Eur. Polym. J.*, 2014, **51**, 159–166.
- 504 M. Unverferth and M. A. R. Meier, Selective formation of C<sub>36</sub>-dimer fatty acids via thiol-ene addition for copolyamide synthesis, *Eur. J. Lipid Sci. Technol.*, 2016, **118**, 1470–1474.
- 505 M. von Czapiewski and M. A. R. Meier, Catalytic Oxyfunctionalization of Methyl 10-undecenoate for the Synthesis of Step-Growth Polymers, *Macromol. Chem. Phys.*, 2017, **218**, 1700153.
- 506 M. von Czapiewski and M. A. R. Meier, Synthesis of Dimer Fatty Acid Methyl Esters by Catalytic Oxidation and Reductive Amination: An Efficient Route to Branched Polyamides, *Eur. J. Lipid Sci. Technol.*, 2018, **120**. DOI: 10.1002/ejlt.201700350.

- 507 M. Firdaus, L. Montero de Espinosa and M. A. R. Meier, Terpene-Based Renewable Monomers and Polymers via Thiol–Ene Additions, *Macromolecules*, 2011, **44**, 7253–7262.
- 508 B. G. G. Lohmeijer, R. C. Pratt, F. Leibfarth, J. W. Logan, D. A. Long, A. P. Dove, F. Nederberg, J. Choi, C. Wade, R. M. Waymouth and J. L. Hedrick, Guanidine and Amidine Organocatalysts for Ring-Opening Polymerization of Cyclic Esters, *Macromolecules*, 2006, **39**, 8574–8583.
- 509 R. M. Shakaroun, P. Jéhan, A. Alaaeddine, J.-F. Carpentier and S. M. Guillaume, Organocatalyzed ring-opening polymerization (ROP) of functional  $\beta$ -lactones: new insights into the ROP mechanism and poly(hydroxyalkanoate)s (PHAs) macromolecular structure, *Polym. Chem.*, 2020, **11**, 2640–2652.
- 510 D. J. Coady, K. Fukushima, H. W. Horn, J. E. Rice and J. L. Hedrick, Catalytic insights into acid/base conjugates: highly selective bifunctional catalysts for the ring-opening polymerization of lactide, *Chem. Commun.*, 2011, **47**, 3105–3107.
- 511 H. A. Brown, A. G. de Crisci, J. L. Hedrick and R. M. Waymouth, Amidine-Mediated Zwitterionic Polymerization of Lactide, *ACS Macro Lett.*, 2012, **1**, 1113–1115.
- 512 P. R. Schreiner and A. Wittkopp, H-bonding additives act like Lewis acid catalysts, *Org. Lett.*, 2002, **4**, 217–220.
- 513 P. R. Schreiner, Metal-free organocatalysis through explicit hydrogen bonding interactions, *Chem. Soc. Rev.*, 2003, **32**, 289–296.
- 514 Y. Takemoto, Recognition and activation by ureas and thioureas: stereoselective reactions using ureas and thioureas as hydrogen-bonding donors, *Org. Biomol. Chem.*, 2005, **3**, 4299–4306.
- 515 A. Wittkopp and P. R. Schreiner, Metal-Free, Noncovalent Catalysis of Diels–Alder Reactions by Neutral Hydrogen Bond Donors in Organic Solvents and in Water, *Chem. Eur. J.*, 2003, **9**, 407–414.
- 516 K. M. Lippert, K. Hof, D. Gerbig, D. Ley, H. Hausmann, S. Guenther and P. R. Schreiner, Hydrogen-Bonding Thiourea Organocatalysts: The Privileged 3,5-Bis(trifluoromethyl)phenyl Group, *Eur. J. Org. Chem.*, 2012, **2012**, 5919–5927.



- 517 M. T. Robak, M. Trincado and J. A. Ellman, Enantioselective Aza-Henry Reaction with an N-Sulfinyl Urea Organocatalyst, *J. Am. Chem. Soc.*, 2007, **129**, 15110–15111.
- 518 S. Ban, X. Zhu, Z. Zhang, H. Xie and Q. Li, Benzoylthiourea-Pyrrolidine as Another Bifunctional Organocatalyst: Highly Enantioselective Michael Addition of Cyclohexanone to Nitroolefins, *Eur. J. Org. Chem.*, 2013, **2013**, 2977–2980.
- 519 Y. Fan and S. R. Kass, Electrostatically Enhanced Thioureas, *Org. Lett.*, 2016, **18**, 188–191.
- 520 M. Ganesh and D. Seidel, Catalytic enantioselective additions of indoles to nitroalkenes, *J. Am. Chem. Soc.*, 2008, **130**, 16464–16465.
- 521 R. Nickisch, S. M. Gabrielsen and M. A. R. Meier, Novel Access to Known and Unknown Thiourea Catalyst via a Multicomponent-Reaction Approach, *ChemistrySelect*, 2020, **5**, 11915–11920.
- 522 M. Blain, H. Yau, L. Jean-Gérard, R. Auvergne, D. Benazet, P. R. Schreiner, S. Caillol and B. Andrioletti, Urea- and Thiourea-Catalyzed Aminolysis of Carbonates, *ChemSusChem*, 2016, **9**, 2269–2272.
- 523 R. C. Pratt, B. G. G. Lohmeijer, D. A. Long, P. N. P. Lundberg, A. P. Dove, H. Li, C. G. Wade, R. M. Waymouth and J. L. Hedrick, Exploration, Optimization, and Application of Supramolecular Thiourea–Amine Catalysts for the Synthesis of Lactide (Co)polymers, *Macromolecules*, 2006, **39**, 7863–7871.
- 524 A. M. Goldys and D. J. Dixon, Organocatalytic Ring-Opening Polymerization of Cyclic Esters Mediated by Highly Active Bifunctional Iminophosphorane Catalysts, *Macromolecules*, 2014, **47**, 1277–1284.
- 525 T. Okino, Y. Hoashi and Y. Takemoto, Enantioselective Michael reaction of malonates to nitroolefins catalyzed by bifunctional organocatalysts, *J. Am. Chem. Soc.*, 2003, **125**, 12672–12673.
- 526 T. Okino, Y. Hoashi, T. Furukawa, X. Xu and Y. Takemoto, Enantio- and diastereoselective Michael reaction of 1,3-dicarbonyl compounds to nitroolefins catalyzed by a bifunctional thiourea, *J. Am. Chem. Soc.*, 2005, **127**, 119–125.
- 527 A. P. Dove, R. C. Pratt, B. G. G. Lohmeijer, R. M. Waymouth and J. L. Hedrick, Thiourea-Based Bifunctional Organocatalysis: Supramolecular

- Recognition for Living Polymerization, *J. Am. Chem. Soc.*, 2005, **127**, 13798–13799.
- 528 X. Zhang, G. O. Jones, J. L. Hedrick and R. M. Waymouth, Fast and selective ring-opening polymerizations by alkoxides and thioureas, *Nat. Chem.*, 2016, **8**, 1047–1053.
- 529 B. Lin and R. M. Waymouth, Organic Ring-Opening Polymerization Catalysts: Reactivity Control by Balancing Acidity, *Macromolecules*, 2018, **51**, 2932–2938.
- 530 B. Lin and R. M. Waymouth, Urea Anions: Simple, Fast, and Selective Catalysts for Ring-Opening Polymerizations, *J. Am. Chem. Soc.*, 2017, **139**, 1645–1652.
- 531 W. Zhou, C. Xu, Y. Liu and Y. Shen, Preparation of high-molecular-weight polylactide by ring-opening polymerization of L-lactide using base/bisurea binary organocatalyst, *J Polym Res*, 2023, **30**. DOI: 10.1007/s10965-023-03621-w.
- 532 J. U. Pothupitiya, N. U. Dharmaratne, T. M. M. Jouaneh, K. V. Fastnacht, D. N. Coderre and M. K. Kiesewetter, H-Bonding Organocatalysts for the Living, Solvent-Free Ring-Opening Polymerization of Lactones: Toward an All-Lactones, All-Conditions Approach, *Macromolecules*, 2017, **50**, 8948–8954.
- 533 Z. Jiang, J. Zhao and G. Zhang, Ionic Organocatalyst with a Urea Anion and Tetra-n-butyl Ammonium Cation for Rapid, Selective, and Versatile Ring-Opening Polymerization of Lactide, *ACS Macro Lett.*, 2019, **8**, 759–765.
- 534 L. R. Schroeder and S. L. Cooper, Hydrogen bonding in polyamides, *J. Appl. Phys.*, 1976, **47**, 4310–4317.
- 535 S. SHARMA, THE CHEMISTRY OF THIOPHOSGENE, *Sulfur reports*, 1986, **5**, 1–100.
- 536 K. Eschliman and S. Bossmann, Synthesis of Isothiocyanates: An Update, *Synthesis*, 2019, **51**, 1746–1752.
- 537 F. B. Dains, R. Q. Brewster and C. P. Olander, Phenyl Isothiocyanate, *Org. Synth.*, 1926, **6**, 72.
- 538 M. Lipp and I. Meier zu Köcker, Über die Addition von Schwefel und Selen an Isonitrile, *Mh. Chem.*, 1959, **90**, 41–48.
- 539 T. B. Nguyen, L. Ermolenko and A. Al-Mourabit, Three-Component Reaction between Isocyanides, Aliphatic Amines and Elemental Sulfur:

- Preparation of Thioureas under Mild Conditions with Complete Atom Economy, *Synthesis*, 2014, **46**, 3172–3179.
- 540 A. Harsanyi and G. Sandford, Organofluorine chemistry: applications, sources and sustainability, *Green Chem.*, 2015, **17**, 2081–2086.
- 541 Z. Abdel Baki, H. Dib and T. Sahin, Overview: Polycarbonates via Ring-Opening Polymerization, Differences between Six- and Five-Membered Cyclic Carbonates: Inspiration for Green Alternatives, *Polymers*, 2022, **14**. DOI: 10.3390/polym14102031.
- 542 E. F. Connor, G. W. Nyce, M. Myers, A. Möck and J. L. Hedrick, First example of N-heterocyclic carbenes as catalysts for living polymerization: organocatalytic ring-opening polymerization of cyclic esters, *J. Am. Chem. Soc.*, 2002, **124**, 914–915.
- 543 A. P. Dove, R. C. Pratt, B. G. Lohmeijer, D. A. Culkin, E. C. Hagberg, G. W. Nyce, R. M. Waymouth and J. L. Hedrick, N-Heterocyclic carbenes: Effective organic catalysts for living polymerization, *Polymer*, 2006, **47**, 4018–4025.
- 544 I. Nifant'ev, A. Shlyakhtin, V. Bagrov, B. Lozhkin, G. Zakirova, P. Ivchenko and O. Legon'kova, Theoretical and experimental studies of 1,5,7-triazabicyclo[4.4.0]dec-5-ene-catalyzed ring opening/ring closure reaction mechanism for 5-, 6- and 7-membered cyclic esters and carbonates, *Reac. Kinet. Mech. Cat.*, 2016, **117**, 447–476.
- 545 M. Selva, A. Caretto, M. Noè and A. Perosa, Carbonate phosphonium salts as catalysts for the transesterification of dialkyl carbonates with diols. The competition between cyclic carbonates and linear dicarbonate products, *Org. Biomol. Chem.*, 2014, **12**, 4143–4155.
- 546 E. W. P. Tan, J. L. Hedrick, P. L. Arrechea, T. Erdmann, V. Kiyek, S. Lottier, Y. Y. Yang and N. H. Park, Overcoming Barriers in Polycarbonate Synthesis: A Streamlined Approach for the Synthesis of Cyclic Carbonate Monomers, *Macromolecules*, 2021, **54**, 1767–1774.
- 547 M. A. Hillmyer and W. B. Tolman, Aliphatic polyester block polymers: renewable, degradable, and sustainable, *Acc. Chem. Res.*, 2014, **47**, 2390–2396.
- 548 M. Ludwig, Bachelor Thesis, Karlsruhe Institute of Technology, 2021.
- 549 S. S. Canan Koch and A. R. Chamberlin, Modified Conditions for Efficient Baeyer-Villiger Oxidation with m-CPBA, *Synth. Commun.*, 1989, **19**, 829–833.

- 550 H. Hussain, I. R. Green and I. Ahmed, Journey Describing Applications of Oxone in Synthetic Chemistry, *Chem. Rev.*, 2013, **113**, 3329–3371.
- 551 S. Alvi, V. Jayant and R. Ali, Applications of Oxone® in Organic Synthesis: An Emerging Green Reagent of Modern Era, *ChemistrySelect*, 2022, **7**. DOI: 10.1002/slct.202200704.
- 552 P. S. Löser, P. Rauthe, M. A. R. Meier and A. Llevot, Sustainable catalytic rearrangement of terpene-derived epoxides: towards bio-based biscarbonyl monomers, *Phil. Trans. R. Soc. A*, 2020, **378**, 20190267.
- 553 G.-J. ten Brink, I. W. C. E. Arends and R. A. Sheldon, The Baeyer-Villiger Reaction: New Developments toward Greener Procedures, *Chem. Rev.*, 2004, **104**, 4105–4124.
- 554 A. Stamm, A. Biundo, B. Schmidt, J. Brücher, S. Lundmark, P. Olsén, L. Fogelström, E. Malmström, U. T. Bornscheuer and P.-O. Syrén, A Retro-biosynthesis-Based Route to Generate Pinene-Derived Polyesters, *ChemBioChem*, 2019, **20**, 1664–1671.
- 555 A. Stamm, J. Öhlin, C. Mosbech, P. Olsén, B. Guo, E. Söderberg, A. Biundo, L. Fogelström, S. Bhattacharyya, U. T. Bornscheuer, E. Malmström and P.-O. Syrén, Pinene-Based Oxidative Synthetic Toolbox for Scalable Polyester Synthesis, *J. Am. Chem. Soc.*, 2021, **1**, 1949–1960.
- 556 B. Jousseume, C. Laporte, T. Toupance and J.-M. Bernard, Efficient bismuth catalysts for transcarbamylation, *Tetrahedron Lett.*, 2002, **43**, 6305–6307.
- 557 D. Limnios and C. G. Kokotos, in *Sustainable Catalysis*, ed. M. North, Royal Society of Chemistry, Cambridge, 2015, pp. 196–255.
- 558 R. Nickisch, Dissertation, Karlsruhe Institute of Technology, 2022.
- 559 F. C. M. Scheelje and M. A. R. Meier, Non-isocyanate polyurethanes synthesized from terpenes using thiourea organocatalysis and thiol-ene-chemistry, *Commun. Chem.*, 2023, **6**, 239.
- 560 D. Merckle, E. Constant and A. C. Weems, Linalool Derivatives for Natural Product-Based 4D Printing Resins, *ACS Sustainable Chem. Eng.*, 2021, **9**, 12213–12222.
- 561 N. S. Purwanto, Y. Chen and J. M. Torkelson, Reprocessable, Bio-Based, Self-Blowing Non-Isocyanate Polyurethane Network Foams from Cashew Nutshell Liquid, *ACS Appl. Polym. Mater.*, 2023, **5**, 6651–6661.

- 562 N. S. Purwanto, Y. Chen, T. Wang and J. M. Torkelson, Rapidly synthesized, self-blowing, non-isocyanate polyurethane network foams with reprocessing to bulk networks via hydroxyurethane dynamic chemistry, *Polymer*, 2023, **272**, 125858.
- 563 A. Cornille, C. Guillet, S. Benyahya, C. Negrell, B. Boutevin and S. Caillol, Room temperature flexible isocyanate-free polyurethane foams, *Eur. Polym. J.*, 2016, **84**, 873–888.
- 564 R. K. Gupta, M. Ionescu, D. Radojicic, X. Wan and Z. S. Petrovic, Novel Renewable Polyols Based on Limonene for Rigid Polyurethane Foams, *J. Polym. Environ.*, 2014, **22**, 304–309.
- 565 R. Acosta Ortiz, R. S. Sánchez Huerta, A. S. Ledezma Pérez and A. E. García Valdez, Synthesis of a Curing Agent Derived from Limonene and the Study of Its Performance to Polymerize a Biobased Epoxy Resin Using the Epoxy/Thiol-Ene Photopolymerization Technique, *Polymers*, 2022, **14**. DOI: 10.3390/polym14112192.
- 566 L. Breloy, C. A. Ouarabi, A. Brosseau, P. Dubot, V. Brezova, S. Abbad Andaloussi, J.-P. Malval and D.-L. Versace,  $\beta$ -Carotene/Limonene Derivatives/Eugenol: Green Synthesis of Antibacterial Coatings under Visible-Light Exposure, *ACS Sustainable Chem. Eng.*, 2019, **7**, 19591–19604.
- 567 M. Ge, J.-T. Miao, K. Zhang, Y. Wu, L. Zheng and L. Wu, Building biobased, degradable, flexible polymer networks from vanillin via thiol–ene “click” photopolymerization, *Polym. Chem.*, 2021, **12**, 564–571.
- 568 H. Morinaga and M. Sakamoto, Synthesis of multi-functional epoxides derived from limonene oxide and its application to the network polymers, *Tetrahedron Lett.*, 2017, **58**, 2438–2440.

